Discovery and Optimisation of Small-Molecule ERK5 Inhibitors as Cancer Therapeutics

Stephanie May Myers

This thesis is submitted to Newcastle University for the degree of Doctor of Philosophy

September 2012

Declaration

The work carried out contributing to this thesis was conducted between October 2008 and September 2012 in the Medicinal Chemistry laboratories, Bedson Building, Northern Institute for Cancer Research at the Newcastle Cancer Centre, Newcastle University, Newcastle upon Tyne, NE1 7RU. The research was conducted in collaboration with the scientists at Cancer Research Technology Discovery Laboratories, The Cruciform Building, Gower Street, London, WC1E 6BT, the Beatson Institute for Cancer Research, Garscube Estate, Switchback Road, Bearsden, Glasgow, G61 1BD and the Babraham Institute, Babraham Research Campus, Cambridge, CB22 3AT.

All of the research presented in this thesis is original in context, and does not include any material or ideas previously published or presented by other authors except where due reference is given in the text.

No part of this thesis has been previously submitted for a degree, diploma or any qualification at any other university.

Acknowledgements

First and foremost I would like to thank my supervisors, Dr Ian Hardcastle, Dr Celine Cano, Professor Roger Griffin, and Professor Bernard Golding. Without their invaluable knowledge, guidance, encouragement and understanding this thesis would not have been possible. I consider myself extremely lucky to have been given the opportunity to work in such a fantastic research environment. In addition, I would like to thank Ms Ai Ching Wong, Mrs Pamela Lochhead and Dr Simon Cook for giving me the opportunity to gain experience in the field of biology during placements at CRT and the Babraham Institute, respectively. Their patience and support was greatly appreciated during those steep learning curves.

I express my gratitude to all of the collaborators involved in the project, at CRT, the Beatson Institute and the Babraham Institute and to Professor Herbie Newell at the NICR for their continued support surrounding the biological aspects of the project. I would particularly like to thank Ms Ai Ching Wong for the biological evaluation of all compounds in the enzyme assays. Thank you to Lan-Zhen Wang at the NICR for conducting preliminary cell based studies, and to Huw Thomas for conducting *in vivo* studies. Support with homology modelling was provided by Dr Susan Boyd of CRT and Professor Martin Noble at the NICR.

I would like to express my appreciation to Cancer Research UK for the generous financial support throughout my PhD, and for funding the on-going research at the NICR.

Thank you to Dr Karen Haggerty for the technical support including HPLC analysis and purification, and to Carlo Bawn for his invaluable NMR expertise and technical support. I would like to thank all of the members of the lab, past and present for their continuing friendship and emotional support; Dr Tim Blackburn, Dr Ruth Bawn, Dr Tommy Rennison, Dr Betty Cottyn, Dr Sandrine Vidot, Dr Barry Dodd, Dr Andrey Zaytzev, Dr Kate Smith, Dr Charlotte Revill, Dr Sara Payne, Dr Chris Coxon, Dr Elisa Meschini, Dr Mangaleswaran Sivaprakasam, Dr Anna Watson, Dr Chris Wong, Dr Jen Ricci, Duncan Miller, Chris Matheson, David Turner, Lauren Barrett, Sarah Cully, Tristan Reuillon, Andrew Shouksmith, Annalisa Bertoli, Nicholas Charles Martin, Bian Zhang, and Honorine Lebraud. You have all made the experience an amazing one.

Last but not least, thank you to my family and my close friends. My parents, who are so proud of my achievements, have given so much support throughout my education, financially, emotionally and unconditionally.

Abstract

Extracellular signal-regulated kinase 5 (ERK5) is a member of the protein kinase superfamily, which plays an essential role in the transduction of extracellular signals to intracellular effectors. Activation of the ERK5 signalling pathway is associated with cell survival, proliferation, and differentiation, and thus ERK5 over-expression may have implications in carcinogenesis. Therefore, the discovery and development of small molecule inhibitors of ERK5 may offer a novel therapeutic intervention for cancer.

High throughput screening (HTS) of chemical libraries, conducted by Cancer Research Technology, revealed three distinct chemical series as moderate inhibitors of ERK5. Two of these series are described herein i.e.: 3-cyanopyridines (IC_{50} = 0.5 – 31.3 µM); and pyrrole-carboxamides (IC_{50} = 0.66 – 3.5 µM).

Two 3-cyanopyridine based hits (2-(2-((3-cyano-4-(4-fluorophenyl)-6-phenylpyridin-2-yl)thio)acetamido)acetic acid, **68** and 2-((3-cyano-4-(4-fluorophenyl)-6-phenylpyridin-2-yl)thio)-*N*-(2-oxopropyl)acetamide, **67**; IC_{50} values = 1.6 and 0.5 µM, respectively) were resynthesised and were slightly less active at 4.9 and 20.5 µM. The 3-cyanopyridine scaffold was deemed a valid starting point for initiating structure activity relationship (SAR) studies. Three areas were identified for further investigation i.e.: modification to the thioether side-chain; modification to the aryl substituent; and isosteric replacement of the 3-cyano motif. Structure-activity studies did not result in improved potency over the initial hits.

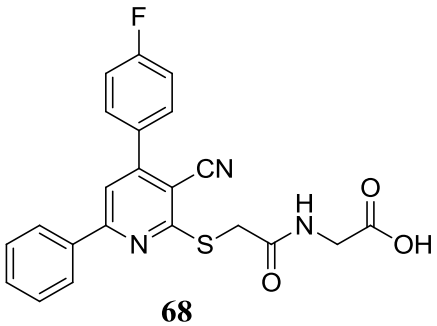

68

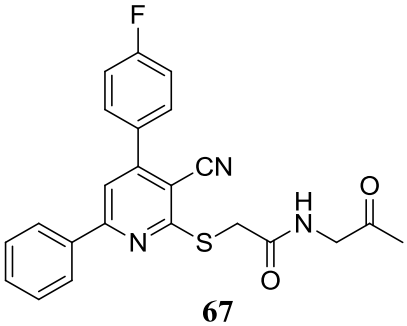

67

Previously, the pyrrole-carboxamide series has been validated successfully. Hit-to-lead studies around the aroyl ring highlighted the importance of substitution pattern for potency, with 2,6-difluoro (or 2,3-dichloro) substituents conferring the greatest potency (4-(2,6-difluorobenzoyl)-*N*-(pyridin-4-ylmethyl)-1*H*-pyrrole-2-carboxamide, **144**; IC_{50} = 2.3 µM) initially. Truncation of the carboxamide side-chain resulted in improved activity (IC_{50} = 0.9

μM) and crucially, ≥100-fold selectivity for ERK5 over the closely related kinase p38α was also achieved e.g. 4-(2,6-difluorobenzoyl)-*N*-(pyridin-4-yl)-1*H*-pyrrole-2-carboxamide, **256**.. Tuning of the aroyl substituents and pyridyl groups resulted in discovery of 4-(2-bromo-6-fluorobenzoyl)-*N*-(pyridin-3-yl)-1*H*-pyrrole-2-carboxamide, **278** a potent and selective ERK5 inhibitor with excellent drug-like properties (i.e.: MW = 388; cLogP = 3.2; LE = 0.35; Aqueous solubility = >100 μM; PPB = 94%). Preliminary *in vivo* studies of lead compound 4-(2-bromo-6-fluorobenzoyl)-*N*-(pyridin-3-yl)-1*H*-pyrrole-2-carboxamide have confirmed efficacy in xenograft tumour models, and satisfactory pharmacokinetic properties in mice. The pyrrole-carboxamide series has now entered the lead optimisation phase of drug discovery, focussing on improvement of cellular activity, and eliminating CYP inhibition, with the aim of providing compounds with suitable potency and properties for clinical trials.

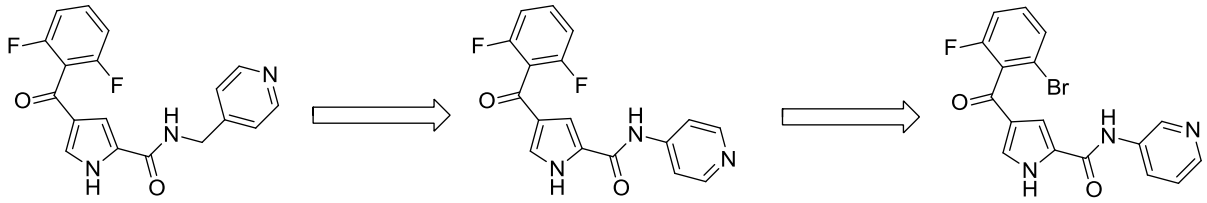

Abbreviations

Å	Ångström
ADMET	Absorption, distribution, metabolism, excretion and toxicology
ALL	Acute lymphoblastic leukaemia
amu	Atomic mass units
AP-1	Activator protein 1
AR	Androgen receptor
AUC	Area under curve
Bad	Bcl-2-associated death promoter
Bcl	B-cell lymphoma
Bem	Bud emergence mediator
BLAST	Basic local alignment search tool
BMK-1	Big MAP kinase
Boc	*tert*-Butoxycarbonyl
br	broad
BRCA	Breast cancer
Caco-2	Human epithelial colorectal adenocarcinoma cell line
CaP	Prostate cancer
CDI	Cabonyldiimidazole
CDK	Cyclin dependant kinase
cLogP	Calculated partition coefficient
CMax	Maximum concentration

CML	Chronic myelogenous leukaemia
CRT	Cancer Research Technology
CTGF	Connective tissue growth factor
CYP	Cytochrome P450 enzymes
d	doublet
DCAMKL	Doublecortin and CaM kinase-like
DHEA	Dehydroepiandrostenedione
DHFR	Dihydrofolate reductase
DHT	5α-dihydrotestosterone
DIPEA	*N*,*N*-diisopropylethylamine
DMAP	4-dimethylaminopyridine
DMCDA	*N*, *N*'-dimethylcyclohexane-1, 2-diamine
DMPK	Drug metabolism and pharmacokinetics
DNA	Deoxyribonucleic acid
DTT	Dithiothreitol
dbpf	Di-*tert*-butylphosphino ferrocene
EAS	Electrophilic aromatic substitution
EDG	Electron donating group
EDTA	Ethylenediaminetetraacetic acid
EGF	Epidermal growth factor
EGFP	Enhanced green fluorescent protein
EGFR	Epidermal growth factor receptor

EGFR-TK	EGFR-tyrosine kinase
EGTA	Ethylene glycol tetraacetic acid
Elk1	Ets-like transcription factor 1
ELSD	Evaporative light scattering detection
ErbB2	V-erb-b2 avian erythroblastic leukemia viral oncogene homologue 2
ERK	Extracellular signal-regulated kinase
c-Ets	c-E twenty-six
EWG	Electron withdrawing group
F	Bioavailability
FAK	Focal adhesion kinase
FBS	Foetal bovine serum
FGF	Fibroblast growth factor
FP	Fluorescence polarisation
FT-IR	Fourier transform infra-red
ΔG	Gibbs free energy
GI	Gastrointestinal
GIST	Gastrointestinal stromal tumour
GnRH	Gonadotropin-releasing hormone
Grb2	Growth factor receptor-bound protein 2
GST	Glutathione *S*-transferase
HAC	Heavy atom count
HBTU	*O*-Benzotriazole-*N*,*N*,*N'*,*N'*-tetramethyl-uronium-hexafluoro-phosphate

HCT116	Human colorectal cancer cell line
HEK293	Human embryonic kidney cell line
HeLa	Human cervical cancer cell line
HER2	Human EGF receptor
hERG	Human ether-a-go-go related gene
HCC	Hepatocellular carcinoma
HMBC	Heteronuclear multiple bond correlation
HOBt	Hydroxybenzotriazole
HPLC	High performance liquid chromatography
HSP	Heat shock protein
HSQC	Heteronuclear single quantum coherence
HTS	High-throughput screening
IC_{50}	Half-maximal inhibitory concentration
Id1	Inhibitor of differentiation 1
IL	Interleukin
IMAP	Immobilised metal affinity polarisation
IP	Intraperitoneally
IP/WB	Immunoprecipitation/Western blotting
IV	Intravenously
JHH-7	Human HCC cell line
JNK	c-Jun *N*-terminal kinase
Ki	Inhibition constant

Km	Michaelis constant
Lad	Lck-associated adaptor
Lck	Lymphocyte-specific protein tyrosine kinase
LCMS	Liquid chromatography/Mass spectrometry
LB	Lysogeny broth
LE	Ligand efficiency
LL	Lewis lung carcinoma
LNCaP	Androgen-sensitive human prostate adenocarcinoma cell line
m	multiplet
MAPK	Mitogen activated protein kinase
MAPKAPK	MAP kinase activated protein kinase
MAPKK	MAP kinase kinase
MAPKKK	MAP kinase kinase kinase
MDA-MB-435	Human breast cancer cell line
MEF2	Myocyte enhancer factor 2
MEK	MAP kinase kinase
MEKK	MAP kinase kinase kinase
MIDA	*N*-methyliminodiacetic acid
MM	Multiple myeloma
MMP	matrix metalloproteinase
MNK	MAP interacting kinase
Mp	Melting point

MPLC	Medium-pressure liquid chromatography
Ms	Mesyl
NBS	*N*-bromosuccinamide
NIS	*N*-iodosuccinamide
ND	No data
NEK2	NIMA (Never in mitosis gene A)-related kinase 2
NES	Nuclear export sequence
NFκB	Nuclear factor kappa-light-chain-enhancer of activated B-cells
NGF	Nerve growth factor
NLK	Nemo-like kinase
NLS	Nuclear localisation sequence
NOE	Nuclear Overhauser effect
NSCLC	Non-small cell lung cancer
PB1	Phox/Bem1 domains
PBS	Phosphate buffered saline
P-gp	Permeability glycoprotein
PC3	Human prostate cancer cell line
PDA	Photodiode array
Phox	Phagocytic oxidase
PI3K	Phosphatidylinositol 3-kinases
PK	Pharmacokinetic
PKA	Protein kinase A

pKa	Acid dissociation constant
PLB	Passive lysis buffer
PLK	Polo-like kinase
PMB	*para*-methoxybenzyl
PML	Promyelocytic leukaemia protein
PO	Orally
POC	Proof-of-concept
PPB	Plasma protein binding
PSA	Prostate specific antigen
PyBOP	Benzotriazol-1-yl-oxytripyrrolidinophosphonium hexafluorophosphate
q	quartet
QSAR	Quantitative SAR
quin	quintet
Raf	Rapidly accelerated fibrosarcoma
Ras	Rat sarcoma
RCC	Renal cell carcinoma
RNA	Ribonucleic acid
rpS6	Ribosomal protein S6
RSK	Ribosomal s6 kinase
RT	Room temperature
s	singlet
SAPK2	Stress-activated protein kinase

SAR	Structure-activity relationship
SEM	2-(Trimethylsilyl)ethoxymethyl
SGK	Serine/threonine kinase
siRNA	Small interfering RNA
SoS	Son of Sevenless
S_NAr	Nucleophilic aromatic substitution
SNU449	Human HCC cell line
Sp1	Specificity protein 1
Stat3	Signal transducer and activator of transcription 3
Stat3-C	Constitutively activated Stat3
t	triplet
T1/2	Half-life
TAD	Transactivation domain
TBAF	Tetra-*n*-butylammonium fluoride
TBAI	Tetra-*n*-butylammonium iodide
TERT	Non-malignant telomerase immortalised breast cancer cell line
TFA	Trifluoroacetic acid
TGF-β	Transforming growth factor β
TIPS	Triisopropylsilyl
TMax	Time at CMax
TMS	trimethylsilyl
TNK	Mouse tyrosine kinase, non-receptor

TPSA	Topological polar surface area
Ts	Tosyl
TSP1	Thrombospondin-1
UPLC	Ultra performance liquid chromatography
UV	Ultraviolet
Vdss	Volume of distribution
VEGF	Vascular endothelium growth factor
wt	Wild-type

Contents

Chapter 1: Overview of Modern Chemotherapy

1.1 Introduction to Cancer

Cancer is an illness characterized by the uncontrolled growth of cells in the body, as a result of mutation in one or more genes. Cells which are free from the usual constraints of proliferation, growth and apoptosis arise through a variety of factors; through complex biological mechanisms, as a result of genetic malfunctions.[1] In 2009, approximately 320,500 new cases of cancer were diagnosed in the UK.[2] There are over 200 classifications of cancer, with breast, lung, colorectal and prostate cancers accounting for 54% of newly diagnosed cases each year (Figure **1**). Advances in cancer research and the development of new treatments have enabled the ten year survival rate to double over the past thirty years. Overall, cancer survival statistics are improving, with around half of people diagnosed with cancer passing the five year survival point, and the cancer death rate has fallen by 10% over the last decade overall in the UK.[3] Despite this improvement, there are still a number of specific cancers where the survival rate is particularly low, and therefore on-going research into new effective chemotherapeutic agents is essential in this disease area.

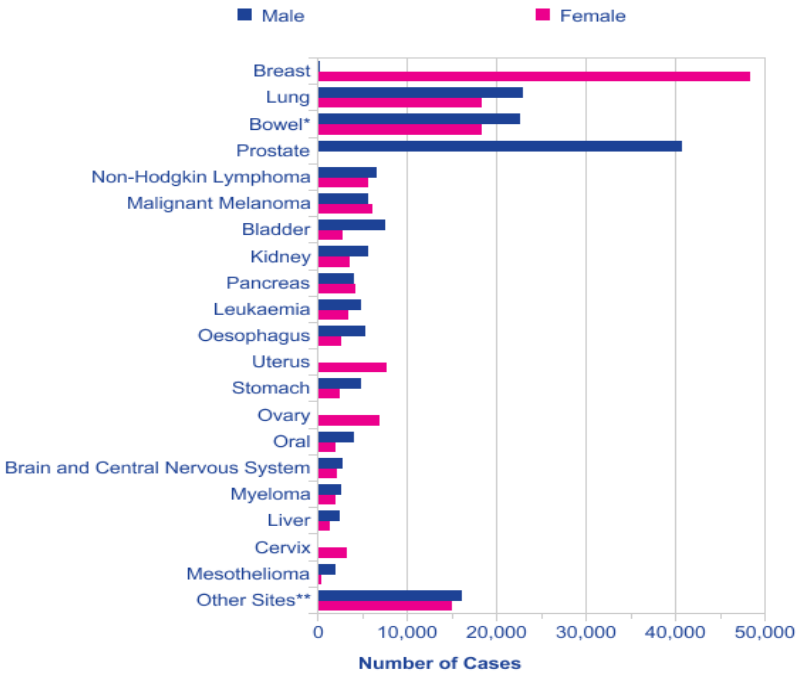

Figure 1: The 20 most commonly diagnosed cancers (excluding non-melanoma skin cancer) in the UK, 2009. * Bowel cancer including anal cancer; ** 4% of female cancers and 3% of male cancers are registered without specification of the primary site. From ref [4].

1.2 The History of Chemotherapy

Until the 1960s the most common treatments for cancer were surgery and radiotherapy, but development of untraced metastases from the primary tumour meant that the overall cure rate was low (33%) following local treatments.[5] The twentieth century saw the beginning of drug development for the treatment of cancer. Investigation into the use of nitrogen mustards began following World War 2, following the observation that levels of bone marrow and lymph tissue were significantly reduced in men who had been exposed to the toxic gases. Pioneering treatment of patients suffering from lymphoma revealed that clinical use of nitrogen mustards was an effective treatment for the disease. Based on this research, DNA alkylating agents such as chlorambucil, **1** were developed.[5] In 1948, Farber *et al* described the effects of administering folic acid to children with acute lymphoblastic leukaemia (ALL). The observed effect was acceleration of the disease. Farber postulated that ALL may therefore be treated using an antagonist of folic acid, aminopterin, which would eventually lead to the discovery of methotrexate, **2**.[6] Methotrexate is known to act as an inhibitor of dihydrofolate reductase (DHFR), an enzyme involved in the biosynthesis of folic acid. Folic acid is required for biosynthesis of thymidine, and therefore the synthesis of DNA. The anti-folate chemotherapeutic agents were some of the first examples of rationally designed anti-cancer drugs used in the clinic.[5] These early discoveries led to the belief that cancer could be treated and ultimately cured using synthetically created compounds.

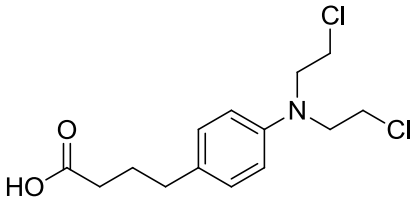

Chlorambucil, **1**

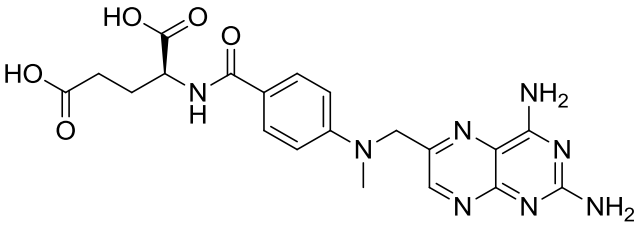

Methotrexate, **2**

1.3 Targeted Drug Discovery

Until recently, drug discovery for new cancer therapeutics largely centred on the development of inhibitors of DNA synthesis, DNA-alkylating agents and anti-metabolites. Although efficacious, these drug classes suffered from severe toxicity profiles due to lack of selectivity for cancer cells over normal tissue.[7] The notion of targeted drug discovery was first described in 1874, when P. Ehrlich hypothesised that the differences between chemoreceptors on microorganisms and cancer cells to those of healthy tissues could be

exploited therapeutically.[8] Despite this, it would take another 100 years for targeted drug discovery to come into practice in cancer treatment. It was not until the early 1980's, when the practice of targeted drug discovery became more prolific, driven by the discovery of oncogenes. One of the first targeted agents to be identified was tamoxifen, **3** approved in 1977 for patients with advanced breast cancer. At the time of its discovery, tamoxifen was not acclaimed as a breakthrough drug, as enthusiasm for cytotoxic chemotherapy was still prevalent.[9] The role of oestrogens in the development of breast cancer is well established; tamoxifen acts as an antagonist of the oestrogen receptor, preventing oestrogenic signalling. Tamoxifen has since become the 'gold standard' of care for the treatment of advanced breast cancers which are positive for the oestrogen receptor.[9] Following the success of tamoxifen for the treatment of female oestrogen dependent cancer, came the launch of bicalutamide, **4** (Casodex) in 1995. The use of anti-androgens for the treatment of advanced prostate cancer is discussed in further detail in Section **3.1.3**.

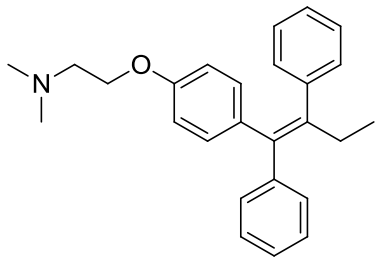

Tamoxifen, **3**

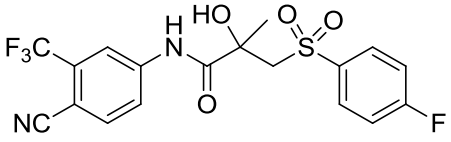

Bicalutamide, **4**

The development of kinase inhibitors has become a prevalent therapeutic area since the discovery of the Bcr-Abl oncogene, which encodes a constitutively active tyrosine kinase in patients with chronic myelogenous leukaemia (CML).[7] The discovery of this oncogene ultimately led to the successful development of imatinib, **5** (Glivec), launched in 2005 for the treatment for patients with CML. This ground-breaking drug proved that it is possible to develop rationally designed, targeted therapeutic agents for the treatment of cancer, where a specific oncogene has been implicated in the onset and progression of the disease.[7]

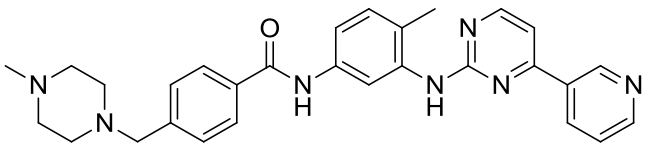

Imatinib, **5**

1.4 Modern Drug Development

The modern drug discovery process typically follows the scheme outlined in Figure **2**. High-throughput screening (HTS) of compound collections is used to identify 'hits' showing good to moderate activity against the biological target. Following hit validation, hit-to-lead studies establish structure-activity relationships (SARs) with respect to potency. Physicochemical properties, synthetic tractability, selectivity for the target and freedom of intellectual property are also considered at this stage. Christopher Lipinski formulated the 'rule of five' in 1997, setting out distinct physicochemical properties required for the development of an orally bioavailable drug. Poor *in vivo* absorption and/or permeation properties are expected for small molecule drugs when one or more of Lipinski's criteria are not met. A molecular weight greater than 500, a logP above 5, and more than 5 H-bond donors/more than 10 H-bond acceptors present in a molecule are all undesirable features, when considering oral bioavailability of a drug.[10] Since Lipinski's computational approach to rational drug design was first published, early assessment of several other parameters have become commonplace in the medicinal chemistry setting. For example topological polar surface area (TPSA) is frequently considered, a factor affecting cell permeation. Typically a TPSA below 140Å^2 is required for adequate cell penetration by a compound.[11] Potent and selective compounds are assessed using a range of *in vitro* ADMET (absorption, distribution, metabolism, elimination, toxicology) assays, and successful fulfilment of criteria results in progression to the lead optimisation stage of development. Ideally, management of drug absorption, metabolic liability and toxicology profile by tuning physicochemical properties should be achieved in the hit-to-lead stage. Table **1** summarises the ADMET *in vitro* techniques typically utilised on a drug discovery project, and are currently being used in hit-to-lead assessment of ERK5 inhibitors.

Table 1: Summary of common ADMET *in vitro* techniques utilised in a drug discovery project

***In Vitro* Technique**	**Rationale**
Turbidimetric solubility assay	Aqueous solubility is an important factor influencing GI tract absorption and therefore oral bioavailability.
Plasma protein binding (PPB) assay	The extent of binding to plasma proteins influences the degree of drug distribution. Extensive PPB also limits the amount of free drug, affecting efficacy.
Microsomal clearance assay	Gives an estimation of intrinsic clearance, by assessing microsomal stability. Excessive clearance indicates a high level of metabolism by CYP enzymes.
Caco-2 permeability assay	Predicts *in vivo* absorption by measuring the rate of transport of drug across the Caco-2 cell line. Measurement of transport in both directions across the cell membrane allows measurement of an efflux ratio. A high ratio suggests compounds are a substrate for the P-glycoprotein (P-gp) efflux pump.
CYP inhibition assay	Compounds which inhibit CYP isoforms are liable to cause drug-drug interactions, by preventing the clearance of other compounds. This may lead to adverse reactions or toxicity.
hERG inhibition assay	Inhibition of the hERG current across a voltage gated potassium channel in the heart causes QT interval prolongation and is associated with cardiotoxicity.

During lead optimisation, proof-of-concept (POC) studies in a preclinical disease model are initiated, which confirm drug efficacy. Optimisation of *in vivo* drug properties is also performed. The predictive *in vitro* tools outlined in Table **1** minimise the risk of progressing compounds which will ultimately fail. However, it is impossible to guarantee success due to the complex nature of biological systems. Assessment of DMPK properties (*in vivo* clearance, volume of distribution, bioavailability and half-life) is often performed in mouse or rat models in the lead optimisation stage. Medicinal chemistry plays a crucial role in three stages of drug discovery; hit validation, hit-to-lead, lead optimisation, prior to candidate selection, preclinical development and ultimately, clinical trials.

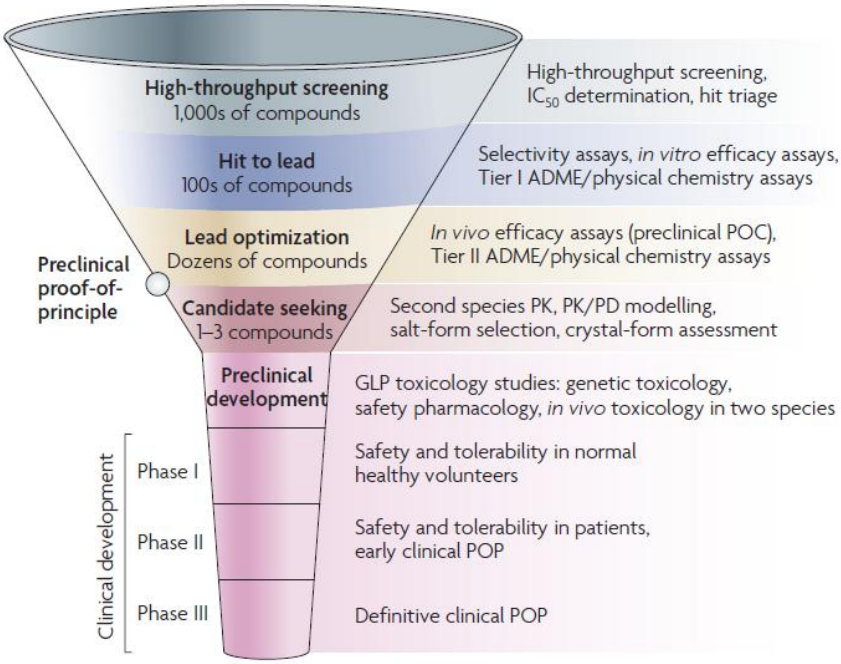

Figure 2: The drug discovery regime. From ref [12].

1.5 The Role of Protein Kinases

Protein kinases are one of the largest superfamilies of homologous genes, encoding proteins sharing common structural features. There are currently 518 known members, many of which whose structures have been elucidated. Protein kinases are structurally related and categorized by their catalytic domains which consist of approximately 250-300 amino acids. Two main subdivisions exist; protein-tyrosine kinases, and protein-serine/threonine kinases of which ERK5 is a member. A third category exists which displays dual functionality, with the ability to phosphorylate all three residues. The characteristic activity and specificity of

kinase activation/inhibition arises from the unique pockets which surround the catalytic domain.

Protein kinases transfer the γ-phosphate group of a purine nucleotide triphosphate, usually adenosine triphosphate (ATP), to the hydroxyl groups of selected amino acid residues of their protein substrates (Figure **3**).[13] Phosphorylation of the substrate results in a functional change, such as onset of enzyme activity. This enables transduction of biochemical signals through the cell. Receptor kinases contain intracellular protein kinase domains which are linked covalently to the ligand binding domain. Upon high affinity binding of a ligand to the receptor ligand binding domain, dimerisation occurs which in turn activates the protein kinase catalytic domain within the cell. A phosphorylation cascade ensues resulting in signal transduction to kinases which control complex cellular processes including progression through the cell cycle.[13] Protein kinases are, therefore, interesting targets for drug discovery, due to the presence of mutations or overexpression in kinase signal transduction pathways resulting in the onset and progression of several cancers. There are currently a number of kinase inhibitors in clinical use for the treatment of several types of human tumours, including imatinib, **5**.

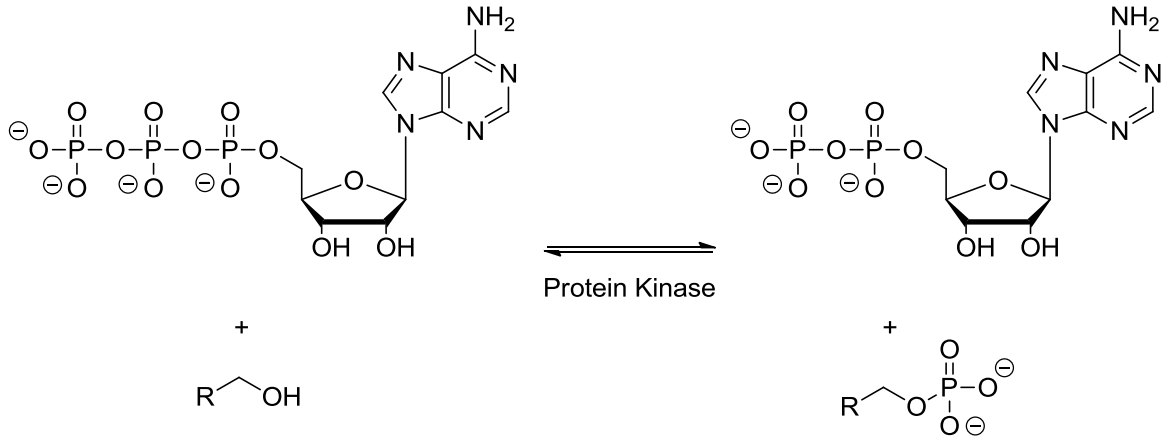

Figure 3: Phosphorylation of a protein substrate (where R = Serine, Threonine or Tyrosine) by a protein kinase.

1.6 Kinase Inhibitors in the Clinic for the Treatment of Cancer

Imatinib, **5** was licenced for the treatment of CML in 2001. CML is characterized by reciprocal translocation of genetic material from chromosomes 9 and 22. This results in the production of a fused Bcr-Abl oncogenic protein which results in unregulated cell proliferation and apoptosis as it lacks the auto-inhibition properties of wild-type Abl protein.

Imatinib is a potent ATP competitive inhibitor of the Abl protein kinase and thus is an effective treatment for CML. This drug also has applications in treating gastrointestinal stromal tumour (GIST) as it was also found to be an inhibitor of c-Kit. Levels of c-kit are elevated in GIST due to genetic mutations.[14] Since the discovery of imatinib, several subsequent kinase inhibitors have been developed and licenced for use in various cancer types (Table 2).

Table 2: Licensed kinase inhibitors for the treatment of cancer

Name	Structure	Year of Approval	Target	Clinical Use
Imatinib, 5 **(Glivec)**	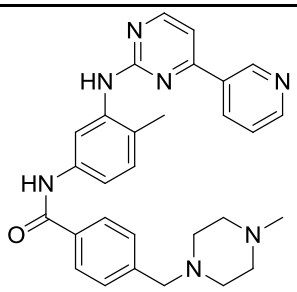	2001[15]	Bcr-Abl fusion	CML, GIST[15]
Gefitinib, 6 **(Iressa)**	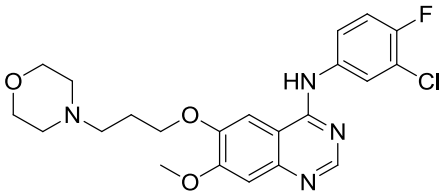	2003[15]	EGFR-TK	Non-small cell lung cancer (NSCLC)[15]
Sorafenib,7 **(Nexavar)**	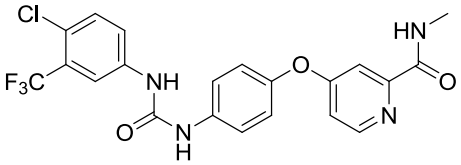	2005[15]	Raf1 (Multi-kinase inhibitor)	Renal cell carcinoma (RCC), hepato-cellular carcinoma (HCC)[15]
Sunitinib, 8 **(Sutent)**	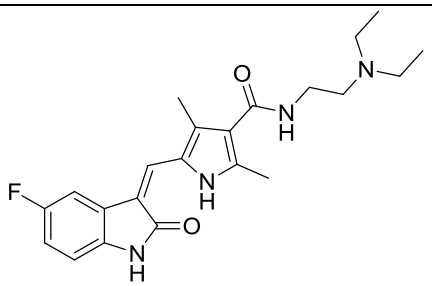	2006[15]	Multi-kinase inhibitor	RCC, imatinib resistant GIST[15]

Erlotinib, 9 **(Tarceva)**	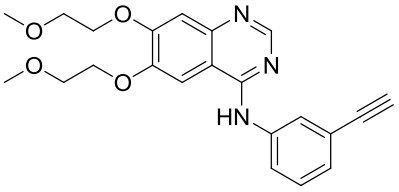	2010[16]	EGFR-TK	Metastatic NSCLC[17]
Dasatinib, 10 **(Sprycel)**	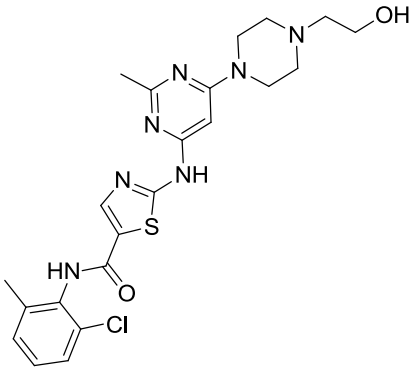	2010[18]	Bcr-Abl fusion (Multi-kinase inhibitor)	CML[18]
Nilotinib, 11 **(Tasigna)**	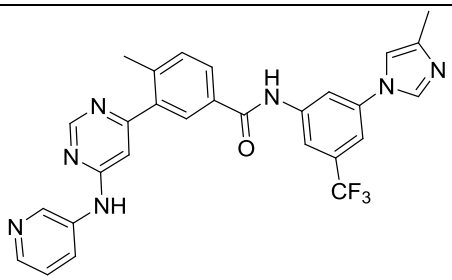	2010[18]	Bcr-Abl fusion (Multi-kinase inhibitor)	CML[18]
Vandetanib, 12 **(Caprelsa)**	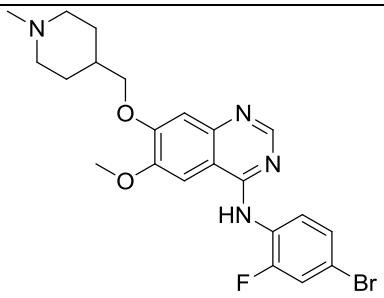	2011[16]	VEGFR/ EGFR	Medullary thyroid cancer[19]
Vemurafenib, 13 **(Zelboraf)**	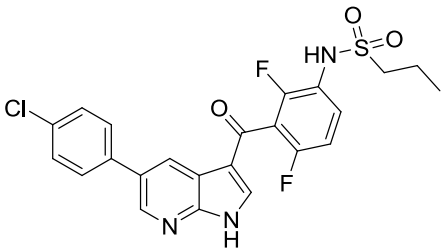	2012[18]	BRaf V600E	Malignant melanoma[18]
Crizotinib, 14 **(Xalkori)**	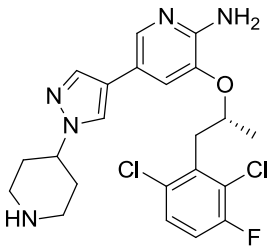	2012 (USA) Expected 2013 (UK)[18]	ALK	NSCLC[18]

The development of resistance to kinase inhibitors has been reported in the clinic. Gefitinib, **6**, an inhibitor of the epidermal growth factor receptor tyrosine kinase (EGFR-TK) was initially found to produce a dramatic response in patients suffering from non-small cell lung cancer (NSCLC). However, despite the initial success of the drug, the majority of tumours become drug-resistant over the course of treatment. Patients whose tumours initially respond to treatment with gefitinib or erlotinib, **9** typically develop resistance within 12 months.

In the case of EGFR-TK inhibitors, over 50% of resistant forms of NSCLC contain a single secondary mutation in the EGFR, with substitution of a methionine residue at position 790 for threonine (T790M).[20, 21] The replacement of the gatekeeper threonine residue has a profound effect on small-molecule binding, as it is this residue which typically allows access to a lipophilic pocket within the ATP binding site in protein kinases. The development of second generation kinase inhibitors which target the T790M variant of the EGFR-TK is in progress, for the treatment of patients which no longer respond to gefitinib or erlotinib treatment. Canertinib, **15,** acts as an irreversible inhibitor of wild type EGFR and $EGFR^{T790M}$ with *in vitro* activities of 0.3 and 26.0 nM respectively. In contrast, gefitinib also inhibits wt-EGFR with an *in vitro* IC_{50} of 0.3 nM, but activity is significantly diminished (IC_{50} = 1013 nM) in the T790M mutant.[22] Canertinib is currently being evaluated in Phase II clinical trials.

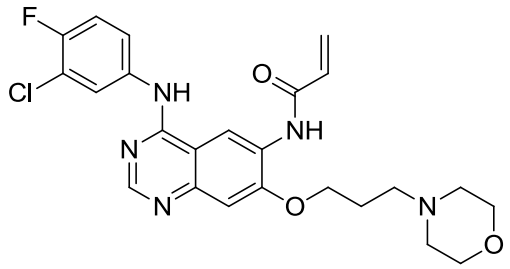

Canertinib, **15**

Identification of a novel mutation (V600E) in BRaf present in human tumours including malignant melanoma has recently led to the development of vemurafenib, **13**, which shows significant anti-tumour effects in cell lines possessing the V600E mutation, but is inactive in wild type BRaf cells.[23] The ability of cancer cell lines to acquire drug resistance *via* secondary mutations, and the marked effect on drug efficacy as a result of single point mutation highlights the necessity for continued genomic investigation and drug discovery for the development of new therapeutic agents.

Chapter 2: Mitogen-Activated Protein Kinases and Their Role in Cancer

2.1 Overview of the MAPK Pathways

The complex process of signal transduction in eukaryotes is mediated *via* a number of pathways. These kinases are responsible for the conversion of extracellular signals to cellular responses. Mitogen-activated protein kinase (MAPK) pathways typically consist of a three tiered kinase module,[24] activated following phosphorylation from a kinase further upstream. Among these pathways are a series of highly conserved proline directed MAPKs, which phosphorylate their substrates at a serine and/or threonine residue.[25]

Eukaryotes possess 14 highly conserved MAP kinases which are categorised into 7 groups. These 7 are further differentiated by the nature of their pathway. Extracellular signal-related kinase (ERK) 1/2, the p38 isoforms, c-Jun amino (*N*)-terminal kinase (JNK) isoforms and ERK5 are referred to as conventional MAPKs, whereas ERKs 3, 4, 7 and 8 and Nemo-like kinase (NLK) are considered atypical MAPKs. The TXY amino acid sequence present in the activation loop of conventional MAPKs varies between the four sub-families (i.e. ERK, TEY; p38, TGY; JNK TPY). Of the conventional MAPKs, ERK5 differs most greatly from the other members. ERK5, or 'Big MAP kinase 1' (BMK-1) contains an *N*-terminus extension, which contains transactivation domain (TAD) and nuclear localisation sequences (NLS).[26]

There is a high level of sequence homology amongst the members of the MAPK family. ERK5 shares 51% and 48% sequence identity with ERK2 and p38α respectively in the kinase domain, and increases to 78% and 56% in the active site region. Due to the highly conserved nature of the MAPK family members, access to counter-screening assays is essential for a project aiming to develop selective ATP-competitive kinase inhibitors. Despite the high sequence homology between ERK5 and ERK2 in the ATP binding pocket, their gatekeeper residues differ significantly in size (ERK2 = Gln; ERK5 = Leu). The gatekeeper residue plays a key role in controlling access to a hydrophobic pocket. This creates an opportunity to design selective inhibitors for ERK5 over ERK2. Although p38α has a lower overall sequence homology, it was anticipated that designing an inhibitor selective for ERK5 over p38α would be more challenging due to the similar sizes of their respective gatekeeper residues (p38α = Thr). The gatekeeper residue in the JNK family of enzymes is methionine, which is also significantlylarger than that of ERK5.

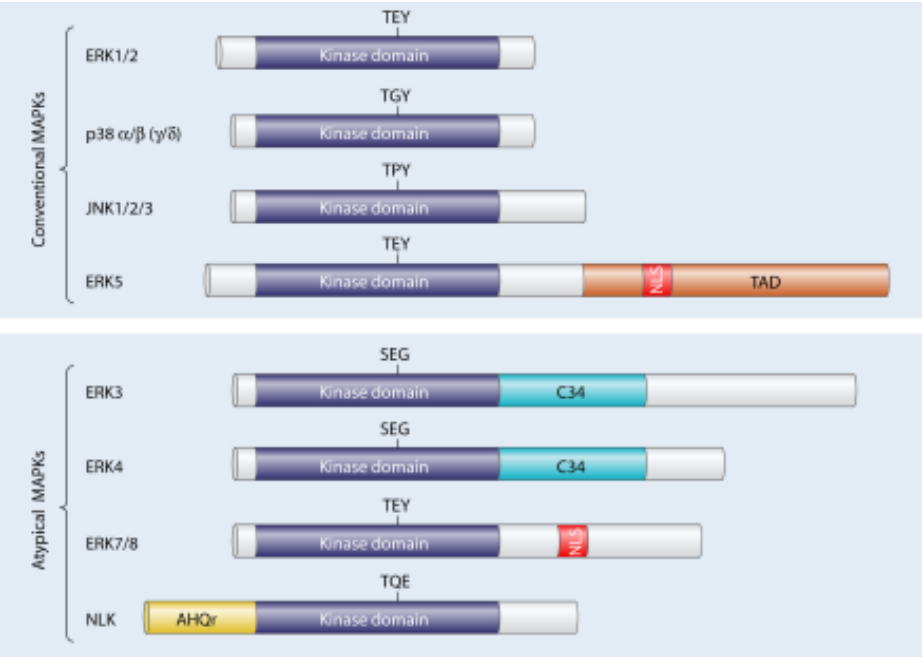

Figure 4: Schematic representation of the structures of conventional and atypical MAPKs. From ref [26].

2.2 Signal Transduction in the MAPK family

The classical Raf/MEK/ERK signal transduction cascade is the most extensively studied of all the known MAPK pathways. This pathway is activated in response to extracellular signals such as the binding of growth factors (e.g. epidermal growth factor (EGF)) to the epidermal growth factor receptor (EGFR).[27] Following binding of a growth factor, receptor dimerization occurs, which results in activation of the intracellular tyrosine kinase. MAPK pathway activation may also be initiated by cytokines, or various cellular stresses (e.g. osmotic stress).[28] Following activation of the intracellular receptor tyrosine kinase, signalling *via* a three-tiered kinase module is induced, assisted by adaptor proteins such as growth factor receptor-bound protein (Grb2) and SoS (Son of Sevenless) which facilitate activation of GTP Ras. A MAPK is activated by a MAPK/ERK kinase (MAPKK, or MEK) which in turn is activated by a MEK kinase (MAPKKK or MEKK) (Figure **5**).[29] The first identified MEKKs were part of the Raf family of enzymes and A-Raf is known to selectively activate MEK1 over MEK2, whereas B-raf and Raf-1 are non-specific for MEKs 1 and 2. MEK1/2 are the only members of the MAPK signalling pathways which are activated by Raf enzymes.[30]

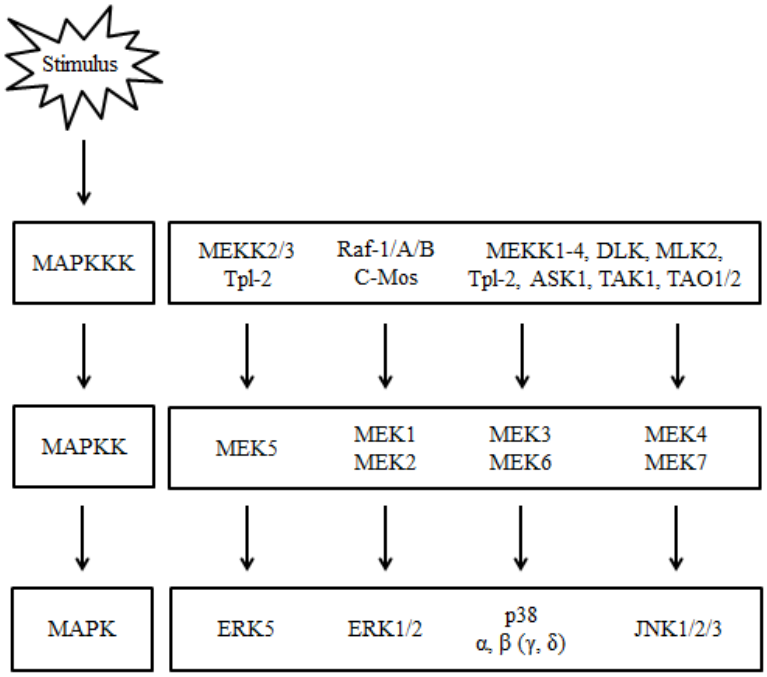

Figure 5: Signalling cascades for the four conventional MAPK sub-families.[29]

2.3 The Ras/Raf/MEK/ERK Signalling Pathway

The activation of ERK1 and 2 proceeds *via* the aforementioned pathway (Section **2.2**), following dual sequential phosphorylation of the conserved TEY motif by MEKs 1 and 2. Dissociation of activated ERK from MEK results in localisation to the nucleus whereby activation of several transcription factors such as c-Ets1, c-Ets-2, MNK1, MNK2, Sp1, E2F, Elk1 and AP-1 occurs. Activation of these transcription factors is associated with a number of processes including cell proliferation, differentiation and apoptosis. Therefore, deregulation of this pathway is associated with the progression of several cancers.[26, 31]

2.3.1 Targeting the Ras/Raf/MEK/ERK1/2 Pathway for the Treatment of Cancer

Initial efforts in drug discovery had focussed on inhibition of the Ras/Raf/MEK/ERK pathway by targeting the extracellular receptors which promote cancer progression following binding of growth factors (e.g. erlotinib, **9**). However, drug resistance to inhibitors of the EGFR-TK is known, due to redundancy of the inhibited pathway.[32] Ras oncoproteins are known to play a major role in the development of cancers, due to their ability to activate signalling pathways such as the MEK/ERK cascade. Ras mutations are present in approximately 30% of all human cancers, and in particular, pancreatic cancer and sporadic

colorectal carcinoma have high incidence of K-Ras mutation, at 90% and 50% respectively.[33] Furthermore, the aberrant overexpression of Raf, MEK and ERK1/2 has proved to be an attractive target for therapeutic intervention.

Several drug discovery groups have embarked upon development of MEK inhibitors for the treatment of cancer. The first MEK1 inhibitor to reach the stages of clinical evaluation was CI-1040, **16**, (PD184352) developed by Pfizer, and was identified following a medicinal chemistry program which was led by a high-throughput screening (HTS) campaign.[34] CI-1040 has been shown to act as an allosteric inhibitor, which enables high specificity for MEK1 over similar kinases such as p38α and JNK2. A *Ki* of 17 nM was measured for MEK1 by CI-1040. Following successful completion of Phase I clinical trials, CI-1040 advanced to Phase II investigating efficacy in patients with metastatic breast cancer, non-small cell lung cancer and pancreatic cancer. Unfortunately, a response was not measured following single agent dosing in each of the three tumour types, therefore further investigation into CI-1040 was terminated.[31] As a result, the second generation MEK inhibitor PD0325901, **17**, was developed which displays significantly improved *in vivo* efficacy and drug-like properties to CI-1040, and an *in vitro* IC_{50} of 1 nM.[35]

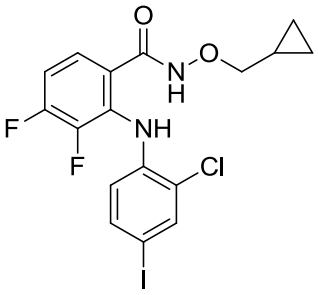

CI-1040, **16**

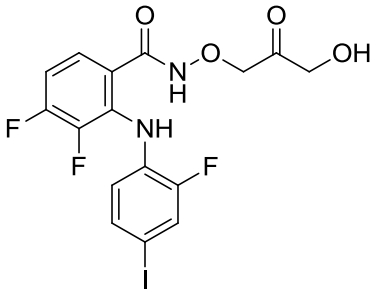

PD0325901, **17**

AZD6244, **18**, (also known as ARRY-142886) was developed by AstraZeneca as a second generation MEK inhibitor; an analogue of CI-1040, it is a potent and selective inhibitor of MEK. AZD6244 has been shown to be particularly effective in cell lines which display BRAF or Ras mutations. AZD6244 has an IC_{50} value of 14 nM against MEK, with an improved pharmacological profile to CI-1040, and Phase II clinical trials have recently been completed.[36, 37] A third analogue of CI-1040 is RO4987655, **19**, currently in Phase II clinical trials for the treatment of advanced solid tumours, following successful Phase I dose escalation studies. A safety profile comparable to other MEK inhibitors was reported in Phase

I, and drug plasma concentrations in the efficacious range as predicted by preclinical models were attained.[38]

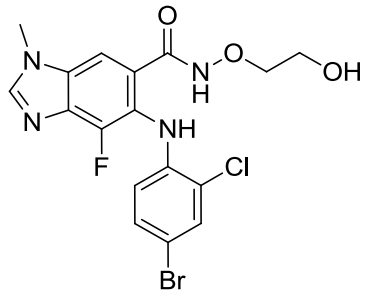

AZD6244, **18**

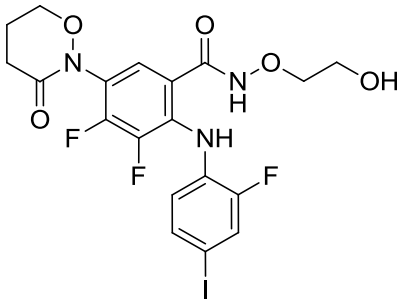

RO4987655, **19**

Pharmacological inhibition of ERK1/2 by small molecules is also an area of interest, although there are far fewer examples of ERK inhibitors described in the literature to date. The discovery of FR180204, **20**, an ATP competitive inhibitor of ERK was reported in 2005. FR180204 inhibits both ERK1 and ERK2 with IC_{50} values of 0.51 and 0.33 μM, respectively. Furthermore, the assessment of **20** in a cell-based functional assay has demonstrated that pharmacological inhibition of ERK1/2 results in inhibition of the AP-1 transcription factor, which is associated with regulation of gene expression. As AP-1 transactivation is associated with the TGF-β pathway, it is suggested that ERKs 1 and 2 play a crucial role in TGF-β mediated signalling.[39]

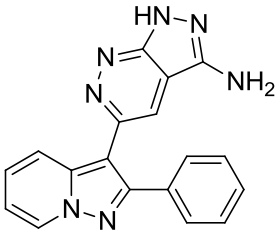

FR180204, **20**

A pyrazolylpyrrole-based hit for ERK1/2, **21** was identified by Vertex pharmaceuticals following a HTS campaign, which displayed micromolar activity against ERK2 (**21**; K_i = 2.3 μM). 3D-QSAR and *in silico* 'side-chain hopping' approaches led to the discovery of several potent ERK inhibitors (summarised in Table **3**).[40] To date, ERK1/2 inhibitors have not reached the clinic.

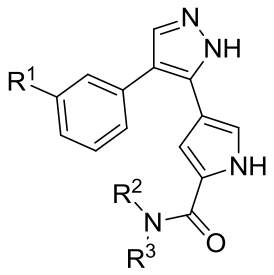

Table 3: Optimisation of potency for pyrazolylpyrrole based inhibitors of ERK.[40]

Compound	R^1	R^2	R^3	K_i ERK2 (μM)
21	H	Me	Me	2.300
22	Cl	H	Benzyl	0.086
23	Cl	H	(*R*)-1-Phenyl-2-hydroxylethyl	0.035
24	Cl	H	(*R*)-1-(3-Cl, 4-FPh)-2-hydroxylethyl	0.002

2.4 The p38 and JNK Signalling Pathways

The p38 subfamily of MAPKs consists of 4 isoforms, α, β, γ and δ. Of these four, p38α is the most widely investigated and therefore, well characterised. It is expressed in the majority of mammalian cells and is involved in the regulation of cytokine expression. The major role of p38α is inactivation and regulation of immune response.[41] Also referred to as stress activated protein kinase 2 (SAPK2), p38α mediates cellular responses to cellular stress including UV, heat, and osmotic shock. Inflammatory cells (e.g. neutrophils, monocytes, and macrophages) predominantly synthesise the p38α isoform. Production of pro-inflammatory cytokines (e.g. Interleukin-1 (IL-1), tumour necrosis factor and IL-6) following activation of the p38 MAPK pathway is associated with the development of inflammatory disease.[42] The p38 pathway is also associated with the regulation of apoptosis, and has recently been identified as a tumour suppressor. It has been demonstrated that induction of p38-dependant apoptosis occurs following treatment with chemotherapeutic agents (i.e. cisplatin, a DNA damaging agent) in different cell lines.[43, 44] Like p38α, the JNK family of enzymes are SAPKs, activated primarily by environmental stress and Figure **5** shows that the MAPKKKs activated in both the p38 and JNK pathways are shared. Activation of the JNK pathway has been associated with tumour formation *via* deregulation of cellular growth.[45]

2.4.1 Targeting the p38 and JNK Pathways for the Treatment of Inflammatory Diseases and Cancer

A number of inhibitors of p38α have entered clinical trials for a number of disease areas driven by inflammatory response. PH797804, **25**, is currently under evaluation in Phase II clinical trials for the treatment of rheumatoid arthritis, and neuropathic pain.[46] Also under investigation in Phase II trials include GW856553, **26** (losmapimod) for the treatment of chronic obstructive pulmonary disease (COPD) and SB-681323, **27**, (dilmapimod) also for the treatment of pain.[47]

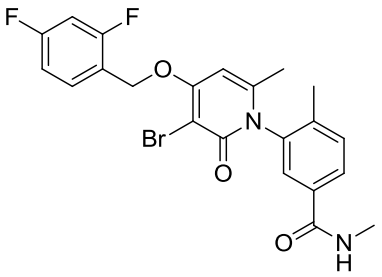

PH797804, **25**

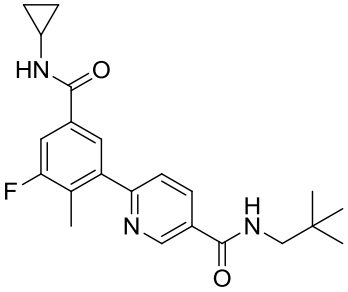

GW856553, **26**

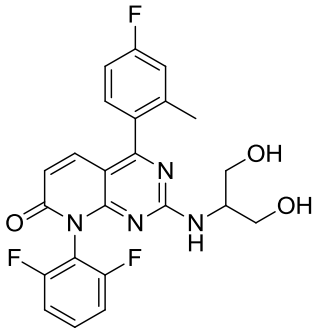

SB-681323, **27**

Only one p38α inhibitor to date has been evaluated clinically for the treatment of cancer. Talmapimod, **28**, (SCIO-469) was reported to be undergoing clinical trials in patients with multiple myeloma (MM) in 2009.[48] It has been reported that talmapimod when dosed as a single agent has little effect on cell viability, although when dosed in combination with a proteasome inhibitor, Velcade, **29**, the reduction in proteasome-induced cell proliferation and metabolism is significantly enhanced. Sensitization to proteasome inhibitors by p38 inhibition is attributed to the reduced activation of MAPK-activated protein kinase-2 (MAPKAPK-2) and activation of the anti-apoptotic heat shock protein 27 (HSP27). Therefore, p38α inhibitors may have a therapeutic application for increasing the sensitivity of resistant or unresponsive tumours to existing chemotherapeutic agents.[49]

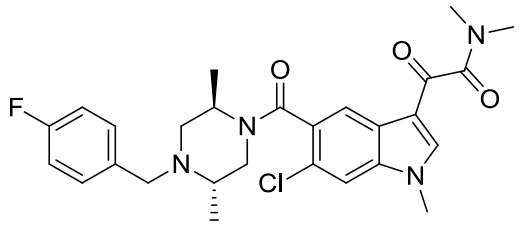

Talmapimod, **28**

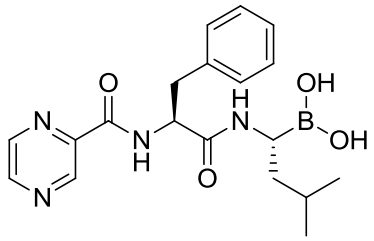

Velcade, **29**

Several inhibitors of the JNK family of MAP kinases have been reported in the literature for use in numerous therapeutic areas. Like p38, JNK is implicated in the progression of inflammatory disease and cancer. However, the biological role of JNK in the progression of neurodegenerative and metabolic disease is also under investigation. There are currently no known clinical candidates whose biological target is the JNK sub-family.[50]

2.5 Introduction to Extracellular Signal Regulated Kinase 5 (ERK5)

Also known as 'Big Map Kinase 1' (BMK-1), ERK5 is almost twice the size of other MAPKs (consisting of 816 amino acids).[51] Activation of the signalling pathway of which ERK5 is a part is associated with cell survival, proliferation, and differentiation, and thus its overexpression may have implications in carcinogenesis.[52]

2.5.1 The MEK5/ERK5 Signalling Pathway

Signalling through the MEK5/ERK5 pathway is stimulated by binding of growth factors EGF, NGF, vascular endothelium growth factor (VEGF) and fibroblast growth factor-2 (FGF-2) to their receptors found on the cell surface. Activation of the signalling pathway can also occur as a result of cellular stresses, or cytokines as is common in the MAPK sub-family (Figure **6**).[53] Unlike the conventional linear Ras/Raf/MEK/ERK pathway (outlined in Section **2.3**), the ERK5 signalling cascade occurs independently of Raf.[54] Cloning of the ERK5 protein was completed in 1995, which first identified MEK5 as a binding partner. ERK5 is activated specifically by MEK5 which is in turn activated by the MAPKKKs, MEKK2/3.[52, 55]

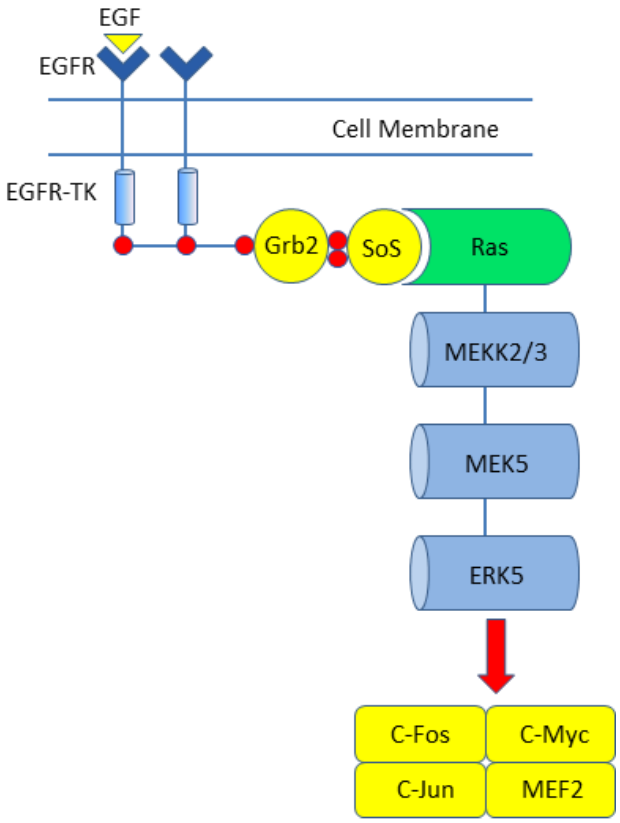

Figure 6: EGF induced signalling cascade through the MEK5/ERK5 pathway to activate cytoplasmic and nuclear transcriptional factors c-Fos, c-Jun, MEF2 and c-Myc.

2.5.2 Adaptor and Scaffold Proteins in the ERK5 pathway

Adaptor and scaffold proteins ensure transmission of the signal to the MAPK, assembling the required components of the cascade in multi-enzyme complexes.[52] An interaction between MEKK2 and Lad (Lck-associated adaptor) assists ERK5 activation, by increasing the binding affinity between MEKK2 and MEK5.[56] MEKKs 2/3 contain a Phox/Bem1 (PB1) domain which may associate with other PB1 containing proteins *via* protein-protein interactions, and it is this interaction which mediates MEK5 activation. Interestingly, ERK5 is the only MAPK to harbour a PB1 domain and it has been demonstrated that MEK5 acts as a scaffold protein by tethering MEKK1/2 to ERK5 *via* its *N*- and *C*-terminal regions of the PB1 domain. The formation of this three-kinase complex is unique to the MAPK family.[57]

2.5.3 Structure and Functional Domains of ERK5

The specificity of the activation of ERK-type kinases can be attributed to their unique tripeptide motif in the activation loop of the kinase. For activation of ERKs to occur, phosphorylation must occur on two sites which are separated by a single amino acid, i.e. in ERK5 the tripeptide sequence Thr-Glu-Tyr is phosphorylated. This motif is common to ERK5 and ERKs 1 and 2. However, BMK-1 is structurally different to the other members of the ERK sub-families. A unique loop-12 structure and extended *C*-terminal domain (~400 amino acids) gives ERK5 its characteristic structure.[52, 53] The *C*-terminal extension harbours both nuclear localisation (NLS) and export (NES) sequences, two proline rich domains, a transcriptional activating domain (TAD) and myocyte enhancer factor 2 (MEF2) interacting region.[58] It has been established that the large *C*-terminal domain present only in ERK5 is auto-phosphorylated at multiple sites, resulting in an increase in transcriptional activity. It is also understood that the *C*-terminus has an auto-inhibitory effect on the ERK5 protein. The long *C*-terminus masks the catalytic domain, thus blocking ERK5 substrates from binding. Following activation of ERK5 by MEK5, a conformational change is apparent, allowing interaction of ERK5 and its substrates. Deletions in the *C*-terminal portion of the kinase results in an increased level of catalytic activity, which supports the hypothesis of an auto-inhibitory function.[52]

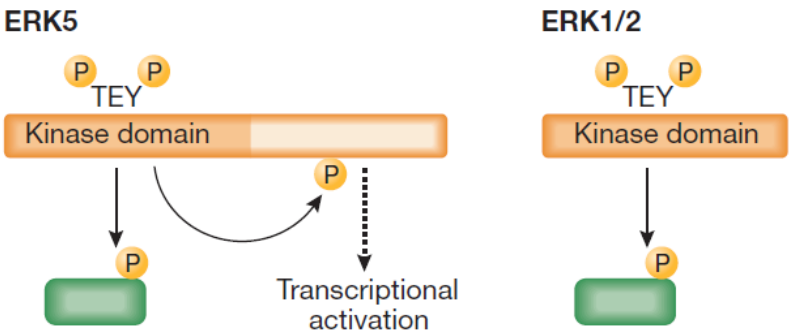

Figure 7: Unique transcriptional activity of the ERK5 arises from the extended C-terminus which does not feature in ERK1/2. From ref [59].

2.5.4 Downstream Effectors of ERK5

Activation of ERK5 results in translocation from the cytoplasm to the nucleus and subsequent activation of a number of transcription factors including MEF2 which control growth factor mediated survival, c-Myc, c-Jun, c-Fos, activating protein 1 (AP-1) and NFκB. Bcl-2 associated death promoter (Bad) and serine/threonine kinase (SGK) are also implicated as ERK5 substrates.[60] ERK5 also phosphorylates and activates the p90 ribosomal s6 kinase (RSK) involved in signal transduction.[61] RSKs are themselves known to activate several cytosolic and nuclear substrates, and are implicated in the regulation of a number of cellular processes associated with the onset and progression of cancer, including cell proliferation, survival, and motility.[62]

2.5.5 Interaction of ERK5 with Promyelocytic Leukaemia Protein (PML)

Investigation into the molecular mechanism by which ERK5 regulates cell proliferation revealed an interaction with PML, a tumour suppressor. Western blot analysis showed co-precipitation of ERK5 and PML, and immunoprecipitation of PML also resulted in isolation of ERK5. Furthermore, p21, a downstream effector of PML, was induced following knockout of the gene encoding ERK5 (MAPK7) by small interfering RNA (siRNA). These data indicate that ERK5 complexes to and phosphorylates PML, resulting in down-regulation of the cell cycle regulator, p21. Pharmacological inhibition of ERK5 has proven to be a successful strategy for increasing p21 expression. The ERK5 inhibitor XMD8-92 which exerts this effect is discussed in more detail in Section **2.5.7.1**.[63]

2.5.6 The Role of ERK5 in the Development of Cancer

In 2000, Hanahan and Weinberg defined six biological capabilities as the ‘hallmarks’ of cancer, differentiating tumours from normal cells. These include; maintenance of proliferative signalling, resistance to apoptosis or immortality, induction of angiogenesis, activation of invasion and metastasis, and evasion of growth suppressors.[1] ERK5 is implicated in a number of these biological processes as will be discussed in more detail in this section.

2.5.6.1 Cell Cycle Progression and Cell Survival

The association of ERK5 overexpression with the activation of several transcription factors leading to cell proliferation is clear. Cervical cancer (HeLa) cells transfected with the dominant negative ERK5 gene (mutation of residues phosphorylated by MEK5 to phenylalanine or alanine) do not undergo cell proliferation, despite stimulation with growth factor EGF.[64] However, the underlying mechanism by which ERK5 controls progression through the cell cycle is less well understood. Kato *et al* suggested in 1998 that ERK5 is involved in the regulation of the transition through the G1/S phase of the cell cycle.[64] This hypothesis has been widely disputed, based on the observation that levels of phospho-ERK5 are scarcely detectable in HeLa cells during G1 or S phase arrest.[65] In contrast, Cude *et al* suggest that ERK5 activation occurs at a maximum level during the G2/M phase of the cell cycle. ERK5 activation was found to be crucial for transition of the cell into mitosis. Furthermore, ERK5 was found to activate the transcription factor NFκB, mediated by RSK2 during the G2/M phase, which is essential for mitotic entry.[65]

In 2007, it was suggested that ERK5 is activated during mitosis, and phosphorylates Bim (a pro-apoptotic BH3-only protein and a member of the Bcl-2 family), thus promoting cell survival.[66] However, in 2012 it was proven by Gilley *et al* that it is CDK1 that mediates Bim phosphorylation rather than ERK5 as previously suggested. Treatment of HeLa cells with Paclitaxel, **30**, or Nocodazole, **31**, results in phosphorylation of Bim, independent of ERK1/2. However, activation of Bim proceeded normally in fibroblast cells which were negative for ERK5 and treatment of the cells with a dual MEK5/ERK5 inhibitor (BIX02189, discussed in further detail in Chapter **4**) did not reverse this effect. Conversely, administration of a selective CDK1 inhibitor did abolish Bim phosphorylation.[67]

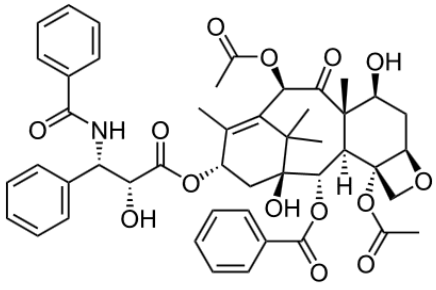

Paclitaxel, **30**

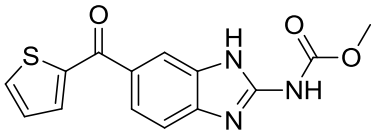

Nocodazole, **31**

2.5.6.2 Angiogenesis

Angiogenesis, the formation of new blood vessels from pre-existing vasculature, is characterised by the proliferation, reorganisation and stabilisation of endothelial cells. It has been established that ERK5 is a regulator of embryonic angiogenesis, and that embryos deficient in ERK5 cannot survive. The MAPK p38α, also implicated in angiogenesis, is unable to compensate for an ERK5 deficiency due to the requirement of ERK5 at an earlier developmental stage than p38.[68] As tumours depend upon the formation of new blood vessels for growth and metastasis, the link between ERK5 mediated angiogenesis and the progression of cancer has been made.

Deletion of the MAPK7 gene which encodes ERK5 in animal studies confirmed that tumour volumes were significantly diminished in ERK5 knockout mice compared with their wild-type counterparts. Furthermore, the vasculature of the tumours was diminished in ERK5-null animals. The reduction in angiogenesis was attributed to the correlation between ERK5 activation and subsequent phosphorylation of ribosomal protein S6 (rpS6), a substrate of RSK. The RSK-rpS6 signalling pathway is associated with cell proliferation and survival, key processes in tumour vascularisation by endothelial cells.[69] More recently, ERK5 has been shown to induce 'inhibitor of differentiation' (Id1), a negative regulator of thrombospondin-1 (TSP1), a known inhibitor of angiogenesis.[70]

2.5.6.3 Migration, Invasion and Metastasis

Metastasis is characterised by the spread of malignant cells from the primary tumour site to secondary areas around the body. Degradation of basement membranes surrounding tumours by matrix metalloproteinase (MMP) enzymes facilitates tumour invasion and is associated with the formation of metastases. As reported previously, ERK5 activates the transcription factor AP-1. The promoters of several MMPs (including MMP-1, 3, 7, 9, 11, 13 and 19) share consensus sequence with AP-1, thus implicating ERK5 in the development of tumour metastases.[71, 72] Furthermore, immunohistochemical data has confirmed the link between MEK5 overexpression and cellular migration and invasion in androgen-sensitive human prostate adenocarcinoma (LNCaP) cells *via* induction of MMP-9.[73]

Focal adhesion kinase (FAK) has been found to activate of ERK2 and ERK5 *via* an integrin mediated pathway. Integrins are a family of receptors implicated in cell attachment and motility. Binding of vitronectin to the extracellular integrin stimulates the ERK pathways in cancer cells. Transfection of MDA-MB-231 breast cancer cells with a dominant negative variant of FAK resulted in ERK5 inhibition and reduced levels of cell adhesion and motility when compared to the wild-type cell line.[74]

2.5.7 Pharmacological Inhibitors of the MEK5/ERK5 Pathway

There are currently three pharmacological inhibitors of the MEK5/ERK5 pathway described in the literature. The first two compounds to be identified are the dual MEK5/ERK5 inhibitors BIX02188 and BIX02189, discovered by Boehringer Ingelheim Pharmaceuticals. These two compounds are described in further detail in Chapter **4**, and were resynthesised for use as a positive control compound in this project.

In 2010, the identification of XMD8-92, **33**, as a selective inhibitor of ERK5 was reported by the Scripps Research Institute. XMD8-92 was discovered serendipitously, following screening of a library subset of compounds initially designed as polo-like kinase (PLK) inhibitors. Expansion of the 6-membered aliphatic ring present in PLK inhibitor BI-2536, **32**, abolished PLK activity but screening of the compound against a panel of 402 protein kinases revealed ERK5 inhibition. Further structure activity relationship (SAR) studies around this scaffold led to the synthesis of XMD8-92. It is reported that XMD8-92 has a dissociation constant (K_D) of 80 nM for ERK5 in an enzymatic assay. Of the 402 kinases screened, only four other kinases were found to be inhibited by **33**, i.e. DCAMKL2, TNK1 and PLK4; K_Ds = 190, 890 and 600 nM, respectively; K_D for DCAMKL1 was not reported, and no inhibition of MEK5 was observed up to a 50 µM drug concentration. A cellular IC_{50} of 1.5 µM in HeLa cells was recorded, it is claimed, with approximately 10-fold selectivity against the most potent off-targets.[63]

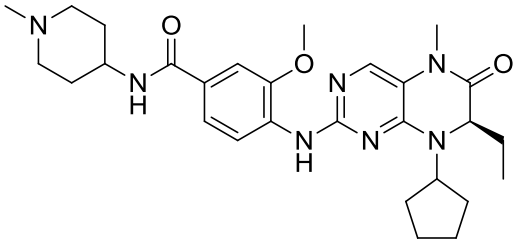

BI-2536, **32**

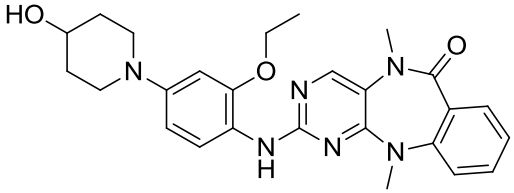

XMD8-92, **33**

2.5.7.1 Effect of ERK5 Inhibition by XMD8-92

The biological effects of XMD8-92, have been demonstrated in tumour-bearing mice. Following the introduction of HeLa or Lewis lung carcinoma (LL/2) cells to test animals, **33** was administered intraperitoneally (IP) twice daily at a dose of 50 mg/kg. Tumour growth was measured at regular time points. Representative animals from each group are pictured in Figure **8**, showing the extent of tumour growth at the end of the experiment. Administration of the ERK5 inhibitor XMD8-92 results in a significant decrease in mean tumour volume in both human tumour xenograft models, when compared to the control. The ability of XMD8-92 to prevent the formation of new vasculature was assessed in an angiogenesis model, *via* implantation of a Matrigel plug. Further details of this assay are provided in Section **6.7.7.4**. A significant decrease in blood vessel formation was detected following 50 mg/kg IP dosing of XMD8-92 compared with animals receiving vehicle only, *via* quantification of haemoglobin concentrations (Figure **9**). The discovery of a novel, selective ERK5 inhibitor has assisted in validating that tumour angiogenesis is mediated by MAPK signalling, particularly *via* ERK5, and that pharmacological inhibition of ERK5 may provide an opportunity for the treatment of invasive and metastatic cancers where ERK5 is deregulated.[63]

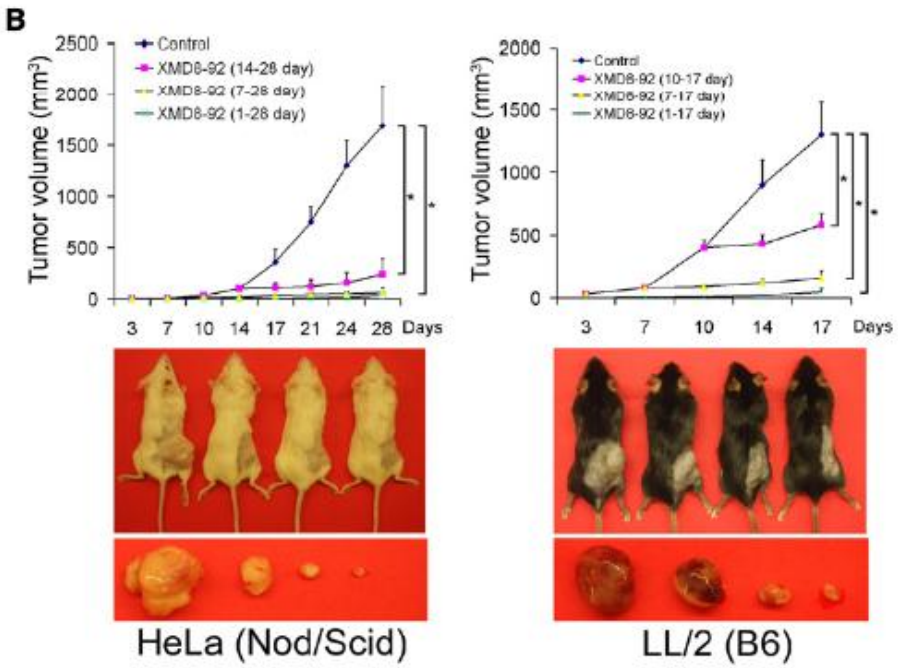

Figure 8: Mouse xenograft model; treatment of tumour-bearing mice (HeLa or LL/2 cell lines) with 50 mg/kg XMD8-92 twice daily IP. From ref [63].

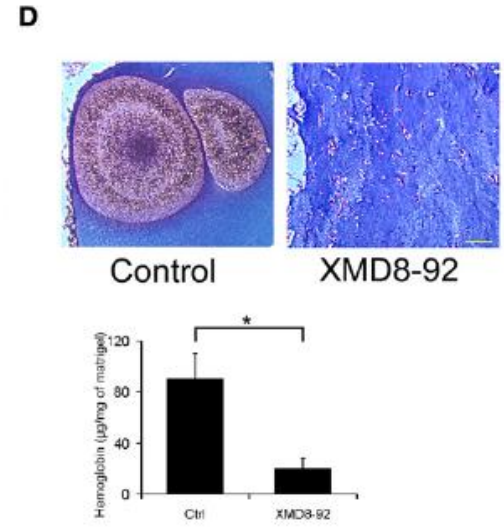

Figure 9: Matrigel plug angiogenesis model; 50 mg/kg XMD8-92 twice daily IP for 6 days. From ref [63].

2.5.7.2 Hit Identification for Novel Inhibitors of ERK5

In 2007, a high-throughput screen (HTS) was conducted by Cancer Research Technology (CRT) laboratories in order to identify novel chemotypes with good to moderate activity against ERK5 as a starting point for drug development. A diverse library of 48,479 compounds and a kinase focused library of 9138 compounds were screened against ERK5 at a concentration of 30 µM. A total of 511 compounds were identified which showed inhibitory activity greater than 50%. Of these 511 compounds, 245 were confirmed as inhibitors of ERK5 using the Immobilised Metal Affinity Polarization (IMAP™) assay format.

Three distinct compound classes were identified; benzo[*d*]thiazoles **34**, 3-cyanopyridines **35**, and pyrrole carboxamides **36**, which were selected for hit validation.

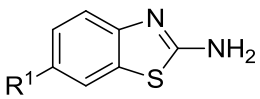

34; 0.06-0.09 µM

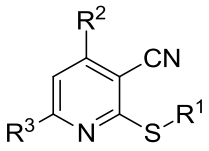

35; 0.45-31.3 µM

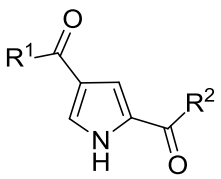

36; 0.66-3.5 µM

Benzo[*d*]thiazole compounds obtained from commercial libraries exhibited excellent inhibitory activity against ERK5 (IC_{50} = 6-9 nM). Research in this series was conducted by Dr Ruth Bawn.[75] Unfortunately, the series was not validated and therefore no further studies

around the benzo[*d*]thiazole scaffold were performed. Hit validation of the 3-cyanopyridine and pyrrole carboxamide series are described in Sections **5.2** and **6.2**.

2.5.7.3 IMAP™ Assay Format

All compounds described herein were evaluated for *in vitro* ERK5 inhibition using the IMAP™ assay format unless otherwise stated. The IMAP™ assay is a generic assay kit obtained from Molecular Devices designed for the screening of compounds against kinases, phosphatases and phosphodiesterases.[76]

The assay is based on the fluorescence polarisation (FP) of a labelled peptide substrate (Figure **10**). Upon phosphorylation by the kinase, the peptide substrate binds to an immobilised metal (III) nanoparticle, thus increasing the fluorescence polarisation observed by reducing rotational speed of the substrate. When no inhibition of the kinase occurs, a maximum amount of FP is observed. Upon inhibition of the kinase by a small molecule the level of FP observed will be significantly lower. The $K_{m\ app}$ of ATP for ERK5 has been determined as 350 μM and thus all IC_{50} determination assays are performed at this concentration of ATP.

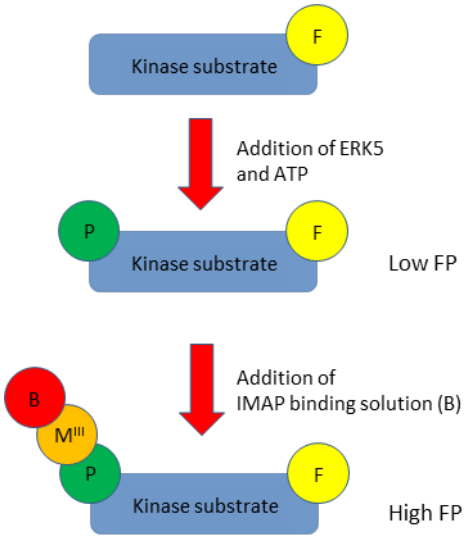

Figure 10: Schematic diagram of the IMAP™ assay.[76]

Chapter 3: Cancer Types Where ERK5 Signalling is De-regulated

3.1 Prostate cancer

3.1.1 Introduction to Prostate Cancer

Prostate cancer typically characterised by abnormal growth of the epithelial cells in the prostate tissue, a small walnut shaped organ involved in the male reproductive system. According to statistics published by Cancer Research UK, prostate cancer (CaP) is the most commonly diagnosed form of cancer in men, with almost 41,000 new cases in the UK in 2009. In 2008, approximately 900,000 cases of prostate cancer were diagnosed worldwide. Fortunately, advances in screening and detection have enabled the majority of patients diagnosed with CaP to reach 5 or 10 year survival points (Figure **11**). However, prostate cancer is still the second leading cause of cancer related deaths, behind lung cancer.[77]

Prostate cancer - UK	Males
Number of new cases (2009)	40,841
Rate per 100,000 population*	106.3
Number of deaths (2010)	10,721
Rate per 100,000 population*	23.8
One-year survival rate (patients diagnosed 2005-2009 in England)	93.5%
Five-year survival rate (patients diagnosed 2005-2009 in England)	81.4%
Ten-year survival rate (predicted survival for patients diagnosed 2007 in England and Wales)	68.5%

**age-standardised to the European population*

Figure 11: Recent prostate cancer statistics according Cancer Research UK. From ref [77].

There are several risk factors associated with the development of prostate cancer, the most prevalent being age. The probability of being diagnosed with prostate cancer increases significantly past the age of 50 (Figure **12**). Genetic predisposition also plays an important role in the development of prostate cancer, and the link between carrying germline mutations in the BRCA2 gene (associated with the onset of breast and ovarian cancers in females) has been established.[78] Several other factors including diet, alcohol intake, and bodyweight have been investigated, but there is currently no evidence to suggest a link with prostate cancer.[77]

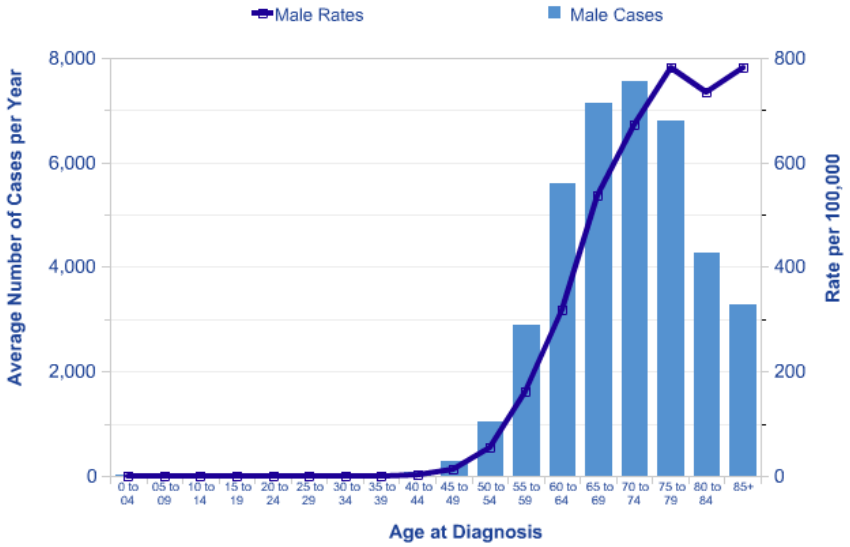

Figure 12: Average number of prostate cancer diagnoses per year, with age-specific incidence rates, 2007-2009. From ref [77].

3.1.2 Screening and Detection of Prostate Cancer

Screening for prostate cancer typically involves a blood test measuring the levels of prostate-specific antigen (PSA) in the bloodstream. This protein is naturally secreted by the prostate. However, elevated levels of this antigen indicates enlargement of the prostate gland. This however is not a diagnostic measure, as elevated PSA levels may also be detected in non-cancerous conditions such as prostatitis, or benign enlargement of the prostate. Paradoxically, many men with prostate cancer do not display elevated PSA levels. The PSA blood test, however, is a non-invasive indicative test which for many men can provide reassurance or lead to early detection of prostate cancer. Should a high PSA level be detected, a recommendation for biopsy may be necessary, which gives a definite diagnosis but is invasive and often painful. If cancerous cells are detected following a biopsy, they are evaluated and graded according to their appearance in terms of abnormality (graded on a scale of 1-5) as viewed through a microscope (Figure **13**). The complication of multiple patterns in one specimen being observed is overcome by using a combined score of the two most prevalent tissue patterns. This technique is referred to as the Gleason sum score.[79]

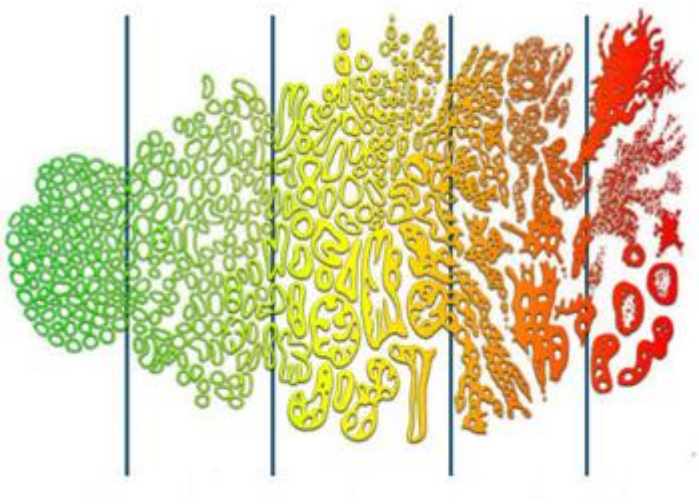

1 2 3 4 5

Figure 13: The Gleason grading system. Grade 1 cells are almost 'normal' displaying closely packed round glands with well-defined edges. Grade 1 cells show no glandular differentiation. From ref [80].

3.1.3 Current Treatments for Advanced Prostate Cancer

Radical prostatectomy is the treatment of choice for patients where their cancer has not spread beyond the prostate. This treatment option allows a normal lifestyle following surgery, without compromising survival of the patient. Radiotherapy is also a treatment option at this stage. For patients with advanced prostate cancer, hormone therapy is usually the first line treatment. This may also be used for patients where cancerous cells have returned following surgery or radiotherapy, the cancer has already spread to secondary sites around the body, or the primary tumour is too large to be treated by surgery or radiotherapy alone.[81] It is estimated that between 80 and 90% of diagnosed prostate cancers are dependent on androgens and the androgen receptor for their development, and expression of the androgen receptor is maintained during prostate cancer progression.[82] Blocking the production of testosterone is a successful approach towards treating such cancers which are dependent on signalling through the androgen receptor. Testosterone is primarily synthesised in the testes, therefore androgen ablation may be achieved *via* orchiectomy; surgical removal of the testes. However, there are currently several drug classes which suppress the action of androgens either by reducing serum testosterone and 5α-dihydrotestosterone (DHT) levels, or by directly inhibiting the androgen receptor (AR), without the need for surgical intervention. Androgen receptor antagonists nilutamide, **37** flutamide, **38** and bicalultamide, **4** act in a

testosterone/DHT competitive manner at the AR in the prostate gland, directly inhibiting the androgen signalling pathway.

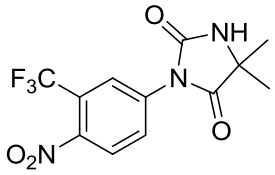

Nilutamide, **37**

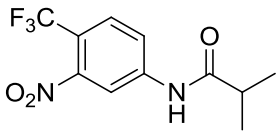

Flutamide, **38**

In contrast, gonadotropin-releasing hormone (GnRH) agonists Leuprolide and Goserelin, **39** act upon the anterior pituitary gland, paradoxically decreasing the release of the luteinising hormone (LH) when administered in high doses, through down-regulation of GnRH receptors. Luteinising hormone stimulates androgen synthesis in the testes, therefore the use of a GnRH agonist such as goserelin, reduces testosterone and DHT serum levels to a concentration comparable with those following orchiectomy.[83] GnRH antagonists (e.g. Abarelix) have also been used clinically for androgen ablation, which does not result in the initial surge in testosterone production which is associated with the GnRH agonists.

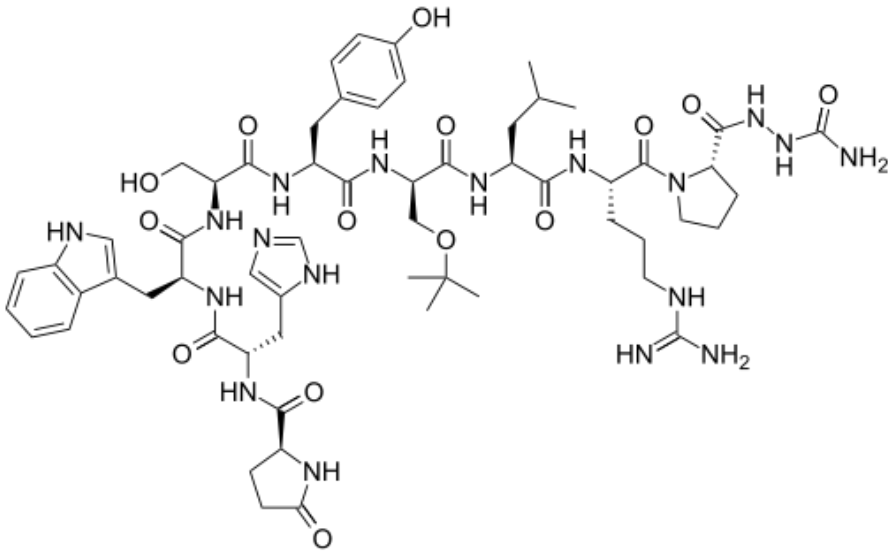

Goserelin, **39**

Unfortunately, approximately 20% of patients will not respond at all to hormonal therapy and for many patients where a response is observed, it is common for resistance to occur resulting in the presence of castrate-resistant tumours.[84] Typically prostate cancers are responsive to hormonal treatments for 12 to 18 months before becoming castrate-resistant and ultimately, metastatic.[85] Once bony metastasis has occurred the survival rate is extremely low, with

patients having a 9 to 12 month life expectancy.[84] At present the treatment of hormone-refractory metastatic tumours is palliative, intending not to cure the disease, but to improve quality of life and relieve pain.[86] Until recently, the only treatments available for these advanced cancers included taxanes, e.g. Docetaxel **40**, which increase survival outcome, reduce serum PSA levels and improve quality of life when used in conjunction with Prednisone, **41**, a corticosteroid drug.[86] In 2011, Abiraterone, **42** was approved as a 17α-hydroxylase and C_{17-20} lyase inhibitor, which prevents androgen biosynthesis, and prolongs the life of patients suffering from terminal prostate cancer.

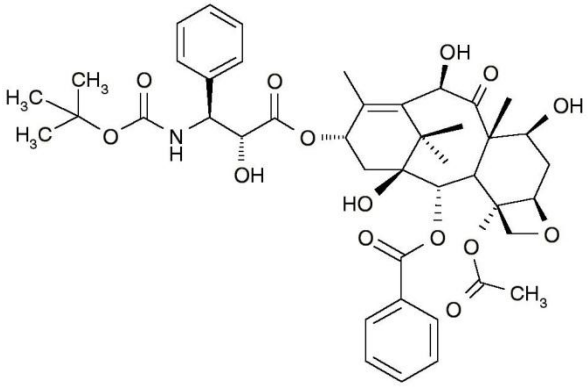

Docetaxel, **40**

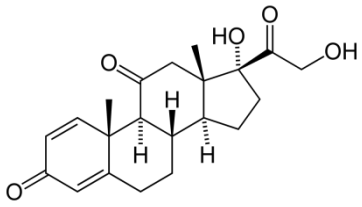

Prednisone, **41**

Despite successful androgen depletion following chemical or surgical castration, approximately 10% of baseline testosterone is still present.[87] Dehydroepiandrostenedione (DHEA) and androstenedione are converted into testosterone by enzymes found in the prostate and other peripheral tissues (Figure **14**). The androgen receptor's sensitivity to testosterone and DHT is often elevated in castrate-resistant prostate cancer. Therefore, the prevention of extra-testicular androgen synthesis by Abiraterone has provided a novel therapy for patients suffering advanced prostate cancer which is no longer responsive to the traditional androgen ablating drugs (i.e. goserelin, nilutamide).[87, 88] The discovery of TAK-700, **43**, (orteronel), a potent and selective non-steroidal imidazole-based inhibitor of C_{17-20} lyase has since been reported, which has an IC_{50} of 28 nM.[89, 90] Orteronel is currently in Phase III clinical trials for the treatment of patients with castrate-resistant metastatic disease.[13,14]

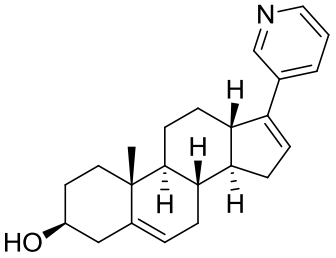

Abiraterone, **42**

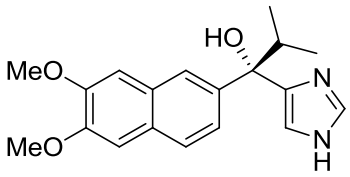

Orteronel, **43**

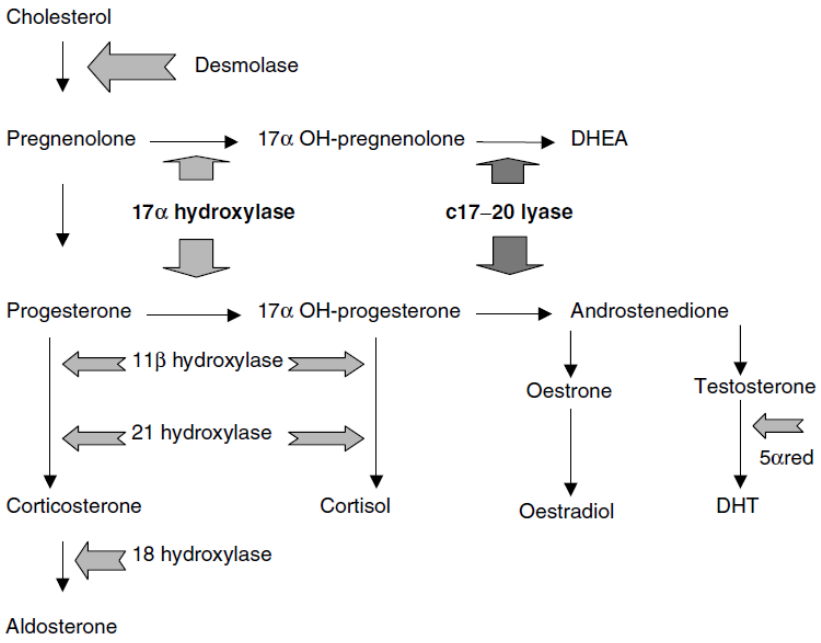

Figure 14: Steroid biosynthesis pathway. Abiraterone acetate inhibits 17α-hydroxylase and $C_{17,20}$-lyase preventing testosterone synthesis. From ref [87].

The development of second-generation anti-androgen treatments is also in progress. One of the known mechanisms of resistance to first-line hormonal therapy is up-regulation of the androgen receptor. Furthermore, in cells which over-express the AR, first generation anti-androgens such as bicalutamide act as partial agonists of the androgen signalling pathway. This clinical liability of the first generation anti-androgens highlights the advantage of identifying progression to the castrate-resistant stage as soon as possible. MDV3100 (enzalutamide, **44**) was optimised as an inhibitor of the AR following a screen of non-steroidal compounds and has a binding affinity for the AR between 5 and 8 times that of bicalutamide, **4**. Enzalutamide also impairs nuclear translocation, and recruitment of co-activators of the AR ligand-receptor complex,[91] and is currently in Phase III clinical trials for

the treatment of castrate-resistant prostate cancer following encouraging anti-tumour activity in Phase II trials.[92]

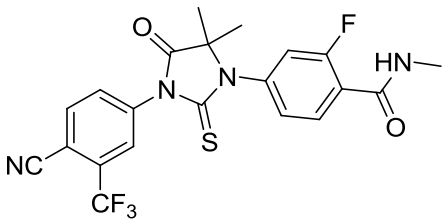

Enzalutamide, **44**

3.1.4 The Implication of MEK5/ERK5 Pathway Deregulation in the Development of Castrate-Resistant Prostate Cancer

Castrate-resistant tumours arise as a result of mutated androgen receptor overexpression which may be activated regardless of anti-androgen therapy by receptor independent mechanisms. Mutated androgen receptors may be deemed 'promiscuous', allowing activation by binding of the anti-androgen drug or other steroid hormones and thirdly, the mutated receptor may be hypersensitive, thus allowing activation despite very low concentrations of androgen present.[88, 93] Expression of the anti-apoptotic gene Bcl-2 has been implicated in the development of castrate-resistance in tumours. Bcl-2 was found to be below detectable levels in androgen dependent cancers. However, high levels of the gene are found in the resistant form of the disease. Presence of this gene allows the cells to evade apoptosis generating a series of cells unresponsive to hormone therapy. Inhibition of the Bcl-2 mediated pro-apoptotic pathway is therefore one potential therapeutic strategy for the treatment of castrate-resistant prostate cancer.[94]

Another validated therapeutic strategy is targeting the MEK5/ERK5 pathway. ERK5 expression is significantly up-regulated in the epithelial cells of advanced prostate cancers when compared with those of benign tumours. It is also found that overexpression strongly correlates with an elevated Gleason sum score, indicating poorly differentiated tumours (Figure **15**).[73, 95] Altered MEK5/ERK5 signalling has also been found to be related to increased metastatic potential of prostate cancer cells, which is directly related to the poor survival outcome associated with the disease (Figure **16**). The exact pathophysiology of bone metastasis is not fully understood although the link between ERK5 overexpression and MMP-9 synthesis has been made (Section **2.5.6.3**). Elevated cytoplasmic and nuclear levels

of ERK5 serve as an independent prognostic marker for advanced prostate cancer, with nuclear ERK5 expression present only in malignant cells.[73]

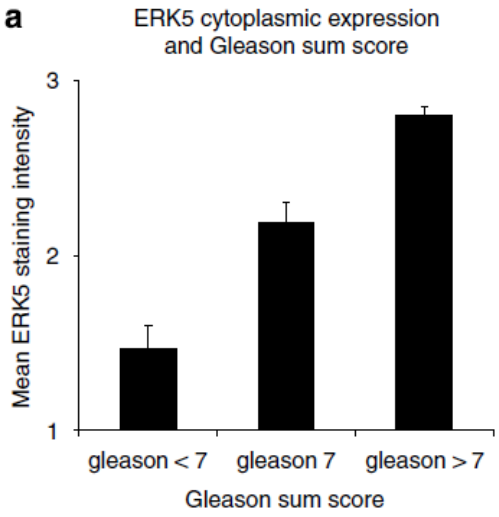

Figure 15: The relationship between ERK5 expression and Gleason sum score.[41] Staining intensity is semi-quantitative, scored as either absent (0), weak (1), moderate (2) or strong (3). From ref [95].

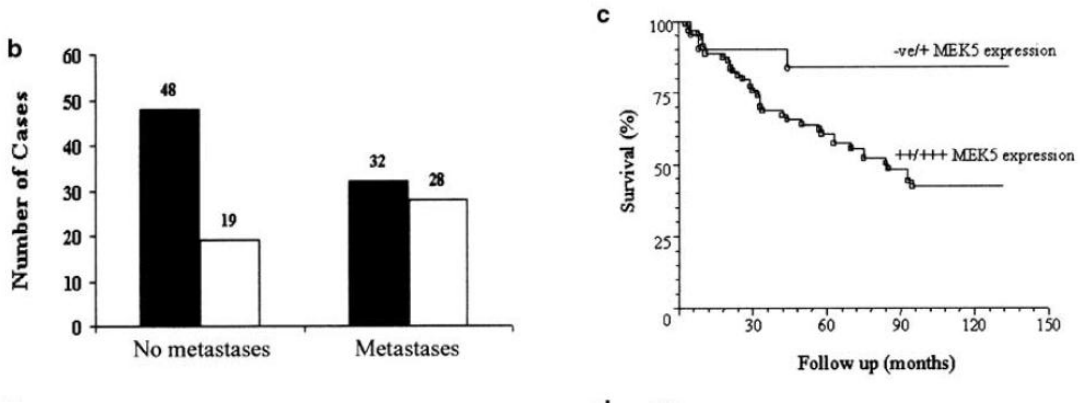

Figure 16: Left: ERK5 expression in the presence and absence of bone metastases. Black = No ERK5 expression detected; White = ERK5 expression detected. Right: Elevated ERK5 expression correlated with disease specific survival. From ref [73].

Definitive confirmation of the link between ERK5 overexpression and aggressive metastatic prostate cancer has been achieved *in vivo*, following mouse xenograft studies. Implanted LNCaP cells transfected with MAPK7, the gene encoding ERK5, proliferated more rapidly when compared those transfected with an empty vector. A significant increase in mean tumour volume at 40 days post implantation was measured, and the rate of migration and

invasion were also notably elevated (Figure **17**), with an increase of 1.8 and 2.1 fold respectively.[73]

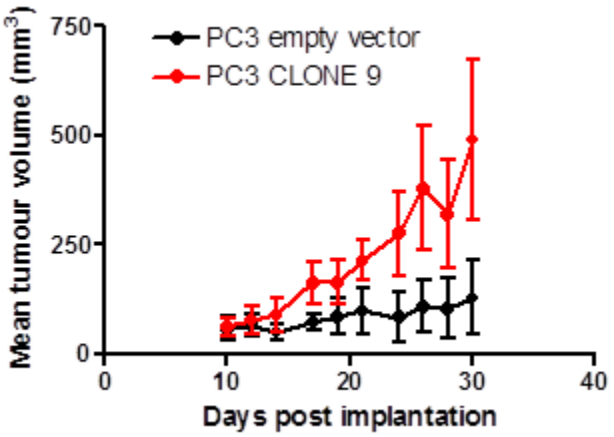

Figure 17: PC3 cells transfected with the MAPK7 gene show a more aggressive phenotype. From ref [73].

3.1.5 The Effects of PD184352 on Prostate Cancer Cell Growth

The small-molecule inhibitor PD184352, **45**, targets MEK1/2 in an allosteric manner. At a low concentration of 0.3 µM, inhibition of ERK1/2 mediated by MEK1/2 was achieved with no measured effect on cell proliferation in PC3 cells. A higher concentration of drug (3 µM) was found to also inhibit ERK5, most likely as a result of action upon MEK5. Treatment of PC3 cells with the elevated concentration of **45** also gave a significant reduction in cell proliferation. These data suggest that effects once attributed to the ERK1/2 pathway may actually be regulated by ERK5, and that clinical inhibition of ERK5 may have a therapeutic application for potentiation of cell proliferation, as well as the prevention of tumour metastasis and angiogenesis.

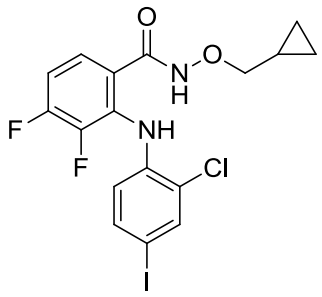

PD184352, **45**

3.2 Breast Cancer

3.2.1 Introduction to Breast Cancer

Whereas prostate cancer is the most frequently diagnosed cancer in men, breast cancer is the most commonly diagnosed cancer in females with approximately 49,000 new cases in the United Kingdom in 2009. Although rare, male breast cancer accounted for approximately 1% of UK cancer diagnoses in 2009.[77] There are several risk factors associated with the onset of breast cancer in females. The age of onset is generally lower than that of prostate cancer, and the risk of developing breast cancer is strongly associated with production of the female hormone oestrogen. Hormonal influences, such as use of the contraceptive pill and reproductive history exert a significant effect on the risk of developing breast cancer. However, the most influential factor is genetic predisposition, with approximately 10% of breast cancers in the Western world resulting from hereditary factors.[96] For example, mutations in the tumour suppressor genes BRCA1 and BRCA2 has been associated with an elevated incidence of breast (and to a lesser extent, ovarian) cancer development, increasing the lifetime risk to ≥80%.[97]

		England	Wales	Scotland	Northern Ireland	UK
Male	**Cases**	**325**	**13**	**24**	**9**	**371**
	Crude Rate	1.3	0.9	1.0	1.0	1.2
	AS Rate	**1.0**	**0.7**	**0.8**	**1.0**	**1.0**
	AS Rate - 95% LCL*	0.9	0.3	0.5	0.3	0.9
	AS Rate - 95% UCL*	1.2	1.0	1.1	1.6	1.1
Female	**Cases**	**40,260**	**2,585**	**4,368**	**1,204**	**48,417**
	Crude Rate	153.1	168.5	163.1	132.3	154.1
	AS Rate	**124.0**	**127.0**	**127.2**	**118.9**	**124.4**
	AS Rate - 95% LCL*	122.8	122.1	123.4	112.2	123.3
	AS Rate - 95% UCL*	125.3	131.9	130.9	125.6	125.5

Figure 18: Recent breast cancer statistics according Cancer Research UK. 95% LCL and UCL are the lower and upper confidence limits around the age-standardised (AS) rate. From ref [77].

3.2.2 Influence of Stat3 on the MEK5/ERK5 Pathway

Stat3 has been classified as an oncogene whose constitutive activation is detected in breast cancer cell lines (Stat3-C). Several genes are reported to be up-regulated by Stat3, including the members of the matrix metalloproteinase family MMP-1 and MMP-10, vascular endothelial growth factor (VEGF), and connective tissue growth factor (CTGF) amongst

others in a non-malignant telomerase immortalised breast cancer (TERT) cell line. Furthermore, expression of Stat3-C in TERT cells resulted in a 22-fold increase in MEK5 induction and activation. In MDA-MB-435 Stat3 expressing breast carcinoma cells, MEK5 expression and activation was inhibited following the use of Stat3 small-interfering RNA (siRNA), which suggests that MEK5 may be directly regulated by Stat3 in some breast cancers.[98]

3.2.3 Expression of ERK5 in HER2-positive Breast Cancer

Overexpression of the HER2 receptor tyrosine kinase oncogene is found in 20-30% of breast cancers, and is associated with a more aggressive phenotype, and poor disease specific survival. The identification of HER2 (or ErbB2) in the 1980's resulted in a large amount of clinical interest, which eventually led to its validation as an anti-cancer target.[99] The monoclonal antibody trastuzamab (Herceptin) and small-molecule inhibitor lapatanib, **46** both target the HER2 protein, and are therefore clinically efficacious in patients with advanced or metastatic breast cancers which are HER2-positive.

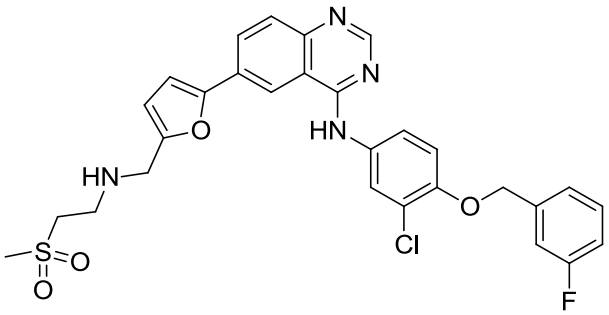

Lapatanib, **46**

The extracellular HER2 receptors mediate signalling *via* several pathways, including those involving the MAPKs, and PI3K (Akt). In breast cancer cells, ERK5 activation is triggered by binding of the substrate neuregulin to the HER2 receptor, and in cancer cell lines where HER2 is expressed, ERK5 has been found to be constitutively elevated. Most interestingly, inhibition of ERK5 in combination with the use of Herceptin appears to sensitize cells to treatment. Furthermore, ERK5 is found to be overexpressed in a number of patients, and recent findings illustrate that ERK5 is an independent prognostic measure in breast cancer (Figure **19**).[100] Therefore, the clinical development of an ERK5 inhibitor may provide a more successful approach for the treatment of advanced breast cancer.

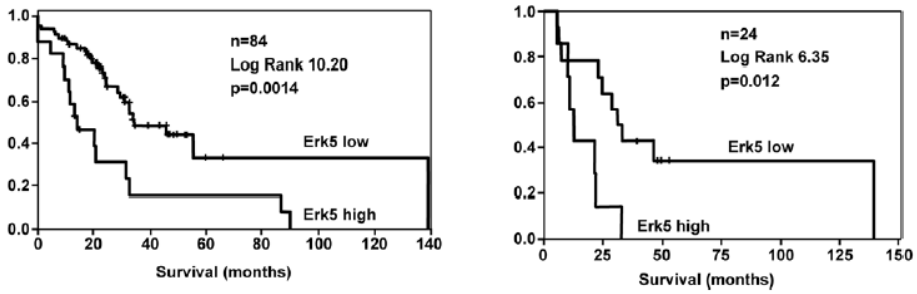

Figure 19: Left: Disease-free survival with respect to ERK5 levels in patients with early stage breast cancer; Right: Disease-free survival with respect to ERK5 levels in patients with HER2 positive early stage breast cancer. From ref [100].

3.3 Hepatocellular Carcinoma (HCC)

3.3.1 Introduction to HCC

HCC is the most commonly diagnosed form of liver cancer, and is the fifth most common cancer type in the world.[101] Unlike breast and prostate cancer, liver cancer in adults often has a poor prognosis at the time of initial diagnosis. The main risk factors associated with the development of liver cancer are exposure to the Hepatitis B and C viruses, and excessive consumption of alcohol. Due to the implication of alcohol abuse in HCC, significant liver cirrhosis is also present at the time of a cancer diagnosis. At this stage, the tumour is deemed inoperable and an average life expectancy of approximately three months is given.[77]

3.3.2 Gene Amplification of ERK5 in HCC

Analysis of HCC cell lines revealed DNA copy number abberations, revealing a novel amplification at the 17p11 chromosome fragment. Amplification of chromosomal DNA is one of the primary mechanisms of protein overexpression associated with the progression of cancer.[101] It is this amplicon at 17p11 which harbours MAPK7, and as a result, cell lines where this amplification was apparent did indeed show overexpression of ERK5 (Figure **20**). A total of 35 of 66 HCC tumours tested contained an increase in MAPK7 copy numbers. Based on this observation, siRNA was used to knockdown the MAPK7 gene in proliferating SNU449 HCC cells, reported to have the greatest amplification of MAPK7. Down-regulation of MAPK7 resulted in a growth inhibitory effect, attributed to prevention of mitotic entry regulated by ERK5 (Figure **21**).[101]

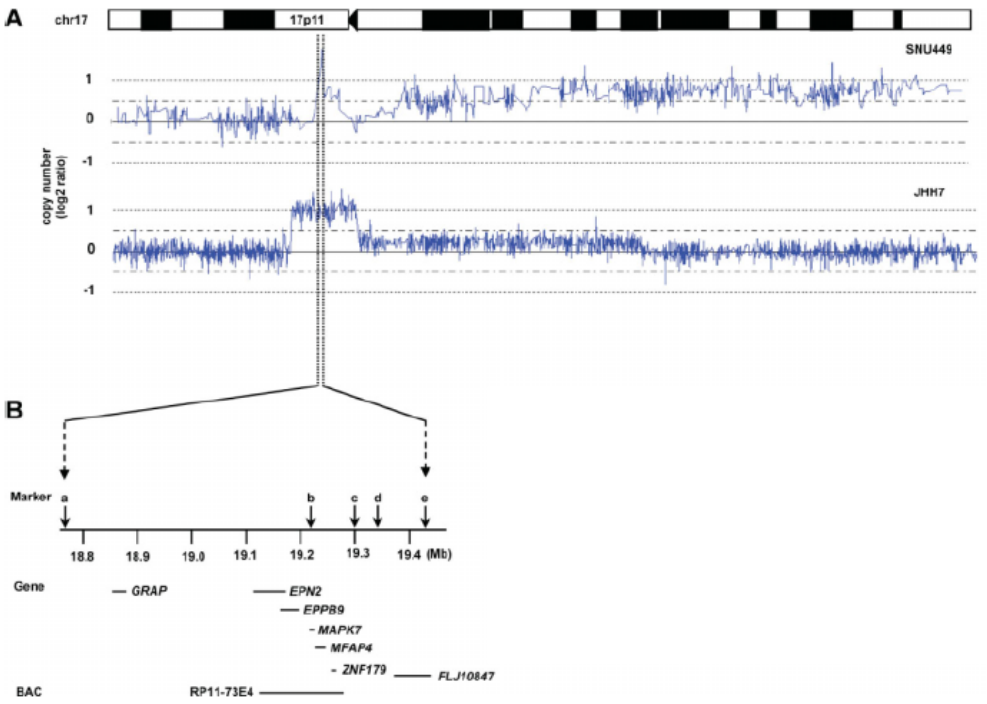

Figure 20: Amplicon map of the 17p11 chromosome in two HCC cell lines; SNU449 and JHH-7. From ref [101].

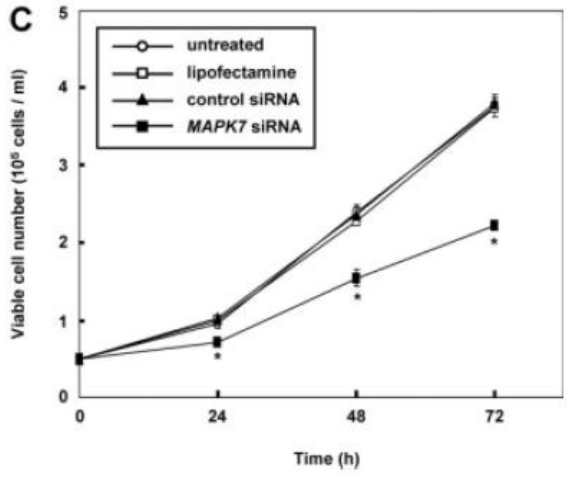

Figure 21: Growth inhibition of SNU449 cells by siRNA knockdown of the MAPK7 gene. From ref [101].

3.4 Multiple Myeloma (MM)

Multiple myeloma (MM) is characterised by the accumulation of neoplastic plasma cells of β-lymphocyte origin, associated with the immune system. Accounting for 10% of all haematological malignancies, MM results in the overproduction of antibodies which are unable to fight infection in the normal fashion.[102, 103] Often, intensive high-dose

chemotherapy is required for treatment, which kills normal and neoplastic cells. The Stat3 protein discussed in Section **3.2.2** has been implicated in the survival of MM cancer cells, in addition to breast cancer cells, and is known to stimulate ERK5 expression. The myeloma growth factor, interleukin 6 (IL-6) has been shown to activate ERK5 in MM cell lines, and IL-6 dependant cell proliferation is down-regulated *via* expression of a dominant negative form of ERK5. As observed in HER2-positive breast cancer (Section **3.2.3**), sensitization to pro-apoptotic agents is observed following knockout of ERK5 activity in MM. A novel therapeutic route for treatment of patients with MM who do not respond to current chemotherapeutic agents is therefore apparent.

Chapter 4: Resynthesis of BIX02188 and BIX02189

4.1 Rationale for the Synthesis of BIX02188 and BIX02189

In 2008, a new class of pharmacological inhibitors of MEK5 were described. The indolinone based inhibitors, BIX02188 (**47**) and BIX02189 (**48**), both exhibit low nanomolar potency against MEK5 with IC_{50} values of 4.3 and 1.5 nM respectively, and are also moderately active against ERK5, (IC_{50} values of 810 and 59 nM respectively).[104] This indolinone class of inhibitors developed by Boehringer Ingelheim Pharmaceuticals are dual-inhibitors of the MEK5/ERK5 signalling pathway. BIX02188 is shown below, drawn as it is illustrated in the literature.[104] It is clear that there is one atom missing from the structure and for the purposes of our investigations it was assumed to be the primary amide.

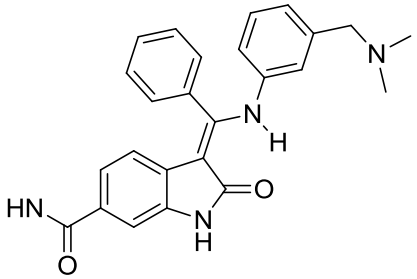

BIX02188, **47**

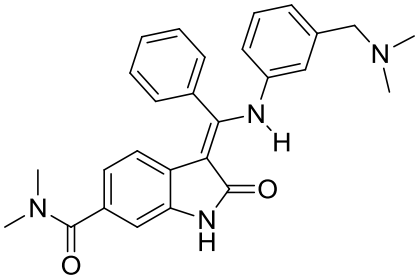

BIX02189, **48**

4.2 Cambrex PKLight™ Protein Kinase Assay

The Cambrex PKLight™ protein kinase assay was used to determine *in vitro* IC_{50} values for BIX02188 and BIX02189. During a kinase reaction, the level of free ATP is depleted as the γ-phosphate group is transferred to the substrate. The reduction in ATP is accurately measured using Cambrex PKLight™ bioluminescent reagents. Upon incubation with an inhibitor, the kinase activity decreases, resulting in a higher concentration of free ATP at the end of the assay. A luminescent signal is emitted at an intensity proportional to the level of ATP present.

The literature procedure used either GST-MEK5 or GST-ERK5 isolated from baculovirus as the kinase, with a 0.75 μM ATP concentration. A 10-point dose titration with a maximum concentration of 10 μM of inhibitor was performed (Figure **22**). IC_{50} values were calculated from % kinase activity relative to a control (where control activity is 100% in the absence of an inhibitor).

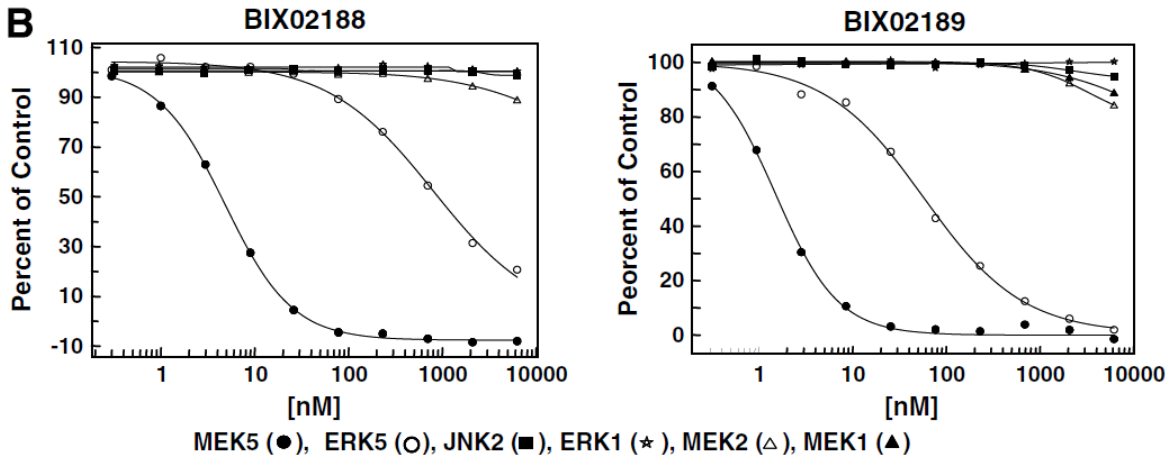

Figure 22: Dose titration curves for BIX02188 and BIX02189 against MEK5, ERK5, JNK2, ERK1, MEK2 and MEK1. Each data point represents an average of two data points. From ref [104].

Importantly, kinase selectivity profiling indicated that **47** and **48** are selective against a range of protein kinases, including other members of the MAPK superfamily (Table **4**). Activity against MEK1/2, ERK1 and JNK2 were all above 6000 nM. Selectivity over the EGF-TK was also achieved. Resynthesis of authentic samples of BIX02188 and BIX02189 was desirable for a number of reasons. Evaluation of these inhibitors in the IMAP™ assay established at CRT would assist in validating the assay format currently being used as the primary assay for prospective ERK5 inhibitors. Furthermore, these compounds are of great interest for the establishment of biomarkers for inhibitors of the MEK5/ERK5 pathway.

Table 4: Selectivity profile of BIX02188 and BIX02189 against closely related kinases. [104]

Kinase	IC_{50} [nM]	
	BIX02188	**BIX02189**
MEK5	4.3	1.5
MEK1	>6300	>6200
MEK2	>6300	>6200
ERK5	810	59
ERK1	>6300	>6200
JNK2	>6300	>6200
TGFβR1	1800	580
EGFR	>6300	>6300
STK16	>6300	>6300

4.3 Synthesis of BIX02188 and BIX02189

BIX02188 and BIX02189 were resynthesised based on the literature protocol published by Boehringer Ingelheim pharmaceuticals (Scheme **1**).[105] Esterification of the commercially available carboxylic acid **49** was performed using thionyl chloride in methanol. Conversion to the corresponding methyl ester was achieved in high yield (85%). Subsequent S_NAr of **50** with dimethyl malonate in the presence of a strong base afforded **51** in 66% yield.

Synthesis of the indolinone scaffold proceeded *via* a one-pot, three-step mechanism under transfer hydrogenation conditions. Firstly, the nitro group is reduced to the corresponding aniline, which cyclises to give dimethyl 2-oxoindoline-3,6-dicarboxylate (not shown). Finally, this intermediate undergoes decarboxylation to afford indolinone **52** in almost quantitative yield. Protection of the amide with an acetyl group followed by a Knovenagel-type condensation with triethyl orthobenzoate afforded **53** as a mixture of *E*- and *Z*- isomers in 79%. Substitution with 3-dimethylamino methylaniline proceeded in moderate yield (52%). At this stage only the *Z*- isomer **54** was observed probably due to the formation of a pseudocycle stabilised by intramolecular hydrogen bonding. Problems were encountered in the last two steps of the reaction scheme. Hydrolysis of the acetyl protecting group and methyl ester were shown to go to completion upon analysis by LCMS and TLC. However, the zwitterionic nature of the resulting product led to complications on workup and purification. Extraction of the product into an organic solvent was extremely difficult, and purification of the carboxylic acid **55** by HPLC was necessary resulting in a low isolated yield of 38%. An alternative method was attempted which did not require an aqueous workup, using potassium trimethylsilanolate in THF,[106] (Scheme **2**) but cleavage of the *N*-acetyl group was detected by LCMS, with no conversion to the corresponding carboxylic acid. The deacetylated product **56** was not isolated.

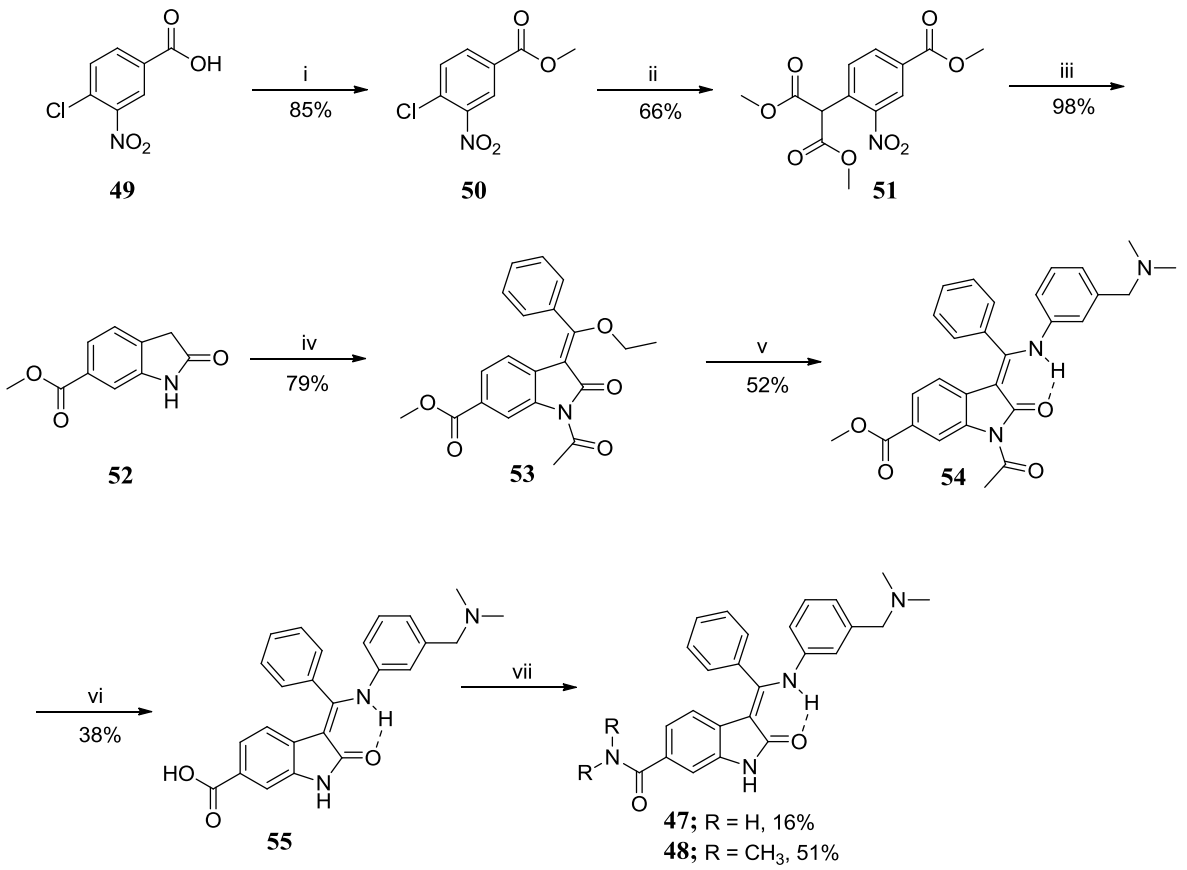

Scheme 1: Resynthesis of BIX02188 and BIX02189. *Reagents and conditions;* i) $SOCl_2$, MeOH, 60 ^oC, 16 h; ii) dimethyl malonate, KO^{t}Bu, NMP, 75 ^oC, 2h; iii) NH_4HCO_2, Pd/C, AcOH, 100 ^oC, 10 min, MW; iv) acetic anhydride, 130 ^oC, 3 h, then triethyl orthobenzoate 100 ^oC, 3 h; v) 3-dimethylamino methylaniline, DMF, 80 ^oC, 3 h; vi) LiOH monohydrate, H_2O, THF, 60 ^oC, 16 h; vii) For R = H; PyBOP, HOBt, Hünig's base, NH_4Cl, DMF, RT, 16 h; For R = CH_3; PyBOP, HOBt, Hünig's base, dimethylamine hydrochloride, DMF, RT, 16 h.

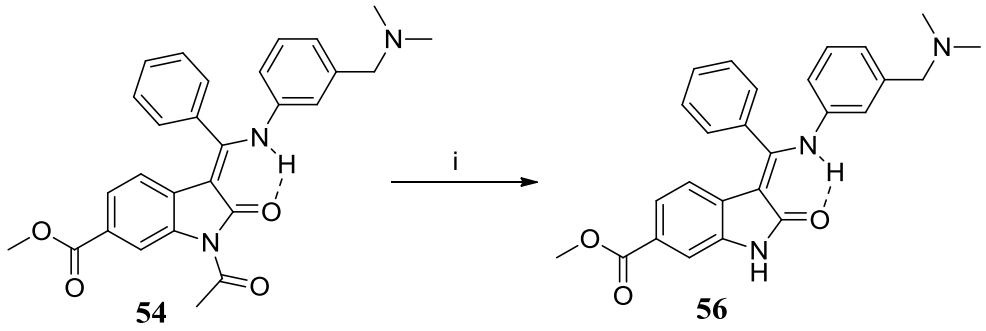

Scheme 2: Cleavage of the *N*-Acetyl protecting group. *Reagents and conditions;* i) potassium trimethylsilanolate, THF, RT, 6 h.[106]

BIX02188 and BIX02189 were obtained following amide coupling reactions using benzotriazol-1-yl-oxytripyrrolidinophosphonium hexafluorophosphate (PyBOP) and hydroxybenzotriazole (HOBt) as an additive in the presence of Hünig's base. Couplings were performed with ammonium chloride and dimethylamine hydrochloride which gave **47** and **48** in 16% and 51% yield, respectively. It is not known why the yield is considerably poorer for the primary amide and purification by semi-preparative HPLC was required for both compounds.

4.4 ERK5 Inhibitory Activity of Indolinone Based Inhibitors

BIX02188 and BIX02189 were submitted for biological evaluation, along with the intermediate carboxylic acid **55** (Table **5**). The activity observed in the literature varies significantly from that measured in the IMAP™ assay. The IMAP™ assay performed at CRT is conducted with an ATP concentration of 350 µM in accordance with the Km of ATP for ERK5. This is an unusually high ATP concentration for an *in vitro* kinase assay and may explain the large variation in IC_{50} values. In the IMAP™ assay, all three indolinone based compounds assessed are equipotent.

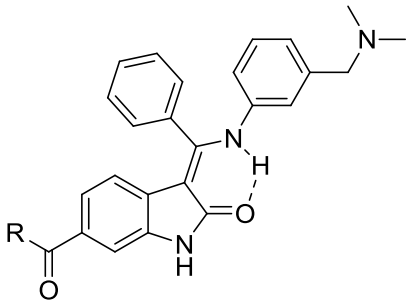

Table 5: Comparison of reported cellular data with IMAP™ assay data

Compound	R	Lit. ERK5 IC_{50} (PKLight™, µM)	Measured ERK5 IC_{50} (IMAP™, µM)
55	OH	-	11.3 ± 2.9
47	NH_2	0.81	10.5 ± 0.3
48	$N(Me)_2$	0.06	9.2 ± 0.9

Cellular based assays were performed in collaboration with Professor Hing Leung at the Beatson Institute, Glasgow. Treatment of SNU449 cells (a HCC cell line), with BIX02189 did not show any reduction in the levels of EGF induced autophospho-ERK5 versus controls

(as shown by the autophospho-ERK5 immunoprecipitation/western blotting (IP/WB) assay) or phospho-ERK5 (as shown by the phospho-ERK5 Western blots, WB), (Figure **23**). Immunoprecipitation was performed as the autophospho-ERK5 antibody is weak, and binds non-specifically to other proteins. This method extracts and concentrates ERK5 protein from cell lysates using an ERK5 antibody. A western blot may then be performed using the autophospho-ERK5 antibody. The SNU449 cell line was used as it is the only cell line tested which has sufficiently high levels of autophosphorylated ERK5 for detection in the IP/WB assay. (Assays were conducted by Dr Lesley McPhail).

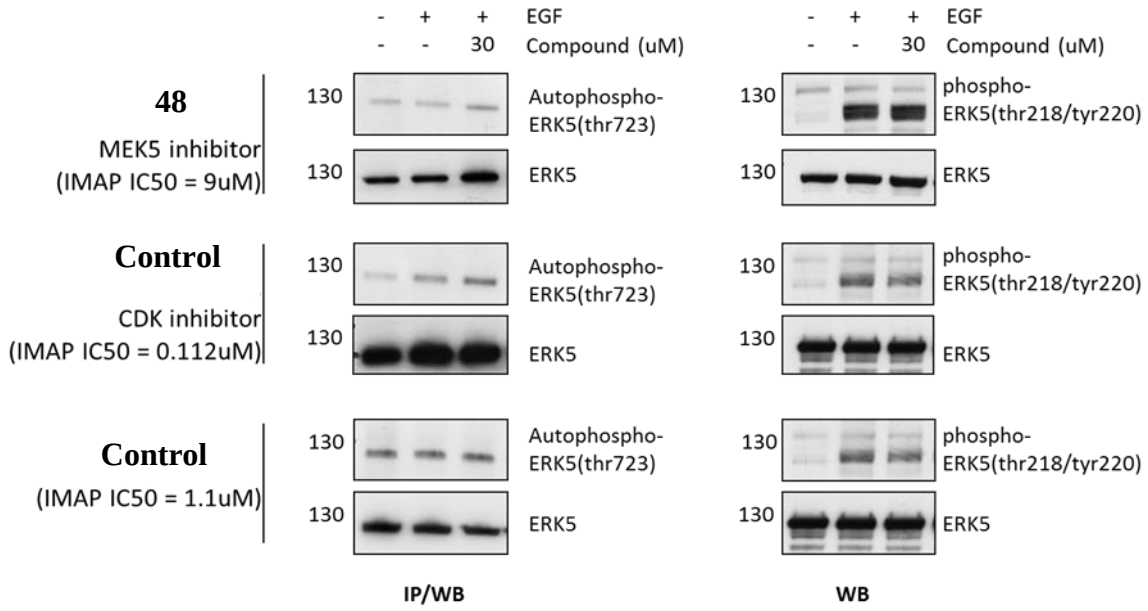

Figure 23: Autophosphorylation/western blotting assay using SNU449 cells with **48**.

In collaboration with Dr Simon Cook of the Babraham Institute, Cambridge, BIX compounds were assessed in a dual-luciferase reporter gene assay. ERK5 IC_{50} values are determined *via* measurement of phosphorylation levels of the downstream transcription factor MEF2D, facilitated by luminescence detection. The dual-luciferase reporter gene assay is described in more detail in Section **7.8**. Assays were conducted by Dr Pamela Lochhead using material resynthesised at Newcastle, and those obtained from Boehringer.

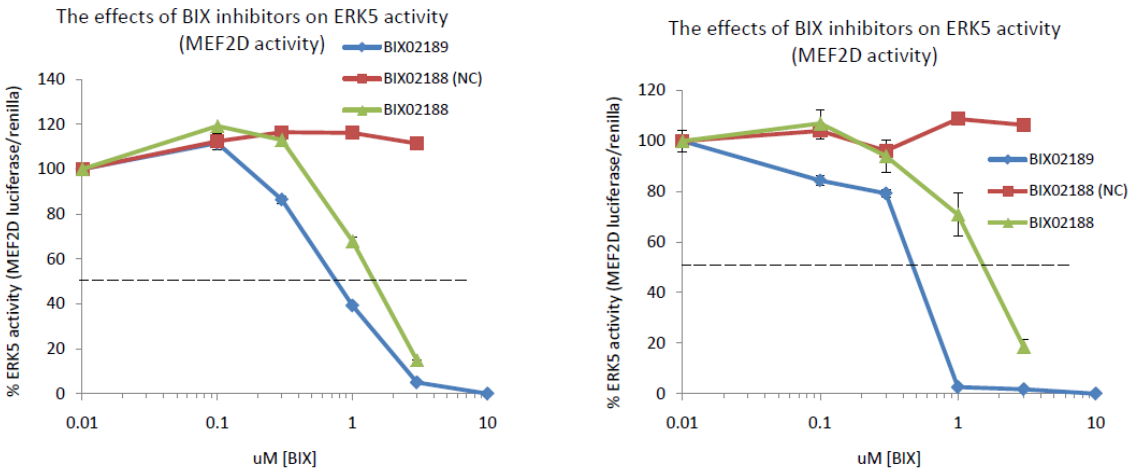

Figure 24: Effects of BIX inhibitors on ERK5 activity in the dual-luciferase reporter gene assay.

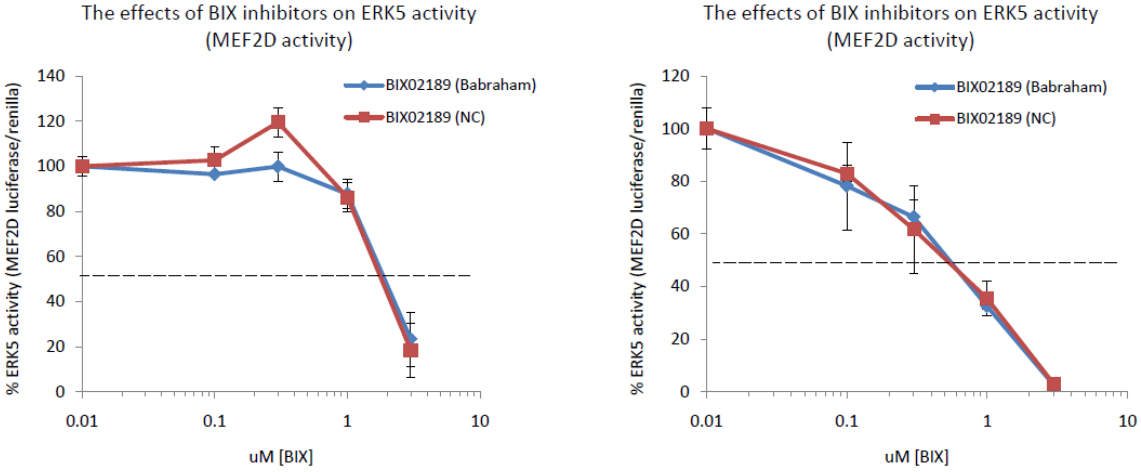

Figure 25: Comparison of BIX02189 resynthesised in-house (NC, red) versus authentic material (Babraham, blue).

Table 6: IC_{50} values for BIX02188 and BIX02189 authentic material versus resynthesised material.

Compound	IC_{50} (μM)	
	Authentic (Babraham)	Resynthesised (Newcastle)
BIX02188	1.2	Inactive
	1.5	Inactive
BIX02189	2	2
	0.5	0.5

A discrepancy was observed when comparing BIX02188 synthesised at Newcastle with that of the commercial supplier (Figure **24**, Table **6**). However, the data obtained for BIX02189 (NC) correlated extremely well with the authentic material (Figure **25**). The MEF2D reporter gene assay determined the IC_{50} for BIX02189 as 1.25 μM as an average of duplicate measurements.

Due to the inactivity of resynthesised BIX02188, **47**, quality control studies were initiated. A small sample of the authentic material was obtained and analysed by LCMS which confirmed a mass difference of 15 amu between the two samples. It was deduced that the correct structure of BIX02188 was the mono-methylated amide **57**, and not the primary amide illustrated in the literature. This demonstrates that the substitution pattern around the amide moiety plays a critical role in cellular activity, likely due to differences in cell permeability.

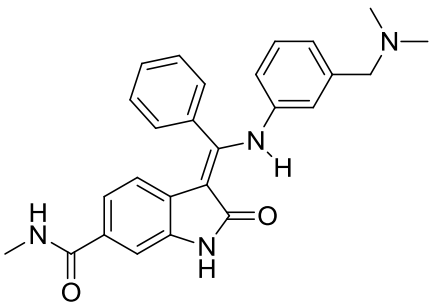

57

BIX02189 has proved to be a powerful molecular tool in the design and validation of both *in vitro* and cell based assays and is currently used as a positive control in the dual-luciferase MEF2D reporter gene assay being conducted at the Babraham Institute.

Chapter 5: The 3-Cyanopyridine Series

5.1 Synthetic Strategy Towards 3-Cyanopyridines

The first synthetic approach which was considered for the synthesis of 3-cyanopyridines was based on the route reported by Shestopalov et al (Figure **26**).[107] 4,6-Diaryl-3-cyanopyridine-2(1*H*)-thiones are key intermediates in the synthesis of hit compounds **67** and **68** and allow diversification at the R^1 position *via* alkylation of the pyridine-thione motif. Aryl substituted pyridine-thiones are accessible from the appropriate α, β-unsaturated ketones.

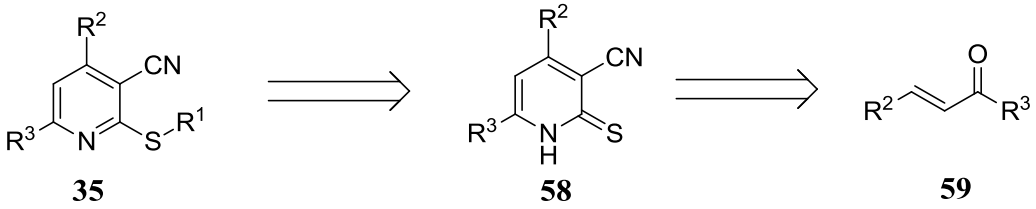

Figure 26: Retrosynthetic analysis of the 3-cyanopyridine scaffold

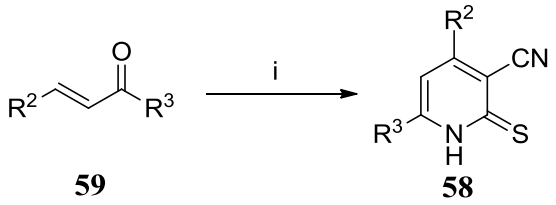

Scheme 3: Shestopalov's synthesis of **58**: *Reagents and Conditions;* i) S_8, morpholine, EtOH, 80 ^oC, 30 min then malononitrile, 80 ^oC, 2 h.

Shestopalov's one-pot synthesis begins with a Michael addition of malononitrile on an α, β-unsaturated ketone (Scheme **3**). The next step is less well defined. Elemental sulfur (as the allotrope S_8) is known to give betaines in the presence of organic bases and ethanol (Scheme **4**).

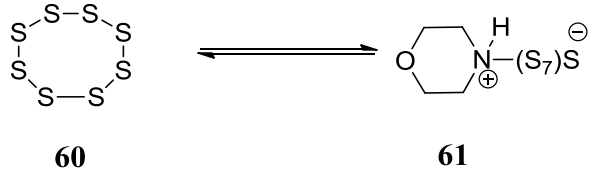

Scheme 4: Reaction of sulfur S_8 with morpholine to give the reactive betaine species.[108] *Reagents and Conditions;* morpholine, EtOH, Δ.

The ketonitrile, **62** resulting from Michael addition with malononitrile is subsequently thiolated at the C(2)-H bond giving **63**, and the transformation which occurs thereafter may proceed by two possible mechanisms. The first involves formation of a thiirene ring followed by rearrangement and finally cyclization by intramolecular condensation (Scheme **5**).

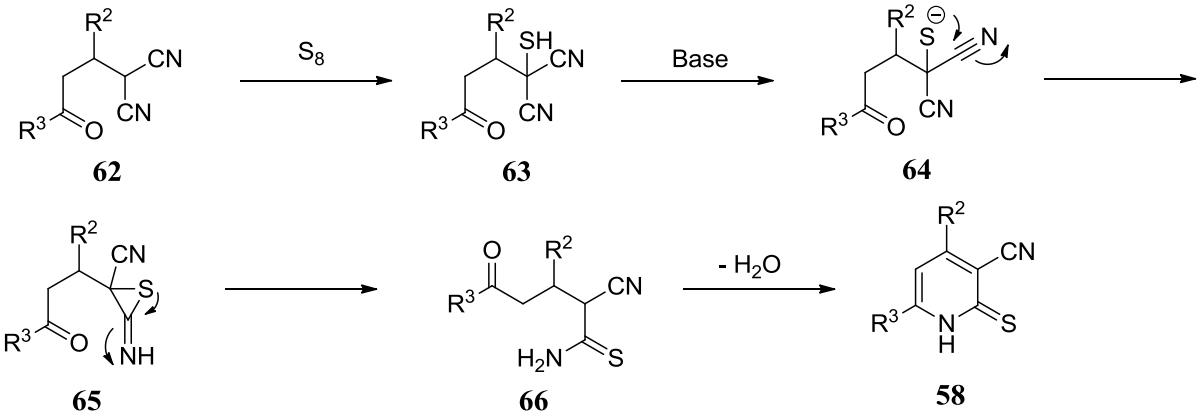

Scheme 5: First possible mechanism for pyridine-thione synthesis.

The alternative mechanism begins with elimination of hydrogen sulfide, which then may add across one of the two nitrile groups to give an unsaturated thioamide. Condensation of the thioamide gave the product (Scheme **6**).

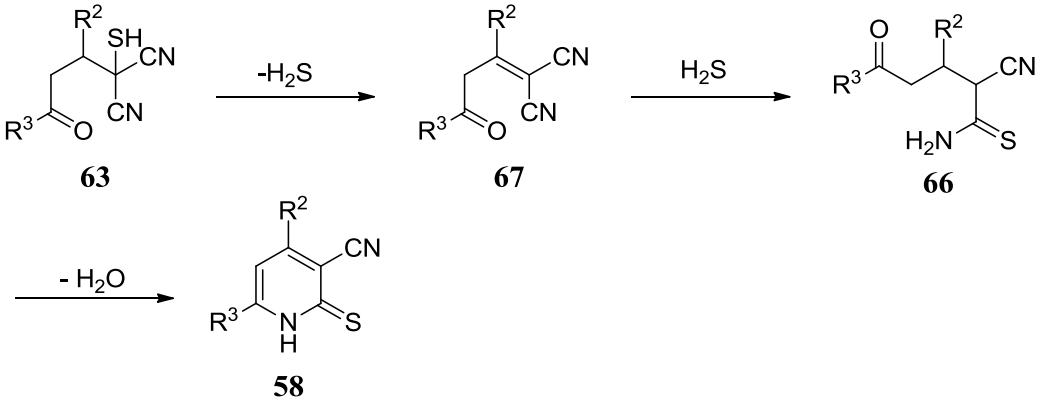

Scheme 6: Second possible mechanism for pyridine-thione synthesis.

Pyridine-thiones may exist in equilibrium between two possible tautomers, but generally prefer to exist as the thione. However, this may be affected by the various ring substituents. This phenomenon has been reported with regards to pyridine-4-thiones, where the presence of an electron-withdrawing group or groups, particularly polyhalogenated species, can influence the compound to exist predominantly as the thiol.[108] The environment in which the pyridine-thiones exist may also dictate their preference for either tautomer. It is generally

accepted that in polar solvents the predominant form is the thione, but in non-polar solvents and in the gaseous phase the thiol may be preferred. Pyridine-2-thiones also readily dimerise *via* a disulfide bond, due to the equilibrium which exists between the thione moiety and its thiophenol tautomer. These properties of the pyridine-thione moiety were considered as potential challenges in the synthesis and isolation of these intermediates.

5.2 Hit Validation of 3-Cyanopyridines

Resyntheses of the two most potent 3-cyanopyridine hits from the HTS (IC_{50} range 0.4-1.6 µM) were performed by Dr Betty Cottyn using the synthetic strategy outlined in Section **5.4.1**. Results of hit validation studies are shown in Table **7**.

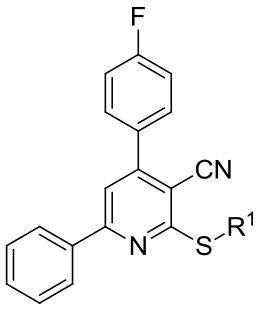

Table 7: IC_{50} values for resynthesised hit compounds

Compound	R^1	IC_{50} HTS (µM)	IC_{50} Resynthesised (µM)[a]
67	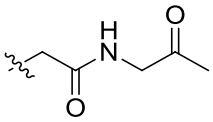	0.4	20.5 ± 1.3
68	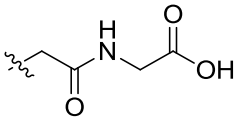	1.6	4.9 ± 0.3

[a] Determinations ± standard deviation (mean of n = 2 unless otherwise stated)

The results show a significant variation between the initial activity observed by HTS to that of the resynthesised material. The reason for the discrepancy between these results has not been established. However, trace impurities are well known to be the cause of false positive results, highlighting the importance of hit validation by resynthesis, and the limitations of the HTS campaign. Despite the diminished activity observed in this series, the 3-cyanopyridine

scaffold was deemed a valid starting point for initiating structure activity relationship (SAR) studies due to its modest potency, synthetic tractability and novelty.

5.3 Proposed Libraries for the 3-Cyanopyridine Series

Following hit validation, areas were identified for further investigation in order to build up structure activity relationships (SAR) around the 3-cyanopyridine scaffold. Key areas are highlighted in Figure **27**.

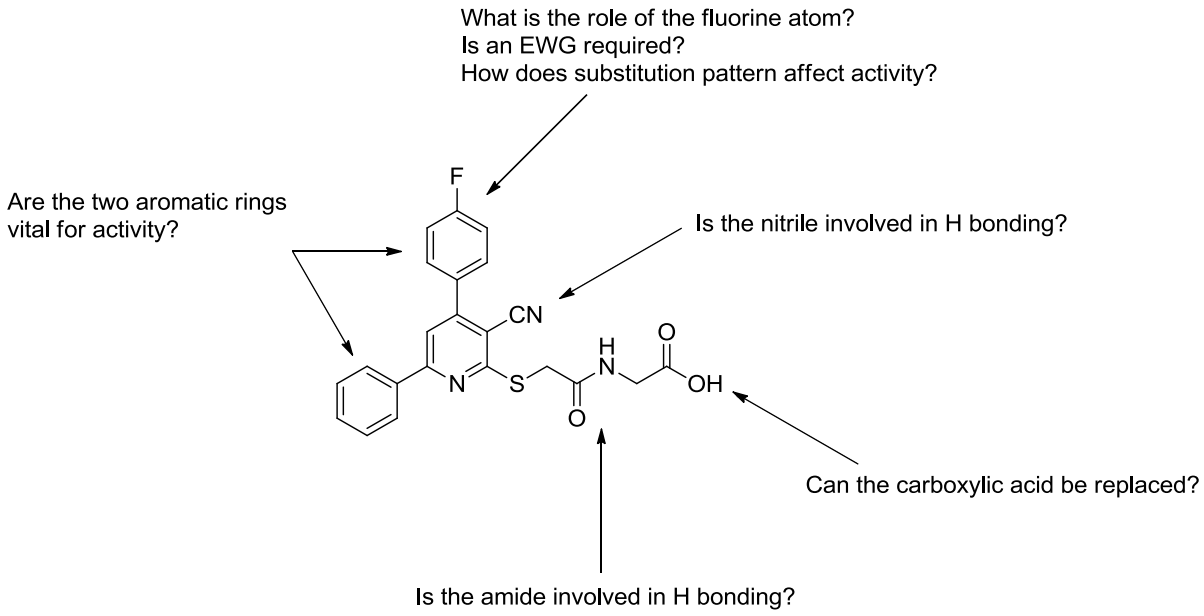

Figure 27: SAR questions posed following hit validation studies

It was determined that the majority of these questions could be answered following the synthesis of three focussed libraries:

Library 1 – Modification to the thioether side-chain (R^1)

Library 2 – Modification to the aryl substituent (R^2 as shown in Figure **26**)

Library 3 – Isosteric replacement of the 3-cyano motif

5.3.1 Library 1 - Modification to the Thioether Side-chain

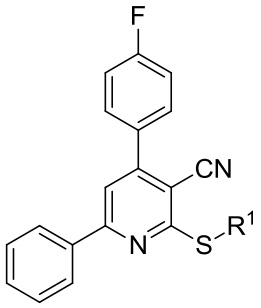

Table 8: Proposed compounds for Library 1 with rationale

Compound	Side-Chain R^1	Rationale
68	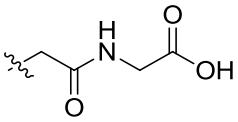	Present in hit compound; synthesis to be optimised
67	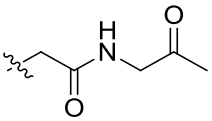	Present in hit compound; methyl ketone is tolerated, indicating carboxylic acid may be replaced
69	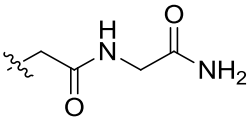	Classical isostere for the carboxylic acid; can the carboxylic acid be replaced?
70	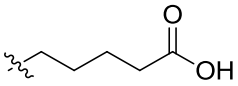	Amide removed; is the amide group crucial for activity?
71	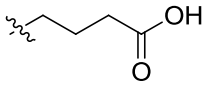	Amide removed plus chain length truncated by one carbon unit; is chain length important?
72	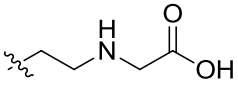	Carbonyl removed; is the carbonyl acting as a H-bond acceptor?

5.3.2 Library 2 - Modification to the Aryl Substituent

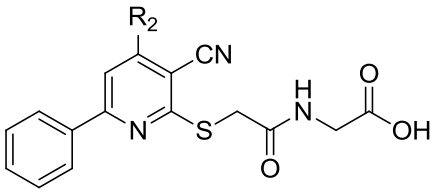

Table 9: Proposed compounds for Library 2

Compound	**73**	**74**	**75**	**76**	**77**	**78**	**79**
R^2	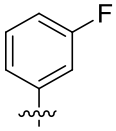	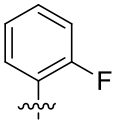	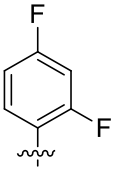	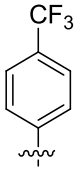	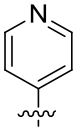	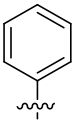	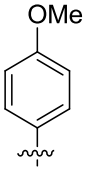

The compounds selected for synthesis in this series aimed to probe regions of the ERK5 ATP binding site around the R^2 aromatic group. In particular, compounds were chosen to investigate the position of the substituent and to compare EWG and EDG properties. Due to the large molecular weight of the hit compounds (>450 g/mol), replacement of the aromatic rings with methyl groups was desirable (compound **80**) in order to establish whether the aromatic groups in positions R^2 and R^3 were part of the pharmacophore. All compounds in this series were synthesised containing the carboxylic acid containing side-chain present in the parent, **68** for comparison purposes. Selected compounds with the methyl ketone side-chain were also synthesised.

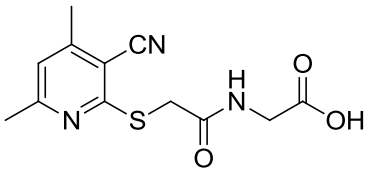

80

5.3.3 Library 3 – Isosteric Replacement of the 3-Cyano Motif

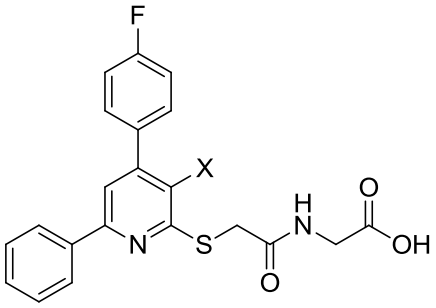

Table 10: Proposed replacements for the cyano group, X.

Compound	81	82	83
X	-H	-Br	-CCH

To determine the nature of the interaction of the nitrile group within the enzyme ATP binding site, a series of replacements were considered. The bromo analogue would have a similar size and lipophilicity but lacks the H-bond acceptor and EWG character. The alkyne is a more classical isostere, occupying the same area of chemical space and possessing sp hybridisation character. However, the alkyne is a weak H-bond donor, whereas the nitrile is an acceptor.

5.4 SAR Studies of the Thioether Side-Chain (R^1)

Preliminary SAR studies aimed to investigate the role of the functional groups present in the thioether side-chain, while keeping aryl groups R^2 and R^3 constant. The first objective was to optimise the chemistry utilised for resynthesis of the initial hits.

5.4.1 Optimisation of the synthesis of 4-(4-fluorophenyl)-6-phenylpyridine-2(1H)-thione 86

4-Fluorochalcone was obtained *via* aldol condensation of acetophenone with 4-fluorobenzaldehyde (Scheme **7**). This reaction proceeded cleanly with ease of purification by recrystallisation in 75%. The key step towards the synthesis of **86** proved challenging. Low isolated yields (≤ 15%) were reported, which have been attributed to the ability of this intermediate to tautomerise, and its readiness to oxidise under atmospheric conditions.[107]

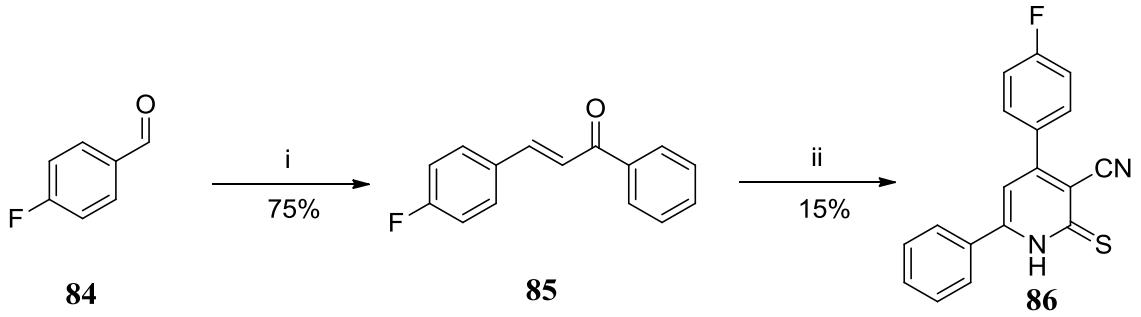

84 **85** **86**

Scheme 7: Initial synthetic strategy towards **86**: *Reagents and Conditions;* i) acetophenone, NaOH, EtOH, RT, 16 h; ii) S_8, morpholine, EtOH, 80 ^oC, 30 min then malononitrile, 80 ^oC, 2 h.

Generation of the betaine species followed by addition of malononitrile and the relevant chalcone, **85** resulted in formation of a complex reaction mixture. The one-pot nature of the cyclisation reaction was thought to add unnecessary complexity so the replacement of the unusual betaine species with 2-cyanothioacetamide for the Michael addition was investigated. Due to the unstable nature of **86** in air, subsequent reactions were performed under an atmosphere of nitrogen. Purification difficulties were overcome by reacting the crude intermediate directly in the alkylation step, with an excess of sodium methoxide to give **89**. *tert*-Butyl 2-(2-bromoacetamido)acetate, **88** was synthesised *via* an efficient one-step procedure, in excellent yield (96%), (Scheme **8**). This improved method (Scheme **9**) led to the isolation of **89** in 54% yield over 2 steps, and the product was easily purified by column chromatography. Deprotection of the *tert*-butyl ester with neat TFA gave acid **68** in near quantitative yield (99%). This methodology was used for the synthesis of all subsequent 3-cyanopyridine compounds.

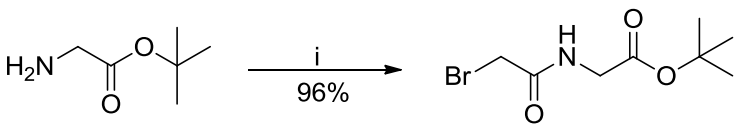

87 **88**

Scheme 8: Synthesis of *tert*-butyl 2-(2-bromoacetamido)acetate, **88**. *Reagents and Conditions;* i) bromoacetyl chloride, Et_3N, DMAP, DCM, 0 ^oC-RT, 3 h.

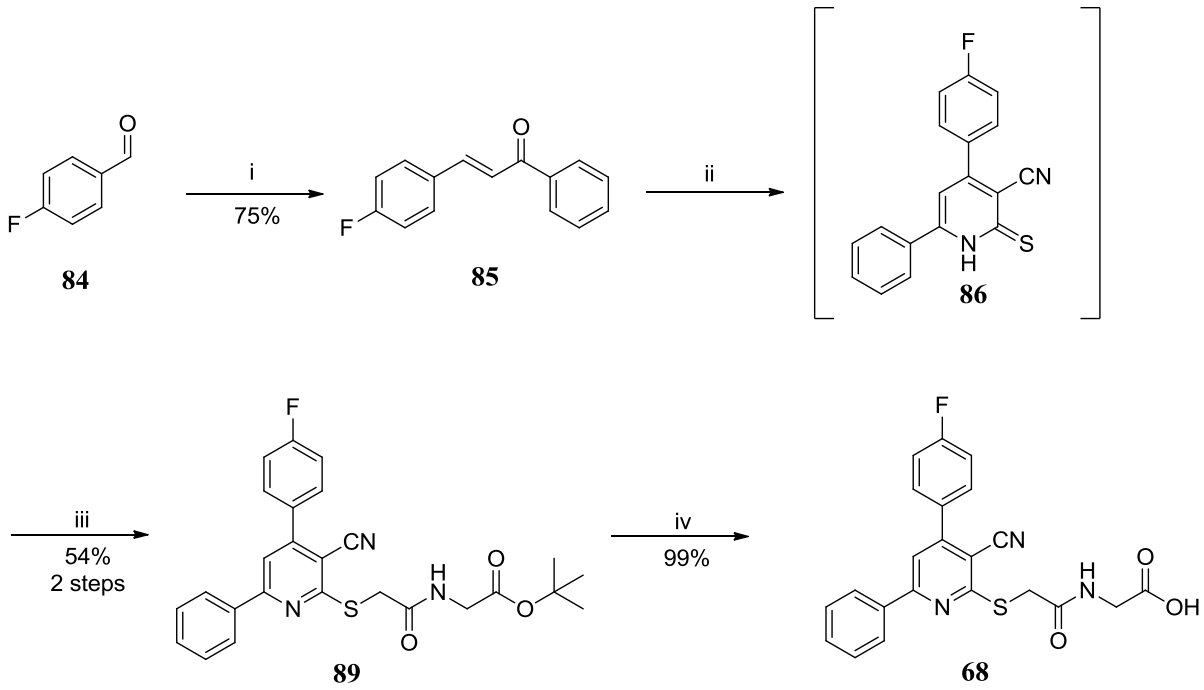

Scheme 9: Optimised synthesis of **68**: *Reagents and Conditions;* i) acetophenone, NaOH, EtOH, RT, 16 h; ii) 2-cyanothioacetamide, 1.6M sodium methoxide solution, 80 ^{o}C, 1.5 h; iii) *tert*-butyl 2-(2-bromoacetamido)acetate, DMF, 100 ^{o}C, 3-4 h; iv) TFA, RT, 30 min.

5.4.2 Isosteric Replacement of the Carboxylic Acid

The most potent compound identified from HTS (**68**) contains a carboxylic acid moiety at the terminus of the thioether side-chain. Replacement of this group was thought to be desirable due to the association of carboxylic acids with poor cell permeability. Extension of Scheme **9** with two further reactions allowed isosteric replacement with an amide (to investigate its importance) (Scheme **10**). Coupling of *p*-methoxybenzylamine in the presence of HBTU gave amide **90** in a moderate yield of 47%. This intermediate was also sent for biological evaluation. Subsequent cleavage of the PMB group was achieved using neat TFA. Reaction monitoring by LCMS indicated a slow conversion to the desired primary amide, with a reaction time of 48 h necessary to reach completion, giving primary amide **69** in 52% yield (unoptimised).

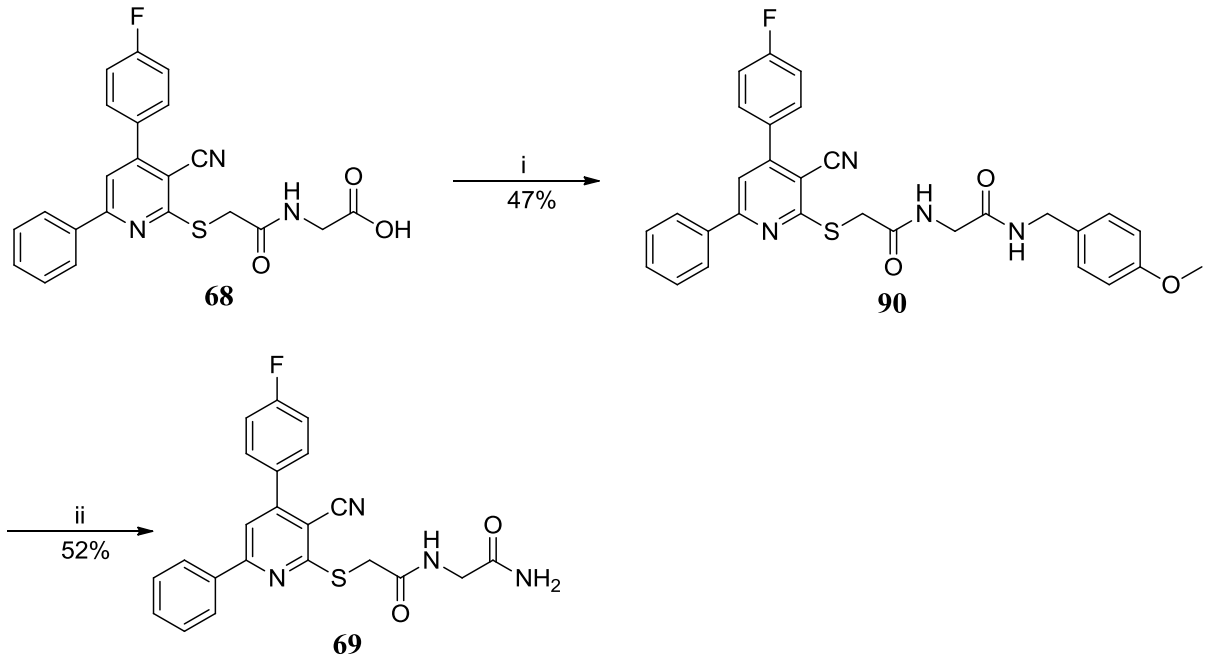

Scheme 10: Synthesis of *N*-(2-amino-2-oxoethyl)-2-((4-(4-fluorophenyl)-6-phenylpyridin-2-yl)thio)acetamide, **69**: *Reagents and Conditions;* i) *p*-methoxybenzylamine, HBTU, DIPEA, DMF, 60 ^{o}C, 4.5 h; ii) TFA, 70 ^{o}C, 48 h.

5.4.3 Modification to the Secondary Amine

The amide group provides one potential hydrogen bond donor and one acceptor. Systematic removal of one or both of these motifs was performed in order to establish which (if any) were involved in key interactions with the binding site of the enzyme. Synthesis of a suitable side-chain containing a secondary amine proved to be challenging (Scheme **11**).

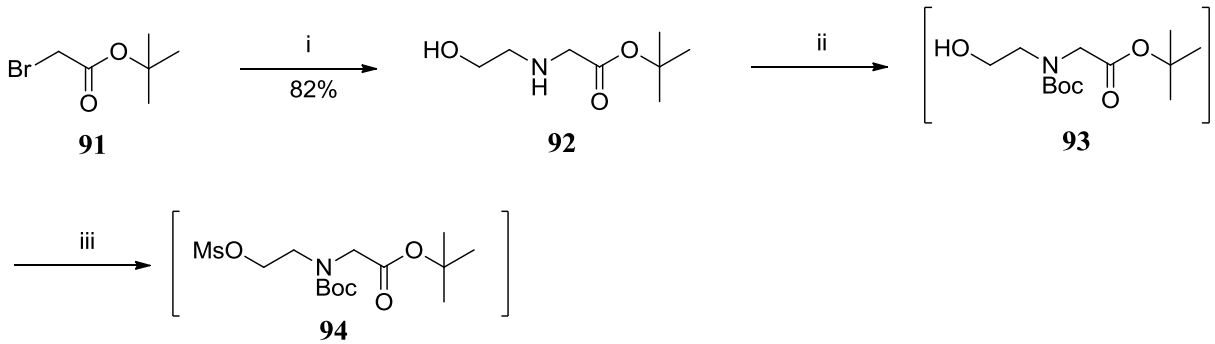

Scheme 11: Synthesis of *tert*-butyl 2-((*tert*-butoxycarbonyl)(2-((methylsulfonyl)oxy)ethyl)amino)acetate, **94**. *Reagents and Conditions;* i) ethanolamine, RT, 72 h; ii) Boc_2O, Et_3N, DMAP, DCM, RT, 3 h; iii) MsCl, Et_3N, DCM, 0 ^{o}C-RT, 16 h.

S_N2 substitution of ethanolamine with *tert*-butyl 2-bromoacetate gave alcohol **92** in good yield (82%). Boc protection of the resulting secondary amine, followed by mesylation gave mesylate **94** which was used immediately in the subsequent alkylation with **86** (Scheme **12**). Purification of intermediates **93** and **94** was not performed, due to concerns of intramolecular lactonisation, or polymerisation. As intermediates **93** and **94** both contain a lone pair on their respective alcohol and mesylate groups, it was suggested that attack of the lone pair on the carbonyl moieties present in the Boc and *tert*-butyl ester groups may be possible.

Substitutions of the 3-cyanopyridine scaffold with *tert*-butyl 5-bromopentanoate and *tert*-butyl 4-bromobutanoate proceeded in moderate yields of 34 and 58% over two steps respectively but comparable to that of *tert*-butyl 2-(2-bromoacetamido)acetate (54% over two steps). However, the reaction with *tert*-butyl 2-((tert-butoxycarbonyl)(2-((methylsulfonyl)oxy)ethyl)amino)acetate afforded **97** in low yield of 12% over 3 steps. Deprotection gave products **70**, **71** and **72** in 54-91%.

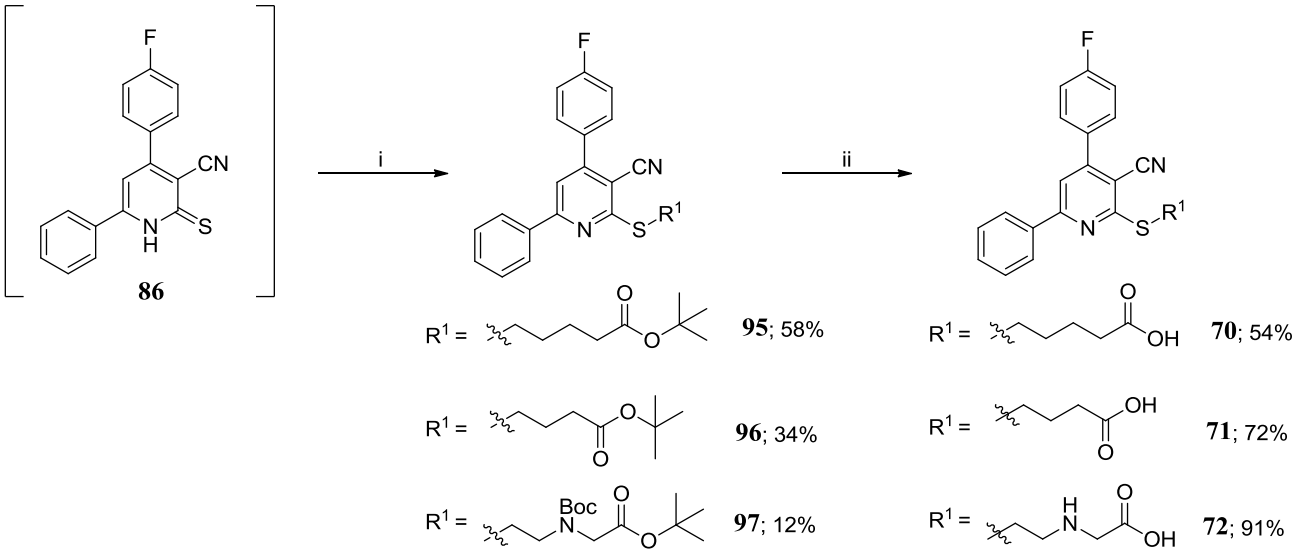

Scheme 12: S_N2 substitution and subsequent deprotection of 3-cyanopyridine side-chains. *Reagents and conditions;* i) relevant bromoalkyl/acetyl species, DMF, 100 ^oC, 3-4 h; ii) TFA, RT, 30 min.

5.4.4 ERK5 Inhibitory Activity of Thioether Analogues

Biological results from the IMAP™ assay for compounds synthesised in this series are shown in Table **11**. Results are expressed as IC_{50} values and as % inhibition at 120 µM. However, it was observed that during the assay, a number of the compounds were insoluble at higher concentrations (indicated in Table **11**) and therefore results for these compounds cannot be considered accurate.

All changes to the thioether side-chain resulted in loss of potency, giving compounds with IC_{50} values greater than 120 µM. Interestingly, the primary amide **69** is much less active than its carboxylic acid and methyl ketone counterparts. Conservation of the peptidic features of the side-chain appears to be crucial, as removal of the carbonyl or amide (compounds **70**, **71** and **72**) appears to abolish activity.

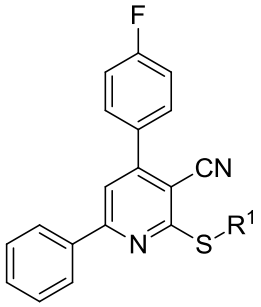

Table 11: SARs for compounds with variation at R^1. NB: Insoluble = Compound precipitated at 1.2 mM in 40% DMSO

Compound	R^1	IC_{50} (µM)[a]	% Inhibition @ 120 µM[a]	Solubility
68	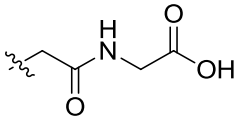	4.9 ± 0.3	89 ± 5.8	
67	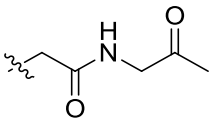	20.5 ± 1.3	72.6 ± 0.2	
90	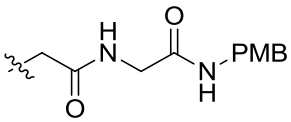	>120	23.6 ± 4.0	Insoluble
69	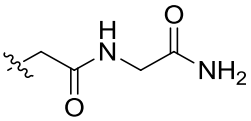	>120	37.6 ± 7.5	

70	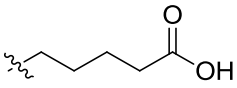	>120	49.0 ± 1.0	Insoluble
71	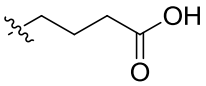	>120	40.8 ± 5.6	Insoluble
72	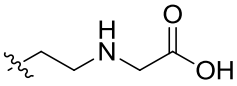	>120	32.8 ± 1.6	

[a] Determinations ± standard deviation (mean of n = 2 unless otherwise stated)

5.5 Modification to the R^2 Aryl Substituent

Both of the hit compounds identified from HTS contained a 4-fluorophenyl group in the R^2 position of the 3-cyanopyridine core. SAR studies were initiated to investigate the importance of this moiety and expand the diversity at this position.

5.5.1 Synthesis of Carboxylic Acid Derivatives

A small library of compounds was prepared using the optimised synthetic route described in Section **5.4.1**, *via* Michael addition of the relevant chalcone with 2-cyanothioacetamide, followed by cyclisation, then alkylation of the resulting thione. Preliminary SAR conducted by Dr Betty Cottyn had revealed that removal of the fluorine atom abolished activity. Hence, replacement with other electron withdrawing groups, and modification to the position of the fluorine atom was explored.

Aldol condensations gave moderate to good yields, with the exception of 4-pyridine carboxaldehyde (10% yield). In this case, synthesis of the relevant chalcone, **106** was achieved *via* a Wittig reaction, using (benzoylmethylene)triphenylphosphorane which gave (*E*)-1-phenyl-3-(pyridin-4-yl)prop-2-en-1-one in an improved yield of 78% (Scheme **13**). Tandem Michael addition/cyclisation and S_N2 substitution reactions all proceeded to give the desired products in variable yield (20-54%; Table **12**).

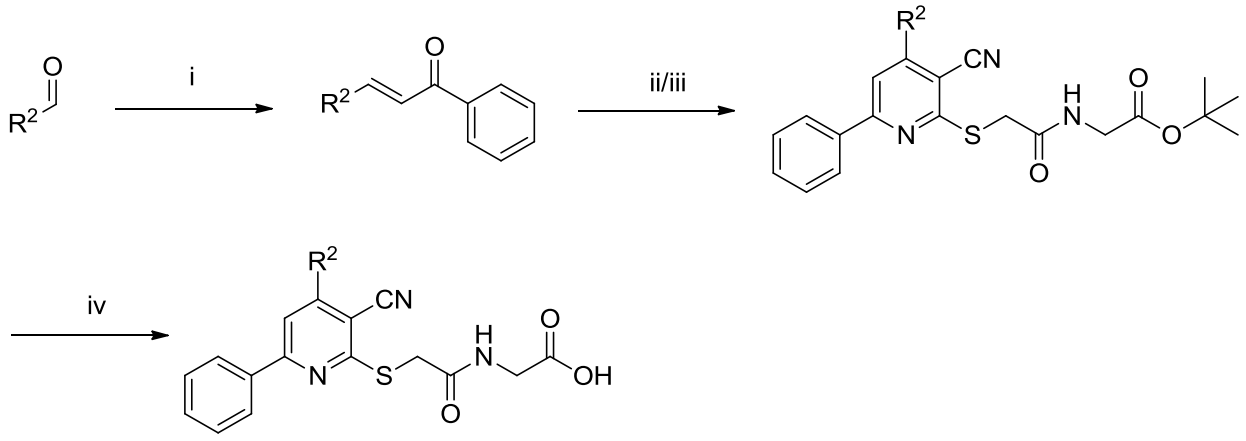

Table 12: Synthesis summary for compounds with variation at R^2. Reagents and conditions are as shown in Scheme **9**, page **77** .

R^2	Aldol Condensation Yield, i (%)	Cyclisation/S_N2 Substitution Yield, ii/iii (%)	Deprotection Yield, iv (%)
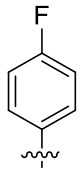	**85**; 75	**89**; 54	**68**; 99
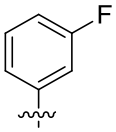	**98**; 64	**99**; 46	**73**; 100
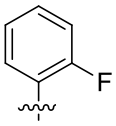	**100**; 56	**101**; 20	**74**; 99
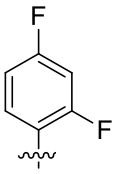	**102**; 80	**103**; 41	**75**; 100
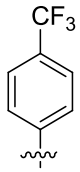	**104**; 73	**105**; 28	**76**; 90
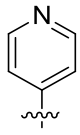	**106**; 10	-	-

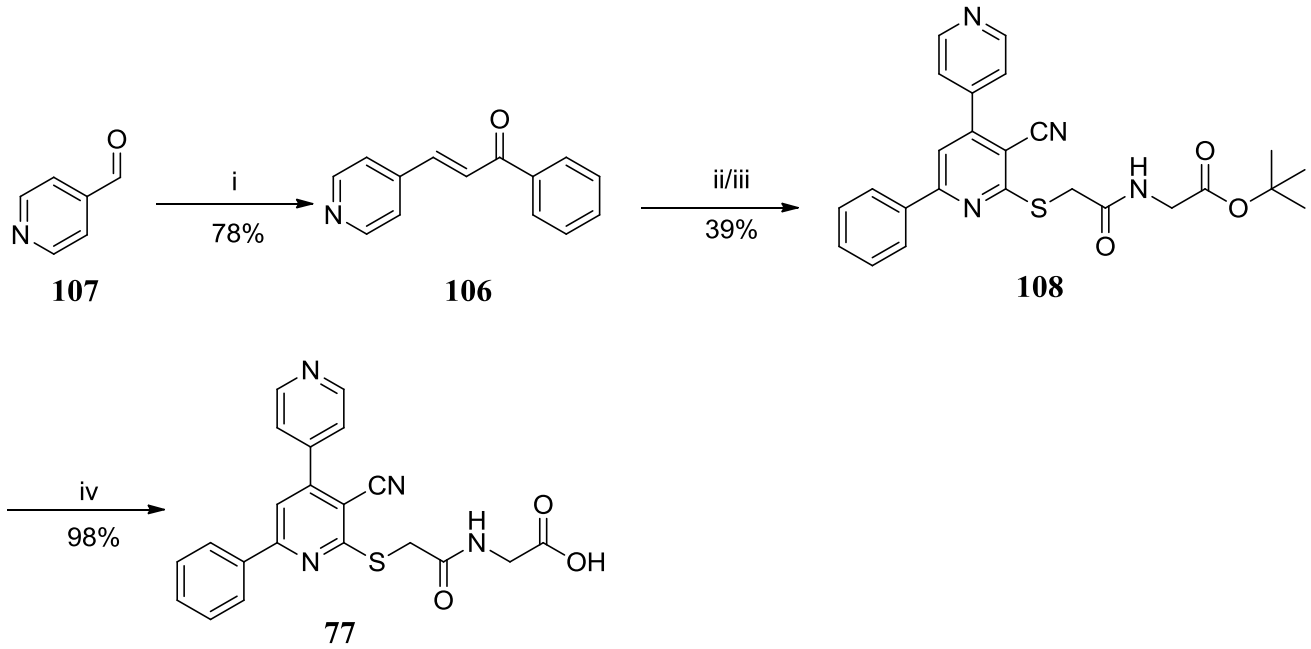

Scheme 13: Synthesis of (*E*)-1-phenyl-3-(pyridin-4-yl)prop-2-en-1-one, **77**. *Reagents and Conditions;* i) (benzoylmethylene)triphenylphosphorane, toluene, 110 ^{o}C, 3 h; ii) 2-cyanothioacetamide, 1.6M sodium methoxide solution, 80 ^{o}C, 1.5 h; iii) *tert*-butyl 2-(2-bromoacetamido)acetate, DMF, 100 ^{o}C, 3-4 h; iv) TFA, RT, 30 min.

5.5.2 Synthesis of Methyl Ketone Derivatives

Incorporation of the methyl ketone side-chain was performed on selected 3-cyanopyridine scaffolds for direct comparison with the carboxylic acid based compounds. 2-Bromo-*N*-(2-oxopropyl)acetamide, **113** was synthesised *via* conversion of 2-((tert-butoxycarbonyl)amino)acetic acid, **109** to the corresponding Weinreb amide **110**, followed by reaction with methyl magnesium bromidegiving methyl ketone **111**. Hydrolysis of the carbamate gave intermediate **112**, which was reacted directly as the hydrochloride salt with bromoacetyl chloride (Scheme **14**). Subsequent alkylations with 2-bromo-*N*-(2-oxopropyl)acetamide **113** are summarised in Table **13**.

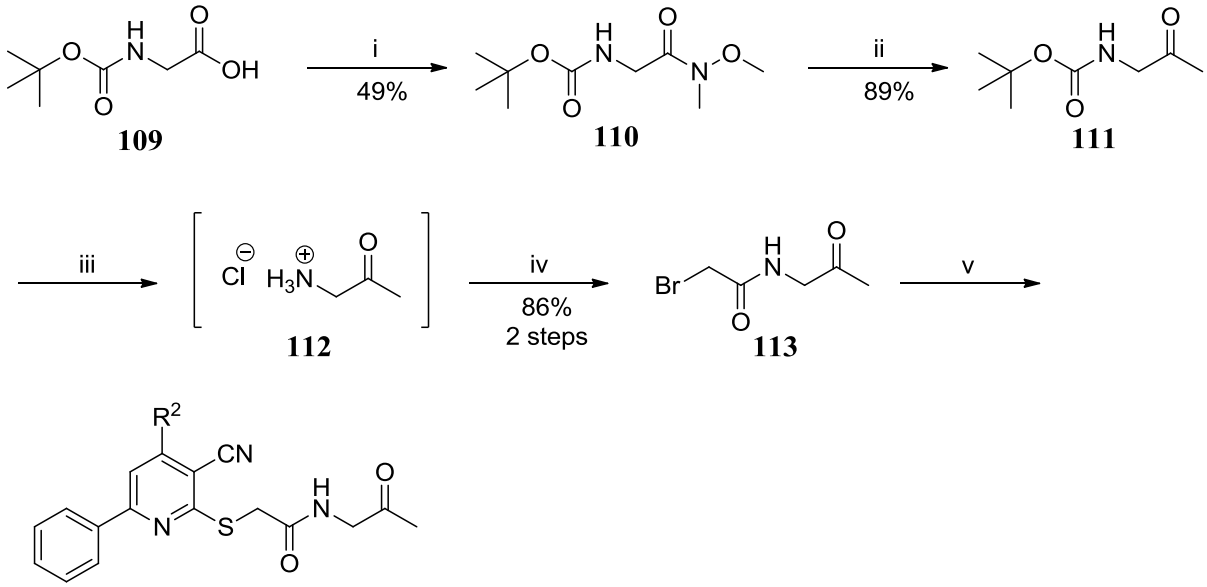

Scheme 14: Synthesis of 2-bromo-*N*-(2-oxopropyl)acetamide, **113,** and subsequent coupling. *Reagents and Conditions;* i) CDI, THF, 70 ^{o}C, 3 h then *N*,*O*-dimethylhydroxylamine hydrochloride, Et_3N, 50 ^{o}C, 3 h; ii) MeMgCl THF, 0 ^{o}C-RT, 16 h; iii) 4M HCl in dioxane, RT, 12 h; iv) bromoacetyl chloride, Et_3N, DMAP, DCM, RT, 12 h, v) Relevant R^2 substituted pyridine-thione (crude mixture), DMF, 100 ^{o}C, 3-4 h.

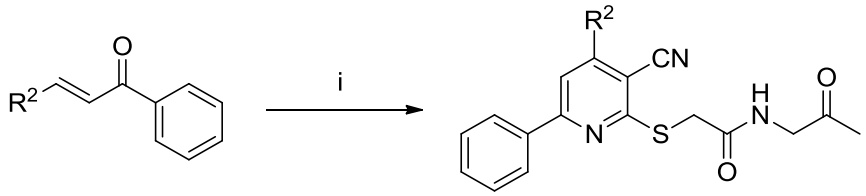

Table 13: Synthesis summary for compounds with variation at R^2

Compound	R^2	Cyclisation/S_N2 Substitution Yield, i (%)
67	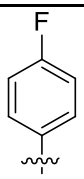	36
114	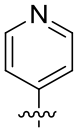	78

5.5.3 Investigation of SAR for the Replacement of the 4- and 6- Aromatic Rings

Substitution of 2-mercapto-4,6-dimethylnicotinonitrile **115** with *tert*-butyl 2-(2-bromoacetamido)acetate using KOH as the base proceeded in a typical yield of 52% and deprotection was quantitative. The corresponding reaction with 2-bromo-*N*-(2-oxopropyl)acetamide, **113** gave 2-((3-cyano-4,6-dimethylpyridin-2-yl)thio)-*N*-(2-oxopropyl)acetamide, **117** in 79%.

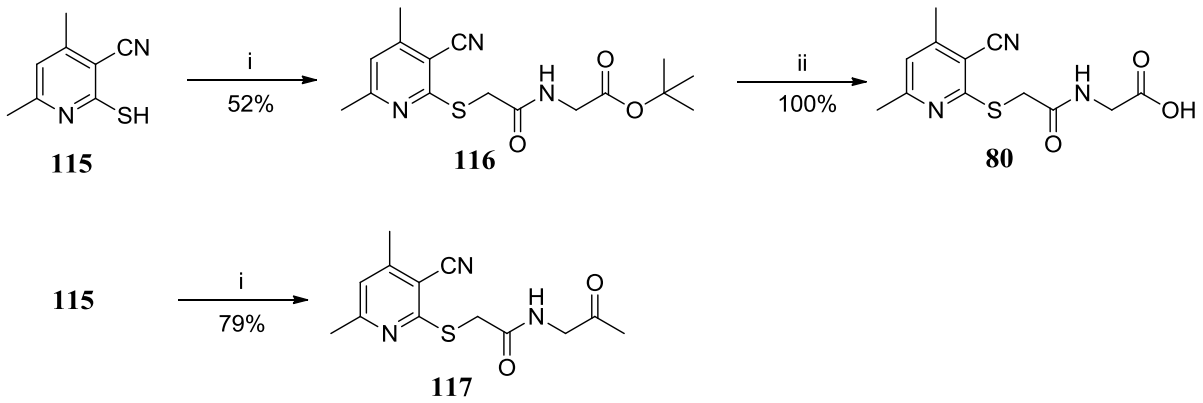

Scheme 15: Synthesis of **80** and **117**. *Reagents and Conditions;* i) relevant bromoacetyl side-chain **113 or 88**, KOH, DMF, 100 ^{o}C, 3 h; ii) TFA, RT, 30 min.

5.5.4 ERK5 Inhibitory Activity of Carboxylic Acid Analogues

Repositioning the fluorine atom to the 3-position of the aryl ring abolished activity. Interestingly, the 2-fluorophenyl analogue showed moderate activity with an IC_{50} value of 34.3 µM (and 100% inhibition of the enzyme at 120 µM). This compound was effective only at concentrations above 10 µM, but inhibitory activity greatly increased above this concentration. At 120 µM, compound **74** is more potent than the initial hit **68**, but has a lower overall IC_{50}. Combining both fluorine atoms in the 2- and 4- positions does not show an additive (or synergistic) effect. Difluoro compound **75** was found to be less active (ERK5 IC_{50} = 73 µM) than both mono-fluorinated analogues. However, this compound suffered from poor solubility in the assay which may have contributed to lower observed activity. Replacement of the 4-fluoro group with a 4-CF_3 moiety, **76** also led to a reduction in potency. The 4-pyridyl derivative, **77**, was also less potent compared to the parent, **68**. Removal of the aryl groups abolished activity, confirming the requirement for aromatic substituents in the 4- and 6-positions of the 3-cyanopyridine scaffold.

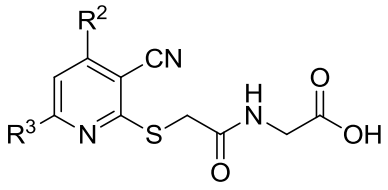

Table 14: ERK5 inhibitory activity for carboxylic acid analogues

Compound	R^2	R^3	IC_{50} (μM)[a]	% Inhibition @ 120 μM[a]	Solubility[b]
68	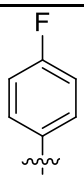	Ph	4.9 ± 0.3	89 ± 5.8	
73	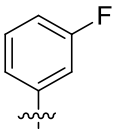	Ph	>120	25.4 ± 2.9	
74	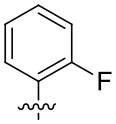	Ph	34.3 ± 6.4	102.1 ± 1.6	
75	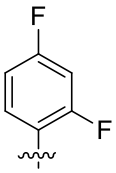	Ph	72.9 ± 26.1	66.9 ± 9.3	Insoluble
76	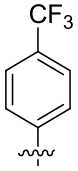	Ph	>120	50.1 ± 15.0	
77	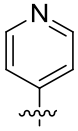	Ph	65.1 ± 12.4	81.7 ± 4.4	
80	Me	Me	>120	14.0 ± 3.8	

[a] Determinations ± standard deviation (mean of n = 2 unless otherwise stated) [b] NB: Insoluble = Compound precipitated at 1.2 mM in 40% DMSO

5.5.5 ERK5 Inhibitory Activity of Methyl Ketone Analogues

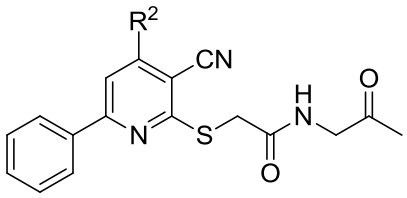

Table 15: ERK5 inhibitory activity of methyl ketone analogues

Compound	R^2	R^3	IC_{50} (µM)[a]	% Inhibition @ 120 µM[a]
67	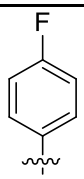	Ph	20.5 ± 1.3	72.6 ± 0.2
114	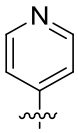	Ph	104.9 ± 6.5	76.1 ± 5.2
117	Me	Me	>120	6.0 ± 1.6

[a] Determinations ± standard deviation (mean of n = 2 unless otherwise stated)

A 4-fold loss in activity was observed between the parent methyl ketone, **67** and the 4-pyridyl and dimethylated derivatives.

5.6 Isosteric Replacement of the 3-Cyano Motif

Previous work had shown that removal of the 3-cyano moiety had a detrimental effect on activity, e.g pyridine **81** showed weak ERK5 inhibition (50% at 120 µM). Replacement of the nitrile with a bromine atom as a steric isostere was performed. It was initially envisaged that the incorporation of a halogen at the 3-position would also allow Sonogashira coupling to introduce an alkyne as a classical isostere if desired.

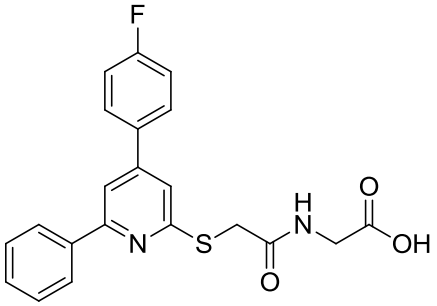

81; ERK5 IC_{50} >120 µM; % Inhibition = 50.4% ± 1.2 @ 120 µM

5.6.1 Synthesis of 3-Bromo and 3-Alkynyl Analogues

Following a similar procedure to the synthesis of 4-(4-fluorophenyl)-6-phenylpyridine-2(1*H*)-thione, **86**, 4-(4-fluorophenyl)-6-phenylpyridin-2(1*H*)-one, **118** was isolated in 34% (Scheme **16**). Bromination of the 3-position of the pyridine was achieved selectively using *N*-bromosuccinamide in acetic acid. Selectivity for bromination of the 3-position was confirmed by a combination of COSY and NOESY NMR experiments of intermediates **118** and **119**. The C(3)-H may only show interaction with one aromatic proton through space in the NOESY spectrum. When the 3-position was brominated, peaks associated with the interaction between C(5)-H and protons present on two different aromatic rings were visible, thus confirming the selectivity for the 3-position. Conversion of the pyridone to pyridine-thione was performed successfully using Lawesson's reagent. Once again, rapid tautomerisation to the thiol form was observed by analysis of the crude mixture by ^{1}H NMR spectroscopy, and so the mixture was subjected to alkylation without further purification. Deprotection of the *tert*-butyl ester proved trivial and gave **82** in 93% yield.

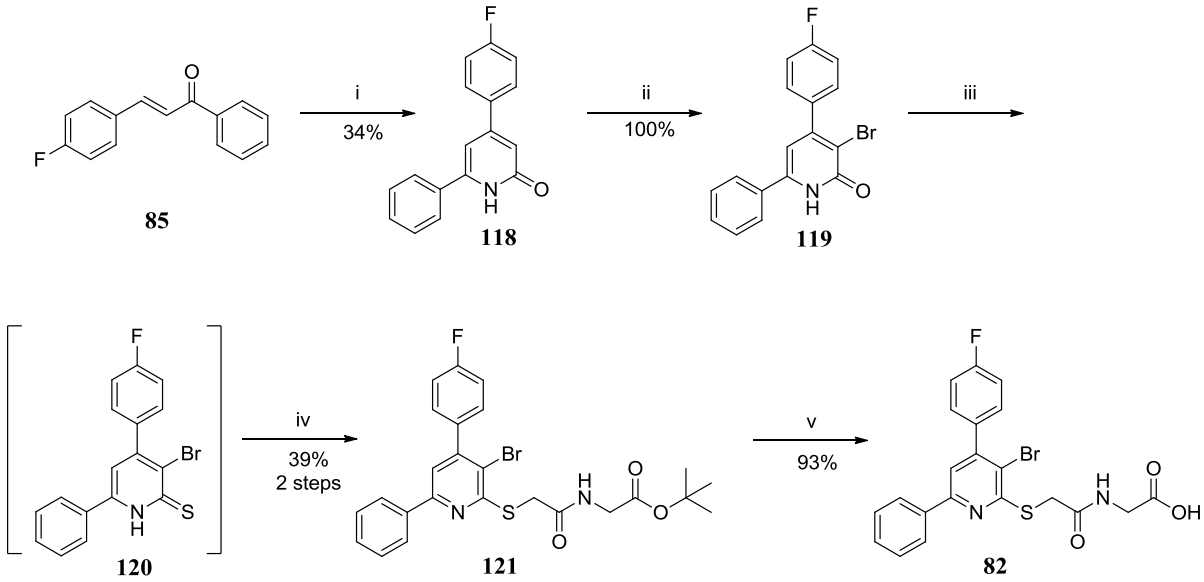

Scheme 16: Synthesis of 2-(2-((3-bromo-4-(4-fluorophenyl)-6-phenylpyridin-2-yl)thio)acetamido)acetic acid, **82**. *Reagents and Conditions;* i) acetamidoacetamide, Cs_2CO_3, DMF, 100 ^oC, 2.5 h; ii) NBS, AcOH, 60 ^oC, 5 h; iii) Lawesson's reagent, toluene, 100 ^oC, 20 h; iv) *tert*-butyl 2-(2-bromoacetamido)acetate, KOH, DMF, 100 ^oC, 4 h; v) TFA, RT, 30 min.

Sonogashira couplings were attempted using intermediate **119** as the bromoaryl species (Scheme **17**). Introduction of the alkyne at this stage would allow continuation of Scheme **16**, *via* conversion to the thione, alkylation of the sulphur and deprotection of the *tert*-butyl ester. Finally, deprotection of the silyl protecting group with TBAF would afford the final carboxylic acid product. Unfortunately, no conversion to the corresponding alkyne was observed. When microwave irradiation was used, reductive dehalogenation occurred (entries 3 and 4; Table **16**).

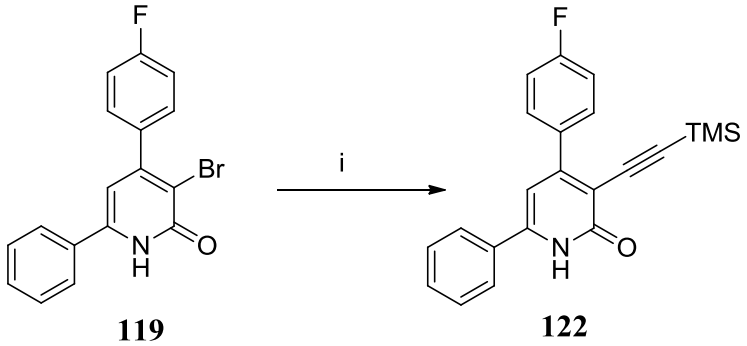

Scheme 17: *Reagents and Conditions;* i) TMS acetylene, $Pd(PPh_3)_2Cl_2$, CuI, Et_3N, THF, See conditions in Table **16**.

Table 16: Sonogashira coupling conditions attempted with intermediate **119**

Attempt	Temp (^{o}C)	Time (h)	Observation
1	RT	16	No conversion
2	80	16	No conversion
3	100 MW	1	No conversion; loss of bromine
4	150 MW	1	No conversion; loss of bromine

Synthesis of the corresponding 3-iodo analogue, **123** was performed to enhance reactivity in the Sonogashira coupling (Scheme **18**). Intermediate **118** was reacted with NIS in quantitative yield. Sonogashira couplings were subsequently attempted (Table **17**). Reaction monitoring by LCMS was used throughout the optimisation process. No conversion to the alkyne was observed with conventional heating, but microwave irradiation at temperatures of 100 ^{o}C and 120 ^{o}C resulted in 18-36% conversion with no reductive dehalogenation. TMS-alkyne **122** was not isolated during optimisation due to the small scale of the reactions undertaken. Further optimisation attempts were to focus on the modification to the catalyst employed, and reaction time at a fixed temperature of 120 ^{o}C (MW). Following optimisation, it was planned that TMS-alkyne **122** would be isolated, then scale-up to be performed. Unfortunately, SAR data indicated that all other structural modifications to the 3-cyanopyridine scaffold abolished activity. Due to the extensive optimisation required, synthesis of the 3-alkynyl analogue was postponed pending further results in this series.

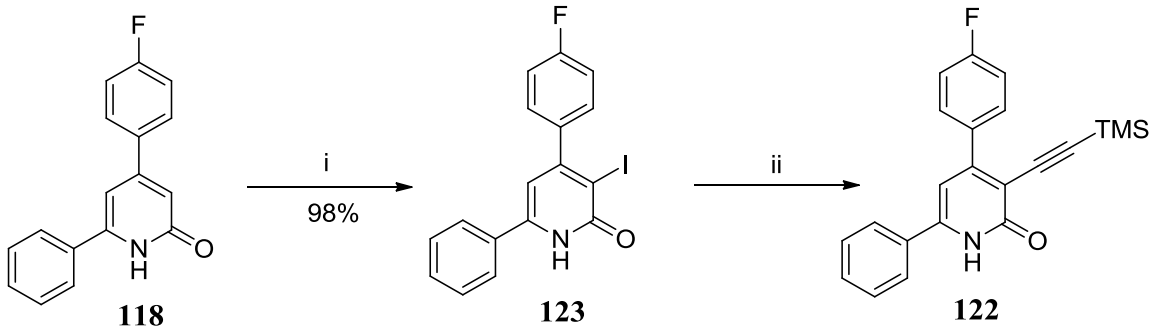

Scheme 18: *Reagents and Conditions;* i) NIS, AcOH, 60 ^{o}C, 5 h; ii) TMS acetylene, $Pd(PPh_3)_2Cl_2$, CuI, Et_3N, THF, See conditions in Table **17**.

Table 17: Sonogashira coupling conditions attempted with intermediate **123**

Attempt	Temp (^{o}C)	Time (h)	Observation
1	RT	16	No conversion
2	80	16	No conversion
3	100, MW	1	18% conversion by LCMS
4	150, MW	1	32% conversion by LCMS; majority –I (m/z 266)
5	120, MW	1	36% conversion by LCMS; No degredation

5.6.2 SAR for Cyano Group Replacement

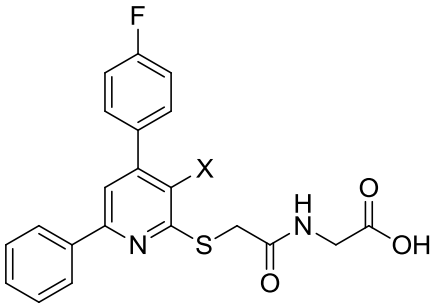

Table 18: NB: Insoluble = Compound precipitated at 1.2 mM in 40% DMSO

Compound	X	IC_{50} (µM)[a]	% Inhibition @ 120 µM[a]	Solubility
68	CN	4.9 ± 0.3	89 ± 5.8	
81	H	>120	50.4 ± 1.2	
82	Br	74.3 [b]	53.2 ± 14.5	Insoluble

[a] Determinations ± standard deviation (mean of n = 2 unless otherwise stated); [b] n = 1

Replacement of the cyano group with a bromine atom acting as a steric isostere did not confer any additional potency against ERK5 versus the parent compound. The brominated analogue was equipotent with compound **81**, suggesting that the nitrile is acting as a hydrogen bond acceptor. However, due to the increased lipophilicity of the brominated analogue (clogP = 5.3 vs 4.3 for X = CN), aqueous solubility of this compound under assay conditions was poor. As such, a definite conclusion regarding the role of the cyano moiety could not be reached.

5.7 Conclusion

Hit validation was performed for two 3-cyanopyridines (**67** and **68**). The resynthesised compounds showed a significant decrease in potency following resynthesis, but with acceptable variation. Structural modifications focussing around components of the thioether side-chain, the R^2-aryl substituent and the 3-cyano moiety were performed. Structure-activity relationships showed that the original hits remained the most potent inhibitors to date (i.e. **68**, ERK5 IC_{50} = 4.9 μM). Many of the compounds synthesised displayed poor solubility in the IMAP™ assay, rendering biological data for such compounds inaccurate. As a result of the limited SARs and poor solubility, further work on this series was discontinued.

Chapter 6: The Pyrrole-Carboxamide series

6.1 Synthetic Strategies Towards Pyrroles

There are several reported synthetic routes towards substituted pyrrole-based compounds. Due the presence of the pyrrole motif in numerous bioactive natural products (e.g. Lamellarin O, **124** and Lukianol A, **125**; effective cytotoxic agents in leukaemia and lymphoma screens)[109] pyrroles are an attractive target for synthetic research. Three classical methods are described herein; the Knorr and Paal-Knorr syntheses, and the Hantzsch pyrrole synthesis.

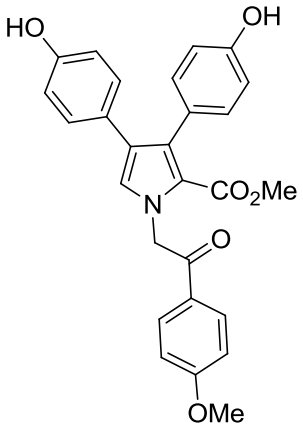

Lamellarin O, **124**

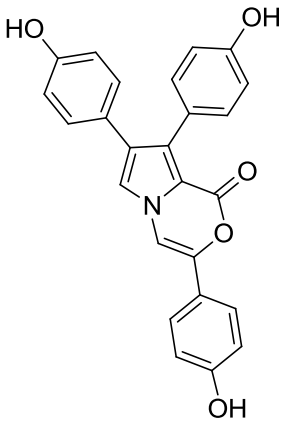

Lukianol A, **125**

6.1.1 Knorr Pyrrole Synthesis

In 1884, Knorr published his synthetic route towards pyrrole-3-carboxylate.[110] An α-aminoketone is reacted with a β-ketoester in the presence of catalytic zinc and acetic acid. Tandem condensation of the amine with the β-ketoester followed by an intramolecular aldol-type condensation gives the desired pyrrole product. Because α-aminoketones readily self-condense, this species is usually prepared *in situ* from the relevant oxime.

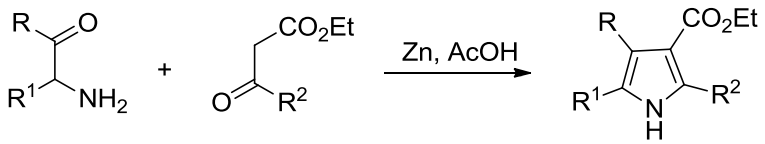

126 **127** **128**

Scheme 19: Knorr Pyrrole Synthesis.

6.1.2 Paal-Knorr Pyrrole Synthesis

One year later (1885), the Paal-Knorr synthesis was simultaneously published by the two chemists.[111] Despite widespread use of the Paal-Knorr method, the mechanism was not fully elucidated until 1991 (Amarnath *et al*).[112] Mechanistic studies revealed that cyclisation proceeds *via* a hemiaminal intermediate, as opposed to an enamine, or imine intermediate. The reaction may be conducted under neutral or slightly acidic conditions with an excess of the amine. However, care must be taken as excessively acidic reaction conditions (below pH 3) result in formation of the corresponding furan.

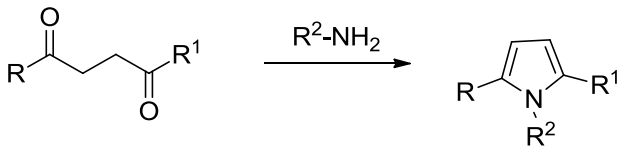

129 **130**

Scheme 20: Paal-Knorr Pyrrole Synthesis.

6.1.3 Hantzsch Pyrrole Synthesis

The multicomponent Hantzsch synthesis was described a few years later (1890). Not unlike the Knorr synthesis, a β-ketoester is reacted with an amine (in this case ammonia). The resulting enamine then reacts with an α-haloketone, followed by cyclisation to give the product (Scheme **21**). Historically, this reaction has not been as widely used, due to reported low yields associated with furan by-products. Solid-phase syntheses have recently been developed to improve yields, which utilise acetoacetylated Rink resin, with the relevant α-haloketone and amine (Scheme **22**) under mild conditions. Hydrolysis of the resin is achieved *via* acid hydrolysis.[113]

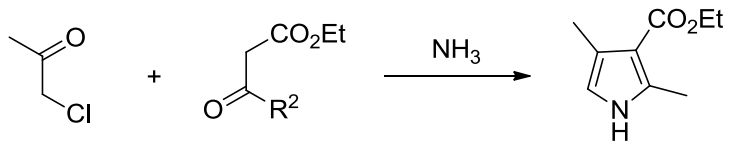

131 **127** **132**

Scheme 21: Hantzsch pyrrole synthesis.

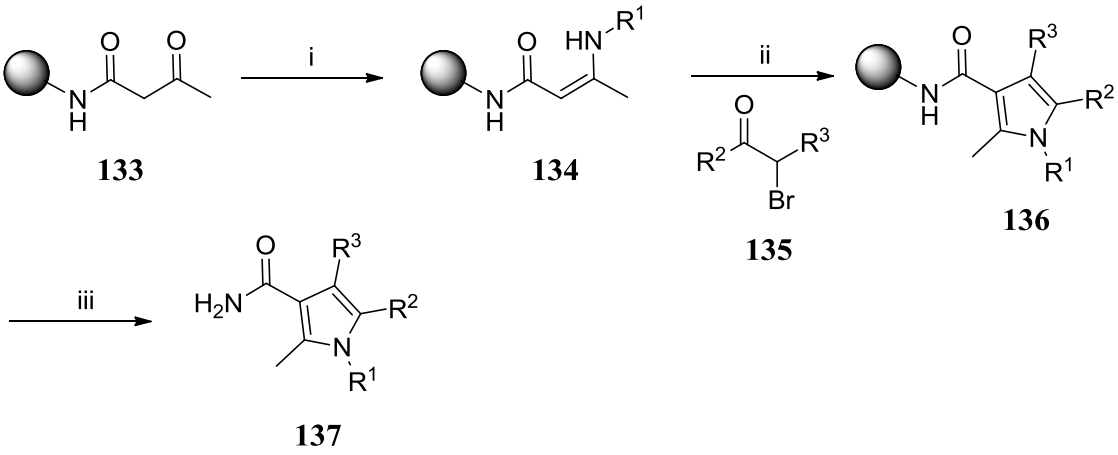

Scheme 22: Hantzsch pyrrole synthesis on solid support.[113] *Reagents and Conditions;* i) R^1NH_2, trimethylorthoformate, DMF, RT, 48 h; ii) 2, 6-di-*tert*-butylpyridine, DMF, RT, 17 h; iii) 20% TFA/DCM, RT, 30 min.

6.2 Pyrrole-Carboxamides Identified from HTS

HTS identified seventeen compounds which fit into the pyrrole-carboxamide class. Of this seventeen, seven were shown to inhibit ERK5 at <10 μM. Validation by resynthesis was performed for four of the most potent hits (Table **19**).

Two of the four hits were shown to be inactive against ERK5 (**139**, **140**; >120 μM), and compound **141** was 10-fold less active. However, the most potent hit identified (**138**) was validated as an inhibitor of ERK5 in the low micromolar range (IC_{50} = 3.7 ± 0.8 μM). SAR studies were initiated following this result.

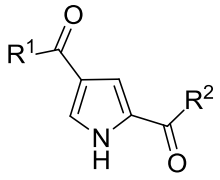

Table 19: IC_{50} values for resynthesised hit compounds

Compound	R^1	R^2	IC_{50} HTS (µM)	IC_{50} Resynthesised (µM)[a]
138	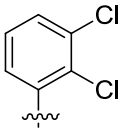	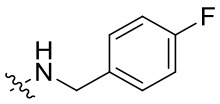	0.7	3.7 ± 0.8
139	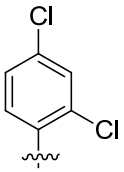		1.9	>120
140	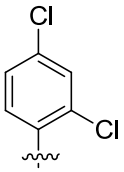	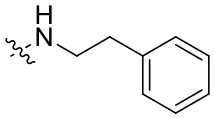	3.5	>120
141	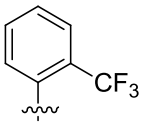		4.3	42.0 ± 3.4

[a] Determinations ± standard deviation (mean of n = 2).

6.3 Existing SAR Around the Pyrrole-Carboxamide Scaffold

Preliminary SAR data was generated by Dr Sandrine Vidot and Dr Ruth Bawn. Modification to the aroyl ring demonstrated that incorporation of a substituent in the *para*-position was not tolerated (**147**, Table **20**). Dihalogenation (2,3-dichloro or 2,6-difluoro) conferred the best potency. *N*-Methylation of the heterocycle abolished activity (ERK5 >120 µM), indicating that the pyrrole NH is acting as a hydrogen bond donor. *N*-Methylation of the carboxamide motif was tolerated, but activity was 5-fold lower than the non-methylated counterpart (**145** versus **146**, Table **20**). Removal of the ketone or reduction to the corresponding secondary alcohol also resulted in loss of activity (ERK5 >120 µM), suggesting presence of a hydrogen bond acceptor in this position is crucial. Finally, 3- and 4-pyridyl substituents were found to

be equipotent with the 4-fluorophenyl moiety present in the carboxamide side-chain of hit compound **138**.

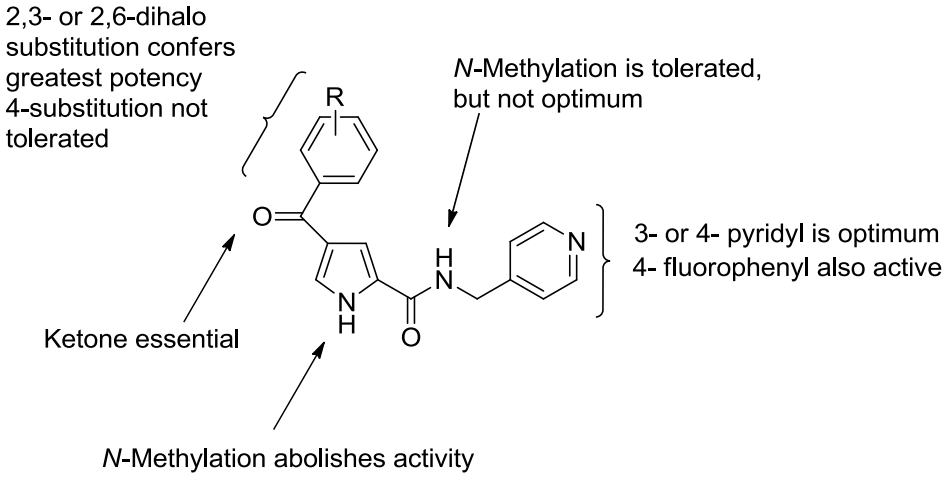

Figure 28: SARs for the pyrrole-carboxamide series

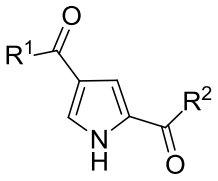

Table 20: Preliminary SAR data around the pyrrole-carboxamide core

Compound	R^1	R^2	IC_{50} (μM)[a]
138	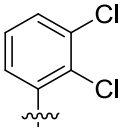	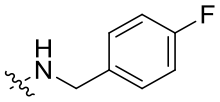	3.7 ± 0.8
142	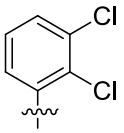	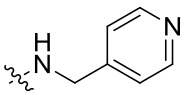	2.0 ± 2.0
143	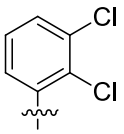	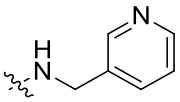	3.8 ± 3.7
144	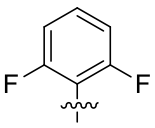	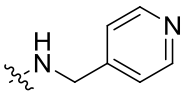	2.3 ± 0.1

145	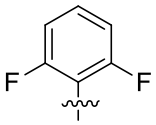	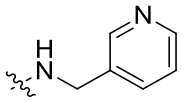	1.8 ± 0.6
146	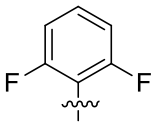	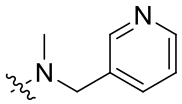	9.0 ± 0.2
147	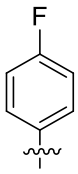	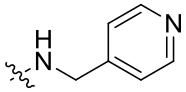	>120

[a] Determinations ± standard deviation (n =2)

6.4 Hit-to-Lead Development Criteria

Following successful hit validation and the establishment of clear preliminary SAR, hit-to-lead studies aimed to develop compounds with improved potency, desirable physicochemical and *in vitro* ADMET properties and finally, *in vivo* efficacy and a suitable DMPK profile. Target parameters identified for a lead compound are shown in Table **21**. These criteria were utilised throughout the hit-to-lead phase. The primary objective following hit validation was to improve ERK5 inhibitory activity (with a target IC_{50} of less than 1 μM), while maintaining drug-like physicochemical properties. Physicochemical property criteria were set according to Lipinski's rule of five; discussed in more detail in Section **6.7.7.1**. Ligand efficiency (LE) was used as a measurement of overall binding energy per heavy atom, with a value greater than 0.3 for LE indicating a high efficiency. Selectivity versus a panel of 131 diverse protein kinases was performed at the International Centre for Kinase Profiling, and routine counter-screening against the closest homologue of ERK5, p38α performed at CRT. An initial target of 10-fold selectivity against all other protein kinases was desirable, in order to attribute efficacious effects observed in subsequent *in vitro* and *in vivo* studies to ERK5, ruling out any off-target effects. In addition, cellular activity was measured for compounds displaying superior *in vitro* activity (<1 μM). The dual luciferase reporter gene assay is described in further detail in Section **7.8**, and is a measure of the ability of the compound to cross cell membranes in a HEK293 (human embryonic kidney) cell-line, and cellular ERK5 inhibition. An initial cellular IC_{50} below 10 μM was deemed an acceptable level of permeation dependent activity. Undesirable inhibitory effects of CYP isoforms and hERG were also monitored, aiming for greater than 10 and 25 μM inhibitory concentrations, respectively, to maximise the elimination of drug-drug interaction and cardiotoxicity liability. A high free

fraction (<99% in PPB assays), low microsomal clearance in human and mouse liver microsomes (<48 µL/min/mg), high aqueous solubility (> 50 µM) and a low efflux ratio in the Caco-2 assay (<2) were prioritised to achieve the best chance of good oral bioavailability, and an acceptable half-life *in vivo*. At this stage, research was guided using homology modelling due to the lack of a protein crystal structure of ERK5.

Table 21: Target criteria for development of a lead compound

Category	Criteria	Lead Compound
Physicochemical properties	Modelling/Crystal Structure	Required
	Molecular weight (MW)	<500
	sLogP	<5
	TPSA	75-100
	H bond donors/acceptors	<5/<10
	PKa	Salt forming
***In Vitro* pharmacology**	ERK5 IC_{50} (µM)	< 1
	LE	>0.3
	Selectivity (over other kinases)	>10 fold
	Cellular ERK5 IC_{50} (µM)	<10
	hERG IC_{50} (µM)	>25
***In Vitro* ADME**	Solubility (µM)	>50
	PPB (%)	<99
	Mouse liver microsomal (MLM) Clearance (µL/min/mg)	<48
	Human liver microsomal (HLM) Clearance (µL/min/mg)	<48
	Caco-2 A2B Papp ($x10^{-6}$ cm/s)	>10
	Efflux Ratio	<2
	CYP1A, CYP2C19, CYP2C9, CYP2D6, CYP3A4 IC_{50} (µM)	All >10
***In Vivo* DMPK and Efficacy**	Clearance (mL/mg/kg)	<30
	Vdss (L/kg)	>1
	Bioavailability (F) (%)	>30
	$t_{1/2}$ Mouse (h)	>1
	$t_{1/2}$ Human (h)	>1
	Biomarker modulation	Required
	Xenograft efficacy	Required

6.5 Structure-Guided Drug Design

Modern drug discovery and optimisation efforts, particularly in the area of kinase inhibitors, have largely relied on crystallographic methods to aid in the design of novel compounds.[114] As a crystal structure was not available for use in structure-guided drug design, the homology model was developed by Dr Susan Boyd of CompChem Solutions, on behalf of CRT. BLAST (Basic Local Alignment Search Tool) searching identified ERK2 as the closest homologue of ERK5, with 51% and 78% sequence identity in the kinase domain and active site regions respectively. Therefore, the original homology model was based on ERK2 (Figure **29**). Three key active site differences between ERK2 and ERK5 were identified as follows: Ile103 (ERK2)/Val134 (ERK5), Gln105 (ERK2)/Leu136 (ERK5) and Cys164 (ERK2)/Gly198 (ERK5). Fus-3, a non-mammalian protein, was identified as the second BLAST hit, followed by p38α which has a 56% sequence identity with the ERK5 binding site. The highly conserved protein structure amongst the MAPK family was considered to be a challenge for the design of selective ERK5 inhibitors.

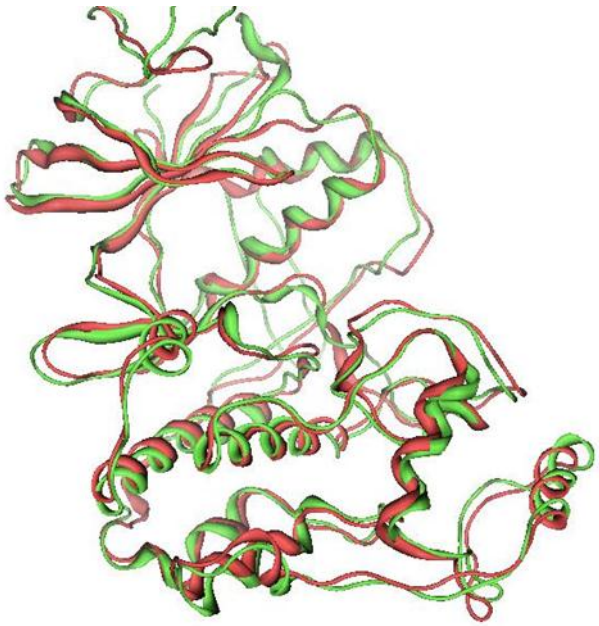

Figure 29: Homology model of ERK5 based on the structure of ERK2; Green = ERK5 model; Red = ERK2 template.

It has been reported that a single mutation of the gatekeeper residue of ERK2 (Gln105) results in the susceptibility of the protein to p38α inhibitors, where selectivity was previously observed in wild-type ERK2.[115] Substitution of Gln105 with threonine or alanine results in pyridinyl imidazole-based inhibitors of p38α conferring potency against mutant ERK2.

SB202190, **148** binding is 25,000-fold greater following mutation of the binding site (Figure **30**).

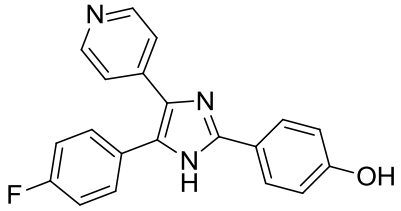

SB202190, **148**

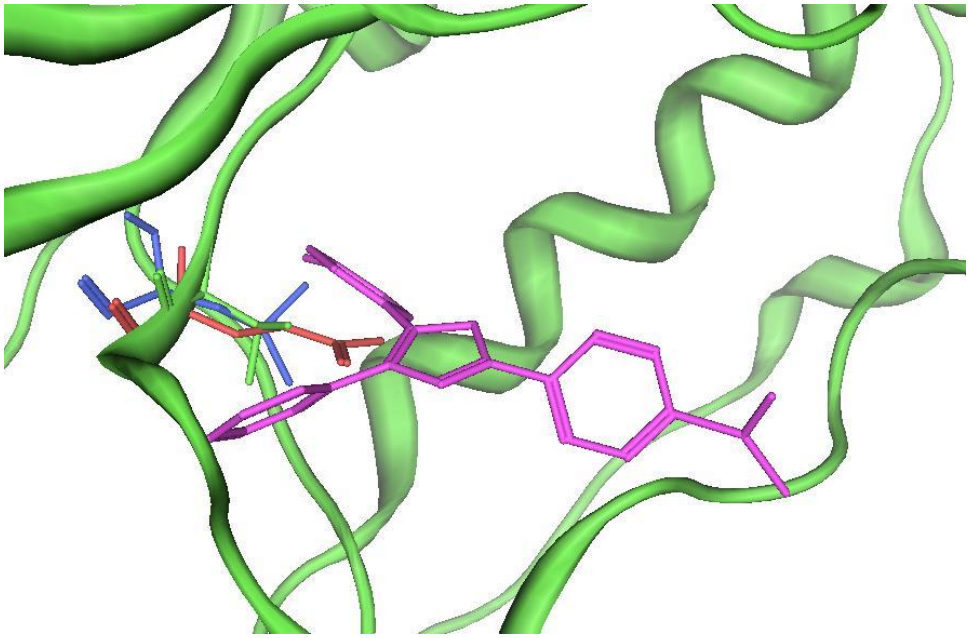

Figure 30: A closely related analogue of SB202190 **148**, bound in the mutant ERK2 active site (Q105T; blue), versus wild-type ERK2 (red).

Comparison of the ERK2, ERK5 (modelled) and p38α protein structures revealed that the differences in gatekeeper residues could be exploited in order to achieve selectivity. The gatekeeper residues in ERK5 and p38α are leucine and threonine respectively. Unfortunately, these two residues are similar in size, increasing the difficulty of achieving selectivity. The homology model was used to propose a binding mode for the pyrrole-carboxamide series, and two potential solutions were found. It is likely that the pyrrole-carboxamide series inhibit ERK5 in an ATP competitive manner. Binding mode 1 (Figures **31**, **32**) suggested that the nitrogen atom of the pyridine ring makes an interaction with the salt bridge lysine residue, leaving the halogenated aroyl moiety pointing out into solvent.

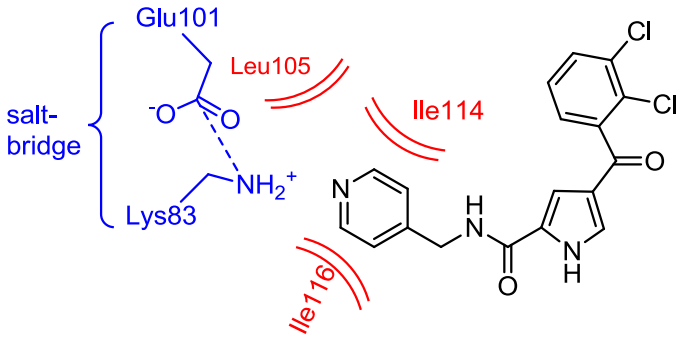

Figure 31: Binding mode 1 prediction; interaction of pyridine with salt bridge lysine residue.

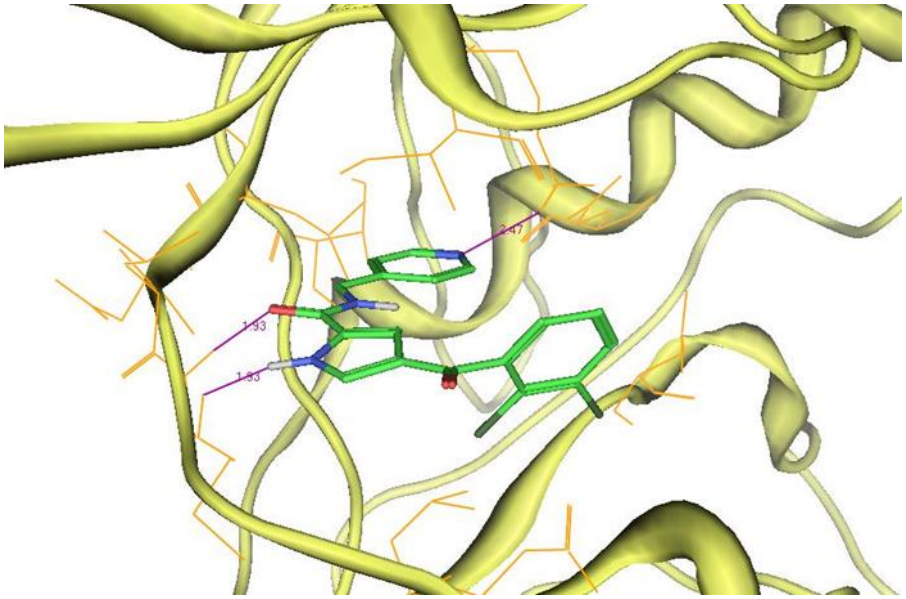

Figure 32: Binding mode 1 prediction; 3D model.

Binding mode 2 (Figures **33**, **34**) suggested that the aroyl group is directed into the hydrophobic pocket, with the carbonyl group making a key interaction with the salt bridge lysine residue. Taking into account the previous SAR data, it is more likely that this is the correct binding mode. The sensitivity of the potency to the substitution pattern around the aroyl substituent implies that there is a limited amount of space in the hydrophobic pocket. For example a loss of activity was observed when *para* substituents (e.g. **147**) were incorporated. In this model, when the aroyl ring is di-*ortho* substituted, steric contacts are maximised with the protein. When no *ortho*-substituent is present, poorer steric contacts and some steric clashes at the *meta*-position are observed. The observed SAR supports the second of the two proposed homology models.

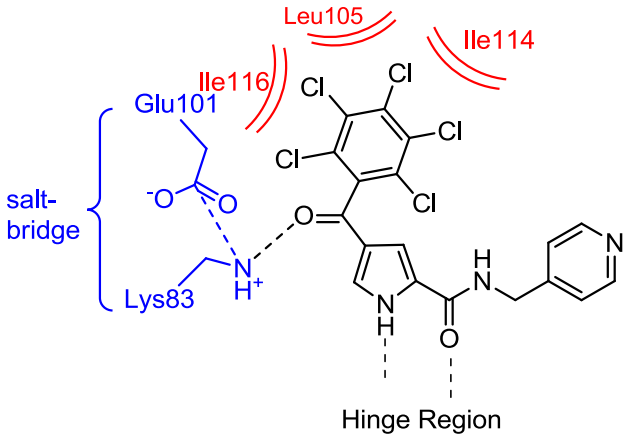

Figure 33: Binding mode 2 prediction; interaction of carbonyl with salt bridge lysine residue; All Cl shown for demonstration purposes.

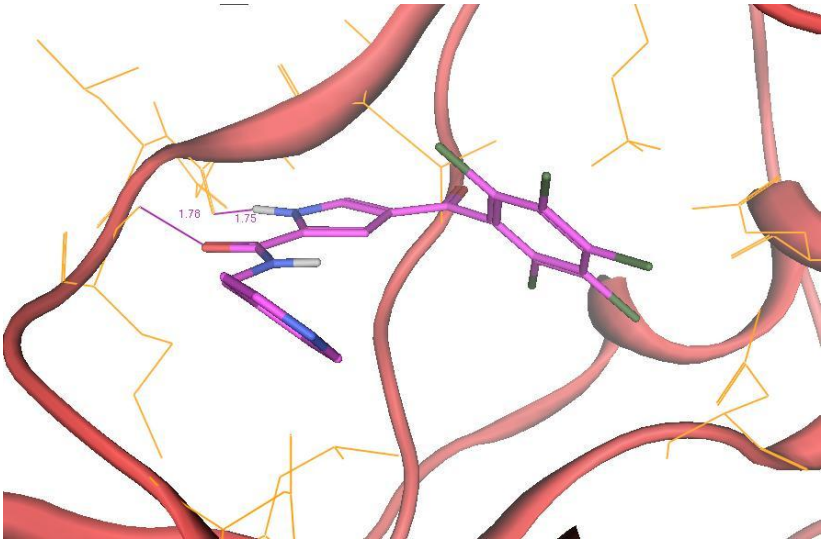

Figure 34: Binding mode 2 prediction; 3D model; All Cl shown for demonstration purposes.

6.6 Selectivity Screening for Hit Compounds

Compound **145** was submitted for selectivity screening against a panel of 63 kinases. Of the 63 screened, 17 showed some degree of inhibition when treated with **145** at a concentration of 10 µM. The majority of kinases were only weakly inhibited. However, six kinases were identified with greater than 15% inhibition (Table **22**).

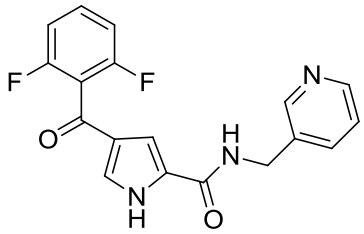

Table 22: Selectivity data of **145**

Kinase	% Inhibition @ 10 µM
JNK1α1	19
MAPK1	20
NEK2	43
PKA	19
SAPK2a/p38α	91
SGK	17

The selectivity data highlighted that pyrrole **145** was active against p38α. An IC_{50} determination for **145** against p38α confirmed activity of 0.41 ± 0.2 µM. It was clear that implementation of a p38α counter-screen would be required for compounds exhibiting significant ERK5 activity. Later in the project, counter-screen data combined with existing knowledge of the p38α structure would assist in the development of a more refined homology model.

6.7 Structure-Activity Relationships for Modifications to the Aroyl Moiety

Preliminary SAR data revealed that the substitution pattern around the aroyl ring (R^1) was crucial for activity. Further investigation of this motif was driven by the ERK2-based homology models.

6.7.1 SAR for Replacement of the Phenyl Ring with Saturated Rings

6.7.1.1 Proposed Series and Rationale

Both binding modes suggested by the homology model indicated that a range of non-aromatic cyclic systems may be tolerated (Figure **35**). The primary objective of the work undertaken at this stage was to improve potency for ERK5. It appeared that there was sufficient space in the binding pocket to accommodate the geometry of the cyclohexane

and/or cyclopentane rings in particular. The incorporation of a non-aromatic ring in the binding site potentially enables formation of interactions with amino acid residues which are not accessible *via* decoration of the planar aromatic ring. It was also envisaged that a range of amide linked 5- or 6- membered heterocycles may be incorporated. The 4-pyridyl side-chain was selected to be incorporated in all target compounds to enable direct comparison of analogues synthesised.

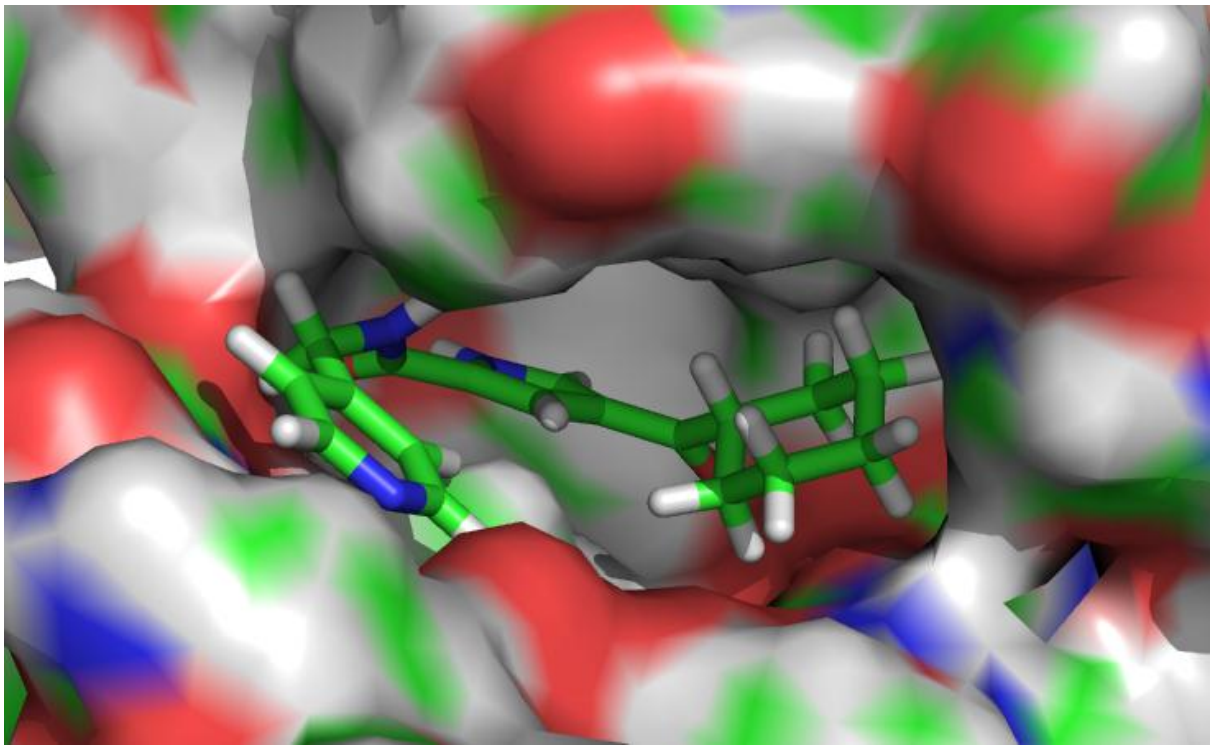

Figure 35: Homology modelling of a 4-cyclohexanone analogue.

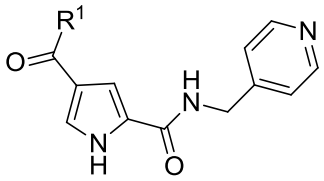

Table 23: Proposed library of non-aromatic derivatives

R[1]				
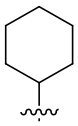		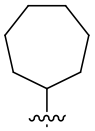	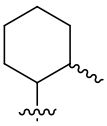	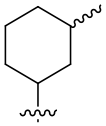
149	**150**	**151**	**152**	**153**
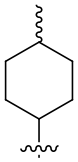	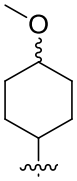	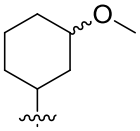	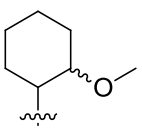	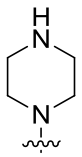
154	**155**	**156**	**157**	**158**
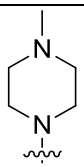	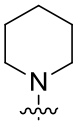	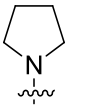	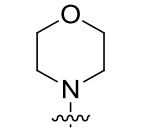	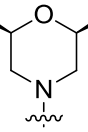
159	**160**	**161**	**162**	**163**

The library aimed to incorporate non-aromatic groups with a range of properties (e.g. variation of sterics, electronics and polarity). Investigation of unsubstituted 5-, 6- and 7-membered rings was performed in order to establish the steric availability in the binding pocket. Methyl or methoxy groups in the 2-, 3- and 4- positions of the 6-membered ring were incorporated to probe the importance of the substitution pattern and whether it was possible to make additional interactions with the protein structure (i.e. hydrogen-bond formation *via* the oxygen lone pair of the methoxy substituent). Finally, a range of heterocycles were introduced. Replacement of the ketone linker with an amide group aimed to enhance the hydrogen bonding capability of the carbonyl *via* a mesomeric effect.[116] The incorporation of additional heteroatoms into the ring creates the possibility additional interactions in the active site.

6.7.1.2 Synthesis of Unsubstituted Alkyl Ring Containing Analogues

Cyclohexane, **149**, cyclopentane, **150**, and cycloheptane **151** derivatives were synthesised *via* the previously established route (Scheme **24**).

Synthesis of target compounds was achieved *via* an efficient 3-step strategy. Friedel-Crafts acylation of commercially available methyl 1*H*-pyrrole-2-carboxylate, **166** with the relevant acid chloride proceeded in excellent yield (80-98%) in all cases. Selectivity for the 4-position is achieved using $AlCl_3$ as the Lewis acid.[117] If necessary, acid chlorides were synthesised from the corresponding carboxylic acid (Scheme **23**). Hydrolysis of the methyl ester was quantitative in all cases. Coupling of carboxylic acids (i.e. **168)** with 4-picolylamine using CDI afforded the target compounds **149**, **150** and **151** in good to excellent yields (60-98%).

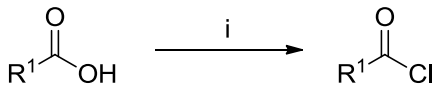

164 **165**

Scheme 23: *Reagents and conditions:* i) $SOCl_2$, DMF (cat), THF, RT, 3 h.

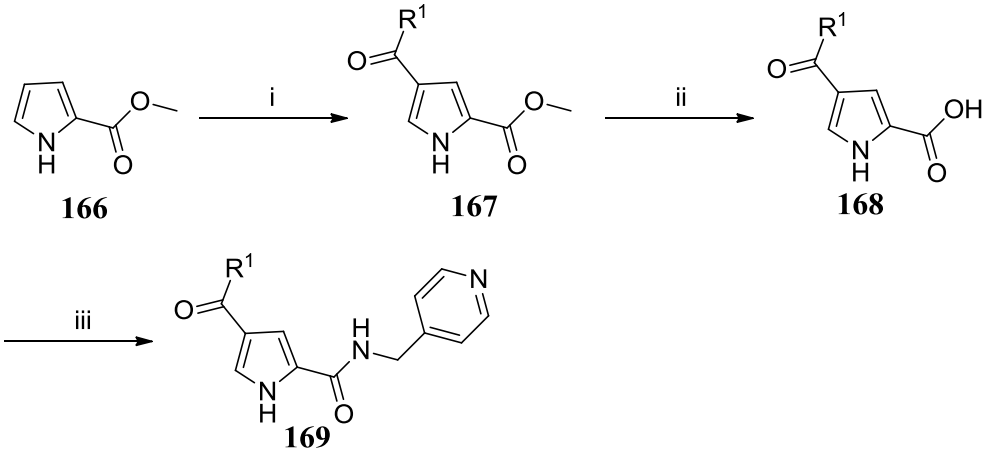

166 **167** **168** **169**

Scheme 24: *Reagents and conditions:* i) R^1COCl, $AlCl_3$, DCM, 0 ^oC-RT, 16 h; ii) LiOH monohydrate, H_2O, THF, 65 ^oC, 16 h; iii) CDI, THF, 70 ^oC, 3 h, then 4-picolylamine, 50 ^oC, 3 h.

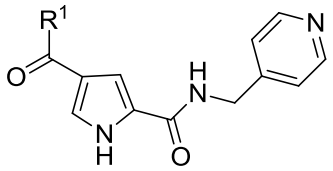

Table 24: Synthesis summary for incorporation of unsubstituted saturated rings

R^1	**Friedel-Crafts Yield (%)**	**Hydrolysis Yield (%)**	**CDI Coupling Yield (%)**
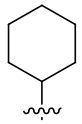	**170**; 81	**171**; 100	**149**; 60
	**172**; 80	**173**; 97	**150**; 63
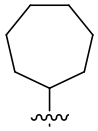	**174**; 98	**175**; 100	**151**; 98

6.7.1.3 Synthesis of Substituted Alkyl Ring Containing Analogues

The importance of substituents around the saturated ring was probed. A methyl group was incorporated into the 2-, 3- and 4- positions following Scheme **24**, to investigate the steric tolerance of the binding pocket. Despite the inactivity of the 4-substituted aryl analogues, 4-substituents on the saturated rings were included as they occupy different space. During the syntheses of these analogues, an interesting phenomenon was observed. Two products were isolated following Friedel-Crafts acylation of methyl 1*H*-pyrrole-2-carboxylate, **166** with 2-, and 3-methylcyclohexanecarbonyl chloride. Due to the presence of two chiral centres in these molecules, it was initially assumed that the two products isolated were the two pairs of diastereoisomers, with *cis* and *trans* geometry respectively. Analysis of the ^{1}H NMR data revealed that the products isolated were the two regioisomers (e.g. **176** and **177**). Table **25** shows a distinctive trend between the proportion of 5-substituted product and position of the methyl group. It is likely that the observed effect is due to the steric hindrance exerted on the intermediate oxonium ion formed in the Friedel-Crafts reaction, by the adjacent methyl group.

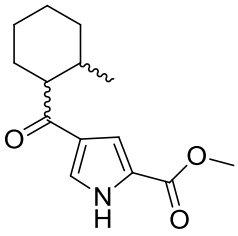

176

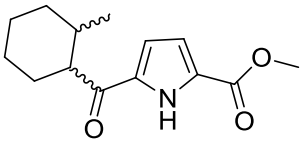

177

Table 25: Chemical yield, selectivity and stereochemical outcome for the 4- regioisomer versus the 5- regioisomer following Friedel-Crafts acylation of methyl 1*H*-pyrrole-2-carboxylate

R^1	4-R^1 Regioisomer Yield (%)	5-R^1 Regioisomer Yield (%)	Selectivity (4- : 5-)	Stereochemistry
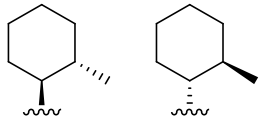	**178/179**; 59	**180/181**; 21	3:1	*trans* only
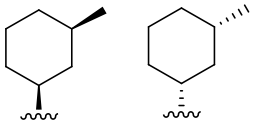	**182/183**; 53	**184/185**; 6	9:1	*cis* only
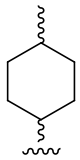	**186**; 59	0	1.0	Mixture; *cis:trans*

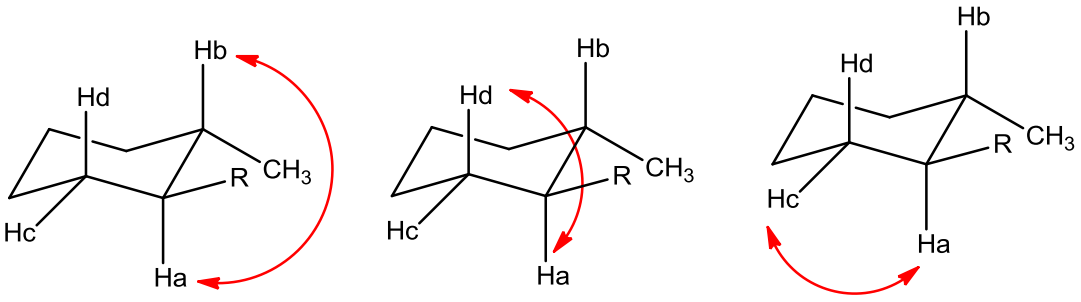

Figure 36: Coupling profile of H_a for compounds **178/179** according to the Karplus equation; H_b (J_{ab} ~12 Hz), H_c (J_{ac} ~3 Hz) and H_d (J_{ad} ~12 Hz).

Use of the Karplus equation allowed elucidation of the stereochemical outcome for the 2-methyl analogues **178/179** and its regioisomers. (Figure **36**).[118] Assignment of the 3-methyl compounds **182/183** was more challenging, where in this instance the C-1 proton (Ha) was

not unequivocally distinguishable as either *cis* nor *trans* by 1D NMR alone. A small-molecule crystal structure was obtained which confirmed that the thermodynamic *cis*-product had been obtained as a mixture of enantiomers (Figure **37**).

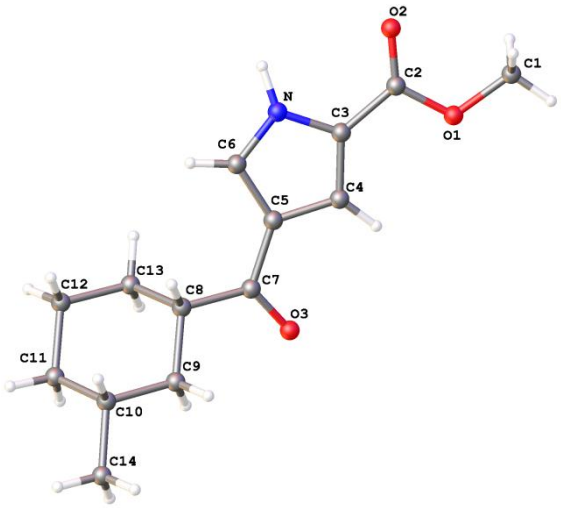

Figure 37: Small-molecule crystal structure of **183**.

Sterics are believed to be the main factor influencing stereochemical outcome. The proton adjacent to the ketone is enolisable, and equilibration to the most thermodynamically stable product is likely to have occurred over the course of the reaction, resulting in the two largest groups both being in the equatorial position. Acylation of **166** with 4-methylcyclohexanecarbonyl chloride proceeded regioselectively for the 4-position of the pyrrole. However, 4-methyl compound **186** was obtained as a mixture of *cis*/*trans* diastereoisomers (Table **25**). When the methyl group is in the 4-position of the acid chloride the steric effect is less significant, resulting in both regioselectivity for the 4-position and an increased proportion of the *cis* diastereoisomer.

Hydrolysis and CDI couplings on the 4-substituted pyrrole scaffold all proceeded in good yield (81-98% and 68-89% respectively; Table **26**). Although initially an undesired reaction product, the 5-substituted regioisomer was carried forward into subsequent hydrolysis and CDI coupling steps, in order for the resulting amides to act as negative control compounds.

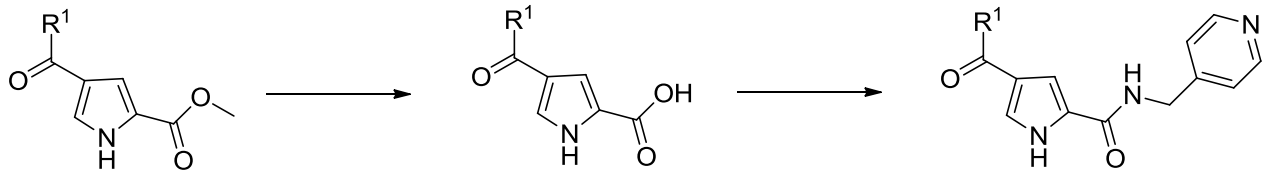

Table 26: Synthesis summary for 4-methylcyclohexane derivatives

R^1	Hydrolysis Yield (%)	CDI Coupling Yield (%)
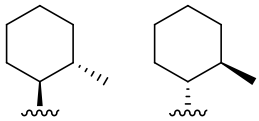	**187/188**; 81	**189/190**; 76
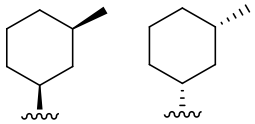	**191/192**; 85	**193/194**; 89
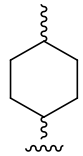	**195**; 98	**154**; 68

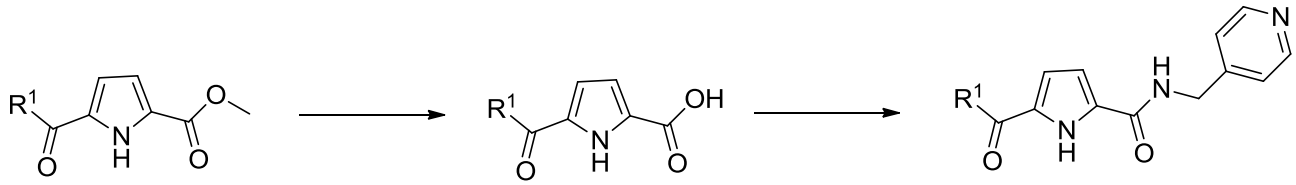

Table 27: Synthesis summary for 5-methylcyclohexane derivatives

R^1	Hydrolysis Yield (%)	CDI Coupling Yield (%)
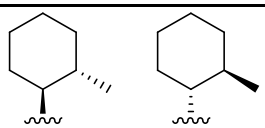	**196/197**; 75%	**198/199**; 83
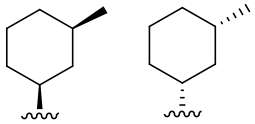	**200/201**; 86	**202/203**; 79

The same strategy as for synthesis of the methylated compounds was employed for the synthesis of methoxy substituted analogues. Synthesis of the 4-substituted analogue, **155** proceeded as expected (Scheme **25**), although an unusually low yield (28%) was obtained for the Friedel-Crafts acylation. Amide **155** was achieved as a mixture of diastereoisomers, in a similar ratio to the 4-methyl analogue **154**.

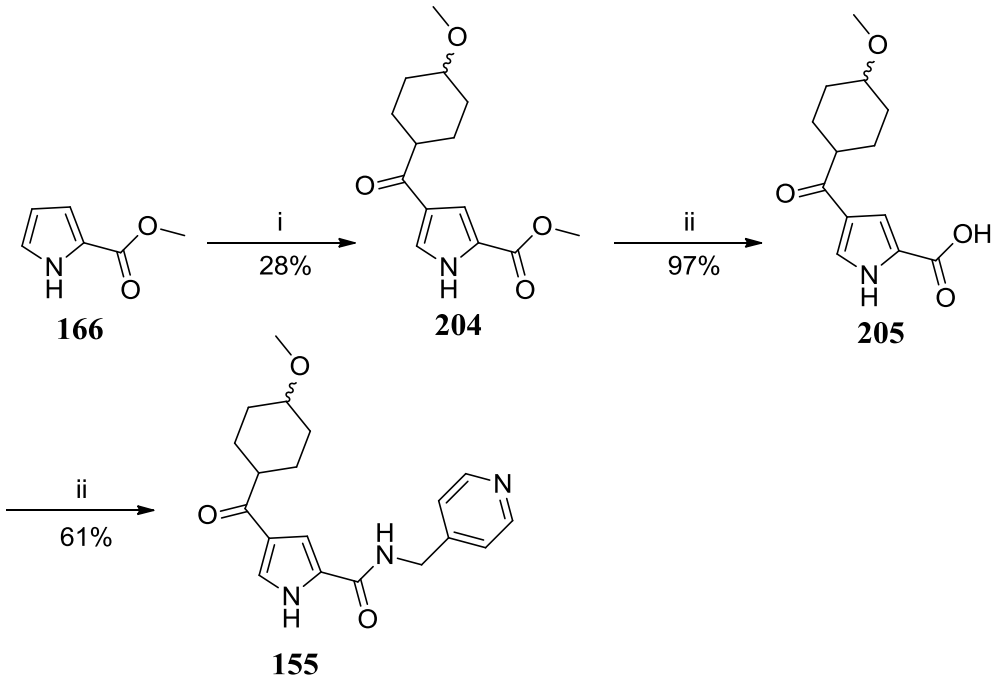

Scheme 25: *Reagents and Conditions;* i) 4-methoxycyclohexanecarbonyl chloride, $AlCl_3$, DCM, 0 ^oC-RT, 16 h; ii) LiOH monohydrate, H_2O, THF, 65 ^oC, 16 h; iii) CDI, THF, 70 ^oC, 3 h, then 4-picolylamine, 50 ^oC, 3 h.

It was noted that Friedel-Crafts acylation of methyl 1*H*-pyrrole-2-carboxylate, **166** with 3-methoxycyclohexane carbonyl chloride did not yield the desired product. ^1H NMR analysis revealed the major product to be the corresponding alcohol, indicating loss of the methyl group under the reaction conditions. In the presence of a Lewis acid, the nucleophilic lone pair of the oxygen atom may attack the carbonyl when both groups are in the axial position, liberating a chloride ion. The chloride ion may then demethylate the positively charged oxygen atom in an S_N2 fashion, similar to that observed in a Krapcho reaction.[119] This could yield a bicyclic lactone, which is able to participate in the Friedel-Crafts acylation of the aromatic species (Scheme **26**) to give the alcohol product. This phenomenon is not observed with the 4-methoxy compound.

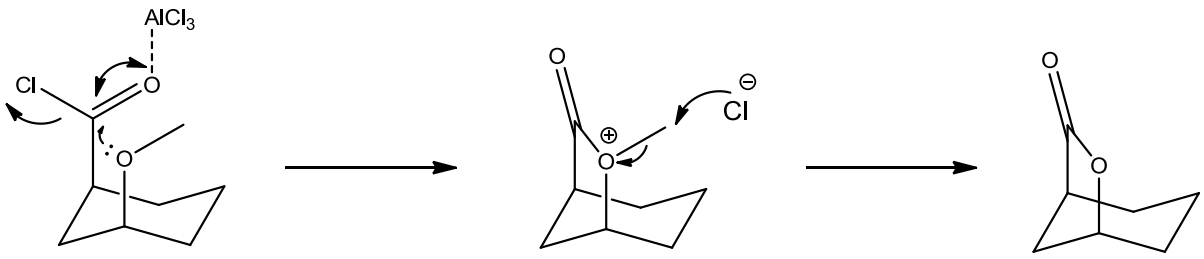

Scheme 26: Formation of a reactive lactone intermediate to afford the 3-hydroxy by-product

Following Friedel-Crafts acylation alcohol **206** was achieved in 48% yield as a single diastereoisomer with *cis* geometry (the thermodynamic product). Silyl protection of this intermediate was performed in order to achieve selectivity during the CDI coupling. Hydrolysis and CDI coupling reactions proceeded well in 80% and 54% respectively. Deprotection using TBAF gave alcohol **210** in 80% yield (Scheme **27**).

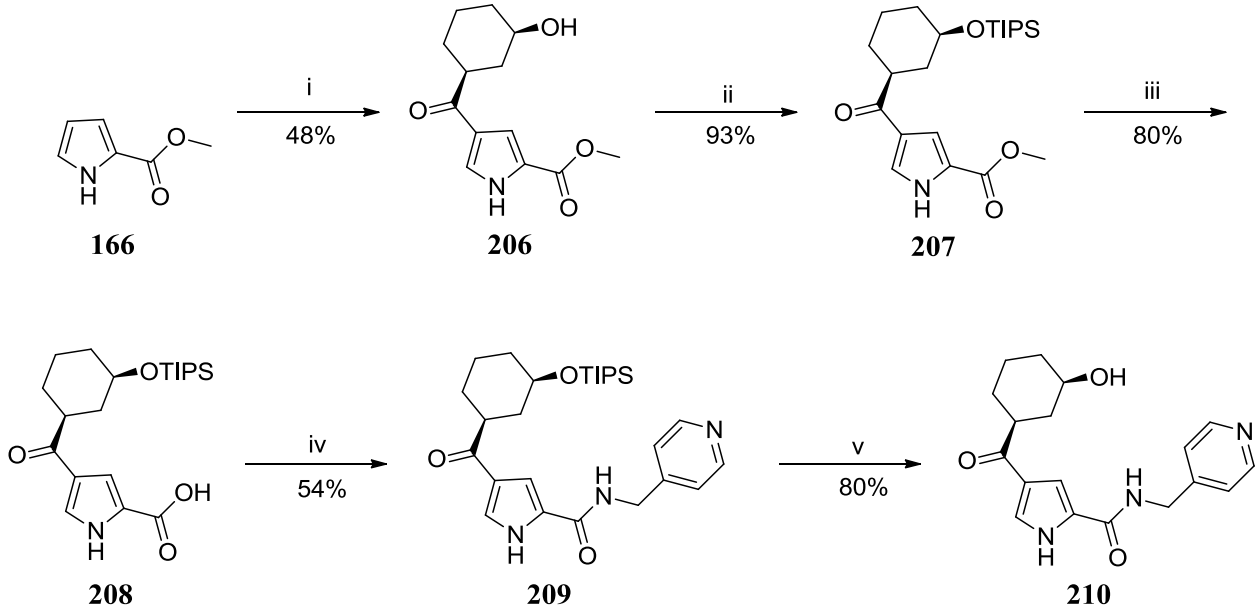

Scheme 27: *Reagents and Conditions;* i) 3-methoxycyclohexane carbonyl chloride, $AlCl_3$, DCM, 0 ^oC-RT, 16 h; ii) TIPSCl, imidazole, DCM, RT, 16 h; iii) LiOH monohydrate, H_2O, THF, 65 ^oC, 16 h; iv) CDI, THF, 70 ^oC, 3 h, then 4-picolylamine, 50 ^oC, 3 h; v) TBAF, THF, RT, 3 h.

It was envisaged that the target methoxy analogue could be synthesised from intermediate **209** with *cis* stereochemistry (Scheme **28**). Protection of the pyrrole nitrogen with a Boc group was intended to enable selective deprotection of the TIPS group using TBAF and so

would allow selective methylation of the alcohol. Unfortunately, upon treatment with TBAF in THF, both the TIPS and the *N*-Boc groups were removed from intermediate **211**.

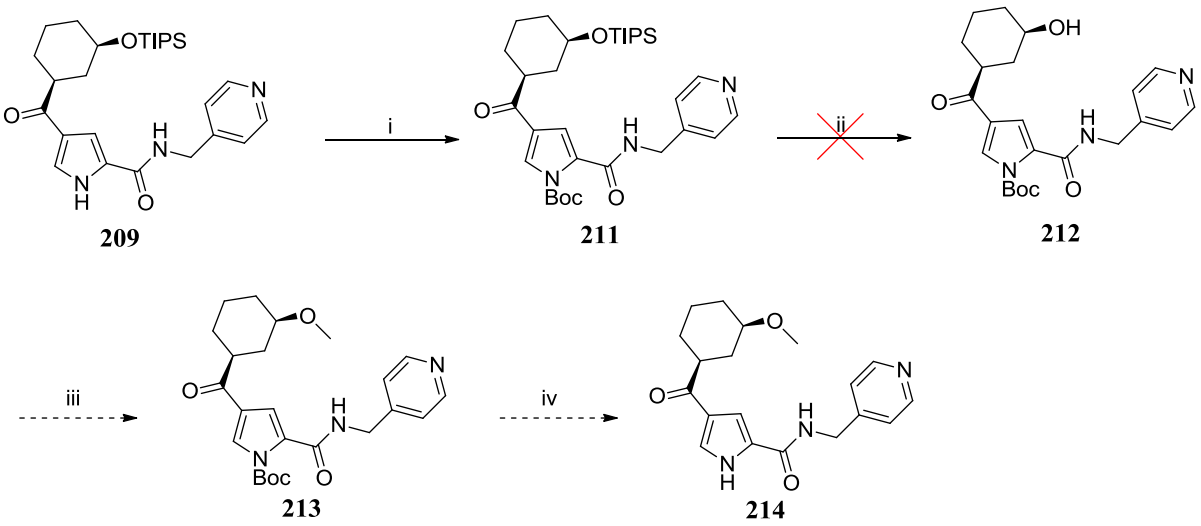

Scheme 28: *Reagents and Conditions;* i) Boc_2O, Et_3N, DMAP, DCM, 0 ^oC-RT, 16 h; ii) TBAF, THF, 0 ^oC, 2 h; iii) *O*-methylation; iv) Boc deprotection.

As it was not possible to synthesise the 3-methoxy analogue **214** *via* this route, it was desirable to synthesise the 4-hydroxy counterpart, **215** so that direct comparisons regarding the substitution pattern between these compounds could be made.

Treatment of the 4-methoxy compound, **155** with BBr_3 resulted in consumption of the starting material (Scheme **29**), but the desired product was not isolated. Two products which could not be separated by column chromatography were evident. The major product had mass/charge ratios (*m/z*) of 389 and 391 amu in a 1:1 ratio, indicative of the presence of a bromine atom. The minor product had an *m/z* of 310 and crude ^1H NMR confirmed the presence of an alkene. Structures of these reaction by-products were therefore elucidated as 4-bromocyclohexane, **216** and 4-cyclohex-3-ene **217** (or its regioisomer) containing analogues. As it was not possible to separate these two products, no further action was taken.

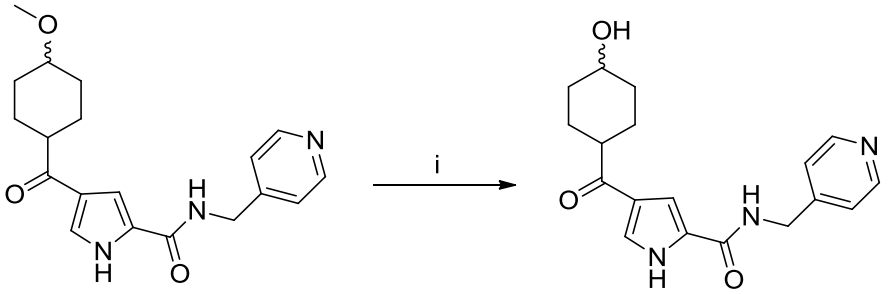

155 **215**

Scheme 29: Conversion of 4-methoxy analogue, **155** to 4-hydroxy compound **215**. *Reagents and Conditions;* i) See conditions in Table **28**.

Table 28: Attempted conditions for the formation of 4-hydroxy analogue **215**.

Attempt	Reagents and conditions	Observation
1	BBr_3, DCM, 0 ^oC-RT, 16 h	No conversion to product; by-products detected
2	$PhSSiMe_3$, ZnI_2, nBu_4NI, DCE, 60 ^oC, 16 h [120]	No conversion

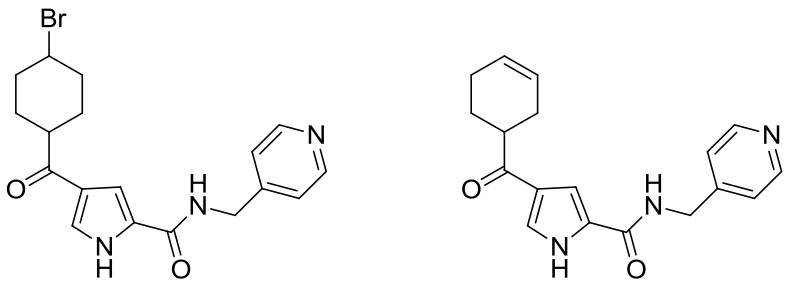

216 **217**

Demethylation was subsequently attempted using an organosilane reagent in the presence of a Lewis acid (ZnI_2) following a literature precedent.[120] Cleavage of the ether may be brought about by treating with a strong oxygenophile (silane), enhanced in the presence of a Lewis acid, with tetrabutylammonium iodide (TBAI) as an additive. Unfortunately, heating at 60 ^oC overnight showed no conversion to the demethylated product. Following the challenges encountered in this series, investigation into the synthesis of 3-methoxy and 4-hydroxy analogues was suspended. The use of alternative pyrrole protecting groups was considered for the synthesis of the 3-methoxy analogue, and alternative Lewis acids (e.g $AlCl_3$) for the

demethylation of **155** but further work was postponed pending biological results on this series.

6.7.1.4 Introduction of Cyclic Tertiary Amides

In order to synthesise tertiary amide based analogues, an alternative strategy was devised (Scheme **30**). The use of 2,2,2-trichloro-1-arylethanones with a range of nitrogen containing nucleophiles is reported as a high yielding strategy towards the synthesis of amides and hydrazides.[121] It was envisaged that the trichloroacetyl group may be introduced to the pyrrole *via* established Friedel-Crafts chemistry, to give a stable intermediate **218** which could be isolated and reacted further with a range of secondary amines.

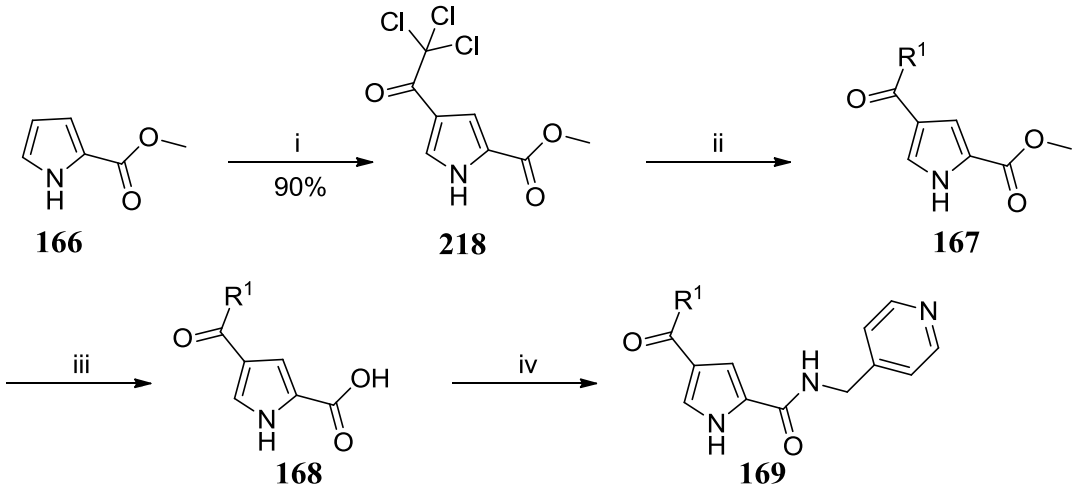

Scheme 30: *Reagents and Conditions;* i) trichloroacetyl chloride, $AlCl_3$, DCM, 0 ^oC-RT, 16 h; ii) R^1H, DMF, 50 ^oC, 4 h; iii) LiOH monohydrate, THF, H_2O, 40 ^oC, 4 h; iv) CDI, THF, 70 ^oC, 3 h, then 4-picolylamine, 50 ^oC, 3 h.

Friedel-Crafts acylation introduced the trichloroacetyl group at the 4-position of the methyl 1*H*-pyrrole-2-carboxylate scaffold. The trichloromethyl moiety acts as an excellent leaving group, yet is stable enough to isolate. S_N2 substitutions on the relevant amine were performed in variable yields (61-99%). Hydrolysis of the ester using the conditions previously used (20 eq. LiOH monohydrate, 65 ^oC, 16 h), were found to also hydrolyse the newly formed amide bond to the corresponding carboxylic acid. Use of lithium chloride in a Krapcho-like demethylation was investigated for ester cleavage with the morpholine analogue **219**, (Scheme **31**). The lithium ion co-ordinates one lone pair of each oxygen, stabilising the resulting negative charge following attack of the methyl group by the chloride ion.[119] A number of impurities were observed, and only 65% conversion to the product achieved.

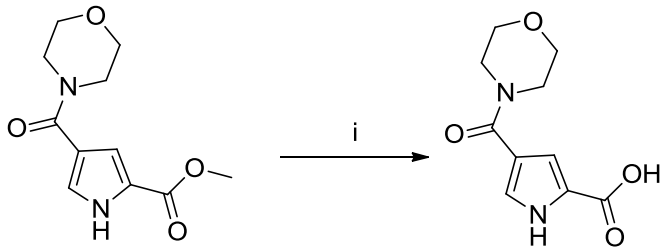

219 **220**

Scheme 31: *Reagents and Conditions;* i) LiCl, DMF, 160 ^{o}C, MW, 3 h.

Optimisation of the hydrolysis conditions (1.5 eq. LiOH monohydrate, 40 ^{o}C, 4 h) achieved selectivity for the ester, leaving the amide intact. CDI couplings were then performed on the resulting carboxylic acids in good to excellent yield (50-95%).

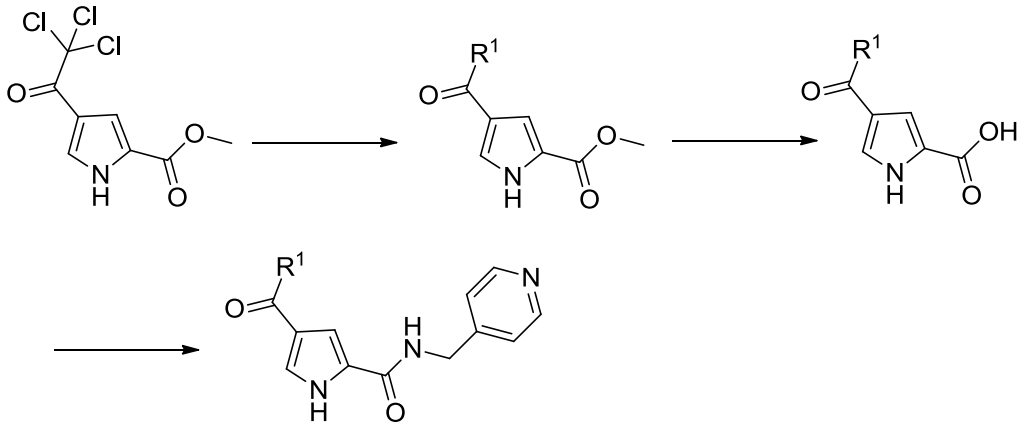

Table 29: Synthesis summary for incorporation of cyclic tertiary amides

R^1	S_N2 Substitution Yield (%)	Hydrolysis Yield (%)	CDI Coupling Yield (%)
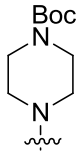	**221**; 61	**222**; 90	**223**; 95
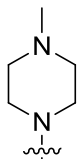	**224**; 63	**225**; 89	**159**; 43
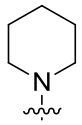	**226**; 75	**227**; 80	**160**; 82

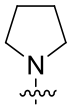	**228**; 99	**229**; 75	**161**; 82
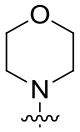	**219**; 88	**220**; 77	**162**; 70
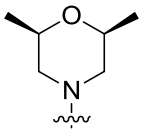	**230**; 90	**231**; 98	**163**; 50

Boc deprotection of **223** using TFA afforded piperazine **158** (Scheme **32**) in a relatively low yield of 46%.

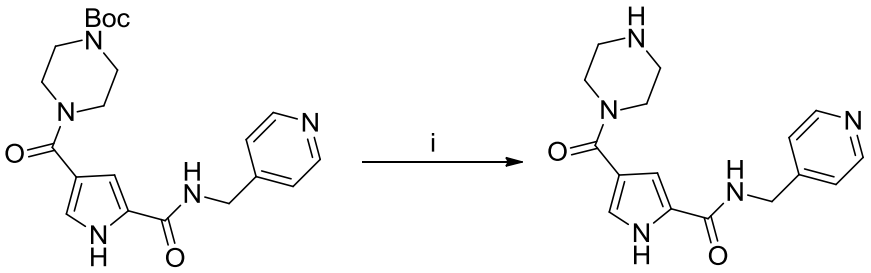

223 **158**

Scheme 32: *Reagents and Conditions;* i) TFA, DCM, RT, 1 h.

6.7.1.5 SARs for Biological Effect of Aromatic Ring Replacement with Non-Aromatic Groups

The cyclopentane, **150** and cycloheptane, **151** analogues were inactive against ERK5. Whereas the cyclohexane analogue **149** was found to be have a similar potency to the corresponding analogue **232**, bearing an unsubstituted aromatic ring (Table **30**). This result indicated that a 6-membered saturated ring is the optimum size and shape for accommodation in the binding pocket. 5-membered and 7-membered rings were deemed too small and too big respectively for satisfactory occupation of the pocket.

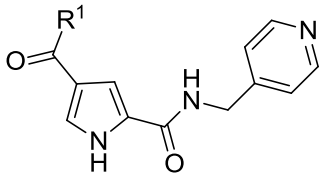

Table 30: ERK5 inhibitory activity of analogues containing alkyl rings

Compound	R^1	IC_{50} (μM)[a]
149	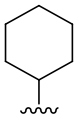	59.3 ± 1.5
150	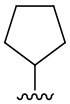	>120
151	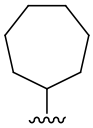	>120
232	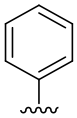	40.4 ± 2.6

[a] Determinations ± standard deviation

Interestingly, in all cases substitution of the cyclohexane ring was not tolerated (Table **30**). In the cases of the 2- and 3- substituted analogues, only one diastereoisomer pair was sent for biological evaluation due to the outcome of the syntheses. It is possible that only one of the four possible isomers is biologically active, and potentially the less stable kinetic product which is favourable. Due to the ability of the compounds to equilibrate to the thermodynamic products *via* the enolisable proton, synthesis of the isomers was not embarked upon. In addition, the 4-substituted diastereoisomeric mixtures did not confer any potency (Table **31**). The 5-substituted regioisomers were also inactive (Table **32**). The homology model indicates that the cyclohexane ring is the optimum size and shape to fit into the binding pocket. The inactivity of these compounds indicates that the electronic nature of the phenyl ring is crucial for activity. The π-system of the aromatic ring present in active compounds may participate in π-stacking interaction within the ERK5 binding site, which is not possible with the non-aromatic analogues. Studies show that electron-withdrawing phenyl substituents confer the greatest potency, which is not examined in this non-aromatic series. However, comparison of

the 2-methylcyclohexane analogues, **189/190** with their aromatic counterpart, **233** reveals that activity is significantly diminished when the phenyl ring is not present.

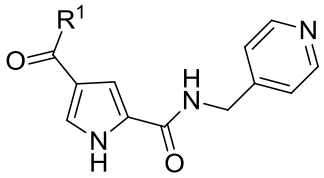

Table 31: ERK5 inhibitory activity of analogues containing substituted alkyl rings

Compound	R^1	IC_{50} (μM)[a]
189/190	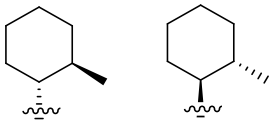	>120
193/194	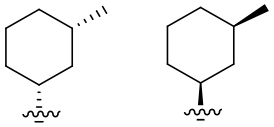	>120
154	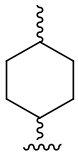 Mixture of *cis/trans*	>120
155	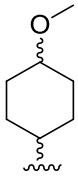 Mixture of *cis/trans*	>120
210	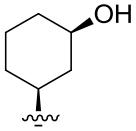	>120
233	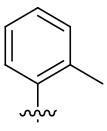	26.5 ± 2.1

[a] Determinations ± standard deviation

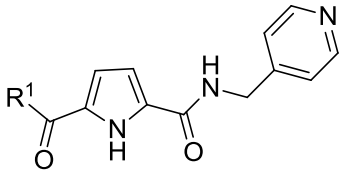

Table 32: ERK5 inhibitory activity of 5-substitued regioisomers

Compound	R^1	IC_{50} (μM)[a]
198/199	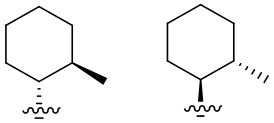	>120
202/203	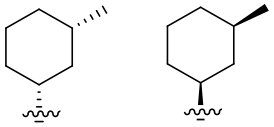	>120

[a] Determinations ± standard deviation

Activity was also abolished when amide linked heterocycles were incorporated. It was initially believed that conversion of the ketone to an amide would increase the hydrogen bonding potential of the carbonyl *via* a mesomeric effect.[116] However, it is possible that the restricted rotation about the amide bond is resulting in an unfavourable conformation. Ketone analogues have the ability to rotate freely, enabling them to adopt a conformation favourable for binding.

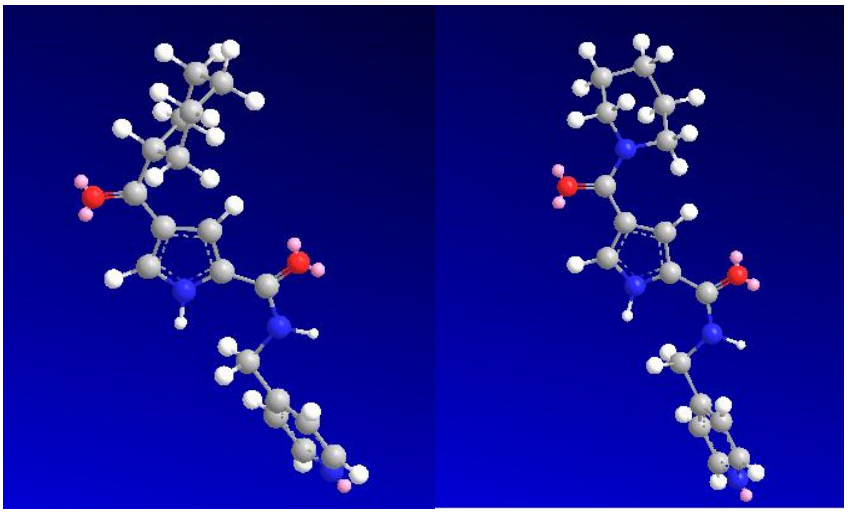

Figure 38: Conformational differences between cyclohexane analogue **149** (left) and piperidine analogue **160** (right) related to restricted rotation of amide bond. Structures are energy minimised using Chem3D, predicted at 31.57 kcal/mol and 31.87 kcal/mol respectively.

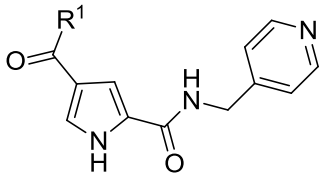

Table 33: ERK5 inhibitory activity of tertiary amide analogues

Compound	R^1	IC_{50} (μM)[a]	Compound	R^1	IC_{50} (μM)[a]
223	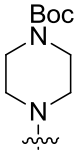	>120	**161**	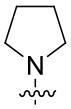	>120
158	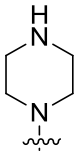	>120	**162**	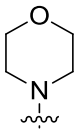	>120
159	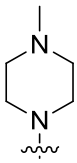	>120	**163**	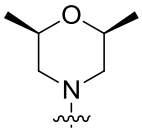	>120
160	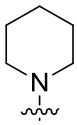	>120			

[a] Determinations ± standard deviation

6.7.2 Phenols as Molecular Probes

The SARs for the non-aromatic libraries showed a loss of potency (Section **6.7.1**), demonstrating that an aromatic group in the 4-position of the pyrrole carboxamide scaffold was essential for potency. For this reason, the remainder of the work conducted in this series focussed on modifications to the aromatic substituent, with the aim of gaining further understanding of the binding interaction and gaining improved potency. Although the SARs relating to the substitution pattern of the aromatic ring were understood in part, it was desirable to explore the chemical space further.

6.7.2.1 Rationale

Studies carried out by Dr Ruth Bawn highlighted that substituents much larger than the fluorine atom were tolerated, when in the *o*- and *m*-positions of the ring (Table **34**). In

particular, the 2-nitro analogue, **237** was equipotent with compound **144**. Electron withdrawing, *ortho*-substituents conferred the greatest potency (i.e. *o*-NO_2; ERK5 IC_{50} = 2.9 μM) compared with those in the *meta* position. Electron donating substituents (i.e. OMe) were not as active, but still tolerated. Phenols are undesirable features in drug molecules due to the possibility of giving rise to toxic quinone-based metabolites,[122] and they are susceptible to phase 2 metabolism processes (e.g. glucuronidation) which results in poor pharmacokinetic properties.[123] However, phenol analogues of **234**, **235** and **236** were deemed desirable targets to understand the importance of substituent size and electronic nature. The phenol group also acts as both a hydrogen-bond donor and acceptor, to probe for hydrogen-bonding with the protein. These compounds were synthetically tractable from the parent methoxy analogues.

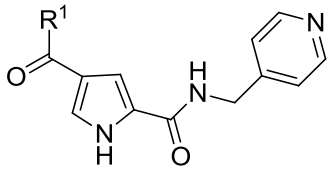

Table 34: ERK5 inhibitory activity of substituted aromatic analogues

Compound	R^1	IC_{50} (μM)[a]
144	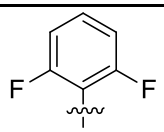	2.3 ± 0.1
234	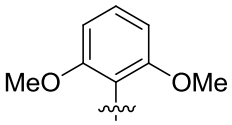	>120
235	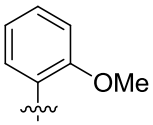	19.1 ± 3.3
236	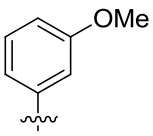	27.0 ± 1.2
237	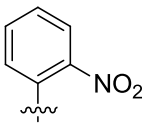	2.9 ± 0.2
238	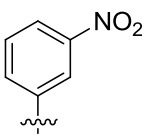	9.9 ± 0.6

[a] Determinations ± standard deviation

6.7.2.2 Synthesis of Phenol Analogues

The previously established route was utilised to synthesise the range of methoxy analogues outlined in Section **6.7.1.2**. Phenol containing target compounds were synthesised in one step from the methoxy precursors **234**, **235**, and **236** by demethylation with boron tribromide (Scheme **33**). Upon treatment of the dimethoxy compound **234** with BBr_3, two compounds were isolated which were identified as the mono- and di-hydroxy products (**239** and **240**). All demethylation reactions proceeded in good yield (66-85% overall) (Table **35**).

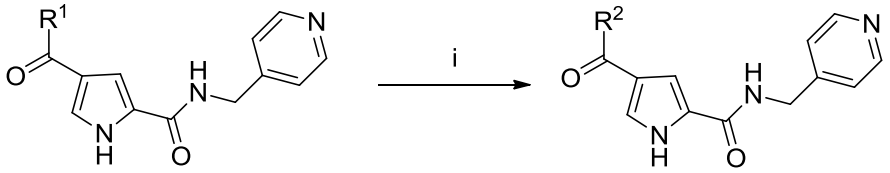

Scheme 33: *Reagents and Conditions;* i) BBr_3, DCM, 0 ^{o}C-RT, 16 h.

Table 35: Synthesis summary for deprotection of methyl ethers

Compound (R^1)	R^1	Compound (R^2)	R^2	Demethylation Yield (%)
234	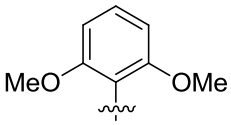	**239**	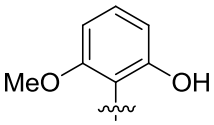	30 (85)
234	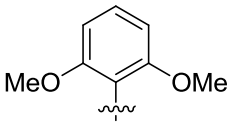	**240**	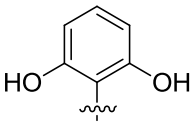	55 (85)
235	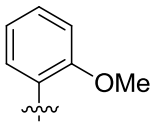	**241**	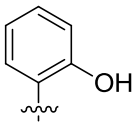	85
236	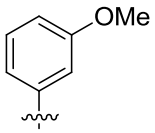	**242**	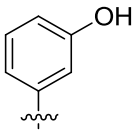	66

6.7.2.3 ERK5 Inhibitory Activity of Phenols

The phenol analogues synthesised were no more active than the corresponding methoxy analogues (Table **36**). Typically, *o*-substituted compounds are more potent than their *m*-substituted counterparts.

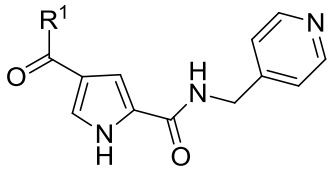

Table 36: ERK5 inhibitory activity of phenol analogues and their methoxy counterparts

Compound	R^1	IC_{50} (μM)[a]	Compound	R^1	IC_{50} (μM)[a]
239	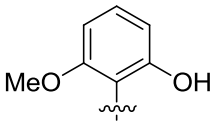	>120	**234**	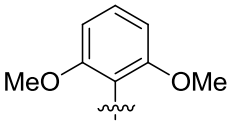	>120
240	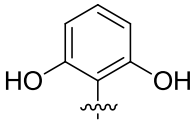	40.7 ± 4.2	**235**	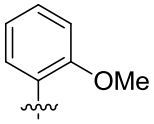	19.1 ± 3.3
241	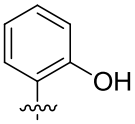	27.7 ± 1.5	**236**	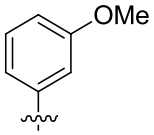	27.0 ± 1.2
242	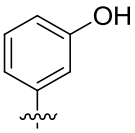	17.1 ± 1.5			

[a] Determinations ± standard deviation (mean of n = 2 unless otherwise stated)

Interestingly, the 3-hydroxy compound, **242** in this series was somewhat more potent than the corresponding 2-substituted analogue. ^{1}H NMR provides an explanation for the slightly improved activity of the 3-substituted compound. When the hydroxyl group resides in the 2-position of the aromatic ring, it may form an intramolecular H-bond with one lone pair of the carbonyl, forming a pseudocycle (Figure **39**). The formation of an intramolecular hydrogen bond would affect the ability of the carbonyl to form the key hydrogen bond with the Lys83 residue of the salt bridge, as shown in binding mode 2 (Figure **33**). Also, H-bonding may lock the aroyl ring in plane of the carbonyl group, where normally the two are not in plane. The chemical shift of the OH peak is at δ 11.05 ppm in the *ortho*-hydroxy compound, **241**. The *meta*-hydroxy proton is observed further upfield (δ 9.74 ppm), supporting this hypothesis. The positions of the aromatic protons, amide NH and pyrrole NH are largely unchanged between the two isomers. Figure **40** shows the differences between the ^{1}H NMR spectra obtained for phenols **241** and **242**.

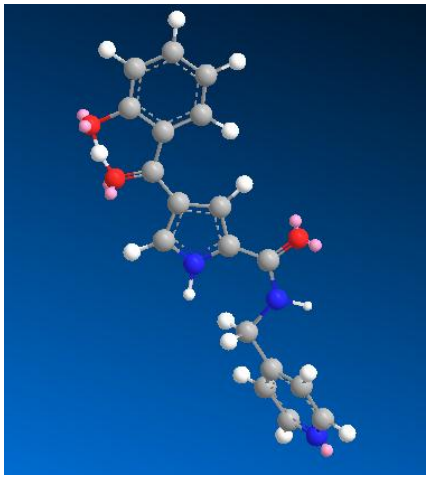

Figure 39: 3D structure of **241**; pseudocycle formation between carbonyl lone pair and phenolic proton. Structure is energy minimised using Chem3D, predicted at 864.92 kcal/mol.

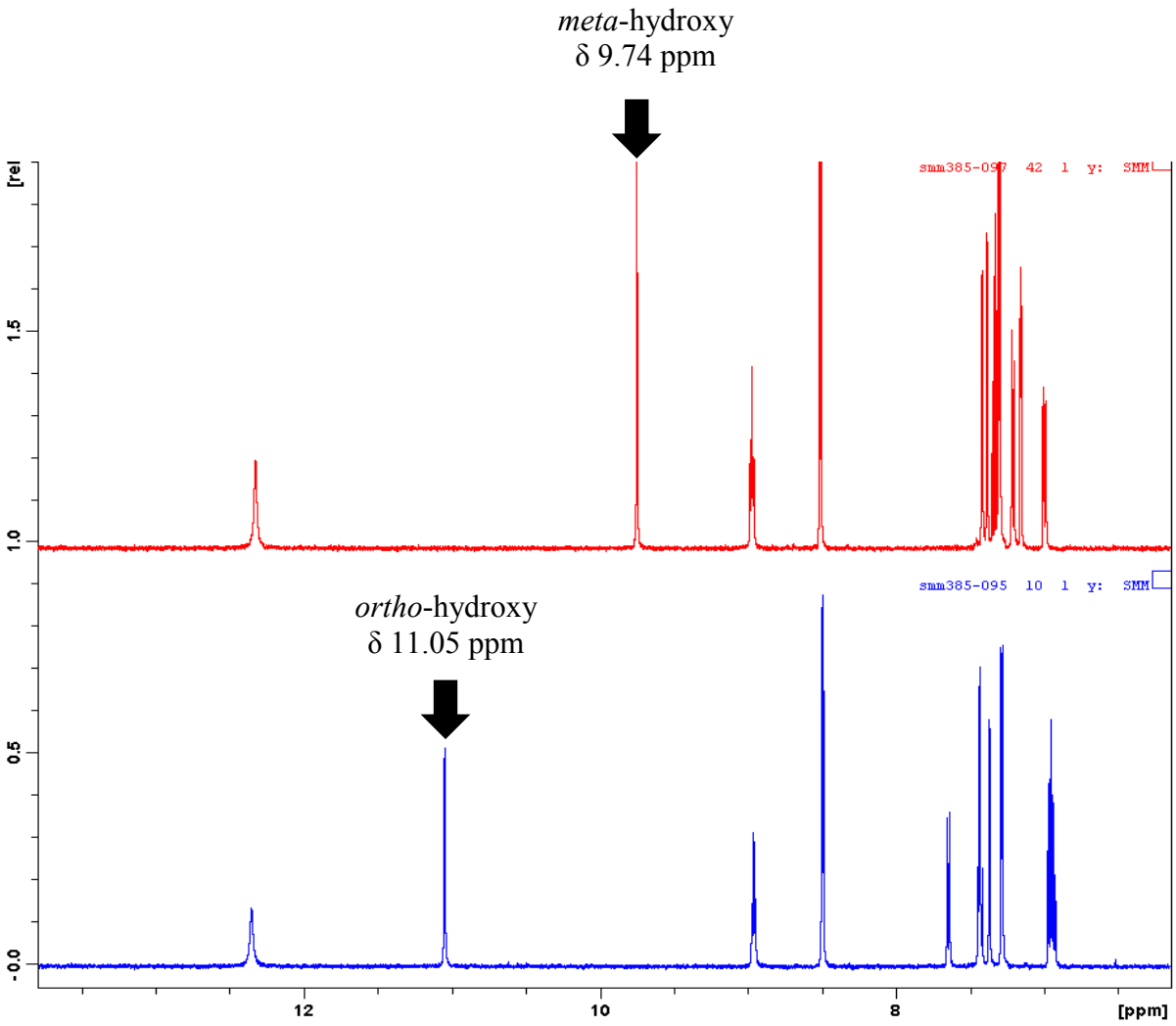

Figure 40: Comparison of ^{1}H NMR for *ortho*- (blue) and *meta*-hydroxy (red) derivatives; a significant change in chemical shift of the hydroxyl proton is observed between the two isomers.

6.7.3 Incorporation of 2-, 3- and 4-Pyridyl Groups

6.7.3.1 Rationale

Binding mode 2, identified by homology modelling, suggested that the aroyl portion of the pyrrole-carboxamides was occupying a largely lipophilic pocket consisting mainly of leucine and isoleucine residues. However, it was desirable to test this hypothesis by incorporating aromatic heterocycles, (i.e. pyridine), which have increased polarity over their phenyl counterparts. The stereoelectronic nature of the 2-pyridyl group is similar to that of the 2, 6-difluorophenyl moiety (Figure **41**). Due to this observation, it was thought that the 2-pyridyl compound may be a suitable isosteric replacement for the difluorophenyl motif. The

synthesis of the 2-pyridyl compound **242** would also probe the importance of steric effect, in addition to electronics. By comparison the unsubstituted phenyl analogue, **232** was found to inhibit ERK5 with an IC_{50} of 40.4 μM.

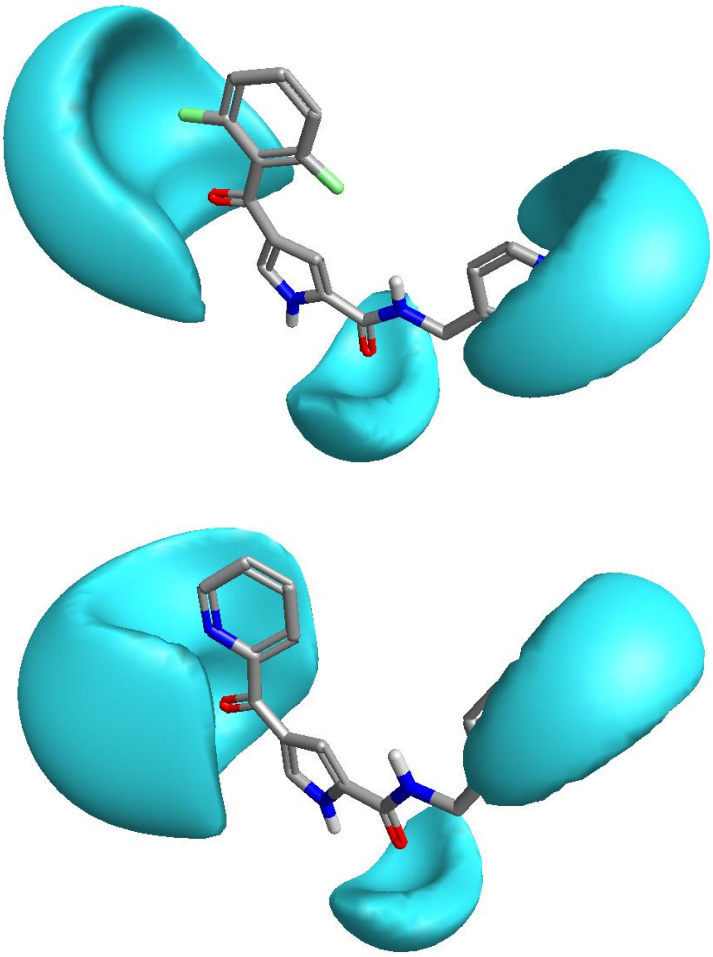

Figure 41: Negative-field surfaces for the 2,6-difluorophenyl analogue **144** (above), and 2-pyridyl analogue **243** (below). Images generated using FieldView software.

6.7.3.2 Synthesis

Friedel-Crafts acylation of methyl 1*H*-pyrrole-2-carboxylate with picolinoyl chloride hydrochloride was not successful (Scheme **34**). No conversion to the desired product was observed. It was believed that the nitrogen lone pair of the pyridine ring was consuming one equivalent of $AlCl_3$ by co-ordination. However, an increase in the number of equivalents did not result in any conversion to the product.

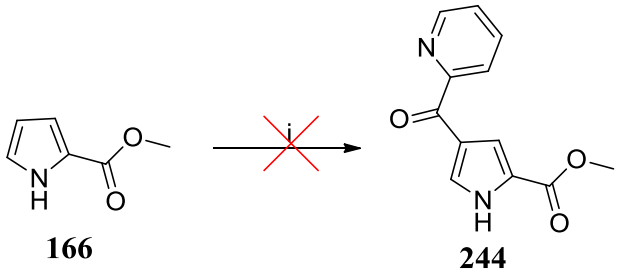

Scheme 34: *Reagents and Conditions;* i) picolinoyl chloride hydrochloride, $AlCl_3$, DCM, 0 ^oC-RT, 16 h.

A review of the literature revealed that regioselective acylation of *N*-(triisopropylsilyl)pyrrole has been achieved using *N*-acylbenzotriazoles in the presence of titanium tetrachloride.[124] Use of the bulky, electron donating TIPS protecting group directs acylation to the 3-position of the pyrrole. Studies by Katritzky *et al* describe the use of a number of *N*-acylbenzotriazole analogues for the synthesis of a variety of 3-acyl pyrroles, including the desired 2-pyridyl compound **244** (Scheme **34**).[124] Several attempts were made to replicate this work, by reacting the relevant *N*-acylbenzotriazole with $TiCl_4$ under anhydrous conditions, followed by the addition of *N*-(triisopropylsilyl)pyrrole **245**, without any success (Scheme **35**, Table **37**). It is known that $TiCl_4$ readily decomposes on contact with air to give hydrochloric acid, which, if present in the reaction mixture would remove the TIPS protecting group. As pyrrole was isolated as the major product from the reaction mixture, it is likely that this is the case. Based on the ability of the TIPS group to direct electrophilic aromatic substitution (EAS) reactions to the 3-position of the pyrrole, classical Friedel-Crafts conditions were attempted (Table **37**). Reaction of picolinoyl chloride with $AlCl_3$ to give the required reactive oxonium ion followed by EAS with *N*-(triisopropylsilyl)pyrrole, resulted in directed acylation in the 3-position of the pyrrole. However, analysis of the reaction mixture by LCMS indicated that slow TIPS deprotection was occurring following acylation giving rise to a mixture of products. Based on this observation, it was decided that the crude mixture would be treated with TBAF to afford pyridin-2-yl(1*H*-pyrrol-3-yl)methanone, **247**. A second Friedel-Crafts acylation on intermediate **247** with trichloroacetyl chloride afforded **250**. The trichloroacetyl group was then substituted with the desired amine to afford amide **243**. The method was applied to the synthesis of 3- and 4-pyridyl derivatives (Scheme **36**). Surprisingly, it was not possible to isolate a pure sample of the 3-pyridyl analogue **253** for biological assay despite purification by HPLC.

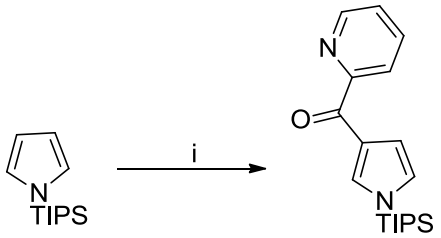

245 **246**

Scheme 35: *Reagents and Conditions;* See conditions in Table **37**.

Table 37: Acylation attempts of TIPS pyrrole

Attempt	Acylating agent	Reagents and conditions	Observation (by LCMS)
1	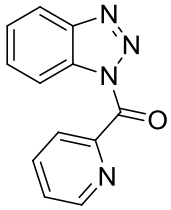	(1*H*-benzo[*d*][1,2,3]triazol-1-yl)(pyridin-2-yl)methanone, $TiCl_4$, DCM, reflux, 24 h.	Isolation of pyrrole; No conversion to product
2	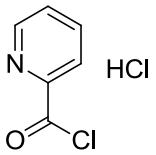	picolinoyl chloride hydrochloride, $AlCl_3$, DCM, 0 ^{o}C-RT, 16 h.	Acylation successful, some loss of TIPS

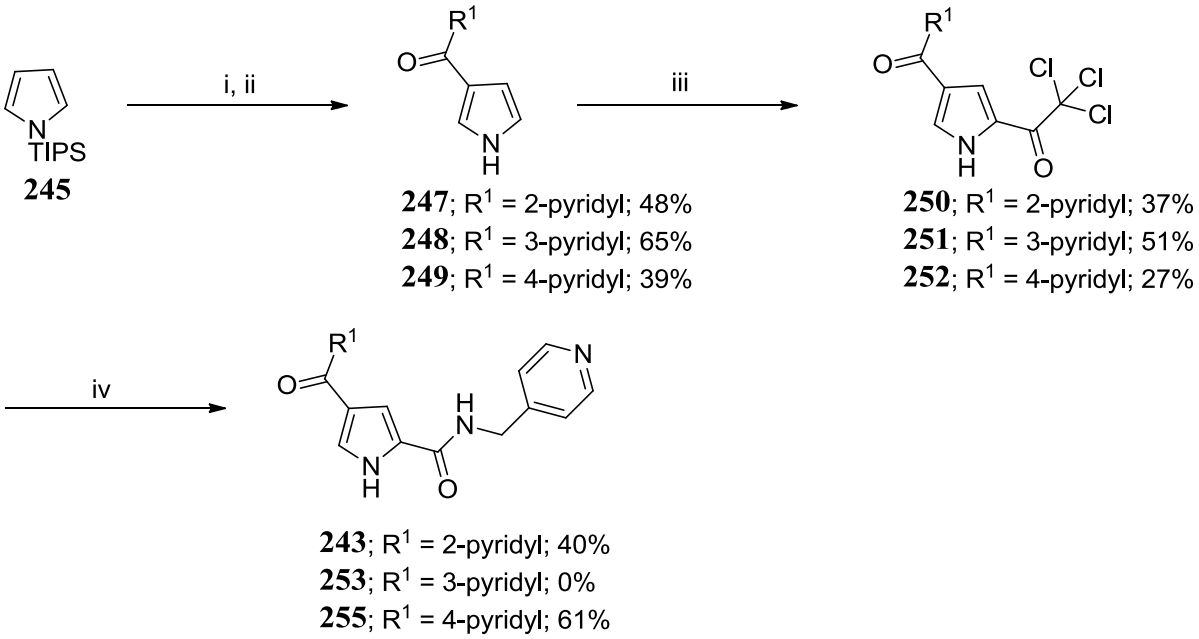

Scheme 36: *Reagents and Conditions;* i) $R^1COCl.HCl$, $AlCl_3$, DCM, 0 ^oC-RT, 16 h; ii) TBAF, THF, RT, 4 h; iii) trichloroacetyl chloride, $AlCl_3$, DCM, 0 ^oC-RT, 16 h; iv) 4-picolylamine, DMF, 50 ^oC, 4 h.

6.7.3.3 ERK5 Inhibitory Activity of Pyridyl Analogues

The unsubstituted phenyl analogue **232**, was considered as the benchmark compound for this series. Incorporation of a nitrogen atom into the 2-position gave no improvement in activity. The 4-pyridyl analogue **255**, displayed a 2-fold improvement in potency over the parent **232**. Further investigation into the role of the 4-pyridyl substituent was required. The activity of the pyridyl analogues **243** and **255** was significantly diminished compared to the 2,6-difluorophenyl analogue **144**. This result indicates that substitution of the phenyl ring in the *ortho*-position is essential for potency, by maximising steric contacts in the protein. The stereoelectronic similarity of the pyridyl motif to the difluorophenyl group alone does not satisfy this requirement.

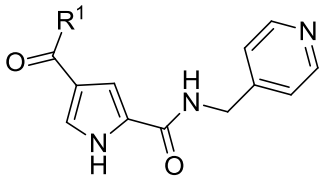

Table 38: ERK5 inhibitory activity of pyridyl analogues

Compound	R^1	IC_{50} (μM)[a]	Compound	R^1	IC_{50} (μM)[a]
232	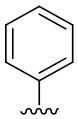	40.4 ± 2.6	**255**	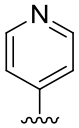	16.1 ± 2.8[b]
243	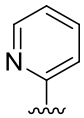	59.0 ± 19.8[b]	**144**	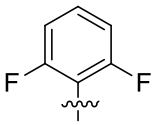	2.3 ± 0.1

[a] Determinations ± standard deviation (mean of n = 2 unless otherwise stated); [b] n = 4

6.7.3.4 A Scaffold-Hopping Approach for a 3, 5-Difluoropyridine Analogue

While investigation of the aroyl motif was continuing, it was discovered that truncation of the carboxamide side-chain resulted in a significant increase in potency. 2,6-Difluoro analogue **256** had an IC_{50} of 0.9 μM, and was the first in the series to display sub-micromolar activity. Furthermore, counter-screening against p38α revealed that the truncated analogues were greater than 100-fold selective for ERK5. It was envisaged that a structural overlay between 2,6-difluoro analogue **256** and 4-pyridyl analogue **255** could improve potency further. Homology modelling (Binding mode 2, Figure **33**) suggested that the 2,6-difluoroaryl motif maximises steric contacts within the protein. A potential further interaction with the 4-pyridyl substituent was probed (Figure **42**).

Table 39: Biological effect of side-chain truncation

Compound	Structure	ERK5 IC_{50} (μM)[a]	p38α IC_{50} (μM)[a]
144	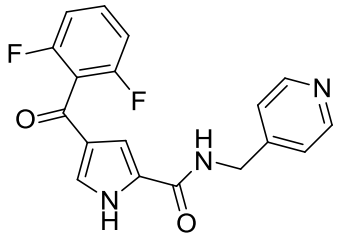	2.3 ± 0.1	0.58 ± 0.27[c]
256	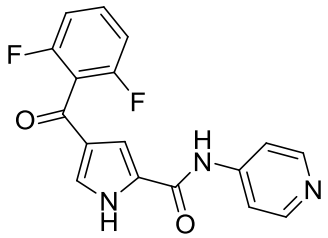	0.9 ± 0.2[b]	>120

[a] Determinations ± standard deviation (mean of n = 2 unless otherwise stated); [b] n = 8; [c] n = 4.

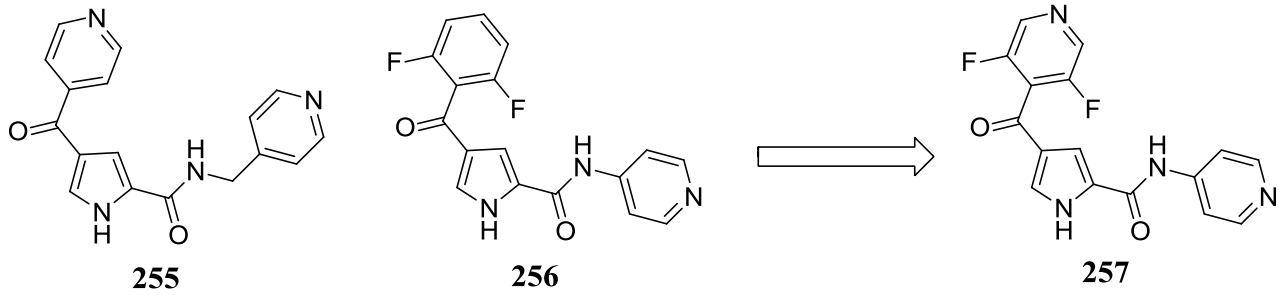

255 **256** **257**

Figure 42: A scaffold-hopping approach towards the 3,5-difluoropyridine analogue **257**

*6.7.3.5 Synthesis of 4-(3,5-Difluoroisonicotinoyl)-N-(pyridin-4-yl)-1H-pyrrole-2-carboxamide **257***

Friedel-Crafts acylation of methyl 1*H*-pyrrole-2-carboxylate with 3,5-difluoroisonicotinoyl chloride proceeded in 31% yield (Scheme **37**). The two electronegative fluorine atoms attenuate the pK_a of the pyridine nitrogen, resulting in less co-ordination of the Lewis acid, and enabling the acylation reaction to proceed. Although relatively low, the yield of the reaction was deemed satisfactory. Hydrolysis of the ester **258** proceeded quantitatively. However, CDI coupling of 4-aminopyridine with carboxylic acid **259** was unsuccessful. Detection of the imidazole intermediate was possible, highlighting that the reactivity of 4-aminopyridine was the problem. In 2009, Colombo *et al* reported the use of phosphorus trichloride mediated amide couplings.[125] The method is particularly useful when using unreactive anilines with strongly electron withdrawing substituents. Microwave-assisted

coupling of carboxylic acid **259** with 4-aminopyridine in the presence of PCl_3 allowed the synthesis of **257** in 30%.

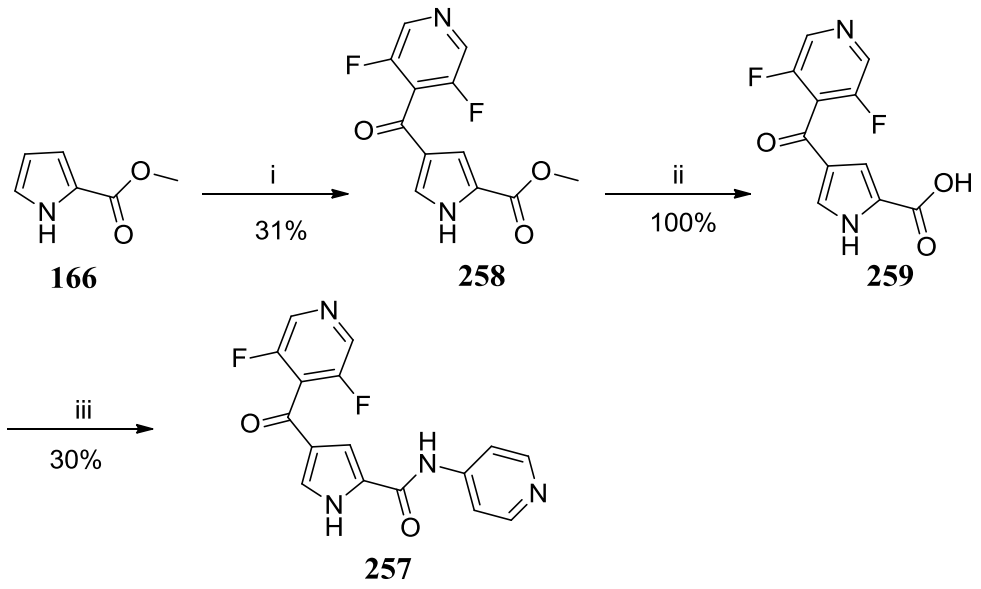

Scheme 37: *Reagents and Conditions;* i) 3,5-difluoroisonicotinoyl chloride, $AlCl_3$, DCM, 0 ^oC-RT, 16 h; ii) LiOH monohydrate, H_2O, THF, 65 ^oC, 16 h; iii) PCl_3, 4-aminopyridine, MeCN, 150 ^oC, MW, 5 min.

*6.7.3.6 ERK5 Inhibitory Activity of 4-(3,5-Difluoroisonicotinoyl)-N-(pyridin-4-yl)-1H-pyrrole-2-carboxamide **257***

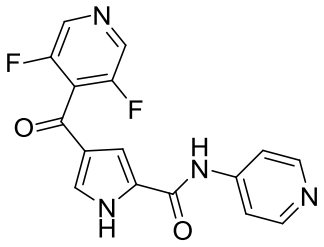

257; ERK5 IC_{50} = 3.9 ± 4.2 µM (n = 2); p38α IC_{50} >120 µM (n = 2).

Compound **257** was found to have an IC_{50} value of 3.9 ± 4.2 µM. Combining the 4-pyridyl and 6-difluorophenyl motifs did not give an additive effect to potency. The additional nitrogen atom in the 4-position is beneficial when the 2,6-difluoro substitution pattern is not present (i.e. comparing with phenyl analogue **232**). However, the difluoroisonicotinoyl compound **257** is equipotent with the 2,6-difluorophenyl analogue **256**. As the two electronegative fluorine atoms present on the pyridyl ring lower the pK_a of the nitrogen lone

pair, it is significantly less available for hydrogen-bonding. This would weaken any possible interactions which were occurring in the unsubstituted analogue, **255**.

6.7.4 Achieving Selectivity Over p38α: Tuning the Aroyl Substituents

Synthesis of two ERK5 selective tool compounds with reasonable potency had been achieved by tuning the carboxamide substituent (Table **40**; Compounds **256** and **260**). Compounds synthesised with large substituents in the *ortho*-position of the aroyl ring (i.e. CF_3) also conferred selectivity over p38α (compounds **261** and **262**), despite the CH_2-linker of the side-chain still being present. It was apparent from these results that there were two possible strategies for achieving selectivity.

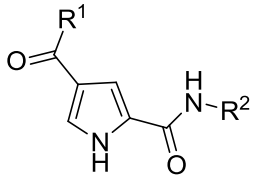

Table 40: Factors affecting selectivity for ERK5 over p38α

Compound	R^1	R^2	ERK5 IC_{50} (μM)[a]	p38α IC_{50} (μM)[a]
256	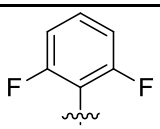	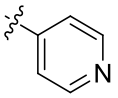	0.9 ± 0.2[b]	>120
260	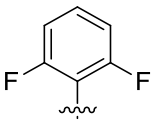	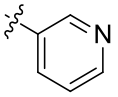	1.1 ± 0.3[c]	33.2 ± 0.9
261	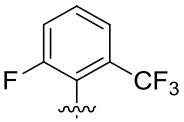	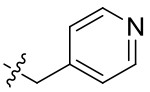	4.9 ± 1.2	66.3 ± 35.0
262	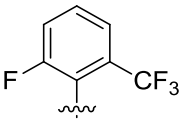	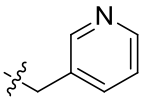	3.5 ± 1.0[d]	28.4 ± 19.9

[a] Determinations ± standard deviation (mean of n = 2 unless otherwise stated); [b] n = 8; [c] n = 6; [d] n = 4.

A library of compounds with substituents of varying sizes at the *ortho*-position was devised. A methyl group was chosen as an isostere for the trifluoromethyl group which confers selectivity over p38α. The size of the *ortho*-halogen was also probed, by incorporating a

chlorine or bromine atom. Homology modelling of a 2-bromo, 6-fluoro analogue **263**, revealed that the larger bromine atom appeared to be tolerated in the binding site of ERK5 (Figure **43**). However, molecular modelling did not predict whether the compounds would be selective over p38α.

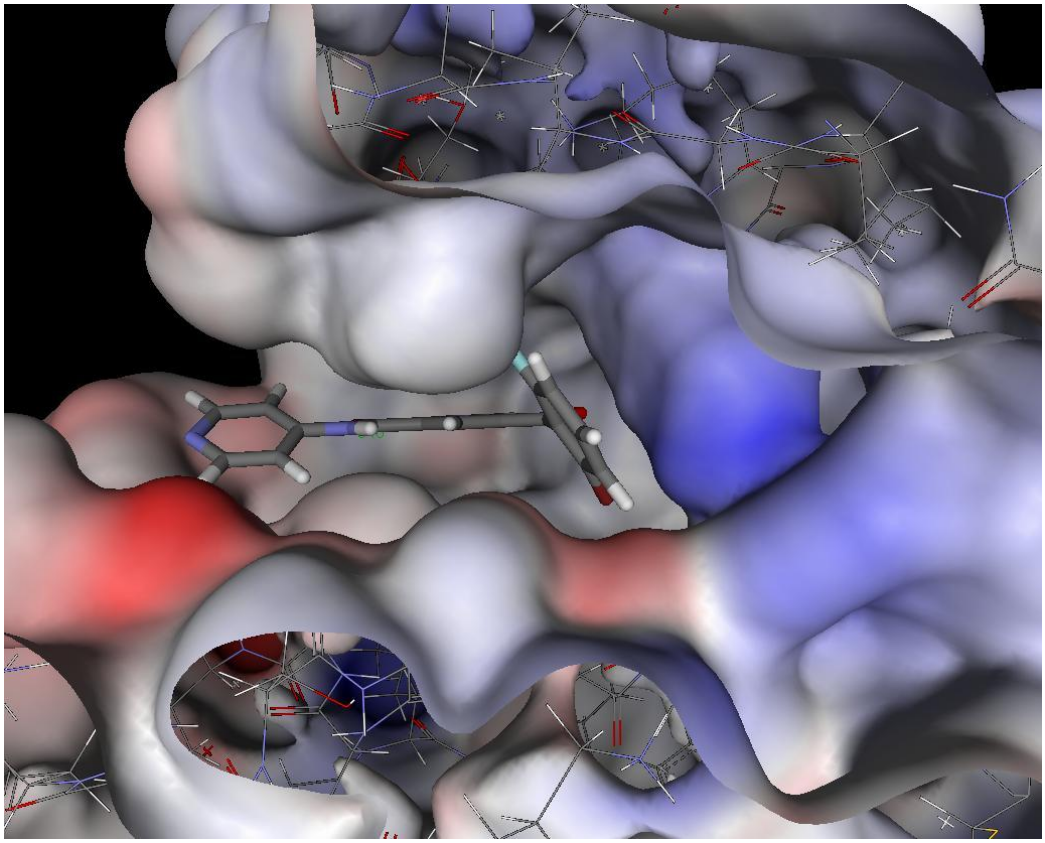

Figure 43: Homology modelling of 2-bromo, 6-fluoro analogue **263.**

6.7.4.1 Synthesis of ortho-Substituted Analogues

Synthesis *via* the efficient route outlined in Scheme **24** was employed. For couplings with 3- and 4-picolylamine, CDI was used, and for amide couplings with electron-poor 3- and 4-aminopyridine, the method using PCl_3 described in Section **6.7.3.5** was necessary (Table **41**). All reactions proceeded in good yield (≥50%).

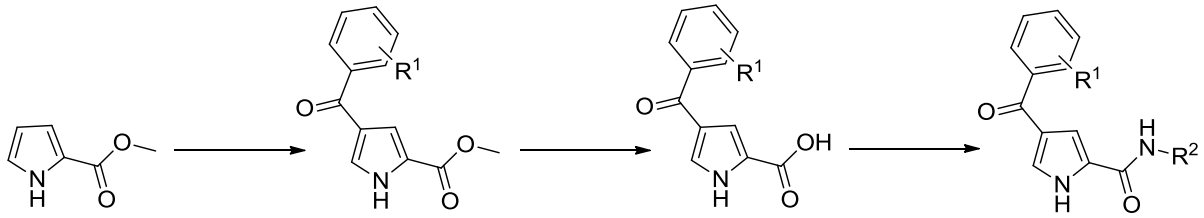

Table 41: Synthesis summary

R^1	R^2	Acylation Yield (%)	Hydrolysis Yield (%)	Amide Coupling Yield (%)
2-F, 6-Me	4-Pyridyl	**264**; 83	**265**; 98	**266**; 70[b]
2-F, 6-Me	3-Pyridyl			**267**; 76[b]
2-F, 6-Me	4-Methylpyridine			**268**; 52[a]
2-F, 6-Me	3-Methylpyridine			**269**; 58[a]
2-Cl, 6-F	4-Pyridyl	**270**; 89	**271**; 99	**272**; 61[b]
2-Cl, 6-F	3-Pyridyl			**273**; 64[b]
2-Cl, 6-F	4-Methylpyridine			**274**; 50[a]
2-Cl, 6-F	3-Methylpyridine			**275**; 68[a]
2-Br, 6-F	4-Pyridyl	**276**; 80	**277**; 90	**263**; 84[b]
2-Br, 6-F	3-Pyridyl			**278**; 76[b]
2-Br, 6-F	4-Methylpyridine			**279**; 55[a]
2-Br, 6-F	3-Methylpyridine			**280**; 68[a]

[a] CDI mediated amide coupling; [b] PCl_3 mediated amide coupling.

6.7.4.2 SARs for Substitution at the ortho-Position

Table **42** shows that compounds with the CH_2-linker present in the carboxamide side-chain were not selective for ERK5. Interestingly, the size of the substituent in the *ortho* position did have some effect on the degree of selectivity. Compounds **279** and **280** (with a bromine atom in the *ortho*-position) were 3-5 fold selective for ERK5 over p38α. However, the observed selectivity is small compared with that resulting from side-chain truncation which abolishes p38α activity. The 3- and 4-pyridyl 2-chloro-6-fluoro analogues **272** and **273** were equipotent with an ERK5 IC_{50} of 600 nM, giving a modest improvement on the initial 2,6-difluoro analogue **256** (ERK5 IC_{50} = 900 nM).

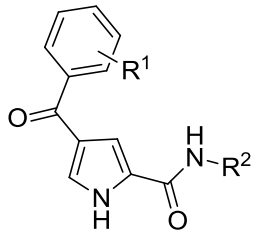

Table 42: ERK5 inhibitory activity of disubstituted pyrrole analogues

Compound	R^1	R^2	ERK5 IC_{50} (μM)[a]	p38α IC_{50} (μM)[a]
266	2-Me, 6-F	4-Pyridyl	1.9 ± 0.4[b]	25.7 ± 5.5
267	2-Me, 6-F	3-Pyridyl	2.6 ± 0.7[b]	54.0 ± 7.1
268	2-Me, 6-F	4-Methylpyridine	5.1 ± 0.7	1.0 ± 0.1
269	2-Me, 6-F	3-Methylpyridine	7.2 ± 1.5	1.2 ± 0.2
272	2-Cl, 6-F	4-Pyridyl	0.60 ± 0.3[b]	>120
273	2-Cl, 6-F	3-Pyridyl	0.60 ± 0.2[b]	93.2 ± 12.5[c]
274	2-Cl, 6-F	4-Methylpyridine	1.5 ± 0.3[b]	2.0 ± 0.1
275	2-Cl, 6-F	3-Methylpyridine	1.6 ± 0.2[b]	1.7 ± 0.0
263	2-Br, 6-F	4-Pyridyl	0.7 ± 0.2[b]	>120
278	2-Br, 6-F	3-Pyridyl	0.82 ± 0.1[b]	>120
279	2-Br, 6-F	4-Methylpyridine	1.9 ± 0.8	9.8 ± 0.2[b]
280	2-Br, 6-F	3-Methylpyridine	1.7 ± 0.6[b]	5.8 ± 0.5[b]

[a] Determinations ± standard deviation (mean of n = 2 unless otherwise stated); [b] n = 4; [c] n = 3

6.7.4.3 Investigation of Non-Aromatic Carboxamide Side-Chains

Discovery of compound **281** revealed that an aromatic group on the terminus of the carboxamide side-chain was not essential for ERK5 activity. Homology modelling suggested that the pyridyl moiety of the molecule points out toward solvent in the binding site of ERK5 (Figure **33**). Whereas the sensitivity of the substitution pattern of the aroyl motif had been shown previously, a wider range of substituents may be tolerated in this position, in particular substituents containing basic residues or those with a strong dipole (e.g. 4-fluorobenzyl compound **138**).

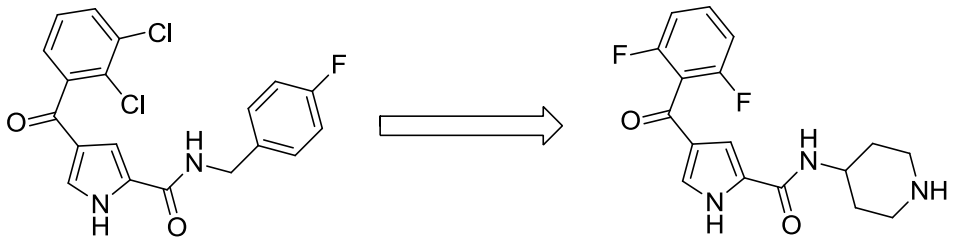

138 **281**

138; ERK5 IC_{50} = 3.7 µM ± 0.8 (n = 2); **281**; ERK5 IC_{50} = 1.3 µM ± 0.4 (n = 6); p38α IC_{50} = 9.8 µM ± 0.5 (n = 2)

Although selectivity for ERK5 over p38α was significantly diminished when substituting the aromatic pyridine moiety for piperidine, further investigation into the SARs around this motif was warranted. Previous studies had confirmed that the selectivity over p38α may be tuned, exploiting the differences in the ERK5 and p38α binding pockets. Scheme **24** was employed; CDI or PCl_3 mediated couplings with the relevant carboxylic acids gave a range of compounds with non-aromatic variation in the R^2 position (Table **43**). All CDI couplings proceeded in good yields (65-89%). The microwave-assisted method was utilised for coupling of *tert*-butyl 4-aminopiperidine-1-carboxylate with carboxylic acids **265** and **271**. However, relatively low yields (37 and 46% respectively) were observed. It was apparent that the harsh reaction conditions of the PCl_3 method were cleaving the Boc protecting group *in situ*. For ease of workup and purification, the cleaner CDI mediated methodology was used wherever possible.

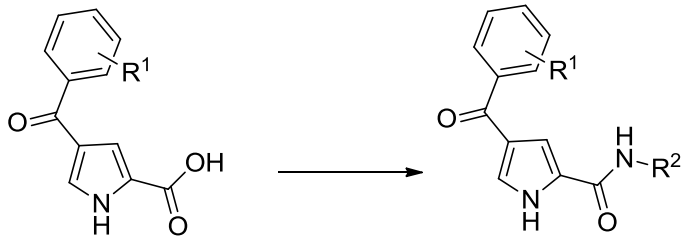

Table 43: Synthesis summary for amide couplings

Compound	R^1	R^2	Amide Coupling Yield (%)[a]
282	2-Me, 6-F	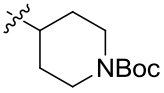	37[b]
283	2-Cl, 6-F	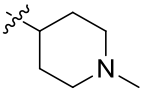	78
284	2-Cl, 6-F	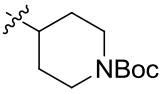	46[b]
285	2-Cl, 6-F	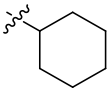	65
286	2-Cl, 6-F	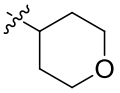	65
287	2-Br, 6-F	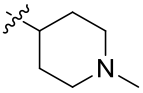	82
288	2-Br, 6-F	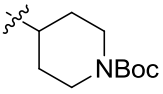	89
289	2-Br, 6-F	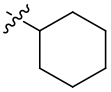	67
290	2-Br, 6-F	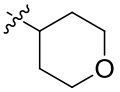	71

[a] Amide couplings performed *via* CDI mediated route (unless otherwise stated); [b] PCl_3 mediated amide coupling

The *tert*-butyloxycarbonyl analogues **282**, **284** and **288** were deprotected to give the corresponding piperidines **291**, **292** and **293** using TFA. In the case of 2-chloro, 6-fluoro analogue **292**, purification proved challenging despite the high purity of the starting material (≥95%). It is reported that the generation of a reactive *tert*-butyl carbocation during Boc

deprotection may be responsible for the occurrence of side-reactions, resulting in several impurities of small quantity.[126] It is not understood why the 2-methyl, 6-fluoro analogue **291** is unaffected. The deprotection was repeated, with the addition of triethylsilane as an additive during the reaction. The use of this additive improved the yield of the reaction significantly, from 51 to 99% yield for compound **289**. All subsequent Boc deprotections were conducted using this optimised method.

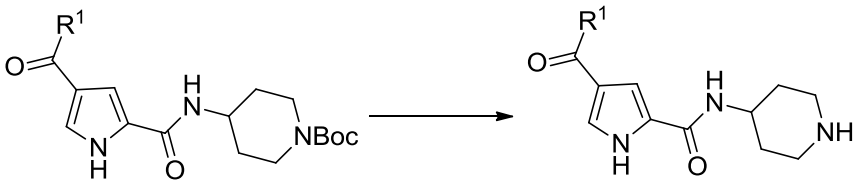

Table 44: Synthesis summary for Boc deprotections

Compound	R^1	Reagents and conditions	Yield (%)
291	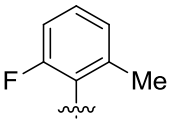	TFA, DCM, RT, 1 h	100
292	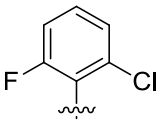	TFA, DCM, RT, 1 h	51
292	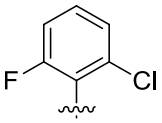	TFA, Et_3SiH (2.5 eq.), DCM, RT, 1 h	99
293	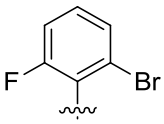	TFA, Et_3SiH (2.5 eq.), DCM, RT, 1 h	100

6.7.4.4 SARs for Pyridyl Group Replacement

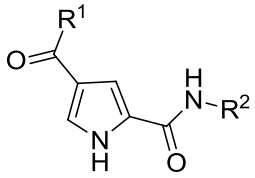

Table 45: Biological effect of side-chain replacement

Compound	R^1	R^2	ERK5 IC_{50} (μM)[a]	p38α IC_{50} (μM)[b]	Selectivity Ratio
291	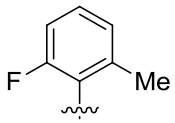	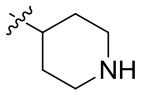	1.4 ± 0.3	5.1 ± 0.6	3-4-fold
283	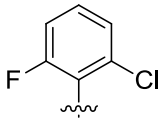	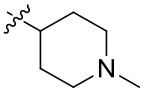	0.20 ± 0.06	8.5 ± 0.2	42-fold
284	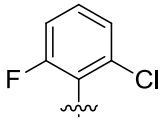	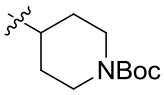	1.1 ± 0.4	99.0[c]	90-fold
292	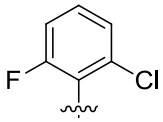	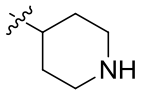	0.49 ± 0.04	11.1 ± 1.0[a]	22-fold
285	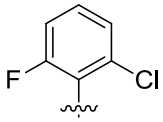	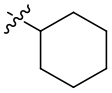	2.5 ± 1.0	>120	>48-fold
286	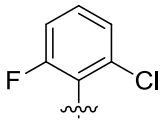	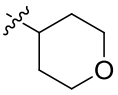	0.80 ± 0.3	12.5 ± 0.9	15-fold
287	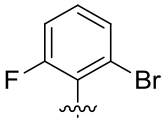	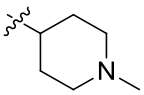	0.29 ± 0.12[d]	11.2 ± 0.2	38-fold
288	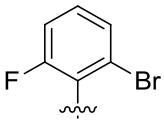	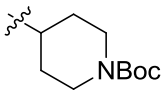	2.7 ± 0.7	>120	>30-fold
293	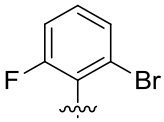	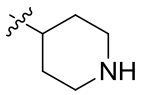	0.39 ± 0.12	18.5 ± 0.3	47-fold

289	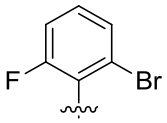	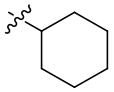	5.5 ± 0.6[b]	>120	>21-fold
290	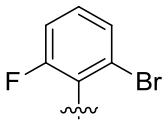	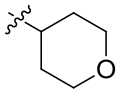	1.2 ± 0.2	18.1 ± 0.4	15-fold

[a] Determinations ± standard deviation (mean of n = 4 unless otherwise stated); [b] n = 2; [c] n = 1; [d] n = 8. NB: Green – ERK5 IC_{50} ≤1.0 µM; Amber – ERK5 IC_{50} = 1.0-2.0 µM; Red – ERK5 IC_{50} >2.0 µM.

Piperidine analogues **292** and **293**, and *N*-methyl piperidine analogues **283** and **287** showed excellent potency (ERK5 IC_{50} range = 200-490 nM). Compound **283** is approximately 42-fold for ERK5 over p38α, which exceeds the criteria set for a lead compound (Table **21**; >10 fold selectivity required for a lead).

6.7.5 Pyrrole-Carboxamide Based Inhibitors of p38α

In 2010, a series of pyrrole-carboxamide based inhibitors of p38α were described in the literature.[127] Although not a validated target in the area of cancer therapeutics, investigation into the discovery of inhibitors of p38α has been undertaken for the potential treatment of inflammatory disease.[127] A virtual screen based on a 3D pharmacophore query, was conducted at GSK using databases of commercially available compounds. Selected hits from the virtual screen were purchased, and assayed against p38α. Several pyrrole-carboxamide based hits were identified which showed sufficient activity for accurate IC_{50} measurement. Compound **294** has a pIC_{50} of 6.6 (n = 9) (IC_{50} = 0.25 µM).

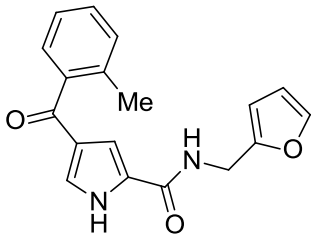

294; p38α IC_{50} = 0.25 µM

Pyrrole **294** was co-crystallised with p38α and an X-ray structure was obtained (Figure **44**). Structure-guided drug design enabled optimisation of the potency (Table **46**). The best activity in the series (IC_{50} = 13 nM) was reported for the 2-fluoro compound **297**, which incorporates a water-solubilising piperazine motif. Interestingly, the data suggests that *para*-

substitution on the aroyl ring is not detrimental to activity (compound **297**), in contrast to the SARs for ERK5. It was also reported that a number of aniline based compounds were prepared (although no structures were disclosed). These analogues all displayed inferior potency, which is attributed to the inflexibility of the aniline. A methionine residue (Met109) is believed to envoke a steric clash in the backbone of the protein with the truncated analogues. This information provides an explanation for the selectivity observed with the truncated aniline ERK5 inhibitors.

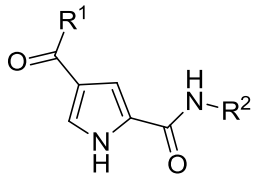

Table 46: Pyrrole-carboxamides as inhibitors of p38α

Compound	R^1	R^2	p38α pIC_{50}[a]	p38α IC_{50} (μM)[a]
294	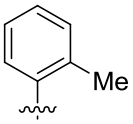	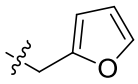	6.6	0.25
295	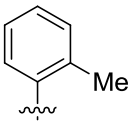	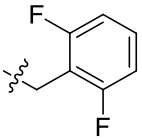	7.0	0.10
296	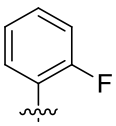	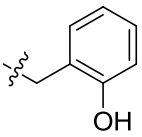	7.3	0.05
297	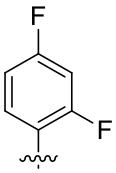	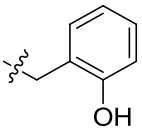	7.5	0.03
298	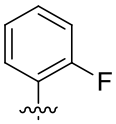	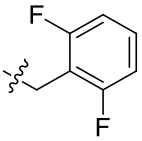	7.6	0.025
299	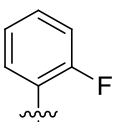	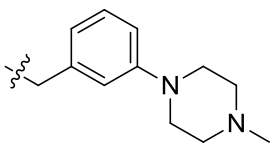	7.9	0.013

[a] Mean of at least three experiments. From ref [127].

The crystal structure of **294** bound to p38α shows a different binding mode of the pyrrole-carboxamide scaffold to that suggested by the ERK2/p38α based homology model for ERK5. The compounds described bear a striking resemblance to those synthesised at Newcastle, and taking into account the conserved nature of the ATP binding site amongst the MAPK family, this alternative binding mode was considered in future studies. The aroyl ring is shown to occupy a small lipophilic pocket, adjacent to the gatekeeper residue (Thr106), although the orientation is different to that shown in the homology model for ERK5 (binding mode 2). In the ERK5 homology model the aroyl carbonyl interacts with a salt bridge lysine, whereas interaction with two water molecules is evident in the p38α crystal structure. A NH-carboxamide-water interaction is also observed. This may explain why the *N*-methyl compound **146**, is tolerated but not optimum for ERK5 inhibition (ERK5 IC_{50} = 9.0 μM). The pyrrole-NH and carboxamide carbonyl motif act as hydrogen bond donor and acceptor respectively in the hinge region of the protein to Met109 and His107.

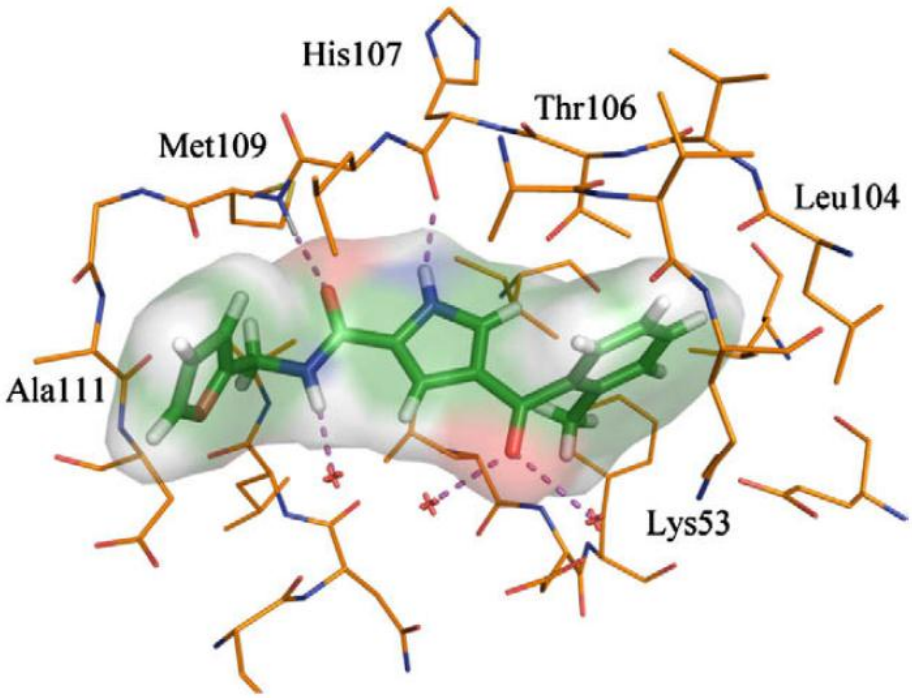

Figure 44: Crystal structure of **294** in complex with p38α. From ref [127]. Magenta dotted lines indicate hydrogen bonds to the inhibitor. Red crosses are water molecules.

6.7.6 Towards the Allosteric Pocket: Tuning the Aroyl Substituents

Molecular docking of pyrrole-carboxamide based ERK5 inhibitors in the updated homology model revealed that it may be possible to access an allosteric binding pocket *via* the 2- or 3-position of the aroyl ring (Figure **45**). The activation loop in protein kinases begins with a conserved DFG (Asp-Phe-Gly) sequence. The structural conformation of this sequence determines whether the kinase is active (DFG-in) or inactive (DFG-out). In the DFG-out conformation an additional binding site adjacent to the ATP binding site is accessible, potentially allowing additional interactions with a small-molecule inhibitor. Probing the allosteric site was therefore an attractive strategy for gaining potency against ERK5. The exceptionally high structural similarity of the pyrrole-carboxamide based p38α inhibitors to our compounds allowed us to make the assumption that these inhibitors bind to both p38α and ERK5 in the same manner. The crystal structure of **294** bound to p38α indicates that the binding mode is different to that of binding modes 1 and 2, which were predicted from the ERK2 based model. The p38α crystal structure was obtained from the protein data bank (PDB) and computationally mutated using MODELLER software to express the amino acid residues present in ERK5, retrieved from the Universal Protein Resource (Uniprot). The pyrrole-carboxamide based inhibitors were docked into the active site of the ERK5 model, according to the binding mode identified from the p38α crystal structure, and used as a template for docking the novel targets. Using COOT software, the novel ligands were inserted into the area of electron density occupied by compound **294**. Finally, energy minimisation of the protein-ligand complex identified the most energetically favourable conformation. The processes involved in creating this homology model (excluding energy minimisation) are summarised in Figure **46**. Crucially, a key difference in the portion of the binding site surrounding the aroyl motif of the ligand was identified. In ERK5, residue 165 is glycine; the smallest amino acid. This gives rise to a deep pocket which differs in shape to that of p38α, offering a third avenue towards achieving selectivity for ERK5 over p38α. Homology modelling using this new strategy suggested that a range of alkyl substituents, namely 2-ethyl, cyclopropyl and ethynyl would be tolerated (Figure **47**) in ERK5.

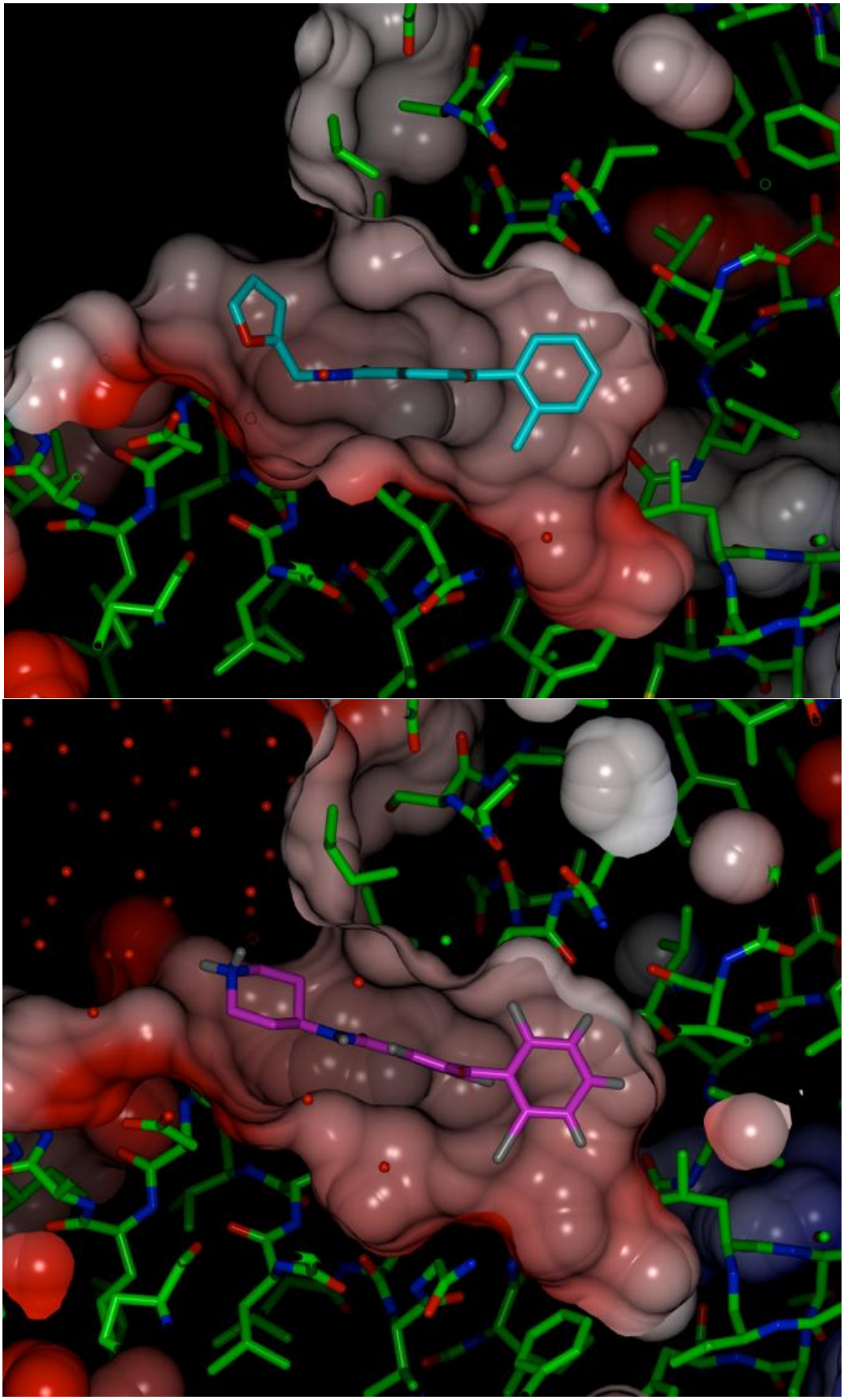

Figure 45: Top; Compound **294** bound in the active site of p38α, using PDB file. Bottom; Compound **292** bound in the active site of ERK5 mutated p38α model.

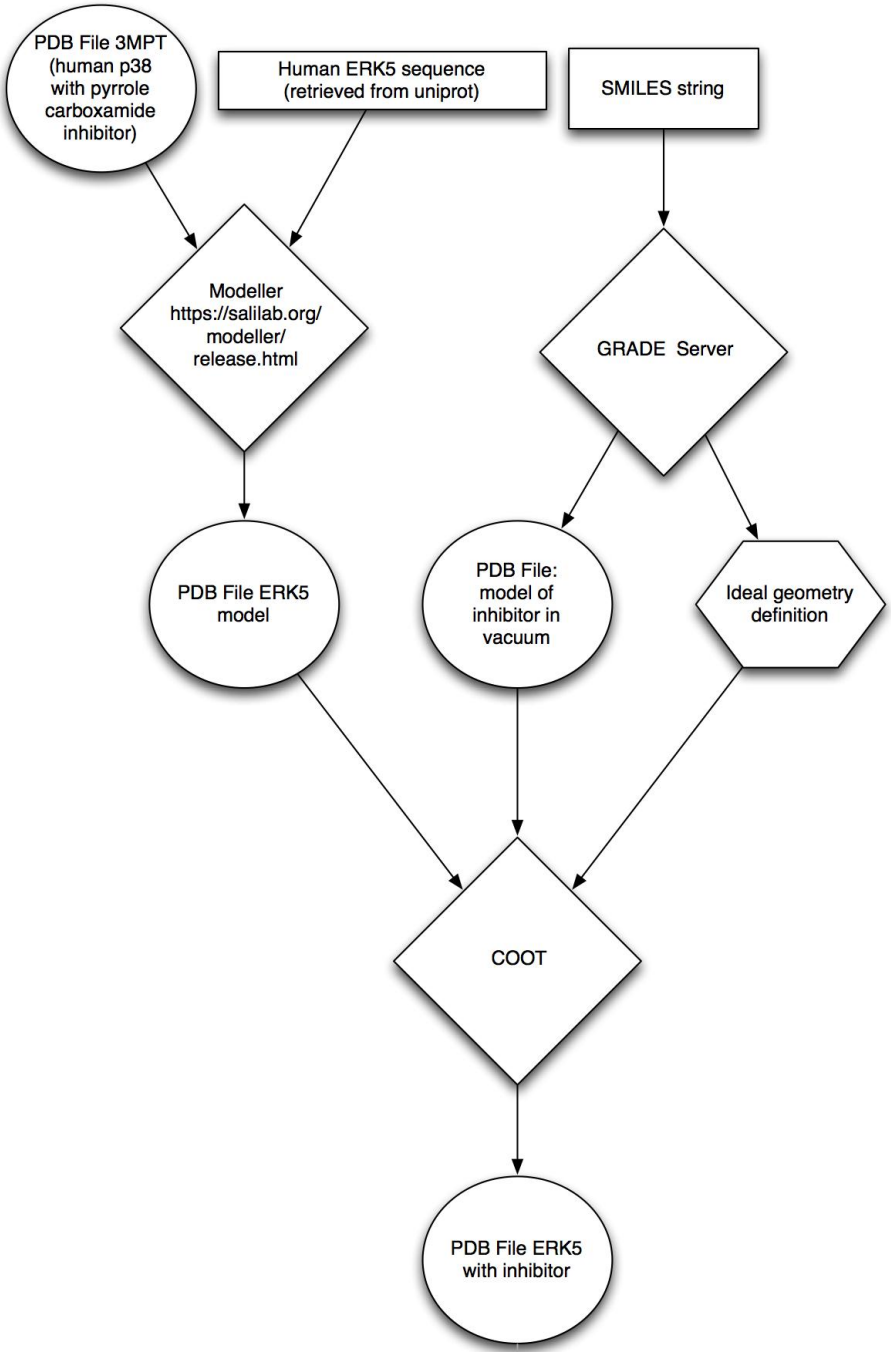

Figure 46: Sequence of processes involved in designing and utilising the current ERK5 homology model

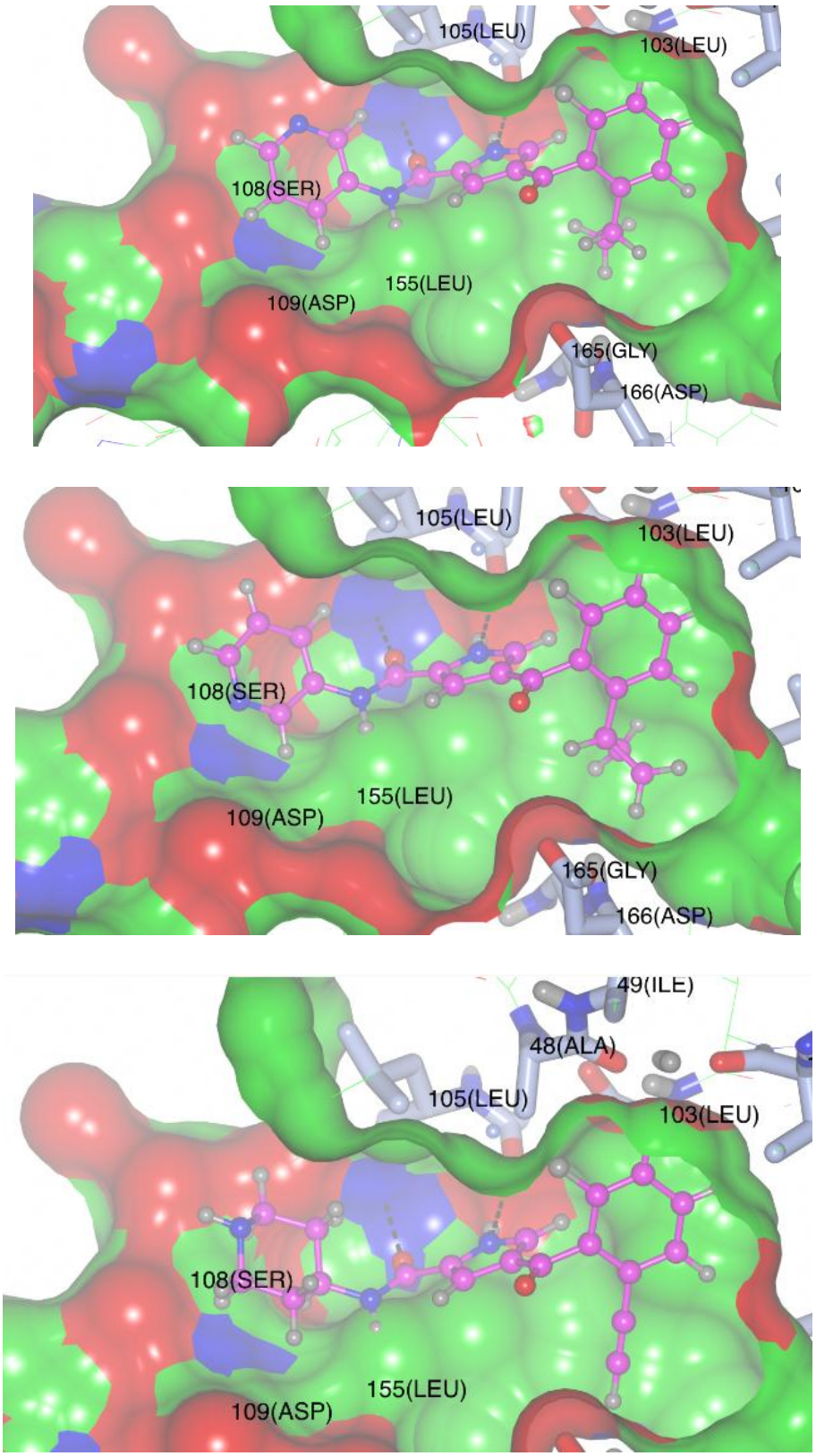

Figure 47: Homology modelling of 2-ethyl **300** (top), 2-cyclopropyl **306** (middle) and 2-ethynyl **310** (bottom) substituted analogues in the ERK5 active site.

Synthesis of 2-methyl, 6-fluoro analogues **266** and **291** indicated that a methyl group was tolerated in the *ortho*-position, but not as active as the di-halogenated analogues. Incorporation of larger alkyl substituents was investigated, which aimed to access the allosteric site *via* the 2-position (Table **47**). The three carboxamide side-chains; 3-pyridyl, piperidine and *N*-methyl piperidine, were selected to achieve the greatest potency, while maintaining desirable physicochemical properties.

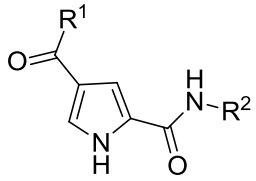

Table 47: Proposed series for investigation of 2-position substituents

Compound	R^1	R^2
300/301/302	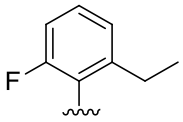	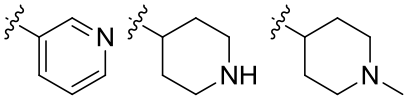
303/304/305	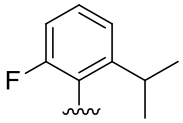	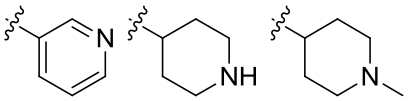
306/307/308	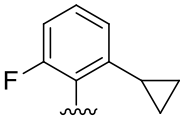	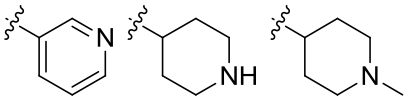
309/310/311	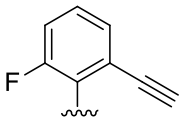	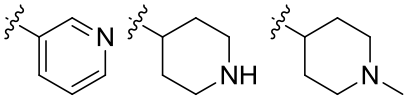

6.7.6.1 Synthesis of ortho-Alkyl Analogues

As a number of compounds had been synthesised with a bromine atom in the 2-position (Section **6.7.4**), it was evident that palladium-mediated couplings could be exploited for the insertion of a range of alkyl or alkynyl substituents. The initial strategy (Scheme **38**) utilised the previously optimised Suzuki coupling conditions to introduce the ethyl group into the *ortho*-position of methyl 2-bromo-6-fluorobenzoate, **313**. Methylation of carboxylic acid **312** using *o*-methyl-*N*,*N*'-diisopropylisourea under microwave irradiation was achieved in 87%. The subsequent Suzuki coupling with ethylboronic acid proceeded in 66%. Ester **314** was

then converted to the corresponding carboxylic acid, **318**. Base-catalysed hydrolysis of ester **314** was attempted using the conditions outlined previously in Scheme **24**. Unfortunately, no conversion to the acid **318** was observed. Demethylation of **314** was achieved *via* a microwave-assisted reaction with lithium chloride in DMF in 75% yield.[119] Conversion to the acid chloride followed by Friedel-Crafts acylation on methyl 1*H*-pyrrole-2-carboxylate **166** gave ester **320** in 83% yield. Hydrolysis of pyrrole-ester **320** proceeded quantitatively, and couplings mediated by CDI or PCl_3 gave amides **300**, **302** and **322** in excellent yields (65-72%). Finally, Boc deprotection to give piperidine analogue **301** proceeded in 93% (Scheme **39**). Following the successful synthesis of the *ortho*-ethyl analogues, the method was applied for synthesis of *ortho*-cyclopropyl and isopropyl analogues. Suzuki coupling with cyclopropylboronic acid and demethylation reactions proceeded in 76% and 64% respectively. However, coupling with isopropylboronic was less successful, achieving a low yield of 16%, attributed to steric hindrance of the boronic acid by the isopropyl group. Isopropenylboronic acid was utilised in the reaction, as it was thought that the boronic acid would be less sterically encumbered than in the isopropyl analogue. Successful conversion to the product was observed by LCMS in approximately 66%. Reduction of the alkene bond was to be performed in the final step of the synthesis, to give both isopropenyl and isopropyl target compounds, to compare the slightly different geometries of the two groups.

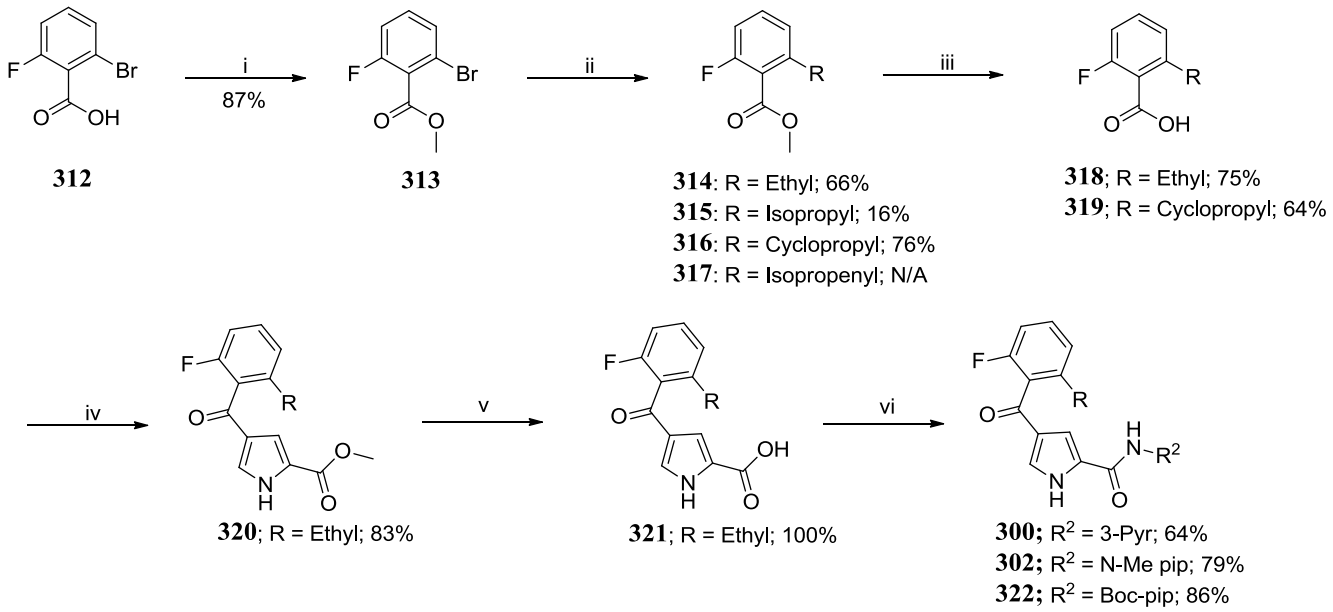

Scheme 38: *Reagents and Conditions;* i) *O*-methyl-*N,N'*-diisopropylisourea, MeCN, 120 ^{o}C, MW, 5 min; ii) $RB(OH)_2$, Cs_2CO_3, $Pd(dtbf)Cl_2$, dioxane, 110 ^{o}C, 16 h; iii) LiCl, DMF, 150 ^{o}C, MW, 1 h; iv) $SOCl_2$, cat DMF, THF, RT, 3 h, then $AlCl_3$, methyl 1*H*-pyrrole-2-carboxylate, DCM, 0 ^{o}C-RT, 16 h; v) LiOH monohydrate, H_2O/THF, 65 ^{o}C, 16 h; vi) For R^2 = 3-pyridyl; PCl_3, 3-aminopyridine, MeCN, 150 ^{o}C, MW, 5 min; For R^2 = Boc-piperidine, *N*-methyl piperidine; CDI, THF, 70 ^{o}C, 3 h then R^2NH_2, 50 ^{o}C, 3 h.

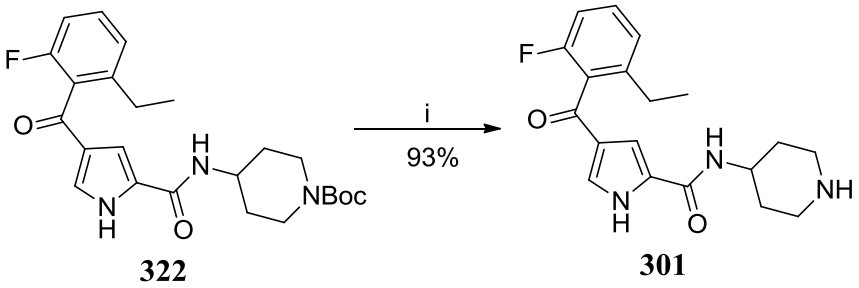

Scheme 39: *Reagents and Conditions;* i) TFA, triethylsilane, DCM, RT, 1 h.

Unfortunately, use of 2-cyclopropyl-6-fluorobenzoyl chloride with $AlCl_3$ in the Friedel-Crafts acylation step did not give any of the desired product, and recovery of starting material was not possible. It is likely that nucleophilic attack of a chloride ion generated during the reaction results in ring-opening of the cyclopropane moiety (E.g. Scheme **40**). Similar problems were predicted during Friedel-Crafts acylation with an isopropenyl analogue and so the synthesis of *ortho*-isopropyl and isopropenyl analogues was suspended, pending

biological results in this series. It was evident that an alternative synthetic strategy would be required for the synthesis of the cyclopropyl analogues **306**, **307** and **308**.

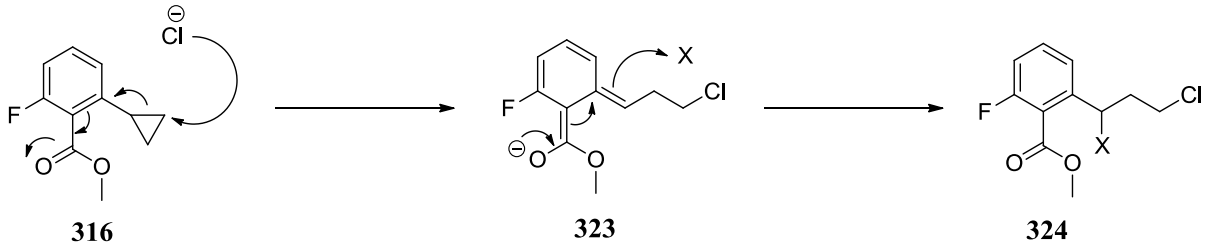

316 **323** **324**

Scheme 40: Proposed cyclopropane ring-opening *via* attack of nucleophilic chloride ion

It was desirable to introduce the cyclopropyl motif after Friedel-Crafts acylation of the relevant pyrrole-species had been performed. Protection of aroyl substituted pyrrole **325** with a tosyl group enabled a Suzuki coupling to be performed under microwave-assisted conditions. Using conventional heating (110 ^{o}C, 16 h), extensive reductive dehalogention occurred. Under the microwave-assisted conditions employed, the tosyl group was found to be partially cleaved, following Suzuki coupling with the relevant boronic acid. Due to this observation, hydrolysis of the ester and remaining tosyl groups was performed, without further purification. Carboxylic acid **326** was obtained in a good yield, 76% over the two steps. CDI couplings with *tert*-butyl 4-aminopiperidine-1-carboxylate and 4-amino-1-methyl piperidine proceeded in excellent yields (74% and 58% respectively). The PCl_3 mediated coupling was much lower yielding than expected (30%). During the course of this reaction HCl is generated, which may have resulted in a similar ring-opening side reaction to that described previously, under the harsh coupling conditions. Deprotection of the Boc-protected piperidine analogue **328** gave the secondary amine **307** in 65% (Scheme **42**). Following successful synthesis of cyclopropyl analogues **306**, **307** and **308** the method was applied for the synthesis of alkynyl analogues, using 2-((*tert*-butyldimethylsilanyl)ethynyl) boronic acid pinacol ester. Monitoring of the Suzuki coupling by LCMS indicated high conversion (>50%). Hydrolysis of the tosyl and ester groups proceeded quantitatively by LCMS, and the silyl protecting group was also cleaved under the reaction conditions. However, purification of the carboxylic acid **327** was challenging, as the compound appeared to be unstable in solution, highlighted by a distinct colour change. Purification by semi-preparative HPLC under neutral conditions gave acid **327** in a low yield of 26%, attributed to the instability of the product. Due to the low yield obtained and the concerns over instability of **327**, only one amide coupling reaction was attempted. A CDI-mediated coupling of acid **327** with 4-amino-1-methyl piperidine was performed at RT, to give amide **311** in 50% yield. The PCl_3 coupling

conditions which would be employed for synthesis of the 3-pyridyl analogue **309**, were deemed too harsh for use with this intermediate.

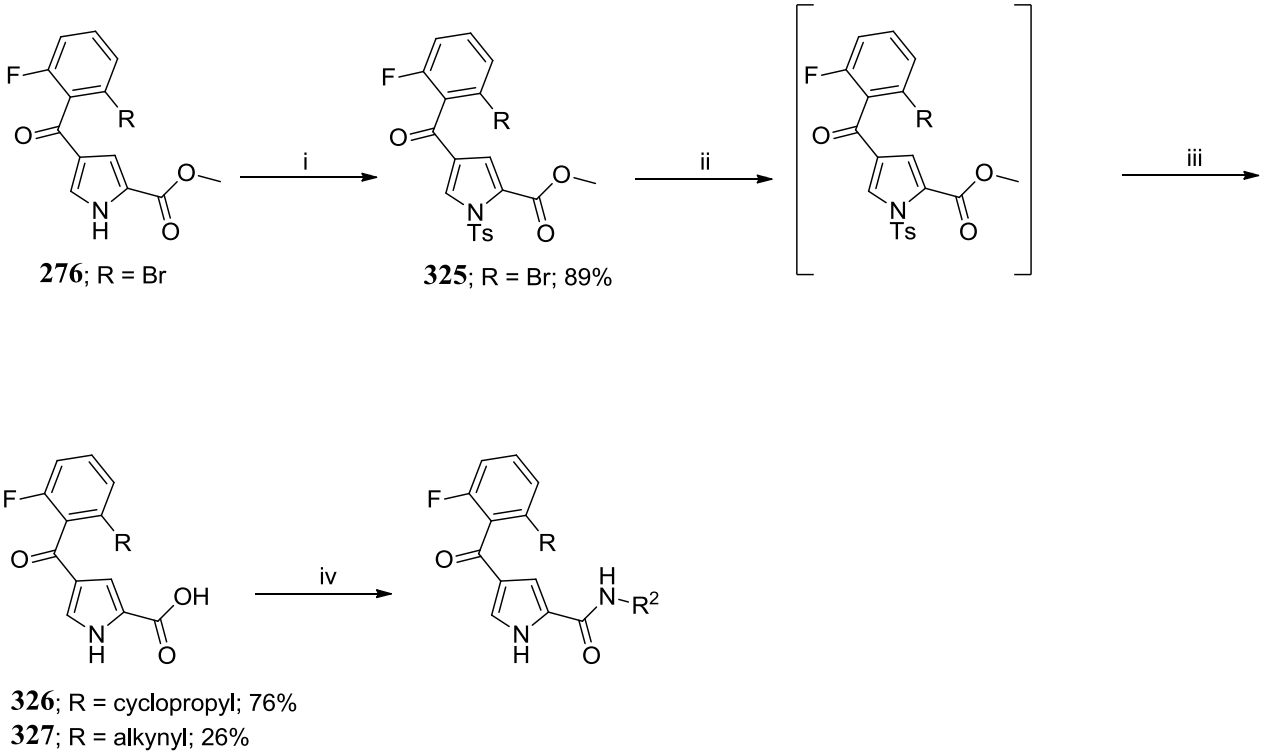

276; R = Br

325; R = Br; 89%

326; R = cyclopropyl; 76%

327; R = alkynyl; 26%

Scheme 41: *Reagents and Conditions;* i) TsCl, KO^{t}Bu, 0 ^{o}C-RT, 16 h; ii) cyclopropylboronic acid or 2-((*tert*-butyldimethylsilanyl)ethynyl) boronic acid pinacol ester, Cs_2CO_3, Pd(dtbf)Cl_2, dioxane, 150 ^{o}C, MW, 1 h; iii) LiOH monohydrate, H_2O/THF, 65 ^{o}C, 16 h; iv) For R^2 = 3-pyridyl; PCl_3, 3-aminopyridine, MeCN, 150 ^{o}C, MW, 5 min; For R^2 = Boc-piperidine, *N*-methyl piperidine; CDI, THF, 70 ^{o}C, 3 h then R^2NH_2, 50 ^{o}C, 3 h.

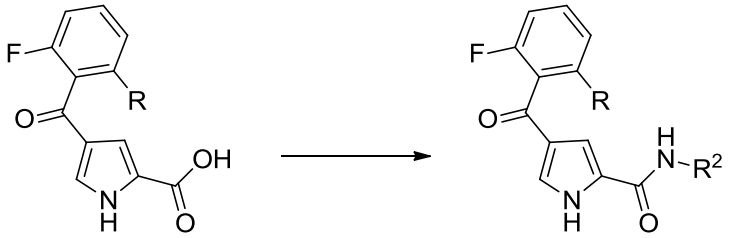

Table 48: Synthesis summary for amide couplings

Compound	R	R^2	Coupling Reagent	Coupling Yield (%)
306		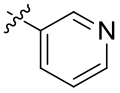	PCl_3	30
328		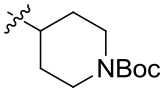	CDI	74
308		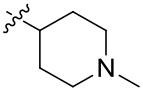	CDI	58
311		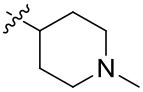	CDI	50

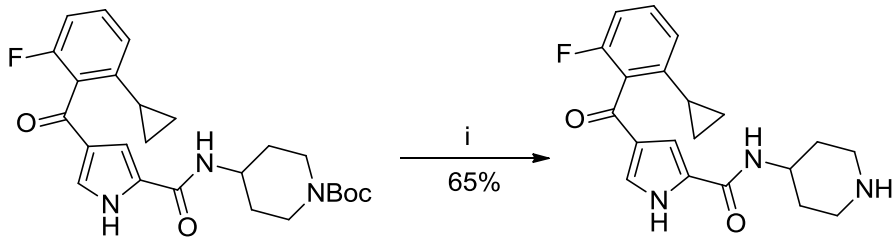

326 **304**

Scheme 42: *Reagents and Conditions;* i) TFA, triethylsilane, DCM, RT, 1 h.

6.7.6.2 Additional SARs Around the ortho-Position

Previous SAR data had revealed that the substitution pattern around the aroyl ring was essential for activity. The most potent compounds in the series to date (i.e. 2-chloro-6-fluoro compound **272** and 2-bromo-6-fluoro compound **278**; IC_{50} values = 0.6 and 0.8 μM; respectively) contain a larger group in one *ortho*-position in the ring, maximising steric contacts with the protein. Introduction of a methyl group is tolerated, but compounds bearing the 2-fluoro, 6-methyl motif are not as potent as their di-halogenated counterparts (e.g. **267**;

IC_{50} = 2.6 μM). Incorporation of larger alkyl substituents aimed to access the allosteric pocket, which seemed possible following homology modelling. Unfortunately, the larger substituents were not tolerated. The addition of ethyl or cyclopropyl groups in the *ortho*-position appears to be particularly detrimental when combined with the rigid 3-pyridyl carboxamide substituent. Analogues containing the more flexible piperidine side-chains are more potent (e.g **302**; IC_{50} = 5.0 μM). However, selectivity over p38α is lost with the piperidine analogues. It is likely that the three-dimensional shape of the side-chain influences the tolerance of the *ortho*-substituent, by subtle changes in overall 3D structure of the inhibitor.

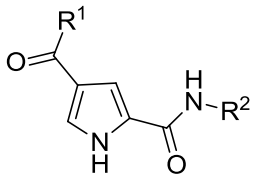

Table 49: ERK5 inhibitory activity of 2-substituted alkyl analogues

Compound	R^1	R^2	ERK5 IC_{50} (μM)[a]	p38α IC_{50} (μM)[a]
267	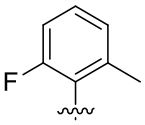	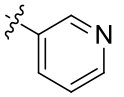	2.6 ± 0.7[b]	54.0 ± 7.1
300	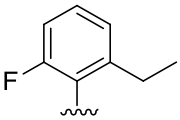	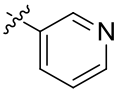	12.7 ± 4.4	>120
301	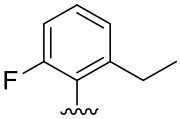	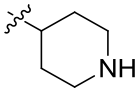	5.0 ± 0.6	43.1 ± 7.9
302	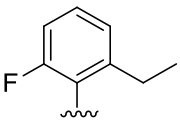	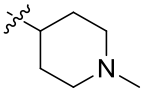	5.0 ± 2.0	45.7 ± 1.9
306	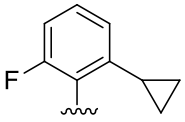	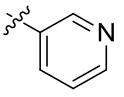	23.0 ± 3.9	>120
307	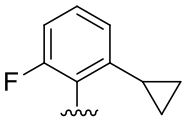	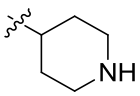	5.8 ± 0.5	45.0 ± 6.2

308	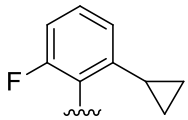	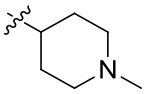	8.2 ± 0.1	57.1 ± 1.2
311	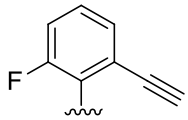	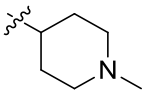	2.6 ± 0.05	52.9 ± 0.01

[a] Determinations ± standard deviation (mean of n = 2 unless otherwise stated); [b] n = 4.

6.7.6.3 Accessing a Possible Allosteric Pocket: Substitution at the meta-Position

Overlay of another p38α inhibitor, **329**, based around a quinazoline scaffold (p38α IC_{50} = 2.4 nM ± 1.3) illustrates the space available for compounds probing the allosteric site, which appears to be accessible *via* the 3-position of the aroyl moiety. Quinazoline **329** makes a hydrogen bond with the backbone NH of an aspartate residue (Asp168), which is present on the activation loop. A second hydrogen bond interaction is between Glu71 and the amide NH of compound **329**.[128]

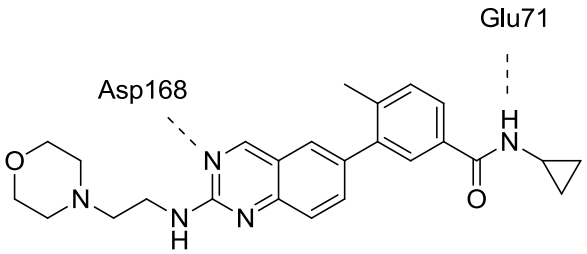

329

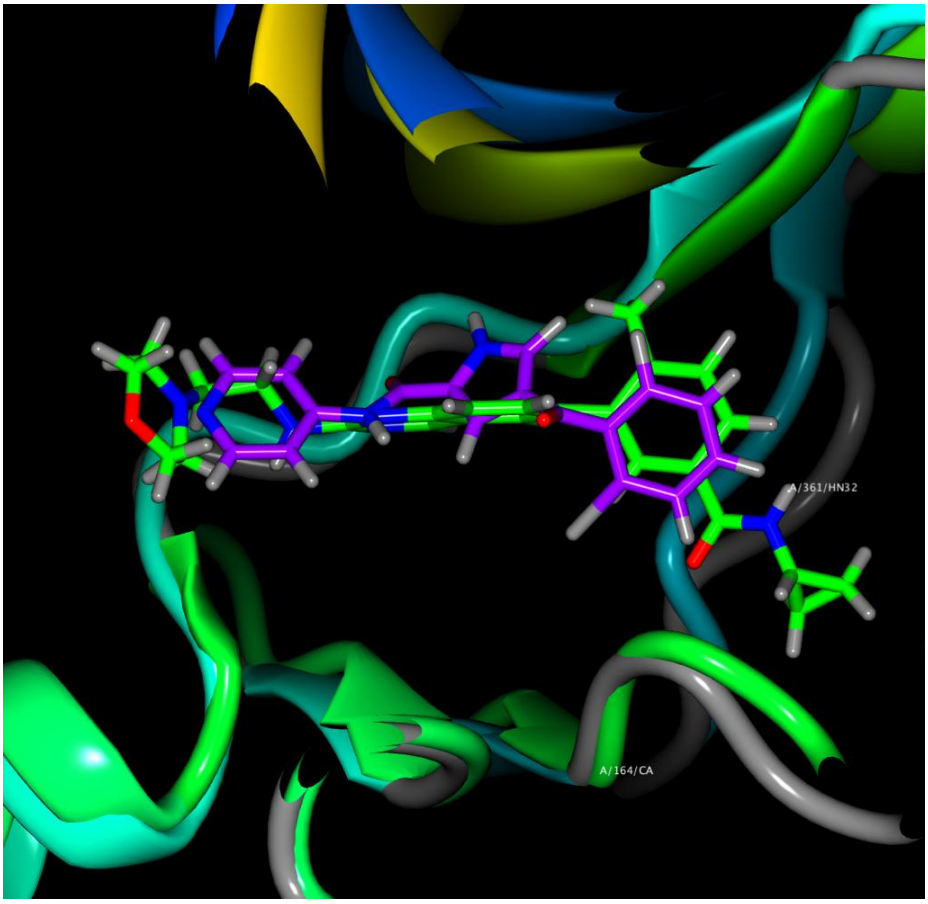

Figure 48: Docking of pyrrole-carboxamide scaffold (magenta) superimposed with quinazoline based p38α inhibitor **329** (green).

A range of analogues were synthesised to investigate whether *meta*-substitution of the aroyl ring was tolerated. Fluoro-, chloro- and methyl groups were incorporated to establish whether further decoration of the aroyl motif would enhance potency. It was envisaged that a halogen in the 3-position (particularly chlorine or bromine) would enable palladium-mediated couplings to install additional functional groups at a later date if desired. At this stage in hit-to-lead drug discovery, it was decided that replacement of the 3-pyridyl motif would be desirable. Inhibition of the CYP family of enzymes *via* interactions of strongly basic and/or acidic groups is a common challenge to overcome in drug discovery. One replacement for pyridine which may reduce the degree of CYP inhibition is the pyrimidine moiety.[129] The pyrimidine group is the same shape and size as the pyridyl, but the pK_a of the nitrogen lone pair is significantly attenuated by the presence of a second electron withdrawing atom in the ring (i.e. pK_a of pyridine = 5.2; pK_a of pyrimidine = 1.1). Other strategies considered for reducing CYP inhibition included incorporation of one or two methyl groups adjacent to the pyridine nitrogen, to sterically encumber the nitrogen lone-pair. However, this would increase

the lipophilicity of the molecule, and so the pyrimidine was considered a more suitable replacement. Pyrimidine analogues were synthesised containing selected aroyl motifs.

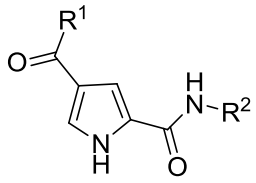

Table 50: Proposed series of compounds with *meta*-substitution

R^1	**R^2**
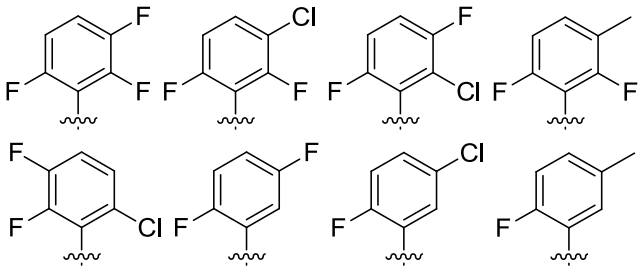	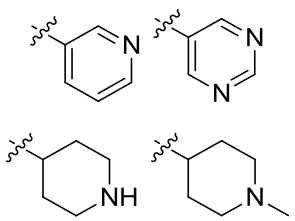

6.7.6.4 Synthesis of Analogues with Substitution at the meta-Position

The optimised Scheme **24** was applied for the parallel synthesis of *meta*-substituted analogues. Friedel-Crafts acylation proceeded successfully in all cases (59-95%) and subsequent hydrolyses were quantitative. PCl_3-mediated amide couplings on the relevant carboxylic acids with 3-aminopyridine were all successful after 5 min at 150 ^oC. However, couplings were significantly slower with 3,5-aminopyrimidine. The reactions with the unreactive pyrimidine were heated in cycles at 150 ^oC for up to 30 min in order to reach completion. Yields were variable, ranging from 41-95%. The CDI mediated amide couplings for piperidine analogues proceeded in variable but good yields (54-100%). Deprotection of the Boc group gave piperidine analogues in greater than 90% in all cases, except with 2-fluoro, 6-methyl compound **383** (Table **52**). In this instance, the product obtained was a hygroscopic solid. Conversion of the free base to the corresponding TFA or HCl salts was attempted, but both forms were also found to be hygroscopic.

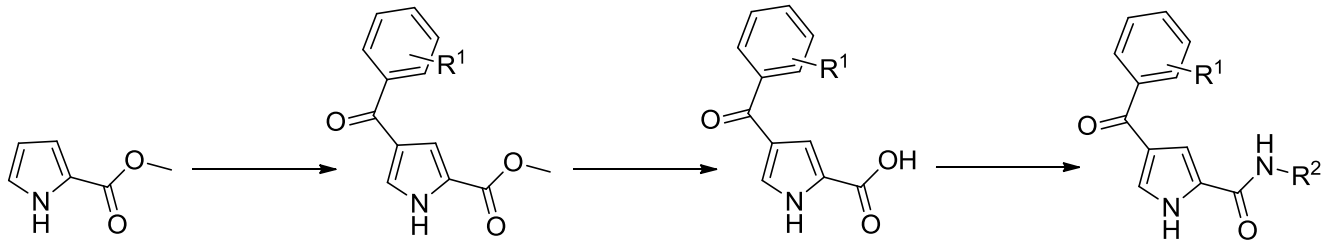

Table 51: Synthesis summary for compounds with *meta*-substitution

R^1	R^2	Friedel-Crafts Yield (%)	Hydrolysis Yield (%)	Amide Coupling Yield (%)
2,3,6-TriF	3-Pyridine	**330**; 95	**331**; 100	**332**; 41[a]
2,3,6-TriF	3,5-Pyrimidine			**333**; 52[a]
2,3,6-TriF	Boc-Piperidine			**334**; 93[b]
2,3,6-TriF	*N*-Me piperidine			**335**; 71[b]
3-Cl, 2,6-DiF	3-Pyridine	**336**; 90	**337**; 100	**335**; 95[a]
3-Cl, 2,6-DiF	3,5-Pyrimidine			**339**; 46[a]
3-Cl, 2,6-DiF	Boc-Piperidine			**340**; 87[b]
3-Cl, 2,6-DiF	*N*-Me piperidine			**341**; 88[b]
2-Cl, 3,6-DiF	3-Pyridine	**342**; 94	**343**; 98	**344**; 58[a]
2-Cl, 3,6-DiF	Boc-Piperidine			**345**; 85[b]
2-Cl, 3,6-DiF	*N*-Me piperidine			**346**; 98[b]
2,6-DiF, 3-Me	3-Pyridine	**347**; 94	**348**; 98	**349**; 92[a]
2,6-DiF, 3-Me	3,5-Pyrimidine			**350**; 51[a]
2,6-DiF, 3-Me	Boc-Piperidine			**351**; 68[b]
2,6-DiF, 3-Me	*N*-Me piperidine			**352**; 88[b]
6-Cl, 2,3-DiF	3-Pyridine	**353**; 59	**354**; 100	**355**; 57[a]
6-Cl, 2,3-DiF	3,5-Pyrimidine			**356**; 55[a]
6-Cl, 2,3-DiF	Boc-Piperidine			**357**; 91[b]
6-Cl, 2,3-DiF	*N*-Me piperidine			**358**; 68[b]
2,5-DiF	3-Pyridine	**359**; 93	**360**; 100	**361**; 41[a]
2,5-DiF	Boc-Piperidine			**362**; 87[b]
2,5-DiF	*N*-Me piperidine			**363**; 100[b]

5-Cl, 2-F	3-Pyridine	**364**; 87	**365**; 98	**366**; 91[a]
5-Cl, 2-F	3,5-Pyrimidine			**367**; 42[a]
5-Cl, 2-F	Boc-Piperidine			**368**; 74[b]
5-Cl, 2-F	*N*-Me piperidine			**369**; 100[b]
2-F, 5-Me	3-Pyridine	**370**; 86	**371**; 99	**372**; 89[a]
2-F, 5-Me	3,5-Pyrimidine			**373**; 49[a]
2-F, 5-Me	Boc-Piperidine			**374**; 54[b]
2-F, 5-Me	*N*-Me piperidine			**375**; 88[b]

[a] PCl_3 mediated amide coupling; [b] CDI mediated amide coupling.

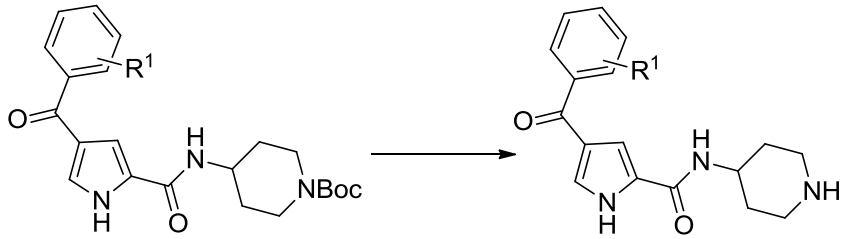

Table 52: Synthesis summary for deprotection of Boc-piperidines

Compound	R^1	Yield (%)
376	2,3,6-TriF	95
377	3-Cl, 2,6-DiF	97
378	2-Cl, 3,6-DiF	94
379	2,6-DiF, 3-Me	93
380	6-Cl, 2,3-DiF	95
381	2,5-DiF	95
382	5-Cl, 2-F	100
383	2-F, 5-Me	NR – Hygroscopic solid

6.7.6.5 SARs for Substitution at the meta-Position

The data show that substitution in both *ortho*-positions is crucial for sub-micromolar ERK5 activity. All compounds with trisubstitution are well tolerated, with IC_{50} values $\leq$ 1.0 μM. The 3-chloro-2, 6-difluoro substitution pattern confers the best overall potency, with all four carboxamide side-chains well tolerated in the binding site (IC_{50} = 140-240 nM). The 6-chloro, 2, 3-difluoroaroyl motif when combined with the *N*-methylpiperidine side-chain, to give

compound **358** also confers high potency (110 nM). However, pyridyl and pyrimidyl side-chains combined with the 6-chloro-2,3-difluoroaroyl scaffold (compounds **355** and **356**) confer significantly less potency (IC_{50} = 0.96 and 0.71 µM, respectively). All compounds containing aromatic side-chains were completely inactive against p38α. Although selectivity for ERK5 over p38α is somewhat reduced when incorporating non-aromatic side-chains, all compounds retain at least 25-fold selectivity, with the exception of the less potent 2-, 5-substituted analogues. No further *in vitro* pharmacology or DMPK studies have been carried out for this set of compounds as of yet, but may be evaluated in future studies.

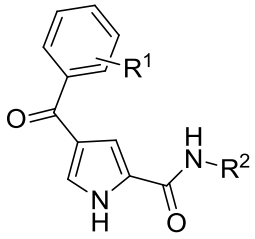

Table 53: ERK5 inhibitory activity of tri- and di-substituted analogues

Compound	R^1	R^2	ERK5 IC_{50} (µM)[a]	p38α IC_{50} (µM)[a]
332	2,3,6-TriF	3-Pyridine	0.40 ± 0.10	>120
333	2,3,6-TriF	3,5-Pyrimidine	0.94 ± 0.14	>120
376	2,3,6-TriF	Piperidine	0.73 ± 0.02	35.9 ± 6.0
335	2,3,6-TriF	*N*-Me piperidine	0.57 ± 0.10	29.3 ± 0.5
338	3-Cl, 2,6-DiF	3-Pyridine	0.20 ± 0.05	>120
339	3-Cl, 2,6-DiF	3,5-Pyrimidine	0.24 ± 0.02	>120
377	3-Cl, 2,6-DiF	Piperidine	0.24 ± 0.01	39.1 ± 7.8
340	3-Cl, 2,6-DiF	*N*-Me piperidine	0.14 ± 0.02	28.9 ± 5.2
344	2-Cl, 3,6-DiF	3-Pyridine	1.00 ± 0.28	>120
378	2-Cl, 3,6-DiF	Piperidine	0.76 ± 0.01	31.9 ± 6.5
346	2-Cl, 3,6-DiF	*N*-Me piperidine	0.80 ± 0.00	20.4 ± 0.7
348	2,6-DiF, 3-Me	3-Pyridine	0.42 ± 0.10	>120
350	2,6-DiF, 3-Me	3,5-Pyrimidine	0.76 ± 0.09	>120
379	2,6-DiF, 3-Me	Piperidine	0.44 ± 0.02	65.9 ± 5.1
352	2,6-DiF, 3-Me	*N*-Me piperidine	0.39 ± 0.02	40.2 ± 3.3

354	6-Cl, 2,3-DiF	3-Pyridine	0.96 ± 0.15	>120
356	6-Cl, 2,3-DiF	3,5-Pyrimidine	0.71 ± 0.02	>120
380	6-Cl, 2,3-DiF	Piperidine	0.21 ± 0.07	38.0 ± 0.09
358	6-Cl, 2,3-DiF	*N*-Me piperidine	0.11 ± 0.00	49.8 ± 6.4
361	2,5-DiF	3-Pyridine	6.0 ± 0.6	>120
381	2,5-DiF	Piperidine	8.6 ± 0.4	52.7[b]
357	2,5-DiF	*N*-Me piperidine	6.2 ± 0.1	52.6 ± 4.9
366	5-Cl, 2-F	3-Pyridine	1.2[b]	>120
367	5-Cl, 2-F	3,5-Pyrimidine	1.6 ± 0.3	>120
382	5-Cl, 2-F	Piperidine	1.7 ± 0.1	44.1 ± 4.8
369	5-Cl, 2-F	*N*-Me piperidine	1.9 ± 0.2	30.9 ± 7.3
372	2-F, 5-Me	3-Pyridine	4.0 ± 0.6	>120
373	2-F, 5-Me	3,5-Pyrimidine	5.2 ± 0.3	>120
375	2-F, 5-Me	*N*-Me piperidine	4.4 ± 0.5	15.9 ± 2.3

[a] Determinations ± standard deviation (mean of n = 2 unless otherwise stated); [b] n = 1. NB: Green – ERK5 $IC_{50} \leq 0.5$ µM; Amber – ERK5 IC_{50} = 0.5-1.0 µM; Red – ERK5 IC_{50} = >1.0 µM.

6.7.7 Evaluation of Di-Substituted Aroyl Analogues as Lead Compounds

Compounds synthesised in this series with potencies ≤1 µM were evaluated according to the criteria outlined in Section **6.4** for their suitability as potential lead compounds.

6.7.7.1 Physicochemical Properties

Analysis of the physicochemical properties of the most potent 2-chloro-6-fluoro analogues indicates that the basic criteria are met. *N*-Methyl piperidine analogue **283** has a slightly lower TPSA than desired, but this was not a cause for concern at this stage. The data for the analogous 2-bromo-6-fluoro compounds were largely the same as those shown in Table **54** and for this reason, are not tabulated here. The Lipinski 'Rule of 5' states that compounds with a molecular weight below 500 amu, ≤ 5 H-bond donors and ≤ 10 H-bond acceptors, and a LogP below 5 have the greatest chance of giving rise to an orally active drug.[130] Topological polar surface area (TPSA) gives an indication of the compound's ability to cross cell membranes, and a value between 75 and 100 $Å^2$ increases the chance of good oral bioavailability, independent of molecular weight.[131]

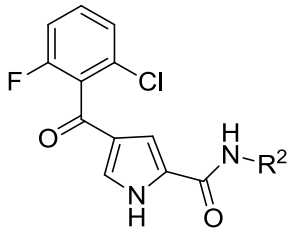

Table 54: Physicochemical properties of potent 2-chloro, 6-fluoro analogues

Compound	Lead	272/273	292	283
R^2	-	3- or 4-Pyridyl	Piperidine	N-Me Piperidine
MW	<500	344	349	363
sLogP	<5	3.1	2.0	2.6
TPSA	75-100	75	74	65
H-Bond Donor/Acceptor	<6/<10	2/5	3/5	2/5
pKa	Salt forming	Y	Y	Y

NB: Green – compound meets critera; Amber – borderline result; Red – compound fails criteria.

6.7.7.2 In Vitro Pharmacology

The *in vitro* pharmacology of the eight selected compounds was investigated. Selected compounds were screened against a panel of 131 diverse protein kinases, which was performed at the International Centre for Kinase Profiling (Dundee). hERG inhibition was measured by Cyprotex, specialists in ADME and toxicology profiling. Cellular activity in HEK293 cells was generated at the Babraham Institute by myself, in collaboration with Dr Simon Cook, assisted by Dr Pamela Lochhead. Further details of the assay procedure are described in Section **7.8**.

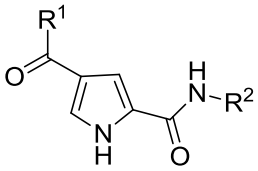

Table 55: *In vitro* pharmacology for potent compounds with pyridyl-carboxamide groups

Compound	Lead	272	273	263	278
R^1	-	2-Chloro, 6-fluoro	2-Chloro, 6-fluoro	2-Bromo, 6-fluoro	2-Bromo, 6-fluoro
R^2	-	4-Pyridyl	3-Pyridyl	4-Pyridyl	3-Pyridyl
ERK5 IC_{50} (µM)	<1	0.60 ± 0.3	0.60 ± 0.2	0.68 ± 0.2	0.82 ± 0.01
LE	>0.3	0.36	0.36	0.36	0.35
Selectivity *vs* other kinases	>10 fold	>120 fold p38α	>120 fold p38α	>120 fold p38α	>120 fold p38α; No inhibition (131 kinases
Cellular Activity (µM)	<10	2.3 ± 1.5	4.0 ± 1.4	4.0 ± 2.8	4.5 ± 2.1
hERG Activity (µM)	>25	ND	ND	ND	>25

NB: Green – compound meets critera; Amber – borderline result; Red – compound fails critera; ND – no data.

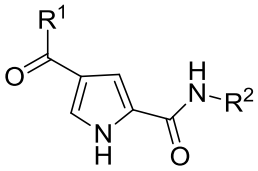

Table 56: *In vitro* pharmacology for potent compounds with piperidine based-carboxamide groups

Compound	Lead	292	283	293	287
R^1	-	2-Chloro, 6-fluoro	2-Chloro, 6-fluoro	2-Bromo, 6-fluoro	2-Bromo, 6-fluoro
R^2	-	Piperidine	*N*-Me Piperidine	Piperidine	*N*-Me Piperidine
ERK5 IC_{50} (μM)	<1	0.49 ± 0.04	0.20 ± 0.06	0.39 ± 0.12	0.29 ± 0.12
LE	>0.3	0.37	0.38	0.38	0.37
Selectivity *vs* other kinases	>10 fold	>20 fold over p38α; No inhibition (131 kinases)	>40 fold over p38α; No inhibition (131 kinases)	>45 fold over p38α.	>35 fold over p38α.
Cellular Activity (μM)	<10	3.5 ± 3.5	1.9 ± 1.0	22.0	ND
hERG Activity (μM)	>25	>25	>25	>25	ND

NB: Green – compound meets critera; Amber – borderline result; Red – compound fails critera; ND – no data.

Compounds selected for selectivity screening were inactive against a wide range of protein kinases (131 in total). In addition, all compounds show at least 20-fold activity over p38α, and no hERG inhibitory activity is detected for compounds containing each of the three selected side-chains (i.e. **292**, **283** and **278**; hERG IC_{50} >25 μM). LE is above 0.35 for all analogues. Cellular activity is below 10 μM in all cases, except piperidine analogue **293** which surprisingly, has a cellular IC_{50} of 22.0 μM (n = 1). Ligand efficiency (LE) was calculated using the formula LE = ΔG/HAC; where ΔG = -1.4 logIC_{50}.

6.7.7.3 In Vitro DMPK Data

Preliminary assessment of drug metabolism and pharmacokinetic properties was assessed *in vitro*. Solubility was assessed in a turbidimetric assay, by Cyprotex. Plasma protein binding (PPB), mouse/human microsomal stability, Caco-2 permeability and CYP inhibition assays were also performed by Cyprotex. Inhibition of the following CYP isoforms was measured; 1A, 2C19, 2C9, 2D6, and 3A4.

Table 57: *In vitro* DMPK data for selected pyridyl analogues

Compound	**Lead**	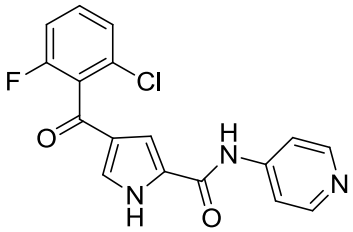 **272**	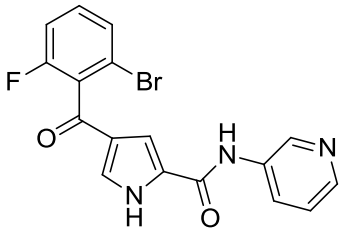 **278**
Solubility (µM)	>50	37.5	>100
PPB (%)	<99	ND	94
MLM Clearance (µL/min/mg)	<48	56	20
HLM Clearance (µL/min/mg)	<48	10	0
Caco-2 A2B Papp ($x10^{-6}$ cm/s)	>10	ND	34
Efflux Ratio	<2	ND	0.82
CYP Inhibition IC_{50} (µM)	All >10	0.07 (2C19), 0.35 (2C9), 1.11 (2D6), 1.24 (3A4)	All >5

NB: Green – compound meets critera; Amber – borderline result; Red – compound fails critera; ND – no data.

Table 58: *In vitro* DMPK data for selected piperidine based analogues

Compound	Lead	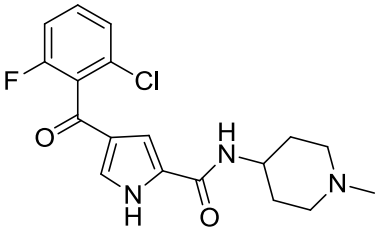 **283**	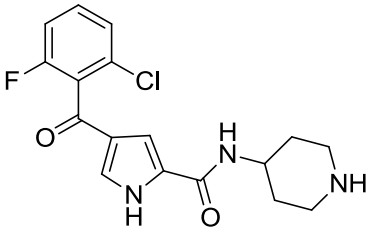 **292**
Solubility (µM)	>50	>100	>100
PPB (%)	<99	68	50
MLM Clearance (µL/min/mg)	<48	8	1
HLM Clearance (µL/min/mg)	<48	0	2
Caco-2 A2B Papp ($x10^{-6}$ cm/s)	>10	3.8	0.38
Efflux Ratio	<2	9.0	8.3
CYP Inhibition IC_{50} (µM)	All >10	All >15	All >10

NB: Green – compound meets critera; Amber – borderline result; Red – compound fails critera; ND – no data.

As anticipated, compounds containing the 4-pyridyl motif (i.e. **272**) were found to be potent inhibitors of the CYP enzymes (0.07-1.24 µM). Interestingly, when the pyridine nitrogen atom is shifted to the 3-position, CYP inhibition is significantly decreased, and microsomal stability increased. It is evident that when in the 4-position, the pyridyl nitrogen lone pair increases the compound's affinity for the CYP enzyme, both as an inhibitor and substrate. Aqueous solubility is also superior for 3-pyridyl analogue **278**. Piperidine analogues **283** and **292** also displayed excellent aqueous solubility (> 100 µM), with seemingly low affinity for CYP, demonstrated by high microsomal stability and lack of CYP inhibition characteristics. Unfortunately, the piperidine analogues both display low permeability properties, as demonstrated by the Caco-2 assay. Furthermore, the efflux ratio suggests that the compounds may be a substrate for P-glycoprotein 1 (P-gp). P-gp efflux is strongly associated with the presence of hydrogen-bond donors, particularly bases.[132] The less basic 3-pyridyl analogue

278 shows no propensity for poor permeability as a result of P-gp efflux, supporting this hypothesis. Based on these observations, it is predicted that pyrimidine analogues will have less affinity for the CYP enzymes, and for P-gp. Considering the data generated investigating *in vitro* DMPK characteristics of pyrrole-carboxamide compounds, 3-pyridyl analogue **278** was progressed for *in vivo* DMPK and efficacy evaluation.

6.7.7.4 In Vivo DMPK and Efficacy Studies

A single 10 or 100 mg/kg oral dose was administered to CD1 mice. Sample collection (plasma and tumour tissue) at five time points following oral dosing, enabled measurement of the pharmacokinetic properties of **278** (Figure **49**). Tumour pharmacokinetic studies were performed using mice bearing a HCT116 human colorectal tumour xenograft. Intravenous and intraperitoneal dosing at 10 and 100 mg/kg was also performed; data is summarised in Table **59**. Oral bioavailability is excellent at 68%, greatly exceeding the lead criteria (30%). In addition, the half-life of compound **278** is measured at 65 minutes. Clearance following oral dosing is higher than desired at 39 mL/min/kg. However, clearance following IV and IP dosing is within the desired range.

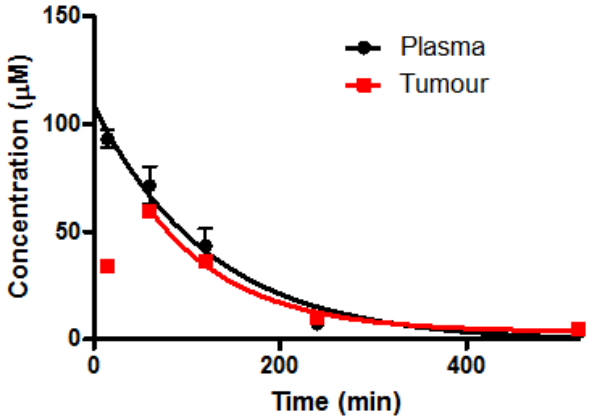

Figure 49: Pharmacokinetic study of compound **278** in CD1 mice, following 10 mg/kg oral dosing for plasma PK and 100 mg/kg for tumour tissue PK (HCT116 human colorectal tumour xenograft).

Table 59: Summary of pharmacokinetic properties of **278** following 10 mg/kg PO, IP or IV dosing.

Parameter	Lead	PO Dosing	IP Dosing	IV Dosing
Dose (mg/kg)	-	10	10	10
AUC inf (µg/mL.min)	-	254	398	372
Cmax (µM)	-	6	12	25
Vdss (L/kg)	>1	-	-	1.2
Tmax (min)	-	15	15	5
Half-life (min)	>60	65	43	38
Clearance (mL/min/kg)	<30	39	25	27
Bioavailability, F (%)	>30	68	108	-

NB: Green – compound meets critera; Amber – borderline result; Red – compound fails critera.

Compound **278** was assessed for *in vivo* efficacy using two techniques; a human tumour xenograft model and a Matrigel plug angiogenesis assay. Comparison with competitor compound XMD8-92, **33** (structure on page **43**) was performed in each case.

6.7.7.4.1 Matrigel Plug Assay

Matrigel may be administered, and solidifies giving a plug; administration of the drug is performed *via* the desired route, i.e. PO, IP, or IV. This allows permeation of the plug by host cells, which form new blood vessels. Administration of an anti-angiogenic agent reduces the degree of blood vessel formation, to the tumour mimic. Histological examination of the plug 7-21 days after dosing allows determination of the extent to which blood vessels have entered the plug.[133] Matrigel containing basic fibroblast growth factor (bFGF) was injected sub-cutanously into 15 CD1 mice which induces angiogenesis. 24 hours post dosing, mice were randomised to receive either vehicle, 50 mg/kg XMD8-92 IP twice daily for 7 days or **278** PO twice daily for 7 days. On day 7, mice were sacrificed; Matrigel plugs were removed and snap frozen in liquid nitrogen. Haemoglobin was measured using the Drabkin's method. Drabkin's reagent (containing sodium bicarbonate, potassium ferricyanide and potassium cyanide) allowed quantitative colorimetric determination of haemoglobin concentrations in blood. Analysis of the Matrigel plugs indicated that inhibition of ERK5 *in vivo* resulted in an

angiogenic effect. A significant reduction in haemoglobin levels detected when CD1 mice received Matrigel with an ERK5 inhibitor (XMD8-92 or **278**) was observed (Figure **50**). This result confirms the anti-angiogenic potential of a clinical ERK5 inhibitor.

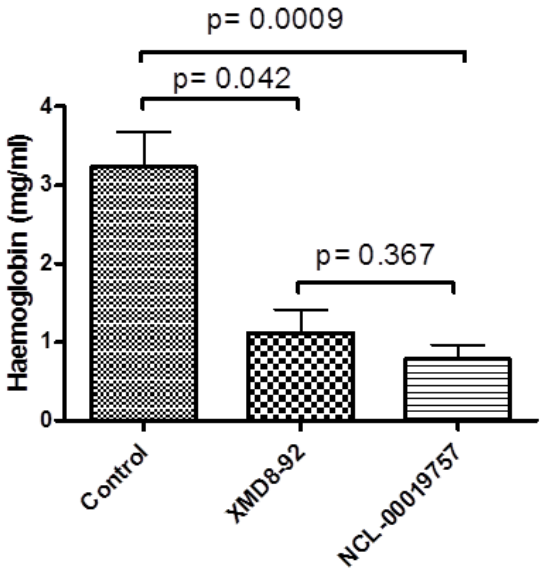

Figure 50: Haemoglobin levels from Matrigel plugs; Animals received vehicle, 50 mg/kg XMD8-92 IP twice daily for 7 days or **278** PO twice daily for 7 days.

6.7.7.4.2 Human Tumour Xenograft Models

CD1 mice were inoculated with A2780 cells (human ovarian carcinoma) cells subcutaneously, and tumour volume was allowed to develop for 7 days to an average volume of 72 mm^3. Mice were randomised to receive either vehicle, 50 mg/kg XMD8-92 IP or 100 mg/kg **278** PO twice daily for 11 days. Tumour volumes were then measured. Nadir weight was monitored as an assessment of drug toxicity. No toxicity was observed in animals dosed with pyrrole-carboxamide **278**. However, one mouse in the XMD8-92 group showed body weight loss (78% of original body weight) at day 10 of the study. Dosing with either XMD8-92 or **278** resulted in a significant decrease in tumour growth compared with the vehicle group. Pyrrole-carboxamide **278** is equipotent with XMD8-92 in terms of slowing tumour progression, but shows an improved toxicity profile (Nadir weight 98% in all cases).

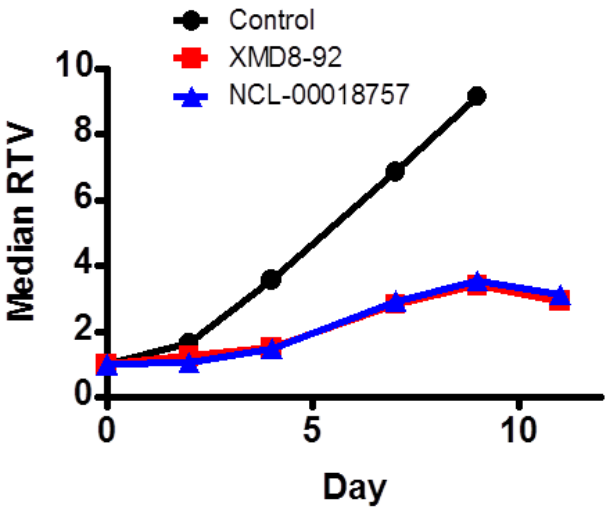

Figure 51: Treatment of CD1 mice bearing A2780 xenograft with XMD8-92 at 50 mg/kg IP or **278** at 100 mg/kg PO twice daily.

6.7.8 Replacement of the Aroyl Substituent

In parallel to the work conducted around the substitution pattern of the aroyl substituent (Sections **6.7.1**-**6.7.7**), investigation into isosteric replacement of the aroyl group was also performed.

6.7.8.1 Rationale

Previous studies had confirmed the importance of the carbonyl group, as removal of the motif or reduction to the corresponding secondary alcohol abolished activity (IC_{50} values >120 μM). The most likely explanation for this observation is the ability of the ketone to act as a hydrogen bond acceptor in the ERK5 binding site. Replacement of the carbonyl group with an isoquinoline group was probed, comparable to aroyl pyrrole **232**. Incorporation of these groups introduced rigidity to the scaffold, while maintaining a lone pair capable of hydrogen bonding. At the time of investigation, it had not yet been discovered that truncation of the carboxamide side-chain resulted in a significant increase in potency. Therefore, the CH_2-linked 4-pyridyl side-chain was incorporated into the target molecule (Figure **52**).

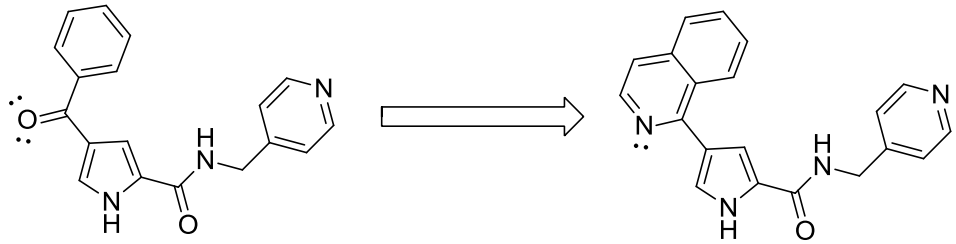

230; ERK5 IC_{50} = 40.4 μM **384**

Figure 52: Comparison of aroyl pyrrole **232** with proposed isoquinoline **384**.

6.7.8.2 Synthetic Strategy

It was initially envisaged that synthesis of isoquinoline pyrrole **384** may be achieved *via* Suzuki coupling of the relevant bromo-pyrrole, **386** with 1-(4,4,5,5-tetramethyl-1,3,2-dioxaborolan-2-yl)isoquinoline. Protection of the pyrrole nitrogen was required, to prevent deprotonation by the base and cross-coupling at this position. Suzuki coupling was performed on the pyrrole ester **387** to minimise the risk of side-reactions (Figure **53**). Initially, optimisation of the reaction with 2-pyridyl boronic acid as a model provided an intermediate towards a second target compound, **390** (Scheme **43**). However, a review of the literature revealed that 2-pyridyl boronic acids and esters are notoriously unstable and present a challenge during cross-couplings, and unsurprisingly the reaction was unsuccessful. Although complex *N*-methyliminodiacetic acid based (MIDA) boronates have been developed which reduce the instability of the boronate species,[134] it was decided in this case to reverse the coupling partners so that 2-bromopyridine was reacted with the pyrrole-3-pinacol boronic ester (Scheme **44**). Previously optimised Suzuki coupling conditions were found to give excellent, reproducible yields over 2 steps.[135] Isolation of boronic ester **389** was not performed.

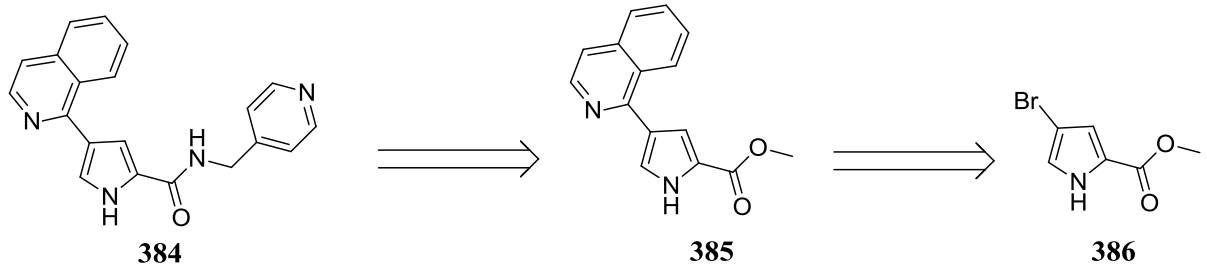

384 **385** **386**

Figure 53: Retrosynthetic analysis of isoquinoline analogue **384**.

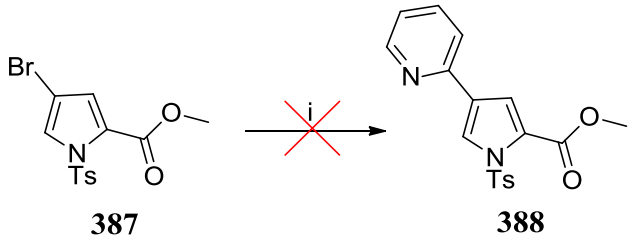

387 **388**

Scheme 43: *Reagents and Conditions;* i) 2-pyridylboronic acid, KOAc, Pd(dbpf)Cl_2, dioxane, 110 ^{o}C, 16 h.

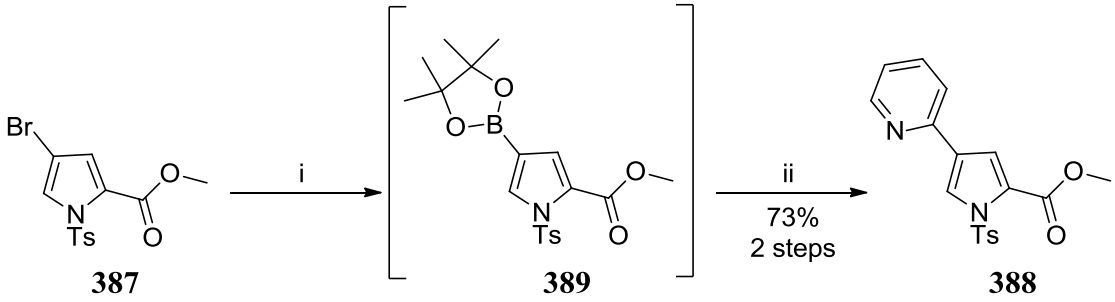

387 **389** **388**

Scheme 44: *Reagents and Conditions;* i) *bis*(pinacolato) diboron, KOAc, Pd(dbpf)Cl_2, dioxane, 110 ^{o}C, 16 h; ii) 2-bromopyridine, Na_2CO_3, $Pd(PPh_3)_4$, dioxane, H_2O, 110 ^{o}C, 16 h.

6.7.8.3 Synthesis of 4-(isoquinolin-1-yl)-N-(pyridin-4-ylmethyl)-1H-pyrrole-2-carboxamide, ***384*** *and 4-(pyridin-2-yl)-N-(pyridin-4-ylmethyl)-1H-pyrrole-2-carboxamide,* ***393***

Tosyl protection of 4-bromopyrrole proceeded in 55% using sodium hydride as the base. The protection strategy was implemented to prevent deprotonation and potential cross-couplings at the pyrrole nitrogen. Suzuki couplings gave the biaryl species **390** and **385** in 73% and 62% respectively. Hydrolysis of the relevant esters proceeded quantitatively by LCMS. However, isolation of the carboxylic acids, **391** and **392** was challenging due to their zwitterionic nature and relatively low yields of 48-52% were achieved, respectively. CDI-mediated couplings of the carboxylic acids **391** and **392** with 4-picolylamine also proved to be problematic. Poor solubility of the 2-pyridyl carboxylic acid in organic solvents resulted in isolation of only 22% of the amide product **393**. The isoquinolyl acid **392** was found to be more soluble under the reaction conditions with 51% of the amide product isolated (Scheme **45**).

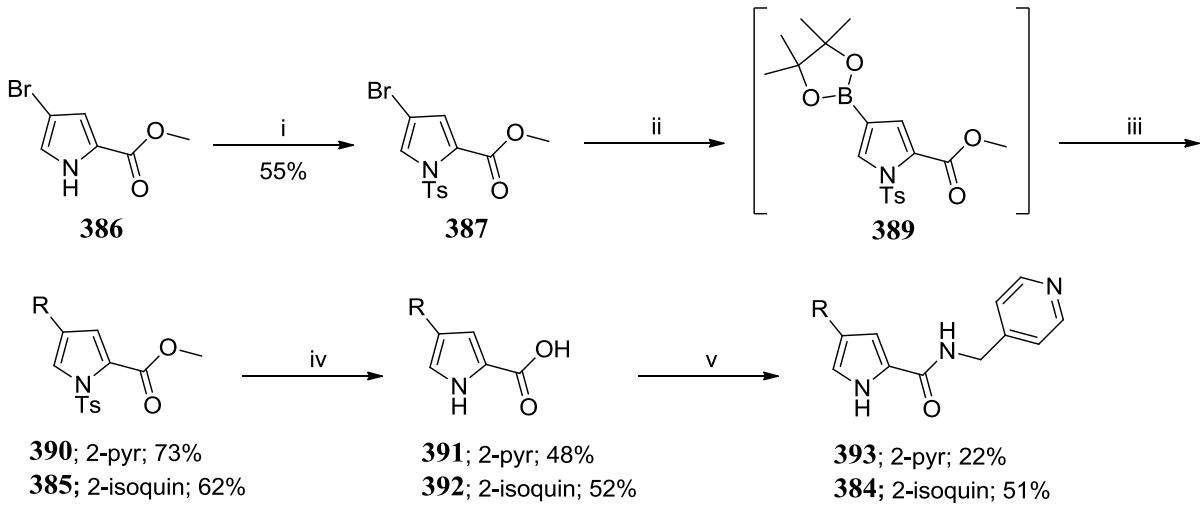

Scheme 45: *Reagents and Conditions;* i) i) NaH, TsCl, THF, 0 ^{o}C-RT, 16 h; ii) *bis*(pinacolato) diboron, KOAc, Pd(dbpf)Cl_2, dioxane, 110 ^{o}C, 16 h; iii) 2-bromopyridine, Na_2CO_3, Pd(PPh_3)$_4$, dioxane, H_2O, 110 ^{o}C, 16 h; iv) LiOH monohydrate, H_2O/THF, 65 ^{o}C, 16 h; v) CDI, THF, 70 ^{o}C, 3 h, then 4-picolylamine, 50 ^{o}C, 3 h.

6.7.8.4 SARs for Isosteric Replacement of the Aroyl Motif

Both biaryl compounds **393** and **384** were found to be inactive against ERK5 (IC_{50} values >120 μM) (Table **60**). This may be due to the planar nature of the biaryl species, whereas the aroyl moiety has the ability to rotate into the correct conformation for binding. Recent data regarding the homology model and the crystal structure of p38α supports this idea. Also, the oxygen atom of the carbonyl group has two lone pairs available for hydrogen bonding. It is currently not known which of these pairs is involved in this interaction. It could be that the lone pair of the pyridine/isoquinoline is in the wrong position to participate in crucial bonding with the salt bridge. As neither compound showed any activity against ERK5, it was not deemed a priority to synthesise analogues without the methylene linker, known to improve potency. Furthermore, the compounds were not counter-screened against p38α due to their lack of ERK5 activity.

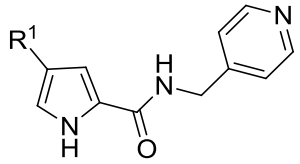

Table 60: ERK5 inhibitory activity of pyridyl and isoquinoline analogues

Compound	R^1	ERK5 IC_{50} (μM)[a]
393	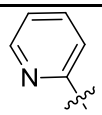	>120
384	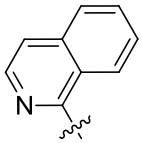	>120
232	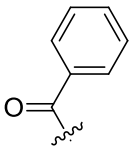	40.4 ± 2.6

[a] Determinations ± standard deviation (mean of n = 2)

6.8 Development of the Pyrrolopyridone Scaffold

Another area of interest which was investigated in parallel with the modification to aroyl substituents was the development of a pyrrolopyridone scaffold.

6.8.1 Rationale

Homology modelling (using the initial ERK2-based model) suggested that incorporation of the pyrrolopyridone heterocycle may lock the carbonyl of the carboxamide motif into a favourable conformation for binding (Figure **54**). Previous SAR studies have shown that although *N*-methylation of the amide nitrogen is detrimental to activity it is not completely lost (**146**; ERK5 IC_{50} = 9.0 μM).

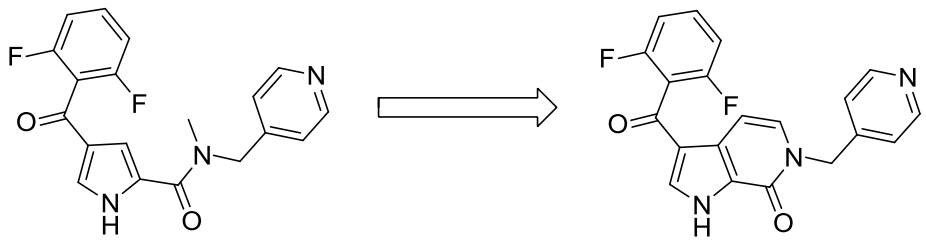

146 **394**

It was hoped that an increase in potency would be obtained as a result of the conformational restraint imposed by the pyrrolopyridone scaffold. When investigation into this series began, the 2.6-difluoroaroyl moeity was present in the most potent compounds, i.e. **144** (ERK5 IC_{50} = 2.3 μM) and the effect of side-chain truncation had not been discovered. Therefore, the CH_2-linked 4-pyridyl carboxamide side-chain was incorporated (Figure **55**).

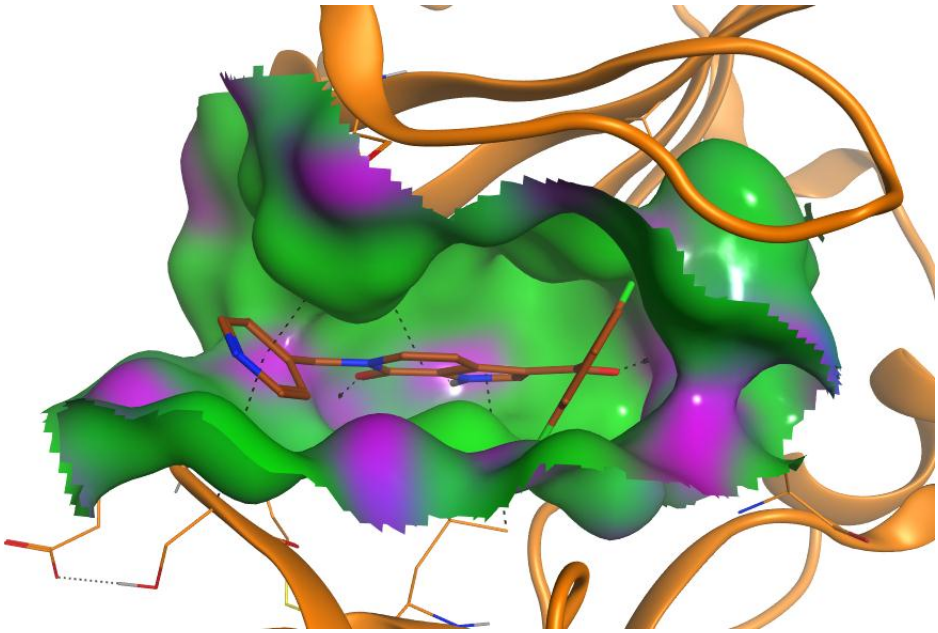

Figure 54: Homology modelling of pyrrolopyridone **394**.

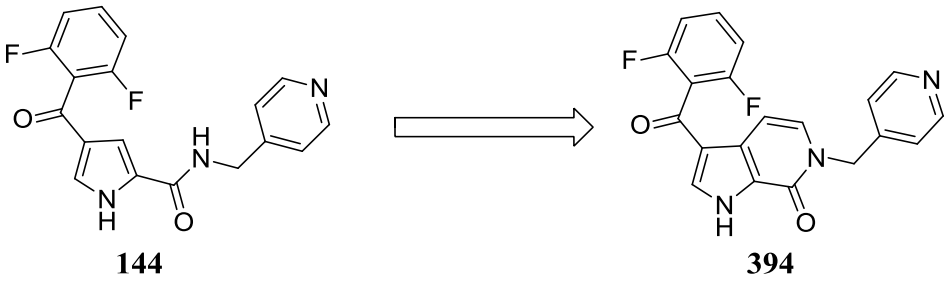

Figure 55: Comparison of pyrrole-carboxamide **144** with pyrrolopyridone target **394**.

6.8.2 Synthetic Strategy

It was envisaged that synthesis of pyrrolopyridone **396** would allow decoration of the scaffold by *N*-methylation of the pyridone, followed by Friedel-Crafts acylation of the pyrrole (Figure **56**).

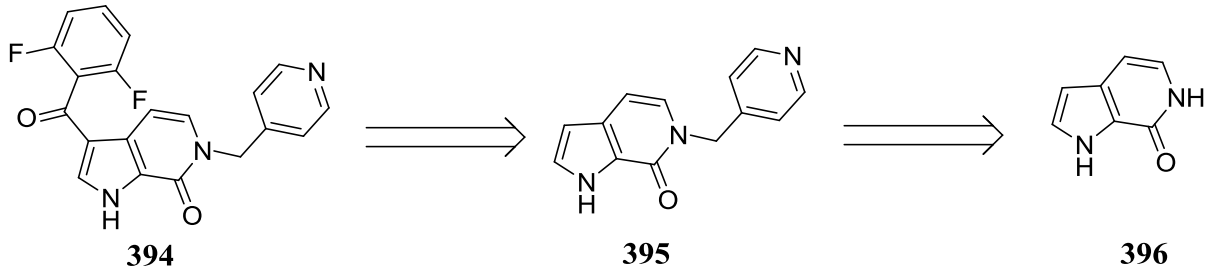

394 **395** **396**

Figure 56: Retrosynthetic analysis of functionalised pyrrolopyridone **394**.

Only one synthetic route towards pyrrolopyridone **396** was present in the literature, when devising the methodology towards substituted pyrrolopyridones.[136] The chlorosulfonium chloride intermediate used in the first step of the reported route was prepared by chlorination of 2-(phenylthio)acetaldehyde dimethyl acetal with liquid chlorine. This was reacted with 2-methoxypyridin-3-amine, in an S_N2 substitution, to give sulfonium chloride intermediate **399**. Treatment with sodium methoxide induced a rearrangement to aniline **400**. Cyclisation under acidic conditions resulted in formation of pyrrolopyridone **402**, *via* the methoxypyridine analogue and reduction of the thioether with Raney nickel gave 1*H*-pyrrolo[2,3-*c*]pyridin-7(6*H*)-one, **396**. Replication of this method using the literature conditions was attempted, however, the synthesis was found to be lengthy and unreliable (Scheme **46**). It was therefore necessary to implement a new strategy towards the synthesis of functionalised pyrrolopyridone compounds.

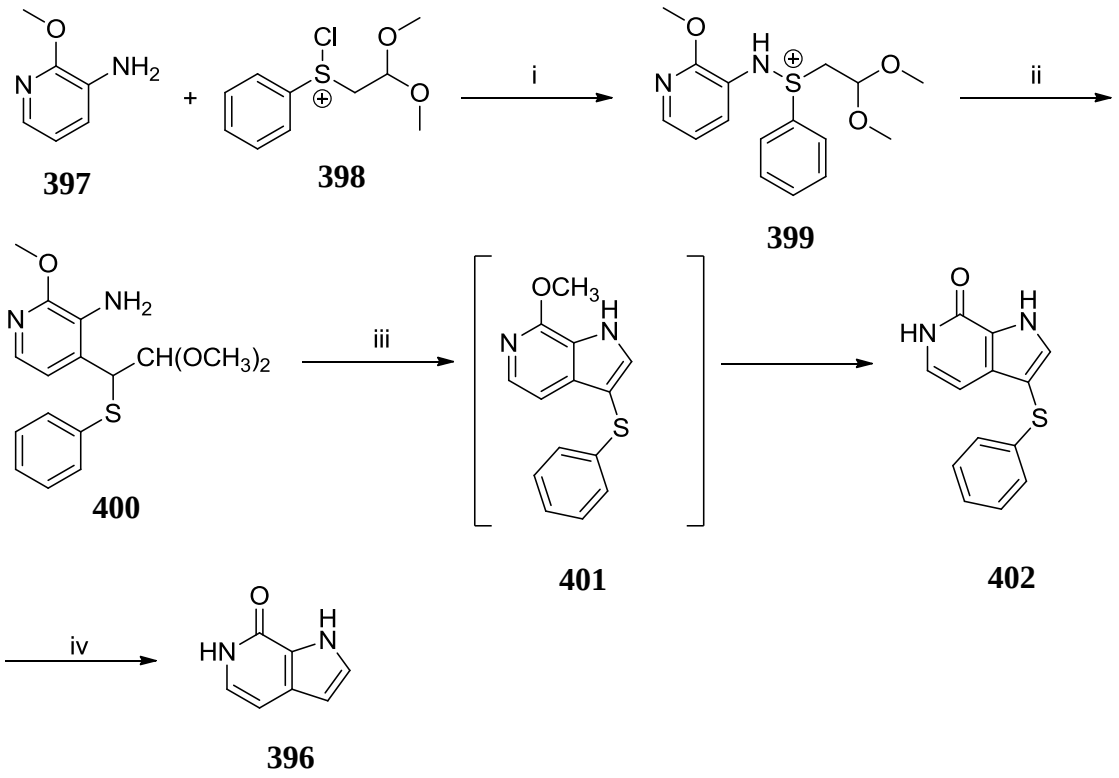

Scheme 46: Reported synthesis of pyrrolopyridone **396**.[136] *Reagents and Conditions;* i) Et_3N, DCM, -70 ^oC, 4 h; ii) NaOMe, MeOH, RT, 18 h; iii) HCl, $CHCl_3$, reflux, 72 h; iv) RaNi, H_2, EtOH, reflux, 72 h.

6.8.3 Synthesis of Substituted Pyrrolopyridones

It was envisaged that cyclisation of the pyridone could be achieved following an intramolecular electrophilic aromatic substitution reaction with an aldehyde, giving a 5-hydroxy-5,6-dihydropyridin-2(1*H*)-one intermediate, **404** (Scheme **47**). Condensation of the 5-hydroxy intermediate was deemed favourable due to the generation of an aromatic species. The aldehyde intermediate was formed *via* acid-catalysed hydrolysis of the corresponding diethyl acetal.

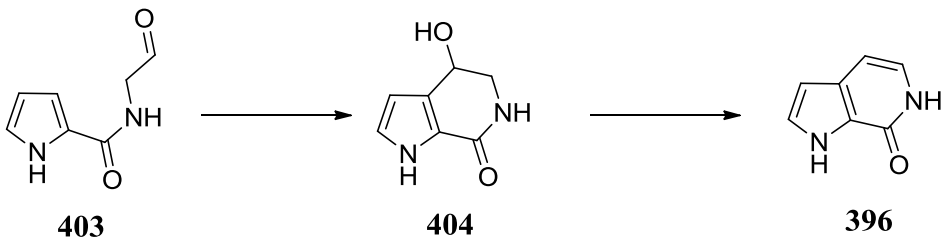

Scheme 47: Pyridone synthesis *via* EAS followed by condensation

Pyrrolopyridone **396** was synthesised from methyl 1*H*-pyrrole-2-carboxylate *via* hydrolysis to the carboxylic acid followed by a CDI-mediated coupling with aminoacetaldehyde diethyl acetal. Under acidic conditions, cleavage of the acetal and subsequent cyclization was achieved at moderate temperature. The desired compound was obtained in good yield at 60% on a small scale (Scheme **48**). However, scale up of the synthesis of **396** resulted in formation of an insoluble solid. It was not possible to analyse the material by ^{1}H NMR due to the insolubility of the polymorph in organic solvents, including DMSO and TFA. The planar nature of the molecule combined with the potential to form intermolecular hydrogen bonds is thought to be responsible for strong crystal packing and poor solubility. Introduction of the pyridyl side-chain prior to acid-catalysed cyclisation was believed to be a reasonable strategy to improve the solubility of the product formed, by increasing the number of rotatable bonds and decreasing its planarity.

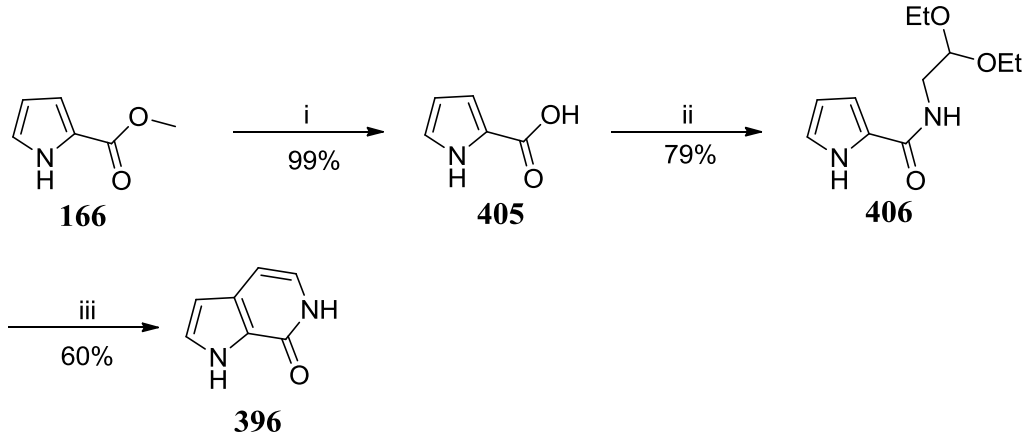

Scheme 48: *Reagents and Conditions:* i) LiOH monohydrate, THF/H_2O, 65 ^{o}C, 16 h; ii) CDI, THF, 70 ^{o}C, 3 h, then aminoacetaldehyde diethyl acetal, 50 ^{o}C, 3 h; iii) TFA:H_2O (1:1), 50 ^{o}C, 16 h.

Synthesis of the required pyridine side-chain, **409** was achieved *via* imine formation of isonicotinaldehyde with aminoacetaldehyde diethyl acetal, followed by reduction, mediated by sodium borohydride (Scheme **49**). Amide coupling of amine **409** with pyrrole-carboxylic acid **405** was unsuccessful using CDI. Conversion of the carboxylic acid **405** to the corresponding acid chloride, followed by substitution with amine **409** gave amide **410** in a low yield of 18%. Acid-catalysed cyclisation of **410** proceeded cleanly using acetic acid, in 83% yield. Unfortunately, Friedel-Crafts acylation of pyrrolopyridone **395** was unsuccessful and a complex reaction mixture was detected by LCMS. Interpretation of the ^{1}H NMR spectrum of amide **410** conducted at RT was not possible. Restricted rotation about the amide

bond resulted in broadening of NMR signals, and some signals were not visible. To resolve the spectrum, a ^{1}H NMR variable temperature experiment was conducted (Figure **57**). The ^{1}H NMR spectrum for amide **410** was conducted at a range of temperatures; 50, 80 and 110 ^{o}C. 80 ^{o}C was found to be the optimum temperature, as the greatest peak intensity was achieved with the best resolution of peaks. Future substituted amides exhibiting restricted rotation in NMR spectra were therefore analysed at this optimum temperature. It was not possible to obtain suitable ^{13}C NMR spectra, as this would involve heating up the NMR probe for prolonged periods of time.

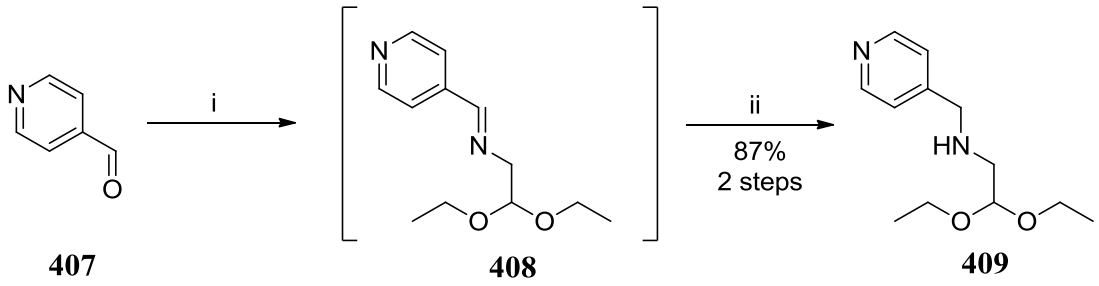

Scheme 49: *Reagents and Conditions;* i) aminoacetaldehyde diethyl acetal, $MgSO_4$, toluene, 110 ^{o}C, 16 h; ii) $NaBH_4$, MeOH, 0 ^{o}C, 4 h.

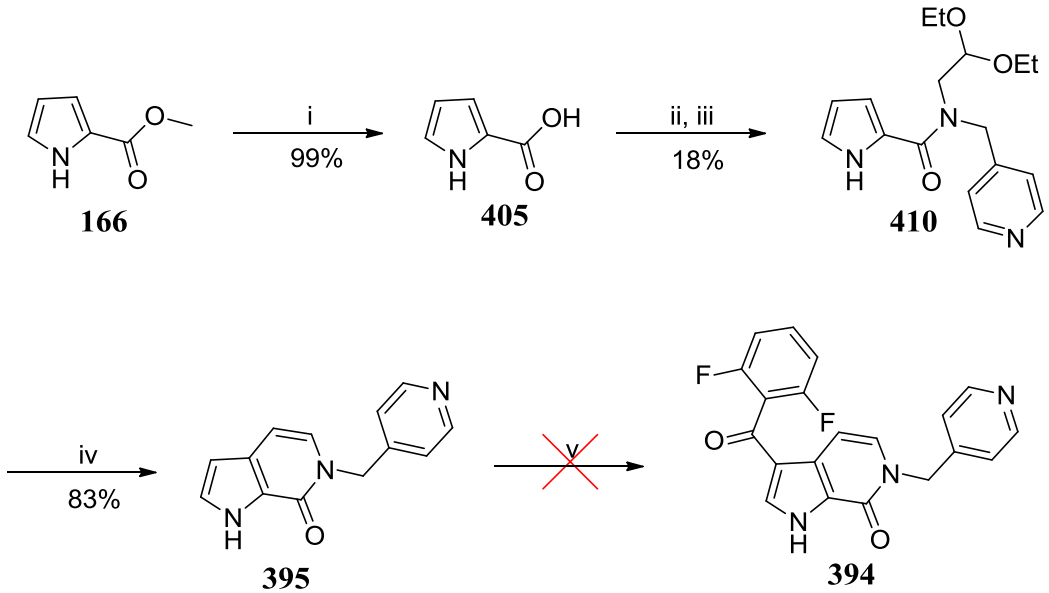

Scheme 50: *Reagents and Conditions;* i) LiOH monohydrate, THF/H_2O, 65 ^{o}C, 16 h; ii) $SOCl_2$, DMF, THF, 0 ^{o}C-RT, 2 h; iii) **409**, DCM, RT, 16 h; iv) acetic acid:H_2O (1:1), 70 ^{o}C, 16 h; v) 2,6-difluorobenzoyl chloride, $AlCl_3$, DCM, 0 ^{o}C-RT, 16 h.

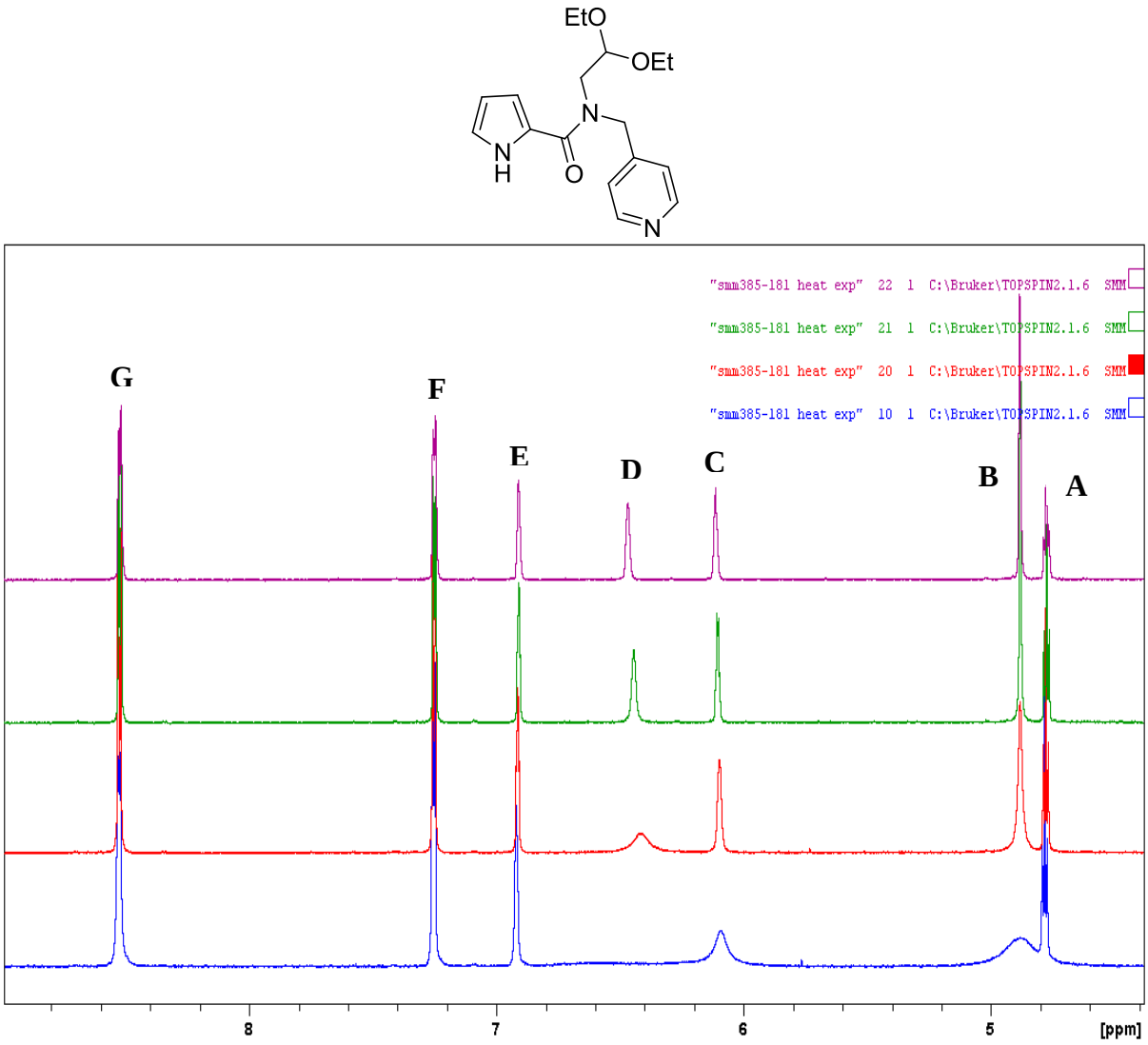

Figure 57: ^{1}H NMR variable temperature experiment of amide **410**, aromatic region. Blue = RT; Red = 50 ^{o}C; Green = 80 ^{o}C; Purple = 110 ^{o}C. **A**: 4.78 (1H, t, *J* = 4.9 Hz, CH); **B**: 4.88 (2H, s, CH_2-pyridine); **C**: 6.10 (1H, dd, *J* = 2.4 and 3.5 Hz, H-4); **D**: 6.45 (1H, s, H-3); **E**: 6.91 (1H, dd, *J* = 1.6 and 2.4 Hz, H-5); **F**: 7.25 (2H, d, *J* = 6.0 Hz, CH-pyridine); **G**: 8.53 (2H, d, *J* = 6.0 Hz, N-CH-pyridine).

Following the failure of the Friedel-Crafts acylation, an alternative strategy was implemented. Acylation of the pyrrole was completed in the first step of the synthesis in 62% yield, which was followed by hydrolysis of ester **411** and coupling of the amine *via* the acid chloride (Scheme **51**). The cyclisation step proved to be much more difficult when the 4-aroyl group was present. The electron withdrawing nature of the aroyl substituent results in a reduction in the pyrrole's electron density making it less reactive for cyclisation. Reaction monitoring by LCMS was used extensively during the optimisation of the reaction. The use

of acetic acid:H_2O was first investigated as this was found to give a cleaner reaction mixture, as opposed to TFA:H_2O. No evidence of cyclisation was observed at 100 ^oC or 120 ^oC under microwave heating, although cleavage of the acetal was observed. The use of TFA was reinstated, using water or TFE as the solvent but reaction was not observed until temperatures were increased to 160 ^oC with microwave heating. Where TFE was used as the solvent, a large impurity peak was observed with *m/z* 466 which corresponds to the addition of trifluoroethanol to the molecule. 1:1 TFA:H_2O showed 90% conversion by LCMS to a product bearing the correct *m/z* ratio (Table **61**).

Table 61: Reaction optimisation – acid-catalysed cyclisation of acetal **413**.

Attempt	Acid	Solvent	Temp (^oC)	Time	Observation
1	Acetic	H_2O	100 conv	16 h	NR
2	Acetic	H_2O	120 mw	30 min	NR
3	TFA	H_2O	100 conv	16 h	NR
4	TFA	H_2O	120 mw	30 min	NR
5	TFA	TFE	120 mw	30 min	NR
6	TFA	TFE	160 mw	30 min	30% conversion; impurity forming *m/z* = product + TFE added
7	TFA	H_2O	160 mw	2 h (in 30 min cycles)	90% conversion to product – no impurities

As the nitrogen atom of pyrrole is not nucleophilic without prior deprotonation, it was assumed that cyclisation about the pyrrole nitrogen would not occur. However, analysis by ^1H NMR, followed by ^1H-^{15}N HSQC and HMBC techniques did not confirm the desired structure, and cyclisation had occurred to give the undesired product **414** instead.

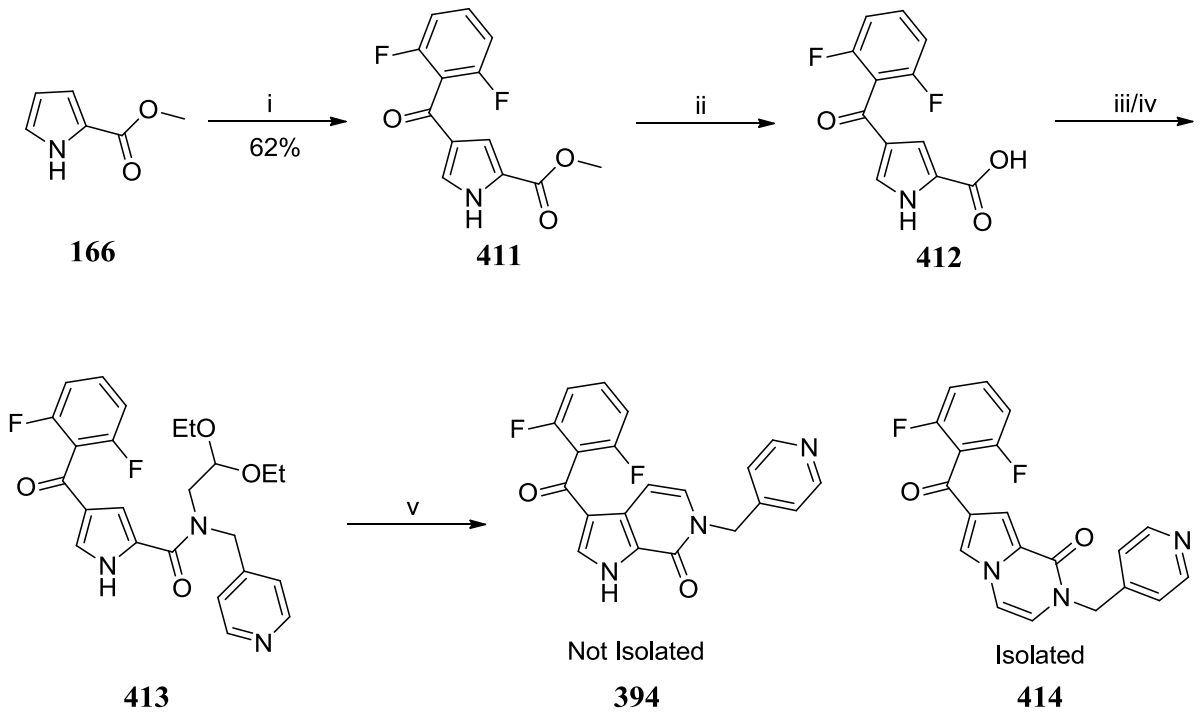

166 411 412 413 394 414

Scheme 51: *Reagents and Conditions;* i) 2,6-difluorobenzoyl chloride, $AlCl_3$, DCM, 0 ^oC-RT, 16 h; ii) LiOH monohydrate, THF/H_2O, 65 ^oC, 16 h; iii) $SOCl_2$, DMF, THF, 0 ^oC-RT, 2 h; iv) **409**, DCM, RT, 16 h; v) TFA:H_2O (1:1), 160 ^oC, MW, 2 h.

In order to prevent cyclisation onto the pyrrole nitrogen, a protection strategy was implemented (Scheme **52**). As the electron withdrawing aroyl moiety makes the cyclisation reaction more difficult, due to the pyrrole being more electron-poor, it was proposed that an electron donating protecting group would be beneficial. The SEM protecting group was chosen due to its apparent robustness to acidic and basic conditions, its electron donating properties, and its ease of removal using a fluoride source. The cyclisation conditions were re-optimised in order to achieve the desired product in the mildest conditions possible (Table **62**). At 60 and 100 ^oC in acetic acid with conventional heating no cyclisation was observed. A small amount of product was observed using microwave heating at 120 ^oC or above. It was noted that during the cyclisation under various conditions (Table **62**, entries 3, 4, 5 and 6), cleavage of the SEM protecting group was observed. This resulted in the formation of the undesired cyclisation product observed previously (Scheme **51**). Following attempts using water as the solvent, it was postulated that use of an aprotic solvent (DME) would improve the ratio of product to impurities. Hydrolysis of the amide bond under the reaction conditions was also observed, giving rise to carboxylic acid and amine by-products. Fortunately, an acceptable proportion of the SEM protected pyrrole withstood the conditions to give the

desired SEM protected cyclised product **418** in 35% yield following column chromatography. Subsequent deprotection of the SEM group was achieved using TBAF in 83% yield.

Table 62: Reaction optimisation – acid-catalysed cyclisation of acetal **417**.

Attempt	Acid	Solvent	Temp (^{o}C)	Time	Observation
1	Acetic	H_2O	60 conv	16 h	NR
2	Acetic	H_2O	100 conv	16 h	NR
3	Acetic	H_2O	120 MW	20 min	V. small product peak, small peak *m/z* 383 (aldehyde, SEM off)
4	Acetic	H_2O	160 MW	20 min	32% product in complex mixture. SEM group off (38%)
5	TFA	DME	120 MW	20 min	V. small product peak, small peak *m/z* 383 (aldehyde, SEM off)
6	TFA	DME	120 MW	1.5 h	Major peak is product. Several other peaks corresponding to various impurities

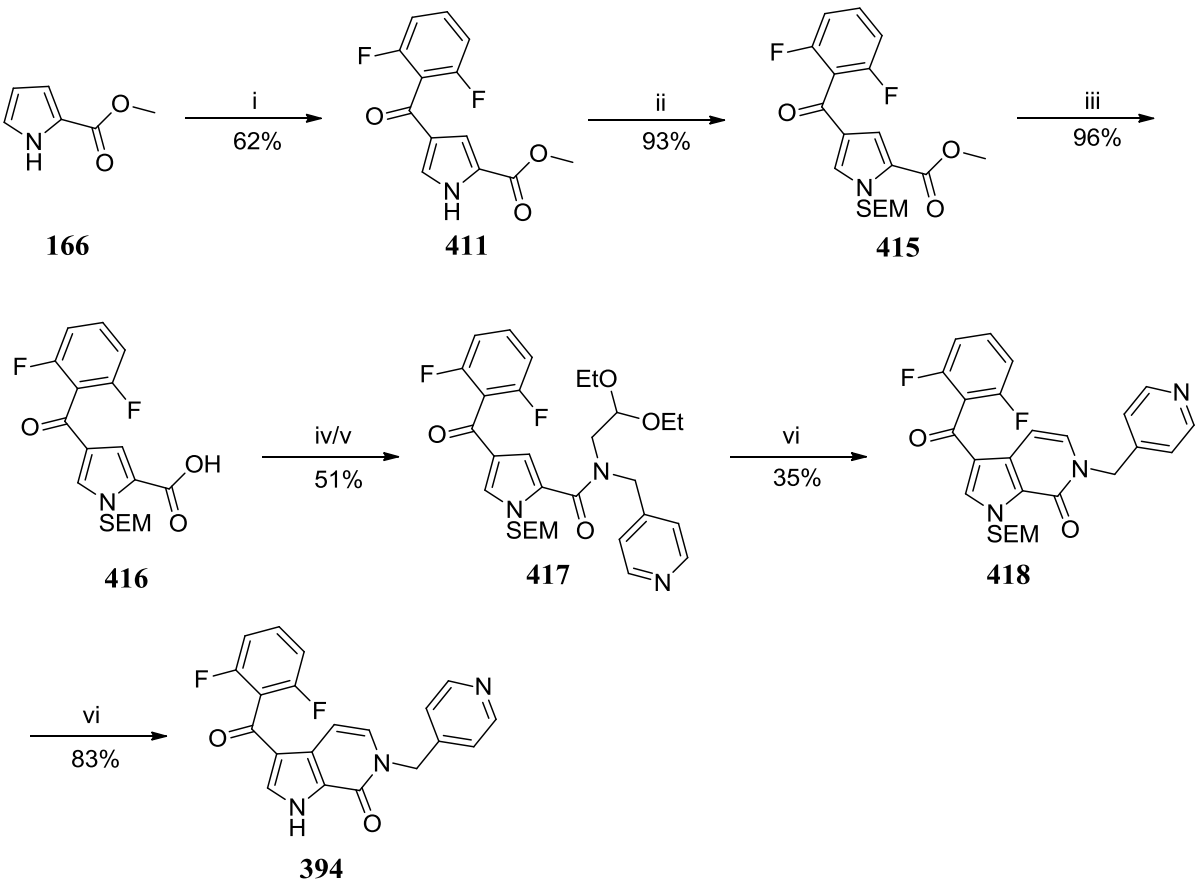

Scheme 52: *Reagents and Conditions;* i) 2,6-difluorobenzoyl chloride, $AlCl_3$, DCM, 0 ^oC-RT, 16 h; ii) SEMCl, Et_3N, DMAP, THF, 0 ^oC-RT, 2 h; iii) LiOH monohydrate, THF/H_2O, 65 ^oC, 16 h; iv) $SOCl_2$, DMF, THF, 0 ^oC-RT, 2 h; v) **409**, DCM, RT, 16 h; vi) 20% TFA in DME, 120 ^oC, 1.5 h; vii) TBAF, THF, 0 ^oC-RT, 16 h.

6.8.4 Discovery of Pyrrolopyridones as Inhibitors of p38α

Subsequent to the optimisation of methodology for the synthesis of substituted pyrrolopyridone **394** we found that discovery of pyrrolopyridone based inhibitors of p38α had been described in a patent by Merck, Sharpe and Dohme.[137] Compounds displaying low nanomolar potency were reported, as summarised in Table **63**. Interestingly, the most potent compounds all feature a 2, 4, 6-trifluoro substitution pattern about the aroyl ring. It is known that *para*-substitution is not tolerated in ERK5, even with a small fluorine atom. All side-chains contained the CH_2-linker, with a 5-, 6-fused heterocycle attached. The most potent compounds contained amide or carboxylic acid based substituents on the 6-membered ring. Based on these results, it was expected that pyrrolopyridone compound **394** would be a p38α inhibitor and so not selective for ERK5.

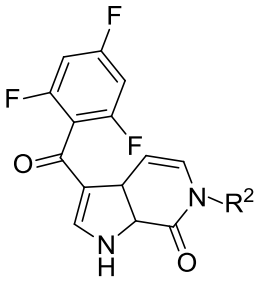

Table 63: Example p38α inhibitors. From ref [137].

Compound	R^2	p38α IC_{50} (nM)
419	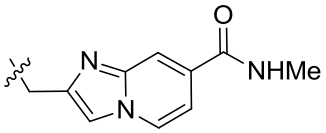	1.0
420	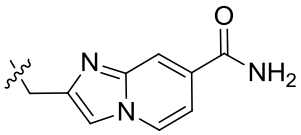	1.3
421	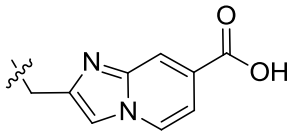	2.0
422	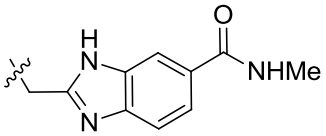	3.0

6.8.5 Biological Evaluation of 3-(2,6-Difluorobenzoyl)-6-(pyridin-4-ylmethyl)-1H-pyrrolo[2,3-c]pyridin-7(6H)-one 394

Pyrrolopyridone **394** was found to be a modest inhibitor of ERK5 with an IC_{50} of 7.7 μM. This result is comparable to the effect of amide *N*-methylation (ERK5 IC_{50} = 9.0 μM). However, counter-screening revealed that **394** was a very potent inhibitor of p38α at 100 nM. As the homology model available for structure-guided drug design is based in part on p38α, it is currently not possible to identify the exact differences in the two binding sites (ERK5 *vs* p38α) which are giving rise to the dramatic differences in potency. Previously reported pyrrole-carboxamide based inhibitors of p38α are known to form a hydrogen bond between their amide NH and a water molecule present in the binding site (i.e. **294**; Section **6.7.5**). It may be that displacement of this water molecule by incorporation of a lipophilic group on the

amide nitrogen is more entropically favoured in p38α than in ERK5. The excellent potency of pyrrolopyridone **394** against p38α and tolerance in ERK5 led us to the investigation of pyrrolopyridone compounds containing truncated side-chains. Evolution of the project had resulted in discovery of truncated 4- and 3-pyridyl side-chains and the 2-bromo-6-fluoro and 2-chloro-6-fluoro aroyl substituents conferring the greatest potency in target molecules during the course of the research into the pyrrolopyridone scaffold.

Table 64: ERK5 inhibitory activity of **394**

Compound	Structure	ERK5 IC_{50} (μM)[a]	p38α IC_{50} (μM)[a]
394	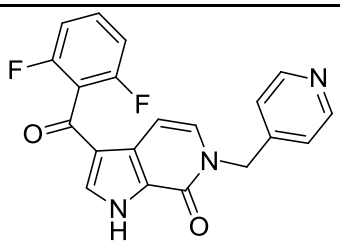	7.7 ± 0.9	0.10 ± 0.01

[a] Determinations ± standard deviation (mean of n = 2)

6.8.6 Synthesis of N-Pyridyl Pyrrolopyridones

The initial synthetic strategy implemented for synthesis of pyrrolopyridones incorporating *N*-pyridyl substituents was (as for the synthesis of pyrrolopyridone **394**), to react the relevant aniline in a substitution reaction with the corresponding acid chloride of carboxylic acid **416**. *N*-(2,2-Diethoxyethyl)pyridin-4-amine, **424** was synthesised *via* S_NAr substitution of 4-chloropyridine hydrochloride **423** with aminoacetaldehyde diethyl acetal (Scheme **53**). Unfortunately, due to the electron poor nature of the amine, the coupling reaction between amine **424** and the acid chloride failed to give the desired product (Scheme **54**). The alternative PCl_3-mediated amide coupling of amine **424** and carboxylic acid **416** was not attempted as previous experience taught that cleavage of the acetal group would undoubtedly occur under the harsh reaction conditions.

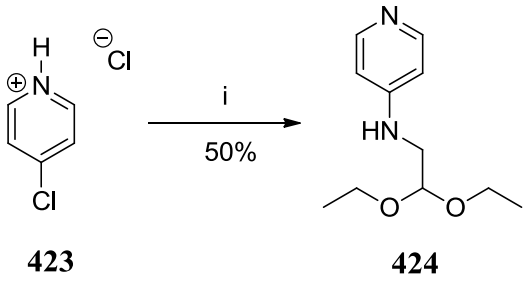

423 **424**

Scheme 53: *Reagents and Conditions;* i) aminoacetaldehyde diethyl acetal, NMP, 130 ^{o}C, MW, 30 min.

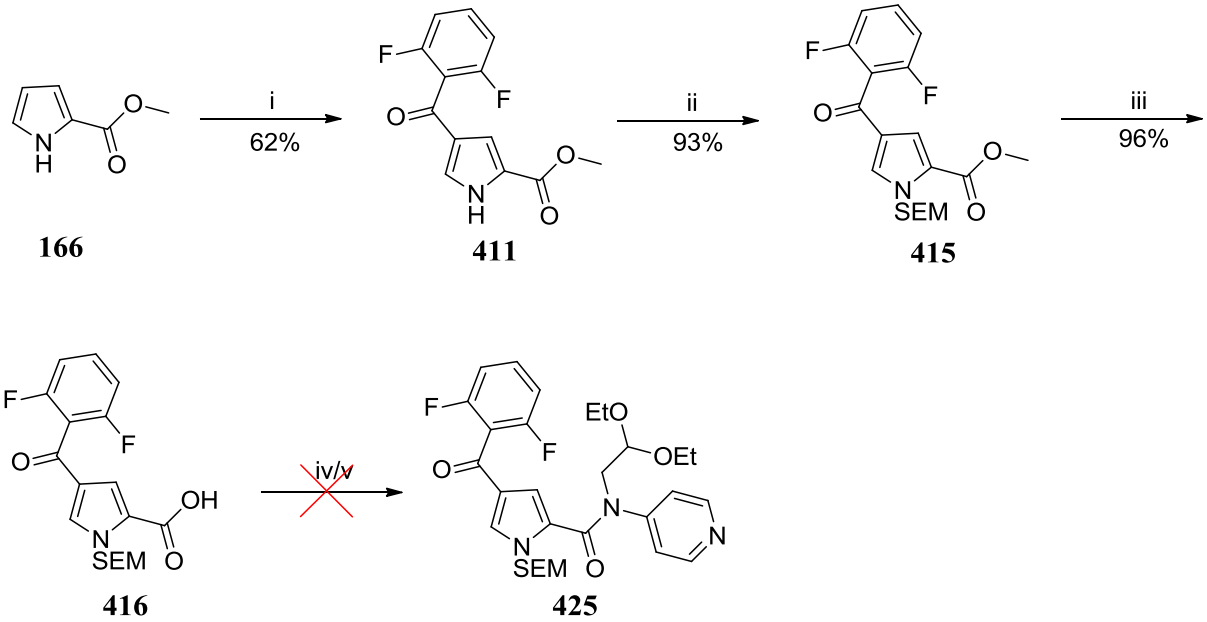

166 **411** **415**

416 **425**

Scheme 54: *Reagents and Conditions;* i) 2,6-difluorobenzoyl chloride, $AlCl_3$, DCM, 0 ^{o}C-RT, 16 h; ii) SEMCl, KO^{t}Bu, THF, 0 ^{o}C-RT, 2 h; iii) LiOH monohydrate, THF/H_2O, 65 ^{o}C, 16 h; iv) $SOCl_2$, DMF, THF, 0 ^{o}C-RT, 2 h; v) **424**, DCM, RT, 16 h.

It was envisaged that, as an alternative, key intermediate **425** could be synthesised by alkylation of the secondary amide, **426**. The electron poor 4-aminopyridine was successfully coupled to carboxylic acid using the PCl_3-mediated approach, and the SEM protecting group remained intact during the course of the reaction, giving amide **426** in 77%. Unfortunately, it was not possible to alkylate amide **426** with bromoacetaldehyde diethyl acetal using potassium *tert*-butoxide as a base (Scheme **55**). A model reaction was conducted, attempting methylation of amide **426** using highly reactive methyl iodide with KO^{t}Bu. *N*-Methyl amide **427** was isolated in 21% yield, confirming that potassium *tert*-butoxide is a strong enough base to deprotonate the amide (Scheme **56**). However, no starting material was recovered,

and no by-products were isolated following an aqueous work-up. It is thought that *N*-methylation of the pyridine, leading to the formation of an aqueous soluble pyridine salt, is occurring more rapidly than *N*-methylation of the amide.

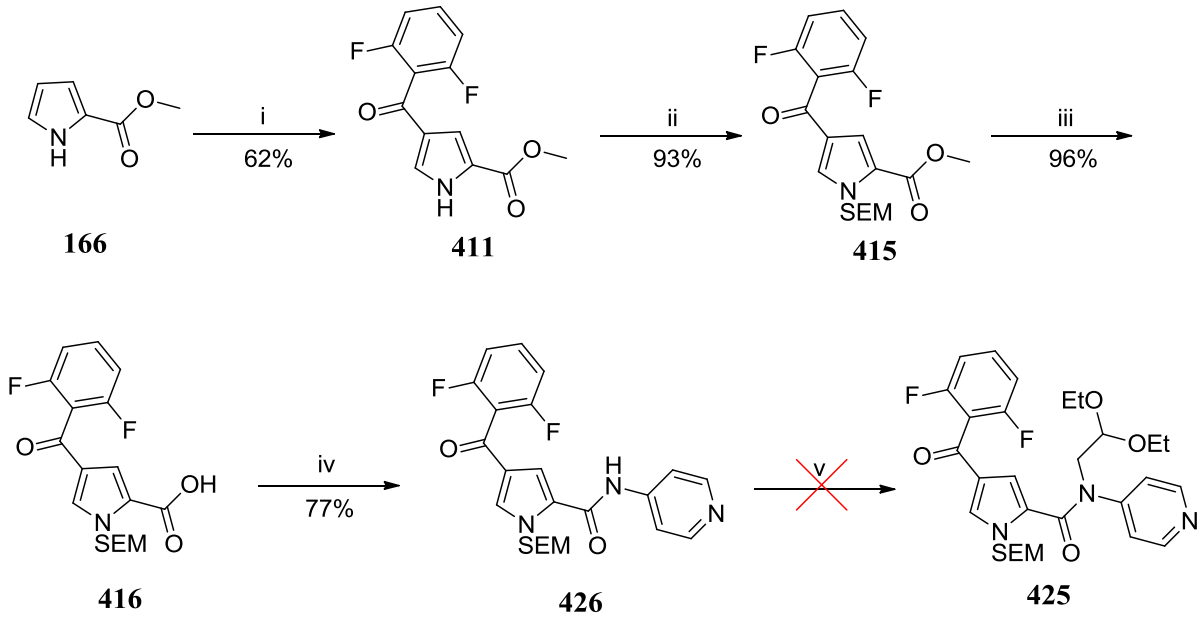

Scheme 55: *Reagents and Conditions;* i) 2,6-difluorobenzoyl chloride, $AlCl_3$, DCM, 0 ^oC-RT, 16 h; ii) SEMCl, KO^{t}Bu, THF, 0 ^oC-RT, 2 h; iii) LiOH monohydrate, THF/H_2O, 65 ^oC, 16 h; iv) PCl_3, 4-aminopyridine, MeCN, 150 ^oC, MW, 5 min; vi) bromoacetaldehyde diethyl acetal, KOtBu, THF, 0 ^oC-RT, 2 h.

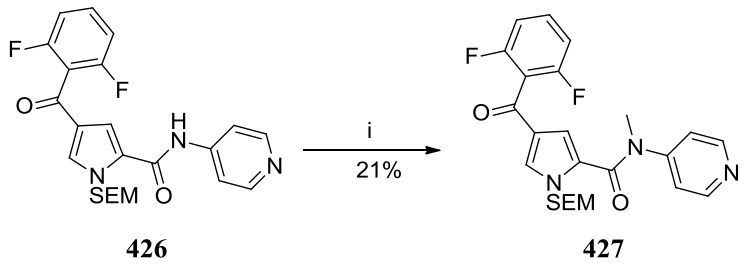

Scheme 56: *Reagents and Conditions;* i) KO^{t}Bu, MeI, THF, 0 ^oC-RT, 2 h.

The final strategy relied on cyclisation of the pyrrolopyridone prior to the addition of the pyridyl group. Amide coupling mediated by CDI of aminoacetaldehyde diethyl acetal with carboxylic acid **412** proceeded in 87% yield. Regioselective acid-catalysed cyclisation was achieved with neat methanesulfonic acid, using the method described in the Merck patent, to give pyrrolopyridone **429** in 46% yield.[137] SEM protection proceeded in 58% yield. There is literature precedent for Ullmann couplings of 2-pyridones with aryl halides.[138] Classical

Ullmann coupling conditions were employed without use of the *N*, *N*'-dimethylcyclohexane-1, 2-diamine (DMCDA) additive described by Wang *et al*, and *N*-arylation was achieved in 21% yield *via* coupling of **430** with 4-bromopyridine hydrochloride. The reaction was unsuccessful when using diamine-based additives. Application of the method for use with 3-bromopyridine was not successful. However, conversion of the pyridine species to the hydrochloride salt prior to coupling resulted in successful and reproducible coupling results. A series of compounds based on this scaffold incorporating features of the most potent pyrrole-carboxamide compounds to date was prepared, summarised in Tables **65** and **66**. It was noted that purification of protected compounds was difficult, which may be responsible for the low yields reported for intermediates bearing the silyl group. Furthermore, during the course of the Ullmann coupling, the SEM group was cleaved in a number of cases. The crude mixtures were deprotected to give the final products. In the case of 2-bromo, 6-fluoro analogue **449**, only 9% of the desired product was isolated following the tandem Ullmann coupling with 4-bromopyridine hydrochloride and silyl deprotection steps. The low yield recorded is attributed to the presence of a second aryl bromide species, which offers an alternative reaction site. Purification *via* semi-preparative HPLC was required due to the presence of closely running impurities. The 3-pyridyl analogue was not able to be synthesised.

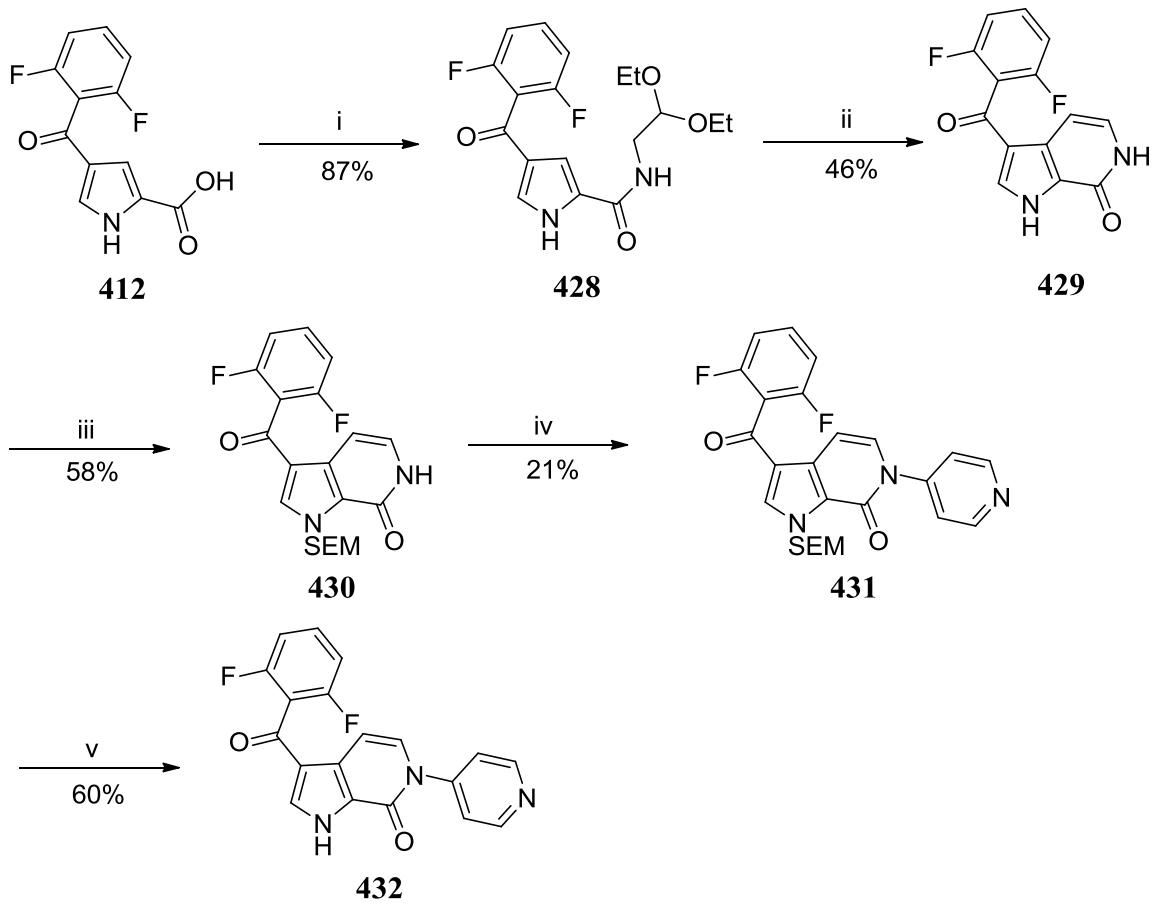

Scheme 57: *Reagents and Conditions;* i) CDI, THF, 70 ^{o}C, 3 h, then aminoacetaldehyde diethyl acetal, 50 ^{o}C, 3 h; ii) $MeSO_3H$, 95 ^{o}C, 1 h; iii) SEMCl, Et_3N, DMAP, THF, RT, 16 h; iv) 4-bromopyridine HCl, K_2CO_3, CuI, DMF, 135 ^{o}C, 48-72 h; v) TBAF, THF, 65 ^{o}C, 16 h.

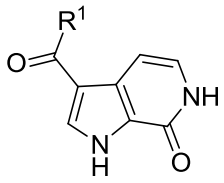

Table 65: Synthesis summary for *N*-pyridyl pyrrolopyridone series, part 1

R^1	Acylation Yield (%)	Hydrolysis Yield (%)	Amide Coupling Yield (%)	Cyclisation Yield (%)	SEM Protection Yield (%)
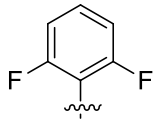	**411**; 62	**412**; 97	**428**; 87	**429**; 46	**430**; 58
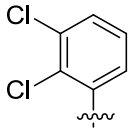	**434**; 79	**435**; 97	**436**; 84	**437**; 55	**438**;72
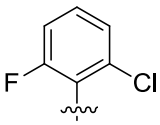	**270**; 89	**271**; 99	**441**; 64	**442**; 53	**443**; 48
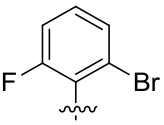	**276**; 80	**277**; 90	**446**; 57	**447**; 59	**448**; 64

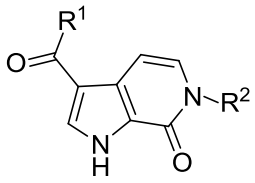

Table 66: Synthesis summary for *N*-pyridyl pyrrolopyridone series, part 2

R^1	R^2	Ullmann Coupling Yield (%)	SEM Deprotection Yield (%)
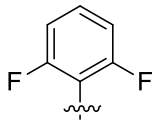	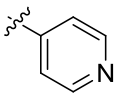	**431**; 21	**432**; 60
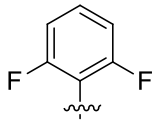	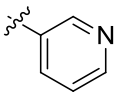	-	**433**; 37
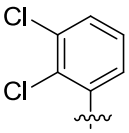	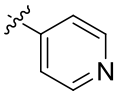	-	**439**; 69
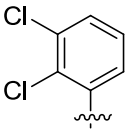	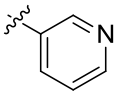	-	**440**; 40
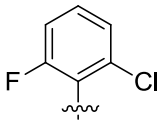	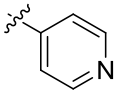	-	**444**; 51
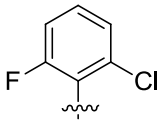	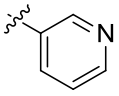	-	**445**; 19
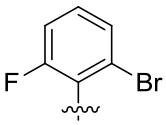	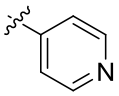	-	**449**; 9

6.8.7 Biological Evaluation of N-Pyridyl Pyrrolopyridones

Unfortunately, all compounds in the *N*-pyridyl pyrrolopyridone series were found to be insoluble at higher concentrations under the IMAP™ assay conditions rendering the interpretation of IC_{50} values unreliable. Despite their insolubility, some ERK5 inhibitory activity was recorded (i.e. **444** ERK5 IC_{50} = 3.0 µM, insoluble in 40% DMSO). We can

compare the pyrrolopyridone-based compounds to their uncyclised counterparts but must consider the caveat of the reduced solubility. It appears that cyclisation does not improve ERK5 activity, but selectivity against p38α is certainly diminished; i.e. Compound **444** is only 3-fold selective for ERK5 over p38α. Conversion of compounds **444** and **449** to their corresponding HCl salts was subsequently performed, and the salts were re-tested. However, no significant improvement in solubility was observed (in order to obtain a reliable IC_{50} measurement). As a result of the poor solubility and selectivity profiles of this series, research into the pyrrolopyridone series was discontinued.

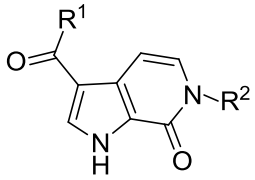

Table 67: ERK5 inhibitory activity of pyrrolopyridone analogues

Compound	R^1	R^2	ERK5 IC_{50} (μM)[a]	p38α IC_{50} (μM)[a]
432	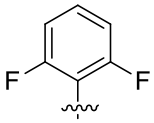	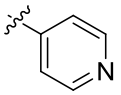	>120	>120
433	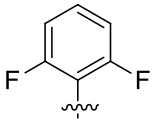	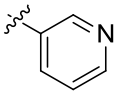	17.9 ± 2.0	15.8[d]
439	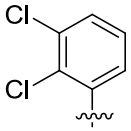	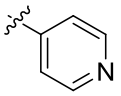	>120	>120
440	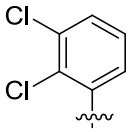	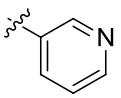	78.6 ± 11.7	>120
444	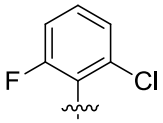	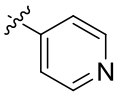	3.0 ± 0.5[b]	8.8 ± 1.0[b]
445	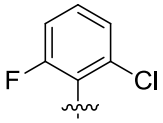	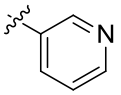	4.4 ± 0.3[c]	15.8 ± 0.5[b]

449	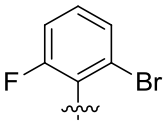	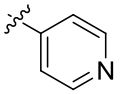	2.8 ± 0.1	13.2 ± 1.1

[a] Determinations ± standard deviation (mean of n = 2, unless otherwise stated); [b] n = 4; [c] n = 3; [d] n = 1

6.9 Future Work and Conclusions

6.9.1 Future Work

The potency of leading compounds in the pyrrole-carboxamide series has been improved by approximately 10 to 20-fold over the course of hit-to-lead optimisation. Future studies aim to improve potency further by probing previously uninvestigated sites in the ERK5 ATP-binding site, ideally below 100 nM in the enzymatic assay. Synthetic efforts to improve ERK5 activity will focus on further investigation around accessing an allosteric pocket *via* the 3-position of the aroyl motif as described in Section **6.7.6**. The presence of a 3-chloro group in the most potent compound to date provides an opportunity to exploit palladium mediated chemistry (i.e. Suzuki, Sonogashira, Buchwald couplings etc), in order to build up SAR around this position. In addition, homology modelling has revealed that access to the ribose pocket may be possible, *via* incorporation of substituents on the 3-position of the pyrrole (Figure **58**).

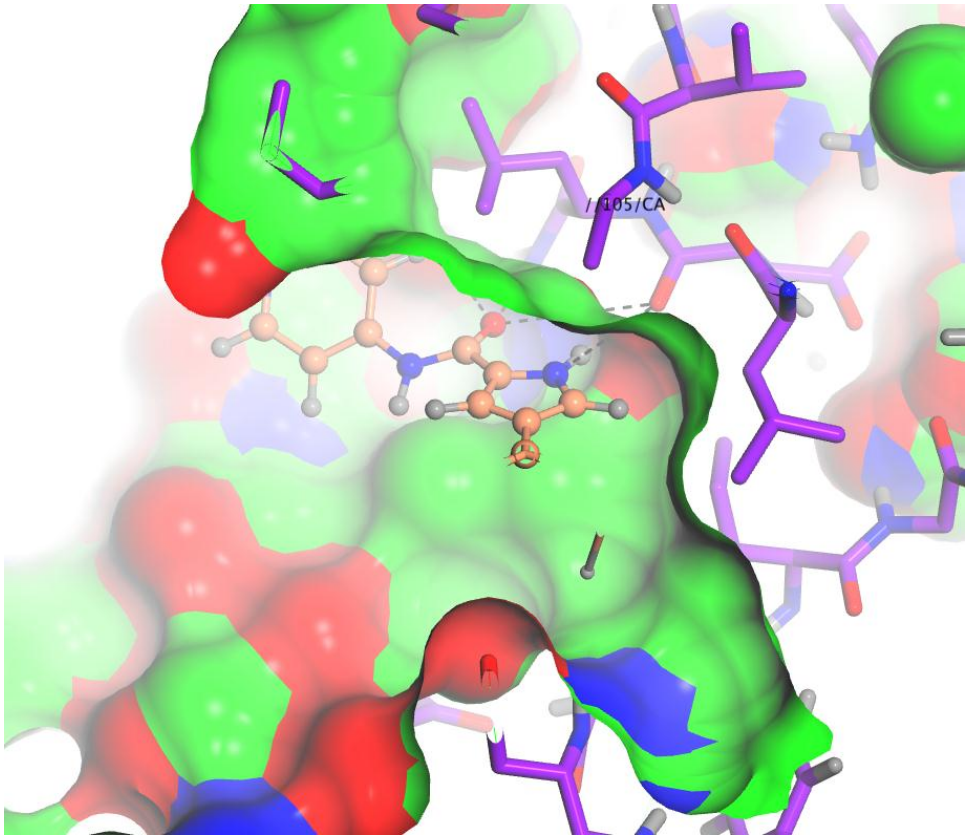

Figure 58: Identification of a ribose pocket in the ERK5 active site, possibly accessible *via* the pyrrole 3-position.

Substitution of the carboxamide side-chain appears to be less constrained than that of the aroyl group, and wider range of substituents may be incorporated. Therefore, it is envisaged that tuning of the ADME properties, primarily CYP inhibition and compound efflux, may be eliminated *via* optimisation of this motif. Figure **59** summarises the ongoing research on the project.

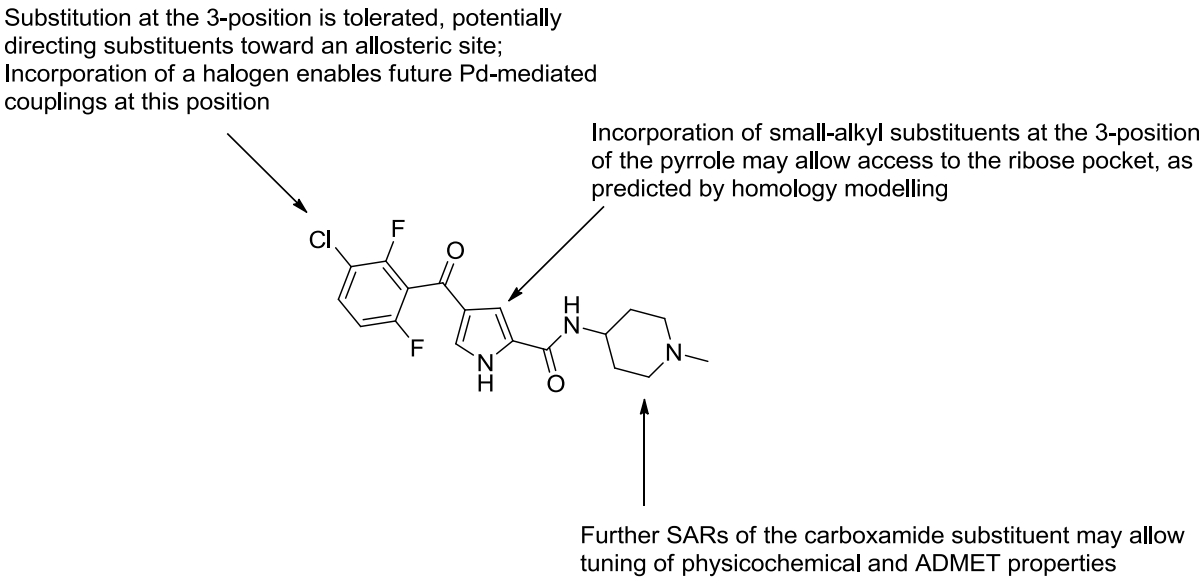

Figure 59: Summary of the future areas for investigation around the pyrrole-carboxamide scaffold.

6.9.2 Conclusions

Structure activity relationships (SARs) around the pyrrole-carboxamide scaffold have been thoroughly investigated, owing to their synthetic tractability. Homology modelling (based on the structures of ERK2, and later, p38α) was the driving force for structure based drug design throughout the project.

Early homology modelling studies suggested that replacement of the aroyl motif with non-aromatic groups may be tolerated in the ERK5 binding site. However, activity was abolished in the majority of cases, with only the unsubstituted cyclohexane analogue, **149** conferring any potency within the limits of the IMAP assay (IC_{50} = 59.3 μM).

Parallel investigation of the substitution pattern of the aroyl ring and carboxamide side-chain motifs led to the discovery of compound **278**, a selective ERK5 inhibitor with sub-micromolar potency (**278**; ERK5 IC_{50} = 0.82 μM; p38α >120 μM; no significant inhibitory activity against a panel of 131 protein kinases). It was discovered that non-aromatic carboxamide substituents, particularly *N*-methyl piperidine, were tolerated i.e. compound **283**; IC_{50} = 0.20 μM.

Owing to the excellent physicochemical properties exhibited (according to Lipinski's rule of 5), compounds **278** and **283** performed well in *in vitro* DMPK studies, and no inhibition of

hERG (IC_{50} >25 μM) was recorded. However, inhibition of the CYP enzymes, attributed to the presence of an unflanked pyridine ring, was observed with compound **272**, and poor cell permeability and high efflux ratio was observed with compound **292**. Pyrrole **278** was progressed into preliminary *in vivo* studies due to the higher probability of cell permeation, and demonstrated efficacy comparable to the competitor compound XMD8-92 in both an angiogenesis model and in tumour xenograft models.

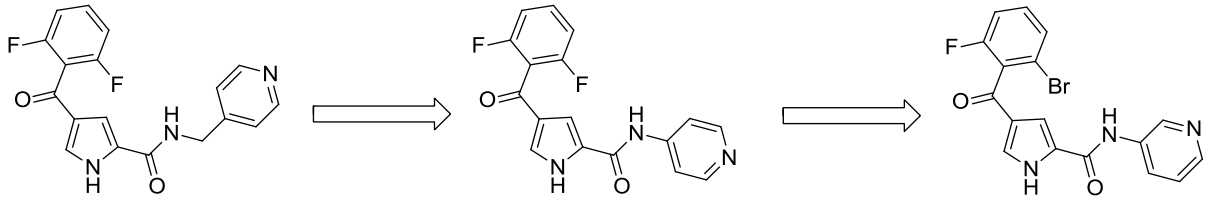

144 **256** **278**

It was hypothesised that access to an allosteric site may be achieved *via* further substitution of the 2- or 3-positions of the aroyl ring. However, incorporation of small alkyl substituents in the 2-position was not well tolerated, with diminished activity observed compared to that of the di-halogenated analogues e.g. **278.** Overlay of pyrrole-carboxamide based compounds with the quinazoline-based p38α inhibitor **341** suggested that substitution of the 3-position was a superior strategy towards accessing the prospective allosteric site. Incorporation of substituents at this position was tolerated, giving the most potent compound to date, **341**, with an IC_{50} of 110 nM.

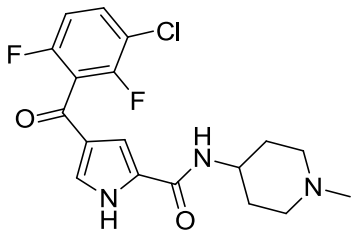

341

Strategies to introduce rigidity to the pyrrole-carboxamide scaffold were also investigated. Replacement of the aroyl motif with a biaryl scaffold, while maintaining the presence of a hydrogen bond acceptor was not tolerated. Furthermore, cyclisation of the pyrrole-carboxamide scaffold to give pyrrolopyridone was extensively investigated. The synthesis of the novel pyrrolopyridones were not trivial, and unfortunately, these compounds suffered from poor aqueous solubility, micromolar potency and reduced selectivity against p38α.

The pyrrole-carboxamide series has now entered the lead optimisation phase of drug discovery following successful hit-to-lead studies. The programme is well positioned to exploit structure-based drug design for rapid lead optimisation with the aim of providing compounds for preclinical development.

Chapter 7: Experimental and Analysis

7.1 Solvents and Reagents

Chemicals were purchased from Sigma-Aldrich Chemical Company and Alfa Aesar unless otherwise stated. Anhydrous DCM, DMF, DMSO, EtOH, MeOH, pyridine and THF were purchased in SureSeal™ bottles from Sigma-Aldrich or Acroseal™ bottles from Acros. Deuterated solvents used for NMR were purchased from Sigma-Aldrich. Unless stated, reactions were carried out under an inert atmosphere of nitrogen.

7.2 Analytical Techniques

The structures of reported compounds were elucidated through use of proton (^{1}H) and carbon (^{13}C) nuclear magnetic resonance techniques and run in the following deuterated solvents; $CDCl_3$, DMSO-d_6 or MeOD. Samples were run on either a Bruker Spectrospin AC 300E (300MHz) NMR spectrometer or a Bruker Avance III (500 MHz) NMR spectrometer. Chemical shifts are reported in parts per million (ppm) and coupling constants in Hertz (Hz). The abbreviations for spin multiplicity are as follows: s = singlet; d = doublet; t = triplet; q = quartet, quin = quintet and m = multiplet. Combinations of these abbreviations are employed to describe more complicated splitting patterns e.g. dd = doublet of doublets; dt = doublet of triplets etc. Where broadening of the peak is observed, spin multiplicity is accompanied by the prefix br = broad.

LC-MS (Liquid Chromatography - Mass Spectrometry) was carried out on a Micromass Platform LC or a Waters Acquity UPLC system with PDA and ELSD employing positive or negative electrospray modes as appropriate to the individual compound. High-resolution mass spectrometry results were obtained from the EPSRC National Mass Spectrometry Service, University of Wales, Singleton Park, Swansea, SAZ 8PP. Analytical purity of compounds were determined using Waters XTerra RP18, 5 μm (4.6 × 150 mm) column at 1 mL/min using either 0.1% aqueous ammonia and acetonitrile or 0.1% aqueous formic acid and acetonitrile with a gradient of 5-100% over 15 minutes.

FTIR spectra were recorded using a Bio-Rad FTS 3000MX diamond ATR as a neat sample. Melting Points were measured on either the Stuart Scientific SMP3 or SMP40 and are uncorrected. Ultraviolet spectra were measured using a Hitachi UV-U2800A spectrophotometer and were performed in EtOH.

7.3 Chromatography

MPLC performed on a Biotage SP4 system used prepacked columns from Biotage or Varian (KP-Sil, KP-NH, KP-C18 or Agilent Si 50 or 35). Thin layer chromatography was performed on Merck TLC silica gel 60 F_{254} plates unless otherwise stated, or NH_2F_{254}s plates on aluminium sheets, which were dried and visualised using short wave (245 nm) ultraviolet light.

Compounds requiring semi-preparative HPLC were purified on one of the following machines: (i) Varian Prostar Modular HPLC system equipped with a binary pumping system, UV detector and fraction collector and controlled by Varian Star software. (ii) Agilent 1200 HPLC system equipped with a binary pump, autosampler, fraction collector and diode array detector and controlled by Agilent ChemStation software.

7.4 Microwave Reactions

All reactions carried out in a microwave were performed in a Biotage Initiator with Sixty robot.

7.5 Crystallography

X-ray crystal structures were obtained by Dr. Ross W. Harrington and Prof. William Clegg at X-ray Crystallography, School of Chemistry, Bedson Building, Newcastle University, Newcastle upon Tyne, NE1 7RU.

7.6 ERK5 IMAP™ Assay Protocol

Preparation of Assay Buffer (1x)

The 0.01% Tween®-20 5x stock was supplied as part of IMAP™ FP Progressive Binding System Kit (Molecular Devices R7436), which was diluted to 1x using miliQ H_2O. 1 µL of a 1M DTT stock was added for every 1 mL of 1x assay buffer to give a final concentration of 1 mM DTT.

Preparation of ERK5 Working Solution

The final dilution was dependent on activity of the enzyme batches. The initial batch (08/08/08) was used at a 1 in 1 in 350 final dilution in assay buffer. A 1:175 dilution of ERK5 stock was performed in 1x assay buffer. For 1 plate, 13 µL of ERK5 stock was added to 2262 µL of 1x assay buffer. ERK5 was expressed and purified at CRT by Leon Pang and Sue Young. Aliquots were stored at –80 °C. Batch PO080808 was used at a stock concentration of 73.4 ng/µl.

Preparation of ATP/Substrate Working Solution

For one plate, ATP disodium salt (90 µL, 20 mM) (Sigma A7699) and FAM-EGFR-derived peptide (15 µL, 100 µM) (LVEPLTPSGEAPNQ(K-5FAM)-COOH) (Molecular Devices RP7129; reconstituted in miliQ H_2O to a stock concentration of 100 µL; Stored at -20°C) was added to 2295 µL of 1x assay buffer.

Preparation of IMAP™ binding solution

For one plate 20.5 µL of IMAP™ binding reagent stock, 1476 µL of 1x binding buffer A (60%), and 984 µL of binding buffer B (40%) (IMAP™ FP Progressive screening express kit (Molecular Devices R8127) was added to 9819.5 µL of milliQ H_2O.

Assay Procedure

1 µL of compound (in 60:40 H_2O/DMSO) or 60:40 H_2O/DMSO (for controls and blanks) were dry-spotted into the relevant wells of a 384-well assay plate using the MATRIX PlateMate® Plus. 5 µL of ERK5 working solution was added to test and control wells, and 5 µL of 1x assay buffer added to blanks; 4 µL of ATP/substrate working solution was added to all wells using a Matrix multichannel pipette. The plate was sealed using DMSO resistant

clear seal and incubated for 2 h at 37 °C. 1 µL of the kinase reaction mixture from the first plate was dry spotted into a second 384-well assay plate using the MATRIX PlateMate® Plus. 9 µL of assay buffer was added, followed by 30 µL of IMAP™ binding solution using a multichannel pipette. The plate was incubated at RT in darkness for 2 h. The assay plate was then read on an Analyst HT plate reader (Molecular Devices) using the settings described below;

Measurement mode = Fluorescence polarisation; Method ID = ERK5; Integration time = 100 ms; Excitation filter = Fluorescein 485-20; Emission filter = 530-25; Dichroic mirror = 505 nm; Plate definition file = Corning 384 black fb; Z-height = 5.715 mm (middle); G-factor = 1; Attenuator = out; Detector counting = Smartread+; Sensitivity = 2.

7.7 p38α LANCE Assay Protocol

Preparation of Assay Buffer (1x)

1x assay buffer was prepared freshly in house, consisting of the following reagents; 250 mM tris(hydroxymethyl)aminomethane (Tris) pH 7.5, 25 mM $MgCl_2$, 2.5 mM ethylene glycol tetraacetic acid (EGTA), 10 mM dithiothreitol (DTT) and 0.05% Triton X100 in milliQ H_2O (NB: 1x buffer final assay concentrations were 5x lower than stated above).

Preparation of p38α/SAPK2 Working Solution

The p38α/SAPK2, active N-terminal GST-tagged recombinant full length protein (Millipore 14-251) was supplied as a 10 µg/4 µL stock. This was diluted to a 10 µg/40 µL (1 µM) concentration by addition of 156 µL of Tris/HCl (pH 7.5, 50 mM), NaCl (150 mM), EGTA (0.1 mM), Brij-35 surfactant (0.03%), glycerol (50%) and 0.1% 2-mercaptoethanol (0.1%). The final dilution was dependent on activity of the enzyme batches. The p38α concentration used in the assay was 1 nM. A 2x working stock solution (2 nM, 500 fold dilution of 1 µM stock) in 1x assay buffer was prepared. For one plate, 9.4 µL of p38α (1 µM) was added to 1870.6 µL of milliQ H_2O.

Preparation of ATP/Substrate working solution

For one plate, ATP disodium salt (17.5 µL, 200 mM stock), (Sigma A7699) and U*light*-MBP Peptide (50 µL, 5 µM stock) (Perkin Elmer TRF0109) was added to 400 µL of 5x assay buffer and 1532.5 µL of milliQ H_2O.

Preparation of EDTA/Antibody Detection Reagent

For one plate, 84 µL of ethylenediaminetetraacetic acid (EDTA) (0.5 M) (Sigma E4378-100G) and 27 µL of Europium-anti-phospho-MBP antibody (0.625 µM) (Perkin Elmer) was added to 420 µL of LANCE detection buffer (1x) and 3669 of milliQ H_2O.

Assay Procedure

1 µL of compound (in 80:20 H_2O/DMSO) or 80:20 H_2O/DMSO was dry-spotted into the relevant wells of a 384-well assay plate using the MATRIX PlateMate® Plus. 5 µL of p38α working solution was added to test and control wells, and 5 µL of assay buffer added to blanks; 4 µL of ATP/substrate working solution was added to all wells using a Thermo Multidrop Combi or Matrix multichannel pipette. The plate was sealed using DMSO resistant clear seal and incubated for 1 h at 37 °C. 10 µL of the EDTA/antibody working solution was added to all wells using a Thermo Multidrop Combi or Matrix multichannel pipette. The plate was incubated at RT in darkness for 2 h. The assay plate was then read on a PheraStar microplate reader using the settings described below;

Pherastar: Measurement mode = TRF; Method ID = LANCE HTRF ERK5; Optic Module: 337, 665, 620 nm. Focal Height = 6.0, Positioning delay, 0.1 sec, Number of flashes per well = 100, Integration start = 60 µs, Integration time = 200 µs, Simultaneous dual emission, Ratio multiplicator = 1000

7.8 Dual-Luciferase Reporter Assay

Preparation of Agar Plates for Bacterial Colony Growth

250 mL of lysogeny broth (LB) agar was spiked with 250 µL of an antibacterial agent (kanomycin or ampicillin), and using a sterile pipette, 25 mL of spiked LB agar was transferred into 12 petri dishes. The *E.Coli* bacteria used to express DNA plasmids are antibiotic resistant; therefore the addition of an antibacterial agent maintains selective bacterial growth.

Growth of Transformed Bacterial Colonies

To a polypropylene tube was added 48 µL of *E. coli* in glycerol stock (prepared in-house at the Babraham Institute), and 2 µL of either the Gal4-Luciferase or MEK5D DNA plasmid. The resulting mixture was incubated at 0 ^{o}C for 15 min. Bacteria were subjected to stress by

heating at 42 ^{o}C for 30 sec, then returning to 0 ^{o}C. 200 µL of LB agar was added at 0 ^{o}C, and the resulting mixture was incubated with shaking for 30 min to 1 h at 37 ^{o}C.

At 37 ^{o}C, 250 µL of the solution containing Gal4-Luciferase transformed bacteria was transferred onto one LB agar/kanomycin plate. 250 µL of the solution containing MEK5D transformed bacteria was transferred onto one LB agar/ampicillin plate. Agar plates were allowed 24 h at 37 ^{o}C for bacterial colony growth.

To a conical flask was added 100 mL LB agar, 100 µL of the relevant antibiotic, and a sample of the bacterial colonies from the relevant petri dish. The flasks were incubated for a further 24 h at 37 ^{o}C, with stirring (150-170 rpm).

DNA Purification

2 x 50 mL portions of the incubated bacteria in agar obtained were transferred into 50 mL Falcon tubes and subjected to centrifugation at 6000 G for 15 min. DNA plasmids were isolated in aqueous media from the remaining bacterial pellet using a Qiagen Plasmid Plus Midi Kit, according to kit instructions.

DNA Quantification

The concentration of the purified aqueous DNA was determined using a NanoDrop 1000 spectrophotometer. DNA stock solutions were at 2419.4 ng/µL and 1965.6 ng/µL for Gal-4-Luciferase and MEK5D plasmid stocks respectively. All other DNA plasmid stocks used were prepared in house at the Babraham Institute by Dr Pamela Lochhead.

Cell Maintenance

HEK293 cells were grown as adherent colonies on tissue culture dishes in Dulbecco's Modified Eagle Medium (DMEM) tissue culture medium (Gibco® 41966) containing L-glutamine (2 mM, Gibco® 1499), penicillin/streptomycin (100 µg/mL, PAA P11-010), foetal bovine serum (FBS) (10%, PAA A15-151) as additives.

Penicillin and streptomycin are antibacterial agents, which minimise the risk of bacterial infection occurring in cell culture. FBS is a serum supplement, which contains growth factors that promote eukaryotic cell growth. L-glutamine is a nutrient which supports the growth of cells which have high energy demands, such as cells which synthesise large amounts of proteins and/or nucleic acids or those which use glucose inefficiently.

Trypsinizing of Adherent Cell Colonies

Cells were regularly passaged in order to maintain optimum colony sizes on plates. In order to do this, and to harvest cells for use in the dual-luciferase reporter assay, adherent cells were lifted from tissue culture dishes. Cell media was removed *via* aspiration, and the cell monolayer was washed with phosphate buffered saline (PBS) solution (10 mL), which was then aspirated. The cells were lifted from the plate through incubation at 37 ^{o}C for 5-10 min with 1 mL trypsin (0.5% trypsin-EDTA (1x), Gibco® 15400054).

PBS (10x): NaCl (4% w/v), KCl (0.1% w/v), $Na_2HPO_4.7H_2O$ (0.6% w/v), KH_2PO_4 (0.1% w/v), NaN_3 (0.01% w/v).

Reverse Transfection of HEK293 cells

Preparation of EGFP Control (C3) Working Solution (For 1 x 96 well plate)

To a 50 mL Falcon tube was added 250 µL Opti-MEM® growth media (reduced serum medium, Invitrogen 31985), and the following DNA plasmids; MEF2D-Gal4 (2.5 µL, 0.25 mg/mL stock), Gal4-Luc (2.5 µL, 1.25 mg/mL stock), Renilla Luciferase (2.5 µL, 0.1 mg/mL stock), EGFP construct, containing no MEK5D (0.25 µL, 0.5 mg/mL stock), and HA-ERK5 wt (2.5 µL, 0.5 mg/mL stock). To this mixture was then added 5 µL of Lipofectamine™ 2000 transfection reagent (Invitrogen 11668) and complexation allowed for 15-20 min.

Preparation of EGFP-MEK5D (5D) Working Solution (For 1 x 96 well plate)

To a 50 mL Falcon tube was added 1500 µL Opti-MEM® growth media (reduced serum medium, Invitrogen 31985), and the following DNA plasmids; MEF2D-Gal4 (15 µL, .25 mg/mL stock), Gal4-Luc (15 µL, 1.25 mg/mL stock), Renilla Luciferase (15 µL, 0.1 mg/mL stock), EGFP-MEK5D construct (1.5 µL, 0.5 mg/mL stock), HA-ERK5 wt (15 µL, 0.5 mg/mL stock). To this mixture was then added 30 µL of Lipofectamine™ 2000 transfection reagent (Invitrogen 11668) and complexation allowed for 15-20 min.

Preparation of HEK293 Cells for Reverse Transfection

Trypsinized HEK293 cells were re-suspended in 19 mL of fresh cell media and counted using haemocytometry. Cells were then diluted with fresh cell media to achieve a final cell concentration of 2 x 10^5 cells/mL. 1237.5 µL and 7425 µL of this cell media was added to the C3 and 5D working solutions respectively. 100 µL of the transfected cells were then

aliquoted into the appropriate wells in a 96-well opaque sided tissue culture plate, and incubated at 37 ^{o}C for 6 h.

Addition of Compounds to HEK293 Cells

Each compound supplied was prepared as a 10 mM working solution in DMSO, from which the following stocks were prepared in DMSO; 3.33 mM, 1 mM, 0.11 mM and 10 µM. 4 compounds was assayed per 96-well plate. For each compound, 1 mL of growth media was added to eight 1.5 mL Eppendorf® tubes. 6 µL of DMSO was added to two tubes for C3 and blank 5D wells, and 6 µL of the relevant compound stock solution was added to the 6 remaining tubes. BIX02189 was added to each plate in varying concentrations as an indicator of assay reliability. Solutions of drug in media were thoroughly mixed, and 100 µL of the relevant compound was transferred (in triplicate) to the 96-well plate containing transfected HEK293 cells using an electronic multichannel pipette with variable tip spacing. Sealed plates were incubated at 37 ^{o}C for 24 h. Final compound concentrations were as follows; 30 µM, 10 µM, 3 µM, 1 µM and 0.3 µM.

Assay Plate Lysis

15 mL of 1x passive lysis buffer (PLB) was prepared using 5x PLB (Dual-Luciferase Reporter Assay System, Promega® E1960), diluting with H_2O. Assay plates prepared were removed from the incubator and the growth media removed by aspiration. 20 µL of 1x PLB was dispensed into each well and the plates shaken for 10 min. Assay plates were sealed and stored at -80 ^{o}C overnight.

Quantification of Cellular Inhibition of ERK5

Cellular inhibition of ERK5 was quantified using the Dual-Luciferase® Reporter Assay System (Promega® E1960). Luciferase assay buffer/Luciferase assay substrate and Stop and Glo® assay buffer/Stop and Glo® substrate were prepared according to kit instructions. 100 µL of the Luciferase system was added to each well using a multichannel pipette, before analysis using an EG&G Berthold Microlumat Plus luminometer. 100 µL of the Stop and Glo® system was subsequently added, and the plate was analysed once again by luminometer. Raw data was processed using Microsoft Excel, enabling generation of IC_{50} values for each compound. IC_{50} values obtained are based on the means of 3 experiments. Each data point is the mean of 3 values ± standard deviation to produce one curve using Microsoft Excel. IC_{50} values were calculated by eye.

7.9 General Procedures

A number of compounds have been synthesised using similar procedures. These general protocols are described below. Quantities used and variations are indicated with the analytical data for a specific compound.

General Procedure A: Aldol Condensation

To a solution of the relevant methyl ketone (1 eq.) in EtOH (1 mL/mmol) was added the relevant aldehyde (1.2 eq.) and KOH (2.4 eq.) at 0 ^{o}C. After 10 min, the mixture was warmed to RT and stirred for 16 h. The resulting solid was filtered and recrystallised from a minimum amount of hot EtOH to give the desired product.

General Procedure B: 3-Cyanopyridine Synthesis

A 1.6M solution of NaOMe was prepared by slowly dissolving sodium metal in MeOH at RT. To the relevant chalcone (1 eq.) and 2-cyanothioacetamide (1 eq.) was added 8.5% w/v NaOMe (2.4 eq.). The resulting solution was heated at 80 ^{o}C for 1.5 h, then allowed to cool to RT and concentrated *in vacuo*. The crude material was redissolved in DMF (1 mL/mmol) and the relevant bromoacetate (1.5 eq.) was added. The solution was heated at 100 ^{o}C for 3-4 h, and monitored by LCMS. The mixture was then cooled and diluted with H_2O (20 mL). The product was extracted with EtOAc (3 x 100 mL), washed with H_2O (3 x 100 mL) and brine (50 mL). Combined organic layers were dried over Na_2SO_4 and concentrated *in vacuo*. Purification *via* column chromatography (silica; 0-50% EtOAc/petrol) gave the desired product.

General Procedure C: Deprotection of a tert-Butyl Ester using TFA

To the relevant *tert*-butyl ester (1 eq.) in DCM (1 mL/mmol) was added TFA (2 eq.) The resulting solution was stirred at RT for 30 min. The mixture was concentrated *in vacuo* and triturated with petrol to give the desired product as the TFA salt. The salt was dissolved in H_2O (10 mL) and neutralised with a 1M aqueous solution of NaOH. Extraction with EtOAc (3 x 30 mL) gave the desired product.

General Procedure D: CDI Mediated Amide Coupling

A solution of carbonyldiimidazole (2.0 eq.) and the relevant carboxylic acid (1.0 eq.) in THF (5 mL/mmol) was heated to 70 ºC for 3 h. The appropriate amine (2.5 eq.) was added and the

mixture heated at 50 °C for 3 h then at RT for 16 h. The product was extracted with EtOAc (2 x 100 mL), washed with brine (100 mL) and dried over Na_2SO_4. Purification *via* column chromatography gave the desired product

General Procedure E: Acid chloride Synthesis

To a solution or suspension of the relevant carboxylic acid (1 eq.) in THF (1 mL/mmol) was added $SOCl_2$ (1.5 eq.) at 0 ^oC, followed by DMF (cat). The resulting mixture was stirred at RT for 3 h, and then concentrated *in vacuo*. The crude material was used in the next step without further purification.

General Procedure F: Friedel-Crafts Acylation

To a suspension of $AlCl_3$ (2.5 eq.) in DCM (1 mL/mmol $AlCl_3$) at 0 ^oC was added the relevant acid chloride (2 eq.) followed by methyl 1*H*-pyrrole-2-carboxylate (1 eq.). The resulting mixture was allowed to reach RT and stirred for 16 h. The reaction was quenched at 0 ^oC with a 1M aqueous solution of HCl (20 mL). The product was extracted with DCM (3 x 100 mL), washed with an aqueous saturated solution of $NaHCO_3$ (2 x 100 mL) and brine (100 mL). Combined organic layers were dried over Na_2SO_4 and concentrated *in vacuo*. Purification *via* column chromatography (silica; 0-50% EtOAc/Petrol) gave the desired product.

General Procedure G: Ester Hydrolysis and/or Tosyl Group Hydrolysis

To a solution of the relevant ester (1 eq.) in THF (8 mL/mmol) was added a solution of LiOH monohydrate (20 eq.) in H_2O (13 mL/mmol). The resulting mixture was heated at 65 ^oC for 16 h, cooled to RT and acidified to pH 3-4 with a 1M aqueous solution of HCl. The product was extracted with EtOAc (3 x 100 mL). Combined organic layers were washed with brine (200 mL), dried over Na_2SO_4 and concentrated *in vacuo* to give the desired product.

General Procedure H: Deprotection of Silyl Protecting Groups

To a solution of the relevant pyrrolopyridone (1 eq.) was added a 1M solution of TBAF in THF (2 mL/mmol). When deprotecting SEM groups, the resulting solution was stirred at 65 ^oC for 16 h. When deprotecting TIPS/TMS groups, the resulting solution was stirred at RT for 4 h. After the allocated time, the mixture was concentrated *in vacuo*. Purification *via* column chromatography gave the desired products.

General Procedure I: Nucleophilic Substitution of Amines

To a solution of methyl 4-(2,2,2-trichloroacetyl)-1*H*-pyrrole-2-carboxylate (1 eq.) in DMF (3 mL/mmol) was added the relevant amine (3 eq.). The resulting mixture was heated at 50 ^{o}C for 4 h. The solution was cooled, diluted with water and extracted with EtOAc (3 x 30 mL). Combined organic layers were washed with brine, dried over Na_2SO_4 and concentrated *in vacuo.* Purification *via* column chromatography or recrystallisation gave the desired product.

General Procedure J: Selective Ester Hydrolysis

To a solution of the relevant methyl ester (1 eq.) in THF (5 mL/mmol) was added a solution of LiOH monohydrate (1.5 eq.) in water (5 mL/mmol). The resulting solution was heated to 40 ^{o}C for 4 h. The mixture was cooled, acidified to pH 5-6 with a 1M aqueous solution of HCl and extracted with EtOAc (3 x 30 mL). Combined organic layers were washed with brine, dried over Na_2SO_4 and concentrated *in vacuo* to give the desired products.

General Procedure K: Deprotection of a Boc Protecting Group with TFA

To a solution of the relevant Boc protected amine (1 eq.) in DCM (5 mL/mmol) was added triethylsilane (2.5 eq.) where indicated, followed by TFA (2 mL/mmol). The resulting solution was stirred at RT for 1 h. The mixture was concentrated *in vacuo,* and triturated with diethyl ether (10 mL) to give the TFA salt. To obtain the free base, the TFA salt was triturated with an aqueous saturated solution of $NaHCO_3$ (10 mL) and the product extracted with EtOAc (2 x 30 mL). Combined organic layers were washed with brine (30 mL), dried over Na_2SO_4 and concentrated *in vacuo* to give the desired product.

General Procedure L: Demethylation of Methyl Ethers with BBr_3

To a 1M solution of BBr_3 in DCM (5 mL/mmol) was added the relevant methyl ether (1 eq.) at 0 ^{o}C. The resulting mixture was warmed to room temperature and stirred for 16 h. The reaction was quenched with water, and adjusted to pH 10 with a 1M aqueous solution of NaOH. The mixture was extracted with EtOAc (3 x 20 mL). Combined organic layers were washed with brine, dried over Na_2SO_4 and concentrated *in vacuo*. Column chromatography gave the desired products.

General Procedure M: PCl_3 Mediated Amide Coupling

A microwave vial was charged with the relevant carboxylic acid (1 eq.), the desired amine (2.5 eq), MeCN (2 mL/mmol) and PCl_3 (1 eq.). The resulting mixture was heated at 150 ^oC with microwave irradiation for 5 min unless otherwise stated. The mixture was quenched with an aqueous saturated solution of $NaHCO_3$ (10 mL) and diluted with H_2O (30 mL). The crude product was extracted with EtOAc (3 x 30 mL). Combined organic layers were washed with brine (50 mL), dried over Na_2SO_4, and concentrated *in vacuo*. Purification *via* column chromatography gave the desired product.

General Procedure N: Suzuki Coupling 1

A microwave vial was charged with the relevant bromoaryl species (1 eq.), Cs_2CO_3 (1.5 eq.) the desired boronic acid (3 eq.), dichloro [1,1'-bis(di-tert-butylphosphino)]ferrocene palladium (II) (10 mol%), and dioxane (10 mL/mmol). The resulting mixture was degassed for 20 min, and then heated at 150 ^oC under microwave irradiation for 1 h. The mixture was diluted with MeOH (20 mL) and passed through a Celite cartridge to remove metallic impurities. The resulting solution was concentrated *in vacuo* and the crude material was either engaged directly in the next step or purified by column chromatography to give the desired product.

General Procedure O: Suzuki Coupling 2

A microwave vial was charged with the relevant bromoaryl species (1 eq.), KOAc (3 eq.), bis(pinacolato)diboron (1.5 eq.), dichloro [1,1' bis(di-tert-butylphosphino)]ferrocene palladium (II) (10 mol%) and dioxane (10 mL/mmol). The resulting mixture was degassed for 20 min, and then heated at 150 ^oC under microwave irradiation for 15 min. To this mixture was then added 2-bromopyridine (1.5 eq.), Na_2CO_3 (1.2 eq), H_2O (0.2 mL), and tetrakis(triphenylphosphine)palladium (0) (10 mol%). The resulting mixture was degassed for 20 min, and then heated conventionally at 110 ^oC for 16 h. The mixture was diluted with MeOH (20 mL), passed through a Celite cartridge, and the resulting solution concentrated *in vacuo*. Purification *via* column chromatography (silica; 10-50% EtOAc/petrol) gave the desired product.

General Procedure P: Acid-catalysed Cyclisation

To neat methanesulfonic acid (3 mL/mmol) was added the relevant diethyl acetal (1 eq.). The resulting solution was heated at 95 ^{o}C for 1 h. The mixture was then allowed to cool to RT, diluted with H_2O and the product was extracted with EtOAc (3 x 100 mL). Combined organic layers were washed with brine, dried over Na_2SO_4 and concentrated *in vacuo*. Purification *via* column chromatography (silica; 0-10% MeOH/DCM) gave the desired product.

General Procedure Q: SEM Protection

To a solution of the relevant pyrrolopyridone (1 eq.) in THF (3 mL/mmol) was added SEMCl (1.2 eq), Et_3N (1.2 eq.) and DMAP (10 mol%). The resulting mixture was stirred for 16 h at RT. An additional 1.2 eq. of Et_3N and SEMCl were added if the reaction had not reached completion and the mixture allowed to stir for a further 24 h. The reaction was quenched with H_2O and the product extracted with EtOAc (3 x 50 mL). Combined organic layers were dried over Na_2SO_4 and concentrated *in vacuo*. Purification *via* column chromatography (silica; 10-70% EtOAc/petrol) gave the desired product.

General Procedure R: Ullmann Coupling

To a microwave vial was added the relevant pyrrolopyridone (1 eq.), the relevant bromopyridine hydrochloride (1.3 eq), K_2CO_3 (3.3 eq.) and CuI (10 mol%). The vial was sealed under an inert atmosphere and DMF (1 mL/mmol) was subsequently added. The mixture was degassed for 20 min, heated conventionally at 135 ^{o}C for 48-72 h and monitored by LCMS. The mixture was allowed to cool, filtered through Celite, and washed with EtOAc/MeOH (7:3). The resulting solution was concentrated *in vacuo*. Purification *via* column chromatography (silica; 0-5% MeOH/DCM) gave the product. In cases where some deprotection of the SEM group occurred during the course of the Ullmann reaction, the crude material was engaged directly in the next step without purification.

7.10 Experimental Data

Methyl 4-chloro-3-nitrobenzoate, 50

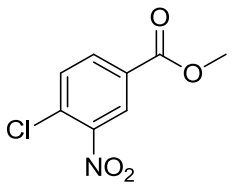

To a solution of 4-chloro-3-nitrobenzoic acid (600 mg, 2.98 mmol) in MeOH (1.5 mL/mmol acid) was added thionyl chloride (0.11 mL, 1.49 mmol) at 0 ^{o}C. The resulting solution was heated at 60 ^{o}C overnight. The mixture was then cooled in an ice bath, resulting in the formation of a precipitate. The solid was filtered and collected *in vacuo*. Recrystallisation (MeOH) gave **50** as beige crystals (550 mg, 85%). R_f 0.83 (1:1 EtOAc/petrol); m.p. 80-81 ˚C (lit.[139] 78-79 ˚C); λ_{max} (EtOH/nm) 230.5; IR υ_{max}/cm^{-1} 3102, 2961, 1714, 1604, 1536; ^{1}H NMR (500 MHz, $CDCl_3$) δ ppm 4.00 (3H, s, O-CH_3), 7.67 (1H, d, *J* = 8.5 Hz, H-5), 8.19 (1H, dd, *J* = 2.0 and 8.5 Hz, H-6), 8.54 (1H, d, *J* = 2.0 Hz, H-2); ^{13}C NMR (125 MHz, $CDCl_3$) δ ppm 53.0 (O-CH_3), 126.7 (C-Ar), 130.1 (C-Ar), 131.7 (C-Ar), 132.2 (C-Ar), 133.6 (C-Ar), 148.7 (C-Ar), 164.2 (CO); MS (ES+) *m/z* 216.5 $[M+H]^+$.

Dimethyl 2-(4-(methoxycarbonyl)-2-nitrophenyl)malonate, 51

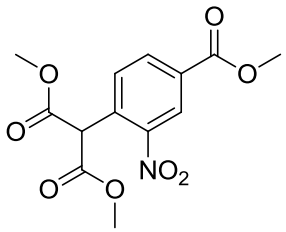

To a solution of potassium *tert*-butoxide (560 mg, 4.98 mmol) in NMP (1 mL/mmol base) was added dimethyl malonate (0.57 mL, 4.98 mmol) and the resulting solution heated at 75 ^{o}C. A solution of methyl 4-chloro-3-nitrobenzoate (540 mg, 2.49 mmol) in NMP (1 mL/mmol ester) was added dropwise and the resulting mixture heated at 75 ^{o}C for 2 h. The solution was allowed to cool, and acidified to pH 2 with a 1M aqueous solution of HCl, and stirred at 0 ^{o}C for a further 2 h. The mixture was diluted with DCM (50 mL), washed with water (50 mL), and brine (30 mL). Combined organic layers were dried over $MgSO_4$ and concentrated *in vacuo*. Purification *via* column chromatography (silica; 0-50% EtOAc/petrol) gave **51** as a yellow oil (500 mg, 66%). R_f 0.66 (1:1 EtOAc/petrol); λ_{max} (EtOH/nm) 228.0; IR υ_{max}/cm^{-1}

2957, 1729, 1620, 1537; ^{1}H NMR (500 MHz, $CDCl_3$) δ ppm 3.74 (6H, s, O-CH_3), 3.91 (3H, s, O-CH_3), 5.30 (1H, s, CH), 7.55 (1H, d, *J* = 8.1 Hz, H-6), 8.21 (1H, dd, *J* = 1.8 and 8.1 Hz, H-5), 8.63 (1H, d, *J* = 1.8 Hz, H-3); ^{13}C NMR (125 MHz, $CDCl_3$) δ ppm 52.9 (O-CH_3), 53.4 (O-CH_3), 54.1 (CH), 126.3 (C-Ar), 131.6 (C-Ar), 131.9 (C-Ar), 132.1 (C-Ar), 134.0 (C-Ar), 148.8 (C-Ar), 164.1 (CO), 167.1 (CO); MS (ES+) *m/z* 311.2 $[M+H]^+$.

Methyl 2-oxoindoline-6-carboxylate, 52

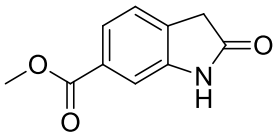

To a solution of dimethyl 2-(4-(methoxycarbonyl)-2-nitrophenyl)malonate (420 mg, 1.35 mmol) in acetic acid (5 mL/mmol malonate) was added ammonium formate (430 mg, 6.75 mmol) and palladium on carbon (10% $^{w}/_{w}$). The resulting mixture was heated at 100 ^{o}C for 10 minutes under microwave irradiation. The mixture was then filtered through Celite and concentrated *in vacuo*. Purification *via* column chromatography (silica; 0-50% EtOAc/petrol) gave **52** as a white solid (310 mg, 98%). R_f 0.23 (6:4 EtOAc/petrol); m.p. 212-215 ^{o}C (lit.[105] 208-211 ^{o}C); λ_{max} (EtOH/nm) 306.0, 222.0; IR υ_{max}/cm^{-1} 3047, 2955, 2923, 2850, 1696, 1628; ^{1}H NMR (500 MHz, $CDCl_3$) δ ppm 3.52 (2H, s, CH_2), 3.85 (3H, s, O-CH_3), 7.23 (1H, d, *J* = 7.8 Hz, H-4), 7.46 (1H, br s, H-7), 7.68 (1H, dd, *J* = 1.3 and 7.8 Hz, H-5), 7.72 (1H, s, NH); MS (ES+) *m/z* 192.2 $[M+H]^+$.

Methyl 1-acetyl-3-(ethoxy(phenyl)methylene)-2-oxoindoline-6-carboxylate (Inseparable mixture of *E* and *Z*), 53

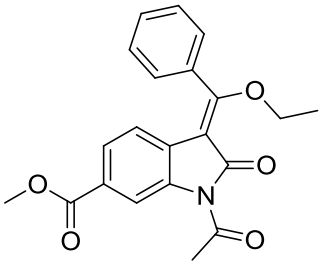

A solution of methyl 2-oxoindoline-6-carboxylate (160 mg, 0.83 mmol) in acetic anhydride (4 mL/mmol) was heated at 130 ^{o}C for 3 h. The mixture was cooled to 100 ^{o}C, triethyl orthobenzoate (0.21 mL, 0.91 mmol) was added and the mixture heated for a further 3 h. The solution was allowed to cool, and diluted with DCM (30 mL). The mixture was washed with water (30 mL) and brine (20 mL). Combined organic layers were dried over $MgSO_4$ and

concentrated *in vacuo*. Purification *via* column chromatography (silica; 0-30% EtOAc/petrol) gave **53** as a yellow solid (240 mg, 79%). R_f 0.80 (1:1 EtOAc/petrol); m.p. 167-169 ^oC; λ_{max} (EtOH/nm) 342.0, 313.5, 266.0, 223.0; IR υ_{max}/cm^{-1} 2994, 2953, 1699, 1621, 1595; ^1H NMR (500 MHz, $CDCl_3$, major isomer) δ ppm 1.44 (3H, t, *J* = 7.1 Hz, CH_2-*CH_3*), 2.58 (3H, s, N-CO-CH_3), 3.94 (3H, s, O-CH_3), 4.00 (2H, q, *J* = 7.1 Hz, *CH_2*-CH_3), 7.40-7.42 (2H, m, H-Ar), 7.56-7.59 (3H, m, H-Ar), 7.97 (1H, dd, *J* = 1.6 and 8.1 Hz, H-5), 8.05 (1H, d, *J* = 8.1 Hz, H-4), 8.84 (1H, d, *J* = 1.6 Hz, H-7); ^{13}C NMR (125 MHz, $CDCl_3$, major isomer) δ ppm 15.1 (CH_3), 26.5 (CH_3), 52.2 (O-CH_3), 67.3 (CH_2), 104.6 (Cq), 115.4 (C-Ar), 122.3 (C-Ar), 125.9 (C-Ar), 127.3 (C-Ar), 128.3 (C-Ar), 128.6 (C-Ar), 128.6 (C-Ar), 130.4 (C-Ar), 130.8 (C-Ar), 136.1 (C-Ar), 166.1 (Cq), 166.1 (CO), 170.8 (CO), 172.3 (CO); MS (ES+) *m/z* = 366.1 $[M+H]^+$.

(*Z*)-Methyl 1-acetyl-3-(((3-((dimethylamino)methyl)phenyl)amino)(phenyl)methylene)-2-oxoindoline-6-carboxylate, 54

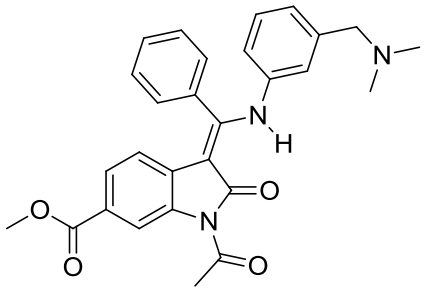

To a solution of methyl 1-acetyl-3-(ethoxy(phenyl)methylene)-2-oxoindoline-6-carboxylate (230 mg, 0.63 mmol) in DMF (5 mL/mmol) was added 3-dimethylamino methylaniline (100 mg, 0.67 mmol) and the resulting mixture heated at 80 ^oC for 3 h. The mixture was allowed to cool, diluted with DCM, and washed with water (30 mL) and brine (20 mL). Combined organic layers were dried over Na_2SO_4 and concentrated *in vacuo*. Purification *via* column chromatography (silica; 0-8% MeOH/DCM) gave **54** as a yellow solid (150 mg, 52%). R_f 0.39 (7:3 EtOAc/petrol); m.p. 157-159 ^oC; λ_{max} (EtOH/nm) 385, 303; IR υ_{max}/cm^{-1} 2927, 2812, 2764, 1699, 1666, 1569; ^1H NMR (500 MHz, MeOD) δ ppm 2.12 (6H, s, N-CH_3), 2.84 (3H, s, N-CO-CH_3), 3.31 (2H, s, CH_2), 3.88 (3H, s, O-CH_3), 5.90 (1H, d, *J* = 8.4 Hz, H-4), 6.93-6.94 (1H, m, H-Ar), 6.96-6.98 (1H, m, H-Ar), 7.11-7.13 (1H, m, H-Ar), 7.23 (1H, dd, *J* = 7.7 and 7.8 Hz, H-Ar), 7.43 (1H, dd, *J* = 1.6 and 8.4 Hz, H-5), 7.46-7.49 (2H, m, H-Ar), 7.56-7.64 (3H, m, H-Ar), 8.88 (1H, d, *J* = 1.6 Hz, H-7); ^{13}C NMR (125 MHz, MeOD) δ ppm Insufficient quantity of material to perform analysis; MS (ES+) *m/z* = 470.4 $[M+H]^+$.

(*Z*)-3-(((3-((Dimethylamino)methyl)phenyl)amino)(phenyl)methylene)-2-oxoindoline-6-carboxylic acid, 55

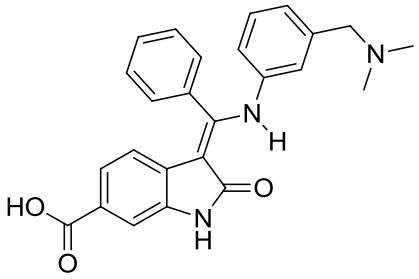

To a solution of (*Z*)-methyl 1-acetyl-3-(((3-((dimethylamino)methyl)phenyl)amino)(phenyl)methylene)-2-oxoindoline-6-carboxylate (100 mg, 0.21 mmol) in THF (5 mL/mmol ester) was added LiOH (180 mg, 4.20 mmol) in water (5 mL/mmol ester) and the resulting mixture heated at 60 ^{o}C overnight. The solution was allowed to cool, and concentrated *in vacuo*. Trituration of the residue with EtOH afforded the crude material. Purification *via* semi-preparative HPLC (55:45 0.1% formic acid (aq)/MeOH) gave **55** as a yellow solid (33 mg, 38%). R_f 0.45 (MeOH); m.p. 278-280 ^{o}C; λ_{max} (EtOH/nm) 387.0; IR υ_{max}/cm^{-1} 3146, 2923, 2853, 1705, 1647, 1582; ^{1}H NMR (500 MHz, DMSO-d_6) δ ppm 2.01 (6H, s, N-CH_3), 3.24 (2H, s, CH_2), 5.83 (1H, d, *J* = 8.2 Hz, H-4), 6.78-6.79 (2H, m, H-Ar), 6.98 (1H, d, *J* = 7.6 Hz, H-Ar), 7.15 (1H, dd, *J* = 7.6 and 7.7 Hz, H-Ar), 7.18 (1H, dd, *J* = 1.5 and 8.2 Hz, H-5), 7.42 (1H, d, *J* = 1.5 Hz, H-7), 7.49-7.51 (2H, m, H-Ar), 7.56-7.62 (3H, m, H-Ar), 10.95 (1H, s, NH), 12.25 (1H, s, NH), COOH not visualised; ^{13}C NMR (125 MHz, DMSO-d_6) δ ppm Insufficient quantity of material to perform analysis; MS (ES+) *m/z* = 414.5 $[M+H]^+$; HRMS calcd for $C_{25}H_{23}N_3O_3$ $[M+H]^+$ 414.1812, found 414.1812.

(*Z*)-3-(((3-((Dimethylamino)methyl)phenyl)amino)(phenyl)methylene)-2-oxoindoline-6-carboxamide, 47

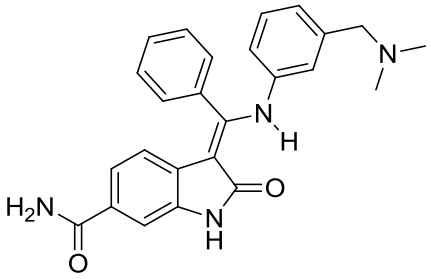

To a suspension of (*Z*)-3-(((3-((dimethylamino)methyl)phenyl)amino)(phenyl)methylene)-2-oxoindoline-6-carboxylic acid (100 mg, 0.22 mmol) in DMF (10 mL/mmol) was added PyBOP (170 mg, 0.33 mmol), HOBt (45 mg, 0.33 mmol), ammonium chloride (24 mg, 0.44 mmol) and DIPEA (0.15 mL, 0.88 mmol). The resulting solution was stirred at RT for 18 h. The solvent was removed *in vacuo*, and the residue triturated with EtOH to give the crude material. Purification by semi-preparative HPLC (3:7 0.1% formic acid (aq)/MeCN) gave **47** as a yellow, hygroscopic solid (16 mg, 16%). R_f 0.45 (95:5 DCM/MeOH); m.p. 120-122 ^{o}C decomp.; λ_{max} (EtOH/nm) 284.5, 386.5; IR υ_{max}/cm^{-1} 3250, 3195, 3118, 3052, 2933, 2837, 1615, 1545; ^{1}H NMR (500 MHz, MeOD) δ ppm 2.56 (6H, s, N-CH_3), 3.99 (2H, s, CH_2), 5.94 (1H, d, *J* = 8.2 Hz, H-4), 6.96-7.02 (2H, m, H-Ar), 7.10 (1H, dd, *J* = 1.6 and 8.2 Hz, H-4), 7.14 (1H, d, *J* = 7.6 Hz, H-Ar), 7.25-7.28 (1H, dd, *J* = 7.6 and 7.7 Hz, H-Ar), 7.43 (1H, d, *J* = 1.6 Hz, H-7), 7.45-7.50 (2H, m, H-Ar), 7.53-7.49-7.54 (3H, m, H-Ar), 8.40 (2H, s, NH_2), NH not visualised; MS (ES+) *m/z* = 413.3 $[M+H]^+$.

(*Z*)-3-(((3-((Dimethylamino)methyl)phenyl)amino)(phenyl)methylene)-*N*,*N*-dimethyl-2-oxoindoline-6-carboxamide, 48

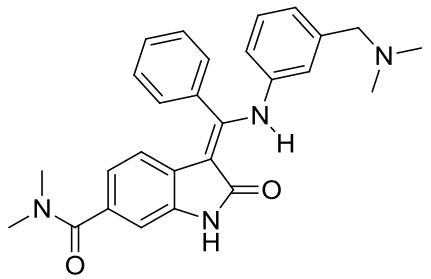

To a suspension of (*Z*)-3-(((3-((dimethylamino)methyl)phenyl)amino)(phenyl)methylene)-2-oxoindoline-6-carboxylic acid (30 mg, 0.07 mmol) in DMF (10 mL/mmol) was added PyBOP (50 mg, 0.10 mmol), HOBt (14 mg, 0.10 mmol), dimethylamine hydrochloride (11

mg, 0.13 mmol) and DIPEA (45 µL, 0.27 mmol). The resulting solution was stirred at room temperature for 18 h. The solvent was removed *in vacuo*, and the residue obtained triturated with EtOH afforded the crude material. Purification by semi-preparative HPLC (95:5 0.1% formic acid (aq)/MeOH) gave **48** as a yellow solid (22 mg, 71 %). R_f 0.59 (95:5 DCM/MeOH); m.p. 108-110 ^oC decomp.; λ_{max} (EtOH/nm) 282.0, 379.0; IR υ_{max}/cm^{-1} 2934, 2817, 2770, 1611, 1573; ^1H NMR (500 MHz, MeOD) δ ppm 1.95 (6H, s, CH_2-N*(CH₃)₂*), 2.89 (6H, br s, CO-N*(CH₃)₂*), 3.15 (2H, s, CH_2), 5.82 (1H, d, *J* = 8.2 Hz, H-4), 6.52 (1H, dd, *J* = 1.5 and 8.2 Hz, H-5), 6.66-6.70 (2H, m, H-Ar), 6.85-6.89 (2H, m, H-Ar), 7.00-7.03 (1H, m, H-Ar), 7.33-7.76 (2H, m, H-Ar), 7.38-7.46 (3H, m, H-Ar), NH not visualised; ^{13}C NMR (125 MHz, MeOD) δ ppm Insufficient quantity of material to perform analysis; MS (ES+) *m/z* = 441.3 $[M+H]^+$.

(*E*)-3-(4-Fluorophenyl)-1-phenylprop-2-en-1-one, 85

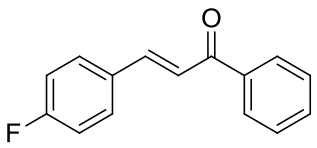

General procedure A: acetophenone (1.03 g, 8.60 mmol), 4-fluorobenzaldehyde (1.07 mL, 10.20 mmol), and NaOH (0.82 g, 20.60 mmol) gave **85** as yellow crystals (1.46 g, 75%). R_f 0.47 (1:9 EtOAc/petrol); m.p. 85-86 ˚C (lit.[140] 88-90 ^oC); λ_{max} (EtOH/nm) 297.0, 379.0; IR υ_{max}/cm^{-1} 1661; ^1H-NMR (500 MHz, $CDCl_3$) δ ppm 7.14 (2H, dd, *J* = 6.6 and 8.5 Hz, H-3 and H-5), 7.48-7.55 (3H, m, CH, H-3' and H-5'), 7.62 (1H, ddd, *J* = 1.2, 1.5 and 7.4 Hz, H-4'), 7.66 (2H, dd, *J* = 5.4 and 8.5 Hz, H-2 and H-6), 7.80 (1H, d, *J* = 15.8 Hz, CO-*CH*), 8.03-8.05 (2H, m, H-2 and H-6'); ^{13}C NMR (125 MHz, $CDCl_3$) δ ppm 116.2 (d, J_{CF} = 22.0 Hz, C-3 and C-5), 121.8 (d, J_{CF} = 2.2 Hz, CH), 128.5 (C-Ar), 128.7 (C-Ar), 130.4 (d, J_{CF} = 8.6 Hz, C-2 and C-6), 131.2 (d, J_{CF} = 3.1 Hz, Cq), 132.9 (C-4'), 138.2 (Cq), 143.5 (CO-*CH*), 164.1 (d, J_{CF} = 251.3, C-F), 190.3 (CO); MS (ES+) *m/z* = 227.0 $[M+H]^+$.

***tert*-Butyl 2-(2-bromoacetamido)acetate, 88**

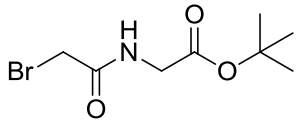

To a solution of bromoacetyl chloride (0.67 mL, 8.1 mmol) in DCM (1 mL/mmol) was added a solution of glycine *tert*-butyl ester (1.0 mL, 7.3 mmol), Et_3N (1.22 mL, 8.8 mmol) and

DMAP (10 mol%) in DCM (1 mL/mmol) at 0 ^{o}C dropwise. The resulting mixture was warmed to RT and stirred for 3 h. Addition of EtOAc (80 mL) resulted in formation of a precipitate, which was filtered and discarded. The filtrate was concentrated *in vacuo* to give **88** as a beige solid (1.66 g, 96%). R_f 0.46 (3:7 EtOAc/petrol); m.p. 67-68 ˚C ; ^{1}H-NMR (300 MHz, $CDCl_3$) δ ppm 1.48 (9H, s, CH_3), 3.92 (2H, s, CH_2), 3.97 (2H, d, J = 5.0 Hz, N-CH_2), 7.04 (1H, br s, NH); ^{13}C-NMR (75 MHz, $CDCl_3$) δ ppm 28.0 (CH_3), 28.6 (CH_2), 46.6 (CH_2), 82.9 (CH), 166.0 (CO), 168.6 (CO); HRMS calcd for $C_8H_{14}{}^{79}BrNO_3$ $[M+NH_4]^+$ 269.0495, found 269.0495.

***tert*-Butyl 2-(2-(3-cyano-4-(4-fluorophenyl)-6-phenylpyridin-2-ylthio)acetamido)acetate, 89**

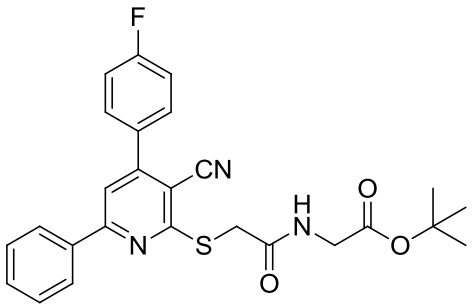

General procedure B: 4-fluorochalcone (88 mg, 0.39 mmol), 8.5% w/v sodium methoxide in MeOH (0.60 mL, 0.94 mmol), 2-cyanothioacetamide (39 mg, 0.39 mmol) followed by *tert*-butyl 2-(2-bromoacetamido)acetate (149 mg, 0.59 mmol) gave **89** as a white solid (71 mg, 38%). R_f 0.75 (1:1 EtOAc/petrol); m.p. 172-174 ˚C; λ_{max} (EtOH/nm) 270.0 and 342.0; IR υ_{max}/cm^{-1} 3279, 2977, 2214, 1740, 1657; ^{1}H NMR (500 MHz, DMSO-d_6) δ ppm 1.39 (9H, s, CH_3), 3.77 (2H, d, J = 5.9 Hz, CH_2-NH), 4.21 (2H, s, S-CH_2), 7.47 (1H, dd, J = 8.3 and 9.1 Hz, H-3' and H-5'), 7.54-7.55 (3H, m, H-2', H-6' and H-4'), 7.84 (2H, dd, J = 5.5 and 8.8 Hz, H-3 and H-5), 7.95 (1H, s, CH-pyridine), 8.29-8.31 (2H, m, H-2 and H-5), 8.65 (1H, t, J = 5.9 Hz, NH); MS (ES+) m/z = 478.2 $[M+H]^+$; HRMS calcd for $C_{26}H_{24}FN_3O_3S$ $[M+H]^+$ 478.1595, found 478.1602.

2-(2-(3-Cyano-4-(4-fluorophenyl)-6-phenylpyridin-2-ylthio)acetamido)acetic acid, 68

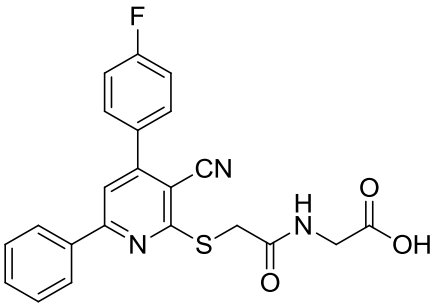

General procedure C: *tert*-butyl 2-(2-(3-cyano-4-(4-fluorophenyl)-6-phenylpyridin-2-ylthio)acetamido)acetate (91 mg, 0.19 mmol), TFA (29 µL, 0.38 mmol) gave **68** as a white solid (80 mg, 99%). R_f 0.37 (EtOH); m.p. 169-172 ˚C; λ_{max} (EtOH/nm) 270.0, 342.0; IR υ_{max}/cm^{-1} 3260, 2215, 1730, 1622; ^{1}H NMR (300 MHz, DMSO-d_6) δ ppm 3.80 (2H, d, J = 5.4 Hz, NH-CH_2), 4.21 (2H, s, S-CH_2),7.43-7.54 (4H, m, H-Ar), 7.82-7.87 (2H, m, H-Ar), 7.94 (1H, s, CH-pyridine), 8.28-8.30 (2H, m, H-Ar), 8.64 (1H, t, J = 5.4 Hz, NH), 12.62 (1H, s, COOH); MS (ES+) m/z = 422.2 $[M+H]^+$; HRMS calcd for $C_{22}H_{16}FN_3O_3S$ $[M+H]^+$ 422.0976, found 422.0969.

2-(3-Cyano-4-(4-fluorophenyl)-6-phenylpyridin-2-ylthio)-*N*-(2-(4 methoxybenzylamino)-2-oxoethyl)acetamide, 90

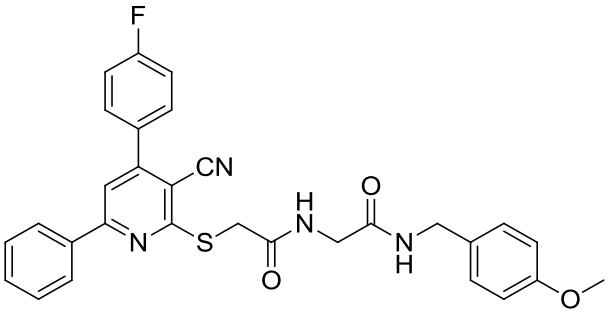

To a solution of 2-(2-(3-cyano-4-(4-fluorophenyl)-6-phenylpyridin-2-ylthio)acetamido)acetic acid (180 mg, 0.43 mmol) in DMF (20 mL) was added HBTU (200 mg, 0.52 mmol), DIPEA (50 µL, 0.52 mmol) and *p*-methoxybenzylamine (0.56 mL, 4.3 mmol). The resulting mixture was heated at 60 ^{o}C for 4.5 h. The mixture was cooled and water (10 mL) added, which resulted in precipitation of the product. Filtration gave **90** as a white solid (110 mg, 47%). R_f 0.52 (EtOH); m.p. 216-220 ˚C; λ_{max} (EtOH/nm) 269.5, 339.0; IR υ_{max}/cm^{-1} 3281, 3069, 2212, 1632, 1547, 1508; ^{1}H NMR (300 MHz, DMSO-d_6) δ ppm 3.71 (3H, s, O-CH_3), 3.77 (2H, d, J = 3.9 Hz, NH-CH_2-CO), 4.17 (2H, d, J = 3.9 Hz, NH-CH_2-Ar), 4.21 (2H, s, S-

CH_2), 6.84 (2H, d, *J* = 8.9 Hz, H-Ar), 7.14 (2H, d, *J* = 8.9 Hz, H-Ar), 7.43-7.53 (5H, m, H-Ar), 7.80-7.83 (2H, m, H-Ar), 7.93 (1H, s, CH-pyridine), 8.21-8.30 (3H, m, NH and H-Ar), 8.63 (1H, t, *J* = 5.9 Hz, NH); MS (ES+) *m/z* = 541.6 $[M+H]^+$; HRMS calcd for $C_{30}H_{25}FN_4O_3S$ $[M+H]^+$ 541.1704, found 541.1700.

_N_-(2-Amino-2-oxoethyl)-2-((3-cyano-4-(4-fluorophenyl)-6-phenylpyridin-2-yl)thio)acetamide, 69

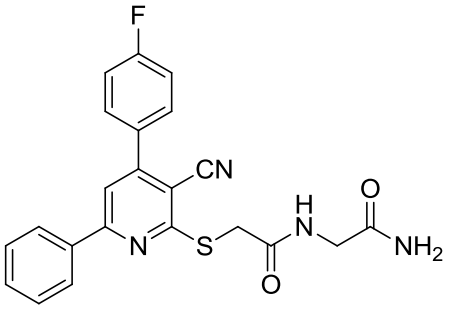

To 2-((3-cyano-4-(4-fluorophenyl)-6-phenylpyridin-2-yl)thio)-*N*-(2-((4-methoxybenzyl)amino)-2-oxoethyl)acetamide (50 mg, 0.093 mmol) was added TFA (5 mL/mmol) and the resulting solution was heated at 70 ^oC for 48 h. The solution was allowed to cool, and concentrated *in vacuo*. The residue was triturated with EtOAc, filtered and washed with petrol to give **69** as a white solid (11 mg, 52%).

R_f 0.36 (MeOH); m.p. 231-232 ˚C; λ_{max} (EtOH/nm) 338.0, 269.5; IR υ_{max}/cm^{-1} 3285, 3073, 2926, 2215, 1653, 1508; ^1H NMR (500 MHz, DMSO-d_6) δ ppm 3.57 (2H, d, *J* = 5.5 Hz, NH-*CH*$_2$), 4.09 (2H, s, S-CH_2), 7.24 (1H, s, NH_2), 7.35 (2H, dd, *J* = 8.6 and 8.7 Hz, H-Ar), 7.42-7.43 (3H, m, H-Ar and H-4'), 7.72 (2H, dd, *J* = 5.4 and 8.6 Hz, H-Ar), 7.83 (1H, s, CH-pyridine), 8.17-8.19 (2H, m, H-Ar), 8.40 (1H, t, *J* = 5.5 Hz, NH); MS (ES+) *m/z* = 421.3 $[M+H]^+$; HRMS calcd for $C_{22}H_{17}FN_4O_2S$ $[M+H]^+$ 421.1129, found 421.1130.

***tert*-Butyl 5-(3-cyano-4-(4-fluorophenyl)-6-phenylpyridin-2-ylthio)pentanoate, 95**

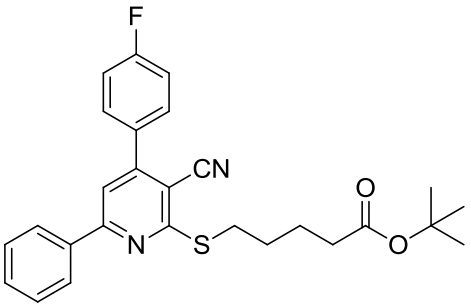

General procedure B: 4-fluorochalcone (118 mg, 0.52 mmol), 8.5% w/v sodium methoxide in MeOH (0.80 mL, 1.25 mmol), 2-cyanothioacetamide (52 mg, 0.52 mmol) followed by *tert*-butyl bromovalerate (185 mg, 0.78 mmol) gave **95** as a white solid (140 mg, 58%). R_f 0.81 (3:7 EtOAc/petrol); m.p. 120-121˚C; λ_{max} (EtOH/nm) 272.0, 347.5; IR υ_{max}/cm^{-1} 2984, 2936, 2214, 1707, 1595, 1566; ^{1}H NMR (300 MHz, $CDCl_3$) δ ppm 1.44 (9H, s, CH_3), 1.80-1.92 (4H, m, CH_2-*CH_2*-*CH_2*-CH_2), 2.30 (2H, t, *J* = 7.3 Hz, S-CH_2), 3.43 (2H, t, *J* = 6.9 Hz, CH_2-CO), 7.25 (2H, dd, *J* = 8.4 and 8.6 Hz, H-3 and H-5), 7.50 (1H, s, CH-pyridine), 7.51-7.56 (3H, m, H-3', H-4' and H-5'), 7.61-7.65 (2H, m, H-2 and H-6), 8.09-8.11 (2H, m, H-2' and H-6'); ^{13}C NMR (125 MHz, $CDCl_3$) δ ppm 24.4 (CH_2), 28.1 (CH_3), 28.7 (CH_2), 30.3 (CH_2), 35.1 (CH_2), 80.3 (Cq), 103.7 (Cq), 115.4 (CH-pyridine), 115.8 (Cq), 116.2 (d, J_{CF} = 23.0 Hz, C-3 and C-5), 127.3 (C-Ar), 129.0 (C-Ar), 130.4 (d, J_{CF} = 8.7 Hz, C-2 and C6), 130.7 (C-4'), 132.3 (d, J_{CF} = 3.4 Hz, Cq), 137.4 (Cq), 153.4 (Cq), 158.6 (Cq), 164.0 (d, J_{CF} = 254.6 Hz, C-F), 164.3 (Cq), 172.7 (CO); MS (ES+) *m/z* = 463.1 $[M+H]^+$; HRMS calcd for $C_{27}H_{27}FN_2O_2S$ $[M+H]^+$ 463.1850, found 463.1848.

***tert*-Butyl 4-(3-cyano-4-(4-fluorophenyl)-6-phenylpyridin-2-ylthio)butanoate, 96**

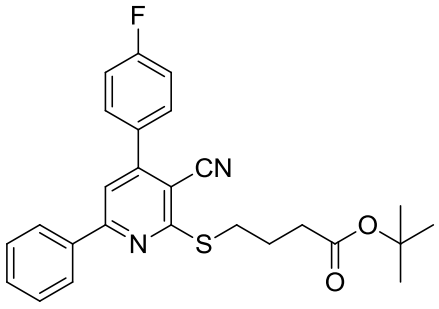

General procedure B: 4-fluorochalcone (75 mg, 0.33 mmol), 8.5% w/v sodium methoxide in MeOH (0.50 mL, 0.80 mmol), 2-cyanothioacetamide (33 mg, 0.33 mmol) followed by *tert*-butyl bromobutyrate (112 mg, 0.50 mmol) gave **96** as a white solid (50 mg, 34%). R_f 0.23

(1:9 EtOAc/petrol); m.p. 104-105 ˚C; λ_{max} (EtOH/nm) 271.0; IR υ_{max}/cm^{-1} 2978, 2930, 2212, 1721, 1603, 1570; ^{1}H NMR (500 MHz, $CDCl_3$) δ ppm 1.46 (9H, s, CH_3), 2.15 (2H, quint, *J* = 7.3 Hz, CH_2-*CH_2*-CH_2), 2.48 (2H, t, *J* = 7.3 Hz, S-CH_2), 3.48 (2H, t, *J* = 7.3 Hz, CH_2-CO), 7.24 (2H, dd, *J* = 8.4 and 8.6 Hz, H-3 and H-5), 7.51-7.55 (4H, m, CH-pyridine, H-3', H-4' and H-5'), 7.61-7.66 (2H, m, H-2 and H-6), 8.09-8.11 (2H, m, H-2' and H-6'); MS (ES+) *m/z* = 449.1 $[M+H]^+$.

5-(3-Cyano-4-(4-fluorophenyl)-6-phenylpyridin-2-ylthio)pentanoic acid, 70

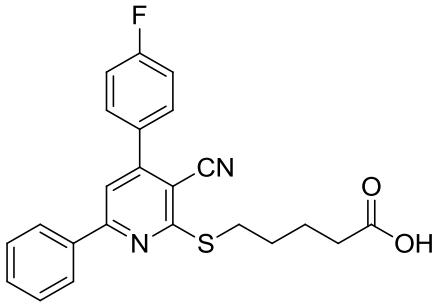

General procedure C: *tert*-butyl 5-(3-cyano-4-(4-fluorophenyl)-6-phenylpyridin-2-ylthio)pentanoate (120 mg, 0.26 mmol), TFA (40 µL, 0.52 mmol) gave **70** as a white solid (58 mg, 54%). R_f 0.65 (EtOH); m.p. 205-206 ˚C; λ_{max} (EtOH/nm) 270.0, 345.5; IR υ_{max}/cm^{-1} 2898, 2210, 1695; ^{1}H NMR (500 MHz, DMSO-d_6) δ ppm 1.69-1.83 (4H, m, CH_2-*CH_2*-*CH_2*-CH_2), 2.30 (2H, t, *J* = 7.4 Hz, S-CH_2), 3.42 (2H, t, *J* = 7.0 Hz, CH_2-CO), 7.44 (2H, dd, *J* = 8.7 and 8.8 Hz, H-Ar), 7.55-7.57 (3H, m, H-Ar), 7.84 (2H, dd, *J* = 5.5 and 8.8 Hz, H-Ar and H-4'), 7.91 (1H, s, CH-pyridine), 8.27-8.30 (2H, m, H-Ar), 12.05 (1H, s, COOH); ^{13}C NMR (125 MHz, DMSO-d_6) δ ppm 23.8 (CH_2), 28.3 (CH_2), 29.6 (CH_2), 33.2 (CH_2), 103.1 (Cq), 115.7 (CH-pyridine), 115.8 (d, J_{CF} = 21.8 Hz, C-3 and C-5), 116.0 (Cq), 127.5 (C-Ar) ,129.0 (C-Ar), 130.8 (C-4'), 131.2 (d, J_{CF} = 8.9 Hz, C-2 and C-6), 132.1 (d, J_{CF} = 2.7 Hz, Cq), 136.7 (Cq), 153.2 (Cq), 157.9 (Cq), 162.7 (Cq), 163.2 (d, J_{CF} = 248.3 Hz, C-F), 174.3 (CO); MS (ES+) *m/z* = 405.2 $[M-H]^-$; HRMS calcd for $C_{23}H_{19}FN_2O_2S$ $[M-H]^-$ 405.41362, found 405.40444.

4-(3-Cyano-4-(4-fluorophenyl)-6-phenylpyridin-2-ylthio)butanoic acid, 71

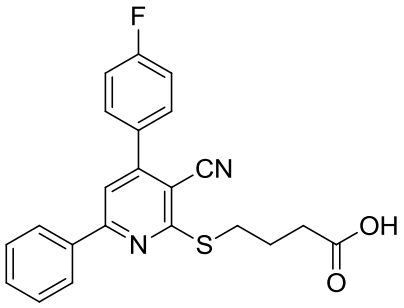

General procedure C: *tert*-butyl 4-(3-cyano-4-(4-fluorophenyl)-6-phenylpyridin-2-ylthio)butanoate (100 mg, 0.22 mmol), TFA (34 µL, 0.44 mmol) gave **71** as a white solid (64 mg, 72%). R_f 0.61 (EtOH); m.p. 160-164 ˚C; λ_{max} (EtOH/nm) 272.0, 346.0; IR υ_{max}/cm^{-1} 2924, 2217, 1711, 1596, 1568, 1525, 1509; ^{1}H NMR (500 MHz, DMSO-d_6) δ ppm 1.95 (2H, quint, *J* = 7.1 Hz, CH_2-*CH_2*-CH_2), 2.38 (2H, t, *J* = 7.1 Hz, S-CH_2), 3.41 (2H, t, *J* = 7.1 Hz, CH_2-CO), 7.40 (2H, dd, *J* = 8.8 and 8.9 Hz, H-3 and H-5), 7.49-7.50 (3H, m, H-Ar), 7.78 (2H, dd, *J* = 5.4 and 8.8 Hz, H-2 and H-6), 7.89 (1H, s, CH-pyridine), 8.24-8.26 (2H, m, H-Ar), 12.12 (1H, s, COOH); MS (ES+) *m/z* = 393.2 $[M+H]^+$; HRMS calcd for $C_{22}H_{17}FN_2O_2S$ $[M+H]^+$ 393.1068, found 393.1069.

***tert*-Butyl 2-(2-hydroxyethylamino)acetate, 92**

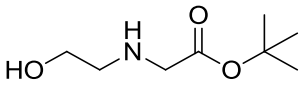

To a solution of ethanolamine (3.0 mL, 49.7 mmol) in THF (0.5 mL/mmol) was added *tert*-butyl bromoacetate (2 mL, 13.5 mmol) dropwise. The resulting solution was stirred at RT for 72 h. The mixture was concentrated *in vacuo* and the residue redissolved in DCM (50 mL). The organic phase was washed with an aqueous solution of saturated $NaHCO_3$ (50 mL) and brine (50 mL), then dried over Na_2SO_4 and concentrated *in vacuo* to give **92** as a yellow oil (1.96 g, 82%). R_f 0.35 (8:2 petol/EtOAc); IR υ_{max}/cm^{-1} 3399, 2970, 1730, 1638; ^{1}H NMR (300 MHz, $CDCl_3$) δ ppm 1.49 (9H, s, CH_3), 2.82 (2H, t, *J* = 5.0 Hz, *CH_2*-NH), 3.36 (2H, s, *CH_2*-CO), 3.65 (2H, t, *J* = 5.0 Hz, *CH_2*-OH), NH and OH not visualised; MS (ES+) *m/z* = 176.2 $[M+H]^+$.

***tert*-Butyl 2-((*tert*-butoxycarbonyl)(2-((3-cyano-4-(4-fluorophenyl)-6-phenylpyridin-2-yl)thio)ethyl)amino)acetate, 97**

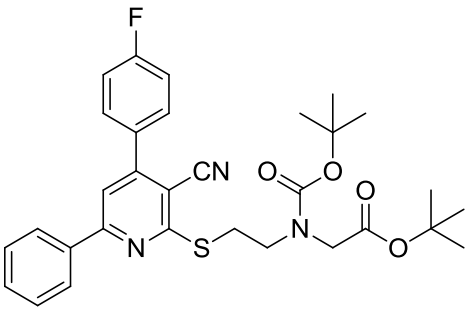

To a solution of *tert*-butyl 2-(2-hydroxyethylamino)acetate (0.53 g, 3.03 mmol) in DCM (3 mL/mmol) was added Boc anhydride (0.80 g, 3.64 mmol), Et_3N (0.51 mL, 3.64 mmol) and DMAP (10 mol%). The resulting solution was stirred at RT for 3 h. The mixture was diluted with water (15 mL) and the product extracted with DCM (2 x 15 mL). Combined organic layers were dried over Na_2SO_4 and concentrated *in vacuo*. The resulting solid was redissolved in DCM (3 mL/mmol). Mesyl chloride (0.28 mL, 3.64 mmol) and triethylamine (0.63 mL, 4.55 mmol) were added at 0 ^oC. The resulting solution was warmed to RT and stirred for 16 h. The reaction mixture was quenched with an aqueous solution of $NaHCO_3$ and extracted with EtOAc (3 x 50 mL). Combined organic layers were washed with brine, dried over Na_2SO_4 and concentrated *in vacuo*. The resulting oil was redissolved in DMF (4 mL) and 4-(4-fluorophenyl)-6-phenyl-2-thioxo-1,2-dihydropyridine-3-carbonitrile (90 mg, 0.29 mmol) and KOH (17 mg, 0.32 mmol) were added. The resulting solution was heated to 100 ^oC for 3 h, cooled, diluted with water and extracted with DCM (3 x 20 mL). Combined organic layers were washed with brine, dried over Na_2SO_4 and concentrated *in vacuo*. Purification *via* column chromatography (silica; 0-50% EtOAc/petrol) gave **97** as a white solid (20 mg, 12%). R_f 0.56 (3:7 EtOAc/petrol); m.p. 152-154 ˚C; λ_{max} (EtOH/nm) 338.0, 270.0; IR υ_{max}/cm^{-1} 3282, 2926, 2215, 1653, 1526, 1508; ^1H NMR (500 MHz, $CDCl_3$) δ ppm 1.25 (9H, s, CH_3), 1.34 (9H, s, CH_3), 3.38 (2H, t, J = 7.0 Hz, S-CH_2), 3.57 (2H, t, J = 7.0 Hz, S-CH_2-CH_2), 4.59 (2H, s, NH-CH_2), 7.17-7.20 (2H, m, dd, J = 8.6 and 8.7 Hz, H-Ar), 7.39-7.42 (3H, m, H-Ar), 7.57-7.80 (3H, m, H-Ar and CH-pyridine), 8.02-8.09 (2H, m, H-Ar); MS (ES+) *m/z* = 564.7 $[M+H]^+$.

2-((2-((3-Cyano-4-(4-fluorophenyl)-6-phenylpyridin-2-yl)thio)ethyl)amino)acetic acid, 72

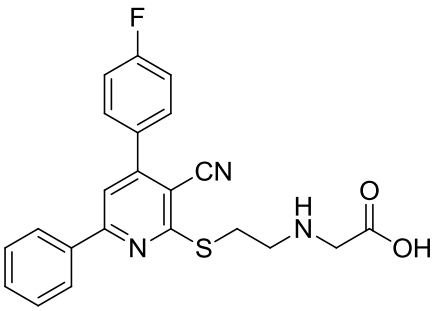

General procedure C: *tert*-butyl 2-((*tert*-butoxycarbonyl)(2-((3-cyano-4-(4-fluorophenyl)-6-phenylpyridin-2-yl)thio)ethyl)amino)acetate (15 mg, 0.027 mmol), TFA (5 µL, 0.054 mmol) gave **72** as a white solid (10 mg, 91%). R_f 0.30 (MeOH); m.p. 193-194 ˚C; λ_{max} (EtOH/nm) 339.0, 269.0; IR υ_{max}/cm^{-1} 3285, 3073, 2926, 2215, 1653, 1508; ^{1}H NMR (500 MHz, MeOD) δ ppm 3.17 (2H, t, *J* = 7.1 Hz, CH_2), 3.31 (2H, s, CH_2), 3.63 (2H, t, *J* = 7.1 Hz, CH_2), 7.45-7.51 (2H, m, H-Ar), 7.54-7.62 (3H, m, H-Ar), 7.83-7.88 (2H, m, H-Ar), 7.97 (1H, s, CH-pyridine), 8.30-8.39 (2H, m, H-Ar); MS (ES+) *m/z* = 408.3 $[M+H]^+$; HRMS calcd for $C_{22}H_{18}FN_3O_2S$ $[M-H]^-$ 406.1031, found 406.1026.

(*E*)-3-(3-Fluorophenyl)-1-phenylprop-2-en-1-one, 98

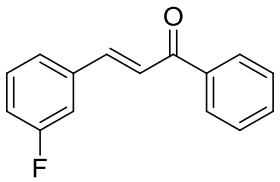

General procedure A: acetophenone (1.03 g, 8.60 mmol), 3-fluorobenzaldehyde (1.07 mL, 10.20 mmol), and NaOH (0.82 g, 20.60 mmol) gave **98** as yellow crystals (1.24 g, 64%). R_f 0.48 (1:9 EtOAc/petrol); m.p. 86-88 ˚C; λ_{max} (EtOH/nm) 297.0, 379.0; IR υ_{max}/cm^{-1} 1661, 1594, 1578, 1481, 1444, 1338, 1313, 1267; ^{1}H NMR (500 MHz, $CDCl_3$) δ ppm 7.06 (1H, dddd, *J* = 1.0, 8.4, 9.3 and 10.8 Hz, H-2), 7.13 (1H, ddd, *J* = 1.0, 7.6 and 8.4 Hz, H-5), 7.29-7.34 (1H, m, H-4), 7.42-7.45 (2H, m, H-3' and H-5'), 7.52 (1H, ddd, *J* = 1.3, 2.0 and 7.3 Hz, H-4'), 7.56-7.59 (2H, m, CH and H-6), 7.83 (1H, d, *J* = 16.0 Hz, CO-*CH*), 7.95-7.97 (2H, m, H-2' and H-6'); ^{13}C NMR (125 MHz, $CDCl_3$) δ ppm 116.3 (d, J_{CF} = 22.2 Hz, C-2), 123.0 (d, J_{CF} = 11.3 Hz, Cq), 124.5 (d, J_{CF} = 3.4 Hz, CH), 124.6 (d, J_{CF} = 7.3 Hz, C-5), 128.6 (C-Ar), 128.7 (C-Ar), 129.8 (d, J_{CF} = 2.9 Hz, C-6), 131.8 (d, J_{CF} = 8.8 Hz, C-4), 132.9 (C-4'), 137.5 (CO-*CH*), 138.0 (Cq), 161.0 (d, J_{CF} = 253.1 Hz, C-F), 190.5 (CO); MS (ES+) *m/z* = 227.0 $[M+H]^+$.

(*E*)-3-(2-Fluorophenyl)-1-phenylprop-2-en-1-one, 100

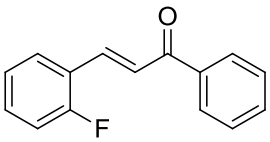

General procedure A: acetophenone (1.03 g, 8.60 mmol), 2-fluorobenzaldehyde (1.07 mL, 10.20 mmol), and NaOH (0.82 g, 20.60 mmol) gave **100** as yellow crystals (1.08 g, 56%). R_f 0.48 (1:9 EtOAc/petrol); m.p. 49-51 ˚C; λ_{max} (EtOH/nm) 302.0, 345.5; IR υ_{max}/cm^{-1} 1659, 1603, 1572; ^{1}H NMR (500 MHz, $CDCl_3$) δ ppm 7.11-7.14 (1H, m, H-Ar), 7.35-7.42 (3H, m, H-Ar), 7.51-7.55 (3H, m, CH and H-Ar), 7.61 (1H, dd, *J* = 7.5 and 7.8 Hz, H-Ar), 7.77 (1H, d, *J* = 15.8 Hz, CH), 8.02-8.04 (2H, m, H-Ar); MS (ES+) *m/z* = 227.0 $[M+H]^+$.

(*E*)-3-(2,4-Difluorophenyl)-1-phenylprop-2-en-1-one, 102

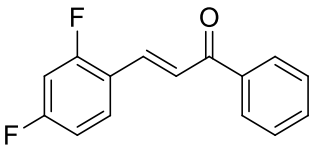

General procedure A: acetophenone (0.82 mL, 7.0 mmol), 2,4-difluorobenzaldehyde (1.3 mL, 7.0 mmol) and NaOH (350 mg, 8.80 mmol) gave **102** as yellow crystals (1.40 g, 80%). R_f 0.58 (3:7 EtOAc/petrol); m.p. 59-61 ˚C; λ_{max} (EtOH/nm) 311.0; IR υ_{max}/cm^{-1} 1659, 1604, 1589, 1497; ^{1}H NMR (500 MHz, $CDCl_3$) δ ppm 7.25 (1H, ddd, *J* = 2.5, 8.5 and 10.9 Hz, H-3), 7.41 (1H, ddd, *J* = 2.5, 9.3 and 11.5 Hz, H-5), 7.58-7.61 (2H, m, H-3' and H-5'), 7.70 (1H, ddd, *J* = 1.2, 1.3 and 7.4 Hz, H-4'), 7.78 (1H, d, *J* = 15.8 Hz, CH), 7.98 (1H, d, *J* = 15.8 Hz, CO-*CH*), 8.15-8.17 (2H, m, H-2' and H-6'), 8.24 (1H, ddd, *J* = 6.8, 9.3 and 15.5 Hz, H-6); ^{13}C NMR (125 MHz, DMSO-d_6) δ ppm 104.6 (dd, J_{CF} = 26.2 and 26.3 Hz, C-3), 112.6 (dd, J_{CF} = 3.5 and 21.7 Hz, C-5), 119.2 (dd, J_{CF} = 3.8 and 11.6 Hz, Cq), 123.8 (dd, J_{CF} = 2.3 and 3.7 Hz, CH), 128.6 (C-Ar), 128.8 (C-Ar), 130.7 (dd, J_{CF} = 3.7 and 10.0 Hz, C-6), 133.4 (H-4'), 134.2 (dd, J_{CF} = 1.4 and 3.7 Hz, Cq), 137.2 (CO-*CH*), 161.1 (dd, J_{CF} = 12.5 and 254.5 Hz, C-F), 163.1 (dd, J_{CF} = 13.1 and 252.1 Hz, C-F), 188.9 (CO); MS (ES+) *m/z* = 245.2 $[M+H]^+$; HRMS calcd for $C_{15}H_{10}F_2O$ $[M+H]^+$ 245.0772, found 245.0771.

(*E*)-1-Phenyl-3-(4-(trifluoromethyl)phenyl)prop-2-en-1-one, 104

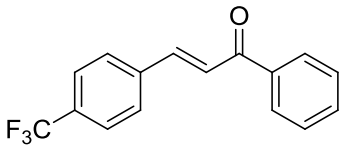

General procedure A: acetophenone (0.87 mL, 7.50 mmol), 4-(trifluoromethyl)benzaldehyde (1.0 mL, 7.50 mmol) and NaOH (380 mg, 9.38 mmol) gave **104** as yellow crystals (1.51 g, 73%). R_f 0.67 (3:7 EtOAc/petrol); m.p. 125-127 ˚C (lit.[140] 129-131 ^{o}C); λ_{max} (EtOH/nm) 220.0, 291.0; IR υ_{max}/cm^{-1} 1663, 1608, 1575; ^{1}H NMR (500 MHz, DMSO-d_6) δ ppm 7.67 (2H, dd, *J* = 7.9 and 8.1 Hz, H-3' and H-5'), 7.77 (1H, ddd, *J* =1.8, 7.9 and 8.1 Hz, H-4'), 7.86-7.90 (3H, m, CH, H-2 and H-6), 8.15-8.21 (3H, m, CH, H-3 and H-5), 8.25-8.27 (2H, m, H-2 and H-6); ^{13}C NMR (125 MHz, DMSO-d_6) δ ppm 123.9 (q, J_{CF} = 272.3 Hz, C-F_3), 124.3 (CH), 125.9 (q, J_{CF} = 3.7 Hz, C-3 and C-5), 128.5 (C-Ar), 128.6 (C-2 and C-6), 128.8 (C-Ar), 131.9 (q, J_{CF} = 32.9 Hz, Cq), 133.2 (C-4'), 137.8 (Cq),

138.3 (Cq), 142.7 (CO-*CH*), 190.0 (CO); MS (ES+) *m/z* = 276.0 $[M+H]^+$; HRMS calcd for $C_{16}H_{11}F_3O$ $[M+H]^+$ 277.0835, found 277.0835.

(*E*)-1-Phenyl-3-(pyridin-4-yl)prop-2-en-1-one, 106

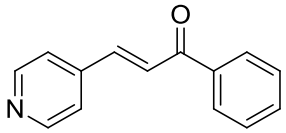

To a solution of 4-pyridine carboxaldehyde (0.56 g, 5.20 mmol), in toluene (1 mL/mmol) was added (benzoylmethylene)triphenylphosphorane (1.97 g, 5.20 mmol) and the resulting mixture was heated at 110 ^oC for 3 h. The mixture was allowed to cool to RT and concentrated *in vacuo*. The resulting residue was triturated with petrol, and the resulting precipitate filtered, washed with a 1M aqueous solution of HCl and discarded. The filtrate was neutralised with a 2.5 M aqueous solution of NaOH, resulting in precipitation. Filtration gave **106** as a yellow solid (0.85 g, 78%). R_f 0.38 (3:7 EtOAc/petrol); m.p. 75-77 ˚C (lit.[141] 77-78 ^oC); λ_{max} (EtOH/nm) 282.5; IR υ_{max}/cm^{-1} 3058, 3034, 1659, 1593, 1578; ^1H NMR (300 MHz, $CDCl_3$) δ ppm 7.41-7.7.56 (5H, m, H-Ar, CH and CO-*CH*), 7.63 (2H, d, *J* = 1.8 Hz, H-Ar), 7.95-7.98 (2H, m, H-Ar), 8.64 (2H, d, *J* = 4.5 Hz, N-CH-pyridine); MS (ES+) *m/z* = 210.0 $[M+H]^+$.

***tert*-Butyl 2-(2-(3-cyano-4-(3-fluorophenyl)-6-phenylpyridin-2-ylthio)acetamido)acetate, 99**

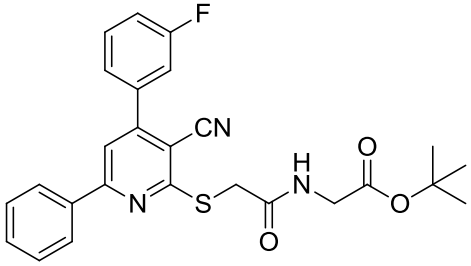

General procedure B: 3-fluorochalcone (88 mg, 0.39 mmol), 8.5% w/v sodium methoxide in MeOH (0.60 mL, 0.94 mmol), 2-cyanothioacetamide (39 mg, 0.39 mmol) followed by *tert*-butyl 2-(2-bromoacetamido)acetate (149 mg, 0.59 mmol) gave **99** as a white solid (86 mg, 46%). R_f 0.54 (1:1 EtOAc/petrol); m.p. 173-174 ˚C; λ_{max} (EtOH/nm) 270.0, 339.5; IR υ_{max}/cm^{-1} 2980, 2932, 2218, 1724, 1649, 1570, 1526, 1483, 1437, 1366; ^1H NMR (500 MHz, $CDCl_3$) δ ppm 1.31 (9H, s, CH_3), 3.84 (2H, d, *J* = 5.1 Hz, NH-CH_2), 4.03 (2H, s, S-CH_2), 7.07 (1H, br s, NH), 7.17-7.20 (1H, m, H-Ar), 7.26 (1H, ddd, *J* = 2.2, 2.3 and 9.1 Hz, H-Ar),

7.36-7.38 (1H, ddd, *J* = 1.0, 2.2 and 7.7 Hz, H-Ar), 7.43-7.49 (4H, m, H-Ar), 7.53 (1H, s, CH-pyridine), 7.99-8.01 (2H, m, H-Ar); MS (ES+) *m/z* = 478.1 $[M+H]^+$.

***tert*-Butyl 2-(2-(3-cyano-4-(2-fluorophenyl)-6-phenylpyridin-2-ylthio)acetamido)acetate, 101**

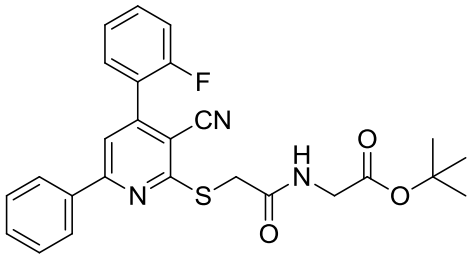

General procedure B: 2-fluorochalcone (54 mg, 0.23 mmol), 8.5% w/v sodium methoxide in MeOH (0.35 mL, 0.55 mmol), 2-cyanothioacetamide (35 mg, 0.23 mmol) followed by *tert*-butyl 2-(2-bromoacetamido)acetate (88 mg, 0.35 mmol) gave **101** as a white solid (22 mg, 20%). R_f 0.50 (1:1 EtOAc/petrol); m.p. 164-168 ˚C; λ_{max} (EtOH/nm) 270.0, 341.5; IR υ_{max}/cm^{-1} 2972, 2216, 1730, 1653, 1616, 1573, 1525, 1485; ^{1}H NMR (500 MHz, $CDCl_3$) δ ppm 1.31 (9H, s, CH_3), 3.84 (2H, d, *J* = 5.1 Hz, NH-*CH_2*), 4.03 (2H, s, S-CH_2), 7.09 (1H, br s, NH), 7.20-7.27 (2H, m, H-Ar), 7.40-7.49 (5H, m, H-Ar), 7.56 (1H, s, CH-pyridine), 7.98-8.00 (2H, m, H-Ar); MS (ES+) *m/z* = 478.1 $[M+H]^+$; HRMS calcd for $C_{26}H_{24}FN_3O_3S$ $[M+H]^+$ 478.1595, found 478.1590.

***tert*-Butyl 2-(2-((3-cyano-4-(2,4-difluorophenyl)-6-phenylpyridin-2-yl)thio)acetamido)acetate, 103**

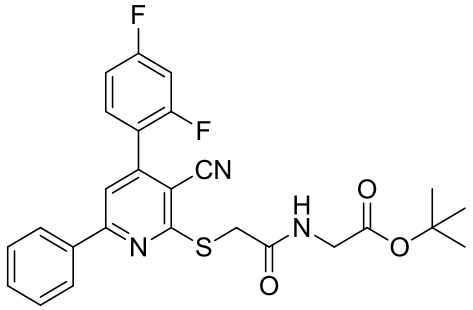

General procedure B: (*E*)-3-(2,4-difluorophenyl)-1-phenylprop-2-en-1-one (590 mg, 2.43 mmol), 8.5% w/v sodium methoxide in MeOH (3.70 mL, 5.83 mmol), 2-cyanothioacetamide (370 mg, 3.65 mmol) and *tert*-butyl 2-(2-bromoacetamido)acetate (1.83 g, 7.29 mmol) gave **103** as a white solid (490 mg, 41%). R_f 0.69 (1:1 EtOAc/petrol); m.p. 156-158 ˚C; λ_{max} (EtOH/nm) 274.0, 328.0, 380.5; IR υ_{max}/cm^{-1} 3326, 2973, 2924, 2218, 1729, 1655, 1618; ^{1}H

NMR (500 MHz, $CDCl_3$) δ ppm 1.30 (9H, s, CH_3), 3.83 (2H, d, *J* = 5.5 Hz, NH-*CH*$_2$), 4.02 (2H, s, S-CH_2), 6.94-7.02 (2H, m, H-Ar), 7.05 (1H, t, *J* = 5.5 Hz, NH), 7.40-7.46 (4H, m, H-5 and H-Ar), 7.51 (1H, d, *J* = 1.5 Hz, H-Ar,), 7.97-7.98 (2H, m, H-Ar); ^{13}C NMR (125 MHz, $CDCl_3$) δ ppm 27.9 (CH_3), 33.9 (NH-CH_2), 42.3 (S-CH_2), 82.3 (Cq), 105.2 (dd, J_{CF} = 25.4 and 25.5 Hz, C-3), 105.3 (Cq), 112.4 (dd, J_{CF} = 3.9 and 21.8 Hz, C-5), 114.7 (CH-pyridine), 117.6 (d, J_{CF} = 1.9 Hz, Cq), 120.0 (dd, J_{CF} = 3.9 and 14.6 Hz, Cq), 127.5 (C-Ar), 129.2 (C-Ar), 131.0 (C-4'), 131.7 (dd, J_{CF} = 3.8 and 10.0 Hz, C-6), 136.5 (Cq), 148.5 (Cq), 159.3 (Cq), 159.7 (dd, J_{CF} = 12.3 and 253.5 Hz, C-F), 161.5 (Cq), 164.2 (dd, J_{CF} = 11.9 and 253.6 Hz, C-F), 167.9 (CO), 168.4 (CO); MS (ES+) *m/z* = 496.3 $[M+H]^+$; HRMS calcd for $C_{26}H_{23}F_2N_3O_3S$ $[M+H]^+$ 496.1501, found 496.1498.

***tert*-Butyl 2-(2-((3-cyano-6-phenyl-4-(4-(trifluoromethyl)phenyl)pyridin-2-yl)thio)acetamido)acetate, 105**

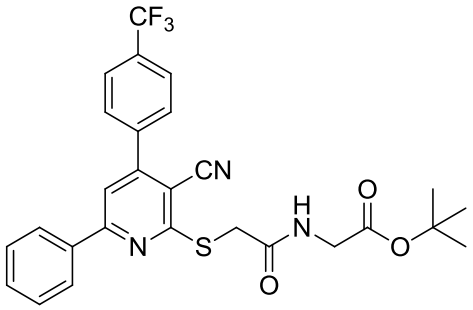

General procedure B: (*E*)-1-phenyl-3-(4-(trifluoromethyl)phenyl)prop-2-en-1-one (320 mg, 1.14 mmol), 8.5% w/v sodium methoxide in MeOH (1.75 mL, 2.74 mmol), 2-cyanothioacetamide (170 mg, 1.71 mmol) and *tert*-butyl 2-(2-bromoacetamido)acetate (860 mg, 3.42 mmol) gave **105** as a white solid (170 mg, 28%). R_f 0.75 (1:1 EtOAc/petrol); m.p. 203-205 ˚C; λ_{max} (EtOH/nm) 269.0, 340.5; IR υ_{max}/cm^{-1} 3294, 2982, 2212, 1743, 1660, 1572, 1525; ^{1}H NMR (500 MHz, $CDCl_3$) δ ppm 1.30 (9H, s, CH_3), 3.83 (2H, d, *J* = 5.1 Hz, NH-*CH*$_2$), 4.03 (2H, s, S-CH_2), 7.03 (1H, t, *J* = 5.1 Hz, NH), 7.43-7.45 (3H, m, H-Ar), 7.53 (1H, s, CH-pyridine), 7.67 (2H, d, *J* = 8.2 Hz, H-Ar), 7.75 (2H, d, *J* = 8.2 Hz, H-Ar), 7.98-8.00 (2H, m, H-Ar); ^{13}C NMR (125 MHz, $CDCl_3$) δ ppm 28.0 (CH_3), 34.0 (NH-CH_2), 42.3 (S-CH_2), 82.3 (Cq), 103.9 (Cq), 114.9 (Cq), 116.5 (CH-pyridine), 126.2 (q, J_{CF} = 3.9 Hz, C-3 and C-5), 127.5 (C-Ar), 128.9 (C-2 and C-6), 129.2 (C-Ar), 131.1 (C-4'), 136.5 (Cq),139.4 (Cq), 153.3 (Cq), 159.5 (Cq), 162.0 (Cq), 167.8 (CO), 168.4 (CO), *C*-F_3, C-*CF*$_3$ and quaternary carbons are not visualised; MS (ES+) *m/z* = 528.3 $[M+H]^+$; HRMS calcd for $C_{27}H_{24}F_3N_3O_3S$ $[M+H]^+$ 528.1563, found 528.1560.

***tert*-Butyl 2-(2-(3-cyano-6-phenyl-4-4'-bipyridin-2-ylthio)acetamido)acetate, 108**

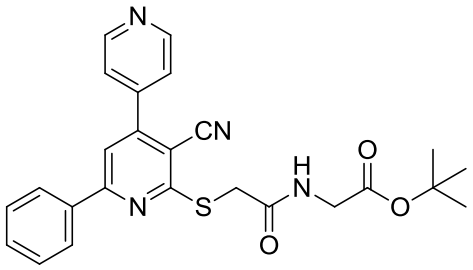

General procedure B: 4-pyrdiylchalcone (140 mg, 0.67 mmol), 8.5% w/v sodium methoxide in MeOH (1.0 mL, 1.68 mmol), 2-cyanothioacetamide (67 mg, 0.67 mmol) followed by *tert*-butyl 2-(2-bromoacetamido)acetate (0.25 g, 1.01 mmol) gave **108** as a white solid (114 mg, 39%). R_f 0.26 (1:1 EtOAc/petrol); m.p. 166-168 ˚C; λ_{max} (EtOH/nm) 221.0, 249.0, 276.5, 347.5; IR υ_{max}/cm^{-1} 2938, 2863, 2212, 1665; ^{1}H NMR (500 MHz, $CDCl_3$) δ ppm 1.40 (9H, s, CH_3), 3.94 (2H, d, *J* = 5.2 Hz, NH-*CH_2*), 4.15 (2H, s, S-CH_2), 7.03 (1H, br s, NH), 7.56-7.57 (3H, m, H-Ar), 7.65 (1H, s, CH-pyridine), 7.90 (2H, d, *J* = 4.6 Hz, H-2 and H-6), 8.10 (2H, dd, *J* = 2.5 and 6.1 Hz, H-Ar), 8.95 (2H, d, *J* = 4.6 Hz, H-3 and H-5); ^{13}C NMR (125 MHz, $CDCl_3$) δ ppm 28.0 (CH_3), 34.0 (NH-CH_2), 42.3 (S-CH_2), 82.5 (Cq), 103.2 (Cq), 114.3 (Cq), 115.8 (CH-pyridine), 121.2 (Cq), 124.5 (C-2 and C-6), 127.7 (C-Ar), 129.4 (C-Ar), 131.6 (C-4'), 136.1 (Cq), 146.7 (Cq), 150.1 (Cq), 160.2 (C-3 and C-5), 162.7 (Cq), 167.4 (CO), 168.5 (CO); MS (ES+) *m/z* = 461.3 $[M+H]^+$; HRMS calcd for $C_{25}H_{24}N_4O_3S$ $[M+H]^+$ 461.1642, found 461.1636.

***tert*-Butyl 2-(2-((3-cyano-4,6-dimethylpyridin-2-yl)thio)acetamido)acetate, 116**

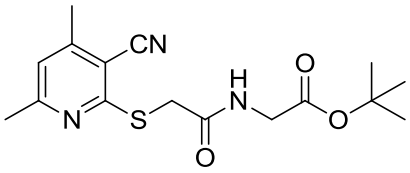

To a solution of 2-mercapto-4,6-dimethylnicotinonitrile (110 mg, 0.69 mmol) in DMF (2 mL/mmol) was added *tert*-butyl 2-(2-bromoacetamido)acetate (210 mg, 0.83 mmol) and KOH (39 mg, 0.69 mmol) and the resulting solution heated at 100 ^{o}C for 3 h. The mixture was allowed to cool, diluted with water and extracted with DCM (3 x 20 mL). Combined organic layers were washed with brine, dried over Na_2SO_4 and concentrated *in vacuo*. Purification *via* column chromatography (silica; 0-60% EtOAc/petrol) gave **116** as a white solid (120 mg, 52%). R_f 0.48 (1:1 EtOAc/petrol); m.p. 132-134 ˚C; λ_{max} (EtOH/nm) 266.0,

302.0; IR υ_{max}/cm^{-1} 2218, 1737, 1652; ^{1}H NMR (500 MHz, $CDCl_3$) δ ppm 1.44 (9H, s, CH_3), 2.47 (3H, s, CH_3), 2.59 (3H, s, CH_3), 3.92-3.93 (4H, m, NH-*CH_2* and S-CH_2), 6.89 (1H, s, CH-pyridine), 7.56 (1H, br s, NH); ^{13}C NMR (125 MHz, $CDCl_3$) δ ppm 20.4 (CH_3), 24.8 (CH_3), 28.4 (CH_3), 33.8 (NH-CH_2), 42.9 (S-CH_2), 82.0 (Cq) 105.8 (Cq), 114.7 (Cq), 121.1 (CH-pyridine), 152.8 (Cq), 162.2 (Cq), 168.9 (CO), 168.9 (CO); MS (ES+) *m/z* = 336.1 $[M+H]^+$; HRMS calcd for $C_{16}H_{21}N_3O_3S$ $[M+H]^+$ 336.1376, found 336.1377.

2-(2-(3-Cyano-4-(3-fluorophenyl)-6-phenylpyridin-2-ylthio)acetamido)acetic acid, 73

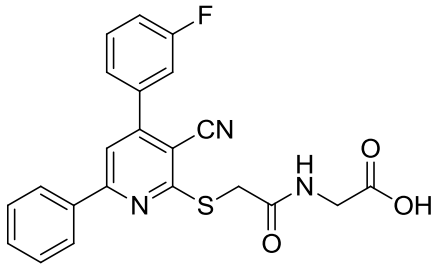

General procedure C: *tert*-butyl 2-(2-(3-cyano-4-(3-fluorophenyl)-6-phenylpyridin-2-ylthio)acetamido)acetate (35 mg, 0.067 mmol), TFA (11 µL, 0.14 mmol) gave **73** as a white solid (28 mg, 100%). R_f 0.50 (EtOH); m.p. 221-224 ˚C; λ_{max} (EtOH/nm) 279.0, 348.5; IR υ_{max}/cm^{-1} 3241, 2217, 2174, 1735, 1624, 1574, 1525; ^{1}H NMR (500 MHz, DMSO-d_6) δ ppm 3.82 (2H, d, *J* = 5.7 Hz, NH-*CH_2*), 4.22 (2H, s, S-CH_2), 7.44-7.48 (1H, m, H-Ar), 7.54-7.58 (3H, m, H-Ar), 7.61-7.71 (3H, m, H-Ar), 7.99 (1H, s, CH-pyridine), 8.31-8.33 (2H, m, H-Ar), 8.68 (1H, t, *J* = 5.7 Hz, NH), 12.67 (1H, s, COOH); MS (ES+) *m/z* = 422.2 $[M+H]^+$, 420.1 $[M-H]^-$; HRMS calcd for $C_{22}H_{16}FN_3O_3S$ $[M+H]^+$ 422.0967, found 422.0967.

2-(2-((3-Cyano-4-(2-fluorophenyl)-6-phenylpyridin-2-yl)thio)acetamido)acetic acid, 74

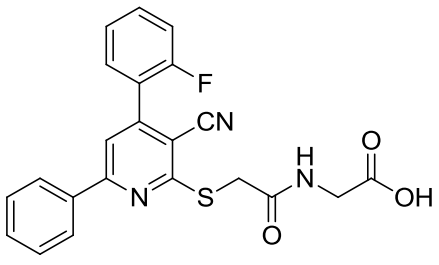

General procedure C: *tert*-butyl 2-(2-(3-cyano-4-(2-fluorophenyl)-6-phenylpyridin-2-ylthio)acetamido)acetate (18 mg, 0.038 mmol), TFA (6 µL, 0.076 mmol) gave **74** as a white solid (16 mg, 99%). R_f 0.51 (EtOH); m.p. 200-202 ˚C; λ_{max} (EtOH/nm) 340.0, 270.5; IR υ_{max}/cm^{-1} 2220,1719, 1653, 1573, 1526; ^{1}H NMR (500 MHz, DMSO-d_6) δ ppm 3.82 (2H, d, *J*

= 5.7 Hz, NH-*CH*$_2$), 4.23 (2H, s, S-CH$_2$), 7.44-7.51 (2H, m, H-Ar), 7.52-7.55 (3H, m, H-Ar and H-4'), 7.64-7.71 (2H, m, H-Ar), 8.00 (1H, s, CH-pyridine), 8.28-8.30 (2H, m, H-Ar), 8.67 (1H, t, *J* = 5.7 Hz, NH), 12.67 (1H, s, COOH); MS (ES+) *m/z* = 422.2 $[M+H]^+$, 420.1 $[M-H]^-$; HRMS calcd for $C_{22}H_{16}FN_3O_3S$ $[M+H]^+$ 422.0967, found 422.0968.

2-(2-((3-Cyano-4-(2,4-difluorophenyl)-6-phenylpyridin-2-yl)thio)acetamido)acetic acid, 75

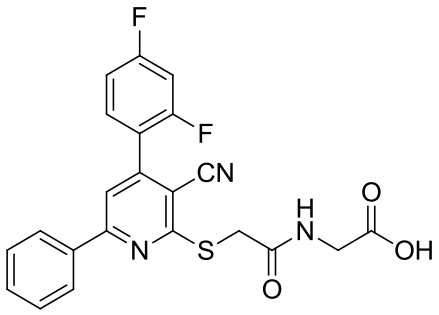

General procedure C: *tert*-butyl 2-(2-((3-cyano-4-(2,4-difluorophenyl)-6-phenylpyridin-2-yl)thio)acetamido)acetate (450 mg, 0.91 mmol), TFA (139 µL, 1.82 mmol) gave **75** as a white solid (400 mg, 100%). R_f 0.23 (MeOH); m.p. 226-227 ˚C; λ_{max} (EtOH/nm) 339.5, 270.5; IR υ_{max}/cm^{-1} 3259, 3079, 2221, 1728, 1619; ^{1}H NMR (500 MHz, DMSO-d_6) δ ppm 3.75 (2H, d, *J* = 5.8 Hz, NH-*CH*$_2$), 4.23 (2H, s, S-CH$_2$), 7.30 (1H, ddd, *J* = 2.1, 8.4 and 10.6 Hz, H-5), 7.53-7.60 (4H, m, H-Ar, H-4' and H-3) 7.77 (1H, ddd, *J* = 6.6, 8.7 and 15.1 Hz, H-6), 7.99 (1H, s, CH-pyridine), 8.27-8.29 (2H, m, H-Ar), 8.60 (1H, t, *J* = 5.8 Hz, NH), 12.62 (1H, s, COOH); ^{13}C NMR (125 MHz, DMSO-d_6) δ ppm 33.7 (NH-CH$_2$), 41.1 (S-CH$_2$), 104.1 (Cq), 104.8 (dd, J_{CF} = 26.8 and 26.9 Hz, C-3), 112.4 (dd, J_{CF} = 3.4 and 21.7 Hz C-5), 115.0 (CH-pyridine), 117.2 (Cq), 120.1 (dd, J_{CF} = 4.0 and 15.0 Hz, Cq) 127.8 (C-Ar), 128.9 (C-Ar), 131.0 (C-4'), 132.8 (dd, J_{CF} = 3.8 and 10.3 Hz, C-6), 136.3 (Cq), 148.1 (Cq), 158.3 (Cq), 159.1 (dd, J_{CF} = 12.7 and 250.3 Hz, C-F), 161.6 (Cq), 163.4 (dd, J_{CF} = 12.3 and 250.7 Hz, C-F), 167.2 (CO), 171.0 (CO); MS (ES+) *m/z* = 440.2 $[M+H]^+$; HRMS calcd for $C_{22}H_{15}F_2N_3O_3S$ $[M+H]^+$ 440.0875, found 440.0874.

2-(2-((3-Cyano-6-phenyl-4-(4-(trifluoromethyl)phenyl)pyridin-2-yl)thio)acetamido)acetic acid, 76

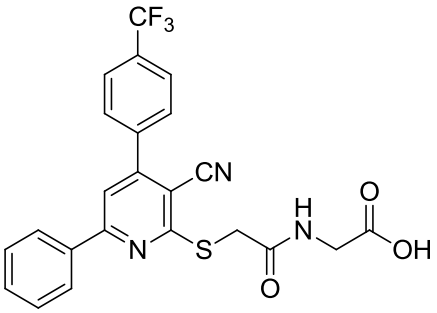

General procedure C: *tert*-butyl 2-(2-((3-cyano-6-phenyl-4-(4-(trifluoromethyl)phenyl)pyridin-2-yl)thio)acetamido)acetate (100 mg, 0.19 mmol), TFA (29 µL, 0.38 mmol) gave **76** as a white solid (80 mg, 90%). R_f 0.25 (MeOH); m.p. 243-244 ˚C; λ_{max} (EtOH/nm) 345.0, 268.0; IR υ_{max}/cm^{-1} 3285, 3069, 2214, 1738, 1667; ^{1}H NMR (500 MHz, DMSO-d_6) δ ppm 3.82 (2H, d, J = 5.7 Hz, NH-*CH*$_2$), 4.23 (2H, s, S-CH_2), 7.54-7.56 (3H, m, H-Ar and H-4'), 7.99-8.01 (5H, m, H-Ar and CH-pyridine) 8.30-8.32 (2H, m, H-Ar), 8.67 (1H, t, J = 5.7 Hz, NH), COOH not visualised; ^{13}C NMR (125 MHz, DMSO-d_6) δ ppm 33.8 (S-CH_2), 41.3 (NH-CH_2), 102.7 (Cq), 115.4 (Cq), 116.0 (CH-pyridine), 124.0 (q, J_{CF} = 273.4 Hz, C-F_3), 125.7 (q, J_{CF} = 3.6 Hz, C-3 and C-5), 127.8 (C-Ar), 128.9 (C-2 and C-6), 129.8 (C-Ar), 130.2 (q, J_{CF} = 32.2 Hz, Cq), 130.9 (C-4'), 136.4 (Cq), 139.7 (Cq), 152.7 (Cq), 158.3 (Cq), 162.1 (Cq), 167.1 (CO), 171.0 (CO); MS (ES+) *m/z* = 472.2 $[M+H]^+$; HRMS calcd for $C_{23}H_{16}F_3N_3O_3S$ $[M+H]^+$ 472.0937, found 472.0932.

2-(2-((3-Cyano-6-phenyl-[4,4'-bipyridin]-2-yl)thio)acetamido)acetic acid, 77

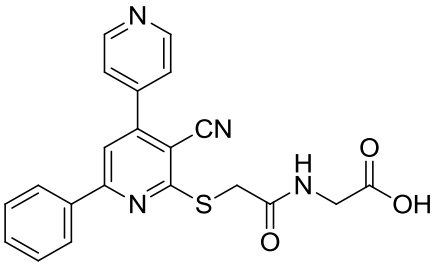

General procedure C: *tert*-butyl 2-(2-(3-cyano-6-phenyl-4-4'-bipyridin-2-ylthio)acetamido)acetate (80 mg, 0.17 mmol), TFA (26 µL, 0.34 mmol) gave **77** as a white solid (67 mg, 98%). R_f 0.35 (EtOH); m.p. 268-271 ^{o}C; λ_{max} (EtOH/nm) 348.5, 276.5, 249.0; IR υ_{max}/cm^{-1} 3267, 2212, 1726, 1665, 1570, 1520; ^{1}H NMR (500 MHz, DMSO-d_6) δ ppm 3.82 (2H, d, J = 5.7 Hz, NH-*CH*$_2$), 4.23 (2H, s, S-CH_2), 7.54-7.57 (3H, m, H-Ar and H-4'),

7.78 (2H, d, *J* = 6.1 Hz, CH-pyridine), 8.02 (1H, s, CH-pyridine), 8.30-8.32 (2H, m, H-Ar), 8.66 (1H, t, *J* = 5.7 Hz, NH), 8.83 (2H, d *J* = 6.1 Hz, N-CH-pyridine), 12.64 (1H, s, COOH); ^{13}C NMR (125 MHz, DMSO-d_6) δ ppm 33.7 (NH-CH_2), 41.1 (S-CH_2), 102.5 (Cq), 115.2 (Cq), 116.0 (CH-pyridine), 123.1 (C-2 and C-5), 127.8 (C-Ar), 128.9 (C-Ar), 131.0 (C-4'), 136.3 (Cq), 143.1 (Cq), 150.2 (C-3 and C-5), 151.6 (Cq), 158.4 (Cq), 162.2 (Cq), 167.2 (CO), 171.0 (CO); MS (ES+) *m/z* = 405.2 $[M+H]^+$; HRMS calcd for $C_{21}H_{16}N_4O_3S$ $[M+H]^+$ 405.1016, found 405.1015.

2-(2-((3-Cyano-4,6-dimethylpyridin-2-yl)thio)acetamido)acetic acid, 80

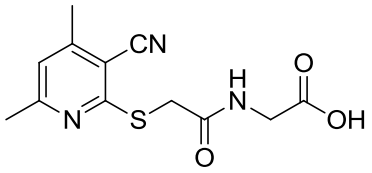

General procedure C: *tert*-butyl 2-(2-((3-cyano-4,6-dimethylpyridin-2-yl)thio)acetamido)acetate (100 mg, 0.29 mmol), TFA (44 µL, 0.58 mmol) gave **80** as a white solid (83 mg, 100%). R_f 0.25 (MeOH); m.p. 225-226 ˚C; λ_{max} (EtOH/nm) 265.0, 304.0; IR υ_{max}/cm^{-1} 3321, 3014, 2216, 1714, 1638; ^{1}H NMR (500 MHz, DMSO-d_6) δ ppm 2.42 (3H, s, CH_3), 2.48 (3H, s, CH_3), 3.78 (2H, d, *J* = 5.9 Hz, NH-*CH*$_2$), 4.03 (2H, s, S-CH_2), 7.13 (1H, s, CH-pyridine), 8.47 (1H, t, *J* = 5.9 Hz, NH,), 12.61 (1H, s, OH); ^{13}C NMR (125 MHz, $CDCl_3$) δ ppm 19.6 (CH_3), 24.2 (CH_3), 33.1 (NH-CH_2), 41.0 (S-CH_2), 103.6 (Cq), 115.0 (CH-pyridine), 120.5 (Cq), 152.4 (Cq), 160.0 (Cq), 161.5 (Cq), 167.4 (CO), 171.0 (CO); MS (ES+) *m/z* = 280.1 $[M+H]^+$; HRMS calcd for $C_{12}H_{13}N_3O_3S$ $[M+H]^+$ 280.0750, found 280.0753.

***tert*-Butyl (2-(methoxy(methyl)amino)-2-oxoethyl)carbamate, 110**

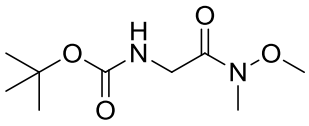

General procedure D: 2-((*tert*-butoxycarbonyl)amino)acetic acid (660 mg, 3.74 mmol), CDI (1.21 g, 7.48 mmol), *N,O*-dimethylhydroxylamine hydrochloride (910 mg, 9.35 mmol) and triethylamine (1.30 mL, 9.35 mmol). Recrystallisation from EtOAc/petrol (7:3) gave **110** as a white solid (400 mg, 49%). R_f 0.59 (1:1 EtOAc/petrol); m.p. 95-97 ˚C (lit.[142] 95-98 ^{o}C); IR υ_{max}/cm^{-1} 3312, 2915, 1618, 1569, 1530; ^{1}H NMR (500 MHz, $CDCl_3$) δ ppm 1.39 (9H, s,

$CH_3)_3$, 3.14 (3H, s, N-CH_3), 3.65 (3H, s, O-CH_3), 4.02 (2H, d, *J* = 3.2 Hz, CH_2), 5.20 (1H, br s, NH).

***tert*-Butyl (2-oxopropyl)carbamate, 111**

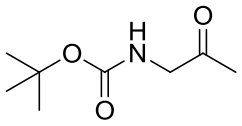

To a solution of *tert*-butyl (2-(methoxy(methyl)amino)-2-oxoethyl)carbamate (260 mg, 1.22 mmol) in THF (5 mL/mmol) was added methyl magnesium chloride (0.84 mL, 2.56 mmol) dropwise at 0 ^{o}C. The reaction mixture was warmed to RT and allowed to stir for 16 h. The reaction was quenched with a 1M aqueous solution of HCl and the product extracted with EtOAc (3 x 50 mL). Combined organic layers were washed with brine, dried over Na_2SO_4 and concentrated *in vacuo*. Purification *via* column chromatography (silica; 0-30% EtOAc/petrol) gave **111** as a yellow oil (190 mg, 89%). R_f 0.63 (1:1 EtOAc/petrol); IR υ_{max}/cm^{-1} 3356, 2978, 2925, 1692, 1514; ^{1}H NMR (500 MHz, $CDCl_3$) δ ppm 1.38 (9H, s, C-CH_3), 2.11 (3H, s, CO-CH_3), 4.05 (2H, s, N-CH_2), 5.16 (1H, s, NH).

2-Bromo-*N*-(2-oxopropyl)acetamide, 113

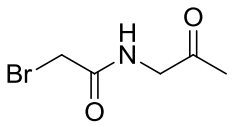

tert-Butyl (2-oxopropyl)carbamate (170 mg, 0.98 mmol) was dissolved in a 4M solution of HCl in dioxane (1 mL/mmol), and the mixture was stirred for 12 h at RT. The solution was concentrated *in vacuo*, the resulting oil redissolved in DCM (3 mL/mmol) and the solution cooled to 0 ^{o}C. An ice cold solution of Et_3N (0.16 mL, 1.18 mmol), DMAP (5 mol%) and bromoacetyl chloride (0.1 mL, 1.08 mmol) in DCM (3 mL/mmol) was added dropwise. The resulting mixture was warmed to RT and stirred for 12 h. The solution was diluted with DCM (30 mL), washed with water (3 x 30 mL) and brine. Combined organic layers were dried over Na_2SO_4 and concentrated *in vacuo*. Recrystallisation from EtOAc/petrol (7:3) gave **113** as a beige solid (160 mg, 86%). R_f 0.57 (1:1 EtOAc/petrol); m.p. 77-79 ˚C; IR υ_{max}/cm^{-1} 3074, 1724, 1643; ^{1}H NMR (500 MHz, $CDCl_3$) δ ppm 2.17 (3H, s, CH_3), 3.84 (2H, s, Br-CH_2), 4.11 (2H, d, *J* = 4.6 Hz, NH-*CH_2*), 7.10 (1H, s, NH); ^{13}C NMR (125 MHz, $CDCl_3$) δ ppm

27.4 (CH_3), 28.5 (CH_2), 50.2 (CH_2), 165.5 (CO), 201.7 (CO); HRMS calcd for $C_5H_8BrNO_2$ $[M-H]^-$ 191.9666, found 191.9671.

2-((3-Cyano-4-(4-fluorophenyl)-6-phenylpyridin-2-yl)thio)-*N*-(2-oxopropyl)acetamide, 67

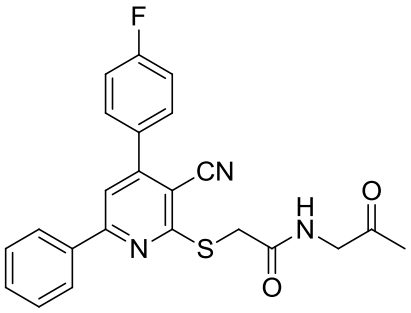

General procedure B: 4-fluorochalcone (15 mg, 0.067 mmol), 8.5% w/v sodium methoxide in MeOH (0.10 mL, 0.16 mmol), 2-cyanothioacetamide (7 mg, 0.067 mmol) and 2-bromo-*N*-(2-oxopropyl)acetamide (20 mg, 0.10 mmol) gave **67** as a white solid (10 mg, 36%). R_f 0.20 (1:1 EtOAc/petrol); m.p. 231-233 ˚C; λ_{max} (EtOH/nm) 270.0, 338.0; IR υ_{max}/cm^{-1} 3281, 2920, 2216, 1732, 1659; ^1H NMR (500 MHz, $CDCl_3$) δ ppm 2.02 (3H, s, CH_3), 4.03 (2H, s, S-CH_2), 4.04 (2H, d, *J* = 5.9 Hz, NH-*CH_2*), 7.16-7.20 (2H, m, H-Ar), 7.26 (1H, br s, NH), 7.44-7.45 (3H, m, H-Ar), 7.52 (1H, s, CH-pyridine), 7.56-7.59 (2H, m, H-Ar), 7.99-8.00 (2H, m, H-Ar); MS (ES+) *m/z* = 420.3 $[M+H]^+$; HRMS calcd for $C_{23}H_{18}FN_3O_2S$ $[M+H]^+$ 420.1177, found 420.1180.

2-((3-Cyano-6-phenyl-[4,4'-bipyridin]-2-yl)thio)-*N*-(2-oxopropyl)acetamide, 114

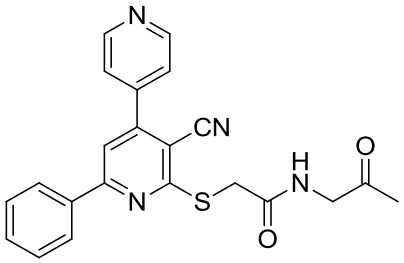

General procedure B: 4-pyridylchalcone (48 mg, 0.23 mmol), 8.5% w/v sodium methoxide in MeOH (0.35 mL, 0.56 mmol), 2-cyanothioacetamide (46 mg, 0.23 mmol) and 2-bromo-*N*-(2-oxopropyl)acetamide (67 mg, 0.35 mmol). Purification *via* column chromatography (silica; 0-15% MeOH/DCM) gave **114** as a white solid (72 mg, 78%). R_f 0.30 (MeOH); m.p. 238-240 ˚C; λ_{max} (EtOH/nm) 345.0, 277.0, 249.0; IR υ_{max}/cm^{-1} 2913, 2213, 1730, 1657, 1570,

1517; ^{1}H NMR (500 MHz, DMSO-d_6) δ ppm 2.03 (3H, s, CH_3), 3.98 (2H, d, *J* = 5.5 Hz, NH-*CH*$_2$), 4.25 (2H, s, S-CH_2), 7.55-7.56 (3H, m, H-Ar and H-4'), 7.78 (2H, d, *J* = 6.9 Hz, CH-pyridine), 8.03 (1H, s, CH-pyridine), 8.30-8.32 (2H, m, H-Ar), 8.61 (1H, t, *J* = 5.5 Hz, NH), 8.83 (2H, d, *J* = 6.9 Hz, N-CH-pyridine); ^{13}C NMR (125 MHz, DMSO-d_6) δ ppm 26.9 (CH_3), 33.7 (CH_2), 49.5 (CH_2), 102.5 (Cq), 115.2 (Cq), 116.0 (CH-pyridine), 123.1 (CH-pyridine), 127.8 (C-Ar), 128.9 (C-Ar), 131.0 (C-4'), 136.3 (Cq), 143.1 (Cq), 150.2 (N-CH-pyridine), 151.6 (Cq), 158.4 (Cq), 162.2 (Cq), 167.2 (CO), 204.3 (CO); MS (ES+) *m/z* = 403.3 $[M+H]^+$; HRMS calcd for $C_{22}H_{18}N_4O_2S$ $[M+H]^+$ 403.1223, found 403.1218.

2-((3-Cyano-4,6-dimethylpyridin-2-yl)thio)-*N*-(2-oxopropyl)acetamide, 117

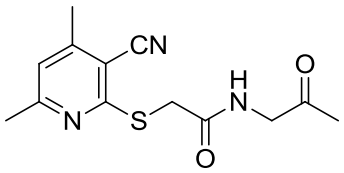

To a solution of 2-mercapto-4,6-dimethylnicotinonitrile (100 mg, 0.61 mmol) in DMF (5 mL/mmol) was added 2-bromo-*N*-(2-oxopropyl)acetamide (153 mg, 0.79 mmol) and KOH (34 mg, 0.61 mmol). The resulting mixture was heated at 100 ^{o}C for 3 h. The solution was cooled, diluted with water, and the product extracted with DCM (3 x 10 mL). Combined organic layers were washed with brine, dried over Na_2SO_4 and concentrated *in vacuo*. Purification *via* column chromatography (silica; 0-50% EtOAc/petrol) gave **117** as a white solid (134 mg, 79%). R_f 0.40 (8:2 petrol/EtOAc); m.p. 147-148 ˚C; λ_{max} (EtOH/nm) 222.0, 266.5, 305.5; IR υ_{max}/cm^{-1} 3325, 2998, 2216, 1709, 1660; ^{1}H NMR (500 MHz, $CDCl_3$) δ ppm 2.09 (3H, s, CH_3), 2.40 (3H, s, CH_3), 2.57 (3H, s, CH_3), 3.84 (2H, s, S-CH_2), 4.08 (2H, d, *J* = 5.9 Hz, NH-*CH*$_2$), 6.83 (1H, s, CH-pyridine), 7.75 (1H, br s, NH); ^{13}C NMR (125 MHz, $CDCl_3$) δ ppm 20.3 (CH_3), 24.7 (CH_3), 27.4 (CH_3), 33.0 (NH-CH_2), 50.4 (S-CH_2), 105.1 (Cq), 114.6 (CH-pyridine), 120.9 (Cq), 152.7 (Cq), 160.6 (Cq), 162.1 (Cq), 169.1 (CO), 202.4 (CO); MS (ES+) *m/z* = 278.1 $[M+H]^+$; HRMS calcd for $C_{13}H_{15}N_3O_2S$ $[M+H]^+$ 278.0958, found 278.0956.

4-(4-Fluorophenyl)-6-phenylpyridin-2(1*H*)-one, 118

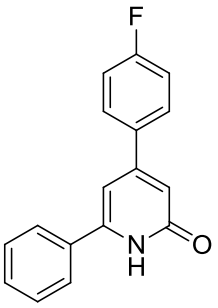

To a solution of 4-fluorochalcone (1.50 g, 6.6 mmol) in DMF (15 mL) was added acetamidoacetamide (0.96 g, 8.3 mmol) and Cs_2CO_3 (2.70 g, 8.3 mmol). The resulting mixture was stirred at 100 ^oC for 2.5 h. The reaction mixture was cooled to RT and poured into a 10% w/v aqueous solution of HCl (40 mL). An orange-brown precipitate formed which was filtered, dried and collected to yield the crude product. Purification *via* column chromatography (silica; 10-70% EtOAc/petrol) and recrystallisation from minimum hot EtOH gave **118** as beige crystals (0.60 g, 34%). R_f 0.60 (1:1 EtOAc/petrol); m.p. 215-217 ˚C; λ_{max} (EtOH/nm) 252.0, 334.5; IR υ_{max}/cm^{-1} 2882, 1634, 1596, 1574, 1528, 1506; ^1H NMR (500 MHz, DMSO-d_6) δ ppm 6.70 (1H, s, H-5 pyridine), 7.01 (1H, s, H-3 pyridine), 7.34 (2H, dd, J = 8.6 and 8.7 Hz, H-Ar), 7.49-7.53 (3H, m, H-Ar and H-4'), 7.89-7.92 (4H, m, H-Ar), 11.72 (1H, s, NH); ^{13}C NMR (125 MHz, $CDCl_3$) δ ppm 115.8 (d, J_{CF} = 21.3 Hz C-3 and C-5), 127.0 (C-Ar), 128.7 (C-Ar), 129.2 (d, J_{CF} = 8.8 Hz, C-2 and C-6), 129.6 (C-4'), 133.8 (d, J_{CF} = 2.8 Hz, Cq), 150.6 (Cq), 163.0 (d, J_{CF} = 245.8 Hz, C-F), 163.6 (CO), CH-pyridines and some quarternary carbons not visualised; MS (ES+) *m/z* = 266.0 $[M+H]^+$.

3-Bromo-4-(4-fluorophenyl)-6-phenylpyridin-2(1*H*)-one, 119

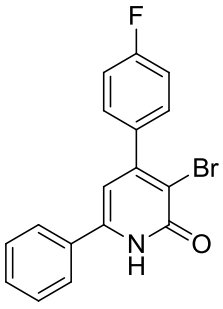

To a solution of 4-(4-fluorophenyl)-6-phenylpyridin-2(1*H*)-one (100 mg, 0.38 mmol) in glacial acetic acid (2.5 mL) was added *N*-bromosuccinamide (0.68 g, 0.38 mmol). The mixure was stirred at RT for 1 h, then at 60 ^oC for a further 5 h. The reaction mixture was

cooled and neutralised with a 2.5 M aqueous solution of NaOH, and precipitation was observed. The resulting solid was filtered, washed with water, dried and collected to give **119** as an off white solid (130 mg, 100%). R_f 0.78 (3:7 EtOAc/petrol); m.p. 257-260 ˚C; λ_{max} (EtOH/nm) 252.0, 339.0; IR υ_{max}/cm^{-1} 2994, 1632, 1601; ^{1}H NMR (500 MHz, DMSO-d_6) δ ppm 6.60 (1H, s, H-5 pyridine), 7.34 (2H, dd, *J* = 8.6 and 8.7 Hz, H-Ar), 7.48-7.52 (3H, m, H-Ar and H-4'), 7.60 (2H, dd, *J* = 5.5 and 8.7 Hz, H-Ar), 7.83-7.84 (2H, m, H-Ar) 12.43 (1H, s, NH); MS (ES+) *m/z* = 344.2 $[(^{79}BrM)+H]^+$, 346.0 2 $[(^{81}BrM)+H]^+$; HRMS calcd for $C_{17}H_{11}{}^{79}BrFNO$ $[M+H]^+$ 344.0081, found 344.0086.

***tert*-Butyl 2-(2-(3-bromo-4-(4-fluorophenyl)-6-phenylpyridin-2-ylthio)acetamido)acetate, 121**

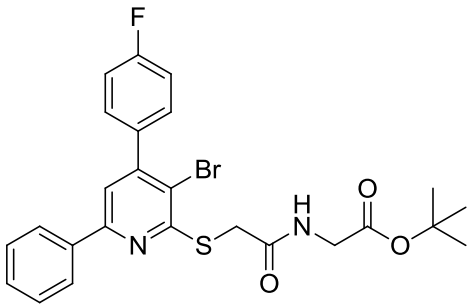

To a solution of 3-bromo-4-(4-fluorophenyl)-6-phenylpyridin-2(1*H*)-one (84 mg, 0.77 mmol) in toluene (6 mL) was added Lawesson's reagent (158 mg, 0.39 mmol). The resulting solution was stirred at 110 ^oC for 20 h. The mixture was allowed to cool, and evaporated to dryness to yield the crude product which was used directly in the next step. To a solution of 3-bromo-4-(4-fluorophenyl)-6-phenylpyridine-2(1*H*)-thione and 3-bromo-4-(4-fluorophenyl)-6-phenylpyridine-2-thiol (280 mg, 0.77 mmol) in DMF (5 mL) was added KOH (43 mg, 0.77 mmol) and *tert*-butyl 2-(2-bromoacetamido)acetate (390 mg, 1.5 mmol). The resulting mixture was heated at 100 ^oC for 4 h. The mixture was cooled and diluted with H_2O. The product was extracted with EtOAc (3 x 20 mL), washed with H_2O (5 x 50 mL) and brine (50 mL). Combined organic layers were dried over Na_2SO_4 and concentrated *in vacuo*. Purification *via* column chromatography (silica; 0-50% EtOAc/petrol) gave **121** as an off white solid (160 mg, 39%). R_f 0.31 (2:8 EtOAc/petrol); m.p. 178-181 ˚C; λ_{max} (EtOH/nm) 250.0, 322.5; IR υ_{max}/cm^{-1} 3071, 2974, 2911, 1718, 1649, 1605, 1555, 1507; ^{1}H NMR (500 MHz, $CDCl_3$) δ ppm 1.30 (9H, s, CH_3), 3.82 (2H, d, *J* = 5.3 Hz, NH-*CH_2*), 3.96 (2H, s, S-CH_2), 7.12 (2H, dd, *J* = 8.6 and 8.7 Hz, H-Ar), 7.20 (1H, br s, NH), 7.35-7.42 (6H, m, H-Ar and CH-pyridine), 7.93-7.95 (2H, m, H-Ar); ^{13}C NMR (75 MHz, $CDCl_3$) δ ppm 28.0 (CH_3),

35.3 (NH-CH_2), 42.3 (S-CH_2), 82.1 (Cq), 115.6 (d, J_{CF} = 22.0 Hz, C-3 and C-5), 117.3 (Cq), 118.7 (CH-pyridine), 126.7 (C-Ar), 129.0 (C-Ar), 129.7 (C-4'), 130.7 (d, J_{CF} = 8.3 Hz, C-2 and C-6), 137.3 (Cq), 150.4 (Cq), 155.3 (Cq), 157.7 (Cq), 168.5 (CO), 168.8 (CO), C-F, and F split quarternary carbon not visualised; MS (ES+) *m/z* = 531.2 [(^{79}BrM)+H]$^+$, 533.2 [(^{81}BrM)+H]$^+$.

2-(2-(3-Bromo-4-(4-fluorophenyl)-6-phenylpyridin-2-ylthio)acetamido)acetic acid, 82

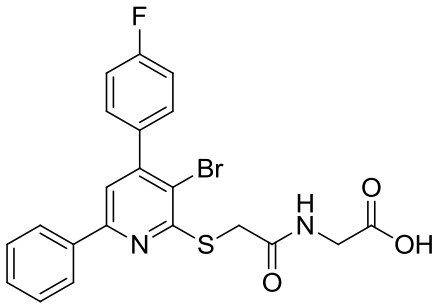

General procedure C: 2-(2-(3-bromo-4-(4-fluorophenyl)-6-phenylpyridin-2-ylthio)acetamido)acetate (80 mg, 0.15 mmol), TFA (23 µL, 0.30 mmol) gave **82** as a white solid (68 mg, 93%). R_f 0.52 (EtOH); m.p. 197-200 ˚C; λ_{max} (EtOH/nm) 248.5, 349.0; IR υ_{max}/cm^{-1} 2955, 2876, 1575, 1500; ^{1}H NMR (500 MHz, $CDCl_3$) δ ppm 3.80 (2H, d, *J* = 5.8 Hz, NH-*CH_2*), 4.08 (2H, s, S-CH_2), 7.39 (2H, dd, *J* = 8.6 and 8.7 Hz, H-Ar), 7.47-7.51 (3H, m, H-Ar and H-4'), 7.59 (2H, dd, *J* = 5.6 and 8.7 Hz, H-Ar), 7.71 (1H, s, CH-pyridine), 8.19-8.21 (2H, m, H-Ar), 8.60 (1H, t, *J* = 5.8 Hz, NH), 12.65 (1H, s, COOH); MS (ES+) *m/z* = 473.1 [(^{79}BrM)+H]$^+$, 475.0 [(^{81}BrM)+H]$^+$; HRMS calcd for $C_{21}H_{16}BrFN_2O_3S$ [M+H]$^+$ 472.9976 [(^{79}BrM)+H]$^+$, 474.9955 [(^{81}BrM)+H]$^+$, found 472.9974 [(^{79}BrM)+H]$^+$, 474.9945 [(^{81}BrM)+H]$^+$.

Methyl 4-(cyclohexanecarbonyl)-1*H*-pyrrole-2-carboxylate, 170

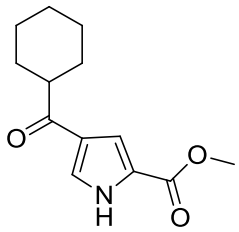

General procedure F: methyl 1*H*-pyrrole-2-carboxylate (300 mg, 2.40 mmol), cyclohexanecarbonyl chloride (0.64 mL, 4.80 mmol) and $AlCl_3$ (800 mg, 6.0 mmol). Purification *via* column chromatography (silica; 0-50% EtOAc/petrol) gave **170** as a white

solid (458 mg, 81%). R_f 0.43 (3:7 EtOAc/petrol); m.p. 164-166 ˚C; λ_{max} (EtOH/nm) 223.0, 273.0; IR υ_{max}/cm^{-1} 3215, 2949, 2859, 1705, 1635, 1554; ^{1}H NMR (500 MHz, $CDCl_3$) δ ppm 1.17-1.29 (4H, m, CH-cyclohexane), 1.39-1.46 (2H, m, CH-cyclohexane), 1.74-1.81 (4H, m, CH-cyclohexane), 2.84 (1H, tt, *J* = 3.2 and 11.6 Hz, CO-CH), 3.81 (3H, s, O-CH_3), 7.21 (1H, dd, *J* = 1.6 and 2.4 Hz, H-3), 7.47 (1H, dd, *J* = 1.6 and 3.3 Hz, H-5), 9.32 (1H, s, NH-pyrrole); ^{13}C NMR (125 MHz, $CDCl_3$) δ ppm 25.8 (C-cyclohexane) 25.9 (C-cyclohexane), 47.6 (C-cyclohexane), 50.9 (CO-*C*-cyclohexane) 51.9 (O-CH_3), 115.0 (C-Ar), 123.8 (C-Ar), 126.1 (C-Ar), 126.4 (C-Ar), 161.2 (CO), 199.4 (CO); MS (ES+) *m/z* = 236.0 $[M+H]^+$.

Methyl 4-(cyclopentanecarbonyl)-1*H*-pyrrole-2-carboxylate, 172

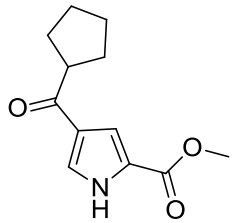

General procedure F: methyl 1*H*-pyrrole-2-carboxylate (300 mg, 2.40 mmol), cyclopentanecarbonyl chloride (0.58 mL, 4.80 mmol) and $AlCl_3$ (800 mg, 6.0 mmol). Purification *via* column chromatography (silica; 0-50% EtOAc/petrol) gave **172** as a white solid (426 mg, 80%). R_f 0.42 (3:7 EtOAc/petrol); m.p. 125-127 ˚C; λ_{max} (EtOH/nm) 223.5, 273.0; IR υ_{max}/cm^{-1} 3213, 2951, 2868, 1702, 1638, 1555; ^{1}H NMR (500 MHz, $CDCl_3$) δ ppm 1.51-1.55 (2H, m, CH-cyclopentane), 1.61-1.68 (2H, m, CH-cyclopentane), 1.80-1.84 (4H, m, CH-cyclopentane), 3.34 (1H, quin, *J* = 7.9 Hz, CO-CH), 3.81 (3H, s, O-CH_3), 7.23 (1H, dd, *J* = 1.6 and 2.4 Hz, H-3), 7.48 (1H, dd, *J* = 1.6 and 3.3 Hz, H-5), 9.51 (1H, s, NH-pyrrole); ^{13}C NMR (125 MHz, $CDCl_3$) δ ppm 26.3 (C-cyclopentane), 29.9 (C-cyclopentane), 48.0 (CO-*C*-cyclopentane), 51.9 (O-CH_3), 115.1 (C-Ar), 123.7 (C-Ar), 126.3 (C-Ar), 127.1 (C-Ar), 161.4 (CO), 198.5 (CO); MS (ES+) *m/z* = 222.0 $[M+H]^+$; HRMS calcd for $C_{12}H_{15}NO_3$ $[M+H]^+$ 222.1125, found 222.1125.

Methyl 4-(cycloheptanecarbonyl)-1*H*-pyrrole-2-carboxylate, 174

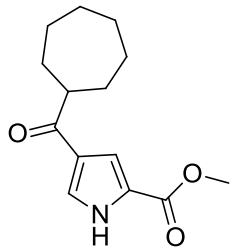

General procedure E: cycloheptane carboxylic acid (1.0 mL, 7.28 mmol) and $SOCl_2$ (0.79 mL, 10.92 mmol) gave cycloheptanecarbonyl chloride which was used directly in the next step. **General procedure F:** methyl 1*H*-pyrrole-2-carboxylate (460 mg, 3.64 mmol), and $AlCl_3$ (1.22 g, 9.10 mmol). Purification *via* column chromatography (silica; 0-50% EtOAc/petrol) gave **174** as a white solid (890 mg, 98%). R_f 0.40 (3:7 EtOAc/petrol); m.p. 110-111 ˚C; λ_{max} (EtOH/nm) 224.0, 273.0; IR υ_{max}/cm^{-1} 3256, 2926, 2855, 1708, 1641, 1553; ^{1}H NMR (500 MHz, DMSO-d_6) δ ppm 1.50-1.56 (6H, m, CH-cycloheptane), 1.57-1.70 (4H, m, CH-cycloheptane), 1.76-1.81 (2H, m, CH-cycloheptane), 3.22 (1H, m, CO-CH), 3.80 (3H, s, O-CH_3), 7.14 (1H, br s, H-3), 7.72 (1H, dd, *J* = 1.6 and 3.2 Hz, H-5), 12.54 (1H, s, NH-pyrrole); ^{13}C NMR (125 MHz, DMSO-d_6) δ ppm 26.1 (C-cycloheptane), 27.9 (C-cycloheptane), 30.6 (C-cycloheptane), 47.2 (CO-*C*-cycloheptane), 51.5 (O-CH_3), 114.5 (C-Ar), 123.4 (C-Ar), 125.0 (C-Ar), 127.9 (C-Ar), 160.6 (CO), 198.8 (CO); MS (ES+) *m/z* = 250.0 $[M+H]^+$; HRMS calcd for $C_{14}H_{19}NO_3$ $[M+H]^+$ 250.1438, found 250.1437.

4-(Cyclohexanecarbonyl)-1*H*-pyrrole-2-carboxylic acid, 171

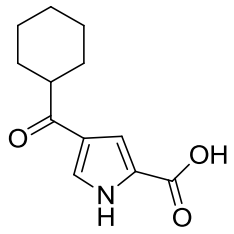

General procedure G: methyl 4-(cyclohexanecarbonyl)-1*H*-pyrrole-2-carboxylate (370 mg, 1.56 mmol) and LiOH monohydrate (1.30 g, 31.23 mmol) gave **171** as a white solid (344 mg, 100%). R_f 0.21 (8:2 DCM/MeOH); m.p. 218-220 ˚C; λ_{max} (EtOH/nm) 224.5, 272.5; IR υ_{max}/cm^{-1} 3270, 2931, 2826, 2609, 1645, 1551, 1435; ^{1}H NMR (500 MHz, DMSO-d_6) δ ppm 1.16-1.40 (6H, m, CH-cyclohexane), 1.65-1.74 (4H, m, CH-cyclohexane), 3.03-3.09 (1H, m, CO-CH), 7.08 (1H, br s, H-3), 7.70 (1H, dd, *J* = 1.6 and 3.3 Hz, H-5), 12.37 (1H, s, NH-pyrrole), 12.71 (1H, s, COOH); ^{13}C NMR (125 MHz, DMSO-d_6) δ ppm 25.1 (C-

cyclohexane), 25.6 (C-cyclohexane), 29.2 (C-cyclohexane), 45.9 (CO-*C*-cyclohexane), 114.0 (C-Ar), 124.7 (C-Ar), 124.9 (C-Ar), 127.5 (C-Ar), 161.6 (CO), 198.3 (CO); MS (ES+) *m/z* = 222.1 $[M+H]^+$; HRMS calcd for $C_{12}H_{15}NO_3$ $[M+H]^+$ 222.1125, found 222.1125.

4-(Cyclopentanecarbonyl)-1*H*-pyrrole-2-carboxylic acid, 173

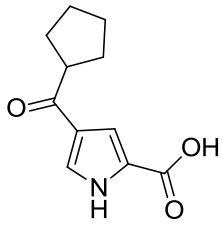

General procedure G: methyl 4-(cyclopentanecarbonyl)-1*H*-pyrrole-2-carboxylate (290 mg, 1.32 mmol) and LiOH monohydrate (1.10 g, 26.40 mmol) gave **173** as a white solid (264 mg, 97%). R_f 0.19 (8:2 DCM/MeOH); m.p. 209-210 ˚C; λ_{max} (EtOH/nm) 223.5, 277.0; IR υ_{max}/cm^{-1} 3246, 2917, 2853, 1704, 1638, 1554; ^{1}H NMR (500 MHz, DMSO-d_6) δ ppm 1.56-1.62 (4H, m, CH-cyclopentane), 1.67-1.73 (2H, m, CH-cyclopentane), 1.79-1.86 (2H, m, CH-cyclopentane), 3.49-3.55 (1H, m, CO-CH), 7.08 (1H, dd, *J* = 1.7 and 2.4 Hz, H-3), 7.68 (1H, dd, *J* = 1.7 and 3.3 Hz, H-5), 12.36 (1H, s, NH-pyrrole), 12.72 (1H, s, COOH); ^{13}C NMR (125 MHz, DMSO-d_6) δ ppm 25.9 (C-cyclopentane), 29.5 (C-cyclopentane), 46.7 (CO-*C*-cyclopentane), 114.1 (C-Ar), 124.6 (C-Ar), 125.6 (C-Ar), 127.6 (C-Ar), 161.6 (CO), 197.3 (CO); MS (ES+) *m/z* = 208.1 $[M+H]^+$; HRMS calcd for $C_{11}H_{13}NO_3$ $[M+H]^+$ 208.0968, found 208.0968.

4-(Cycloheptanecarbonyl)-1*H*-pyrrole-2-carboxylic acid, 175

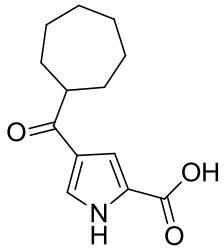

General procedure G: methyl 4-(cycloheptanecarbonyl)-1*H*-pyrrole-2-carboxylate (220 mg, 0.90 mmol) and LiOH monohydrate (0.76 g, 18.00 mmol) gave **175** as a white solid (190 mg, 100%). R_f 0.19 (8:2 DCM/MeOH); m.p. 219-220 ˚C; λ_{max} (EtOH/nm) 229.0, 270.5; IR υ_{max}/cm^{-1} 3290, 2922, 2854, 1655, 1552; ^{1}H NMR (500 MHz, DMSO-d_6) δ ppm 1.42-1.64 (10H, m, CH-cycloheptane), 1.70-1.75 (2H, m, CH-cycloheptane), 3.10-3.15 (1H, m, CO-

CH), 7.00 (1H, br s, H-3), 7.56 (1H, dd, *J* = 1.6 and 3.2 Hz, H-5), 12.19 (1H, s, NH-pyrrole), 12.48 (1H, s, COOH); ^{13}C NMR (125 MHz, DMSO-d_6) δ ppm 26.1 (C-cycloheptane), 28.0 (C-cycloheptane), 30.6 (C-cycloheptane), 47.1 (CO-*C*-cycloheptane), 114.1 (C-Ar), 124.7 (C-Ar), 124.8 (C-Ar), 127.4 (C-Ar), 161.6 (CO), 198.8 (CO); MS (ES+) *m/z* = 236.7 $[M+H]^+$; HRMS calcd for $C_{13}H_{17}NO_3$ $[M-H]^-$ 234.1136, found 234.1129.

4-(Cyclohexanecarbonyl)-*N*-(pyridin-4-ylmethyl)-1*H*-pyrrole-2-carboxamide, 149

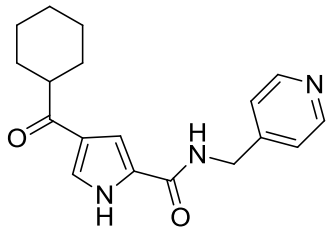

General procedure D: 4-(cyclohexanecarbonyl)-1*H*-pyrrole-2-carboxylic acid (220 mg, 1.01 mmol), CDI (330 mg, 2.03 mmol), and 4-picolylamine (0.26 mL, 2.53 mmol). Purification *via* column chromatography (silica; 0-8% MeOH/DCM) gave **149** as a white solid (188 mg, 60%). R_f 0.66 (95:5 EtOAc/MeOH); m.p. 235-236 ˚C; λ_{max} (EtOH/nm) 397.5, 276.0, 230.0; IR υ_{max}/cm^{-1} 3340, 3188, 3116, 2930, 2852, 1626, 1569; ^{1}H NMR (500 MHz, DMSO-d_6) δ ppm 1.18-1.24 (2H, m, CH-cyclohexane), 1.30-1.42 (4H, m, CH-cyclohexane), 1.66-1.76 (4H, m, CH-cyclohexane), 3.01-3.05 (1H, m, CO-CH), 4.46 (2H, d, *J* = 6.1 Hz, NH-*CH*$_2$), 7.28-7.30 (3H, m, H-3 and CH-pyridine), 7.66 (1H, br s, H-5), 8.50 (2H, d, *J* = 6.0 Hz, N-CH-pyridine), 8.90 (1H, t, *J* = 6.1 Hz, CO-NH), 12.19 (1H, s, NH-pyrrole); ^{13}C NMR (125 MHz, DMSO-d_6) δ ppm 25.2 (C-cyclohexane), 25.6 (C-cyclohexane), 29.3 (C-cyclohexane), 41.0 (NH-CH_2), 46.1 (CO-*C*-cyclohexane), 109.9 (C-Ar), 122.1 (C-Ar), 124.6 (C-Ar), 126.4 (C-Ar), 127.4 (C-Ar), 148.6 (C-Ar), 149.5 (C-Ar), 160.4 (CO), 198.3 (CO); MS (ES+) *m/z* = 312.2 $[M+H]^+$; HRMS calcd for $C_{18}H_{21}N_3O_2$ $[M+H]^+$ 312.1707, found 312.1702.

4-(Cyclopentanecarbonyl)-*N*-(pyridin-4-ylmethyl)-1*H*-pyrrole-2-carboxamide, 150

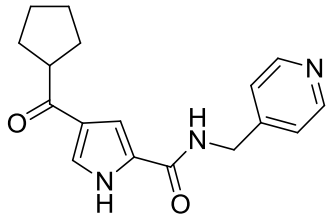

General procedure D: 4-(cyclopentanecarbonyl)-1*H*-pyrrole-2-carboxylic acid (160 mg, 0.75 mmol), CDI (240 mg, 1.50 mmol), and 4-picolylamine (0.19 mL, 1.88 mmol). Purification *via* column chromatography (silica; 0-8% MeOH/DCM) gave **150** as a white solid (140 mg, 63%). R_f 0.65 (95:5 EtOAc/MeOH); m.p. 245-246 ˚C; λ_{max} (EtOH/nm) 275.0, 229.5; IR υ_{max}/cm^{-1} 3346, 3182, 2948, 2867, 1625, 1572; ^{1}H NMR (500 MHz, DMSO-d_6) δ ppm 1.56-1.63 (4H, m, CH-cyclopentane), 1.68-1.74 (2H, m, CH-cyclopentane), 1.80-1.87 (2H, m, CH-cyclopentane), 3.49 (1H, quin, *J* = 7.9 Hz, CO-CH), 4.46 (2H, d, *J* = 5.9 Hz, NH-*CH*$_2$), 7.29 (2H, d, *J* = 6.0 Hz, CH-pyridine), 7.31 (1H, d, *J* = 1.4 Hz, H-3), 7.65 (1H, d, *J* = 1.4 Hz, H-5), 8.51 (2H, d, *J* = 6.0 Hz, N-CH-pyridine), 8.90 (1H, t, *J* = 5.9 Hz, CO-NH), 12.18 (1H, s, NH-pyrrole); ^{13}C NMR (125 MHz, DMSO-d_6) δ ppm 25.9 (C-cyclopentane), 29.7 (C-cyclopentane), 41.0 (NH-CH_2), 46.8 (CO-*C*-cyclopentane), 109.9 (C-Ar), 122.1 (C-Ar), 125.3 (C-Ar), 126.5 (C-Ar), 127.3 (C-Ar), 148.6 (C-Ar), 149.5 (C-Ar), 160.4 (CO), 197.4 (CO); MS (ES+) *m/z* = 298.2 $[M+H]^+$; HRMS calcd for $C_{17}H_{19}N_3O_2$ $[M+H]^+$ 298.1550, found 298.1553.

4-(Cycloheptanecarbonyl)-*N*-(pyridin-4-ylmethyl)-1*H*-pyrrole-2-carboxamide, 151

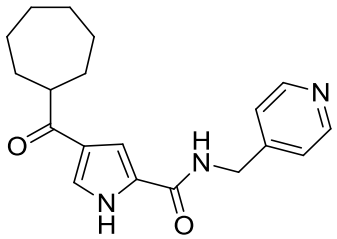

General procedure D: 4-(cycloheptanecarbonyl)-1*H*-pyrrole-2-carboxylic acid (130 mg, 0.54 mmol), CDI (200 mg, 1.22 mmol) and 4-picolylamine (0.15 mL, 1.53 mmol). Purification *via* column chromatography (silica; 0-8% MeOH/DCM) gave **151** as a white solid (190 mg, 98%). R_f 0.65 (95:5 EtOAc/MeOH); m.p. 224-226 ˚C; λ_{max} (EtOH/nm) 274.5, 229.0; IR υ_{max}/cm^{-1} 3344, 3109, 2922, 2856, 1739, 1641; ^{1}H NMR (500 MHz, DMSO-d_6) δ ppm 1.51-1.63 (8H, m, CH-cycloheptane), 1.68-1.72 (2H, m, CH-cycloheptane), 1.77-1.82

(2H, m, CH-cycloheptane), 3.15-3.20 (1H, m, CO-CH), 4.46 (2H, d, *J* = 6.1 Hz, NH-*CH*$_2$), 7.28-7.30 (3H, m, H-3 and CH-pyridine), 7.63 (1H, dd, *J* = 1.5 and 3.1 Hz, H-5), 8.51 (2H, d, *J* = 6.0 Hz, N-CH-pyridine), 8.89 (1H, t, *J* = 6.1 Hz, CO-NH), 12.17 (1H, s, NH-pyrrole); ^{13}C NMR (125 MHz, DMSO-d_6) δ ppm 26.6 (C-cycloheptane), 28.0 (C-cycloheptane), 30.8 (C-cycloheptane), 41.2 (NH-CH_2), 47.5 (CO-*C*-cycloheptane), 110.4 (C-Ar), 122.2 (C-Ar), 125.0 (C-Ar), 126.6 (C-Ar), 127.6 (C-Ar), 148.9 (C-Ar), 149.8 (C-Ar), 160.7 (CO), 199.1 (CO); MS (ES+) *m/z* = 326.2 $[M+H]^+$; HRMS calcd for $C_{19}H_{23}N_3O_2$ $[M-H]^-$ 324.1718, found 324.1715.

Methyl 4-((1*S*,2*S*)-2-methylcyclohexanecarbonyl)-1*H*-pyrrole-2-carboxylate and Methyl 4-((1*R*,2*R*)-2-methylcyclohexanecarbonyl)-1*H*-pyrrole-2-carboxylate, 178/179

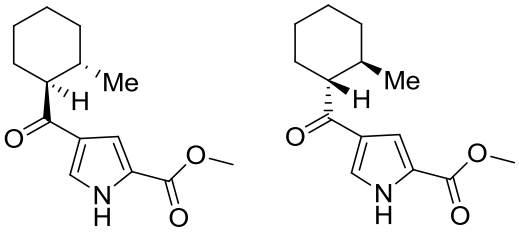

General procedure E: 2-methylcyclohexane carboxylic acid (1.0 mL, 7.10 mmol), and $SOCl_2$ (0.77 mL, 10.64 mmol) gave 2-methylcyclohexanecarbonyl chloride as a colourless oil which was used directly in the next step. **General procedure F:** methyl 1*H*-pyrrole-2-carboxylate (440 mg, 3.55 mmol), and $AlCl_3$ (1.19 g, 8.88 mmol). Purification *via* column chromatography (silica; 0-50% EtOAc/petrol) gave a mixture of **178** and **179** as a white solid (517 mg, 59%). R_f 0.76 (EtOAc); m.p. 123-126 ˚C; λ_{max} (EtOH/nm) 228.5; IR υ_{max}/cm^{-1} 3250, 2921, 2861, 1707, 1639, 1554; ^{1}H NMR (500 MHz, DMSO-d_6) δ ppm 0.73 (3H, d, *J* = 7.1 Hz, CH_3), 1.26-1.72 (8H, m, CH-cyclohexane), 2.10-2.17 (1H, m, CH-cyclohexane), 3.27 (1H, dt, *J* = 3.9 and 10.0 Hz, CO-CH), 3.80 (3H, s, O-CH_3), 7.14 (1H, br s, H-3), 7.72 (1H, br s, H-5), 12.52 (1H, s, NH-pyrrole); ^{13}C NMR (125 MHz, $CDCl_3$) δ ppm 22.8 (CH_3), 24.8, 26.0, 32.3, 32.7, 34.7 (C-cyclohexane), 50.0 (CO-CH), 51.9 (O-CH_3), 115.0 (C-Ar), 123.6 (C-Ar), 126.2 (C-Ar), 126.8 (C-Ar), 161.4 (CO), 198.9 (CO); MS (ES+) *m/z* = 249.99 $[M+H]^+$; HRMS calcd for $C_{14}H_{19}NO_3$ $[M+H]^+$ 250.1438, found 250.1437.

Methyl 5-((1*R*,2*R*)-2-methylcyclohexanecarbonyl)-1*H*-pyrrole-2-carboxylate and Methyl 5-((1*S*,2*S*)-2-methylcyclohexanecarbonyl)-1*H*-pyrrole-2-carboxylate, 180/181

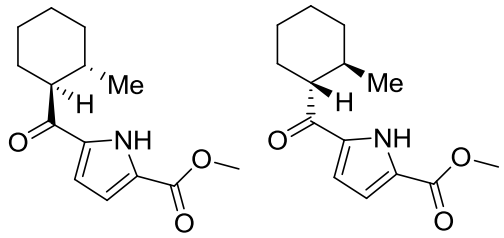

General procedure E: 2-methylcyclohexane carboxylic acid (1.0 mL, 7.10 mmol), and $SOCl_2$ (0.77 mL, 10.64 mmol gave 2-methylcyclohexane carbonyl chloride as a colourless oil which was used directly in the next step. **General procedure F:** methyl 1*H*-pyrrole-2-carboxylate (440 mg, 3.55 mmol), 2-methylcyclohexanecarbonyl chloride (1.14 g, 7.10 mmol) and $AlCl_3$ (1.19 g, 8.88 mmol). Purification *via* column chromatography (silica; 0-50% EtOAc/petrol) gave a mixture of **180** and **181** as a white solid (182 mg, 21%). R_f 0.84 (EtOAc); m.p. 127-130 ^oC; λ_{max} (EtOH/nm) 220.5, 288.5; IR υ_{max}/cm^{-1} 3285, 2926, 2853, 1708, 1655, 1545; ^1H NMR (500 MHz, DMSO-d_6) δ ppm 0.69 (3H, d, *J* = 7.1 Hz, CH_3,), 1.01-1.49 (8H, m, CH-cyclohexane), 1.89-1.91 (1H, m, CH-cyclohexane), 3.25 (1H, dt, *J* = 3.9 and 10.0 Hz, CO-CH), 3.62 (3H, s, O-CH_3), 6.65 (1H, dd, *J* = 1.5 and 3.9 Hz, H-3), 6.81 (1H, d, *J* = 1.5 and 3.9 Hz, H-4), 11.76 (1H, s, NH-pyrrole); 13C NMR (125 MHz, DMSO-d_6) δ ppm Innsufficient quantity of material retained to perform analysis; MS (ES+) *m/z* = 250.0 $[M+H]^+$.

Methyl 4-((1*R*,3*S*)-3-methylcyclohexanecarbonyl)-1*H*-pyrrole-2-carboxylate and methyl 4-((1*S*,3*R*)-3-Methylcyclohexanecarbonyl)-1*H*-pyrrole-2-carboxylate, 182/183

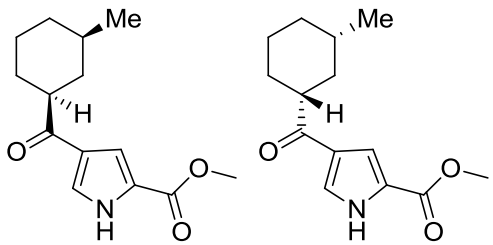

General procedure E: 3-methylcyclohexane carboxylic acid (1.0 mL, 9.96 mmol), and $SOCl_2$ (0.76 mL, 10.44 mmol) gave 3-methylcyclohexane carbonyl chloride as a colourless oil which was used directly in the next step. **General procedure F:** methyl 1*H*-pyrrole-2-carboxylate (440 mg, 3.48 mmol), and $AlCl_3$ (1.17 g, 8.70 mmol). Purification *via* column chromatography (silica; 0-50% EtOAc/petrol) gave a mixture of **182** and **183** as a white solid

(456 mg, 53%). R_f 0.86 (1:1 EtOAc); m.p. 131-134 ˚C; λ_{max} (EtOH/nm) 224.0, 273.5; IR υ_{max}/cm^{-1} 3208, 2926, 2851, 1712, 1642, 1556; ^{1}H NMR (500 MHz, DMSO-d_6) δ ppm 0.88 (3H, d, J = 7.1 Hz, CH_3), 1.16-1.89 (9H, m, CH-cyclohexane), 3.08-3.14 (1H, m, CO-CH), 3.80 (3H, s, O-CH_3), 7.15 (1H, br s, H-3), 7.76 (1H, br s, H-5), 12.55 (1H, s, NH-pyrrole); ^{13}C NMR (125 MHz, $CDCl_3$) δ ppm 22.7 (CH_3), 25.8, 28.9, 32.4, 34.6, 37.7 (C-cyclohexane), 47.7 (CO-CH), 51.9 (O-CH_3), 115.1 (C-Ar), 123.7 (C-Ar), 126.4 (C-Ar), 126.5 (C-Ar), 161.4 (CO), one CO not visualised; MS (ES+) *m/z* = 250.0 $[M+H]^+$; HRMS calcd for $C_{14}H_{19}NO_3$ $[M+H]^+$ 250.1438, found 250.1437.

Methyl 5-((1*R*,3*S*)-3-methylcyclohexanecarbonyl)-1*H*-pyrrole-2-carboxylate and methyl 5-((1*S*,3*R*)-3-Methylcyclohexanecarbonyl)-1*H*-pyrrole-2-carboxylate, 184/185

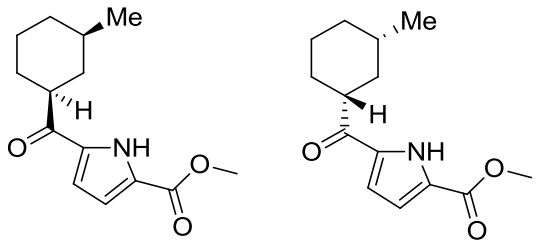

General procedure E: 3-methylcyclohexanecarboxylic acid (1.0 mL, 9.96 mmol), and $SOCl_2$ (0.76 mL, 10.44 mmol) gave 3-methylcyclohexane carbonyl chloride as a colourless oil which was used directly in the next step. **General procedure F:** methyl 1*H*-pyrrole-2-carboxylate (440 mg, 3.48 mmol), and $AlCl_3$ (1.17 g, 8.70 mmol).). Purification *via* column chromatography (silica; 0-50% EtOAc/petrol) gave a mixture of **184** and **185** as a white solid (44 mg, 6%). R_f 0.74 (EtOAc); m.p. 135-137 ^{o}C; λ_{max} (EtOH/nm) 220.5, 287.5; IR υ_{max}/cm^{-1} 3290, 2924, 2855, 1707, 1656, 1546; ^{1}H NMR (500 MHz, DMSO-d_6) δ ppm 0.75 (3H, d, J = 7.1 Hz, CH_3), 1.17-1.91 (9H, m, CH-cyclohexane), 3.12 (1H, m, CO-CH), 3.67 (3H, s, O-CH_3), 6.71 (1H, d, J = 4.0 Hz, H-3), 6.89 (1H, d, J = 4.0 Hz, H-4), 11.86 (1H, s, NH-pyrrole); ^{13}C NMR (125 MHz, DMSO-d_6) δ ppm Insufficient quantity of material obtained to perform analysis; MS (ES+) *m/z* = 250.0 $[M+H]^+$.

Methyl 4-(4-methylcyclohexanecarbonyl)-1*H*-pyrrole-2-carboxylate (*cis*/*trans* 1:4), 186

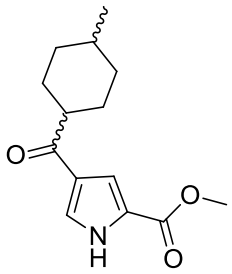

General procedure E: 4-methylcyclohexanecarboxylic acid (0.69 g, 4.80 mmol), $SOCl_2$ (0.52 mL, 7.20 mmol) gave 4-methylcyclohexanecarbonyl chloride as a colourless oil which was used directly in the next step. **General procedure F:** methyl 1*H*-pyrrole-2-carboxylate (300 mg, 2.40 mmol) and $AlCl_3$ (0.80 g, 6.00 mmol). Purification *via* column chromatography (silica; 0-50% EtOAc/petrol) gave **186** as a white solid (350 mg, 59%). R_f 0.32 (9:1 Petrol/EtOAc); m.p. 159-160 ˚C; λ_{max} (EtOH/nm) 273.0, 224.0; IR υ_{max}/cm^{-1} 3330, 3241, 2924, 2855, 1692, 1645, 1558, 1488; ^{1}H NMR (500 MHz, DMSO-d_6) δ ppm 0.72 (3H, d, J = 6.9 Hz, CH_3), 1.15-1.56 (9H, m, CH-cyclohexane), 2.81 (0.2H, dddd, J = 3.2, 3.4 and 11.8 and 12.0 Hz, CO-CH *trans*), 2.94-2.99 (0.8H, m, CO-CH *cis*), 3.61 (3H, s, O-CH_3), 6.96 (1H, br s, H-3), 7.55 (1H, br s, H-5), 12.34 (1H, s, NH-pyrrole); ^{13}C NMR (125 MHz, DMSO-d_6) δ ppm 22.6 (CH_3), 25.2, 28.7, 29.2, 30.6, 31.8, 33.9 (C-cyclohexane *cis* and *trans*), 45.8 (CO-CH), 58.8 (O-CH_3), 114.7 (C-Ar), 123.3 (C-Ar), 125.4 (C-Ar), 128.0 (C-Ar), 160.6 (CO), 198.5 (CO); MS (ES+) *m/z* = 250.1 $[M+H]^+$; HRMS calcd for $C_{14}H_{19}NO_3$ $[M+H]^+$ 250.1438, found 250.1436.

4-((1*R*,2*R*)-2-Methylcyclohexanecarbonyl)-1*H*-pyrrole-2-carboxylic acid and 4-((1*S*,2*S*)-2-Methylcyclohexanecarbonyl)-1*H*-pyrrole-2-carboxylic acid, 187/188

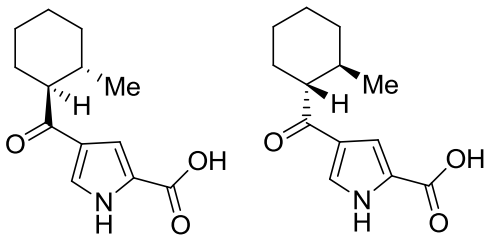

General procedure G: methyl 4-((1*S*,2*S*)-2-methylcyclohexanecarbonyl)-1*H*-pyrrole-2-carboxylate and methyl 4-((1*R*,2*R*)-2-methylcyclohexanecarbonyl)-1*H*-pyrrole-2-carboxylate (500 mg, 2.00 mmol) and LiOH monohydrate (1.68 g, 40.0 mmol) gave a mixture of **187** and **188** as an off-white solid (380 mg, 81%). R_f 0.24 (8:2 DCM/MeOH); m.p. 188-189 ˚C; λ_{max}

(EtOH/nm) 227.0, 273.5; IR υ_{max}/cm^{-1} 3201, 2924, 1642, 1557; ^{1}H NMR (500 MHz, DMSO-d_6) δ ppm 0.73 (3H, d, *J* = 7.1 Hz, CH_3), 1.06-1.71 (9H, m, CH-cyclohexane), 2.76-2.81 (1H, m, CO-CH), 7.09 (1H, br s, H-3), 7.73 (1H, dd, *J* = 1.6 and 3.3 Hz, H-5), 12.38 (1H, s, NH-pyrrole), 12.72 (1H, s, COOH); ^{13}C NMR (125 MHz, DMSO-d_6) δ ppm 20.5 (CH_3), 25.2, 25.7, 30.4, 33.5, 33.9 (C-cyclohexane), 52.6 (CO-CH), 113.9 (C-Ar), 124.8 (C-Ar), 126.4 (C-Ar), 127.6 (C-Ar), 161.6 (CO), 198.6 (CO); MS (ES+) *m/z* = 236.0 $[M+H]^+$; HRMS calcd for $C_{13}H_{17}NO_3$ $[M-H]^-$ 234.1136, found 234.1131.

5-((1*R*,2*R*)-2-Methylcyclohexanecarbonyl)-1*H*-pyrrole-2-carboxylic acid and 5-((1*S*,2*S*)-2-Methylcyclohexanecarbonyl)-1*H*-pyrrole-2-carboxylic acid, 196/197

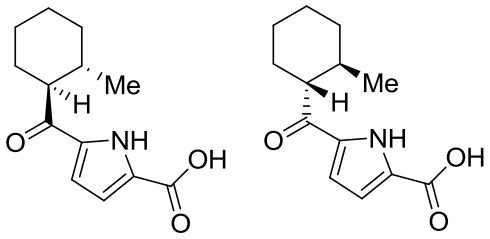

General procedure G: methyl 5-((1*R*,2*R*)-2-methylcyclohexanecarbonyl)-1*H*-pyrrole-2-carboxylate and methyl 5-((1*S*,2*S*)-2-methylcyclohexanecarbonyl)-1*H*-pyrrole-2-carboxylate (170 mg, 0.68 mmol) and LiOH monohydrate (570 mg, 13.65 mmol) gave a mixture of **196** and **197** as an off-white solid (120 mg, 75%). R_f 0.20 (8:2 DCM/MeOH); m.p. 177-179 ˚C; λ_{max} (EtOH/nm) 219.0, 295.5; IR υ_{max}/cm^{-1} 3264, 2923, 2857, 1685, 1648, 1543; ^{1}H NMR (500 MHz, DMSO-d_6) δ ppm 0.74 (3H, d, *J* = 7.1 Hz, CH_3), 1.05-1.75 (9H, m, CH-cyclohexane), 2.92-2.97 (1H, m, CO-CH), 6.78 (1H, d, *J* = 1.9 and 3.8 Hz, H-3), 7.03 (1H, d, *J* = 1.9 and 3.8 Hz H-4), 12.15 (1H, s, NH-pyrrole), 12.91 (1H, s, COOH); 13C NMR (125 MHz, DMSO-d_6) δ ppm Insufficient quantity of material retained to perform analysis; MS (ES+) *m/z* = 236.0 $[M+H]^+$; HRMS calcd for $C_{13}H_{17}NO_3$ $[M-H]^-$ 234.1136, found 234.1129.

4-((1*R*,3*S*)-3-Methylcyclohexanecarbonyl)-1*H*-pyrrole-2-carboxylic acid and 4-((1*S*,3*R*)-3-Methylcyclohexanecarbonyl)-1*H*-pyrrole-2-carboxylic acid, 191/192

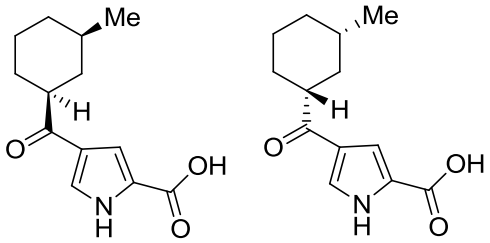

General procedure G: methyl 4-((1*R*,3*S*)-3-methylcyclohexanecarbonyl)-1*H*-pyrrole-2-carboxylate and methyl 4-((1*S*,3*R*)-3-methylcyclohexanecarbonyl)-1*H*-pyrrole-2-carboxylate (430 mg, 1.71 mmol) and LiOH monohydrate (1.44 g, 34.20 mmol) gave a mixture of **191** and **192** as an off-white solid (340 mg, 85%). R_f 0.24 (8:2 DCM/MeOH); m.p. 189-191 ˚C; λ_{max} (EtOH/nm) 226.0, 273.0; IR υ_{max}/cm^{-1} 3200, 2924, 2850, 1671, 1642, 1558; ^{1}H NMR (500 MHz, DMSO-d_6) δ ppm 0.88 (3H, d, *J* = 7.1 Hz, CH_3), 1.17-1.76 (9H, m, CH-cyclohexane), 3.09 (1H, tt, *J* = 3.1 and 12.0 Hz, CO-CH), 7.08 (1H, br s, H-3), 7.70 (1H, dd, *J* = 1.6 and 3.2 Hz, H-5), 12.36 (1H, s, NH-pyrrole), 12.72 (1H, s, COOH); ^{13}C NMR (125 MHz, DMSO-d_6) δ ppm 22.7 (CH_3), 25.0, 28.8, 31.4, 34.3, 37.7 (C-cyclohexane), 46.0 (CO-CH), 113.9 (C-Ar), 124.9 (C-Ar), 127.2 (C-Ar), 127.4 (C-Ar), 161.7 (CO), 198.1 (CO); MS (ES+) *m/z* = 236.0 $[M+H]^+$; HRMS calcd for $C_{13}H_{17}NO_3$ $[M-H]^-$ 234.1136, found 234.1129.

5-((1*R*,3*S*)-3-Methylcyclohexanecarbonyl)-1*H*-pyrrole-2-carboxylic acid and 5-((1*S*,3*R*)-3-Methylcyclohexanecarbonyl)-1*H*-pyrrole-2-carboxylic acid 200/201

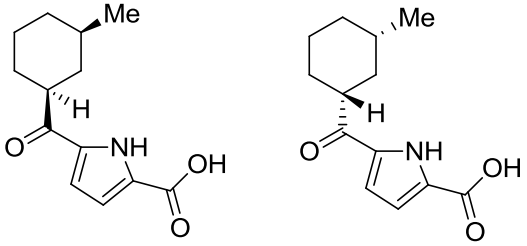

General procedure G: methyl 5-((1*R*,3*S*)-3-methylcyclohexanecarbonyl)-1*H*-pyrrole-2-carboxylate and methyl 5-((1*S*,3*R*)-3-methylcyclohexanecarbonyl)-1*H*-pyrrole-2-carboxylate (40 mg, 0.14 mmol) and LiOH monohydrate (120 mg, 2.89 mmol) gave a mixture of **200** and **201** as an off-white solid (30 mg, 86%). R_f 0.20 (8:2 DCM/MeOH); m.p. 178-180 ˚C; λ_{max} (EtOH/nm) 219.5, 289.5; IR υ_{max}/cm^{-1} 3263, 2922, 2852, 1683, 1547; ^{1}H NMR (500 MHz, DMSO-d_6) δ ppm 0.89 (3H, d, *J* = 7.1 Hz, CH_3), 1.18-1.76 (9H, m, CH-cyclohexane), 3.25

(1H, tt, *J* = 3.2 and 11.9 Hz, CO-CH), 6.78 (1H, dd, *J* = 2.3 and 3.9 Hz, H-3), 7.00 (1H, dd, *J* = 2.3 and 3.9 Hz, H-4), 12.18 (1H, s, NH-pyrrole), 12.88 (1H, s, COOH); MS (ES+) *m/z* = 236.0 $[M+H]^+$; HRMS calcd for $C_{13}H_{17}NO_3$ $[M-H]^-$ 234.1136, found 234.1131.

4-(4-Methylcyclohexanecarbonyl)-1*H*-pyrrole-2-carboxylic acid (*cis*/*trans* 2:3), 195

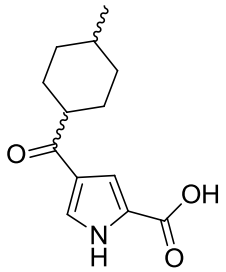

General procedure G: methyl 4-(4-methylcyclohexanecarbonyl)-1*H*-pyrrole-2-carboxylate (319 mg, 1.28 mmol) and LiOH monohydrate (1.08 g, 25.62 mmol) gave **195** as an off-white solid (294 mg, 98%). R_f 0.22 (9:1 Petrol/EtOAc); m.p. 201-202 ˚C; λ_{max} (EtOH/nm) 224.0; IR υ_{max}/cm^{-1} 3331, 2918, 2857, 1646, 1558, 1501, 1451; ^{1}H NMR (500 MHz, DMSO-d_6) δ ppm 0.94-0.97 (3H, m, CH_3), 1.08-1.16 (1H, m, CH-cyclohexane), 1.33-1.45 (2H, m, CH-cyclohexane), 1.56-1.65 (2H, m, CH-cyclohexane), 1.75-1.80 (4H, m, CH-cyclohexane), 3.05 (0.6H, ddd, *J* = 3.2, 3.4 and 11.8 and 12.0 Hz, CO-CH *trans*), 3.16-3.22 (0.4H, m, CO-CH *cis*), 7.12-7.13 (1H, m, H-3), 7.70-7.75 (1H, m, H-5), 12.40 (1H, s, NH-pyrrole), 12.74 (1H, s, COOH); ^{13}C NMR (125 MHz, DMSO-d_6) δ ppm 22.6 (CH_3), 25.2, 28.6, 29.3, 30.6, 31.7, 33.9 (C-cyclohexane *cis* and *trans*), 45.7 (CO-CH), 114.1 (C-Ar), 124.7 (C-Ar), 125.2 (C-Ar), 127.6 (C-Ar), 161.8 (CO), 200.0 (CO); MS (ES+) *m/z* = 236.0 $[M+H]^+$; HRMS calcd for $C_{13}H_{17}NO_3$ $[M+H]^+$ 236.1281, found 236.1283.

4-((1*R*,2*R*)-2-Methylcyclohexanecarbonyl)-*N*-(pyridin-4-ylmethyl)-1*H*-pyrrole-2-carboxamide and 4-((1*S*,2*S*)-2-Methylcyclohexanecarbonyl)-*N*-(pyridin-4-ylmethyl)-1*H*-pyrrole-2-carboxamide, 189/190

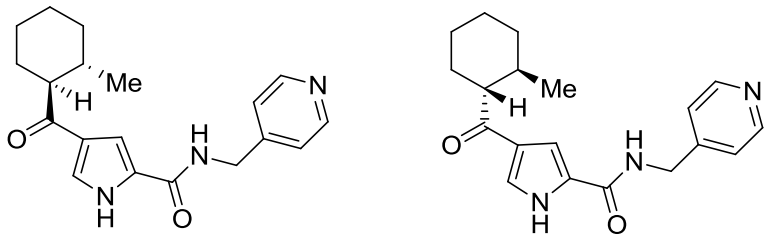

General procedure D: 4-((1*R*,2*R*)-2-methylcyclohexanecarbonyl)-1*H*-pyrrole-2-carboxylic acid and 4-((1*S*,2*S*)-2-methylcyclohexanecarbonyl)-1*H*-pyrrole-2-carboxylic acid (110 mg,

0.45 mmol), CDI (150 mg, 0.90 mmol), and 4-picolylamine (0.11 mL, 1.13 mmol). Purification *via* column chromatography (silica; 0-5% MeOH/DCM) gave **189** and **190** as a white solid (110 mg, 76%). R_f 0.62 (95:5 EtOAc/MeOH); m.p. 218-220 ˚C; λ_{max} (EtOH/nm) 275.0, 230.0; IR υ_{max}/cm^{-1} 3334, 3175, 2924, 2856, 1626, 1571; ^{1}H NMR (500 MHz, DMSO-d_6) δ ppm 0.74 (3H, d, *J* = 6.9 Hz, CH_3), 1.03-1.10 (1H, m, CH-cyclohexane), 1.28-1.74 (8H, m, CH-cyclohexane), 2.72-2.77 (1H, m, CO-CH), 4.46 (2H, d, *J* = 6.1 Hz, NH-*CH*$_2$), 7.29-7.31 (3H, m, H-3 and CH-pyridine), 7.70 (1H, br s, H-5), 8.51 (2H, d, *J* = 6.0 Hz, N-CH-pyridine), 8.88 (1H, t, *J* = 6.1 Hz, CO-NH), 12.19 (1H, s, NH-pyrrole); ^{13}C NMR (125 MHz, DMSO-d_6) δ ppm 20.6 (CH_3), 25.3 (C-cyclohexane), 25.8 (C-cyclohexane), 30.5 (C-cyclohexane), 33.5 (C-cyclohexane), 34.0 (C-cyclohexane), 41.0 (NH-CH_2), 52.8 (CO-*C*-cyclohexane),109.9 (C-Ar), 122.3 (C-Ar), 126.2 (C-Ar), 126.6 (C-Ar), 127.6 (C-Ar), 149.0 (C-Ar), 149.7 (C-Ar), 160.6 (CO), 198.7 (CO); MS (ES+) *m/z* = 326.1 $[M+H]^+$; HRMS calcd for $C_{19}H_{23}N_3O_2$ $[M+H]^+$ 326.1863, found 326.1859.

5-((1*R*,2*R*)-2-Methylcyclohexanecarbonyl)-*N*-(pyridin-4-ylmethyl)-1*H*-pyrrole-2-carboxamide and 5-((1*S*,2*S*)-2-Methylcyclohexanecarbonyl)-*N*-(pyridin-4-ylmethyl)-1*H*-pyrrole-2-carboxamide, 198/199

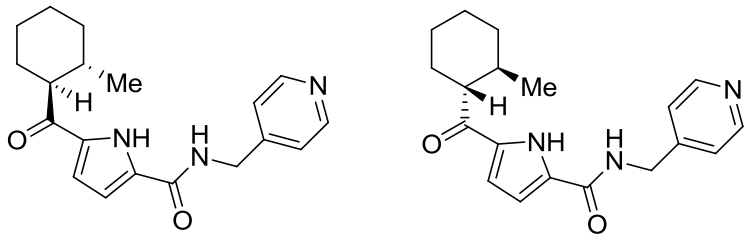

General procedure D: 5-((1*R*,2*R*)-2-methylcyclohexanecarbonyl)-1*H*-pyrrole-2-carboxylic acid and 5-((1*S*,2*S*)-2-methylcyclohexanecarbonyl)-1*H*-pyrrole-2-carboxylic acid (40 mg, 0.18 mmol), CDI (60 mg, 0.36 mmol), and 4-picolylamine (0.09 mL, 0.90 mmol). Purification *via* column chromatography (silica; 0-5% MeOH/DCM) gave **198** and **199** as a white solid (50 mg, 83%). R_f 0.65 (95:5 EtOAc/MeOH); m.p. 197-200 ˚C; λ_{max} (EtOH/nm) 293.5, 220.0; IR υ_{max}/cm^{-1} 3285, 2923, 2850, 1652, 1647; ^{1}H NMR (500 MHz, DMSO-d_6) δ ppm 0.75 (3H, d, *J* = 6.4 Hz, CH_3), 1.04-1.11 (1H, m, CH-cyclohexane), 1.26-1.72 (8H, m, CH-cyclohexane), 2.86-2.92 (1H, m, CO-CH), 4.49 (2H, d, *J* = 5.9 Hz, NH-*CH*$_2$), 6.85 (1H, d, *J* = 3.9 Hz, H-3), 7.08 (1H, d, *J* = 3.9 Hz, H-4), 7.10 (2H, d, *J* = 6.0 Hz CH-pyridine), 8.30 (2H, d, *J* = 6.0 Hz, N-CH-pyridine), 8.77 (1H, t, *J* = 5.9 Hz, CO-NH), 11.73 (1H, s, NH-pyrrole); ^{13}C NMR (125 MHz, DMSO-d_6) δ ppm 20.5 (CH_3), 25.2 (C-cyclohexane), 25.6 (C-

cyclohexane), 30.5 (C-cyclohexane), 33.6 (C-cyclohexane), 34.0 (C-cyclohexane), 41.3 (NH-CH_2), 51.7 (CO-CH), 112.9 (C-Ar), 116.0 (C-Ar), 122.2 (C-Ar), 131.5 (C-Ar), 133.8 (C-Ar), 148.2 (C-Ar), 149.6 (C-Ar), 159.6 (CO), 194.5 (CO); MS (ES+) *m/z* = 326.13 $[M+H]^+$; HRMS calcd for $C_{19}H_{23}N_3O_2$ $[M+H]^+$ 326.1863, found 326.1861.

4-((1*R*,3*S*)-3-Methylcyclohexanecarbonyl)-*N*-(pyridin-4-ylmethyl)-1*H*-pyrrole-2-carboxamide and 4-((1*S*,3*R*)-3-Methylcyclohexanecarbonyl)-*N*-(pyridin-4-ylmethyl)-1*H*-pyrrole-2-carboxamide, 193/194

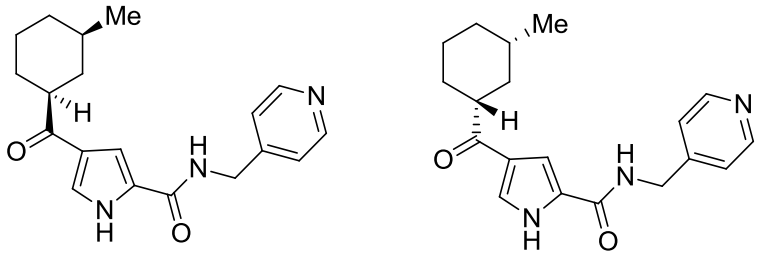

General procedure D: 4-((1*R*,3*S*)-3-methylcyclohexanecarbonyl)-1*H*-pyrrole-2-carboxylic acid and 4-((1*S*,3*R*)-3-methylcyclohexanecarbonyl)-1*H*-pyrrole-2-carboxylic acid (80 mg, 0.35 mmol), CDI (110 mg, 0.70 mmol), and 4-picolylamine (0.085 mL, 0.88 mmol). Purification *via* column chromatography (silica; 0-5% MeOH/DCM) gave **193** and **194** as a white solid (100 mg, 89%). R_f 0.62 (95:5 EtOAc/MeOH); m.p. 222-224 ˚C; λ_{max} (EtOH/nm) 276.5, 229.5; IR υ_{max}/cm^{-1} 3341, 3200, 2926, 2856, 1627, 1573; ^{1}H NMR (500 MHz, DMSO-d_6) δ ppm 0.69 (3H, d, *J* = 6.5 Hz, CH_3), 0.76-0.83 (1H, m, CH-cyclohexane), 1.03-1.56 (8H, m, CH-cyclohexane), 2.86 (1H, tt, *J* = 2.9 and 11.9 Hz, CO-CH), 4.25 (2H, d, *J* = 5.9 Hz, NH-*CH*$_2$), 7.08-7.10 (3H, m, CH-pyridine and H-3), 7.46 (1H, br s, H-5), 8.30 (2H, d, *J* = 6.0 Hz, N-CH-pyridine), 8.68 (1H, t, *J* = 5.9 Hz, CO-NH), 11.98 (1H, s, NH-pyrrole); ^{13}C NMR (125 MHz, DMSO-d_6) δ ppm 22.7 (CH_3), 25.2 (C-cyclohexane), 28.9 (C-cyclohexane), 31.5 (C-cyclohexane), 34.3 (C-cyclohexane), 37.8 (C-cyclohexane), 41.0 (CO-CH), 46.1 (NH-CH_2), 109.9 (C-Ar), 122.1 (C-Ar), 124.6 (C-Ar), 126.4 (C-Ar), 127.4 (C-Ar), 148.6 (C-Ar), 149.5 (C-Ar), 160.4 (CO), 195.6 (CO); MS (ES+) *m/z* = 326.14 $[M+H]^+$; HRMS calcd for $C_{19}H_{23}N_3O_2$ $[M+H]^+$ 326.1863, found 326.1861.

5-((1*R*,3*S*)-3-Methylcyclohexanecarbonyl)-N-(pyridin-4-ylmethyl)-1*H*-pyrrole-2-carboxamide and 5-((1*S*,3*R*)-3-Methylcyclohexanecarbonyl)-*N*-(pyridin-4-ylmethyl)-1*H*-pyrrole-2-carboxamide, 202/203

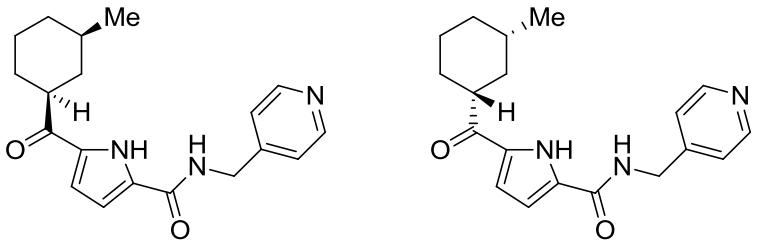

General procedure D: 5-((1*R*,3*S*)-3-methylcyclohexanecarbonyl)-*1H*-pyrrole-2-carboxylic acid and 5-((1*S*,3*R*)-3-methylcyclohexanecarbonyl)-*1H*-pyrrole-2-carboxylic acid (10 mg, 0.04 mmol), CDI (14 mg, 0.09 mmol), and 4-picolylamine (0.01 mL, 0.11 mmol). Purification *via* column chromatography (silica; 0-5% MeOH/DCM) gave **202** and **203** as a white solid (11 mg, 79%). R_f 0.64 (95:5 EtOAc/MeOH); m.p. 198-200 ˚C; λ_{max} (EtOH/nm) 291.0, 221.5; IR υ_{max}/cm^{-1} 3275, 2922, 2848, 1653, 1649; ^{1}H NMR (500 MHz, MeOD) δ ppm 0.80 (3H, d, *J* = 6.5 Hz, CH_3), 0.95-1.73 (9H, m, CH-cyclohexane), 3.03 (1H, tt, *J* = 3.1 and 11.9 Hz, CO-CH), 4.47 (2H, s, NH-*CH_2*), 6.76 (1H, d, *J* = 4.0 Hz, H-3), 6.90 (1H, d, *J* = 4.0 Hz, H-4), 7.26 (2H, d, *J* = 6.0 Hz, CH-pyridine), 8.34 (2H, d, *J* = 6.0 Hz, N-CH-pyridine); 13C NMR (125 MHz, MeOD) δ ppm Insufficient quantity of material obtained to perform analysis; MS (ES+) *m/z* = 326.1 $[M+H]^+$; HRMS calcd for $C_{19}H_{23}N_3O_2$ $[M+H]^+$ 326.1863, found 326.1857.

4-(4-Methylcyclohexanecarbonyl)-*N*-(pyridin-4-ylmethyl)-1*H*-pyrrole-2-carboxamide (*cis*/*trans* 2:3), 154

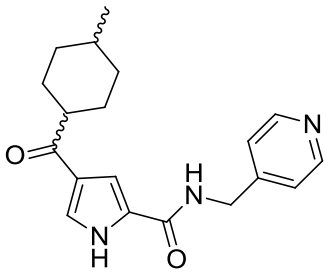

General procedure D: 4-(4-methylcyclohexanecarbonyl)-1*H*-pyrrole-2-carboxylic acid (80 mg, 0.34 mmol), CDI (110 mg, 0.68 mmol) and 4-picolylamine (90 μL, 0.85 mmol). Recrystallisation (9:1 EtOAc/petrol) gave **154** as a white solid (75 mg, 68%). R_f 0.31 (9:1 DCM/MeOH); m.p. 217-219 ˚C; λ_{max} (EtOH/nm) 228.5, 275.0; IR υ_{max}/cm^{-1} 3336, 3113,

3047, 2915, 2850, 1738, 1640, 1606, 1569; ^{1}H NMR (500 MHz, DMSO-d_6) δ ppm 0.95-0.98 (3H, m, CH_3), 0.79-087 (2H, m, CH-cyclohexane), 1.10-1.19 (3H, m, CH-cyclohexane), 1.30-1.53 (4H, m, CH-cyclohexane), 2.73 (0.6H, ddd, *J* = 3.2, 3.4 and 11.8 and 12.0 Hz CO-CH *trans*), 2.86-2.91 (0.4H, m, CO-CH *cis*), 4.23 (2H, d, *J* = 6.0 Hz, NH-*CH*$_2$), 7.06-7.08 (3H, m, H-3 and CH-pyridine), 7.41 (1H, br s, H-5), 8.28 (2H, d, *J* = 6.0 Hz, N-CH-pyridine), 8.66 (1H, t, *J* = 6 Hz, CO-NH), 11.95 (1H, s, NH-pyrrole); ^{13}C NMR (125 MHz, DMSO-d_6) δ ppm 22.6 (CH_3), 25.2, 28.5, 29.3, 30.8, 31.8, 34.0 (C-cyclohexane *cis* and *trans*), 41.1 (NH-CH_2), 45.9 (CO-CH), 109.9 (C-Ar), 122.1 (C-Ar), 126.4 (C-Ar), 148.6 (C-Ar), 149.5 (C-Ar), 160.4 (CO), 200.0 (CO); MS (ES+) *m/z* = 326.1 $[M+H]^+$; HRMS calcd for $C_{19}H_{23}N_3O_2$ $[M+H]^+$ 326.1863, found 326.1866.

Methyl 4-(4-methoxycyclohexanecarbonyl)-1*H*-pyrrole-2-carboxylate (*cis*/*trans* ratio unknown), 204

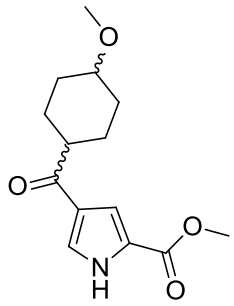

General procedure E: 4-methoxycyclohexanecarboxylic acid (1.01 g, 6.40 mmol), $SOCl_2$ (0.70 mL, 9.60 mmol) gave 4-methoxycyclohexanecarbonyl chloride which was used directly in the next step **General procedure F:** methyl 1*H*-pyrrole-2-carboxylate (400 mg, 3.20 mmol), and $AlCl_3$ (1.07 g, 8.00 mmol). Purification *via* column chromatography (silica; 0-50% EtOAc/petrol) gave **204** as a white solid (240 mg, 28%). R_f 0.37 (9:1 petrol/EtOAc); m.p. 133-134 ˚C; λ_{max} (EtOH/nm) 272.5, 225.5; IR υ_{max}/cm^{-1} 3281, 3112, 2932, 1686, 1652, 1560; ^{1}H NMR (500 MHz, DMSO-d_6) δ ppm 1.09-1.29 (4H, m, CH-cyclohexane), 1.65-1.68 (2H, m, CH-cyclohexane), 1.89-1.92 (2H, m, CH-cyclohexane), 2.90-2.99 (2H, m, CO-CH and *CH*-O-CH_3), 3.12 (3H, s, O-CH_3), 3.67 (3H, s, COO-CH_3), 7.03 (1H, br s, H-3), 7.66 (1H, br s, H-5), 12.44 (1H, s, NH-pyrrole). ^{13}C NMR (125 MHz, DMSO-d_6) δ ppm 27.4 (C-cyclohexane), 30.7 (C-cyclohexane), 45.2 (CO-CH), 51.5 (O-CH_3), 57.1 (COO-*CH*$_3$), 78.1 (*C*-O-CH_3), 114.4 (C-Ar), 123.5 (C-Ar), 125.1 (C-Ar), 128.2 (C-Ar), 160.5 (CO), 200.0 (CO); MS (ES+) *m/z* = 266.3 $[M+H]^+$; HRMS calcd for $C_{14}H_{19}NO_4$ $[M+H]^+$ 266.1387, found 266.1390.

4-(4-Methoxycyclohexanecarbonyl)-1*H*-pyrrole-2-carboxylic acid (*cis*/*trans* 7:3), 205

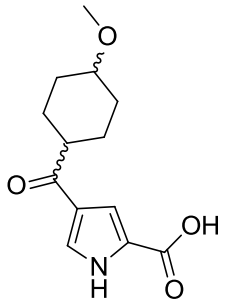

General procedure G: methyl 4-(4-methoxycyclohexanecarbonyl)-1*H*-pyrrole-2-carboxylate (219 mg, 0.83 mmol) and LiOH monohydrate (0.70 g, 16.60 mmol) gave **205** as an off-white solid (203 mg, 97%). R_f 0.20 (9:1 petrol/EtOAc); m.p. 175-176 ˚C; λ_{max} (EtOH/nm) 273.0, 226.5; IR υ_{max}/cm^{-1} 3265, 2938, 2865, 1681, 1645, 1557, 1498, 1437; ^{1}H NMR (500 MHz, DMSO-d_6) δ ppm 1.22-1.67 (5H, m, CH-cyclohexane), 1.76-1.89 (2H, m, CH-cyclohexane), 2.02-2.06 (1H, m, CH-cyclohexane), 3.01-3.14 (2H, m, CO-CH and *CH*-O-CH_3), 3.21-3.25 (3H, m, O-CH_3 *cis* and *trans*), 7.08 (1H, br s, H-3), 7.71 (1H, br s, H-5), 12.37 (1H, s, NH-pyrrole), 12.70 (1H, s, COOH); ^{13}C NMR (125 MHz, DMSO-d_6) δ ppm 27.6 (C-cyclohexane), 30.9 (C-cyclohexane), 45.3 (CO-*CH*), 55.0 (*C*-O-CH_3), 78.4 (O-CH_3), 114.3 (C-Ar), 123.1 (C-Ar), 125.0 (C-Ar), 127.8 (C-Ar), 161.8 (CO), 200.0 (CO); MS (ES+) *m/z* = 252.1 $[M+H]^+$; HRMS calcd for $C_{13}H_{17}NO_4$ $[M-H]^-$ 250.1085, found 250.1078.

4-(4-Methoxycyclohexanecarbonyl)-*N*-(pyridin-4-ylmethyl)-1*H*-pyrrole-2-carboxamide (*cis*/*trans* 75:25), 155

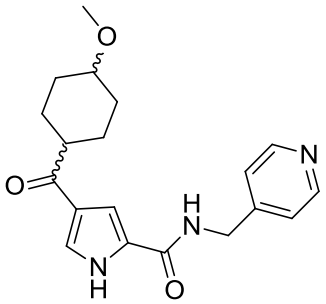

General procedure D: 4-(4-methoxycyclohexanecarbonyl)-1*H*-pyrrole-2-carboxylic acid (136 mg, 0.54 mmol), CDI (174 mg, 1.08 mmol), and 4-picolylamine (130 µL, 1.35 mmol). Purification *via* column chromatography (silica; 0-8% MeOH/DCM) gave **155** as a white solid (112 mg, 61%). R_f 0.35 (9:1 DCM/MeOH); m.p. 198-199 ˚C; λ_{max} (EtOH/nm) 229.0, 275.5; IR υ_{max}/cm^{-1} 3341, 3114, 2930, 2857, 1635, 1606, 1569, 1528; ^{1}H NMR (500 MHz,

DMSO-d_6) δ ppm 1.23-1.54 (4H, m CH-cyclohexane), 1.61-1.92 (3H, m CH-cyclohexane), 2.04-2.07 (1H, m, CH-cyclohexane), 3.00 (0.75H, dddd, *J* = 3.2, 3.4, 11.8 and 12.0 Hz, CO-CH *trans*), 3.05-3.13 (1.25H, m, CO-CH *cis* and *CH*-O-CH_3), 3.21 (0.75H, s, O-CH_3 *cis*), 3.25 (2.25H, s, O-CH_3 *trans*), 4.46 (2H, d, *J* = 6.0 Hz, NH-*CH_2*), 7.28-7.31 (3H, m, H-3 and CH-pyridine), 7.68 (0.25H, dd, *J* = 1.6 and 3.2 Hz, H-5 *cis*), 7.71 (0.75H, dd, *J* = 1.6 and 3.2 Hz, H-5 *trans*,), 8.50 (2H, d, *J* = 6.0 Hz, N-CH-pyridine), 8.90 (1H, t, *J* = 6.0 Hz, CO-NH), 12.21 (1H, s, NH-pyrrole); ^{13}C NMR (125 MHz, DMSO-d_6) δ ppm 26.9 (C-cyclohexane), 30.8 (C-cyclohexane), 41.1 (NH-CH_2), 45.3 (CO-CH), 54.9 (O-CH_3), 78.1 (*C*-OCH_3), 109.8 (C-Ar), 122.1 (C-Ar), 126.6 (C-Ar), 127.5 (C-Ar), 148.6 (C-Ar), 149.5 (C-Ar), 160.4 (CO), 200.0 (CO); MS (ES+) *m/z* = 342.3 $[M+H]^+$; HRMS calcd for $C_{19}H_{23}N_3O_3$ $[M+H]^+$ 342.1812, found 342.1815.

***cis* Methyl 4-(3-hydroxycyclohexanecarbonyl)-1*H*-pyrrole-2-carboxylate, 206**

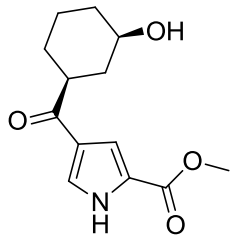

General procedure E: 3-methoxycyclohexanecarboxylic acid (1.01 g, 6.40 mmol), $SOCl_2$ (0.70 mL, 9.60 mmol) gave 3-methoxycyclohexanecarbonyl chloride which was used directly in the next step. **General procedure F:** methyl 1*H*-pyrrole-2-carboxylate (400 mg, 3.20 mmol), and $AlCl_3$ (1.07 g, 8.00 mmol). Purification *via* column chromatography (silica; 30-100% EtOAc/petrol) gave **206** as a white solid (305 mg, 48%). R_f 0.31 (2:8 petrol/EtOAc); m.p. 168-169 ˚C; λ_{max} (EtOH/nm) 274.0, 220.5; IR υ_{max}/cm^{-1} 3421, 3123, 2923, 2859, 1707, 1644, 1559; ^{1}H NMR (500 MHz, DMSO-d_6) δ ppm 0.87-1.08 (3H, m, CH-cyclohexane), 1.21-1.30 (1H, m, CH-cyclohexane), 1.50-1.76 (4H, m, CH-cyclohexane), 2.96-3.05 (1H, m, CO-CH), 3.37-3.43 (1H, m, CH-OH), 3.66 (3H, s, O-CH_3), 4.44 (1H, d, *J* = 4.6 Hz, OH), 7.01 (1H, d, *J* = 1.6 Hz, H-3), 7.62 (1H, d, *J* = 1.6 Hz, H-5), 12.42 (1H, s, NH-pyrrole); ^{13}C NMR (125 MHz, DMSO-d_6) δ ppm 23.3 (C-cyclohexane), 28.4 (C-cyclohexane), 35.2 (C-cyclohexane), 38.6 (C-cyclohexane), 45.1 (C-cyclohexane), 51.7 (CO-*CH*), 68.5 (C-OH), 114.5 (C-Ar), 123.4 (C-Ar), 124.9 (C-Ar), 128.1 (C-Ar),160.5 (CO), 197.2 (CO); MS (ES+) *m/z* = 252.3 $[M+H]^+$; HRMS calcd for $C_{13}H_{17}NO_4$ $[M+H]^+$ 252.1230, found 252.1228.

***cis* Methyl 4-(3-((triisopropylsilyl)oxy)cyclohexanecarbonyl)-1*H*-pyrrole-2-carboxylate, 207**

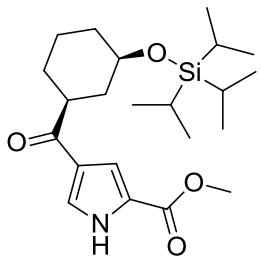

To a suspension of methyl 4-(3-hydroxycyclohexanecarbonyl)-1*H*-pyrrole-2-carboxylate (480 mg, 1.91 mmol) in DCM (8 mL) was added TIPS chloride (0.82 mL, 3.82 mmol) and imidazole (390 mg, 5.73 mmol). The resulting solution was stirred for 16 h at RT. The reaction was quenched with water, and the mixture extracted with EtOAc (3 x 30 mL). Combined organic layers were washed with brine, dried over Na_2SO_4 and concentrated *in vacuo*. Purification *via* column chromatography (silica; 0-30% EtOAc/petrol) gave **207** as a yellow oil (0.72 g, 93%). R_f 0.32 (8:2 petrol/EtOAc); λ_{max} (EtOH/nm) 275.0, 247.0, 223.5; IR υ_{max}/cm^{-1} 3304, 3125, 2939, 2864, 1700, 1650, 1561, 1445; ^{1}H NMR (500 MHz, $CDCl_3$) δ ppm 0.97-0.98 (21H, s, TIPS-CH and TIPS-CH_3), 1.22-1.37 (3H, m, CH-cyclohexane), 1.45-1.52 (1H, m, CH-cyclohexane), 1.73-1.94 (3H, m, CH-cyclohexane), 2.00-2.04 (1H, m, CH-cyclohexane), 2.85-2.91 (1H, m, CO-CH), 3.67-3.73 (1H, m, CH-OSi), 3.82 (3H, s, O-CH_3), 7.20 (1H, dd, *J* = 1.6 and 2.4 Hz, H-3), 7.47 (1H, dd, *J* = 1.6 and 3.2 Hz, H-5), 9.43 (1H, s, NH-pyrrole); ^{13}C NMR (125 MHz, $CDCl_3$) δ ppm 12.4 (TIPS-CH), 18.1 (TIPS-CH_3), 24.2 (C-cyclohexane), 28.6 (C-cyclohexane), 36.0 (C-cyclohexane), 38.7 (C-cyclohexane), 46.4 (CO-CH), 51.9 (O-CH_3), 71.8 (CH-OSi), 114.9 (C-Ar), 123.9 (C-Ar), 126.2 (C-Ar), 161.2 (CO), 197.6 (CO); MS (ES+) *m/z* = 408.3 $[M+H]^+$; HRMS calcd for $C_{22}H_{37}NO_4Si$ $[M+H]^+$ 408.2565, found 408.2566.

***cis* 4-(3-((Triisopropylsilyl)oxy)cyclohexanecarbonyl)-1*H*-pyrrole-2-carboxylic acid, 208**

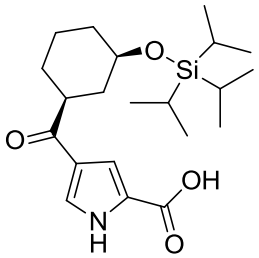

General procedure G: methyl 4-(3-((triisopropylsilyl)oxy)cyclohexanecarbonyl)-1*H*-pyrrole-2-carboxylate (0.71 g, 1.74 mmol) and LiOH monohydrate (110 mg, 2.61 mmol) gave **208** as an off-white solid (0.55 g, 80%). R_f 0.22 (8:2 petrol/EtOAc); m.p. 157-159 ˚C; λ_{max} (EtOH/nm) 280.0, 218.5; IR υ_{max}/cm^{-1} 3268, 2940, 2864, 1649, 1556; ^{1}H NMR (500 MHz, DMSO-d_6) δ ppm 0.79-0.80 (21H, m, TIPS-CH and TIPS-CH$_3$), 0.91-0.99 (2H, m, CH-cyclohexane), 1.03-1.10 (1H, m, CH-cyclohexane), 1.16-1.25 (1H, m, CH-cyclohexane), 1.42-1.54 (2H, m, CH-cyclohexane), 1.66-1.71 (2H, m, CH-cyclohexane), 2.96 (1H, dddd, *J* = 3.2, 3.4 and 11.8 and 12 Hz, CO-CH), 3.58-3.64 (1H, m, CH-OSi), 6.86 (1H, dd, *J* = 1.6 and 2.4 Hz, H-3), 7.48 (1H, dd, *J* = 1.6 and 3.3 Hz, H-5), 12.14 (1H, s, NH-pyrrole), 12.47 (1H, s, COOH); ^{13}C NMR (125 MHz, DMSO-d_6) δ ppm 11.8 (TIPS-CH), 17.9 (TIPS-CH$_3$), 23.4 (C-cyclohexane), 28.4 (C-cyclohexane), 35.8 (C-cyclohexane), 38.9 (C-cyclohexane), 44.6 (CO-CH), 70.4 (C-OSi), 114.1 (C-Ar), 124.7 (C-Ar), 124.8 (C-Ar), 127.6 (C-Ar), 161.6 (CO), 193.9 (CO); MS (ES+) *m/z* = 394.3 $[M+H]^+$; HRMS calcd for $C_{21}H_{35}NO_4Si$ $[M+H]^+$ 394.2408, found 394.2410.

***cis* *N*-(Pyridin-4-ylmethyl)-4-(3-((triisopropylsilyl)oxy)cyclohexanecarbonyl)-1*H*-pyrrole-2-carboxamide, 209**

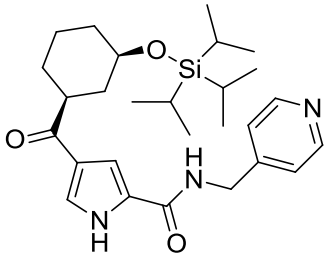

General procedure D: 4-(3-((triisopropylsilyl)oxy)cyclohexanecarbonyl)-1*H*-pyrrole-2-carboxylic acid (390 mg, 0.99 mmol), CDI (321 mg, 1.98 mmol), and 4-picolylamine (240 μL, 2.48 mmol). Purification *via* column chromatography (silica; 0-5% MeOH/DCM) gave **209** as a white solid (256 mg, 54%). R_f 0.36 (9:1 DCM/MeOH); m.p. 190-191 ˚C; λ_{max}

(EtOH/nm) 275.5, 229.0; IR υ_{max}/cm^{-1} 3334, 3202, 2939, 2864 1630, 1574, 1537; ^{1}H NMR (500 MHz, DMSO-d_6) δ ppm 0.78-0.80 (21H, m, TIPS-CH and TIPS-CH_3), 0.90-0.99 (2H, m, CH-cyclohexane), 1.05-1.22 (2H, m, CH-cyclohexane), 1.43-1.55 (2H, m, CH-cyclohexane), 1.67-1.69 (2H, m, CH-cyclohexane), 2.91 (1H, dddd, *J* = 3.2, 3.4, 11.8 and 12.0 Hz, CO-CH), 3.55-3.61 (1H, m, CH-OSi), 4.21 (2H, d, *J* = 6.2 Hz, NH-CH_2), 7.04-7.05 (3H, m, CH-pyridine and H-3), 7.46 (1H, br s, H-5), 8.26 (2H, d, *J* = 6.1 Hz, N-CH-pyridine), 8.64 (1H, t, *J* = 6.2 Hz, CO-NH), 11.94 (1H, s, NH-pyrrole); ^{13}C NMR (125 MHz, DMSO-d_6) δ ppm 11.8 (TIPS-CH), 17.9 (TIPS-CH_3), 23.4 (C-cyclohexane), 28.6 (C-cyclohexane), 35.8 (C-cyclohexane), 41.0 (C-cyclohexane), 42.0 (NH-CH_2), 44.6 (CO-CH), 70.4 (C-OSi), 109.9 (C-Ar), 122.05 (C-Ar), 126.7 (C-Ar), 127.5 (C-Ar), 148.6 (C-Ar), 149.4 (C-Ar), 149.5 (C-Ar), 160.4 (CO), 197.0 (CO); MS (ES+) *m/z* = 484.2 $[M+H]^+$; HRMS calcd for $C_{27}H_{41}N_3O_3Si$ $[M+H]^+$ 484.2990, found 484.2984.

***cis* 4-(3-Hydroxycyclohexanecarbonyl)-*N*-(pyridin-4-ylmethyl)-1*H*-pyrrole-2-carboxamide, 210**

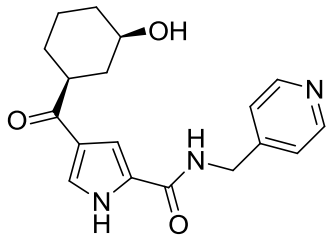

General procedure H: *N*-(pyridin-4-ylmethyl)-4-(3-((triisopropylsilyl)oxy)cyclohexanecarbonyl)-1*H*-pyrrole-2-carboxamide (100 mg, 0.21 mmol) and TBAF (250 μL, 0.25 mmol). Purification *via* column chromatography (silica; 0-8% MeOH/DCM) gave **210** as a white solid (55 mg, 80%). R_f 0.17 (9:1 DCM/MeOH); m.p. 220-221 ˚C; λ_{max} (EtOH/nm) 275.5, 229.5; IR υ_{max}/cm^{-1} 3370, 3208, 2932, 2857, 1632, 1573, 1531; ^{1}H NMR (500 MHz, DMSO-d_6) δ ppm 1.04-1.39 (4H, m, CH-cyclohexane), 1.65-1.91 (4H, m, CH-cyclohexane), 3.08 (1H, dddd, *J* = 3.2, 3.4, 11.8 and 12.0 Hz, CO-CH), 3.50-3.56 (1H, m, CH-OH), 4.46 (2H, d, *J* = 6.0 Hz, NH-CH_2), 4.58 (1H, d, *J* = 4.8 Hz, OH), 7.28-7.29 (3H, m, CH-pyridine and H-3), 7.67 (1H, br s, H-5), 8.50 (2H, d, *J* = 6.0 Hz, N-CH-pyridine), 8.89 (1H, t, *J* = 6.0 Hz, CO-NH), 12.19 (1H, s, NH-pyrrole);^{13}C NMR (125 MHz, DMSO-d_6) δ ppm 23.5 (C-cyclohexane), 28.5 (C-cyclohexane), 35.3 (C-cyclohexane), 38.7 (C-cyclohexane), 41.1 (NH-CH_2), 44.9 (CO-CH), 68.4 (C-OH), 109.9 (C-Ar), 122.1 (C-Ar),

124.5 (C-Ar), 126.5 (C-Ar), 127.5 (C-Ar), 148.6 (C-Ar), 149.5 (C-Ar), 160.4 (CO), 197.3 (CO); MS (ES+) *m/z* = 328.3 $[M+H]^+$; HRMS calcd for $C_{18}H_{21}N_3O_3$ $[M+H]^+$ 328.1656, found 328.1660.

Methyl 4-(2,2,2-trichloroacetyl)-1*H*-pyrrole-2-carboxylate, 218

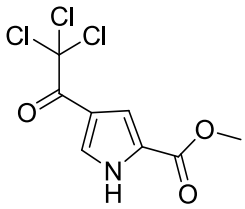

General procedure F: methyl *1H*-pyrrole-2-carboxylate (800 mg, 6.39 mmol), trichloroacetyl chloride (1.44 mL, 12.79 mmol), and $AlCl_3$ (2.14 g, 15.98 mmol). Purification *via* column chromatography (silica; 0-50% EtOAc/petrol) gave **218** as a beige solid (1.55 g, 90%). R_f 0.46 (3:7 EtOAc/petrol); m.p. 122-123 ˚C (lit.[143] 118-119 ^oC); λ_{max} (EtOH/nm) 237.0, 290.0; IR υ_{max}/cm^{-1} 3273, 1683, 1565; ^1H NMR (500 MHz, $CDCl_3$) δ ppm 3.84 (3H, s, O-CH_3), 7.46 (1H, dd, *J* = 1.6 and 2.4 Hz, H-3), 7.80 (1H, dd, *J* = 1.6 and 3.4 Hz, H-5), 9.67 (1H, s, NH-pyrrole); ^{13}C NMR (125 MHz, $CDCl_3$) δ ppm 52.2 (O-CH_3), 117.0 (C-Ar), 117.6 (C-Ar), 124.0 (C-Ar), 130.4 (C-Ar), 161.0 (CO), 176.8 (CO); MS (ES+) *m/z* = 269.8 $[(^{35}ClM)+H]^+$, 271.8 $[(^{37}ClM)+H]^+$.

***tert*-Butyl 4-(5-(methoxycarbonyl)-1*H*-pyrrole-3-carbonyl)piperazine-1-carboxylate, 221**

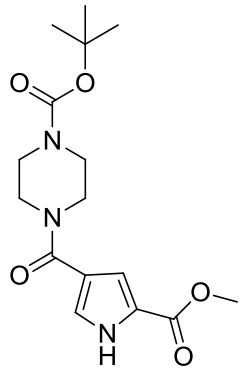

General procedure I: methyl 4-(2,2,2-trichloroacetyl)-1*H*-pyrrole-2-carboxylate (340 mg, 1.25 mmol), and *tert*-butyl piperazine-1-carboxylate (700 mg, 3.75 mmol). Purification *via* column chromatography (silica; 0-30% EtOAc/petrol) gave **221** as a white solid (260 mg, 61%). R_f 0.56 (EtOAc); m.p. 169-171 ˚C; λ_{max} (EtOH/nm) 263.5, 340.5; IR υ_{max}/cm^{-1} 3120, 2923, 2857, 1706, 1589, 1497; ^1H NMR (500 MHz, DMSO-d_6) δ ppm 1.42 (9H, s, C-CH_3),

3.37 (4H, br s, CH-piperazine), 3.57 (4H, br s, CH-piperazine), 3.79 (3H, s, O-CH_3), 6.94 (1H, br s, H-3), 7.33 (1H, br s, H-5), 12.37 (1H, s, NH-pyrrole); ^{13}C NMR (125 MHz, DMSO-d_6) δ ppm 28.0 (C-*CH*$_3$), 51.3 (C-piperazine), 54.9 (O-CH_3), 79.1 (*C*-CH_3), 115.1 (C-Ar), 119.3 (C-Ar), 121.9 (C-Ar), 125.9 (C-Ar), 153.8 (CO), 160.6 (CO), 164.3 (CO); MS (ES+) *m/z* = 338.2 $[M+H]^+$; HRMS calcd for $C_{16}H_{23}N_3O_5$ $[M+H]^+$ 338.1710, found 338.1708.

Methyl 4-(4-methylpiperazine-1-carbonyl)-1*H*-pyrrole-2-carboxylate, 224

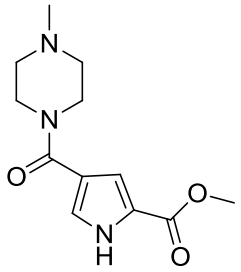

General procedure I: methyl 4-(2,2,2-trichloroacetyl)-1*H*-pyrrole-2-carboxylate (300 mg, 1.11 mmol) and *N*-methyl piperazine (0.37 mL, 3.33 mmol). Recrystallisation from EtOAc/petrol (9:1) gave 224 as white crystals (180 mg, 63%). R_f 0.28 (9:1 DCM/MeOH); m.p. 188-189 ˚C; λ_{max} (EtOH/nm) 210.5, 261.0; IR υ_{max}/cm^{-1} 2950, 2807, 1703, 1607, 1562; ^{1}H NMR (500 MHz, DMSO-d_6) δ ppm 2.09 (3H, s, N-CH_3), 2.19-2.21 (4H, m, CH-piperazine), 3.47-3.49 (4H, m, CH-piperazine), 3.69 (3H, s, O-CH_3), 6.80 (1H, d, *J* = 1.7 Hz, H-3), 7.19 (1H, d, *J* = 1.7 Hz, H-5), 12.23 (1H, s, NH-pyrrole); ^{13}C NMR (125 MHz, DMSO-d_6) δ ppm 45.6 (N-CH_3), 48.6 (C-piperazine), 51.3 (C-piperazine), 54.6 (O-CH_3), 114.9 (C-Ar), 119.5 (C-Ar), 121.8 (C-Ar), 125.8 (C-Ar), 160.6 (CO), 164.1 (CO); MS (ES+) *m/z* = 252.0 $[M+H]^+$; HRMS calcd for $C_{12}H_{17}N_3O_3$ $[M+H]^+$ 252.1343, found 252.1346.

Methyl 4-(piperidine-1-carbonyl)-1*H*-pyrrole-2-carboxylate, 226

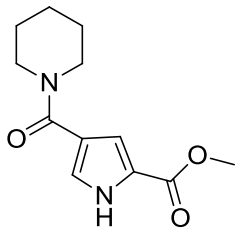

General procedure I: methyl 4-(2,2,2-trichloroacetyl)-1*H*-pyrrole-2-carboxylate (320 mg, 1.16 mmol) and piperidine (0.34 mL, 3.48 mmol). Purification *via* column chromatography (silica; 0-5% MeOH/DCM) gave **226** as a white solid (210 mg, 75%). R_f 0.44 (EtOAc); m.p. 143-144 ˚C; λ_{max} (EtOH/nm) 209.0, 264.0; IR υ_{max}/cm^{-1} 3115, 2939, 2855, 1704, 1581, 1553;

^{1}H NMR (500 MHz, DMSO-d_6) δ ppm 1.48-1.52 (4H, m, CH-piperidine), 1.59-1.64 (2H, m, CH-piperidine), 3.53-3.55 (4H, m, N-CH-piperidine), 3.78 (3H, s, O-CH_3), 6.87 (1H, d, *J* = 1.6 Hz, H-3), 7.26 (1H, d, *J* = 1.6 Hz, H-5), 12.32 (1H, s, NH-pyrrole); ^{13}C NMR (125 MHz, DMSO-d_6) δ ppm 24.2 (C-piperidine), 25.7 (C-piperidine), 48.6 (C-piperidine), 51.3 (O-CH_3), 114.7 (C-Ar), 119.9 (C-Ar), 121.7 (C-Ar), 125.5 (C-Ar), 160.6 (CO), 164.0 (CO); MS (ES+) *m/z* = 237.0 $[M+H]^+$; HRMS calcd for $C_{12}H_{16}N_2O_3$ $[M+H]^+$ 237.1234, found 237.1231.

Methyl 4-(pyrrolidine-1-carbonyl)-1*H*-pyrrole-2-carboxylate, 228

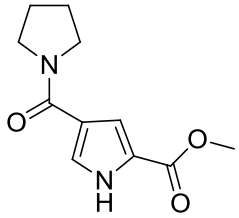

General procedure I: methyl 4-(2,2,2-trichloroacetyl)-1*H*-pyrrole-2-carboxylate (220 mg, 0.81 mmol) and pyrrolidine (0.20 mL, 2.43 mmol). Purification *via* column chromatography (silica; 0-5% MeOH/DCM) gave **228** as a white solid (180 mg, 99%). R_f 0.34 (EtOAc); m.p. 207-208 ˚C; λ_{max} (EtOH/nm) 211.0, 263.0; IR υ_{max}/cm^{-1} 3167, 2953, 2890, 1703, 1590, 1553; ^{1}H NMR (500 MHz, DMSO-d_6) δ ppm 1.84-1.89 (2H, m, CH-pyrrolidine), 1.93-1.98 (2H, m, CH-pyrrolidine), 3.48 (2H, t, *J* = 6.8 Hz, N-CH-pyrrolidine), 3.71 (2H, t, *J* = 6.8 Hz, N-CH-pyrrolidine) 7.13 (1H, d, *J* = 1.6 Hz, H-3), 7.47 (1H, d, *J* = 1.6 Hz, H-5), 12.43 (1H, s, NH-pyrrole); ^{13}C NMR (125 MHz, DMSO-d_6) δ ppm 23.6 (C-pyrrolidine), 26.1 (C-pyrrolidine), 46.4 (C-pyrrolidine), 47.8 (C-pyrrolidine), 51.3 (O-CH_3), 115.4 (C-Ar), 121.0 (C-Ar), 121.9 (C-Ar), 126.2 (C-Ar), 160.7 (CO), 162.6 (CO); MS (ES+) *m/z* = 233.0 $[M+H]^+$; HRMS calcd for $C_{11}H_{14}N_2O_3$ $[M+H]^+$ 223.1077, found 223.1074.

Methyl 4-(morpholine-4-carbonyl)-1*H*-pyrrole-2-carboxylate, 219

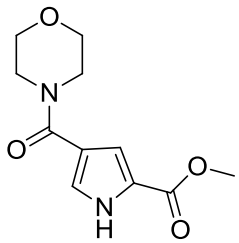

General procedure I: methyl 4-(2,2,2-trichloroacetyl)-1*H*-pyrrole-2-carboxylate (330 mg, 1.20 mmol) and morpholine (0.31 mL, 3.60 mmol). Purification *via* column chromatography (silica; 0-8% MeOH/DCM) gave **219** as a white solid (250 mg, 88%). R_f 0.18 (EtOAc); m.p.

130-131 ˚C; λ_{max} (EtOH/nm) 236.5, 288.5; IR υ_{max}/cm^{-1} 3273, 1683, 1565, 1446; ^{1}H NMR (500 MHz, DMSO-d_6) δ ppm 3.65 (8H, br s, CH_2-N-morpholine and CH_2-O-morpholine), 3.84 (3H, s, O-CH_3), 6.99 (1H, br s, H-3), 7.38 (1H, br s, H-5), 12.42 (1H, s, NH-pyrrole); ^{13}C NMR (125 MHz, DMSO-d_6) δ ppm 51.3 (CH_2-N-morpholine), 59.7 (O-CH_3), 66.2 (CH_2-O-morpholine), 115.1 (C-Ar), 119.2 (C-Ar), 121.9 (C-Ar), 125.9 (C-Ar), 160.6 (CO), 170.3 (CO); MS (ES+) *m/z* = 239.1 $[M+H]^+$; HRMS calcd for $C_{11}H_{14}N_2O_4$ $[M+H]^+$ 239.1026, found 239.1025.

Methyl 4-((2*S*,6*R*)-2,6-dimethylmorpholine-4-carbonyl)-1*H*-pyrrole-2-carboxylate, 230

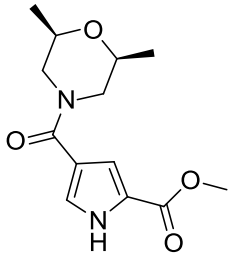

General procedure I: methyl 4-(2,2,2-trichloroacetyl)-1*H*-pyrrole-2-carboxylate (210 mg, 2.34 mmol) and (2*S*,6*R*)-2,6-dimethylmorpholine (290 μL, 2.34 mmol). Recrystallisation (9:1 EtOAc/petrol) gave **230** as white needles (187 mg, 90%). R_f 0.37 (9:1 DCM/MeOH); m.p. 146-147 ˚C; λ_{max} (EtOH/nm) 261.0, 209; IR υ_{max}/cm^{-1} 3076, 3045, 2971, 2856, 1712, 1601, 1566; ^{1}H NMR (500 MHz, DMSO-d_6) δ ppm 1.50 (6H, d, *J* = 5.9 Hz, CH_3), 3.39 (4H, s, N-CH_2-morpholine), 3.53-3.59 (2H, m, CH_2-O-morpholine), 3.84 (3H, s, O-CH_3), 6.98 (1H, br s, H-3), 7.38 (1H, br s, H-5), 12.40 (1H, s, NH-pyrrole); ^{13}C NMR (125 MHz, $CDCl_3$) δ ppm 18.7 (CH_3), 51.8 (CH_2-N-morpholine and O-CH_3), 72.0 (CH_2-O-morpholine), 114.5 (C-Ar), 120.5 (C-Ar), 122.8 (C-Ar), 125.3 (C-Ar), 161.1 (CO) 171.2 (CO); MS (ES+) *m/z* = 267.0 $[M+H]^+$; HRMS calcd for $C_{13}H_{18}N_2O_4$ $[M+H]^+$ 267.1339, found 267.1344.

4-(4-(*tert*-Butoxycarbonyl)piperazine-1-carbonyl)-1*H*-pyrrole-2-carboxylic acid, 222

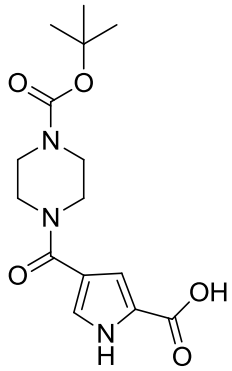

General procedure J: *tert*-butyl 4-(5-(methoxycarbonyl)-1*H*-pyrrole-3-carbonyl)piperazine-1-carboxylate (200 mg, 0.59 mmol) and LiOH monohydrate (500 mg, 11.87 mmol) gave **222** as a white solid (170 mg, 90%). R_f 0.34 (8:2 DCM/MeOH); m.p. 229-230 ˚C; λ_{max} (EtOH/nm) 210.0, 264.5; IR υ_{max}/cm^{-1} 3303, 2964, 2925, 1685, 1553, 1511; ^{1}H NMR (500 MHz, DMSO-d_6) δ ppm 1.42 (9H, s, C-CH_3), 3.37 (4H, br s, CH-piperazine), 3.58 (4H, br s, CH-piperazine), 6.88 (1H, dd, *J* = 1.6 and 2.4 Hz, H-3), 7.27 (1H, dd, *J* = 1.6 and 3.2 Hz, H-5), 12.17 (1H, s, NH-pyrrole), 12.50 (1H, s, COOH); ^{13}C NMR (125 MHz, DMSO-d_6) δ ppm 28.0 (C-CH_3), 65.6 (C-piperazine), 68.3 (C-piperazine), 79.1 (*C*-CH_3), 114.7 (C-Ar), 119.0 (C-Ar), 125.3 (C-Ar), 127.3 (C-Ar), 153.8 (CO), 161.6 (CO), 164.5 (CO); MS (ES+) *m/z* = 324.2 $[M+H]^+$; HRMS calcd for $C_{15}H_{21}N_3O_5$ $[M-H]^-$ 322.1408, found 322.1399.

4-(4-Methylpiperazine-1-carbonyl)-1*H*-pyrrole-2-carboxylic acid, 225

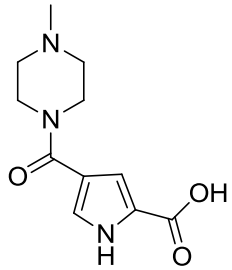

General procedure J with exceptions to the workup: methyl 4-(4-methylpiperazine-1-carbonyl)-1*H*-pyrrole-2-carboxylate (120 mg, 0.48 mmol) and LiOH monohydrate (0.34 g, 0.72 mmol). The mixture was cooled and concentrated *in vacuo*. Purification *via* column chromatography (C_{18} silica; 9:1 H_2O/MeOH, 0.1% formic acid) gave **225** as a white solid (100 mg, 89%). R_f 0.45 (H_2O, reverse phase silica); m.p. 248-250 ˚C; λ_{max} (EtOH/nm) 208.0, 253.0; IR υ_{max}/cm^{-1} 3178, 2946, 2813, 1561, 1504; ^{1}H NMR (500 MHz, DMSO-d_6) δ ppm 2.19 (3H, s, N-CH_3), 2.28-2.30 (4H, m, CH-piperazine), 3.60 (4H, br s, CH-piperazine), 6.43

(1H, d, *J* = 1.6 Hz, H-3), 6.93 (1H, d, *J* = 1.6 Hz, H-5), 11.31 (1H, s, NH-pyrrole), 12.02 (1H, s, COOH); ^{13}C NMR (125 MHz, DMSO-d_6) δ ppm 45.7 (N-CH_3), 47.6 (C-piperazine), 54.8 (C-piperazine), 109.3 (C-Ar), 117.3 (C-Ar), 120.7 (C-Ar), 133.1 (C-Ar), 164.3 (CO), 165.7 (CO); MS (ES+) *m/z* = 238.1 $[M+H]^+$; HRMS calcd for $C_{11}H_{15}N_3O_3$ $[M-H]^-$ 236.1041, found 236.1037.

4-(Piperidine-1-carbonyl)-1*H*-pyrrole-2-carboxylic acid, 227

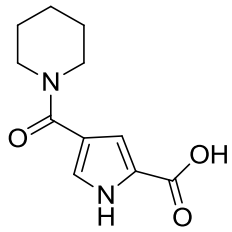

General procedure J: methyl 4-(piperidine-1-carbonyl)-1*H*-pyrrole-2-carboxylate (150 mg, 0.63 mmol) and LiOH monohydrate (41 mg, 0.95 mmol) gave **227** as a white solid (110 mg, 80%). R_f 0.20 (8:2 DCM/MeOH); m.p. 230-233 ˚C; λ_{max} (EtOH/nm) 209.5, 262.5; IR υ_{max}/cm^{-1} 3299, 2927, 2856, 1680, 1543, 1510; ^{1}H NMR (500 MHz, DMSO-d_6) δ ppm 1.52-1.58 (4H, m, CH-piperidine), 1.65-1.69 (2H, m, CH-piperidine), 3.59-3.61 (4H, m, N-CH-piperidine) 6.87 (1H, dd, *J* = 1.6 and 2.4 Hz, H-3), 7.25 (1H, dd, *J* = 1.6 and 3.2 Hz, H-5), 12.16 (1H, s, NH-pyrrole), 12.61 (1H, s, COOH); ^{13}C NMR (125 MHz, DMSO-d_6) δ ppm 24.2 (C-piperidine), 25.7 (C-piperidine), 114.4 (C-piperidine), 119.7 (C-Ar), 122.9 (C-Ar), 124.9 (C-Ar), 161.6 (CO), 164.2 (CO); MS (ES+) *m/z* = 223.0 $[M+H]^+$; HRMS calcd for $C_{11}H_{14}N_2O_3$ $[M-H]^-$ 221.0932, found 221.0928.

4-(Pyrrolidine-1-carbonyl)-1*H*-pyrrole-2-carboxylic acid, 229

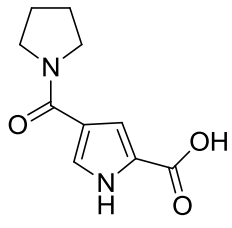

General procedure J: methyl 4-(pyrrolidine-1-carbonyl)-1*H*-pyrrole-2-carboxylate (130 mg, 0.57 mmol) and LiOH monohydrate (40 mg, 0.86 mmol) gave **229** as a white solid (90 mg, 75%). R_f 0.20 (8:2 DCM/MeOH); m.p. 250-252 ˚C; λ_{max} (EtOH/nm) 211.0, 261.5; IR υ_{max}/cm^{-1} 2967, 2882, 1655, 1578, 1554, 1499; ^{1}H NMR (500 MHz, DMSO-d_6) δ ppm 1.84-1.89 (2H, m, CH-pyrrolidine), 1.93-1.98 (2H, m, CH-pyrrolidine), 3.48 (2H, t, *J* = 6.7 Hz, N-

CH-pyrrolidine), 3.70 (2H, t, *J* = 6.7 Hz, N-CH-pyrrolidine), 7.07 (1H, dd, *J* = 1.6 and 2.4 Hz, H-3), 7.41 (1H, dd, *J* = 1.6 and 3.2 Hz, H-5), 12.21 (1H, s, NH-pyrrole), 12.62 (1H, s, COOH); ^{13}C NMR (125 MHz, DMSO-d_6) δ ppm 23.6 (C-pyrrolidine), 26.2 (C-pyrrolidine), 46.4 (C-pyrrolidine), 47.8 (C-pyrrolidine), 115.1 (C-Ar), 120.9 (C-Ar), 123.1 (C-Ar), 125.6 (C-Ar), 161.7 (CO), 162.7 (CO); MS (ES+) *m/z* = 209.0 $[M+H]^+$; HRMS calcd for $C_{10}H_{12}N_2O_3$ $[M-H]^-$ 207.0775, found 207.0772.

4-(Morpholine-4-carbonyl)-1*H*-pyrrole-2-carboxylic acid, 220

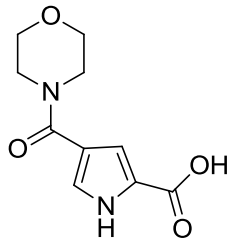

General procedure J: methyl 4-(morpholine-4-carbonyl)-1*H*-pyrrole-2-carboxylate (160 mg, 0.68 mmol) and LiOH monohydrate (43 mg, 1.02 mmol) gave **220** as a white solid (117 mg, 77%). R_f 0.12 (8:2 DCM/MeOH); m.p. 226-228 ˚C; λ_{max} (EtOH/nm) 210.0, 261.5; IR υ_{max}/cm^{-1} 2914, 2680, 1663, 1589, 1561; ^{1}H NMR (500 MHz, DMSO-d_6) δ ppm 3.65 (8H, s, CH_2-N-morpholine and CH_2-O-morpholine), 6.92 (1H, br s, H-3), 7.31 (1H, dd, *J* = 1.6 and 3.2 Hz, H-5), 12.20 (1H, s, NH-pyrrole), 12.64 (1H, s, COOH); ^{13}C NMR (125 MHz, DMSO-d_6) δ ppm 66.2 (CH_2-O-morpholine), 114.7 (C-Ar), 118.9 (C-Ar), 123.3 (C-Ar), 125.3 (C-Ar), 161.6 (CO), 164.5 (CO), CH_2-N-morpholine not visualised; MS (ES+) *m/z* = 224.97 $[M+H]^+$; HRMS calcd for $C_{10}H_{12}N_2O_4$ $[M+H]^+$ 225.0870, found 225.0871.

4-((2*S*,6*R*)-2,6-Dimethylmorpholine-4-carbonyl)-1*H*-pyrrole-2-carboxylic acid, 231

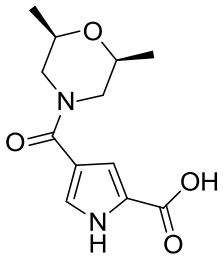

General procedure J: methyl 4-((2*S*,6*R*)-2,6-dimethylmorpholine-4-carbonyl)-1*H*-pyrrole-2-carboxylate (175 mg, 0.66 mmol) and LiOH monohydrate (42 mg, 0.99 mmol) gave **231** as a white solid (163 mg, 98%). R_f 0.24 (9:1 DCM/MeOH); m.p. 205-206 ˚C; λ_{max} (EtOH/nm) 261.0, 209.5; IR υ_{max}/cm^{-1}3285, 2974, 1664, 1559, 1506, 1437; ^{1}H NMR (500 MHz, DMSO-

d_6) δ ppm 1.15 (6H, d, *J* = 5.9 Hz, CH_3), 2.67 (2H, br s, CH_2-N-morpholine), 3.52-3.59 (2H, m, CH_2-O-morpholine), 4.19 (2H, br s, CH_2-N-morpholine), 6.91 (1H, dd, *J* = 1.6 and 2.4 Hz, H-3), 7.32 (1H, dd, *J* = 1.6 and 3.2 Hz, H-5), 12.21 (1H, s, NH-pyrrole), 12.62 (1H, s, COOH); ^{13}C NMR (125 MHz, DMSO-d_6) δ ppm 18.6 (CH_3), 59.7 (N-C-morpholine), 71.2 (C-morpholine), 114.7 (C-Ar), 119.1 (C-Ar), 123.1 (C-Ar), 125.3 (C-Ar), 161.6 (CO), 164.2 (CO); MS (ES+) *m/z* = 253.4 $[M+H]^+$; HRMS calcd for $C_{12}H_{16}N_2O_4$ $[M-H]^-$ 251.1037, found 251.1031.

***tert*-Butyl 4-(5-((pyridin-4-ylmethyl)carbamoyl)-1*H*-pyrrole-3-carbonyl)piperazine-1-carboxylate, 223**

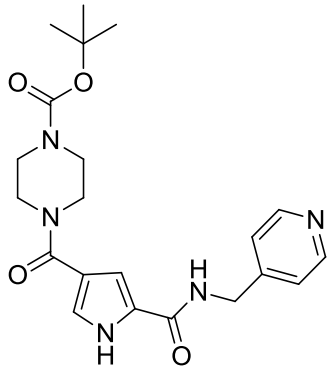

General procedure D: 4-(4-(*tert*-butoxycarbonyl)piperazine-1-carbonyl)-1*H*-pyrrole-2-carboxylic acid (110 mg, 0.34 mmol), CDI (110 mg, 0.67 mmol) and 4-picolylamine (0.08 mL, 0.84 mmol). Purification *via* column chromatography (silica; 0-5% MeOH/DCM) gave **223** as a white solid (130 mg, 95%). R_f 0.23 (95:5 EtOAc/MeOH); m.p. 238-239 ˚C; λ_{max} (EtOH/nm) 263.5; IR υ_{max}/cm^{-1} 3255, 2973, 2906, 2868, 1703, 1645, 1597; ^{1}H NMR (500 MHz, DMSO-d_6) δ ppm 1.42 (9H, s, C-*CH*$_3$), 3.38 (4H, br s, CH-piperazine), 3.60 (4H, br s, CH-piperazine), 4.47 (2H, d, *J* = 5.9 Hz, NH-*CH*$_2$), 7.11 (1H, br s, H-3), 7.21 (1H, dd, *J* = 1.6 and 3.2 Hz, H-5), 7.30 (2H, d, *J* = 6.0 Hz, CH-pyridine), 8.51 (2H, d, *J* = 6.0 Hz, N-CH-pyridine), 8.81 (1H, t, *J* = 5.9 Hz, CO-NH), 11.99 (1H, s, NH-pyrrole); ^{13}C NMR (125 MHz, DMSO-d_6) δ ppm 28.0 (C-*CH*$_3$), 41.0 (NH-CH_2), 42.8 (C-piperazine), 43.9 (C-piperazine), 79.1 (*C*-CH_3), 111.0 (C-Ar), 118.4 (C-Ar), 122.1 (C-Ar), 123.9 (C-Ar), 125.9 (C-Ar), 148.7 (C-Ar), 149.5 (C-Ar), 153.8 (CO), 160.5 (CO), 164.7 (CO); MS (ES+) *m/z* = 414.2 $[M+H]^+$; HRMS calcd for $C_{21}H_{27}N_5O_4$ $[M+H]^+$ 414.2136, found 414.2136.

4-(4-Methylpiperazine-1-carbonyl)-*N*-(pyridin-4-ylmethyl)-1*H*-pyrrole-2-carboxamide, 159

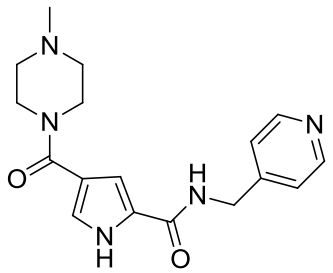

General procedure D: 4-(4-methylpiperazine-1-carbonyl)-1*H*-pyrrole-2-carboxylic acid (50 mg, 0.21 mmol), CDI (70 mg, 0.42 mmol), and 4-picolylamine (0.05 mL, 0.53 mmol). Purification *via* semi-preparative HPLC gave **159** as a white solid (30 mg, 43%) R_f 0.30 (9:1 DCM/MeOH); ^{1}H NMR (500 MHz, DMSO-d_6) δ ppm 2.20 (3H, s, N-CH_3), 2.31-2.33 (4H, m, CH-piperazine), 3.61 (4H, br s, CH-piperazine), 4.46 (2H, d, *J* = 5.9 Hz, NH-CH_2), 7.08 (1H, br s, H-3), 7.17 (1H, br s, H-5), 7.30 (2H, d, *J* = 6.0 Hz, CH-pyridine), 8.51 (2H, d, *J* = 6.0 Hz, N-CH-pyridine), 8.80 (1H, t, *J* = 5.9 Hz, CO-NH), 11.94 (1H, s, NH-pyrrole); MS (ES+) *m/z* = 328.2 $[M+H]^+$; ^{13}C NMR (125 MHz, DMSO-d_6) δ ppm Insufficient quantity of material to perform analysis; HRMS calcd for $C_{17}H_{21}N_5O_2$ $[M+H]^+$ 328.1768, found 328.1772.

4-(Piperidine-1-carbonyl)-*N*-(pyridin-4-ylmethyl)-1*H*-pyrrole-2-carboxamide, 160

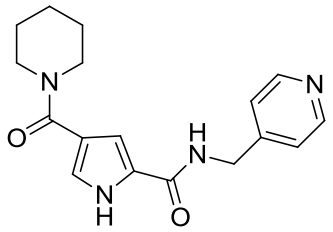

General procedure D: 4-(piperidine-1-carbonyl)-1*H*-pyrrole-2-carboxylic acid (60 mg, 0.27 mmol), CDI (90 mg, 0.54 mmol), and 4-picolylamine (0.07 mL, 0.68 mmol). Recrystallisation from EtOAc/petrol (9:1) gave **160** as a white solid (70 mg, 82%). R_f 0.36 (EtOAc); m.p. 231-233 ˚C; λ_{max} (EtOH/nm) 261.5; IR υ_{max}/cm^{-1} 3248, 2923, 2855, 1643, 1593, 1564, 1534; ^{1}H NMR (500 MHz, DMSO-d_6) δ ppm 1.26-1.31 (4H, m, CH-piperidine), 1.37-1.43 (2H, m, CH-piperidine), 3.34 (4H, br s, N-CH-piperidine), 4.23 (2H, d, *J* = 5.9 Hz, NH-CH_2), 6.83 (1H, dd, *J* = 1.6 and 2.4 Hz, H-3), 6.91 (1H, dd, *J* = 1.6 and 3.2 Hz, H-5), 7.06 (2H, d, *J* = 6.0 Hz, CH-pyridine), 8.28 (2H, d, *J* = 6.0 Hz, N-CH-pyridine), 8.58 (1H, t,

J = 5.9 Hz, CO-NH), 11.68 (1H, s, NH-pyrrole); ^{13}C NMR (125 MHz, DMSO-d_6) δ ppm 24.2 (C-piperidine), 25.8 (C-piperidine), 41.0 (NH-CH_2), 110.7 (C-Ar), 119.1 (C-Ar), 122.1 (C-Ar), 123.4 (C-Ar), 125.7 (C-Ar), 148.8 (C-Ar), 149.5 (C-Ar), 160.5 (CO), 164.4 (CO); MS (ES+) *m/z* = 313.2 $[M+H]^+$; HRMS calcd for $C_{17}H_{20}N_4O_2$ $[M+H]^+$ 313.1659, found 313.1662.

_N_-(Pyridin-4-ylmethyl)-4-(pyrrolidine-1-carbonyl)-1_H_-pyrrole-2-carboxamide, 161

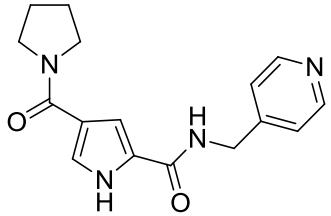

General procedure D: 4-(pyrrolidine-1-carbonyl)-1*H*-pyrrole-2-carboxylic acid (60 mg, 0.30 mmol), CDI (100 mg, 0.60 mmol), and 4-picolylamine (0.07 mL, 0.75 mmol). Recrystallisation (EtOAc/petrol 9:1) gave **161** as a white solid (70 mg, 82%). R_f 0.34 (EtOAc); m.p. 228-230 ˚C; λ_{max} (EtOH/nm) 263.0; IR υ_{max}/cm^{-1} 3232, 2972, 2865, 1627, 1569, 1596; ^{1}H NMR (500 MHz, DMSO-d_6) δ ppm 1.80-1.83 (2H, m, CH-pyrrolidine), 1.90-1.93 (2H, m, CH-pyrrolidine), 3.44 (2H, t, *J* = 6.7 Hz, N-CH-pyrrolidine), 3.67 (2H, t, *J* = 6.7 Hz, N-CH-pyrrolidine), 4.46 (2H, d, *J* = 5.9 Hz, NH-*CH*$_2$), 7.28-7.30 (4H, m, H-3, H-5 and CH-pyridine), 8.51 (2H, d, *J* = 6.0 Hz, N-CH-pyridine), 8.85 (1H, t, *J* = 5.9 Hz, CO-NH), 11.97 (1H, s, NH-pyrrole); ^{13}C NMR (125 MHz, DMSO-d_6) δ ppm 23.6 (C-pyrrolidine), 26.2 (C-pyrrolidine), 41.0 (NH-CH_2), 46.4 (C-pyrrolidine), 47.8 (C-pyrrolidine), 111.4 (C-Ar), 120.4 (C-Ar), 122.1 (C-Ar), 124.1 (C-Ar), 125.8 (C-Ar), 148.8 (C-Ar), 149.5 (C-Ar), 160.6 (CO), 162.9 (CO); MS (ES+) *m/z* = 299.4 $[M+H]^+$; HRMS calcd for $C_{16}H_{18}N_4O_2$ $[M+H]^+$ 299.1503, found 299.1507.

4-(Morpholine-4-carbonyl)-_N_-(pyridin-4-ylmethyl)-1_H_-pyrrole-2-carboxamide, 162

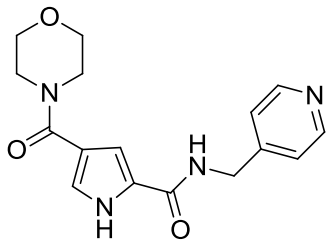

General procedure D: 4-(morpholine-4-carbonyl)-1*H*-pyrrole-2-carboxylic acid (60 mg, 0.25 mmol), CDI (80 mg, 0.50 mmol), and 4-picolylamine (0.06 mL, 0.63 mmol). Recrystallisation from EtOAc/petrol (9:1) gave **162** as a white solid (50 mg, 70%). R_f 0.24

(8:2 DCM/MeOH); m.p. 227-228 ˚C; λ_{max} (EtOH/nm) 262.5; IR υ_{max}/cm^{-1} 3129, 2962, 2920, 2859, 1644, 1597, 1567, 1535; ^{1}H NMR (500 MHz, DMSO-d_6) δ ppm 3.61 (8H, br s, CH_2-N-morpholine and CH_2-O-morpholine), 4.47 (2H, d, *J* = 5.9 Hz, NH-*CH*$_2$), 7.11 (1H, dd, *J* = 1.6 and 2.4 Hz, H-3), 7.21 (1H, dd, *J* = 1.6 and 3.2 Hz, H-5), 7.29 (2H, d, *J* = 6.0 Hz, CH-pyridine), 8.51 (2H, d, *J* = 6.0 Hz, N-CH-pyridine), 8.82 (1H, t, *J* = 5.9 Hz, CO-NH), 11.98 (1H, s, NH-pyrrole); 13C NMR (125 MHz, DMSO-d_6) δ ppm 41.0 (CH_2), 66.3 (CH_2-N-morpholine and CH_2-O-morpholine), 110.9 (C-Ar), 118.3 (C-Ar), 122.1 (C-Ar), 123.9 (C-Ar), 125.9 (C-Ar), 148.7 (C-Ar), 149.5 (C-Ar), 160.5 (CO), 164.7 (CO); MS (ES+) *m/z* = 315.4 $[M+H]^+$; HRMS calcd for $C_{16}H_{18}N_4O_3$ $[M+H]^+$ 315.1452, found 315.1450.

4-((2*S*,6*R*)-2,6-Dimethylmorpholine-4-carbonyl)-*N*-(pyridin-4-ylmethyl)-1*H*-pyrrole-2-carboxamide, 163

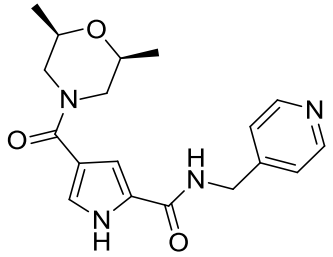

General procedure D: 4-((2*S*,6*R*)-2,6-dimethylmorpholine-4-carbonyl)-1*H*-pyrrole-2-carboxylic acid (115 mg, 0.46 mmol), CDI (149 mg, 0.92 mmol), and 4-picolylamine (110 μL, 1.15 mmol). Purification *via* column chromatography (silica; 0-8% DCM/MeOH) gave **163** as a white solid (55 mg, 50%). R_f 0.29 (9:1 DCM/MeOH); m.p. 262-264 ˚C; λ_{max} (EtOH/nm) 262.5, 340.5; IR υ_{max}/cm^{-1} 3293, 3209, 2924, 2861, 1633, 1600, 1573, 1541; ^{1}H NMR (500 MHz, DMSO-d_6) δ ppm 1.10 (6H, d, *J* = 5.9 Hz, CH_3), 2.61 (2H, br s, CH_2-N-morpholine), 3.48-3.55 (2H, m, CH_2-O-morpholine), 4.19 (2H, br s, CH_2-N-morpholine), 4.46 (2H, d, *J* = 6.0 Hz, NH-*CH*$_2$), 7.09 (1H, dd, *J* = 1.6 and 2.4 Hz, H-3), 7.21 (1H, dd, *J* = 1.6 and 3.2 Hz, H-5), 7.29 (2H, d, *J* = 6.0 Hz, CH-pyridine), 8.51 (2H, d, *J* = 6.0 Hz, N-CH-pyridine), 8.81 (1H, t, *J* = 6.0 Hz, CO-NH), 11.97 (1H, s, NH-pyrrole); ^{13}C NMR (125 MHz, DMSO-d_6) δ ppm 18.6 (CH_3), 41.0 (NH-CH_2), 59.9 (CH_2-N-morpholine), 71.3 (CH_2-O-morpholine), 110.9 (C-Ar), 118.5 (C-Ar), 122.1 (C-Ar), 123.9 (C-Ar), 125.9 (C-Ar), 148.7 (C-Ar), 149.5 (C-Ar), 160.5 (CO), 164.4 (CO); MS (ES+) *m/z* = 343.3 $[M+H]^+$; HRMS calcd for $C_{18}H_{22}N_4O_3$ $[M+H]^+$ 343.1765, found 343.1768.

4-(Piperazine-1-carbonyl)-*N*-(pyridin-4-ylmethyl)-1*H*-pyrrole-2-carboxamide, 158

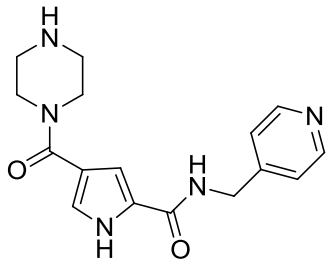

General procedure K: *tert*-butyl 4-(5-((pyridin-4-ylmethyl)carbamoyl)-1*H*-pyrrole-3-carbonyl)piperazine-1-carboxylate (80 mg, 0.19 mmol). Purification *via* column chromatography (NH silica; 0-8% MeOH/DCM) gave **158** as a white solid (30 mg, 46%). R_f 0.26 (9:1 DCM/MeOH); m.p. 43-46˚C; λ_{max} (EtOH/nm) 264.0; IR υ_{max}/cm^{-1} 2918, 2858, 1636, 1603, 1569; ^{1}H NMR (500 MHz, DMSO-d_6) δ ppm 2.60-2.62 (4H, m, CH-piperazine), 3.45 (4H, br s, CH-piperazine), 4.38 (2H, d, *J* = 5.9 Hz, NH-*CH*$_2$), 6.99 (1H, br s, H-3), 7.07 (1H, br s, H-5), 7.21 (2H, d, *J* = 6.0 Hz CH-pyridine), 8.43 (2H, d, *J* = 6.0 Hz, N-CH-pyridine), 8.73 (1H, t, *J* = 5.9 Hz, CO-NH), 11.85 (1H, s, NH-pyrrole); ^{13}C NMR (125 MHz, DMSO-d_6) δ ppm 41.0 (NH-CH_2), 45.8 (C-piperazine), 67.0 (C-piperazine), 110.8 (C-Ar), 118.8 (C-Ar), 122.1 (C-Ar), 123.7 (C-Ar), 125.8 (C-Ar), 148.7 (C-Ar), 149.5 (C-Ar), 160.5 (CO), 164.5 (CO); MS (ES+) *m/z* = 314.1 $[M+H]^+$; HRMS calcd for $C_{16}H_{19}N_5O_2$ $[M+H]^+$ 314.1612, found 314.1612.

4-(2-Hydroxy-6-methoxybenzoyl)-*N*-(pyridin-4-ylmethyl)-1*H*-pyrrole-2-carboxamide, 239

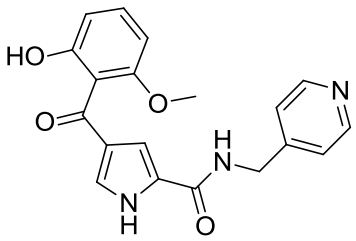

General procedure L: 4-(2,6-dimethoxybenzoyl)-*N*-(pyridin-4-ylmethyl)-1*H*-pyrrole-2-carboxamide (70 mg, 0.19 mmol). Purification *via* column chromatography (silica; 0-8% MeOH/DCM) gave **239** as a white solid (20 mg, 30%). R_f 0.32 (9:1 DCM/MeOH); m.p. 247-249 ˚C; λ_{max} (EtOH/nm) 235.0; IR υ_{max}/cm^{-1} 3315, 3123, 2962, 2838, 1607, 1568, 1535; ^{1}H NMR (500 MHz, DMSO-d_6) δ ppm 3.65 (3H, s, CH_3), 4.45 (2H, d, *J* = 5.9 Hz, NH-*CH*$_2$), 6.53 (2H, dd, *J* = 8.2 and 8.4 Hz, H-3'and H-5'), 7.07 (1H, br s, H-3), 7.15-7.19 (2H, m, H-5

and H-4'), 7.28 (2H, d, *J* = 6.0 Hz, CH-pyridine), 8.50 (2H, d, *J* = 6.0 Hz, N-CH-pyridine), 8.90 (1H, t, *J* = 5.9 Hz, CO-NH), 9.53 (1H, s, OH), 12.09 (1H, s, NH-pyrrole); ^{13}C NMR (125 MHz, DMSO-d_6) δ ppm Insufficient quantity of material to perform analysis; MS (ES+) *m/z* = 352.3 $[M+H]^+$; HRMS calcd for $C_{19}H_{17}N_3O_4$ $[M+H]^+$ 352.1292, found 352.1291.

4-(2,6-Dihydroxybenzoyl)-*N*-(pyridin-4-ylmethyl)-1*H*-pyrrole-2-carboxamide, 240

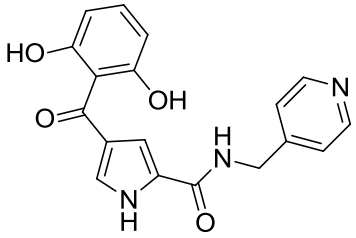

General procedure L: 4-(2,6-dimethoxybenzoyl)-*N*-(pyridin-4-ylmethyl)-1*H*-pyrrole-2-carboxamide (70 mg, 0.19 mmol). Purification *via* Semi-preparative HPLC (75:25 H_2O/MeCN) gave **240** as a white solid (35 mg, 55%). R_f 0.25 (9:1 DCM/MeOH); m.p. 240-241˚C; λ_{max} (EtOH/nm) 234.5; IR υ_{max}/cm^{-1} 3312, 3326, 3129, 2958, 2834, 1606, 1564, 1530; ^{1}H NMR (500 MHz, DMSO-d_6) δ ppm 4.45 (2H, d, *J* = 6.1 Hz, NH-*CH*$_2$), 6.34 (2H, d, *J* = 8.2 Hz, H-3' and H-5'), 6.99 (1H, dd, *J* = 8.1 and 8.2 Hz, H-4'), 7.10 (1H, br s, H-3), 7.18 (1H, br s, H-5), 7.29 (2H, d, *J* = 5.3 Hz, CH-pyridine), 8.50 (2H, d, *J* = 5.3 Hz, N-CH-pyridine), 8.92 (1H, t, *J* = 6.1 Hz, CO-NH), 9.39 (2H, s, OH), 12.07 (1H, s, NH-pyrrole); ^{13}C NMR (125 MHz, DMSO-d_6) δ ppm Insufficient quantity of material to perform analysis; MS (ES+) *m/z* = 338.2 $[M+H]^+$; HRMS calcd for $C_{18}H_{15}N_3O_4$ $[M+H]^+$ 338.1135, found 338.1138.

4-(2-Hydroxybenzoyl)-*N*-(pyridin-4-ylmethyl)-1*H*-pyrrole-2-carboxamide, 241

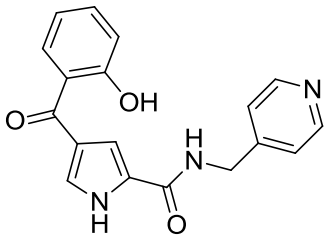

General procedure L: 4-(2-methoxybenzoyl)-*N*-(pyridin-4-ylmethyl)-1*H*-pyrrole-2-carboxamide (31 mg, 0.09 mmol). Purification *via* column chromatography (silica; 0-8% MeOH/DCM) gave **241** as a white solid (25 mg, 85%). R_f 0.26 (9:1 DCM/MeOH); m.p. 191-192 ˚C; λ_{max} (EtOH/nm) 244.5, 331.5; IR υ_{max}/cm^{-1} 3031, 2926, 2853, 1638, 1565, 1542; ^{1}H NMR (500 MHz, DMSO-d_6) δ ppm 4.46 (2H, d, *J* = 6.2 Hz, NH-*CH*$_2$), 6.93-6.98 (2H, m, H-

2'and H-5'), 7.29 (2H, d, *J* = 6.0 Hz, CH-pyridine), 7.37 (1H, d, *J* = 1.6 Hz, H-3), 7.42-7.45 (2H, m, H-5 and H-4'), 7.65 (1H, dd, *J* = 1.6 and 7.8 Hz, H-6'), 8.50 (2H, d, *J* = 6.0 Hz, N-CH-pyridine), 8.96 (1H, t, *J* = 6.2 Hz, CO-NH), 11.05 (1H, s, OH), 12.35 (1H, s, NH-pyrrole); ^{13}C NMR (125 MHz, DMSO-d_6) δ ppm 41.1 (CH_2), 111.4 (C-Ar), 117.1 (C-Ar), 118.9 (C-Ar), 122.1 (C-Ar), 123.7 (C-Ar), 124.3 (C-Ar), 127.4 (C-Ar), 128.0 (C-Ar), 130.4 (C-Ar), 133.4 (C-Ar), 148.6 (C-Ar), 149.5 (C-Ar), 158.4 (C-OH), 160.3 (CO), 191.7 (CO); MS (ES+) *m/z* = 322.2 $[M+H]^+$; HRMS calcd for $C_{18}H_{15}N_3O_4$ $[M+H]^+$ 322.1186, found 322.1188.

4-(3-Hydroxybenzoyl)-*N*-(pyridin-4-ylmethyl)-1*H*-pyrrole-2-carboxamide, 242

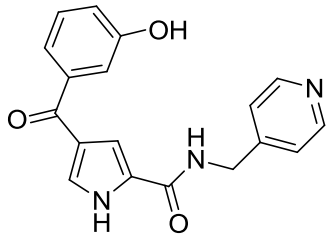

General procedure L: 4-(3-methoxybenzoyl)-*N*-(pyridin-4-ylmethyl)-1*H*-pyrrole-2-carboxamide (112 mg, 0.33 mmol). Purification *via* column chromatography (silica; 0-8% MeOH/DCM) gave **242** as a white solid (70 mg, 66%). R_f 0.26 (9:1 DCM/MeOH); m.p. 261-263 ˚C; λ_{max} (EtOH/nm) 243.0, 289.5, 340.5; IR υ_{max}/cm^{-1} 3346, 3204, 3116, 2674, 1642, 1608, 1575, 1534; ^{1}H NMR (500 MHz, DMSO-d_6) δ ppm 4.46 (2H, s, *J* = 6.0 Hz, NH-CH_2), 6.98 (1H, ddd, *J* = 1.0, 2.5 and 8.1 Hz, H-4'), 7.15 (1H, dd, *J* = 1.6 and 2.5 Hz, H-2'), 7.20 (1H, ddd, *J* = 1.0, 1.2 and 7.6 Hz, H-6'), 7.29 (2H, d, *J* = 6.0 Hz, CH-pyridine), 7.32 (1H, dd, *J* = 7.6 and 8.1 Hz, H-5'), 7.37 (1H, br s, H-3), 7.41 (1H, br s, H-5), 8.50 (2H, d, *J* = 6.0 Hz, N-CH-pyridine), 8.96 (1H, t, *J* = 6.0 Hz, CO-NH), 9.74 (1H, s, OH), 12.32 (1H, s, NH-pyrrole); ^{13}C NMR (125 MHz, DMSO-d_6) δ ppm 41.1 (CH_2), 111.5 (C-Ar), 115.0 (C-Ar), 118.7 (C-Ar), 119.3 (C-Ar), 122.1 (C-Ar), 124.1 (C-Ar), 127.4 (C-Ar), 127.6 (C-Ar), 129.5 (C-Ar), 140.5 (C-Ar), 148.6 (C-Ar), 149.5 (C-Ar), 157.3 (C-OH), 160.3 (CO), 189.2 (CO); MS (ES+) *m/z* = 322.2 $[M+H]^+$; HRMS calcd for $C_{18}H_{15}N_3O_3$ $[M+H]^+$ 322.1186, found 322.1185.

Pyridin-2-yl(1*H*-pyrrol-3-yl)methanone, 247

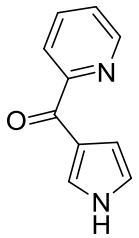

General procedure F: TIPS pyrrole (0.70 mL, 2.81 mmol), picolinoyl chloride (1.09 g, 5.62 mmol) and $AlCl_3$. After quenching with 1M HCl (aq) the mixture was adjusted to pH 9 with 1M NaOH (aq) before extraction. The crude material was used directly in the next step. **General procedure H:** pyridin-2-yl(1-(triisopropylsilyl)-1*H*-pyrrol-3-yl)methanone (0.92 g, 2.81 mmol) and TBAF (562 μL, 5.62 mmol). Purification *via* column chromatography (silica; 0-8% MeOH/DCM) gave **247** as a beige solid (231 mg, 48%). R_f 0.32 (9:1 DCM/MeOH); m.p. 116-117 ˚C; λ_{max} (EtOH/nm) 270.0, 234.5; IR υ_{max}/cm^{-1} 3159, 2865, 1630, 1587, 1564, 1511; ^{1}H NMR (500 MHz, DMSO-d_6) δ ppm 6.73 (1H, br s, H-4), 6.89 (1H, br s, H-5), 7.61 (1H, ddd, *J* = 1.4, 4.7 and 7.4 Hz, CH-pyridine), 7.94-8.02 (3H, m, CH-pyridine and H-2), 8.73 (1H, ddd, *J* = 0.9, 1.7 and 4.7 Hz, N-CH-pyridine), 11.56 (1H, s, NH-pyrrole); ^{13}C NMR (125 MHz, DMSO-d_6) δ ppm 109.7 (C-Ar), 119.5 (C-Ar), 122.9 (C-Ar), 126.1 (C-Ar), 128.3 (C-Ar), 137.3 (C-Ar), 148.5 (C-Ar); MS (ES+) *m/z* = 173.1 $[M+H]^+$; HRMS calcd for $C_{10}H_8N_2O$ $[M+H]^+$ 173.0709, found 173.0708.

Pyridin-4-yl(1*H*-pyrrol-3-yl)methanone, 249

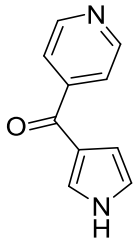

General procedure F: TIPS pyrrole (1.39 mL, 5.62 mmol), isonicotinoyl chloride (2.00 g, 11.23 mmol) and $AlCl_3$ (2.64 g, 19.67 mmol). After quenching with 1M HCl (aq) the mixture was adjusted to pH 9 with 1M NaOH (aq) before extraction. The crude material was used directly in the next step. **General procedure H:** pyridin-4-yl(1-(triisopropylsilyl)-1*H*-pyrrol-3-yl)methanone (1.84 g, 5.62 mmol) and TBAF (1.12 mL, 11.24 mmol). Purification *via* column chromatography (silica; 0-8% MeOH/DCM) gave **249** as a beige solid (380 mg, 39%). R_f 0.32 (9:1 DCM/MeOH); m.p. 114-116 ˚C; λ_{max} (EtOH/nm) 267.5; IR υ_{max}/cm^{-1}

2941, 2831, 1636, 1532, 1492; ^{1}H NMR (500 MHz, DMSO-d_6) δ ppm 6.58 (1H, br s, H-4), 6.96 (1H, br s, H-5), 7.43-7.45 (1H, m, H-2), 7.63 (2H, d, *J* = 6.0 Hz, CH-pyridine), 8.75 (2H, d, *J* = 6.0 Hz, N-CH-pyridine), 11.76 (1H, s, NH-pyrrole);^{13}C NMR (125 MHz, DMSO-d_6) δ ppm 108.9 (C-Ar), 120.7 (C-Ar), 122.0 (C-Ar), 122.9 (C-Ar), 127.1 (C-Ar), 146.5 (C-Ar), 150.1 (C-Ar), 188.1 (CO); MS (ES+) *m/z* = 173.1 $[M+H]^+$; HRMS calcd for $C_{10}H_8N_2O$ $[M+H]^+$ 173.0709, found 173.0707.

2,2,2-Trichloro-1-(4-picolinoyl-1*H*-pyrrol-2-yl)ethanone, 250

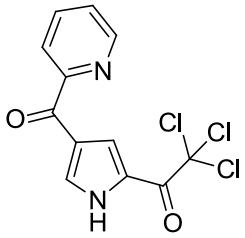

General procedure F: pyridin-2-yl(1*H*-pyrrol-3-yl)methanone (59 mg, 0.34 mmol), trichloroacetyl chloride (76 μL, 0.68 mmol) and $AlCl_3$ (159 mg, 1.19 mmol). After quenching with 1M HCl (aq) the mixture was adjusted to pH 9 with 1M NaOH (aq) before extraction. Purification *via* column chromatography (silica; DCM) gave **250** as a beige solid (40 mg, 37%). R_f 0.38 (95:5 DCM/MeOH); m.p. Degrades >250 ^{o}C; λ_{max} (EtOH/nm) 327.0, 245.0; IR υ_{max}/cm^{-1} 3112, 1679, 1632, 1545, 1498, 1445; ^{1}H NMR (500 MHz, DMSO-d_6) δ ppm 7.67-7.72 (1H, m, CH-pyridine), 7.99 (1H, d, *J* = 1.6 Hz, H-3), 8.06-8.07 (2H, m, CH-pyridine), 8.47 (1H, d, *J* = 1.6 Hz, H-5), 8.80 (1H, ddd, *J* = 1.3, 1.5 and 4.7 Hz, N-CH-pyridine), 13.17 (1H, s, NH-pyrrole); ^{13}C NMR (125 MHz, DMSO-d_6) δ ppm Insufficient quantity of material to perform analysis; MS (ES+) *m/z* = 315.1 $[(^{35}Cl)-H]^-$; HRMS calcd for $C_{12}H_7Cl_3N_2O_2$ $[(^{35}ClM)-H]^-$ 314.9500, found 314.9504.

2,2,2-Trichloro-1-(4-isonicotinoyl-1*H*-pyrrol-2-yl)ethanone, 252

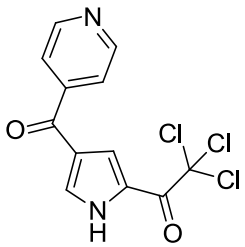

General procedure F: pyridin-3-yl(1*H*-pyrrol-3-yl)methanone (140 mg, 0.81 mmol), trichloroacetyl chloride (180 μL, 1.62 mmol) and $AlCl_3$ (381 mg, 2.84 mmol). After

quenching with 1M HCl (aq) the mixture was adjusted to pH 9 with 1M NaOH (aq) before extraction. Purification *via* column chromatography (silica; DCM) gave **252** as a beige solid (70 mg, 27%). R_f 0.38 (95:5 DCM/MeOH); m.p. Degrades >250 ^{o}C; λ_{max} (EtOH/nm) 314.0, 257.0; IR υ_{max}/cm^{-1} 3115, 1681, 1635, 1545; ^{1}H NMR (500 MHz, DMSO-d_6) δ ppm 7.70 (1H, dd, 1.6 and 2.4 Hz, H-3), 7.71 (2H, d, *J* = 6.0 Hz, CH-pyridine), 7.94 (1H, dd, *J* = 1.5 and 3.2 Hz, H-5), 8.81 (2H, d, *J* = 6.0 Hz, N-CH-pyridine); ^{13}C NMR (125 MHz, DMSO-d_6) δ ppm Insufficient quantity of material to perform analysis; MS (ES+) *m/z* = 316.1, [M-H]$^{-}$; HRMS calcd for $C_{12}H_7Cl_3N_2O_2$ [^{35}ClM-H]$^{-}$ 316.9646, found 316.9652.

4-Picolinoyl-*N*-(pyridin-4-ylmethyl)-1*H*-pyrrole-2-carboxamide, 243

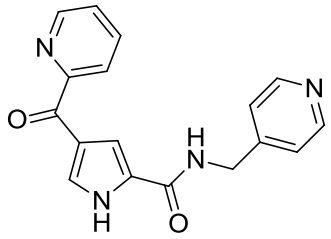

General procedure I: 2,2,2-trichloro-1-(4-picolinoyl-1*H*-pyrrol-2-yl)ethanone (24 mg, 0.08 mmol) and 4-picolylamine (24 μL, 0.24 mmol). Recrystallisation (9:1 EtOAc/petrol) gave **243** as a white solid (10 mg, 40%). R_f 0.15 (9:1 DCM/MeOH); m.p. 194-196 ˚C; λ_{max} (EtOH/nm) 243.0, 309.0; IR υ_{max}/cm^{-1} 3343, 3206, 1623, 1575, 1535, 1494; ^{1}H NMR (500 MHz, MeOD) δ ppm 4.62 (2H, s, NH-*CH*$_2$), 7.43 (2H, d, *J* = 6.0 Hz, CH-pyridine), 7.60-7.63 (2H, m, H-3 and CH-pyridine) 8.00-8.07 (2H, m, CH-pyridine and N-CH-pyridine), 8.18 (1H, d, *J* = 1.6 Hz, H-5), 8.50 (2H, d, *J* = 6.0 Hz, N-CH-pyridine), 8.73-8.75 (1H, m, N-CH-pyridine); ^{13}C NMR (125 MHz, MeOD) δ ppm 43.17 (CH_2), 113.6 (C-Ar), 124.1 (C-Ar), 124.6 (C-Ar), 125.0 (C-Ar), 128.0 (C-Ar), 132.4 (C-Ar), 138.6 (C-Ar), 149.5 (C-Ar), 149.7 (C-Ar), 152.6 (C-Ar), 157.1 (C-Ar), 163.2 (CO), 189.0 (CO); MS (ES+) *m/z* = 307.1 [M+H]$^{+}$; HRMS calcd for $C_{17}H_{14}N_4O_2$ [M+H]$^{+}$ 307.1190, found 307.1193.

4-Isonicotinoyl-*N*-(pyridin-4-ylmethyl)-1*H*-pyrrole-2-carboxamide, 255

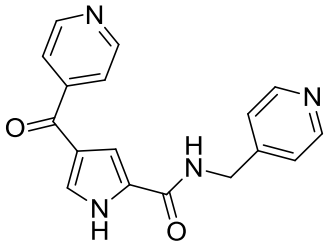

General procedure I: 2,2,2-trichloro-1-(4-isonicotinoyl-1*H*-pyrrol-2-yl)ethanone (25 mg, 0.08 mmol) and 4-picolylamine (24 μL, 0.24 mmol). Recrystallisation (9:1 EtOAc/petrol) gave **255** as an off-white solid (15 mg, 61%). R_f 0.15 (9:1 DCM/MeOH); m.p. 189-192 ˚C; λ_{max} (EtOH/nm) 243.0; IR υ_{max}/cm^{-1} 3323, 3118, 1628, 1566, 1537; ^{1}H NMR (500 MHz, MeOD) δ ppm 4.61 (2H, s, NH-*CH*$_2$), 7.39 (1H, d, *J* = 1.6 Hz, H-3), 7.42 (2H, d, *J* = 6.1 Hz, CH-pyridine), 7.60 (1H, d, *J* = 1.6 Hz, H-5), 7.77 (2H, d, *J* = 6.0 Hz, CH-pyridine), 8.50 (2H, d, *J* = 6.1 Hz, N-CH-pyridine), 8.77 (2H, d, *J* = 6.0 Hz, N-CH-pyridine); ^{13}C NMR (125 MHz, MeOD) δ ppm 42.9 (CH_2), 112.6 (C-Ar), 123.9 (C-Ar), 125.3 (C-Ar), 129.3 (C-Ar), 130.4 (C-Ar), 148.4 (C-Ar), 145.0 (C-Ar), 150.9 (C-Ar), 151.4 (C-Ar), 162.8 (CO), 190.6 (CO); MS (ES+) *m/z* = 307.1 $[M+H]^+$; HRMS calcd for $C_{17}H_{14}N_4O_2$ $[M+H]^+$ 307.1190, found 307.1192.

Methyl 4-(3,5-difluoroisonicotinoyl)-1*H*-pyrrole-2-carboxylate, 258

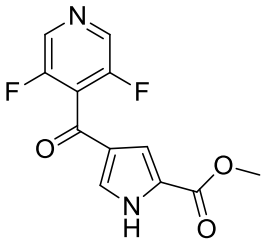

General procedure E: 3,5-difluoroisonicotinic acid (379 mg, 2.38 mmol), $SOCl_2$ (0.43 mL, 5.95 mmol), and DMF (10 mol%) gave 3,5-difluoroisonicotinoyl chloride as a yellow oil which was used directly in the next step. **General procedure F:** methyl 1*H*-pyrrole-2-carboxylate (150 mg, 1.19 mmol), and $AlCl_3$ (0.64 g, 4.76 mmol). Purification *via* column chromatography (silica; 0-60% EtOAc/petrol) gave **258** as a pink solid (99 mg, 31%). R_f 0.10 (80:20 petrol/EtOAc); m.p. 211-212 ˚C; λ_{max} (EtOH/nm) 232.5; IR υ_{max}/cm^{-1} 3120, 3049, 2954, 2926, 2851, 1702, 1654, 1617, 1559; ^{1}H NMR (500 MHz, DMSO-d_6) δ ppm 3.82 (3H, s, O-CH_3), 7.17 (1H, d, *J* = 1.6 Hz, H-3), 7.79 (1H, d, *J* = 1.4 Hz, H-5), 8.70 (2H, s, N-CH-pyridine), 13.00 (1H, s, NH-pyrrole); ^{13}C NMR (125 MHz, DMSO-d_6) δ ppm 51.7 (O-CH_3),

114.5 (C-Ar), 125.0 (C-Ar), 131.4 (C-Ar), 135.2 (dd, J_{CF} = 3.7 and 23.1 Hz, C-Ar), 154.5 (d, J_{CF} = 260.1 Hz, C-F), 160.2 (CO), 179.4 (CO), two C-Ar not visualised; HRMS calcd for $C_{12}H_8F_2N_2O_3$ $[M+H]^+$ 267.0576, found 267.0580.

4-(3,5-Difluoroisonicotinoyl)-1*H*-pyrrole-2-carboxylic acid, 259

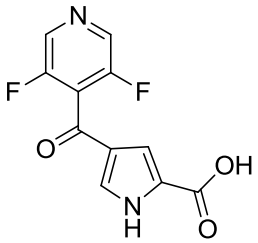

General procedure G: methyl 4-(3,5-difluoroisonicotinoyl)-1*H*-pyrrole-2-carboxylate (90 mg, 3.38 mmol), and LiOH monohydrate (213 mg, 5.07 mmol). Extraction at pH3 gave **259** as a pink solid (85 mg, 100%). R_f 0.13 (9:1 DCM/MeOH); m.p. 242-244 ˚C; λ_{max} (EtOH/nm) 231.0; IR υ_{max}/cm^{-1} 3329, 2785, 2700, 2630, 1699, 1630, 1540; ^{1}H NMR (500 MHz, DMSO-d_6) δ ppm 7.10 (1H, br s, H-3), 7.72 (1H, br s, H-5), 8.70 (2H, s, N-CH-pyridine), 12.83 (1H, s NH-pyrrole), 12.97 (1H, s, COOH); ^{13}C NMR (125 MHz, DMSO-d_6) δ ppm 114.0 (C-Ar), 124.0 (t, J_{CF} = 20.1 Hz, C-Ar), 124.9 (C-Ar), 126.3 (C-Ar), 131.1 (C-Ar), 135.1 (dd, J_{CF} = 3.9 and 22.9 Hz, C-Ar), 154.4 (d, J_{CF} = 260.4 Hz, C-F), 161.2 (CO), 179.4 (CO); Insufficient material retained for HRMS analysis.

4-(3,5-Difluoroisonicotinoyl)-*N*-(pyridin-4-yl)-1*H*-pyrrole-2-carboxamide, 257

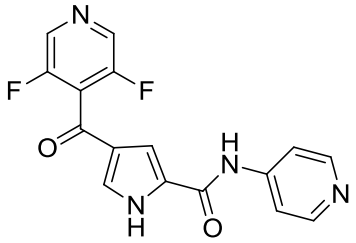

General procedure M: 4-(3,5-Difluoroisonicotinoyl)-1*H*-pyrrole-2-carboxylic acid (43 mg, 0.17 mmol), PCl_3 (14 µL, 0.17 mmol), and 4-aminopyridine (40 mg, 0.43 mmol). Purification *via* column chromatography (silica; 0-8% MeOH/DCM) gave **257** as a pink solid (17 mg, 30%). R_f 0.16 (95:5 DCM/MeOH); m.p. Degrades >250 ˚C; λ_{max} (EtOH/nm) 270.5; IR υ_{max}/cm^{-1} 3112, 2924, 1689, 1649, 1590, 1558, 1509, 1416; ^{1}H NMR (500 MHz, DMSO-d_6) δ ppm 7.65 (1H, br s, H-3), 7.74 (2H, d, *J* = 6.4 Hz, CH-pyridine), 7.78 (1H, br s, H-5), 8.47 (2H, d, *J* = 6.4 Hz, N-CH-pyridine), 8.73 (2H, s, H-3' and H-5'), 10.38 (1H, s, CO-NH),

12.91 (1H, s, NH-pyrrole); ^{13}C NMR (125 MHz, DMSO-d_6) δ ppm 111.8 (C-Ar), 113.7 (C-Ar), 124.1 (t, J_{CF} = 20.8 Hz, C-Ar), 124.9 (C-Ar), 128.4 (C-Ar), 131.2 (C-Ar), 135.2 (dd, J_{CF} = 4.4 and 23.0 Hz, C-Ar), 145.6 (C-Ar), 150.3 (C-Ar), 154.5 (dd, J_{CF} = 2.1 and 261.6 Hz, C-F), 158.9 (CO), 179.6 (CO); HRMS calcd for $C_{16}H_{10}F_2N_4O_2$ $[M+H]^+$ 329.0845, found 329.0847.

Methyl 4-(2-fluoro-6-methylbenzoyl)-1*H*-pyrrole-2-carboxylate, 264

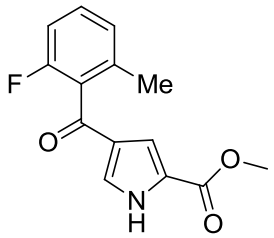

General procedure E: 2-fluoro, 6-methylbenzoic acid (0.73 g, 4.73 mmol), $SOCl_2$ (0.52 mL, 7.10 mmol) and DMF (10 mol%) gave 2-fluoro, 6-methylbenzoyl chloride as a yellow oil which was used directly in the next step. **General procedure F:** methyl 1*H*-pyrrole-2-carboxylate (297 mg, 2.37 mmol), and $AlCl_3$ (0.80 g, 5.93 mmol). Purification *via* column chromatography (silica; 0-50% EtOAc/petrol) gave **264** as a white solid (0.51 g, 83%). R_f 0.22 (8:2 Petrol/EtOAc); m.p. 105-108 ^oC; λ_{max} (EtOH/nm) 282.0, 229.5; IR υ_{max}/cm^{-1} 3125, 3090, 2975, 1709, 1638, 1612, 1550; ^{1}H NMR (500 MHz, DMSO-d_6) δ ppm 2.17 (3H, s, CH_3), 3.80 (3H, s, O-CH_3), 6.96 (1H, br s, H-3), 7.13-7.18 (2H, m, H-3' and H-5'), 7.40-7.44 (2H, m, H-5 and H-4'), 12.80 (1H, s, NH); ^{13}C NMR (125 MHz, DMSO-d_6) δ ppm 18.4 (CH_3), 51.6 (O-CH_3), 112.9 (d, J_{CF} = 21.8 Hz, C-Ar), 114.6 (C-Ar), 124.2 (C-Ar), 126.2 (C-Ar), 126.3 (d, J_{CF} = 2.4 Hz, C-Ar), 128.3 (C-Ar), 129.4 (C-Ar), 130.6 (d, J_{CF} = 8.9 Hz, C-Ar), 136.9 (d, J_{CF} = 3.5 Hz, C-Ar), 158.3 (d, J_{CF} = 243.3 Hz, C-F), 160.3 (CO), 187.5 (CO); HRMS calcd for $C_{14}H_{12}FNO_3$ $[M+H]^+$ 262.0874, found 262.0879.

4-(2-Fluoro-6-methylbenzoyl)-1*H*-pyrrole-2-carboxylic acid, 265

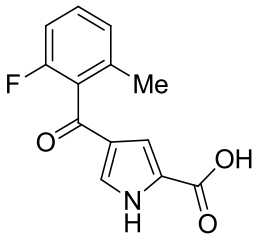

General procedure G: methyl 4-(2-fluoro-6-methylbenzoyl)-1*H*-pyrrole-2-carboxylate (0.50 g, 1.92 mmol) and LiOH monohydrate (0.92 g, 38.30 mmol) gave **265** as a white solid (465 mg, 98%). R_f 0.36 (9:1 DCM/MeOH); m.p. 193-195 ^oC; λ_{max} (EtOH/nm) 280.0, 230.5; IR υ_{max}/cm^{-1} 3337, 2798, 2705, 2626, 1689, 1642, 1561; ^1H NMR (500 MHz, DMSO-d_6) δ ppm 2.17 (3H, s, CH_3), 6.92 (1H, br s, H-3), 7.13-7.18 (2H, m, H-3' and H-5'), 7.34 (1H, br s, H-5), 7.42 (1H, ddd, J = 6.2, 8.3 and 8.4 Hz, H-4'), 12.59 (1H, s, NH), 12.87 (1H, s, COOH); ^{13}C NMR (125 MHz, DMSO-d_6) δ ppm 18.4 (CH_3), 112.9 (d, J_{CF} = 21.5 Hz, C-Ar), 114.1 (C-Ar), 125.6 (C-Ar), 126.1 (C-Ar), 126.2 (d, J_{CF} = 2.5 Hz, C-Ar), 128.3 (d, J_{CF} = 18.3 Hz, C-Ar), 128.9 (C-Ar), 130.5 (d, J_{CF} = 8.5 Hz, C-Ar), 136.9 (d, J_{CF} = 3.3 Hz, C-Ar), 158.3 (d, J_{CF} = 243.2 Hz, C-F), 161.3 (CO), 187.6 (CO); HRMS calcd for $C_{13}H_{10}FNO_3$ $[M-H]^-$ 246.0572, found 246.0562.

4-(2-Fluoro-6-methylbenzoyl)-*N*-(pyridin-4-yl)-1*H*-pyrrole-2-carboxamide, 266

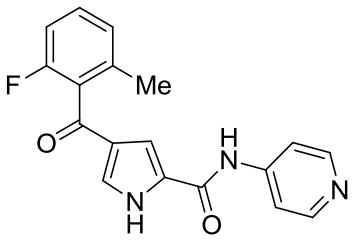

General procedure M: 4-(2-fluoro-6-methylbenzoyl)-1*H*-pyrrole-2-carboxylic acid (50 mg, 0.20 mmol), PCl_3 (17 µL, 0.20 mmol) and 4-aminopyridine (47 mg, 0.50 mmol). Purification *via* column chromatography (silica; 0-8% MeOH/DCM) gave **266** as a white solid (45 mg, 70%). R_f 0.24 (95:5 DCM/MeOH); m.p. 288-290 ^oC; λ_{max} (EtOH/nm) 292.0, 271.0, 210.0; IR υ_{max}/cm^{-1} 3280, 2943, 2845, 1630, 1568, 1535; ^1H NMR (500 MHz, DMSO-d_6) δ ppm 2.19 (3H, s, CH_3), 7.15-7.20 (2H, m, H-3' and H-5'), 7.39 (1H, br s, H-3), 7.43 (1H, ddd, J = 6.2, 8.3 and 8.4 Hz, H-4'), 7.51 (1H, br s, H-5), 7.73 (2H, d, J = 6.4 Hz, CH-pyridine), 8.46 (2H, d, J = 6.4 Hz, N-CH-pyridine), 10.34 (1H, s, CO-NH), 12.66 (NH-pyrrole); ^{13}C NMR (125 MHz, DMSO-d_6) δ ppm 18.4 (CH_3), 112.1 (C-Ar), 113.0 (d, J_{CF} = 21.5 Hz, C-Ar), 113.7 (C-

Ar), 126.2 (C-Ar), 126.3 (d, J_{CF} = 2.3 Hz, C-Ar), 127.7 (C-Ar), 128.4 (d, J_{CF} = 18.7 Hz, C-Ar), 129.1 (C-Ar), 130.5 (d, J_{CF} = 8.7 Hz, C-Ar), 136.9 (d, J_{CF} = 3.5 Hz, C-Ar), 145.7 (C-Ar), 150.3 (C-Ar), 158.4 (d, J_{CF} = 243.6 Hz, C-F), 159.1 (CO), 187.8 (CO); HRMS calcd for $C_{18}H_{14}FN_3O_2$ $[M+H]^+$ 324.1143, found 324.1146.

4-(2-Fluoro-6-methylbenzoyl)-*N*-(pyridin-3-yl)-1*H*-pyrrole-2-carboxamide, 267

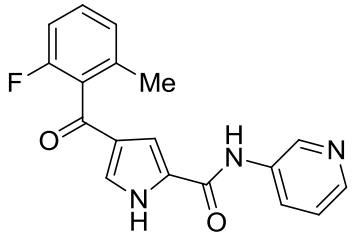

General procedure M: 4-(2-fluoro-6-methylbenzoyl)-1*H*-pyrrole-2-carboxylic acid (50 mg, 0.20 mmol), PCl_3 (17 µL, 0.20 mmol) and 3-aminopyridine (47 mg, 0.50 mmol). Purification *via* column chromatography (silica; 0-8% MeOH/DCM) gave **267** as a white solid (49 mg, 76%). R_f 0.25 (95:5 DCM/MeOH); m.p. 191-193 ^oC; λ_{max} (EtOH/nm) 248.0; IR υ_{max}/cm^{-1} 3280, 2955, 2842, 1629, 1566, 1535; ^1H NMR (500 MHz, DMSO-*d6*) δ ppm 2.20 (3H, s, CH_3), 7.15-7.20 (2H, m, H-3' and H-5'), 7.37-7.40 (2H, m, H-3 and CH-pyridine), 7.43 (1H, ddd, *J* = 6.2, 8.3 and 8.4 Hz, H-4'), 7.47 (1H, br s, H-5), 8.14 (1H, ddd, *J* = 1.5, 2.5 and 8.3 Hz, CH-pyridine), 8.30 (1H, dd, *J* = 1.5 and 4.7 Hz, N-CH-pyridine), 8.89 (1H, d, *J* = 2.5 Hz, N-CH-pyridine), 10.23 (1H, s, CO-NH), 12.60 (1H, s, NH-pyrrole); ^{13}C NMR (125 MHz, DMSO-*d6*) δ ppm 18.4 (CH_3), 111.6 (C-Ar), 112.9 (d, J_{CF} = 21.6 Hz, C-Ar), 123.5 (C-Ar), 126.1 (C-Ar), 126.3 (d, J_{CF} = 2.4 Hz, C-Ar), 127.0 (C-Ar), 127.8 (C-Ar), 128.5 (d, J_{CF} = 18.5 Hz, C-Ar), 128.7 (C-Ar), 130.5 (d, J_{CF} = 8.7 Hz, C-Ar), 135.5 (C-Ar), 136.9 (d, J_{CF} = 3.3 Hz, C-Ar), 141.6 (C-Ar), 144.4 (C-Ar), 158.4 (d, J_{CF} = 243.1 Hz, C-F), 158.8 (CO), 187.8 (CO); HRMS calcd for $C_{18}H_{14}FN_3O_2$ $[M+H]^+$ 324.1143, found 324.1147.

4-(2-Fluoro-6-methylbenzoyl)-*N*-(pyridin-4-ylmethyl)-1*H*-pyrrole-2-carboxamide, 268

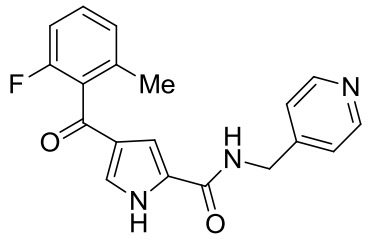

General procedure M: 4-(2-fluoro-6-methylbenzoyl)-1*H*-pyrrole-2-carboxylic acid (50 mg, 0.20 mmol), PCl_3 (17 µL, 0.20 mmol), and 4-picolylamine (51 µL, 0.50 mmol). Purification *via* column chromatography (silica; 0-8% MeOH/DCM) gave **268** as a white solid (35 mg, 52%). R_f 0.30 (95:5 DCM/MeOH); m.p. 209-210 ^oC; λ_{max} (EtOH/nm) 284.0, 234.5; IR υ_{max}/cm^{-1} 3278, 3124, 3080, 2971, 2927, 2865, 1634, 1568, 1538; ^1H NMR (500 MHz, DMSO-d_6) δ ppm 2.18 (3H, s, CH_3), 4.45 (2H, d, J = 6.0 Hz, NH-CH_2), 7.13-7.18 (2H, m, H-3' and H-5'), 7.22 (1H, br s, H-3), 7.26 (1H, br s, H-5), 7.29 (2H, d, J = 6.1 Hz, CH-pyridine), 7.41 (1H, ddd, J = 6.2, 8.3 and 8.4 Hz, H-4'), 8.50 (2H, d, J = 6.1 Hz, N-CH-pyridine), 8.95 (1H, t, J = 6.0 Hz, CO-NH), 12.39 (1H, s, NH-pyrrole); ^{13}C NMR (125 MHz, DMSO-d_6) δ ppm 18.4 (CH_3), 41.1 (CH_2), 110.2 (C-Ar), 112.9 (d, J_{CF} = 21.6 Hz, C-Ar), 122.1 (C-Ar), 126.0 (C-Ar), 126.2 (d, J_{CF} = 2.2 Hz, C-Ar), 127.8 (C-Ar), 128.2 (C-Ar), 128.6 (d, J_{CF} = 18.8 Hz, C-Ar), 130.3 (d, J_{CF} = 8.7 Hz, C-Ar), 136.9 (d, J_{CF} = 3.5 Hz, C-Ar), 148.5 (C-Ar), 149.5 (C-Ar), 158.4 (d, J_{CF} = 242.5 Hz, C-F), 160.2 (CO), 187.7 (CO); HRMS calcd for $C_{19}H_{16}FN_3O_2$ $[M+H]^+$ 338.1299, found 338.1303.

4-(2-Fluoro-6-methylbenzoyl)-*N*-(pyridin-3-ylmethyl)-1*H*-pyrrole-2-carboxamide, 269

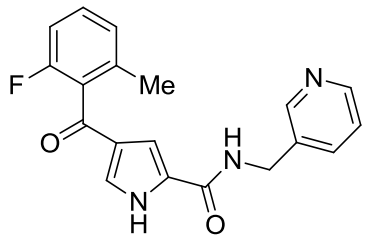

General procedure M: 4-(2-fluoro-6-methylbenzoyl)-1*H*-pyrrole-2-carboxylic acid (50 mg, 0.20 mmol), PCl_3 (17 µL, 0.20 mmol), and 3-picolylamine (51 µL, 0.50 mmol). Purification *via* column chromatography (silica; 0-8% MeOH/DCM) gave **269** as a white solid (39 mg, 58%). R_f 0.28 (95:5 DCM/MeOH); m.p. 233-234 ^oC; λ_{max} (EtOH/nm) 287.0, 235.0; IR υ_{max}/cm^{-1} 3358, 3117, 2953, 2809, 1635, 1564, 1531, 1428, 1283, 1240; ^1H NMR (500 MHz, DMSO-d_6) δ ppm 2.17 (3H, s, CH_3), 4.45 (2H, d, J = 6.0 Hz, NH-CH_2), 7.12-7.18 (2H, m, H-

3, H-3' and H-5'), 7.25 (1H, br s, H-5), 7.36 (1H, dd, *J* = 4.8 and 7.9 Hz, CH-pyridine), 7.40 (1H, ddd, *J* = 6.2, 8.3 and 8.4 Hz, H-4'), 7.70 (1H, dd, *J* = 1.5 and 7.9 Hz, CH-pyridine), 8.46 (1H, dd, *J* = 1.5 and 4.8 Hz, N-CH-pyridine), 8.53 (1H, d, *J* = 2.5 Hz, N-CH-pyridine), 8.90 (1H, t, *J* = 6.0 Hz, CO-NH), 12.37 (1H, s, NH-pyrrole); ^{13}C NMR (125 MHz, DMSO-d_6) δ ppm 18.4 (CH_3), 39.8 (CH_2), 110.1 (C-Ar), 112.9 (d, J_{CF} = 21.6 Hz, C-Ar), 123.5 (C-Ar), 125.9 (C-Ar), 126.2 (d, J_{CF} = 2.3 Hz, C-Ar), 127.7 (C-Ar), 128.2 (C-Ar), 128.6 (d, J_{CF} = 18.7 Hz, C-Ar), 130.3 (d, J_{CF} = 8.7 Hz, C-Ar), 134.9 (C-Ar), 135.1 (C-Ar), 136.8 (d, J_{CF} = 3.7 Hz, C-Ar), 148.1 (C-Ar), 148.8 (C-Ar), 158.3 (d, J_{CF} = 242.4 Hz, C-F), 160.0 (CO), 187.7 (CO); HRMS calcd for $C_{19}H_{16}FN_3O_2$ $[M+H]^+$ 338.1299, found 338.1302.

Methyl 4-(2-chloro-6-fluorobenzoyl)-1*H*-pyrrole-2-carboxylate, 270

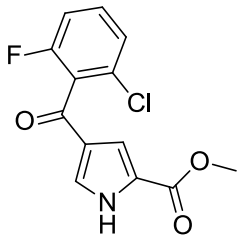

General procedure F: methyl 1*H*-pyrrole-2-carboxylate (2.00 g, 15.98 mmol), 2-chloro, 6-fluorobenzoyl chloride (4.30 mL, 31.96 mmol) and $AlCl_3$ (5.35 g, 39.95 mmol). Purification *via* column chromatography (silica; 0-50% EtOAc/petrol) gave **270** as a white solid (3.99 g, 89%). R_f 0.20 (8:2 Petrol/EtOAc); m.p. 145-146 ^{o}C; ˚C λ_{max} (EtOH/nm) 280.5, 231.5; IR υ_{max}/cm^{-1} 3225, 3141, 3006, 1731, 1639, 1603, 1563, 1508; ^{1}H NMR (500 MHz, DMSO-d_6) δ ppm 3.80 (3H, s, O-CH_3), 7.01 (1H, br s, H-3), 7.37-7.40 (1H, m, H-5'), 7.46 (1H, d, *J* = 8.3 Hz, H-3'), 7.53 (1H, dd, *J* = 1.6 and 3.4 Hz, H-5), 7.58 (1H, ddd, *J* = 6.4, 8.3 and 14.6 Hz, H-4'), 12.89 (1H, s, NH); ^{13}C NMR (125 MHz, DMSO-d_6) δ ppm 51.7 (O-CH_3), 114.6 (C-Ar), 115.0 (d, J_{CF} = 21.4 Hz, C-Ar), 124.5 (C-Ar), 125.4 (C-Ar), 125.8 (d, J_{CF} = 3.1 Hz, C-Ar), 127.7 (d, J_{CF} = 23.1 Hz, C-Ar), 130.1 (C-Ar), 130.3 (d, J_{CF} = 6.1 Hz, C-Ar), 131.9 (d, J_{CF} = 9.2 Hz, C-Ar), 158.6 (d, J_{CF} = 247.3 Hz, C-F), 160.3 (CO), 183.7 (CO); HRMS calcd for $C_{13}H_9{}^{35}ClFNO_3$ $[M+H]^+$ 282.0328, found 282.0331.

4-(2-Chloro-6-fluorobenzoyl)-1*H*-pyrrole-2-carboxylic acid, 271

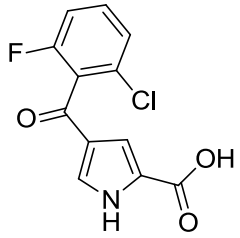

General procedure G: methyl 4-(2-chloro-6-fluorobenzoyl)-1*H*-pyrrole-2-carboxylate (3.98 g, 14.16 mmol), and LiOH monohydrate (11.89 g, 283.27 mmol) gave **271** as a white solid (3.74 g, 99%). R_f 0.36 (95:5 DCM/MeOH); m.p. 209-210 ^{o}C; ˚C λ_{max} (EtOH/nm) 281.0, 233.5; IR υ_{max}/cm^{-1} 3306, 1638, 1556; ^{1}H NMR (500 MHz, DMSO-d_6) δ ppm 6.95 (1H, br s, H-3), 7.36-7.39 (1H, m, H-5'), 7.44-7.45 (2H, m, H-5 and H-3'), 7.56 (1H, ddd, J = 6.3, 8.3 and 8.4 Hz, H-4'), 12.69 (1H, s, NH-pyrrole), 13.15 (1H, br s, COOH); ^{13}C NMR (125 MHz, DMSO-d_6) δ ppm 114.0 (C-Ar), 114.9 (d, J_{CF} = 21.6 Hz, C-Ar), 125.2 (C-Ar), 125.8 (d, J_{CF} = 3.1 Hz, C-Ar), 126.2 (C-Ar), 127.9 (d, J_{CF} = 23.0 Hz, C-Ar), 129.6 (C-Ar), 130.3 (d, J_{CF} = 6.1 Hz, C-Ar), 131.8 (d, J_{CF} = 9.1 Hz, C-Ar), 158.6 (d, J_{CF} = 246.4 Hz, C-F), 161.4 (CO), 183.7 (CO);

4-(2-Chloro-6-fluorobenzoyl)-*N*-(pyridin-4-yl)-1*H*-pyrrole-2-carboxamide, 272

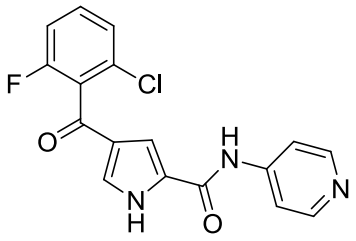

General procedure M: 4-(2-chloro-6-fluorobenzoyl)-1*H*-pyrrole-2-carboxylic acid (75 mg, 0.28 mmol), PCl_3 (25 µL, 0.28 mmol) and 4-aminopyridine (66 mg, 0.70 mmol). Purification *via* column chromatography (silica; 0-8% MeOH/DCM) gave **272** as a white solid (59 mg, 61%). R_f 0.31 (95:5 DCM/MeOH); m.p. Degrades >270 ^{o}C; λ_{max} (EtOH/nm) 341.0, 291.0, 271.5; IR υ_{max}/cm^{-1} 3416, 3354, 1682, 1632, 1586, 1552, 1506; ^{1}H NMR (500 MHz, DMSO-d_6) δ ppm 7.40-7.43 (1H, m, H-5'), 7.47-7.48 (1H, m, H-3'), 7.51 (1H, br s, H-3), 7.55 (1H, br s, H-5), 7.59 (1H, ddd, J = 6.2, 8.3 and 8.4 Hz, H-4'), 7.74 (2H, d, J = 6.3 Hz, CH-pyridine), 8.47 (2H, d, J = 6.3 Hz, N-CH-pyridine), 10.36 (1H, s, CO-NH), 12.76 (1H, s, NH-pyrrole); ^{13}C NMR (125 MHz, DMSO-d_6) δ ppm 112.1 (C-Ar), 113.7 (C-Ar), 115.0 (d, J_{CF} = 21.8 Hz, C-Ar), 125.3 (C-Ar), 125.9 (d, J_{CF} = 2.7 Hz, C-Ar), 127.9 (d, J_{CF} = 23.1 Hz, C-Ar),

128.0 (C-Ar), 129.8 (C-Ar), 130.4 (d, J_{CF} = 6.1 Hz, C-Ar), 131.9 (d, J_{CF} = 9.2 Hz, C-Ar), 145.6 (C-Ar), 150.3 (C-Ar), 158.6 (d, J_{CF} = 247.3 Hz, C-F), 159.0 (CO), 183.9 (CO); HRMS calcd for $C_{17}H_{11}{}^{35}ClFN_3O_2$ $[M+H]^+$ 344.0597, found 344.0592.

4-(2-Chloro-6-fluorobenzoyl)-*N*-(pyridin-3-yl)-1*H*-pyrrole-2-carboxamide, 273

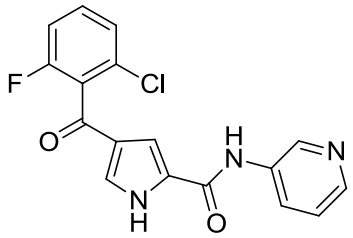

General procedure M: 4-(2-chloro-6-fluorobenzoyl)-1*H*-pyrrole-2-carboxylic acid (75 mg, 0.28 mmol), PCl_3 (25 µL, 0.28 mmol) and 3-aminopyridine (66 mg, 0.70 mmol). Purification *via* column chromatography (silica; 0-8% MeOH/DCM) gave **273** as a white solid (62 mg, 64%). R_f 0.29 (95:5 DCM/MeOH); m.p. Degrades >260 ^oC; λ_{max} (EtOH/nm) 350.0, 248.5; IR υ_{max}/cm^{-1} 3122, 2963, 1635, 1602, 1535; ^1H NMR (500 MHz, DMSO-d_6) δ ppm 7.38-7.43 (2H, m, H-3 and H-5'), 7.47-7.50 (3H, m, H-5, H-3' and CH-pyridine), 7.59 (1H, ddd, J = 6.2, 8.3 and 8.4 Hz, H-4'), 8.14 (1H, ddd, J = 1.5, 2.5 and 8.3 Hz, CH-pyridine), 8.30 (1H, dd, J = 1.5 and 4.7 Hz, N-CH-pyridine), 8.89 (1H, d, J = 2.5 Hz, N-CH-pyridine), 10.24 (1H, s, CO-NH), 12.71 (1H, s, NH-pyrrole); ^{13}C NMR (125 MHz, DMSO-d_6) δ ppm 111.6 (C-Ar), 115.0 (d, J_{CF} = 21.2 Hz, C-Ar), 123.5 (C-Ar), 125.3 (C-Ar), 125.9 (d, J_{CF} = 3.0 Hz, C-Ar), 127.0 (C-Ar), 128.0 (d, J_{CF} = 23.1 Hz, C-Ar), 128.2 (C-Ar), 129.3 (C-Ar), 130.4 (d, J_{CF} = 6.1 Hz, C-Ar), 131.8 (d, J_{CF} = 9.1 Hz, C-Ar), 135.5 (C-Ar), 141.6 (C-Ar), 144.4 (C-Ar), 158.6 (d, J_{CF} = 247.2 Hz, C-F), 158.7 (CO), 183.9 (CO); HRMS calcd for $C_{17}H_{11}{}^{35}ClFN_3O_2$ $[M+H]^+$ 344.0597, found 344.0592.

4-(2-Chloro-6-fluorobenzoyl)-*N*-(pyridin-4-ylmethyl)-1*H*-pyrrole-2-carboxamide, 274

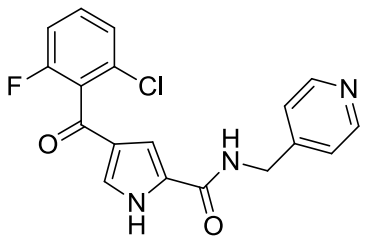

General procedure M: 4-(2-chloro-6-fluorobenzoyl)-1*H*-pyrrole-2-carboxylic acid (75 mg, 0.28 mmol), PCl_3 (25 µL, 0.28 mmol) and 4-picolylamine (71 µL, 0.70 mmol). Purification

via column chromatography (silica; 0-8% MeOH/DCM) gave **274** as a pink solid (50 mg, 50%). R_f 0.24 (95:5 DCM/MeOH); m.p. 200-202 ^oC; λ_{max} (EtOH/nm) 281.5, 235.5; IR υ_{max}/cm^{-1} 3385, 3182, 1622, 1570, 1535; ^1H NMR (500 MHz, DMSO-d_6) δ ppm 4.44 (2H, d, J = 5.9 Hz, NH-CH_2), 7.13 (1H, br s, H-3), 7.29 (2H, d, J = 6.0 Hz, CH-pyridine), 7.31 (1H, br s, H-5), 7.36-7.39 (1H, m, H-5'), 7.43-7.44 (1H, m, H-3'), 7.55 (1H, ddd, J = 6.2, 8.3 and 8.4 Hz, H-4'), 8.49 (2H, d, J = 6.0 Hz, N-CH-pyridine), 9.12 (1H, br s, CO-NH), 13.07 (1H, br s, NH-pyrrole); ^{13}C NMR (125 MHz, DMSO-d_6) δ ppm 41.1 (CH_2), 110.2 (C-Ar), 114.9 (d, J_{CF} = 21.8 Hz, C-Ar), 122.1 (C-Ar), 125.1 (C-Ar), 125.8 (d, J_{CF} = 2.2 Hz, C-Ar), 128.1 (d, J_{CF} = 23.4 Hz, C-Ar), 128.4 (C-Ar), 128.5 (C-Ar), 130.4 (d, J_{CF} = 5.9 Hz, C-Ar), 131.7 (d, J_{CF} = 9.0 Hz, C-Ar), 148.4 (C-Ar), 149.5 (C-Ar), 158.6 (d, J_{CF} = 246.3 Hz, C-F), 160.0 (CO), 183.9 (CO); HRMS calcd for $C_{18}H_{13}{}^{35}ClFN_3O_2$ $[M+H]^+$ 358.0753, found 358.0749.

4-(2-Chloro-6-fluorobenzoyl)-*N*-(pyridin-3-ylmethyl)-1*H*-pyrrole-2-carboxamide, 275

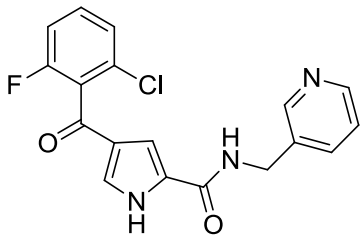

General procedure M: 4-(2-chloro-6-fluorobenzoyl)-1*H*-pyrrole-2-carboxylic acid (75 mg, 0.28 mmol), PCl_3 (25 µL, 0.28 mmol), and 3-picolylamine (71 µL, 0.70 mmol). Purification *via* column chromatography (silica; 0-8% MeOH/DCM) gave **275** as a white solid (68 mg, 68%). R_f 0.26 (95:5 DCM/MeOH); m.p. 258-261 ^oC; λ_{max} (EtOH/nm) 350.0, 284.0, 236.0; IR υ_{max}/cm^{-1} 3366, 3185, 3129, 3087, 1627, 1569, 1537; ^1H NMR (500 MHz, DMSO-*d6*) δ ppm 4.46 (2H, d, J = 6.0 Hz, NH-CH_2), 7.22 (1H, br s, H-3), 7.35-7.39 (3H, m, H-3, H-5' and CH-pyridine), 7.44-7.45 (1H, m, H-3'), 7.56 (1H, ddd, J = 6.2, 8.3 and 8.4 Hz, H-4'), 7.70-7.72 (1H, m, CH-pyridine), 8.47 (1H, dd, J = 1.5 and 4.7 Hz, N-CH-pyridine), 8.54 (1H, d, J = 2.5 Hz, N-CH-pyridine), 8.92 (1H, t, J = 6.0 Hz, CO-NH), 12.48 (1H, s, NH-pyrrole); ^{13}C NMR (125 MHz, DMSO-*d6*) δ ppm 39.8 (CH_2), 110.1 (C-Ar), 114.9 (d, J_{CF} = 21.4 Hz, C-Ar), 123.5 (C-Ar), 125.1 (C-Ar), 125.8 (d, J_{CF} = 2.8 Hz, C-Ar), 128.1 (d, J_{CF} = 22.9 Hz, C-Ar), 128.4 (C-Ar), 128.5 (C-Ar), 130.4 (d, J_{CF} = 6.1 Hz, C-Ar), 131.7 (d, J_{CF} = 9.2 Hz, C-Ar), 134.9 (C-Ar), 135.1 (C-Ar), 148.1 (C-Ar), 148.8 (C-Ar), 158.5 (d, J_{CF} = 246.7 Hz, C-F), 159.9 (CO), 183.8 (CO); HRMS calcd for $C_{18}H_{13}{}^{35}ClFN_3O_2$ $[M+H]^+$ 358.0753, found 358.0749.

Methyl 4-(2-bromo-6-fluorobenzoyl)-1*H*-pyrrole-2-carboxylate, 276

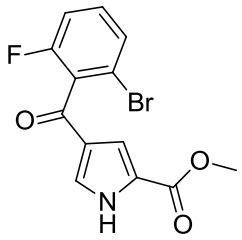

General procedure E: 2-bromo, 6-fluorobenzoic acid (3.00 g, 13.70 mmol), $SOCl_2$ (1.50 mL, 20.55 mmol) and DMF (10 mol%) gave 2-bromo, 6-fluorobenzoyl chloride as a colourless oil. The crude material was used directly in the next step. **General procedure F:** methyl 1*H*-pyrrole-2-carboxylate (0.86 g, 6.85 mmol), 2-bromo,6-fluorobenzoyl chloride (3.25 g, 13.70 mmol) and $AlCl_3$ (2.30g, 17.13 mmol). Purification *via* column chromatography (silica; 0-50% EtOAc/petrol) gave **276** as a white solid (1.78 g, 80%). R_f 0.21 (8:2 Petrol/EtOAc); m.p. 142-144 ^oC; ˚C λ_{max} (EtOH/nm) 286.5, 231.5; IR υ_{max}/cm^{-1} 3230, 3002, 2953, 1730, 1637, 1599, 1564, 1508; ^1H NMR (500 MHz, DMSO-d_6) δ ppm 3.80 (3H, s, O-CH_3), 6.99 (1H, br s, H-3), 7.40 (1H, dd, J = 8.3 and 8.9 Hz, H-5'), 7.48-7.53 (2H, m, H-4' and H-5), 7.59 (1H, d, J = 8.3 Hz, H-3'), 12.88 (1H, s, NH-pyrrole); ^{13}C NMR (125 MHz, DMSO-d_6) δ ppm 51.7 (CH_3), 114.7 (C-Ar), 115.3 (d, J_{CF} = 22.1 Hz, C-Ar), 118.9 (d, J_{CF} = 5.2 Hz, C-Ar), 124.5 (C-Ar), 125.0 (C-Ar), 128.8 (d, J_{CF} = 2.9 Hz, C-Ar), 129.7 (d, J_{CF} = 22.8 Hz, C-Ar), 130.1 (C-Ar), 132.3 (d, J_{CF} = 9.0 Hz, C-Ar), 158.5 (d, J_{CF} = 245.9 Hz, C-F), 160.2 (CO), 184.6 (CO); HRMS calcd for $C_{13}H_9{}^{79}BrFNO_3$ $[M+H]^+$ 325.9823, found 325.9830.

4-(2-Bromo-6-fluorobenzoyl)-1*H*-pyrrole-2-carboxylic acid, 277

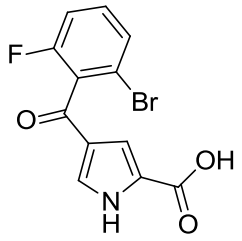

General procedure G: methyl 4-(2-bromo-6-fluorobenzoyl)-1*H*-pyrrole-2-carboxylate (2.88 g, 10.86 mmol), LiOH monohydrate (9.13 g, 217.40 mmol) gave **277** as white solid (2.46 g, 90%). R_f 0.15 (9:1 DCM/MeOH); m.p. 210-211 ^oC; λ_{max} (EtOH/nm) 281.0; IR υ_{max}/cm^{-1} 3342, 1690, 1648, 1561; ^1H NMR (500 MHz, DMSO-d_6) δ ppm 6.94 (1H, br s, H-3), 7.39-7.43 (2H, m, H-5 and H-5'), 7.50 (1H, ddd, J = 6.3, 8.3 and 8.4 Hz, H-4'), 7.59 (1H, d, J =

8.3 Hz, H-3'), 12.68 (1H, s, NH), 12.90 (1H, s, COOH); ^{13}C NMR (125 MHz, DMSO-d_6) δ ppm 114.2 (C-Ar), 115.3 (d, J_{CF} = 21.7 Hz, C-Ar), 118.9 (d, J_{CF} = 5.2 Hz, C-Ar), 124.9 (C-Ar), 125.8 (C-Ar), 128.8 (d, J_{CF} = 3.1 Hz, C-Ar), 129.7 (C-Ar), 129.9 (C-Ar), 132.2 (d, J_{CF} = 8.7 Hz, C-Ar), 158.4 (d, J_{CF} = 249.9 Hz, C-F), 161.3 (CO), 184.6 (CO); HRMS calcd for $C_{12}H_7{}^{79}BrFNO_3$ $[M-H]^-$ 309.9521, found 309.9512.

4-(2-Bromo-6-fluorobenzoyl)-*N*-(pyridin-4-yl)-1*H*-pyrrole-2-carboxamide, 263

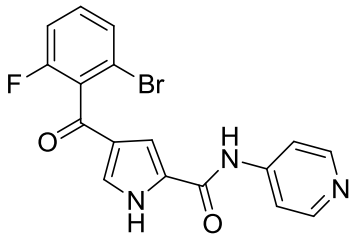

General procedure M: 4-(2-bromo-6-fluorobenzoyl)-1*H*-pyrrole-2-carboxylic acid (50 mg, 0.16 mmol), PCl_3 (14 µL, 0.16 mmol) and 4-aminopyridine (38 mg, 0.40 mmol). Purification *via* column chromatography (silica; 0-8% MeOH/DCM) gave **263** as a white solid (52 mg, 84%). R_f 0.32 (95:5 DCM/MeOH); m.p. Degrades >150 ^oC; λ_{max} (EtOH/nm) 291.5, 270.5; IR υ_{max}/cm^{-1} 3344, 3112, 2958, 1627, 1591, 1557, 1506; ^{1}H NMR (500 MHz, DMSO-*d6*) δ ppm 7.42-7.46 (1H, m, H-5'), 7.49-7.54 (3H, m, H-3, H-4' and H-5), 7.61-7.62 (1H, m, H-3'), 7.73 (2H, d, *J* = 6.4 Hz, CH-pyridine), 8.46 (2H, d, *J* = 6.4 Hz, N-CH-pyridine), 10.35 (1H, s, CO-NH), 12.74 (1H, s, NH-pyrrole); ^{13}C NMR (125 MHz, DMSO-*d6*) δ ppm 112.1 (C-Ar), 113.7 (C-Ar), 115.4 (d, J_{CF} = 21.6 Hz, C-Ar), 119.0 (d, J_{CF} = 5.1 Hz, C-Ar), 125.0 (C-Ar), 128.0 (C-Ar), 128.9 (d, J_{CF} = 2.9 Hz, C-Ar), 129.8 (C-Ar), 132.2 (d, J_{CF} = 8.9 Hz, C-Ar), 145.6 (C-Ar), 150.3 (C-Ar), 158.5 (d, J_{CF} = 247.8 Hz, C-F), 159.0 (CO), 184.9 (CO), one C-Ar not visualised; HRMS calcd for $C_{17}H_{11}{}^{79}BrFN_3O_2$ $[M+H]^+$ 388.0091, found 388.0088.

4-(2-Bromo-6-fluorobenzoyl)-*N*-(pyridin-3-yl)-1*H*-pyrrole-2-carboxamide, 278

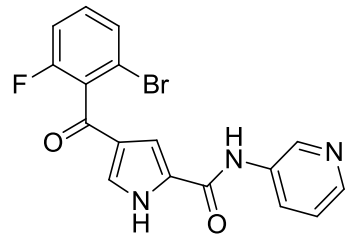

General procedure M: 4-(2-bromo-6-fluorobenzoyl)-1*H*-pyrrole-2-carboxylic acid (50 mg, 0.16 mmol), PCl_3 (14 µL, 0.16 mmol) and 3-aminopyridine (38 mg, 0.40 mmol). Purification

via column chromatography (silica; 0-8% MeOH/DCM) gave **278** as a white solid (47 mg, 76%). R_f 0.31 (95:5 DCM/MeOH); m.p. 138-140 ^oC; λ_{max} (EtOH/nm) 288.0; IR υ_{max}/cm^{-1} 3127, 2960, 1635, 1599, 1534; ^1H NMR (500 MHz, DMSO-*d6*) δ ppm 7.39 (1H, dd, *J* = 4.7 and 8.4 Hz, CH-pyridine), 7.42-7.48 (3H, m, H-3, H-5' and H-5), 7.52 (1H, ddd, *J* = 6.2, 8.3 and 8.4 Hz, H-4'), 7.61-7.63 (1H, m, H-3'), 8.14 (1H, ddd, *J* = 1.5, 2.5 and 8.4 Hz, CH-pyridine), 8.30 (1H, dd, *J* = 1.5 and 4.7 Hz, N-CH-pyridine), 8.89 (1H, d, *J* = 2.5 Hz, N-CH-pyridine), 10.24 (1H, s, CO-NH), 12.70 (1H, s, NH-pyrrole); ^{13}C NMR (125 MHz, DMSO-*d6*) δ ppm 111.7 (C-Ar), 115.4 (d, J_{CF} = 21.7 Hz, C-Ar), 119.0 (d, J_{CF} = 5.2 Hz, C-Ar), 123.6 (C-Ar), 124.9 (C-Ar), 127.0 (C-Ar), 128.8 (d, J_{CF} = 2.5 Hz, C-Ar), 129.4 (C-Ar), 130.0 (C-Ar), 132.1 (d, J_{CF} = 8.7 Hz, C-Ar), 135.5 (C-Ar), 141.6 (C-Ar), 144.4 (C-Ar), 158.5 (d, J_{CF} = 245.6 Hz, C-F), 158.7 (CO), 184.9 (CO), one C-Ar not visualised; HRMS calcd for $C_{17}H_{11}{}^{79}BrFN_3O_2$ $[M+H]^+$ 388.0091, found 388.0090.

4-(2-Bromo-6-fluorobenzoyl)-*N*-(pyridin-4-ylmethyl)-1*H*-pyrrole-2-carboxamide, 279

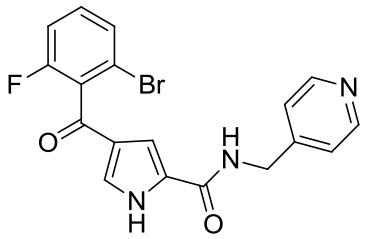

General procedure M: 4-(2-bromo-6-fluorobenzoyl)-1*H*-pyrrole-2-carboxylic acid (55 mg, 0.18 mmol), PCl_3 (16 µL, 0.18 mmol) and *tert*-butyl 4-picolylamine (46 µL, 0.45 mmol). Purification *via* column chromatography (silica; 0-8% MeOH/DCM) gave **279** as a white solid (40 mg, 55%). R_f 0.66 (9:1 DCM/MeOH); m.p. 141-143 ^oC; λ_{max} (EtOH/nm) 384.5, 236.0; IR υ_{max}/cm^{-1} 3076, 2922, 2861, 1628, 1601, 1567, 1535; ^1H NMR (500 MHz, DMSO-d_6) δ ppm 4.46 (2H, d, *J* = 6.0 Hz, NH-CH_2), 7.25 (1H, br s, H-3), 7.29 (2H, d, *J* = 6.0 Hz, CH-pyridine), 7.34 (1H, br s, H-5), 7.41-7.43 (1H, m, H-5'), 7.50 (1H, ddd, *J* = 6.2, 8.3 and 8.4 Hz, H-4'), 7.58-7.59 (1H, m, H-3'), 8.51 (2H, d, *J* = 6.0 Hz, N-CH-pyridine), 8.90 (1H, t, *J* = 6.0 Hz, CO-NH), 12.48 (1H, s, NH-pyrrole); ^{13}C NMR (125 MHz, DMSO-d_6) δ ppm 41.1 (CH_2), 110.3 (C-Ar), 115.3 (d, J_{CF} = 21.5 Hz, C-Ar), 119.0 (d, J_{CF} = 5.2 Hz, C-Ar), 122.1 (C-Ar), 124.8 (C-Ar), 128.4 (C-Ar), 128.5 (C-Ar), 128.8 (d, J_{CF} = 2.6 Hz, C-Ar), 130.0 (d, J_{CF} = 22.9 Hz, C-Ar), 132.1 (d, J_{CF} = 8.5 Hz, C-Ar), 148.4 (C-Ar), 149.5 (C-Ar), 158.4 (d, J_{CF} = 246.9 Hz, C-F), 160.1 (CO), 184.8 (CO); HRMS calcd for $C_{18}H_{13}{}^{79}BrFN_3O_2$ $[M+H]^+$ 402.0248, found 402.0242.

4-(2-Bromo-6-fluorobenzoyl)-*N*-(pyridin-3-ylmethyl)-1*H*-pyrrole-2-carboxamide, 280

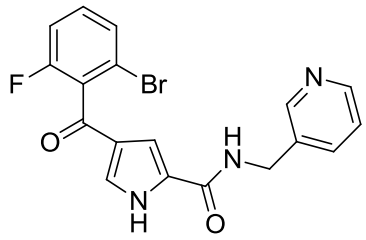

General procedure M: 4-(2-bromo-6-fluorobenzoyl)-1*H*-pyrrole-2-carboxylic acid (56 mg, 0.18 mmol), PCl_3 (16 µL, 0.18 mmol) and *tert*-butyl 3-picolylamine (46 µL, 0.45 mmol). Purification *via* column chromatography (silica; 0-8% MeOH/DCM) gave **280** as a white solid (49 mg, 68%). R_f 0.65 (9:1 DCM/MeOH); m.p. 128-130 ^oC; λ_{max} (EtOH/nm) 290.5, 238.0; IR υ_{max}/cm^{-1} 3121, 2867, 1626, 1566, 1534; ^1H NMR (500 MHz, DMSO-d_6) δ ppm 2.44 (2H, d, J = 6.0 Hz, NH-CH_2), 7.19 (1H, br s, H-3), 7.32 (1H, br s, H-5), 7.35 (1H, dd, J = 4.7 and 7.8 Hz, CH-pyridine), 7.39-7.41 (1H, m, H-5'), 7.48 (1H, ddd, J = 6.2, 8.3 and 8.4 Hz, H-4'), 7.57-7.58 (1H, m, H-3'), 7.69 (1H, dd, J = 1.5 and 7.8 Hz, CH-pyridine), 8.45 (1H, dd, J = 1.5 and 4.7 Hz, N-CH-pyridine), 8.53 (1H, d, J = 2.5 Hz, N-CH-pyridine), 8.91 (1H, t, J = 6.0 Hz, CO-NH), 12.45 (NH-pyrrole); ^{13}C NMR (125 MHz, DMSO-d_6) δ ppm 40.1 (CH_2), 110.2 (C-Ar), 115.3 (d, J_{CF} = 22.3 Hz, C-Ar), 119.0 (d, J_{CF} = 5.4 Hz, C-Ar), 123.5 (C-Ar), 124.7 (C-Ar), 128.4 (C-Ar), 128.5 (C-Ar), 128.7 (d, J_{CF} = 2.8 Hz, C-Ar), 130.0 (d, J_{CF} = 23.1 Hz, C-Ar), 132.0 (d, J_{CF} = 8.7 Hz, C-Ar), 134.9 (C-Ar), 135.1 (C-Ar), 148.1 (C-Ar), 148.8 (C-Ar), 158.4 (d, J_{CF} = 248.5 Hz, C-F), 159.9 (CO), 184.8 (CO); HRMS calcd for $C_{18}H_{13}{}^{79}BrFN_3O_2$ $[M+H]^+$ 402.0248, found 402.0243.

***tert*-Butyl 4-(4-(2-fluoro-6-methylbenzoyl)-1*H*-pyrrole-2-carboxamido)piperidine-1-carboxylate, 282**

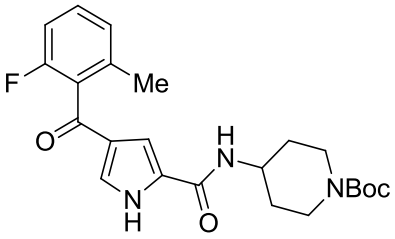

General procedure M: 4-(2-fluoro-6-methylbenzoyl)-1*H*-pyrrole-2-carboxylic acid (100 mg, 0.40 mmol), PCl_3 (35 µL, 0.20 mmol) and *tert*-butyl 4-aminopiperidine-1-carboxylate (200 mg, 1.00 mmol). Purification *via* column chromatography (silica; 30-70% EtOAc/petrol) gave **282** as a colourless oil (64 mg, 37%). R_f 0.67 (9:1 DCM/MeOH); λ_{max}

(EtOH/nm) 284.0, 234.0; IR υ_{max}/cm^{-1} 3126, 2976, 2935, 2867, 1616, 1568, 1534, 1464, 1429, 1394, 1366, 1316, 1276, 1238; ^{1}H NMR (500 MHz, DMSO-*d6*) δ ppm 1.31-1.40 (2H, m, CH-piperidine), 1.41 (9H, s, C-*CH*$_3$), 1.74-1.77 (2H, m, CH-piperidine), 2.17 (3H, s, CH_3), 2.84 (2H, br s, N-CH-piperidine), 3.89-3.96 (3H, m, N-CH-piperidine), 7.12-7.17 (3H, m, H-3, H-3' and H-5'), 7.22 (1H, br s, H-5), 7.41 (1H, ddd, *J* = 6.2, 8.3 and 8.4 Hz, H-4'), 8.11 (1H, d, *J* = 7.8 Hz, CO-NH), 12.31 (1H, s, NH-pyrrole); ^{13}C NMR (125 MHz, $CDCl_3$) δ ppm 19.0 (d, J_{CF} = 2.0 Hz, CH_3), 28.4 (C-*CH*$_3$), 32.1 (C-piperidine), 42.7 (C-piperidine), 47.1 (C-piperidine), 79.8 (*C*-CH_3), 108.8 (C-Ar), 113.0 (d, J_{CF} = 21.8 Hz, C-Ar), 126.1 (d, J_{CF} = 2.5 Hz, C-Ar), 127.5 (C-Ar), 127.8 (C-Ar), 130.4 (d, J_{CF} = 8.7 Hz, C-Ar), 137.8 (d, J_{CF} = 3.2 Hz, C-Ar), 154.7 (CO), 159.7 (CO), 188.8 (CO), 2 C-Ar and C-F not visualised; HRMS calcd for $C_{23}H_{28}FN_3O_4$ $[M+H]^+$ 430.2137, found 430.2138.

4-(2-Fluoro-6-methylbenzoyl)-*N*-(piperidin-4-yl)-1*H*-pyrrole-2-carboxamide, 291

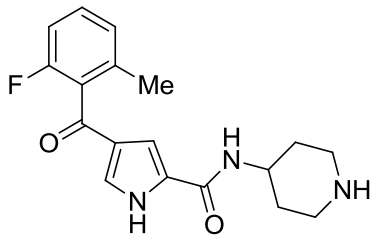

General procedure K: *tert*-butyl 4-(4-(2-fluoro-6-methylbenzoyl)-1*H*-pyrrole-2-carboxamido)piperidine-1-carboxylate (40 mg, 0.09 mmol), TFA (11 µL, 0.14 mmol). Purification *via* column chromatography (NH silica; 0-5% MeOH/DCM) gave **291** as a white solid (30 mg, 100%). R_f 0.45 (9:1 DCM/MeOH, NH silica); m.p. 251-252 ^{o}C; λ_{max} (EtOH/nm) 235.0, 210.0; IR υ_{max}/cm^{-1} 3295, 2949, 2852, 1626, 1568, 1532; ^{1}H NMR (500 MHz, DMSO-d_6) δ ppm 1.35 (2H, m, CH-piperidine), 1.68-1.71 (2H, m, CH-piperidine), 2.17 (3H, s, CH_3), 2.46-2.51 (2H, m, N-CH-piperidine), 2.92-2.96 (2H, m, N-CH-piperidine), 3.72-3.80 (1H, m, N-CH-piperidine), 7.12-7.20 (4H, m, H-3, H-3', H-5' and H-5), 7.41 (1H, ddd, *J* = 6.2, 8.3 and 8.4 Hz, H-4'), 8.08 (1H, d, *J* = 8.0 Hz, CO-NH), 12.33 (1H, br s, NH-pyrrole); ^{13}C NMR (125 MHz, DMSO-d_6) δ ppm 18.4 (CH_3), 33.1 (C-piperidine), 45.3 (C-piperidine), 46.9 (N-C-piperidine), 109.8 (C-Ar), 112.9 (d, J_{CF} = 21.4 Hz, C-Ar), 125.8 (C-Ar), 126.2 (d, J_{CF} = 2.4 Hz, C-Ar), 127.4 (C-Ar), 128.6 (C-Ar), 128.8 (C-Ar), 130.3 (d, J_{CF} = 8.6 Hz, C-Ar), 136.8 (d, J_{CF} = 3.7 Hz, C-Ar), 158.4 (d, J_{CF} = 243.2 Hz, C-F), 158.9 (CO), 187.8 (CO); HRMS calcd for $C_{18}H_{20}FN_3O_2$ $[M+H]^+$ 330.1612, found 330.1615.

4-(2-Chloro-6-fluorobenzoyl)-*N*-(1-methylpiperidin-4-yl)-1*H*-pyrrole-2-carboxamide, 283

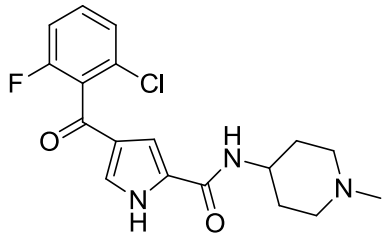

General procedure D: 4-(2-chloro-6-fluorobenzoyl)-1*H*-pyrrole-2-carboxylic acid (200 mg, 0.75 mmol), CDI (243 mg, 1.50 mmol), and 4-amino-1-methyl piperidine (235 µL, 1.88 mmol). Purification *via* column chromatography (NH silica; 0-8% MeOH/DCM) gave **283** as a white solid (212 mg, 78%).

R_f 0.17 (9:1 DCM/MeOH); m.p. Degrades above 260 ^{o}C; λ_{max} (EtOH/nm) 285.5, 236.5; IR υ_{max}/cm^{-1} 3358, 3122, 2937, 2854, 2788, 1614, 1570, 1535; ^{1}H NMR (500 MHz, DMSO-d_6) δ ppm 1.48-1.56 (2H, m, CH-piperidine), 1.71-1.74 (2H, m, CH-piperidine), 1.88-1.95 (2H, m, N-CH-piperidine), 2.16 (3H, s, CH_3), 2.74-2.77 (2H, m, N-CH-piperidine), 3.64-3.70 (1H, m, N-CH-piperidine), 7.20 (1H, br s, H-3), 7.32 (1H, br s, H-5), 7.37-7.40 (1H, m, H-5'), 7.45-7.46 (1H, m, H-3'), 7.57 (1H, ddd, J = 6.4, 8.2 and 8.3 Hz, H-4'), 8.10 (1H, d, J = 8.0 Hz, CO-NH), 12.40 (1H, s, NH-pyrrole); ^{13}C NMR (125 MHz, DMSO-d_6) δ ppm 31.5 (C-piperidine), 45.9 (C-piperidine), 54.4 (CH_3), 109.9 (C-Ar), 114.9 (d, J_{CF} = 21.6 Hz, C-Ar), 125.0 (C-Ar), 125.8 (d, J_{CF} = 2.7 Hz, C-Ar), 128.0 (C-Ar), 128.2 (d, J_{CF} = 23.7 Hz, C-Ar), 128.9 (C-Ar), 130.4 (d, J_{CF} = 6.2 Hz, C-Ar), 131.7 (d, J_{CF} = 9.2 Hz, C-Ar), 158.7 (d, J_{CF} = 246.8 Hz, C-F), 159.0 (CO), 183.9 (CO); HRMS calcd for $C_{18}H_{19}{}^{35}ClFN_3O_2$ $[M+H]^+$ 364.1223, found 364.1226.

***tert*-Butyl 4-(4-(2-chloro-6-fluorobenzoyl)-1*H*-pyrrole-2-carboxamido)piperidine-1-carboxylate, 284**

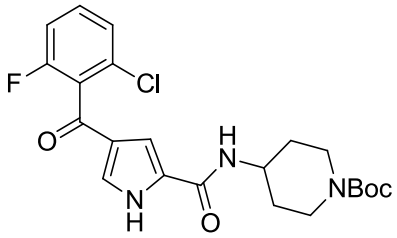

General procedure M: 4-(2-chloro-6-fluorobenzoyl)-1*H*-pyrrole-2-carboxylic acid (100 mg, 0.37 mmol), PCl_3 (31 µL, 0.37 mmol) and *tert*-butyl 4-aminopiperidine-1-carboxylate (185 mg, 0.93 mmol). Purification *via* column chromatography (silica; 30-70% EtOAc/petrol) gave **284** as a white solid (77 mg, 46%). R_f 0.69 (9:1 DCM/MeOH); m.p. 153-155 ^oC; λ_{max} (EtOH/nm) 283.5, 235.5; IR υ_{max}/cm^{-1} 3130, 2976, 2932, 2862, 1623, 1569, 1535; ^1H NMR (500 MHz, DMSO-d_6) δ ppm 1.31-1.39 (2H, m, CH-piperidine), 1.41 (9H, s, C-CH_3), 1.75-1.78 (2H, m, CH-piperidine), 2.84 (2H, br s, N-CH-piperidine), 3.89-3.96 (3H, m, N-CH-piperidine), 7.18 (1H, br s, H-3), 7.33 (1H, br s, H-5), 7.37-7.39 (1H, m, H-5'), 7.45-7.46 (1H, m, H-3'), 7.57 (1H, ddd, J = 6.2, 8.3 and 8.4 Hz, H-4'), 8.11 (1H, d, J = 7.8 Hz, CO-NH), 12.42 (1H, s, NH-pyrrole); ^{13}C NMR (125 MHz, DMSO-d_6) δ ppm 28.1 (C-CH_3), 31.4 (C-piperidine), 45.9 (C-piperidine), 78.6 (*C*-CH_3), 109.9 (C-Ar), 114.9 (d, J_{CF} = 21.6 Hz, C-Ar), 125.0 (C-Ar), 125.8 (d, J_{CF} = 2.7 Hz, C-Ar), 128.1 (C-Ar), 128.2 (d, J_{CF} = 23.0 Hz, C-Ar), 128.8 (C-Ar), 130.4 (d, J_{CF} = 5.9 Hz, C-Ar), 131.7 (d, J_{CF} = 9.1 Hz, C-Ar), 153.9 (CO), 158.5 (d, J_{CF} = 246.8 Hz, C-F), 159.0 (CO), 183.9 (CO); HRMS calcd for $C_{22}H_{25}{}^{35}ClFN_3O_4.NH_4$ $[M+NH_4]^+$ 467.1856, found 467.1855.

4-(2-Chloro-6-fluorobenzoyl)-*N*-cyclohexyl-1*H*-pyrrole-2-carboxamide, 285

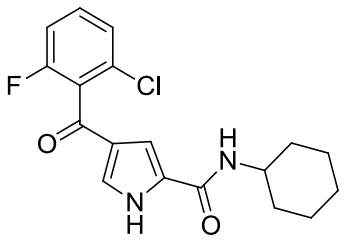

General procedure D: 4-(2-chloro-6-fluorobenzoyl)-1*H*-pyrrole-2-carboxylic acid (200 mg, 0.75 mmol), CDI (243 mg, 1.50 mmol), and cyclohexylamine (0.22 mL, 1.88 mmol). Purification *via* column chromatography (silica; 30-70% EtOAc/petrol) gave **285** with cyclohexylamine contamination. The crude sample was redissolved in DCM (10 mL) and

passed through a MP-TsOH isolute cartridge to give **285** as a white solid (170 mg, 65%). R_f 0.45 (95:5 DCM/MeOH); m.p. 288-290 ^oC; λ_{max} (EtOH/nm) 287.0, 236.5; IR υ_{max}/cm^{-1} 3361, 3161, 3123, 2929, 2854, 1617, 1570, 1533; ^1H NMR (500 MHz, DMSO-d_6) δ ppm 1.07-1.15 (1H, m, CH-cyclohexane), 1.21-1.34 (4H, m, CH-cyclohexane), 1.59-1.62 (1H, m, CH-cyclohexane), 1.71-1.80 (4H, m, CH-cyclohexane), 3.67-3.75 (1H, m, N-CH-cyclohexane), 7.20 (1H, br s, H-3), 7.31 (1H, br s, H-5), 7.37-7.40 (1H, m, H-5'), 7.45-7.46 (1H, m, H-3'), 7.57 (1H, ddd, *J* = 6.3, 8.3 and 8.4 Hz, H-4'), 8.07 (1H, d, *J* = 8.0 Hz, CO-NH), 12.38 (1H, s, NH-pyrrole); ^{13}C NMR (125 MHz, DMSO-d_6) δ ppm 24.9 (C-cyclohexane), 25.2 (C-cyclohexane), 32.5 (C-cyclohexane), 47.7 (N-C-cyclohexane), 109.8 (C-Ar), 114.9 (d, J_{CF} = 21.8 Hz, C-Ar), 124.9 (C-Ar), 125.8 (d, J_{CF} = 2.6 Hz, C-Ar), 128.0 (C-Ar), 128.2 (d, J_{CF} = 23.4 Hz, C-Ar), 129.1 (C-Ar), 130.4 (d, J_{CF} = 6.2 Hz, C-Ar), 131.7 (d, J_{CF} = 9.0 Hz, C-Ar), 158.6 (d, J_{CF} = 247.1 Hz, C-F), 158.8 (CO), 183.9 (CO); HRMS calcd for $C_{18}H_{18}{}^{35}ClFN_2O_2$ $[M+H]^+$ 349.1114, found 349.1118.

4-(2-Chloro-6-fluorobenzoyl)-*N*-(tetrahydro-*2H*-pyran-4-yl)-1*H*-pyrrole-2-carboxamide, 286

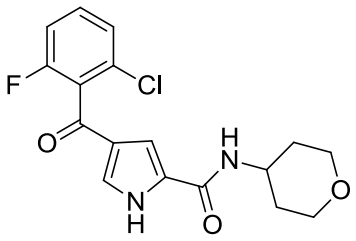

General procedure D: 4-(2-chloro-6-fluorobenzoyl)-1*H*-pyrrole-2-carboxylic acid (200 mg, 0.75 mmol), CDI (243 mg, 1.50 mmol) and 4-aminotetrahydro-2*H*-pyran (0.19 mL, 1.88 mmol). Purification *via* column chromatography (silica; 30-70% EtOAc/petrol) gave **286** as a white solid (172 mg, 65%). R_f 0.42 (95:5 DCM/MeOH); m.p. 246-248 ^oC; λ_{max} (EtOH/nm) 285.5, 238.0; IR υ_{max}/cm^{-1} 3356, 3129, 2951, 2849, 1622, 1570, 1535; ^1H NMR (500 MHz, DMSO-d_6) δ ppm 1.48-1.57 (2H, m, CH-THP), 1.72-1.75 (2H, m, CH-THP), 3.34-3.40 (2H, m, O-CH-THP), 3.35-3.88 (2H, m, O-CH-THP), 3.91-3.99 (1H, m, N-CH-THP), 7.21 (1H, br s, H-3), 7.33 (1H, br s, H-5), 7.37-7.41 (1H, m, H-5'), 7.45-7.47 (1H, m, H-3'), 7.57 (1H, ddd, *J* = 6.3, 8.3 and 8.4 Hz, H-4'), 8.17 (1H, d, *J* = 8.0 Hz, CO-NH), 12.43 (1H, s, NH-pyrrole); ^{13}C MR (125 MHz, DMSO-d_6) δ ppm 32.5 (C-THP), 45.2 (C-THP), 66.1 (N-C-THP), 109.9 (C-Ar), 114.9 (d, J_{CF} = 21.7 Hz, C-Ar), 125.0 (C-Ar), 125.8 (d, J_{CF} = 2.8 Hz, C-Ar), 128.1 (C-Ar), 128.2 (d, J_{CF} = 20.0 Hz, C-Ar), 128.9 (C-Ar), 130.4 (d, J_{CF} = 6.1 Hz, C-

Ar), 131.7 (d, J_{CF} = 8.7 Hz, C-Ar), 158.7 (d, J_{CF} = 246.4 Hz, C-F), 159.0 (CO), 183.9 (CO); HRMS calcd for $C_{17}H_{16}{}^{35}ClFN_2O_3$ $[M+H]^+$ 351.0906, found 351.0910.

4-(2-Chloro-6-fluorobenzoyl)-*N*-(piperidin-4-yl)-1*H*-pyrrole-2-carboxamide, 292

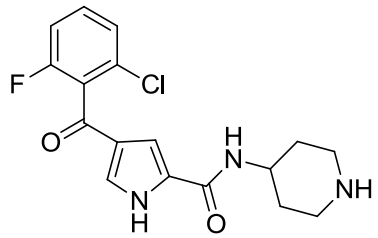

General procedure K: *tert*-butyl 4-(4-(2-chloro-6-fluorobenzoyl)-1*H*-pyrrole-2-carboxamido)piperidine-1-carboxylate (310 mg, 0.69 mmol), triethylsilane (0.27 mL, 1.73 mmol) and TFA (2 mL/mmol) gave **292** as a white solid (238 mg, 99%). R_f 0.42 (9:1 DCM/MeOH, NH silica); m.p. 177-179 ^oC; λ_{max} (EtOH/nm) 287.0, 237.0; IR υ_{max}/cm^{-1} 3300, 2944, 2848, 1628, 1571, 1532; ^1H NMR (500 MHz, $CDCl_3$) δ ppm 1.39-1.47 (2H, m, CH-piperidine), 2.01-2.05 (2H, m, CH-piperidine), 2.74-2.79 (2H, m, N-CH-piperidine), 3.12-3.16 (2H, m, N-CH-piperidine), 4.01-4.09 (1H, m, N-CH-piperidine), 6.98 (1H, d, *J* = 1.5 Hz, H-3), 7.11-7.12 (1H, m, H-5'), 7.30-7.32 (2H, m, H-5 and H-3'), 3.39 (1H, ddd, *J* = 6.2, 8.3 and 8.4 Hz, H-4'), 9.66 (1H, br s, CO-NH), 12.62 (1H, br s, NH-pyrrole); ^{13}C NMR (125 MHz, DMSO-d_6) δ ppm 32.3 (C-piperidine), 44.8 (C-piperidine), 46.3 (C-piperidine), 109.9 (C-Ar), 114.9 (d, J_{CF} = 21.7 Hz, C-Ar), 124.9 (C-Ar), 125.8 (d, J_{CF} = 2.6 Hz, C-Ar), 128.1 (C-Ar), 128.3 (C-Ar), 128.9 (C-Ar), 130.4 (d, J_{CF} = 6.1 Hz, C-Ar), 131.7 (d, J_{CF} = 8.9 Hz, C-Ar), 158.6 (d, J_{CF} = 247.5 Hz, C-Ar), 158.9 (CO), 183.9 (CO); HRMS calcd for $C_{17}H_{17}{}^{35}ClFN_3O_2$ $[M+H]^+$ 350.1066, found 350.1071.

4-(2-Bromo-6-fluorobenzoyl)-*N*-(1-methylpiperidin-4-yl)-1*H*-pyrrole-2-carboxamide, 287

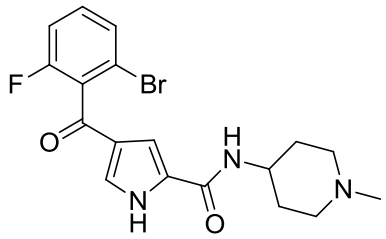

General procedure D: 4-(2-bromo-6-fluorobenzoyl)-1*H*-pyrrole-2-carboxylic acid (200 mg, 0.64 mmol), CDI (207 mg, 1.28 mmol) and 4-amino-1-methyl piperidine (200 µL, 1.60

mmol). Purification *via* column chromatography (NH silica; 0-8% MeOH/DCM) gave **287** as a white solid (214 mg, 82%). R_f 0.15 (9:1 DCM/MeOH); m.p. Degrades above 250 ^oC; λ_{max} (EtOH/nm) 288.5, 234.5; IR υ_{max}/cm^{-1} 3558, 3180, 3127, 2941, 2851, 2797, 1658, 1615, 1569, 1546; ^1H NMR (500 MHz, DMSO-d_6) δ ppm 1.48-1.56 (2H, m, CH-piperidine), 1.72-1.74 (2H, m, CH-piperidine), 1.90-1.94 (2H, N-CH-piperidine), 2.15 (3H, s, CH_3), 2.74-2.77 (2H, m, N-CH-piperidine), 3.64-3.70 (1H, m, N-CH-piperidine), 7.19 (1H, br s, H-3), 7.30 (1H, br s, H-5), 7.40-7.43 (1H, m, H-5'), 7.49 (1H, ddd, J = 6.3, 8.3 and 8.4 Hz, H-4'), 7.58-7.60 (1H, m, H-3'), 8.10 (1H, d, J = 7.8 Hz, CO-NH), 12.39 (1H, s, NH-pyrrole); ^{13}C NMR (125 MHz, DMSO-d_6) δ ppm 31.6 (C-piperidine), 45.9 (C-piperidine), 54.4 (CH_3), 110.0 (C-Ar), 115.3 (d, J_{CF} = 21.4 Hz, C-Ar), 119.0 (d, J_{CF} = 4.8 Hz, C-Ar), 124.6 (C-Ar), 128.1 (C-Ar), 128.8 (d, J_{CF} = 2.7 Hz, C-Ar), 129.0 (C-Ar), 130.1 (d, J_{CF} = 22.7 Hz, C-Ar), 132.0 (d, J_{CF} = 8.3 Hz, C-Ar), 158.5 (d, J_{CF} = 248.0 Hz, C-F), 159.1 (CO), 184.8 (CO); HRMS calcd for $C_{18}H_{19}{}^{79}BrFN_3O_2$ $[M+H]^+$ 408.0717, found 408.0719.

***tert*-Butyl 4-(4-(2-bromo-6-fluorobenzoyl)-1*H*-pyrrole-2-carboxamido)piperidine-1-carboxylate, 288**

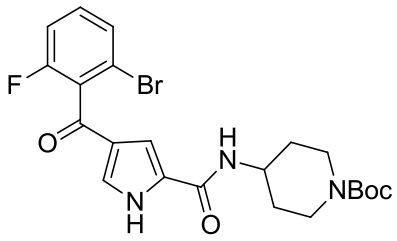

General procedure D: 4-(2-bromo-6-fluorobenzoyl)-1*H*-pyrrole-2-carboxylic acid (100 mg, 0.32 mmol), CDI (103 mg, 0.64 mmol), and *tert*-butyl 4-aminopiperidine-1-carboxylate (160 mg, 0.80 mmol). Purification *via* column chromatography (silica; 30-70% EtOAc/petrol) gave **288** as a white solid (141 mg, 89%). R_f 0.66 (9:1 DCM/MeOH); m.p. 205-207 ^oC; λ_{max} (EtOH/nm) 286.5, 236.5; IR υ_{max}/cm^{-1} 3359, 3177, 3121, 2976, 2934, 2859, 1693, 1660, 1618, 1567, 1535; ^1H NMR (500 MHz, DMSO-d_6) δ ppm 1.31-1.40 (2H, m, CH-piperidine), 1.41 (9H, s, C-CH_3), 1.75-1.78 (2H, m, CH-piperidine), 2.84 (2H, br s, N-CH-piperidine), 3.89-3.97 (3H, m, N-CH-piperidine), 7.18 (1H, br s, H-3), 7.30 (1H, br s, H-5), 7.39-7.43 (1H, m, H-5'), 7.49 (1H, ddd, J = 6.2, 8.3 and 8.4 Hz, H-4'), 7.58-7.60 (1H, m, H-3'), 8.12 (1H, d, J = 8.0 Hz, CO-NH), 12.40 (1H, s, NH-pyrrole); ^{13}C NMR (125 MHz, DMSO-d_6) δ ppm 28.1 (C-*CH3*), 31.4 (C-piperidine), 45.9 (C-piperidine), 78.6 (*C*-CH_3), 110.0 (C-Ar), 115.3 (d, J_{CF} = 21.7 Hz, C-Ar), 119.0 (d, J_{CF} = 5.1 Hz, C-Ar), 124.7 (C-Ar), 128.1 (C-Ar),

128.8 (C-Ar), 130.1 (d, J_{CF} = 23.2 Hz, C-Ar), 132.0 (d, J_{CF} = 8.9 Hz, C-Ar), 153.9 (CO), 158.5 (d, J_{CF} = 246.8 Hz, C-F), 159.0 (CO), 184.8 (CO), one F split C-Ar not visualised; HRMS calcd for $C_{22}H_{25}{}^{79}BrFN_3O_4$ $[M+H]^+$ 494.1085, found 494.1082.

4-(2-Bromo-6-fluorobenzoyl)-*N*-cyclohexyl-1*H*-pyrrole-2-carboxamide, 289

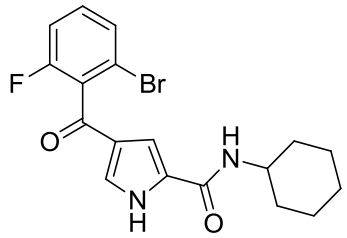

General procedure D: 4-(2-bromo-6-fluorobenzoyl)-1*H*-pyrrole-2-carboxylic acid (200 mg, 0.64 mmol), CDI (207 mg, 1.28 mmol and cyclohexylamine (180 µL, 1.60 mmol). Purification *via* column chromatography (silica; 30-70% EtOAc/petrol) gave **289** with cyclohexylamine contamination. The crude sample was redissolved in DCM (10 mL) and passed through a MP-TsOH isolute cartridge to give **289** as a white solid (169 mg, 67%). R_f 0.43 (95:5 DCM/MeOH); m.p. 296-298 ^oC; λ_{max} (EtOH/nm) 286.5, 236.5; IR υ_{max}/cm^{-1} 3356, 3118, 3055, 2928, 2854, 1615, 1569, 1537; ^1H NMR (500 MHz, DMSO-d_6) δ ppm 1.07-1.15 (1H, m, CH-cyclohexane), 1.12-1.34 (4H, m, CH-cyclohexane), 1.58-1.62 (1H, m, CH-cyclohexane), 1.71-1.80 (4H, m, CH-cyclohexane), 3.68-3.75 (1H, m, N-CH-cyclohexane), 7.20 (1H, br s, H-3), 7.29 (1H, br s, H-5), 7.40-7.43 (1H, m, H-5'), 7.49 (1H, ddd, J = 6.3, 8.3 and 8.4 Hz, H-4'), 7.58-7.60 (1H, m, H-3'), 8.07 (1H, d, J = 8.0 Hz, CO-NH), 12.37 (1H, s, NH-pyrrole); ^{13}C NMR (125 MHz, DMSO-d_6) δ ppm 24.9 (C-cyclohexane), 25.2 (C-cyclohexane), 32.5 (C-cyclohexane), 47.7 (N-C-cyclohexane), 109.8 (C-Ar), 115.3 (d, J_{CF} = 21.5 Hz, C-Ar), 119.1 (d, J_{CF} = 5.1 Hz, C-Ar), 124.6 (C-Ar), 128.0 (C-Ar), 128.8 (d, J_{CF} = 2.5 Hz, C-Ar), 129.0 (C-Ar), 130.1 (d, J_{CF} = 22.8 Hz, C-Ar), 132.0 (d, J_{CF} = 8.8 Hz, C-Ar), 158.6 (d, J_{CF} = 247.4 Hz, C-F), 158.8 (CO), 184.8 (CO); HRMS calcd for $C_{18}H_{18}{}^{79}BrFN_2O_2$ $[M+H]^+$ 393.0608, found 393.0612.

4-(2-Bromo-6-fluorobenzoyl)-*N*-(tetrahydro-2*H*-pyran-4-yl)-1*H*-pyrrole-2-carboxamide, 290

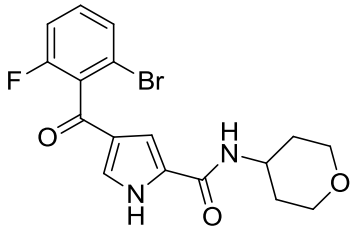

General procedure D: 4-(2-bromo-6-fluorobenzoyl)-1*H*-pyrrole-2-carboxylic acid (200 mg, 0.64 mmol), CDI (207 mg, 1.28 mmol), and 4-aminotetrahydro-2*H*-pyran (170 µL, 1.60 mmol). Purification *via* column chromatography (silica; 30-70% EtOAc/petrol) gave **290** as a white solid (180 mg, 71%). R_f 0.39 (95:5 DCM/MeOH); m.p. 250-251 ^oC; λ_{max} (EtOH/nm) 287.0, 236.0; IR υ_{max}/cm^{-1} 3352, 3179, 3122, 2956, 2852, 1734, 1619, 1568, 1536; ^1H NMR (500 MHz, DMSO-d_6) δ ppm 1.48-1.56 (2H, m, CH-THP), 1.72-1.75 (2H, m, CH-THP), 3.35-3.40 (2H, m, O-CH-THP), 3.85-3.88 (2H, m, O-CH-THP), 3.91-3.99 (1H, m, N-CH-THP), 7.20 (1H, br s, H-3), 7.31 (1H, br s, H-5), 7.40-7.44 (1H, m, H-5'), 7.49 (1H, ddd, *J* = 6.3, 8.2 and 8.3 Hz, H-4'), 7.59-7.60 (1H, m, H-3'), 8.17 (1H, d, *J* = 8.0 Hz, CO-NH), 12.42 (1H, s, NH-pyrrole); ^{13}C NMR (125 MHz, DMSO-d_6) δ ppm 32.5 (C-THP), 45.2 (C-THP), 66.1 (N-C-THP), 110.0 (C-Ar), 115.3 (d, J_{CF} = 21.8 Hz, C-Ar), 119.0 (d, J_{CF} = 5.3 Hz, C-Ar), 124.6 (C-Ar), 128.1 (C-Ar), 128.7 (C-Ar), 128.8 (d, J_{CF} = 2.7 Hz, C-Ar), 130.1 (d, J_{CF} = 22.9 Hz, C-Ar), 132.0 (d, J_{CF} = 9.0 Hz, C-Ar), 158.6 (d, J_{CF} = 247.4 Hz, C-F), 159.0 (CO), 184.8 (CO); HRMS calcd for $C_{17}H_{16}{}^{79}BrFN_2O_3$ $[M+H]^+$ 395.0401, found 395.0403.

4-(2-Bromo-6-fluorobenzoyl)-*N*-(piperidin-4-yl)-1*H*-pyrrole-2-carboxamide, 293

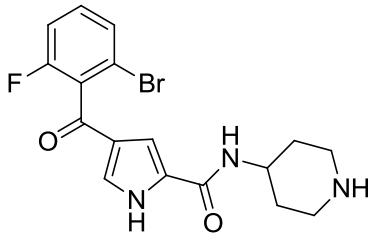

General procedure K: *tert*-butyl 4-(4-(2-bromo-6-fluorobenzoyl)-1*H*-pyrrole-2-carboxamido)piperidine-1-carboxylate (130 mg, 0.26 mmol), triethylsilane (0.10 mL, 0.65 mmol) and TFA (2 mL/mmol) gave **293** as a white solid (102 mg, 100%). R_f 0.50 (9:1 DCM/MeOH, NH silica); m.p. 250-252 ^oC; λ_{max} (EtOH/nm) 281.0, 236.0; IR υ_{max}/cm^{-1} 3301, 2945, 2844, 1626, 1600, 1568, 1530; ^1H NMR (500 MHz, DMSO-d_6) δ ppm 1.33-1.41 (2H,

m, CH-piperidine), 1.69-1.73 (2H, m, CH-piperidine), 2.48-2.54 (2H, m, N-CH-piperidine), 2.94-2.98 (2H, m, N-CH-piperidine), 3.74-3.81 (1H, m, N-CH-piperidine), 7.21 (1H, br s, H-3), 7.29 (1H, br s, H-5), 7.39-7.43 (1H, m, H-5'), 7.49 (1H, ddd, J = 6.2, 8.2 and 8.3 Hz, H-4'), 7.58-7.60 (1H, m, H-3'), 8.10 (1H, d, J = 8.0 Hz, CO-NH), NH-pyrrole not observed; ^{13}C NMR (125 MHz, DMSO-d_6) δ ppm 32.8 (C-piperidine), 45.1 (C-piperidine), 46.7 (C-piperidine), 109.9 (C-Ar), 115.3 (d, J_{CF} = 21.7 Hz, C-Ar), 119.0 (d, J_{CF} = 5.3 Hz, C-Ar), 124.6 (C-Ar), 128.1 (C-Ar), 128.8 (d, J_{CF} = 2.9 Hz, C-Ar), 129.0 (C-Ar), 130.1 (d, J_{CF} = 22.5 Hz, C-Ar), 132.0 (d, J_{CF} = 8.6 Hz, C-Ar), 158.5 (d, J_{CF} = 246.9 Hz, C-F), 158.8 (CO), 184.8 (CO); HRMS calcd for $C_{17}H_{17}{}^{79}BrFN_3O_2$ $[M+H]^+$ 394.0561, found 394.0564.

Methyl 2-bromo-6-fluorobenzoate, 313

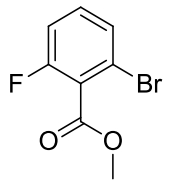

To a solution of methyl 2-bromo-6-fluorobenzoic acid (1.00 g, 4.56 mmol) in MeCN (2 mL/mmol) was added *O*-methyl-*N,N'*-diisopropylisourea (1.00 mL, 5.48 mmol). The resulting solution was heated at 120 ^{o}C with microwave irradiation for 5 min. The crude mixture was filtered under suction, washing with diethyl ether (2 x 10 mL) and the precipitate discarded. Purification *via* column chromatography (silica; 0-10% EtOAc/petrol) gave **313** as a colourless oil (0.92 g, 87%). R_f 0.42 (8:2 Petrol/EtOAc); λ_{max} (EtOH/nm) 272.0; IR υ_{max}/cm^{-1} 2954, 1738, 1605, 1573, 1449, 1282; ^{1}H NMR (500 MHz, $CDCl_3$) δ ppm 3.90 (3H, s, O-CH_3), 7.00-7.03 (1H, m, H-5), 7.19 (1H, ddd, J = 5.8, 8.2 and 8.3 Hz, H-4), 7.31-7.33 (1H, m, H-3); ^{13}C NMR (125 MHz, $CDCl_3$) δ ppm 53.0 (CH_3), 115.0 (d, J_{CF} = 21.4 Hz, C-Ar), 120.3 (d, J_{CF} = 4.1 Hz, C-Ar), 124.6 (d, J_{CF} = 19.9 Hz, C-Ar), 128.6 (d, J_{CF} = 3.5 Hz, C-Ar), 132.0 (d, J_{CF} = 8.9 Hz, C-Ar), 159.6 (d, J_{CF} = 254.0 Hz, C-F), 164.4 (CO); MS (ES+) *m/z* = 233.2 $[(^{79}BrM)+H]^+$.

Methyl 2-ethyl-6-fluorobenzoate, 314

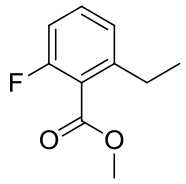

General procedure N: methyl 2-bromo-6-fluorobenzoate (250 mg, 1.07 mmol), ethylboronic acid (237 mg, 3.21 mmol), Cs_2CO_3 (522 mg, 1.61 mmol), and $Pd(dtbf)Cl_2$ (10 mol%). Purification *via* column chromatography (silica; 0-15% EtOAc/petrol) gave **314** as a colourless oil (129 mg, 66%). R_f 0.52 (8:2 Petrol/EtOAc); λ_{max} (EtOH/nm) 269.5; IR υ_{max}/cm^{-1} 1736, 1616, 1581; ^1H NMR (500 MHz, $CDCl_3$) δ ppm 1.14 (3H, t, *J* = 7.4 Hz, CH_3), 2.63 (2H, q, *J* = 7.4 Hz, CH_2), 3.86 (3H, s, O-CH_3), 6.85-6.89 (1H, m, H-5), 6.95-6.97 (1H, m, H-3), 7.25 (1H, ddd, *J* = 5.8, 8.2 and 8.3 Hz, H-4); ^{13}C NMR (125 MHz, $CDCl_3$) δ ppm 15.5 (CH_3), 26.6 (CH_2), 52.4 (O-CH_3), 113.2 (d, J_{CF} = 21.6 Hz, C-Ar), 121.2 (d, J_{CF} = 16.0 Hz, C-Ar), 124.4 (d, J_{CF} = 2.8 Hz, C-Ar), 131.4 (d, J_{CF} = 8.9 Hz, C-Ar), 144.8 (d, J_{CF} = 1.8 Hz, C-Ar), 159.8 (d, J_{CF} = 250.4 Hz, C-F), 166.4 (CO); HRMS calcd for $C_{10}H_{11}FO_2$ $[M+H]^+$ 183.0816, found 183.0813.

2-Ethyl-6-fluorobenzoic acid, 318

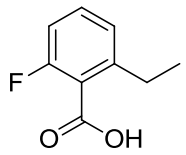

A microwave *via*l was charged with methyl 2-ethyl-6-fluorobenzoate (1.14 g, 6.26 mmol), LiCl (1.33 g, 31.30 mmol) and DMF (5 mL). The resulting mixture was heated at 150 ^oC with microwave irradiation for 1 h. Water was added (50 mL) and adjusted to pH10 with a 1M aqueous solution of NaOH, and washed with EtOAc (50 mL). The aqueous phase was then acidified (pH2-3) with a 1M aqueous solution of HCl and the product extracted into EtOAc (2 x 50 mL). Combined organic layers were washed with brine, dried over Na_2SO_4 and concentrated *in vacuo* to give **318** as a colourless oil (0.79 g, 75%). R_f 0.15 (9:1 DCM/MeOH); λ_{max} (EtOH/nm) 268.5; IR υ_{max}/cm^{-1} 2970, 2877, 2651, 2541, 1690, 1616, 1579; ^1H NMR (500 MHz, $CDCl_3$) δ ppm 1.29 (3H, t, *J* = 7.5 Hz, CH3), 2.86 (2H, q, J = 7.5 Hz, CH2), 7.00-7.03 (1H, m, H-5), 7.10-7.11 (1H, m, H-3), 7.40 (1H, ddd, J = 5.8, 8.2 and 8.3 Hz, H-4), 10.73 (1H, br s, COOH); ^{13}C NMR (125 MHz, $CDCl_3$) δ ppm 15.7 (CH_3), 26.8

(CH_2), 113.5 (d, J_{CF} = 22.3 Hz, C-Ar), 119.8 (d, J_{CF} = 14.4 Hz, C-Ar), 124.8 (d, J_{CF} = 3.1 Hz, C-Ar), 132.2 (d, J_{CF} = 9.2 Hz, C-Ar), 145.6 (C-Ar), 160.4 (d, J_{CF} = 252.7 Hz, C-F), 170.7 (CO); HRMS calcd for $C_9H_9FO_2$ $[M-H]^-$ 167.0514, found 167.0514.

Methyl 4-(2-ethyl-6-fluorobenzoyl)-1*H*-pyrrole-2-carboxylate, 320

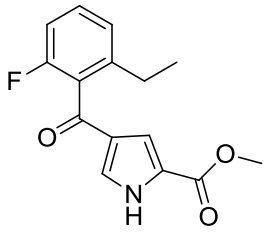

General procedure E: 2-ethyl-6-fluorobenzoic acid (486 mg, 2.89 mmol), $SOCl_2$ (316 µL, 4.34 mmol) and DMF (10 mol%) gave 2-ethyl-6-fluorobenzoyl chloride as a yellow oil which was used directly in the next step. **General procedure F:** methyl 1*H*-pyrrole-2-carboxylate (242 mg, 1.93 mmol) and $AlCl_3$ (0.65 g, 4.84 mmol). Purification *via* column chromatography (silica; 0-50% EtOAc/petrol) gave **320** as a colourless oil (441 mg, 83%). R_f 0.25 (8:2 Petrol/EtOAc); λ_{max} (EtOH/nm) 283.0, 231.5; IR υ_{max}/cm^{-1} 3259, 3136, 2972, 2879, 1709, 1613, 1635, 1558; ^{1}H NMR (500 MHz, $CDCl_3$) δ ppm 1.17 (3H, t, J = 7.5 Hz, CH_3), 2.62 (2H, q, J = 7.5 Hz, CH_2), 3.90 (3H, s, O-CH_3), 6.97-7.00 (1H, m, H-5'), 7.10-7.12 (1H, m, H-3'), 7.22 (1H, br s, H-3), 7.36 (1H, ddd, J = 5.9, 8.2 and 8.3 Hz, H-4'), 7.44 (1H, dd, J = 1.3 and 3.2 Hz, H-5), 9.54 (1H, s, NH-pyrrole); ^{13}C NMR (125 MHz, $CDCl_3$) δ ppm 15.7 (CH_3), 26.0 (CH_2), 52.0 (O-CH_3), 113.0 (d, J_{CF} = 21.6 Hz, C-Ar), 115.5 (C-Ar), 124.4 (C-Ar), 124.5 (d, J_{CF} = 2.7 Hz, C-Ar), 127.9 (C-Ar), 128.2 (C-Ar), 130.6 (d, J_{CF} = 8.4 Hz, C-Ar), 144.2 (d, J_{CF} = 2.8 Hz, C-Ar), 159.0 (d, J_{CF} = 244.5 Hz, C-F), 161.2 (CO), 188.8 (CO), one C-Ar not visualised; HRMS calcd for $C_{15}H_{14}FNO_3$ $[M+H]^+$ 276.1030, found 276.1035.

4-(2-Ethyl-6-fluorobenzoyl)-1*H*-pyrrole-2-carboxylic acid, 321

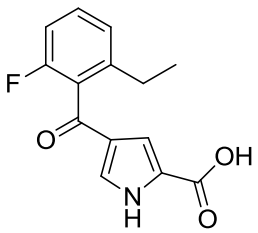

General procedure G: methyl 4-(2-ethyl-6-fluorobenzoyl)-1*H*-pyrrole-2-carboxylate (400 mg, 1.45 mmol), and LiOH monohydrate (1.22 g, 29.00 mmol) gave **321** as a white solid (378 mg, 100%). R_f 0.21 (9:1 DCM/MeOH); m.p. 179-181 ^oC; λ_{max} (EtOH/nm) 275.5, 230.5;

IR υ_{max}/cm^{-1} 3338, 2961, 2921, 2852, 2705, 2625, 1688, 1641, 1560; ^{1}H NMR (500 MHz, DMSO-d_6) δ ppm 1.07 (3H, t, J = 7.5 Hz, CH_3), 2.48 (2H, q, J = 7.5 Hz, CH_2), 6.91 (1H, br s, H-3), 7.13-7.17 (1H, m, H-5'), 7.19-7.21 (1H, m, H-3'), 7.34 (1H, br s, H-5), 7.45 (1H, ddd, J = 6.2, 8.3 and 8.4 Hz, H-4'), 12.61 (1H, s, NH-pyrrole), 12.86 (1H, s, COOH); ^{13}C NMR (125 MHz, DMSO-d_6) δ ppm 15.6 (CH_3), 25.3 (CH_2), 112.9 (d, J_{CF} = 21.5 Hz, C-Ar), 114.2 (C-Ar), 124.8 (d, J_{CF} = 2.2 Hz, C-Ar), 125.5 (C-Ar), 126.5 (C-Ar), 127.9 (d, J_{CF} = 18.2 Hz, C-Ar), 128.9 (C-Ar), 130.7 (d, J_{CF} = 8.4 Hz, C-Ar), 143.2 (d, J_{CF} = 2.9 Hz, C-Ar), 158.2 (d, J_{CF} = 243.5 Hz, C-F), 161.3 (CO), 187.6 (CO); HRMS calcd for $C_{14}H_{12}FNO_3$ $[M-H]^-$ 260.0728, found 260.0718.

4-(2-Ethyl-6-fluorobenzoyl)-*N*-(pyridin-3-yl)-1*H*-pyrrole-2-carboxamide, 300

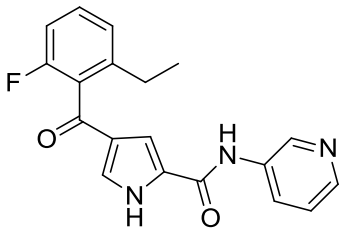

General procedure M: 4-(2-ethyl-6-fluorobenzoyl)-1*H*-pyrrole-2-carboxylic acid (50 mg, 0.19 mmol), PCl_3 (16 µL, 0.19 mmol), and 3-aminopyridine (45 mg, 0.48 mmol). Purification *via* column chromatography (silica; 0-8% MeOH/DCM) gave **300** as a white solid (41 mg, 64%). R_f 0.29 (95:5 DCM/MeOH); m.p. 197-200 ^{o}C; λ_{max} (EtOH/nm) 292.5, 248.5; IR υ_{max}/cm^{-1} 3295, 3117, 2969, 2937, 2876, 1641, 1535; ^{1}H NMR (500 MHz, DMSO-d_6) δ ppm 1.10 (3H, t, J = 7.5 Hz, CH_3), 2.49 (2H, t, J = 7.5 Hz, CH_2), 7.16-7.19 (1H, m, H-5'), 7.22-7.24 (1H, m, H-3'), 7.37 (1H, br s, H-3), 7.39 (1H, dd, J = 4.7 and 8.4 Hz, CH-pyridine), 7.45-7.50 (2H, m, H-5 and H-4'), 3.14 (1H, ddd, J = 1.5, 2.5, and 8.4 Hz, CH-pyridine), 8.30 (1H, dd, J = 1.5 and 4.7 Hz, N-CH-pyridine), 8.89 (1H, d, J = 2.5 Hz, N-CH-pyridine), 10.24 (1H, s, CO-NH), 12.62 (1H, s, NH-pyrrole); ^{13}C NMR (125 MHz, DMSO-d_6) δ ppm 15.6 (CH_3), 25.4 (CH_2), 111.6 (C-Ar), 113.0 (d, J_{CF} = 21.5 Hz, C-Ar), 123.5 (C-Ar), 124.8 (d, J_{CF} = 2.5 Hz, C-Ar), 126.5 (C-Ar), 127.0 (C-Ar), 127.8 (C-Ar), 128.0 (d, J_{CF} = 18.7 Hz, C-Ar), 128.6 (C-Ar), 130.7 (d, J_{CF} = 8.8 Hz, C-Ar), 135.5 (C-Ar), 141.6 (C-Ar), 143.6 (d, J_{CF} = 3.3 Hz, C-Ar), 144.4 (C-Ar), 158.3 (d, J_{CF} = 242.4 Hz, C-F), 158.8 (CO), 187.8 (CO); HRMS calcd for $C_{19}H_{16}FN_3O_2$ $[M+H]^+$ 338.1300, found 338.1304.

***tert*-Butyl 4-(4-(2-ethyl-6-fluorobenzoyl)-1*H*-pyrrole-2-carboxamido)piperidine-1-carboxylate, 322**

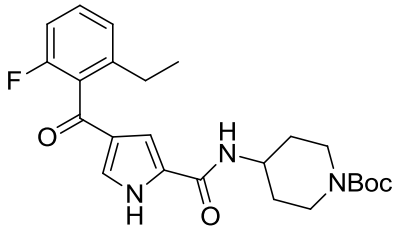

General procedure D: 4-(2-ethyl-6-fluorobenzoyl)-1*H*-pyrrole-2-carboxylic acid (86 mg, 0.33 mmol), CDI (107 mg, 0.66 mmol) and *tert*-butyl 4-aminopiperidine-1-carboxylate (166 mg, 0.83 mmol). Purification *via* column chromatography (silica; 30-70% EtOAc/petrol) gave **322** as a white solid (126 mg, 86%). R_f 0.66 (9:1 DCM/MeOH); m.p. 133-135 ^oC; λ_{max} (EtOH/nm) 282.5, 235.0; IR υ_{max}/cm^{-1} 3194, 3127, 2973, 2933, 2873, 1614, 1568, 1533; ^1H NMR (500 MHz, DMSO-d_6) δ ppm 1.07 (3H, t, J = 7.5 Hz, CH_3), 1.31-1.39 (2H, m, CH-piperidine), 1.41 (9H, s, C-CH_3), 1.74-1.77 (2H, m, CH-piperidine), 2.49 (2H, q, J = 7.5 Hz, CH_2), 2.84 (2H, br s, N-CH-piperidine), 3.88-3.96 (3H, m, N-CH-piperidine), 7.13-7.21 (4H, m, H-3, H-5, H-3' and H-5'), 7.45 (1H, ddd, J = 6.3, 8.3 and 8.4 Hz, H-4'), 8.11 (1H, d, J = 8.0 Hz, CO-NH), 12.31 (1H, s, NH-pyrrole); ^{13}C NMR (125 MHz, $CDCl_3$) δ ppm 15.7 (CH_3), 26.0 (CH_2), 28.4 (C-CH_3), 32.1 (C-piperidine), 42.7 (C-piperidine), 47.0 (C-piperidine), 79.8 (*C*-CH_3), 108.8 (C-Ar), 113.0 (d, J_{CF} = 21.4 Hz, C-Ar), 127.7 (C-Ar), 127.8 (d, J_{CF} = 13.8 Hz, C-Ar), 130.6 (d, J_{CF} = 8.5 Hz, C-Ar), 144.1 (C-Ar), 154.7 (CO), 159.7 (CO), 188.9 (CO), three C-Ar and C-F not visualised; HRMS calcd for $C_{24}H_{30}FN_3O_4$ $[M+H]^+$ 444.2293, found 444.2289.

4-(2-Ethyl-6-fluorobenzoyl)-*N*-(piperidin-4-yl)-1*H*-pyrrole-2-carboxamide smm435-001

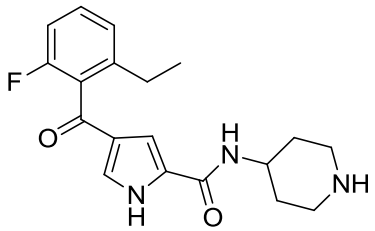

General procedure K: *tert*-butyl 4-(4-(2-ethyl-6-fluorobenzoyl)-1*H*-pyrrole-2-carboxamido)piperidine-1-carboxylate (100 mg, 0.23 mmol), triethylsilane (92 µL, 0.58 mmol) and TFA (2 mL/mmol) gave **301** as a white solid (73 mg 93%). R_f 0.60 (9:1 DCM/MeOH, NH silica); m.p. 172-174 ^oC; λ_{max} (EtOH/nm) 234.0, 206.5; IR υ_{max}/cm^{-1} 3377,

2978, 2855, 2748, 1778, 1664, 1614, 1564, 1533, 1501; ^{1}H NMR (500 MHz, DMSO-d_6) δ ppm 1.03 (3H, t, J = 7.5 Hz, CH_3), 1.58-1.67 (2H, m, CH-piperidine), 1.89-1.93 (2H, m, CH-piperidine), 2.45 (2H, q, J = 7.5 Hz, CH_2), 2.95-3.01 (2H, m, N-CH-piperidine), 3.26-3.29 (2H, m, N-CH-piperidine), 3.95-4.02 (1H, m, N-CH-piperidine), 7.09-7.12 (1H, m, H-5'), 7.15-7.16 (1H, m, H-3'), 7.41 (1H, ddd, J = 6.3, 8.3 and 8.4 Hz, H-4'), 8.24 (1H, d, J = 8.0 Hz, CO-NH), 8.33 (1H, br s, H-3), 8.56 (1H, br s, H-5), 12.30 (1H, s, NH); ^{13}C NMR (125 MHz, DMSO-d_6) δ ppm 15.6 (CH_3), 25.3 (CH_2), 28.3 (C-piperidine), 42.3 (C-piperidine), 43.7 (C-piperidine), 110.1 (C-Ar), 112.9 (d, J_{CF} = 21.6 Hz, C-Ar), 124.7 (d, J_{CF} = 2.2 Hz, C-Ar), 126.2 (C-Ar), 127.7 (C-Ar), 128.1 (d, J_{CF} = 18.7 Hz, C-Ar), 128.3 (C-Ar), 130.6 (d, J_{CF} = 8.5 Hz, C-Ar), 143.2 (d, J_{CF} = 2.8 Hz, C-Ar), 158.2 (d, J_{CF} = 243.0 Hz, C-F), 159.4 (CO), 187.8 (CO); HRMS calcd for $C_{19}H_{22}FN_3O_2$ $[M+H]^+$ 344.1769, found 344.1771.

4-(2-Ethyl-6-fluorobenzoyl)-*N*-(1-methylpiperidin-4-yl)-1*H*-pyrrole-2-carboxamide, 302

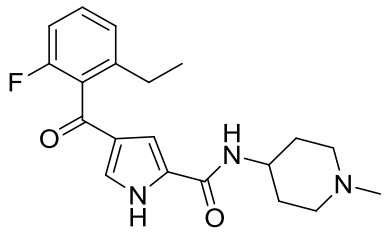

General procedure D: 4-(2-ethyl-6-fluorobenzoyl)-1*H*-pyrrole-2-carboxylic acid (50 mg, 0.19 mmol), CDI (62 mg, 0.38 mmol), and 4-amino-1-methyl piperidine (60 µL, 0.48 mmol). Purification *via* column chromatography (NH silica; 0-8% MeOH/DCM) gave **302** as a white solid (54 mg, 79%). R_f 0.16 (9:1 DCM/MeOH); m.p. 183-186 ^{o}C; λ_{max} (EtOH/nm) 283.0, 237.0, 207.0; IR υ_{max}/cm^{-1} 3354, 3120, 2935, 2863, 2792, 2684, 1614, 1571, 1537; ^{1}H NMR (500 MHz, DMSO-d_6) δ ppm 1.07 (3H, t, J = 7.5 Hz, CH_3), 1.48-1.56 (2H, m, CH-piperidine), 1.71-1.75 (2H, m, CH-piperidine), 1.89-1.95 (2H, m, N-CH-piperidine), 2.16 (3H, s, N-CH_3), 2.49 (2H, q, J = 7.5 Hz, CH_2), 2.74-2.76 (2H, m, N-CH-piperidine), 3.63-3.71 (1H, m, N-CH-piperidine), 6.92 (1H, br s, H-3), 7.12-7.21 (3H, m, H-5, H-3', H-5'), 7.45 (1H, ddd, J = 6.3, 8.3 and 8.4 Hz, H-4'), 8.09 (1H, d, J = 8.0 Hz, CO-NH), 12.01 (1H, s, NH-pyrrole); ^{13}C NMR (125 MHz, DMSO-d_6) δ ppm 15.6 (CH_3), 25.3 (CH_2), 31.5 (C-piperidine), 45.9 (N-CH_3), 46.0 (C-piperidine), 54.4 (C-piperidine), 109.9 (C-Ar), 112.9 (d, J_{CF} = 21.8 Hz, C-Ar), 126.2 (C-Ar), 127.3 (C-Ar), 128.2 (d, J_{CF} = 18.8 Hz, C-Ar), 128.6 (C-Ar), 130.5 (d, J_{CF} = 8.6 Hz, C-Ar), 135.1 (C-Ar), 143.2 (C-Ar), 158.1 (d, J_{CF} = 243.2 Hz, C-F), 159.2 (CO), 187.8 (CO); HRMS calcd for $C_{20}H_{24}FN_3O_2$ $[M+H]^+$ 358.1925, found 358.1929.

Methyl 4-(2-bromo-6-fluorobenzoyl)-1-tosyl-1*H*-pyrrole-2-carboxylate, 325

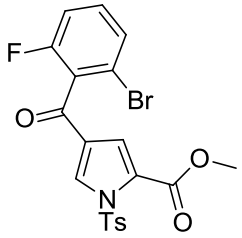

To a solution of methyl 4-(2-bromo-6-fluorobenzoyl)-1*H*-pyrrole-2-carboxylate (1.23 g, 3.77 mmol), in THF (1 mL/mmol) was added KO^{t}Bu (0.51 g, 4.52 mmol) at 0 ^{o}C. The resulting mixture was warmed to RT and stirred for 15 min. TsCl (0.86 g, 4.52 mmol) was then added, and the solution stirred for 16 h. The product was extracted with EtOAc (3 x 100 mL), and washed with brine (100 mL). Combined organic layers were dried over Na_2SO_4 and concentrated *in vacuo.* Purification *via* column chromatography (silica; 0-50% EtOAc/petrol) gave **325** as a white solid (1.60 g, 89%). R_f 0.20 (8:2 Petrol/EtOAc); m.p. 158-160 ^{o}C; λ_{max} (EtOH/nm) 236.5; IR υ_{max}/cm^{-1} 3140, 2956, 1733, 1660, 1598, 1549; ^{1}H NMR (500 MHz, DMSO-d_6) δ ppm 2.43 (3H, s, CH_3), 3.73 (3H, s, O-CH_3), 7.27 (1H, d, J = 2.0 Hz, H-3), 7.47-7.50 (1H, m, H-5), 7.52 (2H, d, J = 8.3 Hz, CH-tosyl), 7.58 (1H, ddd, J = 6.3, 8.3 and 8.4 Hz, H-4'), 7.65-7.67 (1H, m, H-3'), 8.05 (2H, d, J = 8.3 Hz, CH-tosyl), 8.32 (1H, d, J = 2.0 Hz, H-5); ^{13}C NMR (125 MHz, DMSO-d_6) δ ppm 26.4 (CH_3), 57.7 (O-CH_3), 120.9 (d, J_{CF} = 21.4 Hz, C-Ar), 124.2 (d, J_{CF} = 4.7 Hz, C-Ar), 125.2 (C-Ar), 129.5 (C-Ar), 131.6 (C-Ar), 133.6 (d, J_{CF} = 21.6 Hz, C-Ar), 133.8 (C-Ar), 133.9 (C-Ar), 134.4 (d, J_{CF} = 3.2 Hz, C-Ar), 135.2 (C-Ar), 138.3 (d, J_{CF} = 8.6 Hz, C-Ar), 138.7 (C-Ar), 139.3 (C-Ar), 151.7 (CO), 163.5 (CO), 163.8 (d, J_{CF} = 245.9 Hz, C-F); HRMS calcd for $C_{20}H_{15}{}^{79}BrFNO_5S$ $[M+H]^+$ 479.9911, found 479.9908.

4-(2-Cyclopropyl-6-fluorobenzoyl)-1*H*-pyrrole-2-carboxylic acid, 326

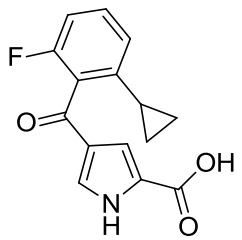

General procedure N: methyl 4-(2-bromo-6-fluorobenzoyl)-1-tosyl-1*H*-pyrrole-2-carboxylate (286 mg, 0.59 mmol), cyclopropylboronic acid (152 mg, 1.77 mmol), Cs_2CO_3 (290 mg, 0.89 mmol), and Pd(dtbf)Cl_2 (10 mol%). The crude material was used directly in

the next step. General procedure G: LiOH monohydrate (496 mg, 11.80 mmol) gave **326** as a white solid (161 mg, 76%). R_f 0.20 (9:1 DCM/MeOH); m.p. Degrades >150 ^oC; λ_{max} (EtOH/nm) 282.5, 227.0; IR υ_{max}/cm^{-1} 3360, 3005, 2793, 2705, 2629, 1682, 1650, 1617, 1561; ^1H NMR (500 MHz, MeOD) δ ppm 0.58-0.61 (2H, m, CH-cyclopropane), 0.75-0.79 (2H, m, CH-cyclopropane), 1.66-1.71 (1H, m, CH-cyclopropane), 6.74-6.75 (1H, m, H-3'), 6.88-6.92 (1H, m, H-5'), 7.03 (1H, d, J = 1.5 Hz, H-3), 7.23 (1H, d, J = 1.5 Hz, H-5), 7.27 (1H, ddd, J = 6.3, 8.3 and 8.4 Hz, H-4'), NH-pyrrole and COOH not visualised; ^{13}C NMR (125 MHz, MeOD) δ ppm 12.2 (C-cyclopropane), 16.4 (d, J_{CF} = 2.8 Hz, C-cyclopropane), 116.1 (d, J_{CF} = 21.6 Hz, C-Ar), 118.7 (C-Ar), 123.8 (d, J_{CF} = 2.8 Hz, C-Ar), 129.6 (C-Ar), 131.1 (C-Ar), 132.8 (d, J_{CF} = 18.4 Hz, C-Ar), 133.2 (C-Ar), 134.5 (d, J_{CF} = 8.7 Hz, C-Ar), 147.3 (d, J_{CF} = 3.7 Hz, C-Ar), 162.6 (d, J_{CF} = 245.0 Hz, C-F), 166.1 (CO), 193.8 (CO); HRMS calcd for $C_{15}H_{12}FNO_3$ $[M-H]^-$ 272.0728, found 272.0718.

4-(2-Cyclopropyl-6-fluorobenzoyl)-*N*-(pyridin-3-yl)-1*H*-pyrrole-2-carboxamide, 306

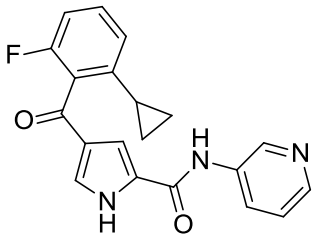

General procedure M: 4-(2-cyclopropyl-6-fluorobenzoyl)-1*H*-pyrrole-2-carboxylic acid (21 mg, 0.08 mmol), PCl_3 (7 μL, 0.08 mmol), and 3-aminopyridine (18 mg, 0.19 mmol). Purification *via* column chromatography (silica; 0-8% MeOH/DCM) gave **306** as a white solid (8 mg, 30%). R_f 0.27 (95:5 DCM/MeOH); m.p. Degrades >250 ^oC; λ_{max} (EtOH/nm) 264.5; IR υ_{max}/cm^{-1} 3417, 3123, 2957, 2923, 1633, 1556, 1534; ^1H NMR (500 MHz, MeOD) δ ppm 0.59-0.62 (2H, m, CH-cyclopropane), 0.75-0.79 (2H, m, CH-cyclopropane), 1.69-1.75 (1H, m, CH-cyclopropane), 6.75-6.77 (1H, m, H-3'), 6.90-6.93 (1H, m, H-5'), 7.26-7.34 (4H, m, H-4', H-3, H-5 and CH-pyridine), 8.11 (1H, ddd, *J* = 1.5, 2.5 and 8.3 Hz, CH-pyridine), 8.16 (1H, dd, *J* = 1.5 and 4.7 Hz, N-CH-pyridine), 8.77 (1H, d, *J* = 2.5 Hz, N-CH-pyridine), CO-NH and NH-pyrrole not visualised; ^{13}C NMR (125 MHz, MeOD) δ ppm Insufficient quantity of material obtained to perform analysis; Insufficient quantity of material to perform HRMS analysis.

***tert*-Butyl 4-(4-(2-cyclopropyl-6-fluorobenzoyl)-1*H*-pyrrole-2-carboxamido)piperidine-1-carboxylate, 328**

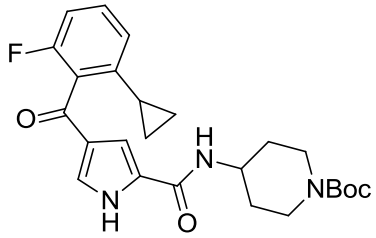

General procedure D: 4-(2-cyclopropyl-6-fluorobenzoyl)-1*H*-pyrrole-2-carboxylic acid (47 mg, 0.17 mmol), CDI (55 mg, 0.34 mmol), and *tert*-butyl 4-aminopiperidine-1-carboxylate (86 mg, 0.43 mmol). Purification *via* column chromatography (silica; 30-70% EtOAc/petrol) gave **328** as a white solid (57 mg, 74%). R_f 0.68 (9:1 DCM/MeOH); m.p. 145-146 ^oC; λ_{max} (EtOH/nm) 285.5, 234.0; IR υ_{max}/cm^{-1} 3332, 3126, 2973, 2928, 2858, 1691, 1619, 1567, 1534; ^1H NMR (500 MHz, $CDCl_3$) δ ppm 0.69-0.72 (2H, m, CH-cyclopropane), 0.85-0.89 (2H, m, CH-cyclopropane), 1.35-1.43 (2H, m, CH-piperidine), 1.49 (9H, s, C-*CH*$_3$), 1.84-1.89 (1H, m, CH-cyclopropane), 1.95-1.98 (2H, m, N-CH-piperidine), 2.85-2.90 (2H, m, N-CH-piperidine), 4.04-4.11 (3H, m, N-CH-piperidine), 6.25 (1H, d, *J* = 7.9 Hz, CO-NH), 6.76-6.77 (1H, m, H-3'), 6.94-6.97 (1H, m, H-5'), 7.21 (1H, br s, H-3), 7.30-7.34 (2H, m, H-5 and H-4'), 9.96 (1H, s, NH-pyrrole); ^{13}C NMR (125 MHz, $CDCl_3$) δ ppm 9.4 (C-cyclopropane), 13.0 (d, J_{CF} = 2.3 Hz, C-cyclopropane), 28.5 (C-*CH*$_3$), 32.0 (C-piperidine), 42.6 (C-piperidine), 47.0 (C-piperidine), 79.7 (*C*-CH_3), 108.8 (C-Ar), 112.7 (d, J_{CF} = 21.5 Hz, C-Ar), 120.0 (C-Ar), 127.8 (C-Ar), 127.9 (d, J_{CF} = 9.1 Hz, C-Ar), 128.9 (d, J_{CF} = 18.6 Hz, C-Ar), 130.1 (C-Ar), 130.6 (d, J_{CF} = 8.4 Hz, C-Ar), 143.7 (CO), 154.6 (CO), 158.9 (d, J_{CF} = 243.6 Hz, C-F), 188.9 (CO), one C-Ar not visualised; HRMS calcd for $C_{25}H_{30}FN_3O_4$ $[M+H]^+$ 456.2293, found 456.2293.

4-(2-Cyclopropyl-6-fluorobenzoyl)-*N*-(piperidin-4-yl)-1*H*-pyrrole-2-carboxamide, 307

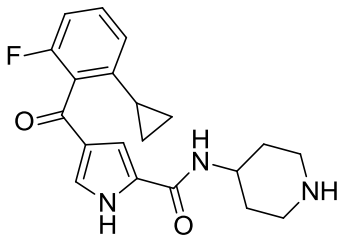

General procedure K: *tert*-Butyl 4-(4-(2-cyclopropyl-6-fluorobenzoyl)-1*H*-pyrrole-2-carboxamido)piperidine-1-carboxylate (50 mg, 0.11 mmol), triethylsilane (45 µL, 0.28

mmol) and TFA (2 mL/mmol) gave **307** as a white solid (26 mg, 65%). R_f 0.58 (9:1 DCM/MeOH, NH silica); m.p. Degrades >250 ^oC; λ_{max} (EtOH/nm) 234.0; IR υ_{max}/cm^{-1} 3266, 2951, 2851, 1623, 1566, 1532; ^1H NMR (500 MHz, DMSO-d_6) δ ppm 0.67-0.68 (2H, m, CH-cyclopropane), 0.83-0.86 (2H, m, CH-cyclopropane), 1.31-1.39 (2H, m, CH-piperidine), 1.67-1.72 (3H, m, CH-cyclopropane and CH-piperidine), 2.46-2.50 (2H, m, N-CH-piperidine), 2.92-2.96 (2H, m, N-CH-piperidine), 3.72-3.80 (1H, m, N-CH-piperidine), 6.83-6.84 (1H, m, H-3'), 7.08-7.11 (1H, m, H-5'), 7.20 (1H, br s, H-3), 7.22 (1H, br s, H-5), 7.39 (1H, ddd, *J* = 6.3, 8.3 and 8.4 Hz, H-4'), 8.10 (1H, d, *J* = 8.0 Hz, CO-NH), 12.26 (1H, br s, NH-pyrrole); ^{13}C NMR (125 MHz, DMSO-d_6) δ ppm 9.3 (C-cyclopropane), 12.6 (C-cyclopropane), 32.9 (C-piperidine), 45.1 (C-piperidine), 46.7 (C-piperidine), 109.9 (C-Ar), 112.4 (d, J_{CF} = 21.3 Hz, C-Ar), 119.8 (C-Ar), 126.3 (C-Ar), 127.5 (C-Ar), 128.7 (C-Ar), 129.0 (d, J_{CF} = 19.0 Hz, C-Ar), 130.5 (d, J_{CF} = 8.6 Hz, C-Ar), 142.9 (d, J_{CF} = 3.8 Hz, C-Ar), 158.0 (d, J_{CF} = 242.6 Hz, C-F), 159.0 (CO), 187.8 (CO); HRMS calcd for $C_{20}H_{22}FN_3O_2$ $[M+H]^+$ 56.1769, found 356.1774.

4-(2-Cyclopropyl-6-fluorobenzoyl)-*N*-(1-methylpiperidin-4-yl)-1*H*-pyrrole-2-carboxamide, 308

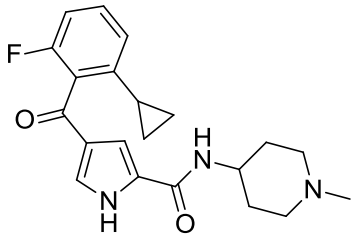

General procedure D: 4-(2-cyclopropyl-6-fluorobenzoyl)-1*H*-pyrrole-2-carboxylic acid (20 mg, 0.07 mmol), CDI (24 mg, 0.15 mmol), and 4-amino-1-methyl piperidine (23 µL, 0.18 mmol). Semi-preparative HPLC gave **308** as a white solid (15 mg, 58%). R_f 0.17 (9:1 DCM/MeOH); m.p. Degrades >250 ^oC; λ_{max} (EtOH/nm) 234.5; IR υ_{max}/cm^{-1} 3357, 2781, 1619, 1568, 1534; ^1H NMR (500 MHz, MeOD) δ ppm 0.57-0.60 (2H, m, CH-cyclopropane), 0.74-0.76 (2H, m, CH-cyclopropane), 1.51-1.59 (2H, m, CH-piperidine), 1.66-1.72 (1H, m, CH-cyclopropane), 1.79-1.84 (2H, m, CH-piperidine), 2.06-2.11 (2H, m, N-CH-piperidine), 2.21 (3H, s, N-CH_3), 2.80-2.84 (2H, m, N-CH-piperidine), 3.70-3.76 (1H, m, N-CH-piperidine), 6.73-6.75 (1H, m, H-3'), 6.87-6.91 (1H, m, H-5'), 7.02 (1H, d, *J* = 1.3 Hz, H-3), 7.23-7.28 (2H, m, H-5 and H-4'), NH peaks not observed; ^{13}C NMR (125 MHz, MeOD) δ ppm 9.7 (C-cyclopropane), 13.9 (C-cyclopropane), 32.2 (C-piperidine), 46.0 (N-CH_3), 47.5

(C-piperidine), 55.6 (C-piperidine), 111.8 (C-Ar), 113.6 (d, J_{CF} = 21.5 Hz, C-Ar), 121.3 (C-Ar), 128.4 (C-Ar), 129.6 (C-Ar), 130.4 (C-Ar), 131.8 (d, J_{CF} = 8.6 Hz, C-Ar), 144.8 (C-Ar), 160.1 (d, J_{CF} = 244.2 Hz, C-F), 162.1 (CO), 191.4 (CO), one C-Ar not visualised; Insufficient quantity of material to perform HRMS analysis.

4-(2-Ethynyl-6-fluorobenzoyl)-1*H*-pyrrole-2-carboxylic acid, 327

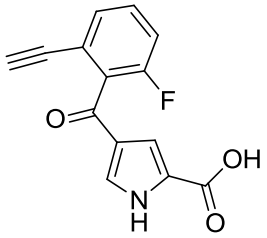

General procedure N: methyl 4-(2-bromo-6-fluorobenzoyl)-1-tosyl-1*H*-pyrrole-2-carboxylate (237 mg, 0.49 mmol), tert-butyldimethyl((4,4,5,5-tetramethyl-1,3,2-dioxaborolan-2-yl)ethynyl)silane (333 mg, 1.47 mmol), Cs_2CO_3 (240 mg, 0.74 mmol), Pd(dtbf)Cl_2 (10 mol%). The crude material was used directly in the next step. General procedure G: LiOH monohydrate (411 mg, 9.80 mmol) gave **327** as a white solid following purification *via* semi-preparative HPLC (33 mg, 26%). R_f 0.24 (9:1 DCM/MeOH); m.p. Degrades >250 ^oC; λ_{max} (EtOH/nm) 285.5, 232.0; IR υ_{max}/cm^{-1} 3280, 3136, 1687, 1632, 1605, 1560; ^1H NMR (500 MHz, DMSO-d_6) δ ppm 4.28 (1H, s, C-CH), 6.89 (1H, br s, H-3), 7.33 (1H, br s, H-5), 7.40-7.46 (2H, m, H-3' and H-5'), 7.52-7.56 (1H, m, H-4'), 12.57 (1H, s, NH-pyrrole), 12.92 (1H, s, COOH); ^{13}C NMR (125 MHz, DMSO-d_6) δ ppm Insufficient quantity of material obtained to perform analysis; HRMS calcd for $C_{14}H_8FNO_3$ $[M+H]^+$ 258.0561, found 258.0559.

4-(2-Ethynyl-6-fluorobenzoyl)-*N*-(1-methylpiperidin-4-yl)-1*H*-pyrrole-2-carboxamide, 311

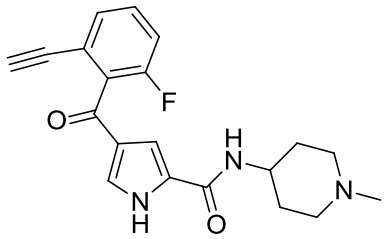

General procedure D with exceptions to the method: 4-(2-ethynyl-6-fluorobenzoyl)-1*H*-pyrrole-2-carboxylic acid (21 mg, 0.08 mmol), CDI (26 mg, 0.16 mmol) and 4-amino-1-

methyl piperidine (25 µL, 0.20 mmol) at RT. Purification via semi-preparative HPLC (1:1 0.1% NH_3 (aq)/MeCN) gave **311** as a white solid (20 mg, 71%). R_f 0.18 (9:1 DCM/MeOH); m.p. Degrades >130 ^oC; λ_{max} (EtOH/nm) 286.5, 235.5; IR υ_{max}/cm^{-1} 3568, 3198, 3128, 2923, 2851, 2796, 1620, 1570, 1545; ^1H NMR (500 MHz, DMSO-d_6) δ ppm 1.53-1.60 (2H, m, CH-piperidine), 1.75-1.77 (2H, m, CH-piperidine), 2.07-2.12 (2H, m, N-CH-piperidine), 2.24 (1H, s, C-CH-alkyne), 2.84-2.86 (2H, m, N-CH-piperidine), 3.68-3.76 (1H, m, N-CH-piperidine), 7.20 (1H, br s, H-3), 7.25 (1H, br s, H-5), 7.40-7.45 (2H, m, H-3' and H-5'), 7.51-7.56 (1H, m, H-4'), 8.14 (1H, d, J = 7.7 Hz, CO-NH), 12.34 (1H, s, NH-pyrrole); ^{13}C NMR (125 MHz, DMSO-d_6) δ ppm 31.1 (C-piperidine), 45.4 (N-CH_3), 45.6 (C-piperidine), 54.1 (C-piperidine), 79.9 (d, J_{CF} = 3.7 Hz, C-alkyne), 85.2 (CH-alkyne), 110.0 (C-Ar), 116.8 (d, J_{CF} = 21.8 Hz, C-Ar), 120.9 (d, J_{CF} = 6.0 Hz, C-Ar), 125.3 (C-Ar), 127.9 (C-Ar), 128.6 (C-Ar), 128.9 (d, J_{CF} = 2.5 Hz, C-Ar), 131.0 (d, J_{CF} = 8.8 Hz, C-Ar), 131.5 (d, J_{CF} = 21.2 Hz, C-Ar), 158.0 (d, J_{CF} = 244.2 Hz, C-F), 159.2 (CO), 185.5 (CO); HRMS calcd for $C_{20}H_{20}FN_3O_2$ $[M+H]^+$ 354.1612, found 354.1610.

Methyl 4-(2,3,6-trifluorobenzoyl)-1*H*-pyrrole-2-carboxylate, 330

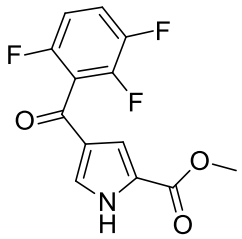

General procedure F: methyl 1*H*-pyrrole-2-carboxylate (322 mg, 2.57 mmol), 2,3,6-trifluorobenzoyl chloride (1.00 g, 5.14 mmol), and $AlCl_3$ (0.86 g, 6.43 mmol). Purification *via* column chromatography (silica; 0-50% EtOAc/petrol) gave **330** as a white solid (0.69 g, 95%). R_f 0.23 (8:2 Petrol/EtOAc); m.p. 168-170 ^oC; λ_{max} (EtOH/nm) 281.5, 234.5; IR υ_{max}/cm^{-1} 3280, 3118, 1683, 1640, 1560; ^1H NMR (500 MHz, DMSO-d_6) δ ppm 3.81 (3H, s, O-CH_3), 7.13 (1H, d, J = 1.5 Hz, H-3), 7.28-7.32 (1H, m, H-5'), 7.65-7.72 (1H, m, H-4'), 7.78 (1H, d, J = 1.5 Hz, H-5), 12.96 (1H, s, NH-pyrrole); ^{13}C NMR (125 MHz, $CDCl_3$) δ ppm 52.1 (O-CH_3), 111.7 (ddd, J_{CF} = 4.5, 4.9 and 24.3 Hz, C-Ar), 115.6 (C-Ar), 118.5 (dd, J_{CF} = 9.6 and 19.5 Hz, C-Ar), 124.7 (C-Ar), 127.0 (C-Ar), 128.3 (C-Ar), 147.1 (m, C-F), 151.5 (m, C-F), 154.7 (m, C-F), 161.1 (CO), 181.0 (CO); HRMS calcd for $C_{13}H_8F_3NO_3$ $[M+H]^+$ 284.0529, found 284.0529.

4-(2,3,6-Trifluorobenzoyl)-1*H*-pyrrole-2-carboxylic acid, 331

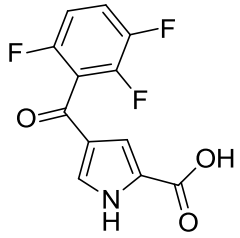

General procedure G: Methyl 4-(2,3,6-trifluorobenzoyl)-1*H*-pyrrole-2-carboxylate (0.66 g, 2.33 mmol) and LiOH monohydrate (1.96 g, 46.60 mmol) gave **331** as a white solid (0.62 g, 100%). R_f 0.32 (9:1 DCM/MeOH); m.p. 205-207 ^oC; λ_{max} (EtOH/nm) 285.5, 232.0; IR υ_{max}/cm^{-1} 3358, 3141, 3083, 1692, 1654, 1627, 1594, 1562; ^1H NMR (500 MHz, DMSO-d_6) δ ppm 7.07 (1H, br s, H-3), 7.27-7.32 (1H, m, H-5'), 7.64-7.71 (2H, m, H-5 and H-4'), 12.76 (1H, s, NH-pyrrole), 12.98 (1H, s, COOH); ^{13}C NMR (125 MHz, DMSO-d_6) δ ppm 112.5 (ddd, J_{CF} = 4.4, 6.0 and 25.5 Hz, C-Ar), 114.1 (C-Ar), 119.0 (dd, J_{CF} = 9.6 and 19.6 Hz, C-Ar), 125.4 (C-Ar), 126.1 (C-Ar), 146.4 (d, J_{CF} = 252.4 Hz, C-F), 153.9 (d, J_{CF} = 248.5 Hz, C-F), 161.3 (CO), 180.2 (CO), one C-F and one C-Ar not visualised; HRMS calcd for $C_{12}H_6F_3NO_3$ $[M+H]^+$ 270.0373, found 270.0373.

***N*-(Pyridin-3-yl)-4-(2,3,6-trifluorobenzoyl)-1*H*-pyrrole-2-carboxamide, 332**

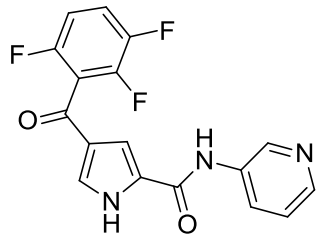

General procedure M: 4-(2,3,6-trifluorobenzoyl)-1*H*-pyrrole-2-carboxylic acid (100 mg, 0.37 mmol), PCl_3 (32 µL, 0.37 mmol), and 3-aminopyridine (88 mg, 0.93 mmol). Purification *via* column chromatography (NH silica; 0-8% MeOH/DCM) gave **332** as a white solid (52 mg, 41%). R_f 0.31 (95:5 DCM/MeOH); m.p. Degrades >250 ^oC; λ_{max} (EtOH/nm) 292.0, 260.0; IR υ_{max}/cm^{-1} 3350, 3239, 3121, 3013, 1628, 1599, 1558, 1533; ^1H NMR (500 MHz, DMSO-d_6) δ ppm 7.31-7.35 (1H, m, H-5'), 7.40 (1H, dd, J = 4.7 and 8.3 Hz, CH-pyridine), 7.58 (1H, d, J = 1.4 Hz, H-3), 7.67-7.74 (2H, m, H-5 and H-4'), 8.15 (1H, ddd, J = 1.5, 2.5 and 8.3 Hz, CH-pyridine), 8.31 (1H, dd, J = 1.5 and 4.7 Hz, N-CH-pyridine), 8.90 (1H, d, J = 2.5 Hz, N-CH-pyridine), 10.26 (1H, s, CO-NH), 12.00 (1H, br s, NH-pyrrole); ^{13}C NMR (125 MHz, DMSO-d_6) δ ppm 111.5 (C-Ar), 112.6 (m, C-Ar), 119.1 (m, C-Ar), 123.6 (C-Ar),

125.4 (C-Ar), 127.0 (C-Ar), 128.3 (C-Ar), 130.4 (C-Ar), 135.5 (C-Ar), 141.6 (C-Ar), 144.4 (C-Ar), 158.7 (CO), 180.4 (CO), one C-Ar and three C-F not visualised; HRMS calcd for $C_{17}H_{10}F_3N_3O_2$ $[M+H]^+$ 346.0798, found 346.0800.

***N*-(Pyrimidin-5-yl)-4-(2,3,6-trifluorobenzoyl)-1*H*-pyrrole-2-carboxamide, 333**

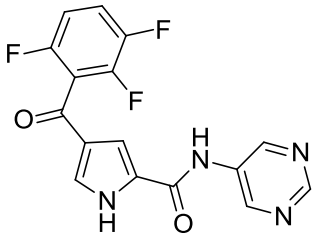

General procedure M with exceptions to the method: 4-(2,3,6-trifluorobenzoyl)-1*H*-pyrrole-2-carboxylic acid (52 mg, 0.19 mmol), PCl_3 (17 μL, 0.19 mmol), and 5-aminopyrimidine (46 mg, 0.48 mmol) for 30 min. Purification *via* column chromatography (silica; 0-8% MeOH/DCM) gave **333** as a yellow solid (34 mg, 52%). R_f 0.58 (9:1 DCM/MeOH); m.p. Degrades >250 ^oC; λ_{max} (EtOH/nm) 242.0; IR υ_{max}/cm^{-1} 3331, 3247, 3119, 3037, 1626, 1590, 1555, 1526; ^1H NMR (500 MHz, DMSO-d_6) δ ppm 7.32-7.35 (1H, m, H-5'), 7.58 (1H, br s, H-3), 7.68-7.73 (2H, m, H-4' and H-5), 8.93 (1H, s, N-CH-pyrimidine), 9.14 (2H, s, N-CH-pyrimidine), 10.46 (1H, s, CO-NH), 12.89 (1H, s, NH-pyrrole); ^{13}C NMR (125 MHz, DMSO-d_6) δ ppm 112.0 (C-Ar), 112.6 (m, C-Ar), 119.0 (m, C-Ar), 125.5 (C-Ar), 127.8 (C-Ar), 130.7 (C-Ar), 134.3 (C-Ar), 147.8 (C-Ar), 153.2 (C-Ar), 158.8 (CO), 180.4 (CO), one C-Ar and three C-F not visualised; HRMS calcd for $C_{16}H_9F_3N_4O_2$ $[M+H]^+$ 347.0750, found 347.0755.

***tert*-Butyl 4-(4-(2,3,6-trifluorobenzoyl)-1*H*-pyrrole-2-carboxamido)piperidine-1-carboxylate, 334**

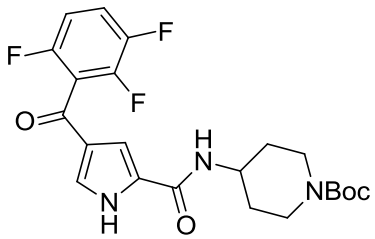

General procedure D: 4-(2,3,6-trifluorobenzoyl)-1*H*-pyrrole-2-carboxylic acid (100 mg, 0.37 mmol), CDI (120 mg, 0.74 mmol), and *tert*-butyl 4-aminopiperidine-1-carboxylate (186 mg, 0.93 mmol). Purification *via* column chromatography (silica; 30-100% EtOAc/petrol)

gave **334** as a white solid (155 mg, 93%). R_f 0.70 (9:1 DCM/MeOH); m.p. 148-150 ^oC; λ_{max} (EtOH/nm) 285.5, 236.0; IR υ_{max}/cm^{-1} 3128, 2976, 2863, 1667, 1624, 1567, 1535; ^1H NMR (500 MHz, $CDCl_3$) δ ppm 1.39-1.45 (2H, m, CH-piperidine), 1.49 (9H, s, C-*CH*$_3$), 1.98-2.00 (2H, m, CH-piperidine), 2.87-2.93 (2H, m, N-CH-piperidine), 4.06-4.14 (3H, m, N-CH-piperidine), 6.12 (1H, d, *J* = 7.9 Hz, CO-NH), 6.95-7.00 (1H, m, H-5'), 7.11 (1H, dd, *J* = 1.5 and 2.4 Hz, H-3), 7.25-7.31 (1H, m, H-4'), 7.39 (1H, br s, H-5), 10.20 (NH-pyrrole); ^{13}C NMR (125 MHz, $CDCl_3$) δ ppm 28.4 (C-*CH*$_3$), 31.9 (C-piperidine), 42.7 (C-piperidine), 47.1 (C-piperidine), 79.8 (*C*-CH_3), 109.6 (C-Ar), 111.7 (ddd, J_{CF} = 4.5, 5.8 and 24.4 Hz, C-Ar), 118.4 (dd, J_{CF} = 9.9 and 19.3 Hz, C-Ar), 119.6 (dd, J_{CF} = 18.6 and 24.6 Hz, C-Ar), 126.5 (C-Ar), 128.5 (C-Ar), 129.0 (C-Ar), 147.0 (dd, J_{CF} = 9.2 and 244.0 Hz, C-F), 147.2 (dd, J_{CF} = 15.7 and 244.9 Hz, C-F), 154.5 (ddd, J_{CF} = 3.1, 5.5 and 247.6 Hz, C-F), 154.7 (CO), 160.1 (CO), 181.2 (CO); HRMS calcd for $C_{22}H_{24}F_3N_3O_4$ $[M+H]^+$ 452.1792, found 452.1790.

***N*-(Piperidin-4-yl)-4-(2,3,6-trifluorobenzoyl)-1*H*-pyrrole-2-carboxamide, 376**

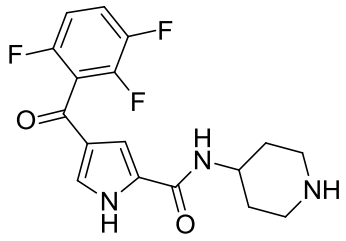

General procedure K: *tert*-butyl 4-(4-(2,3,6-trifluorobenzoyl)-1*H*-pyrrole-2-carboxamido)piperidine-1-carboxylate (140 mg, 0.31 mmol), triethylsilane (124 μL, 0.78 mmol), and TFA (2 mL/mmol) gave **376** as a white solid (103 mg, 95%). R_f 0.45 (9:1 DCM/MeOH, NH silica); m.p. 214-216 ^oC; λ_{max} (EtOH/nm) 286.5, 236.5; IR υ_{max}/cm^{-1} 3280, 2943, 2845, 1630, 1568, 1535; ^1H NMR (500 MHz, DMSO-d_6) δ ppm 1.41-1.49 (2H, m, CH-piperidine), 1.77-1.80 (2H, m, CH-piperidine), 2.62-2.68 (2H, m, N-CH-piperidine), 3.04-3.07 (2H, m, N-CH-piperidine), 3.81-3.89 (1H, m, N-CH-piperidine), 7.28-7.33 (2H, m, H-3 and H-5'), 7.51 (1H, d, *J* = 1.5 Hz, H-5), 7.65-7.72 (1H, m, H-4'), 8.17 (1H, d, *J* = 7.8 Hz, CO-NH); ^{13}C NMR (125 MHz, DMSO-d_6) δ ppm 31.0 (C-piperidine), 43.9 (C-piperidine), 45.6 (C-piperidine), 110.0 (C-Ar), 112.5 (ddd, J_{CF} = 3.3, 5.9 and 24.2 Hz, C-Ar), 118.8 (dd, J_{CF} = 9.9 and 19.5 Hz, C-Ar), 119.5 (dd, J_{CF} = 19.6 and 25.9 Hz, C-Ar), 125.1 (C-Ar), 129.0 (C-Ar), 129.1 (C-Ar), 146.2 (m, C-F), 146.4 (m, C-F), 153.8 (dd, J_{CF} = 5.1 and 244.7 Hz, C-F), 158.9 (CO), 180.3 (CO); HRMS calcd for $C_{17}H_{16}F_3N_3O_2$ $[M+H]^+$ 352.1267, found 352.1268.

***N*-(1-Methylpiperidin-4-yl)-4-(2,3,6-trifluorobenzoyl)-1*H*-pyrrole-2-carboxamide, 335**

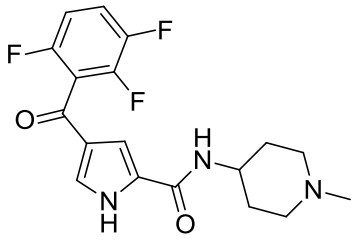

General procedure D: 4-(2,3,6-trifluorobenzoyl)-1*H*-pyrrole-2-carboxylic acid (100 mg, 0.37 mmol), CDI (120 mg, 0.74 mmol), and 4-amino-1-methyl piperidine (116 µL, 0.93 mmol). Purification *via* column chromatography (NH silica; 0-8% MeOH/DCM) gave **335** as a white solid (96 mg, 71%). R_f 0.17 (9:1 DCM/MeOH); m.p. Degrades >250 ^oC; λ_{max} (EtOH/nm) 236.5; IR υ_{max}/cm^{-1} 3368, 2943, 2852, 2798, 1638, 1566, 1517; ^1H NMR (500 MHz, DMSO-d_6) δ ppm 1.49-1.57 (2H, m, CH-piperidine), 1.72-1.75 (2H, m, CH-piperidine), 1.90-1.95 (2H, m, N-CH-piperidine), 2.16 (3H, s, N-CH_3), 2.74-2.77 (2H, m, N-CH-piperidine), 3.64-3.72 (1H, m, N-CH-piperidine), 7.28-7.33 (2H, m, H-3 and H-5'), 7.51 (1H, br s, H-5), 7.65-7.71 (1H, m, H-4'), 8.10 (1H, d, J = 7.8 Hz, CO-NH), 12.47 (1H, s, NH-pyrrole); ^{13}C NMR (125 MHz, DMSO-d_6) δ ppm 31.6 (C-piperidine), 45.9 (N-CH_3), 46.0 (C-piperidine), 54.4 (C-piperidine), 109.8 (C-Ar), 112.5 (m, C-Ar), 118.8 (dd, J_{CF} = 9.4 and 19.6 Hz, C-Ar), 119.5 (m, C-Ar), 125.1 (C-Ar), 129.0 (C-Ar), 129.1 (C-Ar), 146.2 (m, two C-F), 153.8 (m, C-F), 159.0 (CO), 180.3 (CO); HRMS calcd for $C_{18}H_{18}F_3N_3O_2$ $[M+H]^+$ 366.1424, found 366.1430.

Methyl 4-(3-chloro-2,6-difluorobenzoyl)-1*H*-pyrrole-2-carboxylate, 336

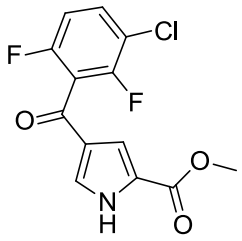

General procedure F: methyl 1*H*-pyrrole-2-carboxylate (593 mg, 4.74 mmol), 3-chloro, 2,6-difluorobenzoyl chloride (2.00 g, 9.48 mmol) and $AlCl_3$ (1.59 g, 11.85 mmol). Purification *via* column chromatography (silica; 0-50% EtOAc/petrol) gave **336** as a white solid (1.28 g, 90%). R_f 0.27 (8:2 Petrol/EtOAc); m.p. 143-145 ^oC; λ_{max} (EtOH/nm) 289.0; IR υ_{max}/cm^{-1} 3256, 3147, 3090, 2998, 2956, 1693, 1650, 1615, 1561; ^1H NMR (500 MHz, DMSO-d_6) δ ppm 3.81 (3H, s, O-CH_3), 7.12 (1H, br s, H-3), 7.34 (1H, dd, J = 8.9 and 10.2 Hz, H-5'), 7.72

(1H, dd, J = 1.5 and 3.4 Hz, H-5), 7.80-7.85 (1H, m, H-4'), 12.95 (1H, s, NH-pyrrole); ^{13}C NMR (125 MHz, DMSO-d_6) δ ppm 51.7 (O-CH_3), 113.6 (dd, J_{CF} = 3.7 and 23.4 Hz, C-Ar), 114.6 (C-Ar), 116.1 (dd, J_{CF} = 3.8 and 17.9 Hz, C-Ar), 118.8 (t, J_{CF} =24.2 Hz, C-Ar), 124.7 (C-Ar), 125.5 (C-Ar), 131.0 (C-Ar), 132.2 (d, J_{CF} = 9.8 Hz, C-Ar), 153.7 (dd, J_{CF} = 8.6 and 249.5 Hz, C-F), 157.2 (dd, J_{CF} = 7.0 and 248.6 Hz, C-F), 160.3 (CO), 180.4 (CO); HRMS calcd for $C_{13}H_8{}^{35}ClF_2NO_3$ $[M+H]^+$ 300.0234, found 300.0236.

4-(3-Chloro-2,6-difluorobenzoyl)-1*H*-pyrrole-2-carboxylic acid, 337

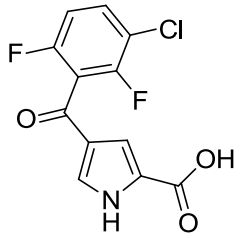

General procedure G: methyl 4-(3-chloro-2,6-difluorobenzoyl)-1*H*-pyrrole-2-carboxylate (1.20 g, 4.00 mmol), and LiOH monohydrate (3.36 g, 80.00 mmol) gave **337** as a white solid (1.14 g, 100%). R_f 0.36 (9:1 DCM/MeOH); m.p. 235-237 ^oC; λ_{max} (EtOH/nm) 282.5, 231.5; IR υ_{max}/cm^{-1} 3358, 3238, 3134, 1676, 1630, 1613, 1555; ^{1}H NMR (500 MHz, DMSO-d_6) δ ppm 7.06 (1H, br s, H-3), 7.33 (1H, dd, J = 8.8 and 10.0 Hz, H-5'), 7.65 (1H, dd, J = 1.5 and 3.4 Hz, H-5), 7.79-7.84 (1H, m, H-4'), 12.77 (1H, s, NH-pyrrole), 12.95 (1H, s, COOH); ^{13}C NMR (125 MHz, DMSO-d_6) δ ppm 113.6 (dd, J_{CF} = 3.8 and 23.2 Hz, C-Ar), 114.1 (C-Ar), 116.1 (dd, J_{CF} = 3.8 and 17.9 Hz, C-Ar), 118.9 (m, C-Ar), 125.4 (C-Ar), 126.0 (C-Ar), 130.6 (C-Ar), 132.1 (d, J_{CF} = 9.7 Hz, C-Ar), 153.7 (dd, J_{CF} = 8.3 and 248.8 Hz, C-F), 157.2 (dd, J_{CF} = 6.9 and 248.2 Hz, C-F), 161.3 (CO), 180.3 (CO); HRMS calcd for $C_{12}H_6{}^{35}ClF_2NO_3$ $[M-H]^-$ 283.9932, found 283.9922.

4-(3-Chloro-2,6-difluorobenzoyl)-*N*-(pyridin-3-yl)-1*H*-pyrrole-2-carboxamide, 338

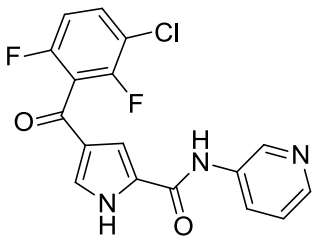

General procedure M: 4-(3-chloro-2,6-difluorobenzoyl)-1*H*-pyrrole-2-carboxylic acid (51 mg, 0.18 mmol), PCl_3 (16 µL, 0.18 mmol), and 3-aminopyridine (42 mg, 0.45 mmol).

Purification *via* column chromatography (NH silica; 0-8% MeOH/DCM) gave **338** as a white solid (62 mg, 95%). R_f 0.32 (95:5 DCM/MeOH); m.p. 269-272 ^oC; λ_{max} (EtOH/nm) 305.0; IR υ_{max}/cm^{-1} 3359, 3235, 1642, 1613, 1561, 1535; ^1H NMR (500 MHz, DMSO-d_6) δ ppm 7.35-7.41 (2H, m, H-5' and CH-pyridine), 7.57 (1H, br s, H-3), 7.68 (1H, br s, H-5), 7.82-7.86 (1H, m, H-4'), 8.15 (1H, ddd, J = 1.5, 2.5 and 8.3 Hz, CH-pyridine), 8.31 (1H, dd, J = 1.5 and 4.6 Hz, N-CH-pyridine), 8.90 (1H, d, J = 2.5 Hz, N-CH-pyridine), 10.26 (1H, s, CO-NH), 12.80 (1H, s, NH-pyrrole); ^{13}C NMR (125 MHz, DMSO-d_6) δ ppm 111.5 (C-Ar), 113.6 (dd, J_{CF} = 3.3 and 23.4 Hz, C-Ar), 116.1 (dd, J_{CF} = 3.5 and 18.4 Hz, C-Ar), 119.0 (t, J_{CF} = 23.4 Hz, C-Ar), 123.6 (C-Ar), 125.4 (C-Ar), 127.0 (C-Ar), 128.4 (C-Ar), 130.4 (C-Ar), 132.1 (d, J_{CF} = 9.7 Hz, C-Ar), 135.5 (C-Ar), 141.6 (C-Ar), 144.4 (C-Ar), 153.7 (dd, J_{CF} = 9.1 and 248.7 Hz, C-F), 157.2 (dd, J_{CF} = 6.8 and 248.5 Hz, C-F), 158.7 (CO), 180.5 (CO); HRMS calcd for $C_{17}H_{10}{}^{35}ClF_2N_3O_2$ $[M+H]^+$ 362.0502, found 362.0503.

4-(3-Chloro-2,6-difluorobenzoyl)-*N*-(pyrimidin-5-yl)-1*H*-pyrrole-2-carboxamide, 339

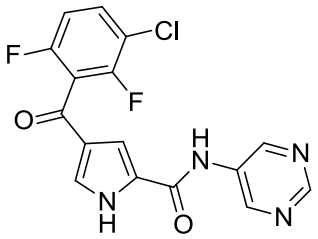

General procedure M with exceptions to the method: 4-(3-chloro-2,6-difluorobenzoyl)-1*H*-pyrrole-2-carboxylic acid (100 mg, 0.35 mmol), PCl_3 (31 μL, 0.35 mmol), and 5-aminopyrimidine (84 mg, 0.88 mmol) for 15 min. Purification *via* column chromatography (silica; 0-8% MeOH/DCM) gave **339** as a yellow solid (58 mg, 46%). R_f 0.62 (9:1 DCM/MeOH); m.p. 322-324 ^oC; λ_{max} (EtOH/nm) 267.5; IR υ_{max}/cm^{-1} 3076, 2922, 2861, 1628, 1601, 1567, 1535; ^1H NMR (500 MHz, DMSO-d_6) δ ppm 7.37 (1H, dd, J = 7.6 and 9.0 Hz, H-5'), 7.57 (1H, br s, H-3), 7.73 (1H, br s, H-5), 7.83-7.87 (1H, m, H-4'), 8.93 (1H, s, CH-pyrimidine), 9.14 (2H, s, CH-pyrimidine), 10.45 (1H, s, CO-NH), 12.89 (1H, s, NH-pyrrole); ^{13}C NMR (125 MHz, DMSO-d_6) δ ppm 112.0 (C-Ar), 113.7 (dd, J_{CF} = 3.9 and 23.6 Hz, C-Ar), 116.1 (m, C-Ar), 119.0 (m, C-Ar), 125.4 (C-Ar), 127.8 (C-Ar), 130.6 (C-Ar), 132.2 (d, J_{CF} = 9.8 Hz, C-Ar), 134.3 (C-Ar), 147.8 (C-Ar), 153.2 (C-Ar), 153.7 (dd, J_{CF} = 9.2 and 249.4 Hz, C-F), 157.2 ((dd, J_{CF} = 7.5 and 248.2 Hz, C-F), 158.8 (CO), 180.5 (CO); HRMS calcd for $C_{16}H_9{}^{35}ClF_2N_4O_2$ $[M+H]^+$ 363.0455, found 363.0460.

***tert*-Butyl 4-(4-(3-chloro-2,6-difluorobenzoyl)-1*H*-pyrrole-2-carboxamido)piperidine-1-carboxylate, 340**

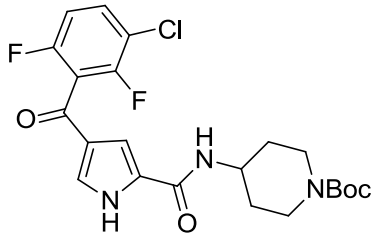

General procedure D: 4-(3-chloro-2,6-difluorobenzoyl)-1*H*-pyrrole-2-carboxylic acid (117 mg, 0.41 mmol), CDI (133 mg, 0.82 mmol), *tert*-butyl 4-aminopiperidine-1-carboxylate (206 mg, 1.03 mmol). Purification *via* column chromatography (silica; 30-70% EtOAc/petrol) gave **340** as a white solid (167 mg, 87%). R_f 0.71 (9:1 DCM/MeOH); m.p. 135-137 ^oC; λ_{max} (EtOH/nm) 290.0, 233.5; IR υ_{max}/cm^{-1} 2960, 2930, 2865, 1663, 1618, 1567, 1535; ^1H NMR (500 MHz, DMSO-d_6) δ ppm 1.40-1.49 (11H, m, CH-piperidine and C-CH_3), 1.98-2.01 (2H, m, CH-piperidine), 2.87-2.93 (2H, m, N-CH-piperidine), 4.07-4.15 (3H, m, N-CH-piperidine), 6.10 (1H, d, J = 7.7 Hz, CO-NH), 7.00 (1H, dd, J = 7.9 and 9.0 Hz, H-5'), 7.08 (1H, br s, H-3), 7.38 (1H, br s, H-5), 7.58-7.52 (1H, m, H-4'), 10.17 (1H, s, NH-pyrrole); ^{13}C NMR (125 MHz, DMSO-d_6) δ ppm 28.4 (C-CH_3), 32.1 (C-piperidine), 42.6 (C-piperidine), 47.1 (C-piperidine), 79.8 (*C*-CH_3), 108.9 (C-Ar), 112.7 (dd, J_{CF} = 4.2 and 23.3 Hz, C-Ar), 117.4 (m, C-Ar), 119.3 (t, J_{CF} = 22.6 Hz, C-Ar), 126.8 (C-Ar), 128.0 (C-Ar), 128.1 (C-Ar), 131.7 (d, J_{CF} = 9.5 Hz, C-Ar), 154.7 (CO), 154.9 (dd, J_{CF} = 8.7 and 253.8 Hz, C-F), 157.8 (dd, J_{CF} = 6.8 and 251.9 Hz, C-F), 159.5 (CO), 181.1 (CO); HRMS calcd for $C_{22}H_{24}{}^{35}ClF_2N_3O_4$ $[M+H]^+$ 468.1496, found 468.1495.

4-(3-Chloro-2,6-difluorobenzoyl)-N-(piperidin-4-yl)-1*H*-pyrrole-2-carboxamide, 377

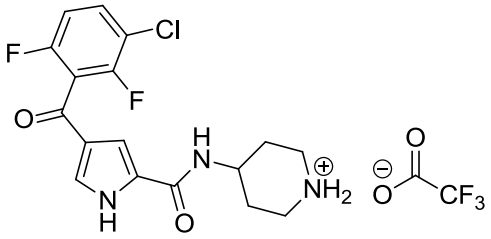

General procedure K: *tert*-butyl 4-(4-(3-chloro-2,6-difluorobenzoyl)-1*H*-pyrrole-2-carboxamido)piperidine-1-carboxylate (100 mg, 0.21 mmol), triethylsilane (84 μL, 0.53 mmol), and TFA (2 mL/mmol) gave **377** as a white solid (98 mg, 97%). R_f 0.01 (9:1 DCM/MeOH, NH silica); m.p. 185-187 ^oC; λ_{max} (EtOH/nm) 286.0, 235.5; IR υ_{max}/cm^{-1} 3452,

3267, 2829, 2738, 1754, 1699, 1662, 1638, 1616, 1576; ^{1}H NMR (500 MHz, DMSO-d_6) δ ppm 1.65-1.73 (2H, m, CH-piperidine), 1.95-1.98 (2H, m, CH-piperidine), 2.30-2.37 (2H, m, N-CH-piperidine), 3.32-3.34 (2H, m, N-CH-piperidine), 4.00-4.07 (1H, m, N-CH-piperidine), 7.33-7.36 (2H, m, H-3 and H-5'), 7.54 (1H, br s, H-5), 7.78-7.84 (1H, m, H-4'), 8.32 (1H, d, J = 7.4 Hz, CO-NH), 8.61 (1H, br s, NH-piperidine), 8.78 (1H, br s, NH-piperidine), 12.52 (1H, s, NH-pyrrole); ^{13}C NMR (125 MHz, DMSO-d_6) δ ppm 28.3 (C-piperidine), 42.2 (C-piperidine), 43.8 (C-piperidine), 110.2 (C-Ar), 113.5 (dd, J_{CF} = 3.1 and 23.3 Hz, C-Ar), 116.0 (dd, J_{CF} = 3.5 and 17.8 Hz, C-Ar), 116.0 (q, J_{CF} = 293.0 Hz, CF_3), 119.3 (d, J_{CF} = 5.8 Hz, C-Ar), 125.1 (C-Ar), 128.7 (C-Ar), 129.3 (C-Ar), 132.0 (d, J_{CF} = 9.5 Hz, C-Ar), 153.7 (dd, J_{CF} = 8.4 and 249.1 Hz, C-F), 157.1 (dd, J_{CF} = 7.0 and 247.9 Hz, C-F), 158.6 (d, J_{CF} = 34.9 Hz, CO), 159.2 (CO), 180.4 (CO); HRMS calcd for $C_{17}H_{16}{}^{35}ClF_2N_3O_2$ $[M+H]^+$ 368.0972, found 368.0971.

4-(3-Chloro-2,6-difluorobenzoyl)-*N*-(1-methylpiperidin-4-yl)-1*H*-pyrrole-2-carboxamide, 341

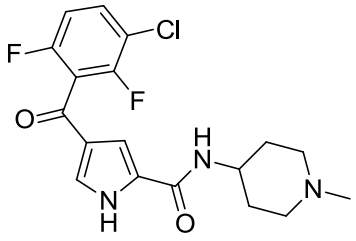

General procedure D: 4-(3-chloro-2,6-difluorobenzoyl)-1*H*-pyrrole-2-carboxylic acid (50 mg, 0.17 mmol), CDI (55 mg, 0.34 mmol), and 4-amino-1-methyl piperidine (54 µL, 0.43 mmol). Purification *via* column chromatography (NH silica; 0-8% MeOH/DCM) gave **341** as a white solid (57 mg, 88%). R_f 0.20 (9:1 DCM/MeOH); m.p. 200-203 ^{o}C; λ_{max} (EtOH/nm) 292.0, 236.5; IR υ_{max}/cm^{-1} 3241, 3073, 2940, 2850, 2801, 2689, 1625, 1578, 1518; ^{1}H NMR (500 MHz, DMSO-d_6) δ ppm 1.49-1.56 (2H, m, CH-piperidine), 1.73-1.75 (2H, m, CH-piperidine), 1.90-1.95 (2H, m, N-CH-piperidine), 2.16 (3H, m, N-CH_3), 2.74-2.78 (2H, m, N-CH-piperidine), 3.64-3.72 (1H, m, N-CH-piperidine), 7.27 (1H, br s, H-3), 7.35 (1H, dd, J = 7.9 and 9.2 Hz, H-5'), 7.51 (1H, br s, H-5), 7.79-7.84 (1H, m, H-4'), 8.10 (1H, d, J = 7.9 Hz, CO-NH), 12.47 (1H, s, NH-pyrrole); ^{13}C NMR (125 MHz, DMSO-d_6) δ ppm 31.5 (C-piperidine), 45.9 (N-CH_3), 46.0 (C-piperidine), 54.4 (C-piperidine), 109.8 (C-Ar), 113.6 (dd, J_{CF} = 3.3 and 22.9 Hz, C-Ar), 115.9 (dd, J_{CF} = 3.5 and 17.8 Hz, C-Ar), 125.1 (C-Ar), 129.0 (C-Ar), 129.1 (C-Ar), 132.0 (d, J_{CF} = 9.5 Hz, C-Ar), 159.0 (CO), 180.4 (CO) one C-Ar and

two C-F not visualised; HRMS calcd for $C_{18}H_{18}{}^{35}ClF_2N_3O_2$ $[M+H]^+$ 382.1128, found 382.1130.

Methyl 4-(2-chloro-3,6-difluorobenzoyl)-1*H*-pyrrole-2-carboxylate, 342

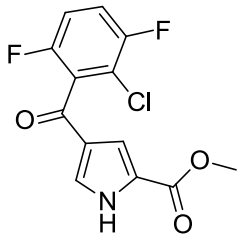

General procedure F: methyl 1*H*-pyrrole-2-carboxylate (297 mg, 2.37 mmol), 2-chloro, 3, 6-difluorobenzoyl chloride (1.00 g, 4.74 mmol), and $AlCl_3$ (0.76 g, 5.93 mmol). Purification *via* column chromatography (silica; 0-50% EtOAc/petrol) gave **342** as a white solid (0.67 g, 94%).

R_f 0.25 (8:2 Petrol/EtOAc); m.p. 123-125 ^oC; λ_{max} (EtOH/nm) 279.5, 232.5; IR υ_{max}/cm^{-1} 3257, 3106, 2994, 2952, 1697, 1659, 1561; ^1H NMR (500 MHz, DMSO-d_6) δ ppm 3.81 (3H, s, O-CH_3), 7.08 (1H, d, J = 1.6 Hz, H-3), 7.44-7.48 (1H, m, H-5'), 7.61-7.66 (2H, m, H-4' and H-5), 12.94 (NH-pyrrole); ^{13}C NMR (125 MHz, DMSO-d_6) δ ppm 51.7 (O-CH_3), 114.6 (C-Ar), 116.4 (dd, J_{CF} = 7.8 and 24.3 Hz, C-Ar), 118.3 (dd, J_{CF} = 9.1 and 23.7 Hz, C-Ar), 124.9 (d, J_{CF} = 26.7 Hz, C-Ar), 129.0 (d, J_{CF} = 25.1 Hz, C-Ar), 130.9 (C-Ar), 154.1 (d, J_{CF} = 244.0 Hz, C-F), 154.3 (d, J_{CF} = 247.6 Hz, C-F), 160.3 (CO), 182.4 (CO), two C-Ar not visualised; HRMS calcd for $C_{13}H_8{}^{35}ClF_2NO_3$ $[M+H]^+$ 300.0234, found 300.0237.

4-(2-Chloro-3,6-difluorobenzoyl)-1*H*-pyrrole-2-carboxylic acid, 343

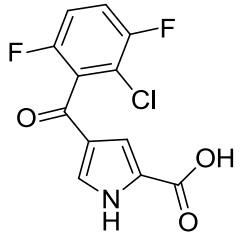

General procedure G: methyl 4-(2-chloro-3,6-difluorobenzoyl)-1*H*-pyrrole-2-carboxylate (0.60 g, 2.01 mmol), and LiOH monohydrate (1.69 g, 40.20 mmol) gave **343** as a white solid (0.56 g, 98%). R_f 0.32 (9:1 DCM/MeOH); m.p. 226-228 ^oC; λ_{max} (EtOH/nm) 276.5, 233.0; IR υ_{max}/cm^{-1} 3368, 3137, 3093, 1682, 1650, 1559; ^1H NMR (500 MHz, DMSO-d_6) δ ppm 7.03 (1H, br s, H-3), 7.43-7.48 (1H, m, H-5'), 7.58 (1H, br s, H-5), 7.60-7.65 (1H, m, H-4'), 12.75

(1H, s, NH-pyrrole), 12.95 (1H, s, COOH); ^{13}C NMR (125 MHz, DMSO-d_6) δ ppm 114.1 (C-Ar), 116.3 (dd, J_{CF} = 7.7 and 24.3 Hz, C-Ar), 117.5 (dd, J_{CF} = 6.9 and 21.3 Hz, C-Ar), 118.2 (dd, J_{CF} = 9.2 and 23.7 Hz, C-Ar), 124.9 (C-Ar), 126.1 (C-Ar), 129.1 (d, J_{CF} = 25.5 Hz, C-Ar), 130.4 (C-Ar), 154.0 (dd, J_{CF} = 1.5 and 243.1 Hz, C-F), 154.2 (dd, J_{CF} = 5.6 and 240.8 Hz, C-F), 161.3 (CO), 182.4 (CO); HRMS calcd for $C_{12}H_6{}^{35}ClF_2NO_3$ $[M-H]^-$ 283.9932, found 283.9921.

4-(2-Chloro-3,6-difluorobenzoyl)-*N*-(pyridin-3-yl)-1*H*-pyrrole-2-carboxamide, 344

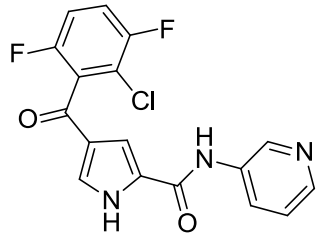

General procedure M: 4-(2-chloro-3,6-difluorobenzoyl)-1*H*-pyrrole-2-carboxylic acid (100 mg, 0.35 mmol), PCl_3 (31 µL, 0.35 mmol), and 3-aminopyridine (83 mg, 0.88 mmol). Purification *via* column chromatography (silica; 0-8% MeOH/DCM) gave **344** as a white solid (73 mg, 58%). R_f 0.34 (95:5 DCM/MeOH); m.p. 177-178 ^oC; λ_{max} (EtOH/nm) 292.0, 268.0; IR υ_{max}/cm^{-1} 3120, 2817, 2708, 1639, 1593, 1557, 1530, 1501; ^{1}H NMR (500 MHz, DMSO-d_6) δ ppm 7.39 (1H, dd, J = 4.7 and 8.4 Hz, CH-pyridine), 7.47-7.51 (1H, m, H-5'), 7.54 (1H, br s, H-3), 7.61 (1H, br s, H-5), 7.63-7.68 (1H, m, H-4'), 8.14 (1H, ddd, J = 1.5, 2.5 and 8.4 Hz, CH-pyridine), 8.31 (1H, dd, J = 1.5 and 4.7 Hz, N-CH-pyridine), 8.99 (1H, d, J = 2.5 Hz, N-CH-pyridine), 10.25 (1H, s, CO-NH), 12.79 (1H, s, NH-pyrrole); ^{13}C NMR (125 MHz, DMSO-d_6) δ ppm 111.5 (C-Ar), 116.4 (dd, J_{CF} = 7.5 and 24.4 Hz, C-Ar), 118.2 (dd, J_{CF} = 9.4 and 23.9 Hz, C-Ar), 119.6 (C-Ar), 123.6 (C-Ar), 124.8 (C-Ar), 127.0 (C-Ar), 128.4 (C-Ar), 129.2 (d, J_{CF} = 25.7 Hz, C-Ar), 130.1 (C-Ar), 135.5 (C-Ar), 141.6 (C-Ar), 144.4 (C-Ar), 154.1 (d, J_{CF} = 241.9 Hz, C-F), 154.4 (d, J_{CF} = 241.9 Hz, C-F), 158.7 (CO), 182.6 (CO); HRMS calcd for $C_{17}H_{10}{}^{35}ClF_2N_3O_2$ $[M+H]^+$ 362.0502, found 362.0508.

***tert*-Butyl 4-(4-(2-chloro-3,6-difluorobenzoyl)-1*H*-pyrrole-2-carboxamido)piperidine-1-carboxylate, 345**

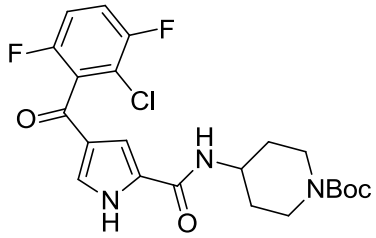

General procedure D: 4-(2-chloro-3,6-difluorobenzoyl)-1*H*-pyrrole-2-carboxylic acid (104 mg, 0.36 mmol), CDI (117 mg, 0.72 mmol), and *tert*-butyl 4-aminopiperidine-1-carboxylate (180 mg, 0.90 mmol). Purification *via* column chromatography (silica; 30-70% EtOAc/petrol) gave **345** as a white solid (143 mg, 85%). R_f 0.71 (9:1 DCM/MeOH); m.p. 159-161 ^oC; λ_{max} (EtOH/nm) 281.0, 236.0; IR υ_{max}/cm^{-1} 3190, 2976, 2935, 2865, 1666, 1622, 1565, 1535; ^1H NMR (500 MHz, $CDCl_3$) δ ppm 1.38-1.46 (2H, m, CH-piperidine), 1.49 (9H, s, C-*CH*$_3$), 1.97-2.00 (2H, m, CH-piperidine), 2.87-2.92 (2H, m, N-CH-piperidine), 4.05-4.12 (3H, m, N-CH-piperidine), 6.14 (1H, d, *J* = 8.0 Hz, CO-NH), 7.07-7.13 (2H, m, H-3 and H-5'), 7.22-7.27 (1H, m, H-4'), 7.33 (1H, br s, H-5), 10.20 (1H, s, NH-pyrrole); ^{13}C NMR (125 MHz, $CDCl_3$) δ ppm 28.4 (C-*CH*$_3$), 31.9 (C-piperidine), 42.7 (C-piperidine), 47.1 (C-piperidine), 79.8 (*C*-CH$_3$), 109.5 (C-Ar), 115.4 (dd, J_{CF} = 7.1 and 24.1 Hz, C-Ar), 117.6 (dd, J_{CF} = 8.9 and 23.9 Hz, C-Ar), 119.2 (dd, J_{CF} = 6.4 and 21.2 Hz, C-Ar), 126.0 (C-Ar), 128.6 (C-Ar), 128.9 (C-Ar), 129.4 (d, J_{CF} = 24.4 Hz, C-Ar), 154.6 (CO), 154.7 (dd, J_{CF} = 2.8 and 244.0 Hz, C-F), 154.8 (d, J_{CF} = 244.0 Hz, C-F), 160.1 (CO), 183.5 (CO); HRMS calcd for $C_{22}H_{24}{}^{35}ClF_2N_3O_4$ $[M+H]^+$ 468.1496, found 468.1495.

4-(2-Chloro-3,6-difluorobenzoyl)-*N*-(piperidin-4-yl)-1*H*-pyrrole-2-carboxamide, 378

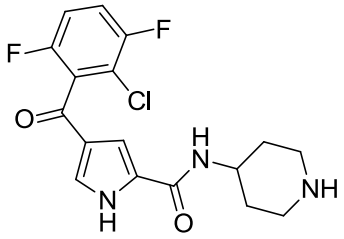

General procedure K: *tert*-butyl 4-(4-(2-chloro-3,6-difluorobenzoyl)-1*H*-pyrrole-2-carboxamido)piperidine-1-carboxylate (130 mg, 0.28 mmol), triethylsilane (112 µL, 0.70 mmol), and TFA (2 mL/mmol) gave **378** as a white solid (97 mg, 94%). R_f 0.53 (9:1 DCM/MeOH, NH silica); m.p. 223-225 ^oC; λ_{max} (EtOH/nm) 283.5, 237.0; IR υ_{max}/cm^{-1} 3280,

2955, 2842, 1629, 1566, 1535; ^{1}H NMR (500 MHz, DMSO-d_6) δ ppm 1.48-1.56 (2H, m, CH-piperidine), 1.82-1.86 (2H, m, CH-piperidine), 2.74-2.80 (2H, m, N-CH-piperidine), 3.12-3.16 (2H, m, N-CH-piperidine), 3.87-3.95 (1H, m, N-CH-piperidine), 7.27 (1H, br s, H-3), 7.45-7.49 (2H, m, H-3 and H-5'), 7.61-7.66 (1H, m, H-4'), 8.20 (1H, d, J = 7.8 Hz, CO-NH), NH-pyrrole not observed. ^{13}C NMR (125 MHz, DMSO-d_6) δ ppm 30.2 (C-piperidine), 43.4 (C-piperidine), 45.1 (C-piperidine), 110.0 (C-Ar), 116.3 (dd, J_{CF} = 7.6 and 24.4 Hz, C-Ar), 117.5 (dd, J_{CF} = 7.0 and 21.1 Hz, C-Ar), 118.0 (dd, J_{CF} = 9.0 and 23.6 Hz, C-Ar), 124.6 (C-Ar), 129.0 (C-Ar), 129.4 (d, J_{CF} = 25.7 Hz, C-Ar), 154.1 (d, J_{CF} = 242.5 Hz, C-F), 154.2 (d, J_{CF} = 242.5 Hz, C-Ar), 159.0 (CO), 182.5 (CO), one C-Ar not visualised; HRMS calcd for $C_{17}H_{16}{}^{35}ClF_2N_3O_2$ $[M+H]^+$ 368.0972, found 368.0977.

4-(2-Chloro-3,6-difluorobenzoyl)-*N*-(1-methylpiperidin-4-yl)-1*H*-pyrrole-2-carboxamide, 346

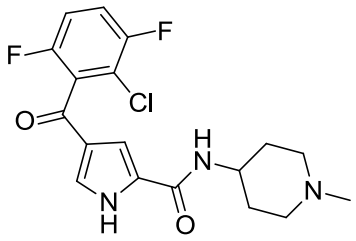

General procedure D: 4-(2-chloro-3,6-difluorobenzoyl)-1*H*-pyrrole-2-carboxylic acid (109 mg, 0.38 mmol), CDI (123 mg, 0.76 mmol), and 4-amino-1-methyl piperidine (119 µL, 0.95 mmol). Purification *via* column chromatography (NH silica; 0-8% MeOH/DCM) gave **346** as a white solid (142 mg, 98%). R_f 0.20 (9:1 DCM/MeOH); m.p. Degrades >250 ^{o}C; λ_{max} (EtOH/nm) 281.5, 237.0; IR υ_{max}/cm^{-1} 3196, 3124, 2945, 2852, 2796, 1668, 1620, 1566, 1529; ^{1}H NMR (500 MHz, DMSO-d_6) δ ppm 1.49-1.56 (2H, m, CH-piperidine), 1.72-1.75 (2H, m, CH-piperidine), 1.90-1.95 (2H, m, N-CH-piperidine), 2.16 (3H, s, N-CH_3), 2.74-2.77 (2H, m, N-CH-piperidine), 3.64-3.72 (1H, m, N-CH-piperidine), 7.24 (1H, br s, H-3), 7.44-7.48 (2H, m, H-5 and H-5'), 7.61-7.65 (1H, m, H-4'), 8.09 (1H, d, J = 7.8 Hz, CO-NH), 12.46 (1H, s, NH-pyrrole); ^{13}C NMR (125 MHz, DMSO-d_6) δ ppm 31.5 (C-piperidine), 45.9 (N-CH_3), 46.0 (C-piperidine), 54.4 (C-piperidine), 109.8 (C-Ar), 116.3 (dd, J_{CF} = 7.5 and 24.5 Hz, C-Ar), 117.5 (dd, J_{CF} = 7.2 and 21.4 Hz, C-Ar), 118.0 (dd, J_{CF} = 8.9 and 23.7 Hz, C-Ar), 124.6 (C-Ar), 128.7 (C-Ar), 129.1 (C-Ar), 129.4 (d, J_{CF} = 25.6 Hz, C-Ar), 154.0 (d, J_{CF} = 244.5 Hz, C-F), 154.2 (d, J_{CF} = 242.4 Hz, C-F), 159.0 (CO), 182.5 (CO); HRMS calcd for $C_{18}H_{18}{}^{35}ClF_2N_3O_2$ $[M+H]^+$ 382.1128, found 382.1134.

Methyl 4-(2,6-difluoro-3-methylbenzoyl)-1*H*-pyrrole-2-carboxylate, 347

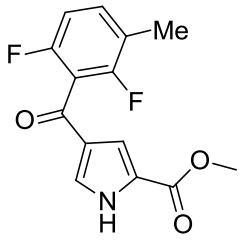

General procedure F: methyl 1*H*-pyrrole-2-carboxylate (330 mg, 2.63 mmol), 2,6- difluoro, 3- methylbenzoyl chloride (1.00 g, 5.25 mmol), and $AlCl_3$ (0.88 g, 6.58 mmol). Purification *via* column chromatography (silica; 0-50% EtOAc/petrol) gave **347** as a colourless oil (0.69 g, 94%). R_f 0.25 (8:2 Petrol/EtOAc); λ_{max} (EtOH/nm) 277.5, 233.5; IR υ_{max}/cm^{-1} 3277, 2955, 2923, 1709, 1643, 1625, 1559; ^{1}H NMR (500 MHz, $CDCl_3$) δ ppm 2.30 (3H, s, CH_3), 3.90 (3H, s, O-CH_3), 6.90 (1H, dd, *J* = 8.6 and 9.7 Hz, H-5'), 7.24-7.27 (2H, m, H-3 and H-4'), 7.51 (1H, dd, *J* = 1.5 and 3.3 Hz, H-5), 9.63 (1H, s, NH-pyrrole); ^{13}C NMR (125 MHz, $CDCl_3$) δ ppm 14.1 (d, J_{CF} = 2.9 Hz, CH_3), 52.0 (O-CH_3), 111.2 (dd, J_{CF} = 3.9 and 21.5 Hz, C-Ar), 115.8 (C-Ar), 117.4 (t, J_{CF} = 22.2 Hz, C-Ar), 121.3 (dd, J_{CF} = 3.5 and 17.6 Hz, C-Ar), 124.4 (C-Ar), 127.5 (C-Ar), 128.3 (C-Ar), 132.6 (dd, J_{CF} = 6.8 and 9.1 Hz, C-Ar), 157.5 (dd, J_{CF} = 7.8 and 250.0 Hz, C-F), 157.7 (dd, J_{CF} = 7.3 and 248.8 Hz, C-F), 161.2 (CO), 183.1 (CO); HRMS calcd for $C_{14}H_{11}F_2NO_3$ $[M+H]^+$ 280.0780, found 280.0780.

4-(2,6-Difluoro-3-methylbenzoyl)-1*H*-pyrrole-2-carboxylic acid, 348

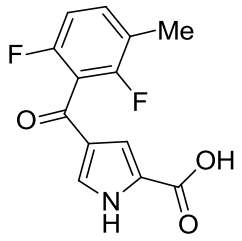

General procedure G: methyl 4-(2,6-difluoro-3-methylbenzoyl)-1*H*-pyrrole-2-carboxylate (0.60 g, 2.15 mmol), and LiOH monohydrate (1.81 g, 43.00 mmol) gave **348** as a white solid (0.55 g, 98%). R_f 0.27 (9:1 DCM/MeOH); m.p. 222-224 ^oC; λ_{max} (EtOH/nm) 282.0, 231.5; IR υ_{max}/cm^{-1} 3294, 2882, 2703, 2623, 2546, 1626, 1552, 1506; ^{1}H NMR (500 MHz, DMSO-d_6) δ ppm 2.26 (3H, s, CH_3), 6.99 (1H, br s, H-3), 7.14 (1H, dd, J = 8.6 and 9.4 Hz, H-5'), 7.45-7.50 (2H, m, H-5 and H-4'), 12.69 (1H, s, NH-pyrrole), 12.92 (1H, s, COOH); ^{13}C NMR (125 MHz, DMSO-d_6) δ ppm 13.6 (d, J_{CF} = 2.7 Hz, CH_3), 111.5 (dd, J_{CF} = 3.5 and 21.2 Hz, C-Ar), 114.2 (C-Ar), 117.2 (t, J_{CF} = 23.6 Hz, C-Ar), 121.1 (dd, J_{CF} = 3.5 and 17.8 Hz, C-Ar), 125.7

(C-Ar), 125.9 (C-Ar), 129.7 (C-Ar), 132.9 (dd, J_{CF} = 6.8 and 9.4 Hz, C-Ar), 156.6 (dd, J_{CF} = 7.6 and 246.7 Hz, C-F), 156.7 (dd, J_{CF} = 7.6 and 245.1 Hz, C-F), 161.3 (CO), 182.0 (CO); HRMS calcd for $C_{13}H_9F_2NO_3$ $[M-H]^-$ 264.0478, found 264.0466.

4-(2,6-Difluoro-3-methylbenzoyl)-*N*-(pyridin-3-yl)-1*H*-pyrrole-2-carboxamide, 349

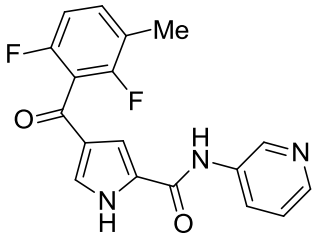

General procedure M: 4-(2,6-difluoro-3-methylbenzoyl)-1*H*-pyrrole-2-carboxylic acid (55 mg, 0.21 mmol), PCl_3 (18 µL, 0.21 mmol), and 3-aminopyridine (50 mg, 0.53 mmol). Purification *via* column chromatography (NH silica; 0-8% MeOH/DCM) gave **349** as a white solid (66 mg, 92%). R_f 0.31 (95:5 DCM/MeOH); m.p. 254-256 ^oC; λ_{max} (EtOH/nm) 293.5, 253.5; IR υ_{max}/cm^{-1} 3356, 3254, 3118, 1705, 1631, 1599, 1533; ^1H NMR (500 MHz, DMSO-d_6) δ ppm 2.27 (3H, s, CH_3), 7.17 (1H, dd, J = 8.6 and 8.7 Hz, H-5'), 7.39 (1H, dd, J = 4.7 and 8.2 Hz, CH-pyridine), 4.47-4.53 (3H, m, H-3, H-5 and H-4'), 8.14-8.16 (1H, m, CH-pyridine), 8.30 (1H, dd, J = 1.5 and 4.7 Hz, N-CH-pyridine), 8.90 (1H, d, J = 2.5 Hz, N-CH-pyridine), 10.25 (1H, s, CO-NH), 12.71 (1H, s, NH-pyrrole); ^{13}C NMR (125 MHz, DMSO-d_6) δ ppm 13.7 (CH_3), 111.5 (C-Ar), 111.6 (C-Ar), 117.4 (m, C-Ar), 121.1 (dd, J_{CF} = 3.0 and 18.6 Hz, C-Ar), 123.6 (C-Ar), 125.9 (C-Ar), 127.0 (C-Ar), 132.9 (m, C-Ar), 135.5 (C-Ar), 141.6 (C-Ar), 144.4 (C-Ar), 156.5 (dd, J_{CF} = 7.5 and 245.9 Hz, C-F), 156.6 (dd, J_{CF} = 7.1 and 244.5 Hz, C-F), 158.7 (CO), 182.2 (CO), two C-Ar not visualised; HRMS calcd for $C_{18}H_{13}F_2N_3O_2$ $[M+H]^+$ 342.1049, found 342.1049.

4-(2,6-Difluoro-3-methylbenzoyl)-*N*-(pyrimidin-5-yl)-1*H*-pyrrole-2-carboxamide, 350

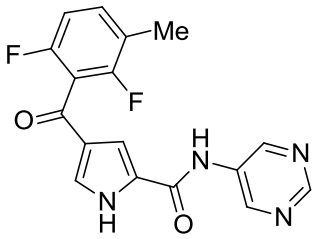

General procedure M with exceptions to the method: 4-(2,6-difluoro-3-methylbenzoyl)-1*H*-pyrrole-2-carboxylic acid (85 mg, 0.32 mmol), PCl_3 (28 µL, 0.32 mmol), and 5-

aminopyrimidine (76 mg, 0.80 mmol) for 15 min. Purification *via* column chromatography (silica; 0-8% MeOH/DCM) gave **350** as a yellow solid (56 mg, 51%). R_f 0.60 (9:1 DCM/MeOH); m.p. 317-319 ^oC; λ_{max} (EtOH/nm) 290.0; IR υ_{max}/cm^{-1} 3331, 3257, 3118, 2982, 1666, 1626, 1589, 1554, 1525; ^1H NMR (500 MHz, DMSO-d_6) δ ppm 2.27 (3H, s, CH_3), 7.17 (1H, dd, *J* = 8.6 and 8.7 Hz, H-5'), 7.57-7.53 (2H, m, H-3 and H-4'), 7.58 (1H, br s, H-5), 8.92 (1H, s, CH-pyrimidine), 9.13 (2H, s, CH-pyrimidine), 10.44 (1H, s, CO-NH), 12.81 (1H, s, NH-pyrrole); ^{13}C NMR (125 MHz, DMSO-d_6) δ ppm 13.7 (CH_3), 111.6 (dd, J_{CF} = 2.9 and 20.5 Hz, C-Ar), 112.2 (C-Ar), 117.3 (t, J_{CF} = 23.9 Hz, C-Ar), 121.1 (dd, J_{CF} = 2.8 and 17.5 Hz, C-Ar), 125.9 (C-Ar), 127.5 (C-Ar), 129.7 (C-Ar), 133.0 (dd, J_{CF} = 6.1 and 8.1 Hz, C-Ar), 134.3 (C-Ar), 147.8 (C-Ar), 153.2 (C-Ar), 156.6 (m, C-F), 158.8 (CO), 182.2 (CO), one C-F not visualised; HRMS calcd for $C_{17}H_{12}F_2N_4O_2$ $[M+H]^+$ 343.1001, found 343.1003.

***tert*-Butyl 4-(4-(2,6-difluoro-3-methylbenzoyl)-1*H*-pyrrole-2-carboxamido)piperidine-1-carboxylate, 351**

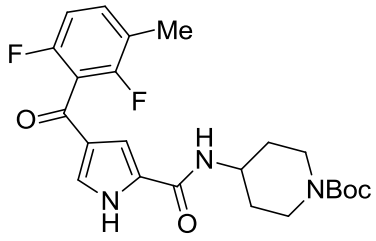

General procedure D: 4-(2,6-difluoro-3-methylbenzoyl)-1*H*-pyrrole-2-carboxylic acid (101 mg, 0.38 mmol), CDI (123 mg, 0.76 mmol), and *tert*-butyl 4-aminopiperidine-1-carboxylate (190 mg, 0.95 mmol). Purification *via* column chromatography (silica; 30-100% EtOAc/petrol) gave **351** as a white solid (115 mg, 68%). R_f 0.71 (9:1 DCM/MeOH); m.p. 231-232 ^oC; λ_{max} (EtOH/nm) 288.0, 237.0; IR υ_{max}/cm^{-1} 3355, 3167, 3125, 2973, 2931, 2864, 1696, 1621, 1568, 1531; ^1H NMR (500 MHz, $CDCl_3$) δ ppm 1.38-1.46 (2H, m, CH-piperidine), 1.49 (9H, s, C-*CH*$_3$), 1.97-1.80 (2H, m, CH-piperidine), 2.30 (3H, s, CH_3), 2.86-2.92 (2H, m, N-CH-piperidine), 4.05-4.12 (3H, m, N-CH-piperidine), 6.15 (1H, br s, CO-NH), 6.91 (1H, dd, *J* = 7.6 and 8.6 Hz, H-5'), 7.14 (1H, br s, H-3), 7.24-7.28 (1H, m, H-4'), 7.36 (1H, d, *J* = 2.5 Hz, H-5), 10.02 (1H, s, NH-pyrrole); ^{13}C NMR (125 MHz, $CDCl_3$) δ ppm 14.1 (d, J_{CF} = 2.9 Hz, CH_3), 28.4 (C-*CH*$_3$), 32.0 (C-piperidine), 42.8 (C-piperidine), 47.1 (C-piperidine), 79.8 (*C*-CH_3), 109.2 (C-Ar), 111.2 (dd, J_{CF} = 3.8 and 21.2 Hz, C-Ar), 117.5 (t, J_{CF} =22.7 Hz, C-Ar), 121.3 (dd, J_{CF} = 3.4 and 17.9 Hz, C-Ar), 127.3 (C-Ar), 128.0 (C-Ar),

128.3 (C-Ar), 132.6 (dd, J_{CF} = 6.9 and 8.8 Hz, C-Ar), 154.7 (CO), 157.5 (dd, J_{CF} = 7.5 and 249.2 Hz, C-F), 157.6 (dd, J_{CF} = 7.1 and 248.3 Hz, C-F), 159.9 (CO), 183.1 (CO); HRMS calcd for $C_{23}H_{27}F_2N_3O_4$ $[M+H]^+$ 448.2042, found 448.2043.

4-(2,6-Difluoro-3-methylbenzoyl)-*N*-(piperidin-4-yl)-1*H*-pyrrole-2-carboxamide, 379

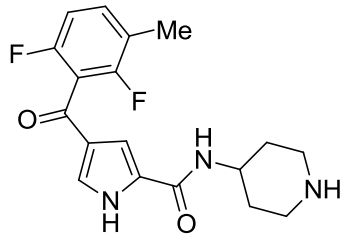

General procedure K: *tert*-butyl 4-(4-(2,6-difluoro-3-methylbenzoyl)-1*H*-pyrrole-2-carboxamido)piperidine-1-carboxylate (80 mg, 0.17 mmol), triethylsilane (69 μL, 0.43 mmol) and TFA (2 mL/mmol) gave **379** as a white solid (55 mg, 93%). R_f 0.61 (9:1 DCM/MeOH, NH silica); m.p. 212-213 ^oC; λ_{max} (EtOH/nm) 283.0, 234.5; IR υ_{max}/cm^{-1} 2935, 2862, 1624, 1566, 1535; ^1H NMR (500 MHz, DMSO-d_6) δ ppm 1.46-1.53 (2H, m, CH-piperidine), 1.79-1.82 (2H, m, CH-piperidine), 2.25 (3H, s, CH_3), 2.69-2.74 (2H, m, N-CH-piperidine), 3.09-3.12 (2H, m, N-CH-piperidine), 3.85-3.91 (1H, m, N-CH-piperidine), 7.12-7.16 (1H, dd, *J* = 7.6 and 8.6 Hz, H-5'), 7.26 (1H, br s, H-3), 7.37 (1H, br s, H-5), 7.43-7.49 (1H, m, H-4'), 8.20 (1H, d, *J* = 7.9 Hz, CO-NH); ^{13}C NMR (125 MHz, DMSO-d_6) δ ppm 13.6 (d, J_{CF} = 2.3 Hz, CH_3), 31.0 (C-piperidine), 43.9 (C-piperidine), 45.5 (C-piperidine), 110.1 (C-Ar), 111.5 (dd, J_{CF} = 3.1 and 21.3 Hz, C-Ar), 117.5 (t, J_{CF} = 23.3 Hz, C-Ar), 121.0 (dd, J_{CF} = 3.0 and 17.5 Hz, C-Ar), 125.6 (C-Ar), 128.2 (C-Ar), 128.7 (C-Ar), 132.7 (dd, J_{CF} = 6.4 and 8.4 Hz, C-Ar), 156.5 (dd, J_{CF} = 8.2 and 246.5 Hz, C-F), 156.7 (dd, J_{CF} = 7.8 and 244.8 Hz, C-F), 159.0 (CO), 182.2 (CO); HRMS calcd for $C_{18}H_{19}F_2N_3O_2$ $[M+H]^+$ 348.1518, found 348.1520.

4-(2,6-Difluoro-3-methylbenzoyl)-*N*-(1-methylpiperidin-4-yl)-1*H*-pyrrole-2-carboxamide, 352

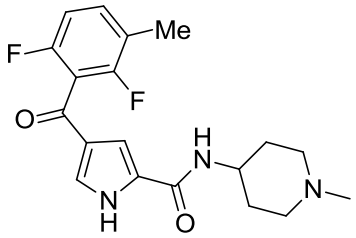

General procedure D: 4-(2,6-difluoro-3-methylbenzoyl)-1*H*-pyrrole-2-carboxylic acid (50 mg, 0.17 mmol), CDI (55 mg, 0.34 mmol), and 4-amino-1-methyl piperidine (54 µL, 0.43 mmol). Purification *via* column chromatography (NH silica; 0-8% MeOH/DCM) gave **352** as a white solid (57 mg, 88%). R_f 0.19 (9:1 DCM/MeOH); m.p. 275-278 ^oC; λ_{max} (EtOH/nm) 295.0, 235.5; IR υ_{max}/cm^{-1} 3243, 2940, 2803, 1622, 1582; ^1H NMR (500 MHz, DMSO-d_6) δ ppm 1.48-1.56 (2H, m, CH-piperidine), 1.72-1.75 (2H, m, CH-piperidine), 1.90-1.95 (2H, m, N-CH-piperidine), 2.16 (3H, s, N-CH_3), 2.26 (3H, s, CH_3), 2.74-2.77 (2H, m, N-CH-piperidine), 3.64-3.72 (1H, m, N-CH-piperidine), 7.14 (1H, dd, J = 8.6 and 9.1 Hz, H-5'), 7.24 (1H, br s, H-3), 7.36 (1H, br s, H-5), 7.44-7.49 (1H, m, H-4'), 8.09 (1H, d, J = 7.9 Hz, CO-NH), 12.37 (1H, s, NH-pyrrole); ^{13}C NMR (125 MHz, DMSO-d_6) δ ppm 13.7 (d, J_{CF} = 2.3 Hz, CH_3), 31.6 (C-piperidine), 45.9 (N-CH_3), 46.0 (C-piperidine), 54.4 (C-piperidine), 109.9 (C-Ar), 111.5 (dd, J_{CF} = 3.8 and 20.7 Hz, C-Ar), 121.0 (dd, J_{CF} = 3.4 and 17.5 Hz, C-Ar), 125.6 (C-Ar), 128.1 (C-Ar), 128.8 (C-Ar), 132.7 (m, C-Ar), 156.5 (m, two C-F), 159.1 (CO), 182.2 (CO), one C-F not visualised; HRMS calcd for $C_{19}H_{21}F_2N_3O_2$ $[M+H]^+$ 362.1675, found 362.1674.

Methyl 4-(6-chloro-2,3-difluorobenzoyl)-1*H*-pyrrole-2-carboxylate, 353

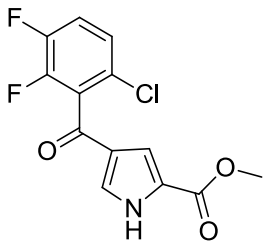

General procedure E: 6-chloro, 2,3-difluorobenzoic acid (1.12 g, 5.83 mmol), $SOCl_2$ (0.64 mL, 8.75 mmol) and DMF (10 mol%) gave 6-chloro, 2,3-difluorobenzoyl chloride as a yellow oil which was used directly in the next step. **General procedure F:** methyl 1*H*-pyrrole-2-carboxylate (365 mg, 2.92 mmol), and $AlCl_3$ (0.98 g, 7.30 mmol). Purification *via*

column chromatography (silica; 0-50% EtOAc/petrol) gave **353** as a white solid (0.51 g, 59%). R_f 0.19 (8:2 Petrol/EtOAc); m.p. 176-178 ^oC; λ_{max} (EtOH/nm) 281.0, 232.5, 211.5; IR υ_{max}/cm^{-1} 3260, 3162, 3037, 2967, 1691, 1656, 1557; ^1H NMR (500 MHz, $CDCl_3$) δ ppm 3.91 (3H, s, O-CH_3), 7.21-7.25 (3H, m, H-3, H-4' and H-5'), 7.49 (1H, dd, *J* = 1.6 and 2.4 Hz, H-5), 9.79 (1H, s, NH-pyrrole); ^{13}C NMR (125 MHz, $CDCl_3$) δ ppm 52.1 (O-CH_3), 115.6 (C-Ar), 118.5 (d, J_{CF} = 18.5 Hz, C-Ar), 124.8 (C-Ar), 125.7 (dd, J_{CF} = 4.3 and 5.0 Hz, C-Ar), 126.1 (dd, J_{CF} = 3.4 and 3.5 Hz, C-Ar), 126.4 (C-Ar), 128.4 (C-Ar), 129.9 (d, J_{CF} = 18.6 Hz, C-Ar), 147.4 (dd, J_{CF} = 12.9 and 248.9 Hz, C-F), 149.2 (dd, J_{CF} = 12.8 and 249.5 Hz, C-F), 161.1 (CO), 183.2 (CO); HRMS calcd for $C_{13}H_8{}^{35}ClF_2NO_3$ $[M+H]^+$ 300.0234, found 300.0240.

4-(6-Chloro-2,3-difluorobenzoyl)-1*H*-pyrrole-2-carboxylic acid, 354

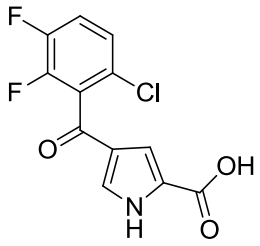

General procedure G: methyl 4-(6-chloro-2,3-difluorobenzoyl)-1*H*-pyrrole-2-carboxylate (480 mg, 1.61 mmol), and LiOH monohydrate (1.35 g, 32.2 mmol) gave **354** as a white solid (459 mg, 100%). R_f 0.21 (9:1 DCM/MeOH); m.p. 253-255 ^oC; λ_{max} (EtOH/nm) 283.0, 234.5; IR υ_{max}/cm^{-1} 3334, 2674, 2626, 2605, 1685, 1651, 1558; ^1H NMR (500 MHz, DMSO-d_6) δ ppm 7.05 (1H, br s, H-3), 7.48 (1H, ddd, J = 1.8, 4.0 and 9.1 Hz, H-5'), 7.60-7.67 (2H, m, H-5 and H-4'), 12.76 (1H, s, NH-pyrrole), 12.93 (1H, s, COOH); ^{13}C NMR (125 MHz, DMSO-d_6) δ ppm 114.1 (C-Ar), 119.1 (d, J_{CF} = 19.0 Hz, C-Ar), 124.8 (C-Ar), 125.0 (dd, J_{CF} = 3.4 and 3.5 Hz, C-Ar), 126.1 (C-Ar), 126.4 (dd, J_{CF} = 4.1 and 6.8 Hz, C-Ar), 129.5 (d, J_{CF} = 19.4 Hz, C-Ar), 130.6 (C-Ar), 146.6 (dd, J_{CF} = 12.7 and 247.5 Hz, C-F), 148.6 (dd, J_{CF} = 13.0 and 247.9 Hz, C-F), 161.3 (CO), 182.3 (CO); HRMS calcd for $C_{12}H_6{}^{35}ClF_2NO_3$ $[M+H]^+$ 286.0077, found 286.0082.

4-(6-Chloro-2,3-difluorobenzoyl)-*N*-(pyridin-3-yl)-1*H*-pyrrole-2-carboxamide, 355

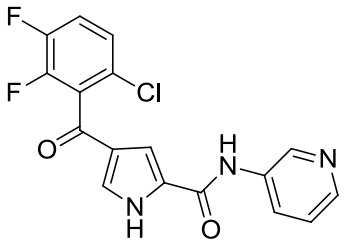

General procedure M: 4-(6-chloro-2,3-difluorobenzoyl)-1*H*-pyrrole-2-carboxylic acid (54 mg, 0.19 mmol), PCl_3 (17 µL, 0.19 mmol), and 3-aminopyridine (45 mg, 0.48 mmol). Purification *via* column chromatography (silica; 0-8% MeOH/DCM) gave **355** as a white solid (39 mg, 57%). R_f 0.31 (95:5 DCM/MeOH); m.p. 228-229 ^oC; λ_{max} (EtOH/nm) 290.5, 253.5; IR υ_{max}/cm^{-1} 3319, 3123, 3095, 2979, 2930, 2875, 1647, 1593, 1516; ^1H NMR (500 MHz, DMSO-d_6) δ ppm 7.40 (1H, dd, *J* = 4.7 and 8.4 Hz, CH-pyridine), 7.52 (1H, ddd, *J* = 1.8, 4.1 and 9.1 Hz, H-5'), 7.55 (1H, br s, H-3), 7.64-7.70 (2H, m, H-5 and H-4'), 8.14 (1H, ddd, *J* = 1.5, 2.5 and 8.3 Hz, CH-pyridine), 8.31 (1H, dd, *J* = 1.5 and 4.7 Hz, N-CH-pyridine), 8.90 (1H, d, *J* = 2.5 Hz, N-CH-pyridine), 10.25 (1H, s, CO-NH), 12.79 (1H, s, NH-pyrrole); ^{13}C NMR (125 MHz, DMSO-d_6) δ ppm 111.5 (C-Ar), 119.1 (d, J_{CF} = 18.0 Hz, C-Ar), 123.6 (C-Ar), 124.8 (C-Ar), 125.1 (dd, J_{CF} = 4.6 and 5.7 Hz, C-Ar), 126.4 (dd, J_{CF} = 3.7 and 5.9 Hz, C-Ar), 127.0 (C-Ar), 128.4 (C-Ar), 129.7 (d, J_{CF} = 20.1 Hz, C-Ar), 130.4 (C-Ar), 135.5 (C-Ar), 141.6 (C-Ar), 158.7 (CO), 182.4 (CO), two C-F and one C-Ar not visualised; HRMS calcd for $C_{17}H_{10}{}^{35}ClF_2N_3O_2$ $[M+H]^+$ 362.0502, found 362.0503.

4-(6-Chloro-2,3-difluorobenzoyl)-*N*-(pyrimidin-5-yl)-1*H*-pyrrole-2-carboxamide, 356

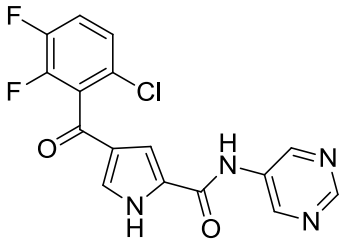

General procedure M with exceptions to the method: 4-(6-chloro-2,3-difluorobenzoyl)-1*H*-pyrrole-2-carboxylic acid (59 mg, 0.21 mmol), PCl_3 (18 µL, 0.21 mmol), and 5-aminopyrimidine (50 mg, 0.53 mmol) for 30 min. Purification *via* column chromatography (silica; 0-8% MeOH/DCM) gave **356** as a yellow solid (42 mg, 55%). R_f 0.58 (9:1 DCM/MeOH); m.p. 277-279 ^oC; λ_{max} (EtOH/nm) 291.0, 267.5; IR υ_{max}/cm^{-1} 3309, 3125, 3079, 2868, 1644, 1588, 1555, 1533; ^1H NMR (500 MHz, DMSO-d_6) δ ppm 7.51-7.54 (2H,

m, H-5' and H-3), 7.65-7.70 (2H, m, H-4' and H-5), 8.93 (1H, s, N-CH-pyrimidine), 9.13 (2H, s, N-CH-pyrimidine), 10.45 (1H, s, CO-NH), 12.88 (1H, s, NH-pyrrole); ^{13}C NMR (125 MHz, DMSO-d_6) δ ppm 112.0 (C-Ar), 119.2 (d, J_{CF} = 18.6 Hz, C-Ar), 124.9 (C-Ar), 125.1 (dd, J_{CF} = 3.8 and 4.0 Hz, C-Ar), 126.5 (dd, J_{CF} = 3.6 and 5.9 Hz, C-Ar), 127.9 (C-Ar), 129.6 (d, J_{CF} = 19.2 Hz, C-Ar), 130.6 (C-Ar), 134.3 (C-Ar), 146.5 (dd, J_{CF} = 14.4 and 248.3 Hz, C-F), 147.8 (C-Ar), 148.8 (dd, J_{CF} = 11.6 and 235.6 Hz, C-F), 153.2 (C-Ar), 158.8 (CO), 182.4 (CO); HRMS calcd for $C_{16}H_9{}^{35}ClF_2N_4O_2$ $[M+H]^+$ 363.0455, found 363.0472.

***tert*-Butyl 4-(4-(6-chloro-2,3-difluorobenzoyl)-1*H*-pyrrole-2-carboxamido)piperidine-1-carboxylate, 357**

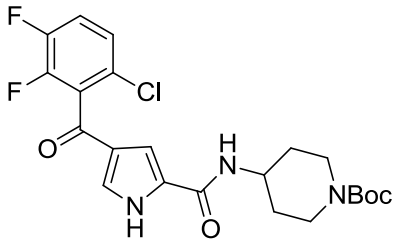

General procedure D: 4-(6-chloro-2,3-difluorobenzoyl)-1*H*-pyrrole-2-carboxylic acid (100 mg, 0.35 mmol), CDI (113 mg, 0.70 mmol), and *tert*-butyl 4-aminopiperidine-1-carboxylate (176 mg, 0.88 mmol). Purification *via* column chromatography (silica; 30-100% EtOAc/petrol) gave **357** as a colourless oil (150 mg, 91%). R_f 0.65 (9:1 DCM/MeOH); λ_{max} (EtOH/nm) 288.0, 236.5; IR υ_{max}/cm^{-1} 1662, 1619, 1568, 1534; ^{1}H NMR (500 MHz, $CDCl_3$) δ ppm 1.37-1.45 (2H, m, CH-piperidine), 1.48 (9H, s, C-*CH*$_3$), 1.97-2.00 (2H, m, CH-piperidine), 2.86-2.92 (2H, m, N-CH-piperidine), 4.04-4.12 (3H, m, N-CH-piperidine), 5.93 (1H, d, J = 7.9 Hz, CO-NH), 7.00 (1H, br s, H-3), 7.22-7.24 (2H, m, H-4' and H-5'), 7.33 (1H, br s, H-5), 9.90 (1H, s, NH-pyrrole); ^{13}C NMR (125 MHz, $CDCl_3$) δ ppm 28.4 (C-*CH*$_3$), 32.1 (C-piperidine), 42.7 (C-piperidine), 47.1 (C-piperidine), 79.8 (*C*-CH$_3$), 108.8 (C-Ar), 118.5 (d, J_{CF} = 18.8 Hz, C-Ar), 125.8 (dd, J_{CF} = 4.2 and 5.8 Hz, C-Ar), 126.2 (d, J_{CF} = 6.8 Hz, C-Ar), 128.0 (C-Ar), 128.2 (C-Ar), 154.7 (CO), 159.4 (CO), two C-F, two C-Ar and one CO not visualised; HRMS calcd for $C_{22}H_{24}{}^{35}ClF_2N_3O_4$ $[M+NH_4]^+$ 485.1762, found 485.1754.

4-(6-Chloro-2,3-difluorobenzoyl)-*N*-(piperidin-4-yl)-1*H*-pyrrole-2-carboxamide, 380

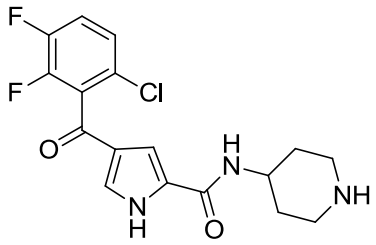

General procedure K: *tert*-butyl 4-(4-(6-chloro-2,3-difluorobenzoyl)-1*H*-pyrrole-2-carboxamido)piperidine-1-carboxylate (140 mg, 0.30 mmol), triethylsilane (120 µL, 0.75 mmol) and TFA (2 mL/mmol) gave **380** as a white solid (105 mg, 95%). R_f 0.43 (9:1 DCM/MeOH, NH silica); m.p. 154-156 ^oC; λ_{max} (EtOH/nm) 286.5, 236.5; IR υ_{max}/cm^{-1} 3123, 2941, 2854, 1620, 1566, 1533; ^1H NMR (500 MHz, DMSO-d_6) δ ppm 1.32-1.39 (2H, m, CH-piperidine), 1.69-1.72 (2H, m, CH-piperidine), 2.46-2.51 (2H, m, N-CH-piperidine), 2.93-2.96 (2H, m, N-CH-piperidine), 3.73-3.81 (1H, m, N-CH-piperidine), 7.25 (1H, br s, H-3), 7.46 (1H, br s, H-5), 7.49 (1H, ddd, *J* = 1.7, 4.0 and 9.1 Hz, H-5'), 7.62-7.67 (1H, m, H-4'), 8.10 (1H, d, *J* = 7.7 Hz, CO-NH), NH-piperidine and NH-pyrrole not visualised; ^{13}C NMR (125 MHz, $CDCl_3$) 33.0 (C-piperidine), 45.2 (C-piperidine), 46.8 (C-piperidine), 109.8 (C-Ar), 118.9 (d, J_{CF} = 18.6 Hz, C-Ar), 124.5 (C-Ar), 125.1 (C-Ar), 126.4 (dd, J_{CF} = 3.6 and 5.7 Hz, C-Ar), 129.1 (m, C-Ar), 129.4 (C-Ar), 129.9 (d, J_{CF} = 19.6 Hz, C-Ar), 146.5 (dd, J_{CF} = 14.8 and 247.5 Hz, C-F), 148.7 (dd, J_{CF} = 11.9 and 248.5 Hz, C-F), 158.8 (CO), 182.3 (CO); HRMS calcd for $C_{17}H_{16}{}^{35}ClF_2N_3O_2$ $[M+H]^+$ 368.0972, found 368.0976.

4-(6-Chloro-2,3-difluorobenzoyl)-*N*-(1-methylpiperidin-4-yl)-1*H*-pyrrole-2-carboxamide, 358

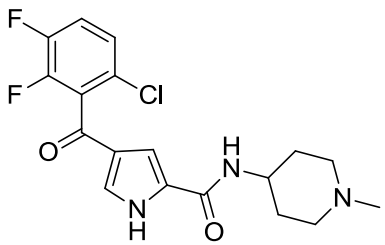

General procedure D: 4-(6-chloro-2,3-difluorobenzoyl)-1*H*-pyrrole-2-carboxylic acid (71 mg, 0.25 mmol), CDI (81 mg, 0.50 mmol), and 4-amino-1-methyl piperidine (79 µL, 0.63 mmol). Purification *via* column chromatography (NH silica; 0-5% MeOH/DCM) gave **358** as a white solid (65 mg, 68%).

R_f 0.17 (9:1 DCM/MeOH); m.p. 188-190 ^oC; λ_{max} (EtOH/nm) 286.0, 238.0; IR υ_{max}/cm^{-1} 3562, 3200, 3131, 2947, 2852, 2801, 1665, 1616, 1579, 1549; ^1H NMR (500 MHz, DMSO-d_6) δ ppm 1.49-1.57 (2H, m, CH-piperidine), 1.72-1.75 (2H, m, CH-piperidine), 1.90-1.95 (2H, m, N-CH-piperidine), 2.16 (3H, s, N-CH_3), 2.74-2.78 (2H, m, N-CH-piperidine), 3.64-3.72 (1H, m, N-CH-piperidine), 7.25 (1H, br s, H-3), 7.47-7.51 (2H, m, H-5 and H-5'), 7.62-7.67 (1H, m, H-4'), 8.10 (1H, d, J = 7.9 Hz, CO-NH), 12.47 (1H, s, NH-pyrrole); ^{13}C NMR (125 MHz, DMSO-d_6) δ ppm 31.5 (C-piperidine), 45.9 (N-CH_3), 46.0 (C-piperidine), 54.4 (C-piperidine), 109.8 (C-Ar), 119.0 (d, J_{CF} = 18.3 Hz, C-Ar), 124.5 (C-Ar), 125.1 (dd, J_{CF} = 3.8 and 3.9 Hz, C-Ar), 126.4 (dd, J_{CF} = 3.0 and 5.6 Hz, C-Ar), 129.0 (C-Ar), 129.2 (C-Ar), 129.8 (d, J_{CF} = 19.8 Hz, C-Ar), 146.4 (dd, J_{CF} = 14.4 and 247.2 Hz, C-F), 148.7 (dd, J_{CF} = 12.2 and 248.3 Hz, C-F), 159.0 (CO), 182.3 (CO); HRMS calcd for $C_{18}H_{18}{}^{35}ClF_2N_3O_2$ $[M+H]^+$ 382.1128, found 382.1130.

Methyl 4-(2,5-difluorobenzoyl)-1*H*-pyrrole-2-carboxylate, 359

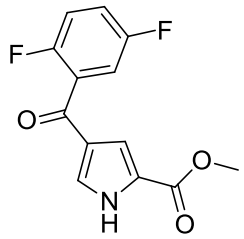

General procedure F: methyl 1*H*-pyrrole-2-carboxylate (0.51 g, 4.05 mmol), 2,5-difluorobenzoyl chloride (1.43 mL, 8.10 mmol, and $AlCl_3$ (1.36 g, 10.13 mmol). Purification *via* column chromatography (silica; 0-50% EtOAc/petrol) gave **359** as a white solid (0.97 g, 93%). R_f 0.17 (8:2 Petrol/EtOAc); m.p. 151-153 ^oC; λ_{max} (EtOH/nm) 284.5, 234.5.; IR υ_{max}/cm^{-1} 3321, 3090, 2957, 1719, 1630, 1590, 1557, 1508; ^1H NMR (500 MHz, DMSO-d_6) δ ppm 3.81 (3H, s, O-CH_3), 7.09 (1H, br s, H-3), 7.40-7.49 (3H, m, H-3', H-4' and H-6'), 7.58 (1H, br s, H-5), 12.84 (1H, s, NH-pyrrole); ^{13}C NMR (125 MHz, $CDCl_3$) δ ppm 52.1 (O-CH_3), 116.1 (C-Ar), 116.5 (dd, J_{CF} = 3.7 and 25.2 Hz, C-Ar), 117.8 (dd, J_{CF} = 8.3 and 25.1 Hz, C-Ar), 119.1 (dd, J_{CF} = 8.5 and 24.1 Hz, C-Ar), 124.3 (C-Ar), 126.4 (C-Ar), 128.4 (C-Ar), 129.0 (dd, J_{CF} = 6.5 and 18.0 Hz, C-Ar), 155.5 (dd, J_{CF} = 2.3 and 247.6 Hz, C-F), 160.3 (d, J_{CF} = 232.9 Hz, C-F), 161.2 (CO), 185.5 (CO); HRMS calcd for $C_{13}H_9F_2NO_3$ $[M+H]^+$ 266.0623, found 266.0628.

4-(2,5-Difluorobenzoyl)-1*H*-pyrrole-2-carboxylic acid, 360

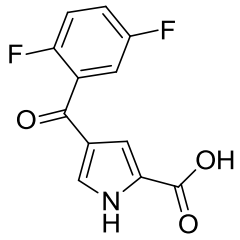

General procedure G: methyl 4-(2,5-difluorobenzoyl)-1*H*-pyrrole-2-carboxylate (0.90 g, 3.40 mmol), and LiOH monohydrate (2.86 g, 68.00 mmol) gave **360** as a white solid (0.85 g, 100%). R_f 0.30 (9:1 DCM/MeOH); m.p. 209-210 ^oC; λ_{max} (EtOH/nm) 285.0, 233.0; IR υ_{max}/cm^{-1} 3672, 3447, 3360, 3317, 3074, 1676, 1630, 1558; ^1H NMR (500 MHz, DMSO-d_6) δ ppm 7.04 (1H, br s, H-3), 7.39-7.48 (3H, m, H-3', H-4' and H-6'), 7.50 (1H, br s, H-5), 12.65 (1H, s, NH-pyrrole), 12.90 (1H, s, COOH); ^{13}C NMR (125 MHz, DMSO-d_6) δ ppm 114.7 (C-Ar), 116.0 (dd, J_{CF} = 3.7 and 25.4 Hz, C-Ar), 118.1 (dd, J_{CF} = 8.4 and 24.9 Hz, C-Ar), 118.9 (dd, J_{CF} = 8.7 and 24.1 Hz, C-Ar), 124.9 (C-Ar), 125.4 (C-Ar), 129.2 (dd, J_{CF} = 7.0 and 19.2 Hz, C-Ar), 129.9 (C-Ar), 154.8 (d, J_{CF} = 243.8 Hz, C-F), 157.8 (d, J_{CF} = 241.8 Hz, C-F), 161.4 (CO), 184.6 (CO); HRMS calcd for $C_{12}H_7F_2NO_3$ $[M+H]^+$ 252.0467, found 252.0467.

4-(2,5-Difluorobenzoyl)-*N*-(pyridin-3-yl)-1*H*-pyrrole-2-carboxamide, 361

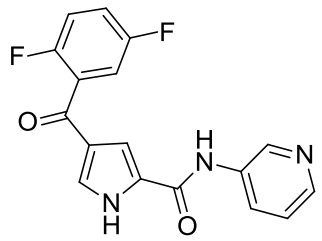

General procedure M: 4-(2,5-difluorobenzoyl)-1*H*-pyrrole-2-carboxylic acid (100 mg, 0.37 mmol), PCl_3 (32 µL, 0.37 mmol), and 3-aminopyridine (88 mg, 0.93 mmol). Purification *via* column chromatography (NH silica; 0-8% MeOH/DCM) gave **361** as a white solid (52 mg, 41%). R_f 0.25 (95:5 DCM/MeOH); m.p. 276-277 ^oC; λ_{max} (EtOH/nm) 265.5; IR υ_{max}/cm^{-1} 3238, 3079, 1668, 1635, 1562, 1545; ^1H NMR (500 MHz, DMSO-d_6) δ ppm 7.40 (1H, dd, J = 4.7 and 8.3 Hz, CH-pyridine), 7.42-7.50 (3H, m, H-3', H-4' and H-6'), 7.54 (1H, br s, H-3), 7.58 (1H, br s, H-5), 8.15 (1H, ddd, J = 1.5, 2.5 and 8.3 Hz, CH-pyridine), 8.30 (1H, dd, J = 1.5 and 4.7 Hz, N-CH-pyridine), 8.91 (1H, d, J = 2.5 Hz, N-CH-pyridine), 10.25 (1H, s, CO-NH), 12.68 (1H, s, NH-pyrrole); ^{13}C NMR (125 MHz, DMSO-d_6) δ ppm 112.1 (C-Ar), 116.0 (dd, J_{CF} = 3.4 and 25.2 Hz, C-Ar), 118.1 (dd, J_{CF} = 8.5 and 25.1 Hz, C-Ar), 118.9 (dd, J_{CF} =

8.8 and 24.2 Hz, C-Ar), 123.6 (C-Ar), 124.9 (C-Ar), 126.9 (C-Ar), 127.8 (C-Ar), 129.4 (dd, J_{CF} = 6.4 and 19.1 Hz, C-Ar), 129.6 (C-Ar), 135.5 (C-Ar), 141.6 (C-Ar), 144.4 (C-Ar), 154.8 (d, J_{CF} = 243.8 Hz, C-F), 157.8 (d, J_{CF} = 243.5 Hz, C-F), 158.8 (CO), 184.8 (CO); HRMS calcd for $C_{17}H_{11}F_2N_3O_2$ $[M+H]^+$ 328.0892, found 328.0897.

***tert*-Butyl 4-(4-(2,5-difluorobenzoyl)-1*H*-pyrrole-2-carboxamido)piperidine-1-carboxylate, 362**

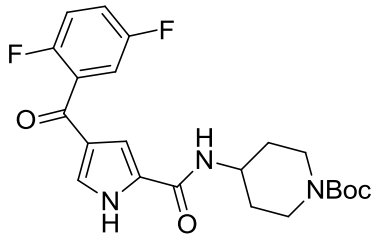

General procedure D: 4-(2,5-difluorobenzoyl)-1*H*-pyrrole-2-carboxylic acid (102 mg, 0.41 mmol), CDI (133 mg, 0.82 mmol), and *tert*-butyl 4-aminopiperidine-1-carboxylate (206 mg, 1.03 mmol). Purification *via* column chromatography (silica; 30-100% EtOAc/petrol) gave **362** as a white solid (154 mg, 87%). R_f 0.69 (9:1 DCM/MeOH); m.p. 133-135 ^oC; λ_{max} (EtOH/nm) 286.0, 238.0; IR υ_{max}/cm^{-1} 3127, 2975, 2932, 2866, 1623, 1565, 1533; ^1H NMR (500 MHz, $CDCl_3$) δ ppm 1.39-1.47 (2H, m, CH-piperidine), 1.49 (9H, s, C-*CH*$_3$), 1.97-2.00 (2H, m, CH-piperidine), 2.87-2.92 (2H, m, N-CH-piperidine), 4.06-4.14 (3H, m, N-CH-piperidine), 6.25 (1H, d, *J* = 7.9 Hz, CO-NH), 7.14-7.23 (3H, m, H-3, H-3', H-6'), 7.26 (1H, dddd, *J* = 3.4, 3.5, 8.0 and 8.1 Hz, Hz, H-4'), 7.40 (1H, br s, H-5), 10.41 (1H, s, NH-pyrrole); ^{13}C NMR (125 MHz, $CDCl_3$) δ ppm 28.4 (C-*CH*$_3$), 32.1 (C-piperidine), 42.7 (C-piperidine), 47.1 (C-piperidine), 79.8 (*C*-CH_3), 109.6 (C-Ar), 116.4 (dd, J_{CF} = 3.1 and 24.9 Hz, C-Ar), 117.8 (dd, J_{CF} = 8.1 and 25.0 Hz, C-Ar), 119.0 (dd, J_{CF} = 8.4 and 23.9 Hz, C-Ar), 126.0 (C-Ar), 127.8 (C-Ar), 128.2 (C-Ar), 129.1 (dd, J_{CF} = 6.1 and 18.7 Hz, C-Ar), 154.7 (CO), 155.5 (d, J_{CF} = 248.0 Hz, C-F), 158.3 (d, J_{CF} = 244.8 Hz, C-F), 159.8 (CO), 185.6 (CO); HRMS calcd for $C_{22}H_{25}F_2N_3O_4$ $[M+H]^+$ 434.1886, found 434.1888.

4-(2,5-Difluorobenzoyl)-*N*-(piperidin-4-yl)-1*H*-pyrrole-2-carboxamide, 381

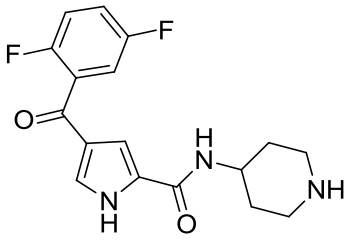

General procedure K: *tert*-butyl 4-(4-(2,5-difluorobenzoyl)-1*H*-pyrrole-2-carboxamido)piperidine-1-carboxylate (140 mg, 0.32 mmol), triethylsilane (127 µL, 0.73 mmol), and TFA (2 mL/mmol) gave **381** as a white solid (101 mg, 95%). R_f 0.45 (9:1 DCM/MeOH, NH silica); m.p. 198-200 ^oC; λ_{max} (EtOH/nm) 289.0, 238.0; IR υ_{max}/cm^{-1} 3124, 2940, 2834, 2742, 1675, 1628, 1567, 1535; ^1H NMR (500 MHz, DMSO-d_6) δ ppm 1.46-1.54 (2H, m, CH-piperidine), 1.80-1.84 (2H, m, CH-piperidine), 2.70-2.75 (2H, m, N-CH-piperidine), 3.09-3.13 (2H, m, N-CH-piperidine), 3.86-3.92 (1H, m, N-CH-piperidine), 7.30 (1H, d, *J* = 1.5 Hz, H-3), 7.38 (1H, br s, H-5), 7.39-7.49 (3H, m, H-2', H-4' and H-5'), 8.19 (1H, d, *J* = 7.8 Hz, CO-NH), 12.35 (1H, br s, NH-pyrrole); ^{13}C NMR (125 MHz, DMSO-d_6) δ ppm 30.8 (C-piperidine), 43.8 (C-piperidine), 45.4 (C-piperidine), 110.6 (C-Ar), 115.9 (dd, J_{CF} = 2.9 and 25.6 Hz, C-Ar), 118.0 (dd, J_{CF} = 8.6 and 24.9 Hz, C-Ar), 118.7 (dd, J_{CF} = 8.3 and 23.8 Hz, C-Ar), 124.6 (C-Ar), 128.4 (C-Ar), 129.5 (m, C-Ar), 154.8 (d, J_{CF} = 243.2 Hz, C-F), 157.8 (d, J_{CF} = 224.3 Hz, C-F), 159.1 (CO), 184.9 (CO), one C-Ar not visualised; HRMS calcd for $C_{17}H_{17}F_2N_3O_2$ $[M+H]^+$ 334.1362, found 334.1364.

4-(2,5-Difluorobenzoyl)-*N*-(1-methylpiperidin-4-yl)-1*H*-pyrrole-2-carboxamide, 363

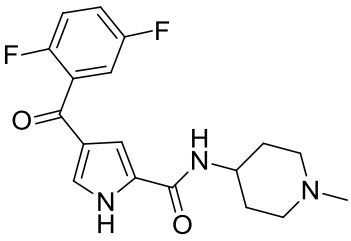

General procedure D: 4-(2,5-difluorobenzoyl)-1*H*-pyrrole-2-carboxylic acid (108 mg, 0.43 mmol), CDI (139 mg, 0.86 mmol), and 4-amino-1-methyl piperidine (135 µL, 1.08 mmol). Purification *via* column chromatography (NH silica; 0-8% MeOH/DCM) gave **363** as a white solid (149 mg, 100%). R_f 0.15 (9:1 DCM/MeOH); m.p. 211-213 ^oC; λ_{max} (EtOH/nm) 288.0, 238.0; IR υ_{max}/cm^{-1} 2934, 2798, 1637, 1563, 1516; ^1H NMR (500 MHz, DMSO-d_6) δ ppm 1.49-1.57 (2H, m, CH-piperidine), 1.72-1.75 (2H, m, CH-piperidine), 1.90-1.95 (2H, m, N-

CH-piperidine), 2.16 (3H, s, N-CH_3), 2.75-2.77 (2H, m, N-CH-piperidine), 3.64-3.72 (1H, m, N-CH-piperidine), 7.27 (1H, d, *J* = 1.5 Hz, H-3), 7.37 (1H, br s, H-5), 7.39-7.47 (3H, m, H-2', H-4' and H-5'), 8.10 (1H, d, *J* = 7.9 Hz, CO-NH), 12.34 (1H, s, NH-pyrrole); ^{13}C NMR (125 MHz, DMSO-d_6) δ ppm 31.5 (C-piperidine), 45.9 (N-CH_3), 46.0 (C-piperidine), 54.4 (C-piperidine), 110.4 (C-Ar), 115.9 (dd, J_{CF} = 3.9 and 25.4 Hz, C-Ar), 118.0 (dd, J_{CF} = 8.4 and 25.1 Hz, C-Ar), 118.7 (dd, J_{CF} = 9.0 and 24.2 Hz, C-Ar), 124.6 (C-Ar), 128.3 (C-Ar), 128.5 (C-Ar), 129.6 (dd, J_{CF} = 6.7 and 19.1 Hz, C-Ar), 154.8 (dd, J_{CF} = 2.0 and 244.2 Hz, C-F), 157.8 (dd, J_{CF} = 2.0 and 242.0 Hz, C-F), 159.1 (CO), 184.9 (CO); HRMS calcd for $C_{18}H_{19}F_2N_3O_2$ $[M+H]^+$ 348.1518, found 348.1520.

Methyl 4-(5-chloro-2-fluorobenzoyl)-1*H*-pyrrole-2-carboxylate, 364

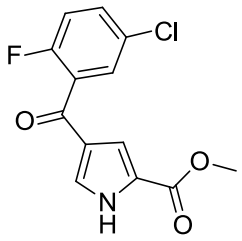

General procedure F: methyl 1*H*-pyrrole-2-carboxylate (0.95 g, 7.57 mmol), 5-chloro, 6-fluorobenzoyl chloride (2.00 mL, 15.13 mmol), and $AlCl_3$ (2.54 g, 18.93 mmol). Purification *via* column chromatography (silica; 0-50% EtOAc/petrol) gave **364** as a white solid (1.85 g, 87%). R_f 0.17 (8:2 Petrol/EtOAc); m.p. 156-157 ^oC; λ_{max} (EtOH/nm) 283.5, 236.0; IR υ_{max}/cm^{-1} 3284, 3143, 3074, 2993, 2947, 1720, 1637, 1605, 1561; ^{1}H NMR (500 MHz, DMSO-d_6) δ ppm 3.81 (O-CH_3), 7.09 (1H, br s, H-3), 7.42 (1H, dd, *J* = 8.8 and 9.2 Hz, H-3'), 7.58 (1H, br s, H-5), 7.60 (1H, dd, *J* = 2.7 and 5.9 Hz, H-6'), 7.66 (1H, ddd, *J* = 2.7, 4.4 and 8.8 Hz, H-4'), 12.84 (1H, s, NH-pyrrole); ^{13}C NMR (125 MHz, DMSO-d_6) δ ppm 51.6 (O-CH_3), 115.1 (C-Ar), 118.4 (d, J_{CF} = 24.3 Hz, C-Ar), 124.1 (C-Ar), 125.0 (C-Ar), 128.5 (d, J_{CF} = 2.8 Hz, C-Ar), 129.0 (d, J_{CF} = 3.6 Hz, C-Ar), 129.5 (d, J_{CF} = 18.2 Hz, C-Ar), 130.3 (C-Ar), 132.2 (d, J_{CF} = 8.5 Hz, C-Ar), 157.4 (d, J_{CF} = 248.2 Hz, C-F), 160.4 (CO), 184.4 (CO); HRMS calcd for $C_{13}H_9{}^{35}ClFNO_3$ $[M+H]^+$ 282.0328, found 282.0333.

4-(5-Chloro-2-fluorobenzoyl)-1*H*-pyrrole-2-carboxylic acid, 365

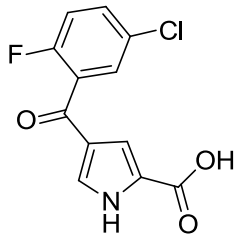

General procedure G: methyl 4-(5-chloro-2-fluorobenzoyl)-1*H*-pyrrole-2-carboxylate (1.80 g, 6.41 mmol), and LiOH monohydrate (5.38 g, 128.20 mmol) gave **365** as a white solid (1.68 g, 98%). R_f 0.35 (9:1 DCM/MeOH); m.p. 237-239 ^oC; λ_{max} (EtOH/nm) 281.5, 234.0; IR υ_{max}/cm^{-1} 3410, 3131, 3027, 2876, 2634, 2555, 1673, 1635, 1604, 1560; ^1H NMR (500 MHz, DMSO-d_6) δ ppm 7.03 (1H, br s, H-3), 7.42 (1H, dd, J = 8.8 and 9.2 Hz, H-3'), 7.51 (1H, br s, H-5), 7.60 (1H, dd, J = 2.8 and 5.9 Hz, H-6'), 7.66 (1H, ddd, J = 2.8, 4.4 and 8.8 Hz, H-4'), 12.65 (1H, s, NH-pyrrole), 12.89 (1H, s, COOH); ^{13}C NMR (125 MHz, DMSO-d_6) δ ppm 114.7 (C-Ar), 118.3 (d, J_{CF} = 23.9 Hz, C-Ar), 124.9 (C-Ar), 125.5 (C-Ar), 128.5 (d, J_{CF} = 2.4 Hz, C-Ar), 129.0 (d, J_{CF} = 3.5 Hz, C-Ar), 129.6 (d, J_{CF} = 18.2 Hz, C-Ar), 129.9 (C-Ar), 132.2 (d, J_{CF} = 8.6 Hz, C-Ar), 157.4 (d, J_{CF} = 248.4 Hz, C-F), 161.4 (CO), 184.5 (CO); HRMS calcd for $C_{12}H_7{}^{35}ClFNO_3$ $[M-H]^-$ 266.0026, found 266.0017.

4-(5-Chloro-2-fluorobenzoyl)-*N*-(pyridin-3-yl)-1*H*-pyrrole-2-carboxamide, 366

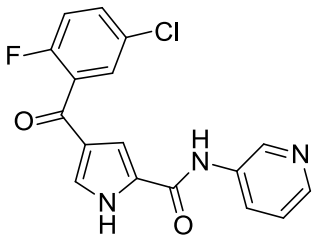

General procedure M: 4-(5-chloro-2-fluorobenzoyl)-1*H*-pyrrole-2-carboxylic acid (69 mg, 0.26 mmol), PCl_3 (23 µL, 0.26 mmol), and 3-aminopyridine (61 mg, 0.65 mmol). Purification *via* column chromatography (NH silica; 0-8% MeOH/DCM) gave **366** as a white solid (81 mg, 91%). R_f 0.27 (95:5 DCM/MeOH); m.p. 263-265 ^oC; λ_{max} (EtOH/nm) 263.5; IR υ_{max}/cm^{-1} 3230, 3076, 2984, 1668, 1603, 1545; ^1H NMR (500 MHz, DMSO-d_6) δ ppm 7.39-7.47 (2H, m, H-6' and H-3'), 7.54 (1H, br s, H-3), 7.58 (1H, br s, H-5), 7.64-7.69 (2H, m, H-4' and CH-pyridine), 8.16 (1H, ddd, J = 1.5, 2.5 and 8.3 Hz, CH-pyridine), 8.31 (1H, br s, N-CH-pyridine), 8.92 (1H, br s, N-CH-pyridine), 10.26 (1H, s, CO-NH), 12.69 (1H, s, NH-pyrrole); ^{13}C NMR (125 MHz, DMSO-d_6) δ ppm 112.1 (C-Ar), 118.4 (d, J_{CF} = 23.6 Hz, C-Ar), 123.6

(C-Ar), 124.9 (C-Ar), 127.0 (C-Ar), 127.8 (d, J_{CF} = 2.7 Hz, C-Ar), 129.0 (d, J_{CF} = 3.3 Hz, C-Ar), 129.7 (C-Ar), 129.8 (C-Ar), 132.1 (d, J_{CF} = 8.5 Hz, C-Ar), 135.6 (C-Ar), 141.5 (C-Ar), 144.3 (C-Ar), 157.5 (d, J_{CF} = 248.7 Hz, C-F), 158.8 (CO), 184.7 (CO), one C-Ar not visualised; HRMS calcd for $C_{17}H_{11}{}^{35}ClFN_3O_2$ $[M+H]^+$ 344.0597, found 344.0599.

4-(5-Chloro-2-fluorobenzoyl)-*N*-(pyrimidin-5-yl)-1*H*-pyrrole-2-carboxamide, 367

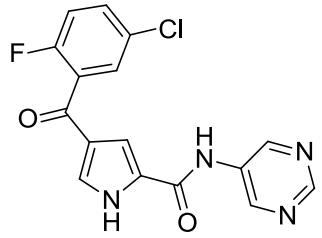

General procedure M with exceptios to the method: 4-(5-chloro-2-fluorobenzoyl)-1*H*-pyrrole-2-carboxylic acid (106 mg, 0.40 mmol), PCl_3 (35 µL, 0.40 mmol), and 5-aminopyrimidine (95 mg, 1.00 mmol) for 15 min. Purification *via* column chromatography (silica; 0-8% MeOH/DCM) gave **367** as a white solid (58 mg, 42%). R_f 0.59 (9:1 DCM/MeOH); m.p. Degrades >250 ^oC; λ_{max} (EtOH/nm) 297.5; IR υ_{max}/cm^{-1} 3504, 3307, 3227, 3116, 3051, 2981, 2922, 2860, 1652, 1622, 1584, 1554, 1525; ^1H NMR (500 MHz, DMSO-d_6) δ ppm 7.45 (1H, dd, J = 8.9 and 9.1 Hz, H-3'), 7.57 (1H, br s, H-3), 7.59 (1H, br s, H-5), 7.64-7.70 (2H, m, H-5' and H-4'), 8.92 (1H, s, CH-pyrimidine), 9.15 (2H, s, CH-pyrimidine), 10.51 (1H, s, CO-NH), 12.67 (1H, s, NH-pyrrole); ^{13}C NMR (125 MHz, DMSO-d_6) δ ppm 112.7 (C-Ar), 118.4 (d, J_{CF} = 24.3 Hz, C-Ar), 125.0 (C-Ar), 127.3 (C-Ar), 128.5 (d, J_{CF} = 2.9 Hz, C-Ar), 129.0 (d, J_{CF} = 3.1 Hz, C-Ar), 129.7 (d, J_{CF} = 18.0 Hz, C-Ar), 130.0 (C-Ar), 132.2 (d, J_{CF} = 8.5 Hz, C-Ar), 134.4 (C-Ar), 147.8 (C-Ar), 153.1 (C-Ar), 157.5 (d, J_{CF} = 249.5 Hz, C-F), 158.9 (CO), 184.7 (CO); HRMS calcd for $C_{16}H_{10}{}^{35}ClFN_4O_2$ $[M+H]^+$ 345.0549, found 345.0555.

***tert*-Butyl 4-(4-(5-chloro-2-fluorobenzoyl)-1*H*-pyrrole-2-carboxamido)piperidine-1-carboxylate, 368**

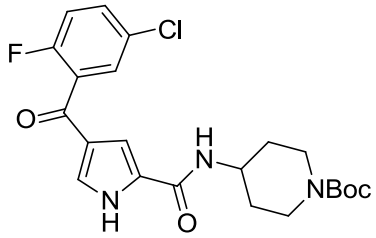

General procedure D: 4-(5-chloro-2-fluorobenzoyl)-1*H*-pyrrole-2-carboxylic acid (75 mg, 0.28 mmol), CDI (91 mg, 0.56 mmol), and *tert*-butyl 4-aminopiperidine-1-carboxylate (140 mg, 0.95 mmol). Purification *via* column chromatography (silica; 30-100% EtOAc/petrol) gave **368** as a white solid (93 mg, 74%). R_f 0.68 (9:1 DCM/MeOH); m.p. 134-135 ^oC; λ_{max} (EtOH/nm) 294.0, 242.5; IR υ_{max}/cm^{-1} 3122, 2959, 2869, 1621, 1566, 1534; ^1H NMR (500 MHz, $CDCl_3$) δ ppm 1.40-1.49 (11H, m, CH-piperidine and C-CH_3), 1.98-2.01 (2H, m, CH-piperidine), 2.87-2.93 (2H, m, N-CH-piperidine), 4.07-4.13 (3H, m, N-CH-piperidine), 6.18 (1H, d, J = 7.7 Hz, CO-NH), 7.13-7.17 (2H, m, H-3 and H-3'), 7.40 (1H, br s, H-5), 7.45-7.48 (1H, m, H-4'), 7.53 (1H, dd, J = 2.6 and 5.7 Hz, H-6'), 10.31 (1H, s, NH-pyrrole); ^{13}C NMR (125 MHz, $CDCl_3$) δ ppm 28.4 (C-CH_3), 32.1 (C-piperidine), 42.7 (C-piperidine), 47.1 (C-piperidine), 79.8 (*C*-CH_3), 109.4 (C-Ar), 117.9 (d, J_{CF} = 24.1 Hz, C-Ar), 126.1 (C-Ar), 127.8 (C-Ar), 129.6 (C-Ar), 129.7 (d, J_{CF} = 2.9 Hz, C-Ar), 132.2 (d, J_{CF} = 7.8 Hz, C-Ar), 154.7 (CO), 158.1 (d, J_{CF} = 251.1 Hz, C-F), 159.7 (CO), 185.4 (CO), two C-Ar not visualised; HRMS calcd for $C_{22}H_{25}{}^{35}ClFN_3O_4$ $[M+H]^+$ 450.1590, found 450.1590.

4-(5-Chloro-2-fluorobenzoyl)-*N*-(piperidin-4-yl)-1*H*-pyrrole-2-carboxamide, 382

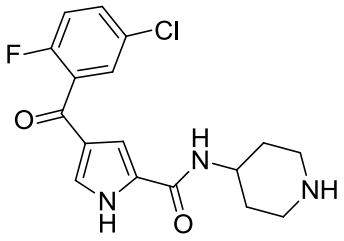

General procedure K: *tert*-butyl 4-(4-(5-chloro-2-fluorobenzoyl)-1*H*-pyrrole-2-carboxamido)piperidine-1-carboxylate (80 mg, 0.17 mmol), triethylsilane (69 µL, 0.43 mmol) and TFA (2 mL/mmol) gave **382** as a white solid (61 mg, 100%). R_f 0.42 (9:1 DCM/MeOH, NH silica); m.p. 208-210 ^oC; λ_{max} (EtOH/nm) 238.5; IR υ_{max}/cm^{-1} 3299, 2939, 2824, 2745, 1627, 1568, 1533; ^1H NMR (500 MHz, DMSO-d_6) δ ppm 1.39-1.44 (2H, m, CH-

piperidine), 1.73-1.76 (2H, m, CH-piperidine), 2.55-2.60 (2H, m, N-CH-piperidine), 2.99-3.01 (2H, m, N-CH-piperidine), 3.78-3.85 (1H, m, N-CH-piperidine), 7.29 (1H, br s, H-3), 7.38 (1H, br s, H-5), 7.41-7.45 (1H, m, H-6'), 7.58-7.60 (1H, m, H-3'), 7.65-7.68 (1H, m, H-4'), 8.14 (1H, d, J = 7.9 Hz, CO-NH); ^{13}C NMR (125 MHz, DMSO-d_6) δ ppm 32.3 (C-piperidine), 44.8 (C-piperidine), 46.4 (C-piperidine), 110.4 (C-Ar), 118.3 (d, J_{CF} = 23.9 Hz, C-Ar), 124.6 (C-Ar), 128.3 (C-Ar), 128.4 (C-Ar), 128.6 (C-Ar), 128.9 (d, J_{CF} = 3.1 Hz, C-Ar), 130.0 (d, J_{CF} = 18.5 Hz, C-Ar), 131.9 (d, J_{CF} = 8.6 Hz, C-Ar), 157.4 (d, J_{CF} = 248.9 Hz, C-F), 159.0 (CO), 184.7 (CO); HRMS calcd for $C_{17}H_{17}{}^{35}ClFN_3O_2$ $[M+H]^+$ 350.1066, found 350.1073.

4-(5-Chloro-2-fluorobenzoyl)-*N*-(1-methylpiperidin-4-yl)-1*H*-pyrrole-2-carboxamide, 369

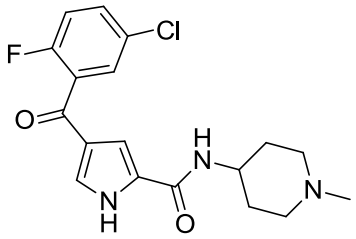

General procedure D: 4-(5-chloro-2-fluorobenzoyl)-1*H*-pyrrole-2-carboxylic acid (63 mg, 0.24 mmol), CDI (78 mg, 0.48 mmol), and 4-amino-1-methyl piperidine (75 µL, 0.60 mmol). Purification *via* column chromatography (NH silica; 0-8% MeOH/DCM) gave **369** as a white solid (76 mg, 87%). R_f 0.17 (9:1 DCM/MeOH); m.p. Degrades >250 ^oC; λ_{max} (EtOH/nm) 290.0, 238.0; IR υ_{max}/cm^{-1} 3104, 2935, 2848, 2794, 2689, 1637, 1564, 1516; ^{1}H NMR (500 MHz, DMSO-d_6) δ ppm 1.49-1.57 (2H, m, CH-piperidine), 1.72-1.75 (2H, m, CH-piperidine), 1.90-1.95 (2H, m, N-CH-piperidine), 2.16 (3H, s, N-CH_3), 2.74-2.77 (2H, m, N-CH-piperidine), 3.64-3.72 (1H, m, N-CH-piperidine), 7.27 (1H, br s, H-3), 7.37 (1H, br s, H-5), 7.42 (1H, dd, J = 9.0 and 9.1 Hz, H-3'), 7.58 (1H, dd, J = 2.7 and 5.8 Hz, H-6'), 7.64-7.67 (1H, m, H-4'), 8.09 (1H, d, J = 7.9 Hz, CO-NH), 12.35 (1H, s, NH-pyrrole); ^{13}C NMR (125 MHz, DMSO-d_6) δ ppm 31.6 (C-piperidine), 45.9 (N-CH_3), 46.0 (C-piperidine), 54.4 (C-piperidine), 110.4 (C-Ar), 118.3 (d, J_{CF} = 23.5 Hz, C-Ar), 124.6 (C-Ar), 128.3 (C-Ar), 128.4 (d, J_{CF} = 2.6 Hz, C-Ar), 128.6 (C-Ar), 128.9 (d, J_{CF} = 3.5 Hz, C-Ar), 130.0 (d, J_{CF} = 18.5 Hz, C-Ar), 131.9 (d, J_{CF} = 9.0 Hz, C-Ar), 157.4 (d, J_{CF} = 248.2 Hz, C-F), 159.1 (CO), 184.7 (CO); HRMS calcd for $C_{18}H_{19}{}^{35}ClFN_3O_2$ $[M+H]^+$ 364.1223, found 364.1225.

Methyl 4-(2-fluoro-5-methylbenzoyl)-1*H*-pyrrole-2-carboxylate, 370

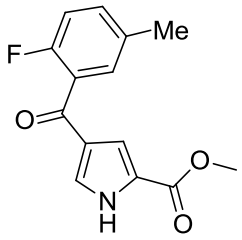

General procedure E: 2-fluoro, 6-methylbenzoic acid (2.00 g, 13.07 mmol), $SOCl_2$ (1.43 mL, 19.61 mmol), and DMF (10 mol%) gave 2-fluoro, 6-methylbenzoyl chloride as a yellow oil which was used directly in the next step. **General procedure F:** methyl 1*H*-pyrrole-2-carboxylate (0.82 g, 6.54 mmol), and $AlCl_3$ (2.19 g, 16.35 mmol). Purification *via* column chromatography (silica; 0-50% EtOAc/petrol) gave **370** as a white solid (1.47 g, 86%). R_f 0.19 (8:2 Petrol/EtOAc); m.p. 115-117 ^oC; λ_{max} (EtOH/nm) 286.0, 233.5; IR υ_{max}/cm^{-1} 3296, 3139, 3067, 2998, 2955, 1794, 1701, 1645, 1611, 1561; ^1H NMR (500 MHz, DMSO-d_6) δ ppm 2.34 (3H, s, CH_3), 3.81 (3H, s, O-CH_3), 7.06 (1H, br s, H-3), 7.23 (1H, dd, *J* = 8.6 and 10.0 Hz, H-3'), 7.34 (1H, dd, *J* = 2.0 and 6.5 Hz, H-6'), 7.38-7.41 (1H, m, H-4'), 7.50 (1H, br s, H-5), 12.78 (1H, s, NH-pyrrole); ^{13}C NMR (125 MHz, DMSO-d_6) δ ppm 20.0 (CH_3), 51.6 (O-CH_3), 115.2 (C-Ar), 115.9 (d, J_{CF} = 21.8 Hz, C-Ar), 123.9 (C-Ar), 125.5 (C-Ar), 127.5 (d, J_{CF} = 15.9 Hz, C-Ar), 129.7 (d, J_{CF} = 2.7 Hz, C-Ar), 129.8 (C-Ar), 132.9 (d, J_{CF} = 8.0 Hz, C-Ar), 133.8 (d, J_{CF} = 3.0 Hz, C-Ar), 157.0 (d, J_{CF} = 245.7 Hz, C-F), 160.4 (CO), 186.1 (CO); HRMS calcd for $C_{14}H_{12}FNO_3$ $[M+H]^+$ 262.0874, found 262.0878.

4-(2-Fluoro-5-methylbenzoyl)-1*H*-pyrrole-2-carboxylic acid, 371

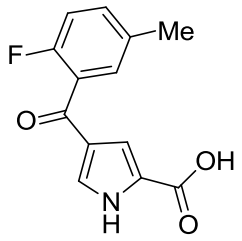

General procedure G: methyl 4-(2-fluoro-5-methylbenzoyl)-1*H*-pyrrole-2-carboxylate (1.40 g, 5.36 mmol), and LiOH monohydrate (4.50 g, 107.20 mmol) gave **371** as a white solid (1.31 g, 99%). R_f 0.27 (9:1 DCM/MeOH); m.p. 189-190 ^oC; λ_{max} (EtOH/nm) 285.0, 233.0; IR υ_{max}/cm^{-1} 3302, 2978, 2877, 2701, 2618, 2550, 1668, 1629, 1553; ^1H NMR (500 MHz, DMSO-d_6) δ ppm 2.34 (3H, s, CH_3), 7.01 (1H, br s, H-3), 7.22 (1H, dd, *J* = 8.5 and 9.9 Hz, H-3'), 7.33 (1H, dd, *J* = 1.8 and 6.6 Hz, H-6'), 7.37-7.40 (1H, m, H-4'), 7.43 (1H, br s, H-5),

12.58 (1H, s, NH-pyrrole), 12.84 (1H, s, COOH); ^{13}C NMR (125 MHz, DMSO-d_6) δ ppm 20.0 (CH_3), 114.8 (C-Ar), 115.9 (d, J_{CF} = 21.8 Hz, C-Ar), 125.1 (C-Ar), 125.4 (C-Ar), 127.6 (d, J_{CF} = 16.1 Hz, C-Ar), 129.3 (C-Ar), 129.7 (d, J_{CF} = 2.6 Hz, C-Ar), 132.8 (d, J_{CF} = 7.9 Hz, C-Ar), 133.7 (d, J_{CF} = 2.9 Hz, C-Ar), 157..0 (d, J_{CF} = 245.1 Hz, C-F), 161.4 (CO), 186.2 (CO); HRMS calcd for $C_{13}H_{10}FNO_3$ $[M-H]^-$ 246.0572, found 246.0562.

4-(2-Fluoro-5-methylbenzoyl)-*N*-(pyridin-3-yl)-1*H*-pyrrole-2-carboxamide, 372

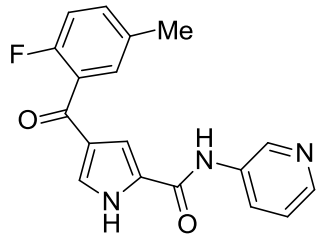

General procedure M: 4-(2-fluoro-5-methylbenzoyl)-1*H*-pyrrole-2-carboxylic acid (65 mg, 0.26 mmol), PCl_3 (23 µL, 0.26 mmol), and 3-aminopyridine (61 mg, 0.65 mmol).). Purification *via* column chromatography (NH silica; 0-8% MeOH/DCM) gave **372** as a white solid (75 mg, 89%). R_f 0.28 (95:5 DCM/MeOH); m.p. 251-253 ^oC; λ_{max} (EtOH/nm) 303.5; IR υ_{max}/cm^{-1} 3334, 3238, 3117, 3038, 2977, 1625, 1557, 1532; ^{1}H NMR (500 MHz, DMSO-d_6) δ ppm 2.36 (3H, s, CH_3), 7.25 (1H, dd, J = 8.2 and 8.3 Hz, H-3'), 7.36-7.41 (3H, m, H-6', H'4' and CH-pyridine), 7.46 (1H, br s, H-3), 7.57 (1H, br s, H-5), 8.15-8.17 (1H, m, CH-pyridine), 8.30 (1H, br s, N-CH-pyridine), 8.92 (1H, br s, N-CH-pyridine), 10.24 (1H, s, CO-NH), 12.61 (1H, s, NH-pyrrole); ^{13}C NMR (125 MHz, DMSO-d_6) δ ppm 20.0 (CH_3), 112.2 (C-Ar), 115.9 (d, J_{CF} = 21.7 Hz, C-Ar), 123.6 (C-Ar), 125.4 (C-Ar), 126.9 (C-Ar), 127.5 (C-Ar), 127.8 (d, J_{CF} = 15.7 Hz, C-Ar), 129.1 (C-Ar), 129.7 (C-Ar), 132.8 (d, J_{CF} = 8.0 Hz, C-Ar), 133.8 (d, J_{CF} = 2.6 Hz, C-Ar), 135.6 (C-Ar), 141.5 (C-Ar), 144.3 (C-Ar), 157.0 (d, J_{CF} = 245.8 Hz, C-F), 158.9 (CO), 186.4 (CO); HRMS calcd for $C_{18}H_{14}FN_3O_2$ $[M+H]^+$ 324.1143, found 324.1145.

4-(2-Fluoro-5-methylbenzoyl)-*N*-(pyrimidin-5-yl)-1*H*-pyrrole-2-carboxamide, 373

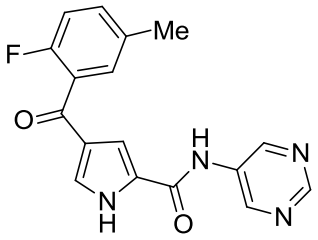

General procedure M with exceptions to the method: 4-(2-fluoro-5-methylbenzoyl)-1*H*-pyrrole-2-carboxylic acid (113 mg, 0.46 mmol), PCl_3 (40 µL, 0.46 mmol), and 5-aminopyrimidine (109 mg, 1.15 mmol) for 15 min. Purification *via* column chromatography (silica; 0-8% MeOH/DCM) gave **373** as a yellow solid (73 mg, 49%). R_f 0.61 (9:1 DCM/MeOH); m.p. 287-288 ^oC; λ_{max} (EtOH/nm) 294.5, 249.5; IR υ_{max}/cm^{-1} 3238, 3115, 3050, 2979, 2927, 2868, 1622, 1584, 1553, 1525; ^1H NMR (500 MHz, DMSO-d_6) δ ppm 2.36 (3H, s, CH_3), 7.25 (1H, dd, J = 8.6 and 8.7 Hz, H-3'), 7.37-7.41 (2H, m, H-4' and H-6'), 7.50 (1H, br s, H-3), 7.56 (1H, br s, H-5), 8.92 (1H, s, CH-pyrimidine), 9.15 (2H, s, CH-pyrimidine), 10.44 (1H, s, CO-NH), 12.70 (1H, s, NH-pyrrole); ^{13}C NMR (125 MHz, DMSO-d_6) δ ppm 20.0 (CH_3), 112.7 (C-Ar), 116.0 (d, J_{CF} = 21.9 Hz, C-Ar), 125.5 (C-Ar), 127.0 (C-Ar), 127.7 (d, J_{CF} = 16.1 Hz, C-Ar), 129.4 (C-Ar), 129.7 (d, J_{CF} =2.2 Hz, C-Ar), 132.9 (d, J_{CF} = 8.1 Hz, C-Ar), 133.8 (d, J_{CF} = 2.9 Hz, C-Ar), 134.4 (C-Ar), 147.7 (C-Ar), 153.1 (C-Ar), 157.0 (d, J_{CF} = 246.0 Hz, C-F), 159.0 (CO), 186.4 (CO); HRMS calcd for $C_{17}H_{13}FN_4O_2$ $[M+H]^+$ 325.1095, found 325.1098.

***tert*-Butyl 4-(4-(2-fluoro-5-methylbenzoyl)-1*H*-pyrrole-2-carboxamido)piperidine-1-carboxylate, 374**

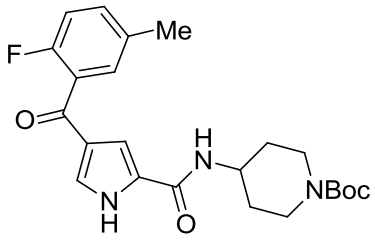

General procedure D: 4-(2-fluoro-5-methylbenzoyl)-1*H*-pyrrole-2-carboxylic acid (74 mg, 0.30 mmol), CDI (97 mg, 0.60 mmol), and *tert*-butyl 4-aminopiperidine-1-carboxylate (150 mg, 0.75 mmol). Purification *via* column chromatography (silica; 30-100% EtOAc/petrol) gave **374** as a white solid (70 mg, 54%). R_f 0.70 (9:1 DCM/MeOH); m.p. 127-130 ^oC; λ_{max} (EtOH/nm) 288.0, 239.0; IR υ_{max}/cm^{-1} 2961, 2927, 2861, 1622, 1566, 1534; ^1H NMR (500

MHz, $CDCl_3$) δ ppm 1.40-1.45 (2H, m, CH-piperidine), 1.47 (9H, s, C-*CH*$_3$), 1.96-1.99 (2H, m, CH-piperidine), 2.37 (3H, s, CH_3), 2.85-2.91 (2H, m, N-CH-piperidine), 4.03-4.15 (3H, m, N-CH-piperidine), 6.05 (1H, d, *J* = 7.8 Hz, CO-NH), 7.04 (1H, dd, J = 8.7 and 9.5 Hz, H-3'), 7.10 (1H, br s, H-3), 7.26-7.29 (1H, m, H-4'), 7.33 (1H, dd, *J* = 2.2 and 6.7 Hz, H-6'), 7.39 (1H, br s, H-5), 9.92 (1H, s, NH-pyrrole); ^{13}C NMR (125 MHz, $CDCl_3$) δ ppm 20.6 (CH_3), 28.5 (C-*CH*$_3$), 32.1 (C-piperidine), 42.8 (C-piperidine), 47.0 (C-piperidine), 79.8 (*C*-CH_3), 109.4 (C-Ar), 116.0 (d, J_{CF} = 21.8 Hz, C-Ar), 126.7 (C-Ar), 127.4 (C-Ar), 127.7 (d, J_{CF} = 15.7 Hz, C-Ar), 127.8 (C-Ar), 130.2 (d, J_{CF} = 2.9 Hz, C-Ar), 133.0 (d, J_{CF} = 7.9 Hz, C-Ar), 133.9 (d, J_{CF} = 3.5 Hz, C-Ar), 154.7 (CO), 157.8 (d, J_{CF} = 248.9 Hz, C-F), 159.8 (CO), 187.4 (CO); HRMS calcd for $C_{23}H_{28}FN_3O_4$ $[M+H]^+$ 430.2137, found 430.2138.

4-(2-Fluoro-5-methylbenzoyl)-*N*-(1-methylpiperidin-4-yl)-1*H*-pyrrole-2-carboxamide, 375

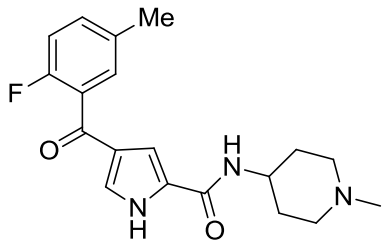

General procedure D: 4-(2-fluoro-5-methylbenzoyl)-1*H*-pyrrole-2-carboxylic acid (75 mg, 0.30 mmol), CDI (97 mg, 0.60 mmol) and 4-amino-1-methyl piperidine (94 µL, 0.75 mmol). Purification *via* column chromatography (NH silica; 0-8% MeOH/DCM) gave **375** as a white solid (91 mg, 88%). R_f 0.18 (9:1 DCM/MeOH); m.p. Degrades > 250 ^oC; λ_{max} (EtOH/nm) 287.5, 237.5; IR υ_{max}/cm^{-1} 3370, 2934, 2850, 2795, 1637, 1562, 1517, 1489, 1432; ^{1}H NMR (500 MHz, $CDCl_3$) δ ppm 1.49-1.57 (2H, m, CH-piperidine), 1.72-1.75 (2H, m, CH-piperidine), 1.90-1.95 (2H, m, N-CH-piperidine), 2.16 (3H, s, N-CH_3), 2.34 (3H, s, CH_3), 2.74-2.78 (2H, m, N-CH-piperidine), 3.64-3.72 (1H, m, N-CH-piperidine), 7.22 (1H, dd, J = 9.0 and 9.1 Hz, H-3'), 7.26 (1H, br s, H-3), 7.29-7.32 (2H, m, H-5 and H-6'), 7.36-7.39 (1H, m, H-4'), 8.09 (1H, d, J = 7.9 Hz, CO-NH), 12.27 (1H, s, NH-pyrrole); ^{13}C NMR (125 MHz, $CDCl_3$) δ ppm 20.0 (CH_3), 31.5 (C-piperidine), 45.9 (N-CH_3 and C-piperidine), 54.4 (C-piperidine), 110.4 (C-Ar), 115.9 (d, J_{CF} = 21.9 Hz, C-Ar), 125.1 (C-Ar), 128.0 (d, J_{CF} = 15.8 Hz, C-Ar), 128.3 (C-Ar), 129.6 (d, J_{CF} = 2.8 Hz, C-Ar), 132.5 (d, J_{CF} = 7.9 Hz, C-Ar), 133.7 (d, J_{CF} = 2.9 Hz, C-Ar), 157.0 (d, J_{CF} = 244.6 Hz, C-F), 159.2 (CO), 186.5 (CO), one C-Ar not visualised; HRMS calcd for $C_{19}H_{22}FN_3O_2$ $[M+H]^+$ 344.1769, found 344.1771.

Methyl 4-bromo-1-tosyl-1*H*-pyrrole-2-carboxylate, 387

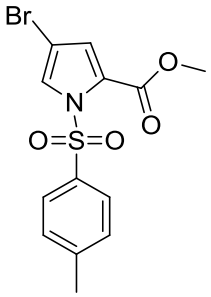

To a solution of methyl 4-bromo-1*H*-pyrrole-2-carboxylate (507 mg, 2.49 mmol) in THF (4 mL/mmol) was added NaH (72 mg, 2.99 mmol) portionwise at 0 ^{o}C. The resulting mixture was stirred for 15 min, then tosyl chloride (0.95 g, 4.98 mmol) was added and the mixture warmed to RT. The mixture was stirred for 16 h. The reaction was quenched with a saturated aqueous solution of $NaHCO_3$ then extracted with DCM (2 x 50 mL). Combined organic layers were washed with brine (50 mL), dried over Na_2SO_4 and concentrated *in vacuo*. Column chromatography (silica; 0-20% EtOAc/petrol) gave **387** as a white solid (0.96 g, 55%). R_f 0.41 (9:1 Petrol/EtOAc); m.p. 123-124 ˚C; λ_{max} (EtOH/nm) 271.0, 237.0; IR υ_{max}/cm^{-1} 3157, 2945, 1730, 1595; ^{1}H NMR (500 MHz, DMSO-d_6) δ ppm: 2.41 (3H, s, CH_3), 3.70 (3H, s, O-CH_3), 7.17 (1H, d, *J* = 1.6 Hz, H-3), 7.50 (2H, d, *J* = 8.1 Hz, H-3 and H-5 tosyl), 7.96 (2H, d, *J* = 8.1 Hz, H-2 and H-6 tosyl), 8.04 (1H, d, *J* = 1.6 Hz, H-5); ^{13}C NMR (125 MHz, DMSO-d_6) δ ppm; 21.1 (CH_3), 52.2 (O-CH_3), 98.7 (C-Ar), 123.9 (C-Ar), 124.8 (C-Ar), 128.0 (C-Ar), 128.1 (C-Ar), 129.9 (C-Ar), 134.4 (C-Ar), 145.8 (C-Ar), 157.9 (CO); MS (ES+) *m/z* = 358 and 360.1 $[M+H]^+$; HRMS calcd for $C_{13}H_{12}{}^{79}BrNO_4S$ $[M+H]^+$ 357.9743, found 357.9750.

Methyl 4-(pyridin-2-yl)-1-tosyl-1*H*-pyrrole-2-carboxylate, 390

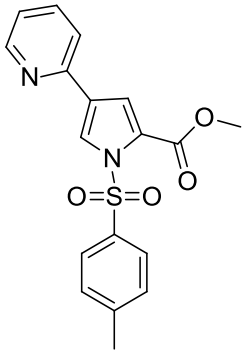

General procedure O: methyl 4-bromo-1-tosyl-1*H*-pyrrole-2-carboxylate (150 mg, 0.42 mmol), bis(pinacolato) diboron (160 mg, 0.63 mmol), KOAc (123 mg, 1.26 mmol) and

polymer-supported dichloro[1,1'-bis(di-tert-butylphosphino)ferrocene]palladium (II) (10 mol%). Then 2-bromopyridine (60 μL, 0.63 mmol), Na_2CO_3 (53 mg, 0.50 mmol) and polymer-supported tetrakis(triphenylphosphine)palladium (0) (10 mol%). Column chromatography (silica; 10-50% EtOAc/petrol) gave **390** as a white solid (110 mg, 73%). R_f 0.32 (7:3 Petrol/EtOAc); m.p. Degrades >250 ˚C; λ_{max} (EtOH/nm) 239.5; IR υ_{max}/cm^{-1} 2978, 1721, 1597, 1559, 1464; ^{1}H NMR (500 MHz, DMSO-d_6) δ ppm 2.43 (3H, s, CH_3), 3.73 (3H, s, O-CH_3), 7.31 (1H, ddd, *J* = 1.1, 4.9 and 7.4 Hz, CH-pyridine), 7.50 (2H, d, *J* = 8.1 Hz, H-3 and H-5 tosyl), 7.67 (1H, d, *J* = 2.0 Hz, H-3), 7.82-7.86 (1H, m, CH-pyridine), 7.91-7.94 (1H, m, N-CH-pyridine). 7.98 (2H, d, *J* = 8.1 Hz, H-2 and H-6 tosyl), 8.44 (1H, d, *J* = 2.0 Hz, H-5), 8.59 (1H, ddd, *J* = 1.1, 1.8 and 4.9 Hz, N-CH-pyridine); ^{13}C NMR (125 MHz, DMSO-d_6) δ ppm 21.1 (CH_3), 52.0 (O-CH_3), 120.0 (C-Ar), 120.5 (C-Ar), 122.5 (C-Ar), 125.1 (C-Ar), 126.0 (C-Ar), 126.8 (C-Ar), 128.0 (C-Ar), 129.8 (C-Ar), 134.7 (C-Ar), 137.1 (C-Ar), 145.6 (C-Ar), 149.5 (C-Ar), 150.5 (C-Ar), 158.6 (CO); MS (ES+) *m/z* = 357.1 $[M+H]^+$; HRMS calcd for $C_{18}H_{16}N_2O_4S$ $[M+H]^+$ 357.0904, found 357.0906.

4-(Pyridin-2-yl)-1*H*-pyrrole-2-carboxylic acid, 391

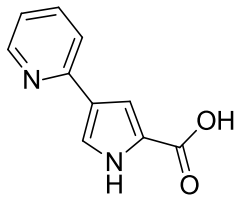

General procedure G: methyl 4-(pyridin-2-yl)-1-tosyl-1*H*-pyrrole-2-carboxylate (134 mg, 0.38 mmol), and LiOH monohydrate (315 mg, 7.50 mmol) gave **391** as an off-white solid (34 mg, 48%). R_f 0.15 (9:1 DCM/MeOH); m.p. Degrades >250 ˚C; λ_{max} (EtOH/nm) 297.0, 234.0; IR υ_{max}/cm^{-1} 3239, 3131, 1624, 1604, 1554; ^{1}H NMR (500 MHz, DMSO-d_6) δ ppm 7.01-7.03 (1H, m, CH-pyridine), 7.15 (1H, br, H-3), 7.48 (1H, br, H-5), 7.59-7.62 (2H, m, CH-pyridine and N-CH-pyridine), 8.35-8.37 (1H, m, N-CH-pyridine), 11.88 (1H, s, NH-pyrrole), 12.30 (1H, s, COOH); ^{13}C NMR (125 MHz, MeOD) δ ppm 114.1 (C-Ar), 121.2 (C-Ar), 122.2 (C-Ar), 123.5 (C-Ar), 139.0 (C-Ar), 149.4 (C-Ar), three C-Ar and CO not visualised; HRMS calcd for $C_{10}H_8N_2O_2$ $[M+H]^+$ 189.0659, found 189.0658.

4-(Pyridin-2-yl)-N-(pyridin-4-ylmethyl)-1*H*-pyrrole-2-carboxamide, 393

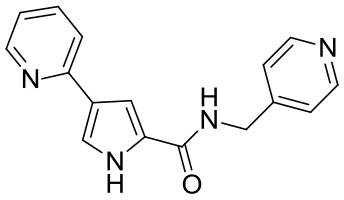

General procedure D: 4-(pyridin-2-yl)-1*H*-pyrrole-2-carboxylic acid (25 mg, 0.13 mmol), CDI (42 mg, 0.26 mmol) and 4-picolylamine (19 μL, 0.20 mmol). Column chromatography (silica; 0-8% MeOH/DCM) gave **393** as a white solid (8 mg, 22%). R_f 0.26 (9:1 DCM/MeOH); m.p. 195-197 ˚C; λ_{max} (EtOH/nm) 295.0, 239.5; IR υ_{max}/cm^{-1} 2936, 2914, 1619, 1589, 1550; ^{1}H NMR (500 MHz, MeOD) δ ppm 4.52 (2H, s, CH_2), 7.10 (1H, ddd, *J* = 1.0, 5.0 and 7.4 Hz, CH-pyridine), 7.23 (1H, d, *J* = 1.6 Hz, H-3), 7.33 (2H, d, *J* = 6.3 Hz, CH-pyridine), 7.48 (1H, d, *J* = 1.6 Hz, H-5), 7.56-7.58 (1H, m, CH-pyridine), 7.67-7.70 (1H, m, N-CH-pyridine), 8.34-8.36 (1H, m, N-CH-pyridine), 8.38 (2H, d, *J* = 6.3 Hz, N-CH-pyridine); ^{13}C NMR (125 MHz, MeOD) δ ppm 42.9 (CH_2), 109.7 (C-Ar), 121.1 (C-Ar), 122.2 (C-Ar), 122.6 (C-Ar), 123.9 (C-Ar), 126.6 (C-Ar), 138.9 (C-Ar), 149.6 (C-Ar), 150.0 (C-Ar), 151.6 (C-Ar), 155.4 (C-Ar), 163.7 (CO), one C-Ar not visualised; HRMS calcd for $C_{16}H_{14}N_4O$ $[M+H]^+$ 279.1240, found 279.1246.

Methyl 4-(isoquinolin-1-yl)-1-tosyl-1H-pyrrole-2-carboxylate, 385

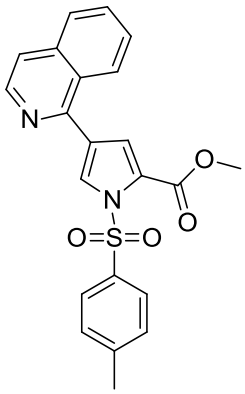

General procedure O: methyl 4-bromo-1-tosyl-1*H*-pyrrole-2-carboxylate (150 mg, 0.42 mmol), bis(pinacolato) diboron (160 mg, 0.63 mmol), KOAc (123 mg, 1.26 mmol) and polymer-supported dichloro[1,1'-bis(di-tert-butylphosphino)ferrocene]palladium (II) (10 mol%). Then, 2-bromoisoquinoline (131 mg, 0.63 mmol), Na_2CO_3 (53 mg, 0.50 mmol) and polymer-supported tetrakis(triphenylphosphine)palladium (0) (10 mol%). Column chromatography (silica; 10-50% EtOAc/petrol) gave **385** as a white solid (105 mg, 62%). R_f

0.32 (8:2 Petrol/EtOAc); m.p. Degrades >250 ˚C; λ_{max} (EtOH/nm) 295.0, 231.0; IR υ_{max}/cm^{-1} 2977, 1718, 1595, 1563; ^{1}H NMR (500 MHz, $CDCl_3$) δ ppm 2.38 (3H, s, CH_3), 3.72 (3H, s, O-CH_3), 7.28 (2H, d, *J* = 8.2 Hz, H-3 and H-5 tosyl), 7.51 (1H, d, *J* = 2.0 Hz, H-3), 7.59-7.62 (2H, m, CH-isoquinoline), 7.67-7.69 (1H, m, CH-isoquinoline), 7.83 (1H, d, *J* = 8.0 Hz, CH-isoquinoline), 7.93 (2H, d, *J* = 8.2 Hz, H-2 and H-6 tosyl), 8.20 (1H, br, H-5), 8.29 (1H, d, *J* = 8.0 Hz, CH-isoquinoline), 8.50 (1H, d, *J* = 5.9 Hz, N-CH-isoquinoline); ^{13}C NMR (125 MHz, $CDCl_3$) δ ppm 21.8 (CH_3), 51.9 (O-CH_3), 120.2 (C-Ar), 124.2 (C-Ar), 124.7 (C-Ar), 126.5 (C-Ar), 126.7 (C-Ar), 127.3 (C-Ar), 127.8 (C-Ar), 128.5 (C-Ar), 128.9 (C-Ar), 129.5 (C-Ar), 130.3 (C-Ar), 135.5 (C-Ar), 136.8 (C-Ar), 142.3 (C-Ar), 145.3 (C-Ar), 153.0 (C-Ar), 159.2 (CO); MS (ES+) *m/z* = 407.3 $[M+H]^+$; HRMS calcd for $C_{22}H_{18}N_2O_4S$ $[M+H]^+$ 407.1060, found 407.1059.

4-(Isoquinolin-1-yl)-1*H*-pyrrole-2-carboxylic acid, 392

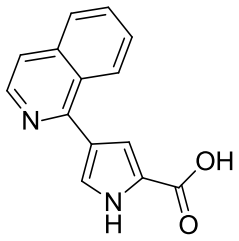

General procedure G: methyl 4-(isoquinolin-1-yl)-1-tosyl-1*H*-pyrrole-2-carboxylate (91 mg, 0.22 mmol), and LiOH monohydrate (188 mg, 4.48 mmol) gave **392** as an off-white solid (33 mg, 57%). R_f 0.17 (9:1 DCM/MeOH); m.p. Degrades >250 ˚C; λ_{max} (EtOH/nm) 339.5, 218.0; IR υ_{max}/cm^{-1} 3197, 1644, 1537, 1499, 1429; ^{1}H NMR (500 MHz, DMSO-d_6) δ ppm 7.25 (1H, br, H-3), 7.53 (1H, dd, *J* = 1.7 and 2.9 Hz, H-5), 7.67-7.70 (2H, m, CH-isoquinoline), 7.77-7.80 (1H, m, CH-isoquinoline), 7.99 (1H, d, *J* = 8.4 Hz, CH-isoquinoline), 8.43 (1H, d, *J* = 8.4 Hz, CH-isoquinoline), 8.48 (1H, d, *J* = 5.6 Hz, N-CH-isoquinoline), 12.22 (1H, s, NH-pyrrole), 12.52 (1H, s, COOH); ^{13}C NMR (125 MHz, DMSO-d_6) δ ppm 115.6 (C-Ar), 118.6 (C-Ar), 124.0 (C-Ar), 124.5 (C-Ar), 125.5 (C-Ar), 126.5 (C-Ar), 127.1 (C-Ar), 127.6 (C-Ar), 130.0 (C-Ar), 136.3 (C-Ar), 142.1 (C-Ar), 154.3 (C-Ar), 161.8 (CO), one C-Ar not visualised; HRMS calcd for $C_{14}H_{10}N_2O_2$ $[M-H]^-$ 237.0670, found 237.0668.

4-(Isoquinolin-1-yl)-*N*-(pyridin-4-ylmethyl)-1*H*-pyrrole-2-carboxamide, 384

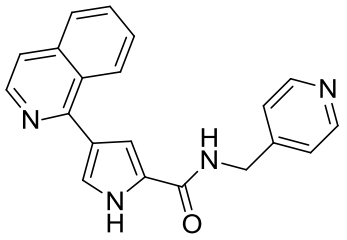

General procedure D: 4-(isoquinolin-1-yl)-1*H*-pyrrole-2-carboxylic acid (15 mg, 0.06 mmol), CDI (21 mg, 0.13 mmol), and 4-picolylamine (16 μL, 0.16 mmol). Column chromatography (silica; 0-8% MeOH/DCM) gave **384** as a white solid (10 mg, 51%). R_f 0.29 (9:1 DCM/MeOH); m.p. 145-147 ˚C; λ_{max} (EtOH/nm) 303.0, 263.5, 218.0; IR υ_{max}/cm^{-1} 2934 1641, 1531; ^{1}H NMR (500 MHz, MeOD) δ ppm 4.53 (2H, s, CH_2), 7.25 (1H, d, *J* = 1.6 Hz, H-3), 7.33 (2H, d, *J* = 6.0 Hz, CH-pyridine), 7.37 (1H, d, *J* = 1.6 Hz, H-5), 7.55-7.59 (1H, m, CH-isoquinoline), 7.60 (1H, d, *J* = 5.9 Hz, CH-isoquinoline), 7.66-7.69 (1H, m, CH-isoquinoline), 7.85 (1H, d, *J* = 8.4 Hz, CH-isoquinoline), 8.28 (1H, d, *J* = 5.9 Hz, CH-isoquinoline), 8.38-8.40 (3H, m, N-CH-pyridine and N-CH-isoquinoline); ^{13}C NMR (125 MHz, DMSO-d_6) δ ppm 42.9 (CH_2), 113.1 (C-Ar), 120.8 (C-Ar), 123.9 (C-Ar), 124.6 (C-Ar), 124.7 (C-Ar), 127.5 (C-Ar), 128.1 (C-Ar), 128.2 (C-Ar), 128.6 (C-Ar), 128.9 (C-Ar), 131.8 (C-Ar), 138.6 (C-Ar), 142.0 (C-Ar), 150.1 (C-Ar), 151.4 (C-Ar), 156.9 (C-Ar), 163.6 (CO); MS (ES+) *m/z* = 327.1 $[M+H]^+$; HRMS calcd for $C_{20}H_{16}N_4O$ $[M+H]^+$ 329.1397, found 329.1394.

2,2-Diethoxy-*N*-(pyridin-4-ylmethyl)ethanamine, 409

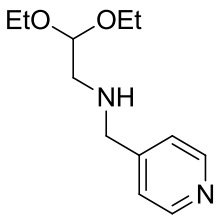

To a solution of aminoacetaldehyde diethyl acetal (0.50 mL, 3.44 mmol) in toluene (1 mL/mmol) was added 4-pyridine carboxaldehyde (0.49 mL, 5.16 mmol) and $MgSO_4$ (300 mg). The resulting mixture was heated at 110 ^{o}C for 16 h. The mixture was cooled, filtered and concentrated in vacuo. The resulting yellow oil, (*E*)-2,2-diethoxy-*N*-(pyridin-4-ylmethylene)ethanamine, was used directly in the next step. To a solution of (*E*)-2,2-diethoxy-*N*-(pyridin-4-ylmethylene)ethanamine (0.76 g, 3.44 mmol) in MeOH (2.5

mL/mmol) was added $NaBH_4$ (156 mg, 4.13 mmol) portionwise at 0 ^oC. The resulting mixture was stirred for 4 h. The reaction was quenched with H_2O (20 mL), neutralised with a saturated aqueous solution of $NaHCO_3$ and the MeOH removed *in vacuo*. The resulting aqueous solution was extracted with EtOAc (2 x 30 mL). Combined organic layers were washed with brine, dried over Na_2SO_4 and concentrated *in vacuo*. Purification *via* column chromatography (silica; 0-8% MeOH/DCM) gave **409** as a yellow oil (0.67 g, 87%). R_f 0.35 (EtOAc); λ_{max} (EtOH/nm) 256-257; IR υ_{max}/cm^{-1} 2975, 2897, 1601, 1561; ^1H NMR (500 MHz, $CDCl_3$) δ ppm 1.22 (6H, t, *J* = 7.1 Hz, CH_3), 1.76 (1H, s, NH), 2.74 (2H, dd, *J* = 1.5 and 5.4 Hz, NH-*CH_2*), 3.52-3.58 (2H, m, CH_2), 3.68-3.75 (2H, m, CH_2), 3.84 (2H, s, N-CH_2-pyridine), 4.62 (1H, t, *J* = 5.4 Hz, CH), 7.27 (2H, d, *J* = 4.5 Hz, CH-pyridine), 8.55 (2H, d, *J* = 4.5 Hz, N-CH-pyridine); ^{13}C NMR (125 MHz, $CDCl_3$) δ ppm 15.4 (CH_3), 51.6 (NH-CH_2), 52.5 (NH-CH_2), 62.6 (CH_2), 102.1 (CH), 122.9 (C-Ar), 149.3 (C-Ar), 149.8 (C-Ar); MS (ES+) *m/z* = 225.3 $[M+H]^+$.

Methyl 4-(2,6-difluorobenzoyl)-1*H*-pyrrole-2-carboxylate, 411

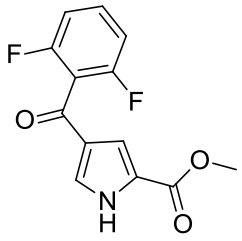

General procedure F: methyl 1*H*-pyrrole-2-carboxylate (1.00 g, 7.99 mmol), 2,6-difluorobenzoyl chloride (2.00 mL, 15.98 mmol) and $AlCl_3$ (2.68 g, 19.98 mmol). Purification *via* column chromatography (silica; 0-50% EtOAc/petrol) gave **411** as a white solid (1.31 g, 62%). R_f 0.17 (8:2 Petrol/EtOAc); m.p. 131-132 ^oC; λ_{max} (EtOH/nm) 281.0, 232.0; IR υ_{max}/cm^{-1} 3335, 2919, 2563, 2224, 2021, 1733; ^1H NMR (500 MHz, DMSO-d_6) δ ppm 3.86 (3H, s, O-CH_3), 7.13 (1H, br s, H-3), 7.31-7.36 (2H, m, H-3' and H-5'), 7.67-7.73 (2H, m, H-5 and H-4'), 12.99 (1H, s, NH); ^{13}C NMR (125 MHz DMSO-d_6) δ ppm 51.7 (O-CH_3), 112.2 (d, J_{CF} = 24.7 Hz, C-Ar), 114.6 (C-Ar), 117.5 (C-Ar), 124.5 (C-Ar), 125.9 (C-Ar), 130.2 (C-Ar), 132.4 (t, J_{CF} = 10.0 Hz, C-Ar), 158.7 (dd, J_{CF} = 8.1 and 247.0 Hz, C-F), 160.3 (CO), 181.6 (CO); MS (ES+) *m/z* = 266.1 $[M+H]^+$.

4-(2,6-Difluorobenzoyl)-1*H*-pyrrole-2-carboxylic acid, 412

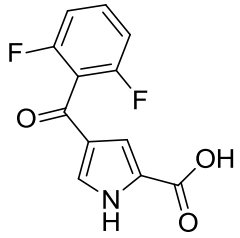

General procedure G: methyl 4-(2,6-difluorobenzoyl)-1*H*-pyrrole-2-carboxylate (1.30 g, 4.91 mmol) and LiOH monohydrate (4.12 g, 98.20 mmol) gave **412** as a white solid (1.19 g, 97%). R_f 0.22 (9:1 DCM/MeOH); m.p. 197-198 ^oC; λ_{max} (EtOH/nm) 283.0, 232.5; IR υ_{max}/cm^{-1} 3772, 3024, 2779, 2612, 2539, 2105, 1753; ^1H NMR (500 MHz DMSO-d_6) δ ppm 7.00 (1H, br s, H-3), 7.23-7.28 (2H, m, H-3' and H-5'), 7.51 (1H, br s, H-5), 7.62 (1H, dddd, J = 6.7, 6.8, 8.3 and 8.4 Hz, H-4'), 12.71 (1H, s, NH), 12.94 (1H, s COOH); ^{13}C NMR (125 MHz, DMSO-d_6) δ ppm 112.2 (d, J_{CF} = 25.2 Hz, C-Ar), 114.2 (C-Ar), 117.6 (t, J_{CF} = 24.5 Hz, C-Ar), 124.3 (C-Ar), 125.8 (C-Ar), 129.7 (C-Ar), 132.3 (t, J_{CF} = 10.0 Hz, C-Ar), 158.6 (dd, J_{CF} = 8.0 and 248.3 Hz, C-F), 161.3 (CO), 181.6 (CO); MS (ES+) *m/z* = 252.2 $[M+H]^+$; HRMS calcd for $C_{12}H_8NF_2O_3$ $[M+H]^+$ 252.0467, found 252.0470.

***N*-(2,2-Diethoxyethyl)-4-(2,6-difluorobenzoyl)-*N*-(pyridin-4-ylmethyl)-1*H*-pyrrole-2-carboxamide, 413**

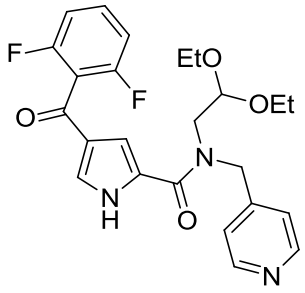

General procedure E: 4-(2,6-difluorobenzoyl)-1*H*-pyrrole-2-carboxylic acid (313 mg, 1.25 mmol), $SOCl_2$ (140 μL, 1.88 mmol) gave 4-(2,6-difluorobenzoyl)-1*H*-pyrrole-2-carbonyl chloride as a colourless oil and used directly in the next step. To a solution of 4-(2,6-difluorobenzoyl)-1*H*-pyrrole-2-carbonyl chloride (336 mg, 1.25 mmol) in DCM (2.5 mL/mmol) was added 2,2-diethoxy-*N*-(pyridin-4-ylmethyl)ethanamine (420 mg, 1.88 mmol). The resulting mixture was stirred at RT for 16 h. The DCM was removed by rotary evaporation and the slurry obtained was diluted with H_2O (10 mL) and adjusted to pH 10 with 1M NaOH (aq). The resulting mixture was extracted with EtOAc (2 x 20 mL).

Combined organic layers were dried over Na_2SO_4 and concentrated *in vacuo*. Purification *via* column chromatography (silica; 30-100% EtOAc/petrol) gave **413** as a white solid (400 mg, 70%). R_f 0.32 (20:80 Petrol/EtOAc); m.p. 84-85 ˚C; λ_{max} (EtOH/nm) 290.5, 234.0; IR υ_{max}/cm^{-1} 2977, 1653, 1620, 1600, 1550; ^{1}H NMR (500 MHz DMSO-d_6, 353 K) δ ppm 1.09 (6H, t, J = 7.3 Hz, CH_3), 3.43-3.49 (2H, m, O-CH_2), 3.60-3.65 (4H, m, O-CH_2 and N-CH_2), 4.75 (1H, t, J = 5.3 Hz, CH), 4.85 (2H, s, N-CH_2-pyridine), 6.85 (1H, br s, H-3), 7.18 (2H, dd, J = 8.1 and 8.2 Hz, H-3'), 7.25 (2H, d, J = 6.0 Hz, CH-pyridine), 7.40 (1H, br s, H-5), 7.60 (1H, m, H-4'), 8.52 (2H, d, J = 6.0 Hz, N-CH-pyridine), 12.21 (1H, s, NH-pyrrole); ^{13}C NMR (125 MHz, DMSO-d_6) δ ppm Use of long VT experiment not possible; MS (ES+) *m/z* = 458.1 $[M+H]^+$; HRMS calcd for $C_{24}H_{25}F_2N_3O_4$ $[M+H]^+$ 458.1186, found 458.1187.

7-(2,6-Difluorobenzoyl)-2-(pyridin-4-ylmethyl)pyrrolo[1,2-a]pyrazin-1(2*H*)-one, 414

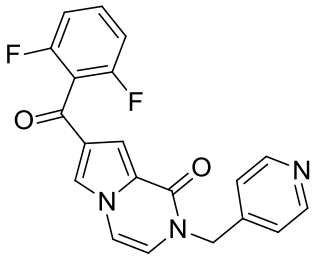

A solution of *N*-(2,2-diethoxyethyl)-4-(2,6-difluorobenzoyl)-N-(pyridin-4-ylmethyl)-1*H*-pyrrole-2-carboxamide (153 mg, 0.40 mmol) in 1:1 TFA:H_2O (3 mL/mmol) was heated with microwave irradiation for 2 h at 160 ^{o}C. The mixture was allowed to cool, diluted with H_2O (10 mL), and adjusted to pH 10 with 2M NaOH (aq). The mixture was extracted with EtOAc (2 x 20 mL). Combined organic layers were washed with brine, dried over Na_2SO_4 and concentrated *in vacuo*. Purification *via* column chromatography (silica; DCM) gave **414** as a greyish solid (133 mg, 90%). R_f 0.34 (DCM); m.p. 77-79 ˚C; λ_{max} (EtOH/nm) 267.0, 223.0; IR υ_{max}/cm^{-1} 3106, 1640, 1622, 1601, 1532; ^{1}H NMR (500 MHz MeOD) δ ppm 5.05 (2H, s, N-CH_2), 6.01 (1H, d, J = 6.0 Hz, CH-pyridone), 7.01-7.06 (2H, m, H-3'), 7.24-7.29 (4H, m, H-3, CH-pyridine and N-CH-pyridone), 7.45-7.51 (1H, m, H-4'), 7.78 (1H, d, J = 1.6 Hz, H-5), 8.40 (2H, m, N-CH-pyridine); ^{13}C NMR (125 MHz, MeOD) δ ppm 50.4 (CH_2), 110.2 (C-Ar), 112.2 (C-Ar), 113.0 (C-Ar), 113.2 (d, J_{CF} = 25.0 Hz, C-Ar), 121.6 (C-Ar), 123.9 (C-Ar), 125.2 (C-Ar), 126.6 (C-Ar), 129.3 (C-Ar), 133.7 (t, J_{CF} = 10.1 Hz, C-Ar), 148.6 (C-Ar), 150.5 (C-Ar), 158.0 (CO), 184.5 (CO), C-F not visualised; MS (ES+) *m/z* = 366.2 $[M+H]^+$; HRMS calcd for $C_{20}H_{13}F_2N_3O_2$ $[M+H]^+$ 366.1049, found 366.1051.

Methyl 4-(2,6-difluorobenzoyl)-1-((2-(trimethylsilyl)ethoxy)methyl)-1*H*-pyrrole-2-carboxylate, 415

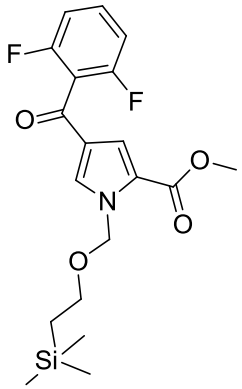

To a solution of methyl 4-(2,6-difluorobenzoyl)-1*H*-pyrrole-2-carboxylate (400 mg, 1.51 mmol) in THF (4 mL/mmol) was added KO^{t}Bu (203 mg, 1.81 mmol) at 0 ^oC. The resulting mixture was stirred for 15 min, and then SEM chloride (0.32 mL, 1.81 mmol) was added dropwise. The mixture was warmed to RT and stirred for 2 h. The reaction was quenched with H_2O (10 mL) and extracted with DCM (2 x 30 mL). Combined organic layers were washed with brine, dried over Na_2SO_4 and concentrated *in vacuo*. Purification *via* column chromatography (silica; 0-30 % EtOAc/petrol) gave **415** as a colourless oil (554 mg, 93%). R_f 0.45 (9:1 Petrol/EtOAc); λ_{max} (EtOH/nm) 279.5, 234.0; IR υ_{max}/cm^{-1} 2954, 2895, 1716, 1659, 1622, 1545; ^1H NMR (500 MHz $CDCl_3$) δ ppm 0.00 (9H, s, CH_3), 0.92-0.96 (2H, m, CH_2-Si), 3.58-3.62 (2H, m, O-CH_2), 3.87 (3H, s, O-CH_3), 5.73 (2H, s, N-CH_2-O), 6.99-7.04 (2H, m, H-3' and H-5'), 7.35 (1H, d, J = 1.6 Hz, H-3), 7.44 (1H, dddd, J = 6.7, 6.8, 8.3 and 8.4 Hz, H-4'), 7.56 (1H, d, J = 1.6 Hz, H-5); ^{13}C NMR (125 MHz, $CDCl_3$) δ ppm 17.8 (Si-CH_3), 22.2 (CH_2-Si), 51.7 (O-CH_3), 67.0 (O-CH_2), 78.0 (N-CH_2-O), 111.9 (d, J_{CF} = 25.2 Hz, C-Ar), 117.2 (t, J_{CF} = 22.2 Hz, C-Ar) 119.1 (C-Ar), 124.0 (C-Ar), 125.1 (C-Ar), 131.6 (t, J_{CF} = 10.2 Hz, C-Ar), 132.8 (C-Ar), 159.7 (dd, J_{CF} = 7.0 and 251.5 Hz, C-F), 161.0 (CO), 182.2 (CO); MS (ES+) *m/z* = 394.2 $[M-H]^-$; HRMS calcd for $C_{19}H_{23}F_2NO_4Si$ $[M+H]^+$ 396.1437, found 396.1437.

4-(2,6-Difluorobenzoyl)-1-((2-(trimethylsilyl)ethoxy)methyl)-1*H*-pyrrole-2-carboxylic acid, 416

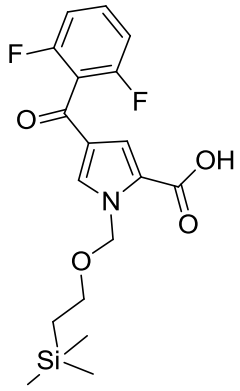

General procedure G: methyl 4-(2,6-difluorobenzoyl)-1-((2-(trimethylsilyl)ethoxy)methyl)-1*H*-pyrrole-2-carboxylate (540 mg, 1.37 mmol) and LiOH monohydrate (1.15 g, 27.30 mmol) gave **416** as a colourless oil which solidified as a white solid upon cooling (501 mg, 96%). R_f 0.25 (9:1 Petrol/EtOAc); m.p. 125-126 ^{o}C; λ_{max} (EtOH/nm) 279.0, 233.0; IR υ_{max}/cm^{-1} 2952, 1663, 1624, 1589, 1547; ^{1}H NMR (500 MHz $CDCl_3$) δ ppm 0.00 (9H, s, Si-CH_3), 0.93-0.96 (2H, m, CH_2-Si), 3.58-3.62 (2H, m, O-CH_2), 5.71 (2H, s, N-CH_2-O), 6.99-7.04 (2H, m, H-3' and H-5'), 7.45 (1H, dddd, *J* = 6.7, 6.8, 8.3 and 8.4 Hz, H-4'), 7.49 (1H, d, *J* = 1.6 Hz, H-3), 7.61 (1H, d, *J* = 1.6 Hz, H-5), COOH not visualised; ^{13}C NMR (125 MHz, $CDCl_3$) δ ppm 17.8 (Si-CH_3), 21.1 (CH_2-Si), 67.2 (O-CH_2), 78.2 (N-CH_2-O), 112. (d, J_{CF} = 24.7 Hz, C-Ar), 117.7 (t, J_{CF} = 22.0 Hz, C-Ar), 121.3 (C-Ar), 123.1 (C-Ar), 125.3 (C-Ar), 131.7 (t, J_{CF} = 10.4 Hz, C-Ar), 133.5 (C-Ar), 159.7 (dd, J_{CF} = 7.0 and 251.7 Hz, C-F), 164.5 (CO), 182.2 (CO); MS (ES+) *m/z* = 382.2 $[M+H]^+$; HRMS calcd for $C_{18}H_{21}F_2NO_4Si$ $[M+H]^+$ 382.1281, found 382.1283.

***N*-(2,2-Diethoxyethyl)-4-(2,6-difluorobenzoyl)-*N*-(pyridin-4-ylmethyl)-1-((2-(trimethylsilyl)ethoxy)methyl)-1*H*-pyrrole-2-carboxamide, 417**

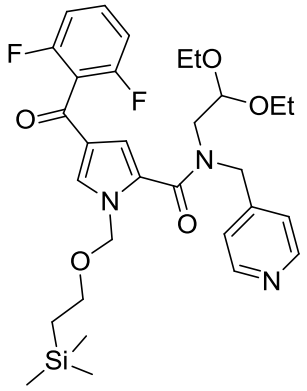

General procedure E: 4-(2,6-difluorobenzoyl)-1-((2-(trimethylsilyl)ethoxy)methyl)-1*H*-pyrrole-2-carboxylic acid (490 mg, 1.29 mmol), and $SOCl_2$ (140 μL, 1.94 mmol) gave 4-(2,6-difluorobenzoyl)-1-((2-(trimethylsilyl)ethoxy)methyl)-1*H*-pyrrole-2-carbonyl chloride as a colourless oil which was used directly in the next step. To a solution of 4-(2,6-difluorobenzoyl)-1-((2-(trimethylsilyl)ethoxy)methyl)-1*H*-pyrrole-2-carbonyl chloride (0.51 g, 1.29 mmol) in DCM (3 mL/mmol) was added 2,2-diethoxy-*N*-(pyridin-4-ylmethyl)ethanamine (347 mg, 1.55 mmol) at RT. The resulting mixture was stirred for 16 h. The reaction was quenched with H_2O, and adjusted to pH 10 with 1M NaOH (aq). The mixture was extracted with DCM (2 x 30 mL). Combined organic layers were washed with brine, dried over Na_2SO_4 and concentrated *in vacuo*. Purification *via* column chromatography (silica; 0-50% EtOAc/petrol) gave **417** as a pale yellow oil (389 mg, 51%). R_f 0.45 (1:1 Petrol/EtOAc); λ_{max} (EtOH/nm) 236.0; IR υ_{max}/cm^{-1} 2896, 1736, 1622, 1546, 1497, 1463; ^1H NMR (500 MHz, DMSO-d_6, 353 K) δ ppm 0.04 (s, 9H, Si-CH_3), 0.81 (2H, t, J = 8 Hz, CH_2-Si), 1.10 (6H, t, J = 7.3 Hz, CH_3), 3.43-3.47 (4H, m, CH_2 and O-CH_2), 3.51 (2H, d, J = 5.5 Hz, N-CH_2), 3.59-3.62 (2H, m, CH_2), 4.73 (1H, t, J = 5.5 Hz, CH), 4.80 (2H, s, CH_2-pyridine), 5.47 (2H, s, N-CH_2-O), 6.90 (1H, br s, H-3), 7.17-7.21 (2H, m, H-3' and H-5'), 7.28 (2H, d, J = 6 Hz, CH-pyridine), 7.60 (1H, dddd, J = 6.7, 6.8, 8.3 and 8.4 Hz, H-4'), 7.71 (1H, d, J = 1.5 Hz, H-5), 8.52 (2H, d, J = 6 Hz, CH-N-pyridine); ^{13}C NMR (125 MHz, DMSO-d_6) δ ppm Use of long VT experiment not possible; MS (ES+) *m/z* = 588.3 $[M+H]^+$; HRMS calcd for $C_{30}H_{39}F_2N_3O_5Si$ $[M+H]^+$ 588.2700, found 588.2694.

3-(2,6-Difluorobenzoyl)-6-(pyridin-4-ylmethyl)-1-((2-(trimethylsilyl)ethoxy)methyl)-1*H*-pyrrolo[2,3-c]pyridin-7(6*H*)-one, 418

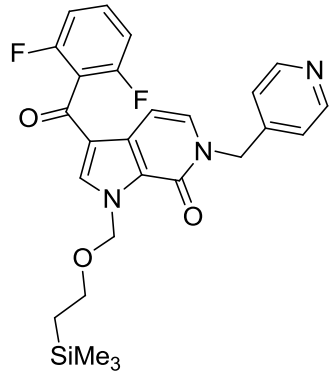

N-(2,2-Diethoxyethyl)-4-(2,6-difluorobenzoyl)-*N*-(pyridin-4-ylmethyl)-1-((2(trimethylsilyl)ethoxy)methyl)-1*H*-pyrrole-2-carboxamide (350 mg, 0.60 mmol) was dissolved in a 5% TFA solution in DME (6 mL/mmol). The resulting solution was heated at 120 ^{o}C for 1.5 h under microwave irradiation. The reaction mixture was diluted with water (10 mL), and adjusted to pH 10 with 1M NaOH (aq). The mixture was extracted with EtOAc (2 x 30 mL). Combined organic layers were washed with brine, dried over Na_2SO_4 and concentrated *in vacuo*. Purification *via* column chromatography (silica; 0-5% DCM/MeOH then NH silica; 30-100% EtOAc/petrol) gave **418** as a colourless oil (103 mg, 35%). R_f 0.37 (8:2 Petrol/EtOAc); λ_{max} (EtOH/nm) 260.0, 223.5; IR υ_{max}/cm^{-1}2954, 2899, 1648, 1623, 1590, 1519; ^{1}H NMR (500 MHz DMSO-d_6) δ ppm 0.00 (9H, s, Si-CH_3), 0.90 (2H, t, *J* = 8 Hz, CH_2-Si), 3.65 (2H, t, *J* = 8 Hz, O-CH_2), 5.41 (2H, s, CH_2-pyridine), 5.97 (2H, s, N-CH_2-O), 7.22 (1H, d, *J* = 7 Hz, CH), 7.34 (2H, d, *J* = 6 Hz, CH-pyridine), 8.41-8.45 (2H, m, H-3' and H-5'), 7.79-7.83 (2H, m, H-4' and N-CH), 8.23 (1H, s, H-5), 8.65 (2H, d, *J* = 6.1 Hz, CH-N-pyridine); ^{13}C NMR (125 MHz, DMSO-d_6) δ ppm 17.2 (Si-CH_3), 49.9 (CH_2-Si), 65.3 (O-CH_2), 76.5 (N-CH_2-O), 100.5 (C-Ar), 112.3 (dd, J_{CF} = 4.3 and 20.7 Hz, C-Ar), 117.5 (C-Ar), 122.1 (C-Ar), 123.5 (C-Ar), 130.7 (C-Ar), 132.5 (t, J_{CF} = 10.3 Hz, C-Ar), 134.0 (C-Ar), 140.1 (C-Ar), 146.5 (C-Ar), 149.7 (C-Ar), 154.0 (CO), 158.7 (dd, J_{CF} = 7.8 and 247.7 Hz, C-F), 181.8 (CO), one C-Ar and N-CH_2 not visualised; MS (ES+) *m/z* = 496.3 $[M+H]^+$; HRMS calcd for $C_{26}H_{27}F_2N_3O_3Si$ $[M+H]^+$ 496.1863, found 496.1855.

3-(2,6-Difluorobenzoyl)-6-(pyridin-4-ylmethyl)-1*H*-pyrrolo[2,3-c]pyridin-7(6*H*)-one, 394

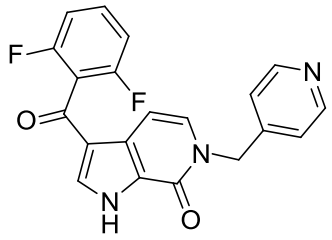

General procedure H: 3-(2,6-difluorobenzoyl)-6-(pyridin-4-ylmethyl)-1-((2-(trimethylsilyl)ethoxy)methyl)-1*H*-pyrrolo[2,3-c]pyridin-7(6*H*)-one (90 mg, 0.18 mmol). Purification *via* column chromatography (silica; 0-8% DCM/MeOH) followed by recrystallisation from a minimum amount of hot ethanol gave **394** as a white solid (55 mg, 83%). R_f 0.30 (95:5 DCM/MeOH); m.p 271-272 ^oC; λ_{max} (EtOH/nm) 393.5, 258.5, 222.5; IR υ_{max}/cm^{-1} 3040, 2916, 1649, 1619, 1587, 1518; ^1H NMR (500 MHz DMSO-d_6) δ ppm 5.34 (2H, s, CH_2), 7.03 (1H, d, *J* = 7.1 Hz, CH), 7.25 (2H, d, *J* = 6.0 Hz, CH-pyridine), 7.29-7.34 (2H, m, H-3' and H-5'), 7.61 (1H, d, *J* = 7.1 Hz, N-CH), 7.68 (1H, m, H-4'), 7.84 (1H, s, H-5), 8.56 (2H, d, *J* = 6.0 Hz, N-CH-pyridine), 13.2 (1H, s, NH-pyrrole); ^{13}C NMR (125 MHz, DMSO-d_6) δ ppm 49.6 (CH_2), 100.8 (C-Ar), 112.3 (dd, J_{CF} = 4.7 and 21.3 Hz, C-Ar), 117.9 (t, J_{CF} = 22.3 Hz, C-Ar), 118.6 (C-Ar), 122.0 (C-Ar), 125.2 (C-Ar), 129.3 (C-Ar), 132.2 (t, J_{CF} = 9.8 Hz, C-Ar), 133.0 (C-Ar), 135.9 (C-Ar), 146.6 (C-Ar), 149.8 (C-Ar), 154.0 (CO), 158.6 (dd, J_{CF} = 7.8 and 247.8 Hz, C-F), 181.7 (CO); MS (ES+) *m/z* = 366.2 $[M+H]^+$; HRMS calcd for $C_{20}H_{13}F_2N_3O_2$ $[M+H]^+$ 366.1049, found 366.1051.

***N*-(2,2-Diethoxyethyl)-4-(2,6-difluorobenzoyl)-1*H*-pyrrole-2-carboxamide, 428**

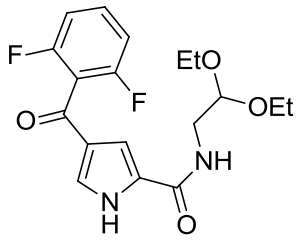

General procedure D: 4-(2,6-Difluorobenzoyl)-1*H*-pyrrole-2-carboxylic acid (0.50 g, 1.99 mmol), CDI (0.65 g, 3.98 mmol) and aminoacetaldehyde diethyl acetal (0.72 mL, 4.98 mmol). Purification *via* column chromatography (10-70% EtOAc/petrol) gave **428** as a white solid (0.63 g, 87%). R_f 0.47 (9:1 DCM/MeOH); m.p. 144-146 ^oC; $^{\circ}C$ λ_{max} (EtOH/nm) 285.5, 235.0; IR υ_{max}/cm^{-1} 3379, 3191, 2976, 2888, 1621, 1572, 1536; ^1H NMR (500 MHz, DMSO-d_6) δ ppm 1.12 (6H, t, *J* = 7.1 Hz, CH_3), 3.29 (2H, dd, *J* = 5.5 and 5.8 Hz, NH-CH_2), 3.46-

3.52 (2H, m, CH_2), 3.60-3.66 (2H, m, CH_2), 4.58 (1H, t, *J* = 5.5 Hz, CH), 7.23-7.28 (3H, m, H-3, H-3' and H-5'), 7.38 (1H, br s, H-5), 7.61 (1H, dddd, *J* = 6.7, 6.8, 8.3 and 8.4 Hz, H-4'), 8.42 (1H, t, *J* = 5.8 Hz, CO-NH), 12.42 (1H, s, NH-pyrrole); ^{13}C NMR (125 MHz, DMSO-d_6) δ ppm 15.3 (CH_3), 41.6 (NH-CH_2), 61.5 (CH_2), 100.2 (CH), 112.2 (d, J_{CF} = 24.7 Hz, C-Ar), 117.9 (t, J_{CF} = 23.5 Hz, C-Ar), 125.6 (C-Ar), 128.4 (C-Ar), 128.6 (C-Ar), 132.1 (t, J_{CF} = 9.8 Hz, C-Ar), 158.6 (dd, J_{CF} = 8.0 and 247.6 Hz, C-F), 159.9 (CO), 181.8 (CO); HRMS calcd for $C_{18}H_{20}F_2N_2O_4$ $[M-H]^-$ 365.1318, found 365.1308

3-(2,6-Difluorobenzoyl)-1*H*-pyrrolo[2,3-c]pyridin-7(6*H*)-one, 429

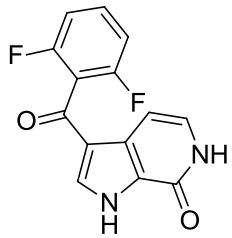

General procedure P: *N*-(2,2-diethoxyethyl)-4-(2,6-difluorobenzoyl)-1*H*-pyrrole-2-carboxamide (1.30 g, 3.56 mmol). Purification *via* column chromatography (silica; 0-5% MeOH/DCM) gave **429** as a white solid (450 mg, 46%). R_f 0.41 (9:1 DCM/MeOH); m.p. 289-290 ^oC; ˚C λ_{max} (EtOH/nm) 259.0, 217.0; IR υ_{max}/cm^{-1} 2911, 1772, 1622, 1531; ^{1}H NMR (500 MHz, DMSO-d_6) δ ppm 6.88 (1H, d, *J* = 6.8 Hz, CH-pyridone), 7.14 (1H, dd, *J* = 5.9 and 6.8 Hz, NH-*CH*-pyridone), 7.24-7.28 (2H, m, H-3' and H-5'), 7.62 (1H, dddd, *J* = 6.7, 6.8, 8.3 and 8.4 Hz, H-4'), 7.72 (1H, s, H-5), 11.37 (1H, br s, CO-NH), 13.02 (1H, s, NH-pyrrole); ^{13}C NMR (125 MHz, DMSO-d_6) δ ppm 99.9 (C-pyridone), 112.2 (d, J_{CF} = 24.8 Hz, C-Ar), 118.0 (t, J_{CF} = 23.0 Hz, C-Ar), 118.6 (C-pyridone), 125.6 (C-Ar), 128.6 (C-Ar), 129.8 (C-Ar), 132.1 (t, J_{CF} = 9.8 Hz, C-Ar), 135.3 (C-Ar), 154.6 (CO), 158.6 (dd, J_{CF} = 8.1 and 247.3 Hz, C-F), 181.6 (CO); HRMS calcd for $C_{14}H_8F_2N_2O_2$ $[M+H]^+$ 275.0627, found 275.0631.

3-(2,6-Difluorobenzoyl)-1-((2-(trimethylsilyl)ethoxy)methyl)-1*H*-pyrrolo[2,3-c]pyridin-7(*6H*)-one, 430

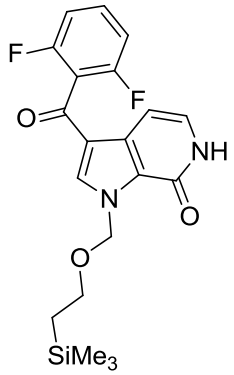

General procedure Q: 3-(2,6-difluorobenzoyl)-1*H*-pyrrolo[2,3-c]pyridin-7(*6H*)-one (0.59 g, 2.15 mmol), SEMCl (0.46 mL, 0.94 mmol), Et_3N (0.36 mL, 2.58 mmol) and DMAP (10 mol%). Purification *via* column chromatography (silica; 0-70% EtOAc/petrol) gave **430** as a colourless oil (0.50 g, 58%). R_f 0.37 (8:2 Petrol/EtOAc); λ_{max} (EtOH/nm) 260.0, 219.5; IR υ_{max}/cm^{-1} 2957, 2900, 1642, 1622, 1588, 1521, 1463, 1374, 1309, 1246; ^1H NMR (500 MHz, $CDCl_3$) δ ppm 0.01 (9H, s, CH_3), 0.90-0.0.94 (2H, m, Si-CH_2), 3.63-3.66 (2H, m, O-CH_2), 5.98 (2H, s, N-CH_2-O), 7.00-7.04 (2H, m, H-3' and H-5'), 7.14 (1H, dd, *J* = 5.9 and 7.2 Hz, NH-*CH*-pyridone), 7.33 (1H, d, J = 7.2 Hz, CH-pyridone), 7.45 (1H, dddd, *J* = 6.7, 6.8, 8.3 and 8.4 Hz, H-4'), 7.56 (1H, s, H-5), 10.28 (1H, s, CO-NH); ^{13}C NMR (125 MHz, $CDCl_3$) δ ppm 17.8 (CH_2), 66.8 (O-CH_2), 74.7 (N-CH_2-O), 102.5 (C-pyridone), 112.0 (d, J_{CF} = 24.9 Hz, C-Ar), 119.3 (C-pyridone), 124.3 (C-Ar), 127.8 (C-Ar), 129.8 (C-Ar), 132.1 (t, J_{CF} = 9.8 Hz, C-Ar), 134.7 (C-Ar), 156.1 (CO), 159.6 (dd, J_{CF} = 7.6 and 251.1 Hz, C-F), 182.1 (CO), one F split C-Ar not visualised; HRMS calcd for $C_{20}H_{22}F_2N_2O_3Si$ $[M+H]^+$ 405.1441, found 405.1442.

3-(2,6-Difluorobenzoyl)-6-(pyridin-4-yl)-1-((2-(trimethylsilyl)ethoxy)methyl)-1*H*-pyrrolo[2,3-c]pyridin-7(*6H*)-one, 431

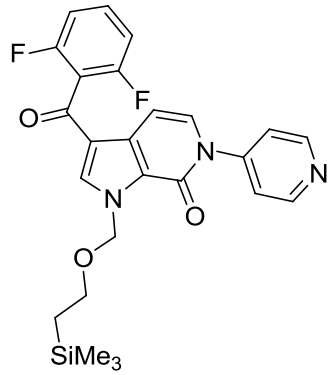

General procedure R: 3-(2,6-difluorobenzoyl)-1-((2-(trimethylsilyl)ethoxy)methyl)-1*H*-pyrrolo[2,3-c]pyridin-7(*6H*)-one (200 mg, 0.50 mmol), 4-bromopyridine (126 mg, 0.65 mmol), K_2CO_3 (228 mg, 1.65 mmol and CuI (10 mol%). Purification *via* column chromatography (silica; 20-100% EtOAc/petrol) gave **431** as a colourless oil (50 mg, 21%). R_f 0.18 (8:2 Petrol/EtOAc); λ_{max} (EtOH/nm) 309.5, 284.0; IR υ_{max}/cm^{-1} 2964, 1651, 1623, 1581, 1517, 1464, 1380, 1274; ^{1}H NMR (500 MHz, $CDCl_3$) δ ppm 0.04 (9H, s, CH_3), 0.90-0.93 (2H, m, Si-CH_2), 3.64-3.67 (2H, m, O-CH_2), 5.95 (2H, s, N-CH_2-O), 7.02-7.06 (2H, m, H-3' and H-5'), 7.21 (1H, d, *J* = 7.3 Hz, CH-pyridone), 7.43 (1H, d, *J* = 7.3 Hz, N-CH-pyridone), 7.45-7.50 (3H, m, H-4' and CH-pyridine), 7.60 (1H, s, H-5), 8.80 (2H, br s, N-CH-pyridine); ^{13}C NMR (125 MHz, $CDCl_3$) δ ppm 17.9 (CH_2), 67.0 (O-CH_2), 77.4 (N-CH_2-O), 103.4 (C-pyridone), 112.0 (d, J_{CF} = 25.2 Hz, C-Ar), 119.2 (C-pyridone), 121.7 (m, C-Ar), 124.0 (C-Ar), 131.1 (C-Ar), 131.6 (C-Ar), 131.8 (t, J_{CF} = 9.7 Hz, C-Ar), 137.6 (C-Ar), 148.0 (C-Ar), 151.0 (C-Ar), 154.4 (CO), 159.7 (dd, J_{CF} = 7.1 and 250.7 Hz, C-F), 182.1 (CO) one C-Ar not visualised; HRMS calcd for $C_{25}H_{25}F_2N_3O_3Si$ $[M+H]^+$ 482.1706, found 482.1701.

3-(2,6-Difluorobenzoyl)-6-(pyridin-4-yl)-*1H*-pyrrolo[2,3-c]pyridin-7(*6H*)-one, 432

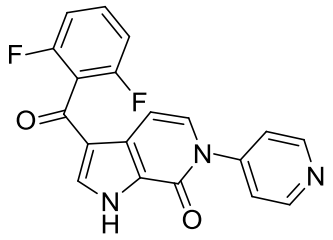

General procedure H: 3-(2,6-difluorobenzoyl)-6-(pyridin-4-yl)-1-((2-(trimethylsilyl)ethoxy)methyl)-1*H*-pyrrolo[2,3-c]pyridin-7(6*H*)-one (50 mg, 0.10 mmol), 1M TBAF in THF (0.15 mL, 0.15 mmol). Purification *via* column chromatography (silica; 0-8% MeOH/DCM) gave **432** as a white solid (21 mg, 60%). R_f 0.23 (9:1 DCM/MeOH); m.p. Degrades >200 ^oC; λ_{max} (EtOH/nm) 256.5, 223.5; IR υ_{max}/cm^{-1} 3055, 2986, 2917, 1668, 1641, 1620, 1579, 1518, 1479, 1457; ^1H NMR (500 MHz, DMSO-*d6*) δ ppm 7.03 (1H, d, *J* = 7.1 Hz, CH-pyridone), 7.27-7.30 (2H, m, H-3' and H-5'), 7.50 (1H, d, *J* = 7.1 Hz, N-CH-pyridone), 7.61-7.67 (3H, m, CH-pyridine and H-4'), 7.87 (1H, s, H-5), 8.76 (2H, d, *J* = 6.1 Hz, N-CH-pyridine), 13.28 (1H, s, NH-pyrrole); ^{13}C NMR (125 MHz, DMSO-*d6*) δ ppm 101.4 (C-pyridone), 112.3 (d, J_{CF} = 24.7 Hz, C-Ar), 118.7 (C-pyridone), 121.9 (C-Ar), 125.0 (C-Ar), 129.3 (C-Ar), 132.0 (C-Ar), 132.5 (t, J_{CF} = 9.6 Hz, C-Ar), 147.6 (C-Ar), 150.7 (C-Ar), 153.4 (CO), 158.6 (dd, J_{CF} = 8.1 and 247.6 Hz, C-F), 181.8 (CO), one F split C-Ar not visualised; HRMS calcd for $C_{19}H_{11}F_2N_3O_2$ $[M+H]^+$ 352.0892, found 352.0895.

3-(2,6-Difluorobenzoyl)-6-(pyridin-3-yl)-1*H*-pyrrolo[2,3-c]pyridin-7(6*H*)-one, 433

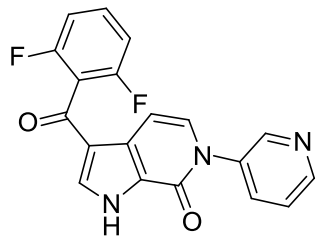

General procedure R: 3-(2,6-difluorobenzoyl)-1-((2-(trimethylsilyl)ethoxy)methyl)-1*H*-pyrrolo[2,3-c]pyridin-7(6*H*)-one (110 mg, 0.27 mmol), 3-bromopyridine HCl (68 mg, 0.35 mmol), K_2CO_3 (123 mg, 0.89 mmol) and CuI (10 mol%) gave 3-(2,6-difluorobenzoyl)-6-(pyridin-3-yl)-1-((2-(trimethylsilyl)ethoxy)methyl)-1*H*-pyrrolo[2,3-c]pyridin-7(6*H*)-one which was used directly in the next step. General procedure H: 1M TBAF in THF (0.41 mL, 0.41 mmol). Purification *via* column chromatography (silica; 0-5% MeOH/DCM) gave **433** as a white solid (35 mg, 37%).R_f 0.22 (9:1 DCM/MeOH); m.p Degrades >200 ^oC; λ_{max}

(EtOH/nm) 262.5, 221.5; IR υ_{max}/cm^{-1} 3111, 3045, 1651, 1620, 1594, 1573; ^{1}H NMR (500 MHz, DMSO-d_6) δ ppm 7.01 (1H, d, *J* = 7.1 Hz, CH-pyridone), 7.27-7.30 (2H, m, H-3' and H-5'), 7.50 (1H, d, *J* = 7.1 Hz, N-CH-pyridone), 7.60-7.68 (2H, m, CH-pyridine and H-4'), 7.87 (1H, s, H-5), 7.99 (1H, ddd, *J* = 1.5, 2.5 and 8.1 Hz, CH-pyridine), 8.67 (1H, dd, *J* = 1.5 and 4.5 Hz, N-CH-pyridine), 8.72 (1H, d, *J* = 2.5 Hz, N-CH-pyridine), 13.27 (1H, s, NH-pyrrole); ^{13}C NMR (125 MHz, DMSO-d_6) δ ppm 100.6 (C-pyridone), 112.3 (d, J_{CF} = 24.7 Hz, C-Ar), 118.8 (C-pyridone), 123.9 (C-Ar), 125.0 (C-Ar), 129.4 (C-Ar), 132.3 (t, J_{CF} = 9.8 Hz, C-Ar), 132.8 (C-Ar), 134.9 (C-Ar), 136.0 (C-Ar), 137.2 (C-Ar), 147.9 (C-Ar), 148.8 (C-Ar), 153.9 (CO), 158.6 (dd, J_{CF} = 8.1 and 247.3 Hz, C-F), 181.7 (CO); HRMS calcd for $C_{19}H_{11}F_2N_3O_2$ $[M+H]^+$ 352.0892, found 352.0896.

Methyl 4-(2,3-dichlorobenzoyl)-1*H*-pyrrole-2-carboxylate, 434

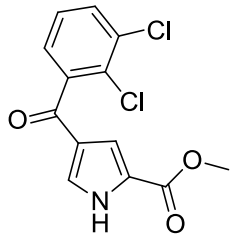

General procedure F: methyl 1*H*-pyrrole-2-carboxylate (1.50 g, 11.99 mmol), 2,3-dichlorobenzoyl chloride (5.00 g, 23.98 mmol), and $AlCl_3$ (4.02 g, 29.98 mmol). Purification *via* column chromatography (silica; 0-50% EtOAc/petrol) gave **434** as a white solid (2.25 g, 79%). R_f 0.18 (8:2 Petrol/EtOAc); m.p. 188-190 ^{o}C; ˚C λ_{max} (EtOH/nm) 282.5, 228.0; IR υ_{max}/cm^{-1} 3281, 3118, 2956, 1687, 1655, 1560; ^{1}H NMR (500 MHz, DMSO-d_6) δ ppm 3.80 (3H, s, O-CH_3), 7.02 (1H, br s, H-3), 7.44-7.50 (3H, m, H-6', H-5 and H-5'), 7.78 (1H, dd, *J* = 1.7 and 7.8 Hz, H-4'), 12.84 (1H, s, NH); ^{13}C NMR (125 MHz, DMSO-d_6) δ ppm 51.6 (O-CH_3), 115.0 (C-Ar), 124.3 (C-Ar), 124.8 (C-Ar), 126.9 (C-Ar), 127.5 (C-Ar), 128.6 (C-Ar), 130.4 (C-Ar), 131.5 (C-Ar), 132.3 (C-Ar), 141.3 (C-Ar), 160.3 (CO), 187.2 (CO); HRMS calcd for $C_{13}H_9{}^{35}Cl_2NO_3$ $[M+H]^+$ 298.0032, found 298.0037.

4-(2,3-Dichlorobenzoyl)-1*H*-pyrrole-2-carboxylic acid, 435

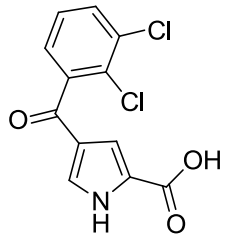

General procedure G: methyl 4-(2,3-dichlorobenzoyl)-1*H*-pyrrole-2-carboxylate (2.20 g, 7.38 mmol) and LiOH monohydrate (6.20 g, 147.60 mmol) gave **435** as a white solid (2.04 g, 97%). R_f 0.25 (9:1 DCM/MeOH); m.p. Degrades >150 ^{o}C; ˚C λ_{max} (EtOH/nm) 282.5, 230.0; IR υ_{max}/cm^{-1} 3300, 3128, 2786, 2685, 2619, 2412, 1672, 1639, 1550, 1501; ^{1}H NMR (500 MHz, DMSO-d_6) δ ppm 6.97 (1H, dd, *J* = 1.8 and 2.2 Hz, H-3), 7.38 (1H, dd, *J* = 1.8 and 3.4 Hz, H-5), 7.44 (1H, dd, *J* = 1.8 and 7.6 Hz, H-6'), 7.48 (1H, dd, *J* = 7.7 and 7.8 Hz, H-5'), 7.78 (1H, dd, *J* = 1.8 and 7.8 Hz, H-4'), 12.64 (1H, s, NH), 12.90 (1H, s, COOH); ^{13}C NMR (125 MHz, DMSO-d_6) δ ppm 114.6 (C-Ar), 124.6 (C-Ar), 125.6 (C-Ar), 126.9 (C-Ar), 127.5 (C-Ar), 128.5 (C-Ar), 130.0 (C-Ar), 131.4 (C-Ar), 132.3 (C-Ar), 141.5 (C-Ar), 161.3 (CO), 187.2 (CO); HRMS calcd for $C_{12}H_7{}^{35}Cl_2NO_3$ $[M+H]^+$ 283.9876, found 283.9880.

4-(2,3-Dichlorobenzoyl)-*N*-(2,2-diethoxyethyl)-1*H*-pyrrole-2-carboxamide, 436

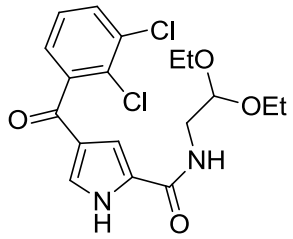

General procedure D: 4-(2,3-Dichlorobenzoyl)-1*H*-pyrrole-2-carboxylic acid (2.00 g, 7.04 mmol), CDI (2.28 g, 14.08 mmol) and aminoacetaldehyde diethyl acetal (2.56 mL, 17.60 mmol). Purification *via* column chromatography (silica; 10-70% EtOAc/petrol) gave **436** as a white solid (2.36 g, 84%). R_f 0.50 (9:1 DCM/MeOH); m.p. 160-162 ^{o}C; λ_{max} (EtOH/nm) 295.0; IR υ_{max}/cm^{-1} 3365, 3180, 3130, 2975, 2931, 2894, 1617, 1573, 1534; ^{1}H NMR (500 MHz, DMSO-d_6) δ ppm 1.12 (6H, t, *J* = 7.0 Hz, CH_3), 3.29 (2H, dd, *J* = 5.4 and 5.8 Hz, NH-CH_2), 3.46-3.52 (2H, m, CH_2), 3.60-3.67 (2H, m, CH_2), 4.58 (1H, t, *J* = 5.4 Hz, CH), 7.21 (1H, d, *J* = 1.5 Hz, H-3), 7.27 (1H, d, *J* = 1.5 Hz, H-5), 7.44 (1H, dd, *J* = 1.6 and 7.5 Hz, H-6'), 7.49 (1H, dd, *J* = 7.5 and 7.8 Hz, H-5'), 7.78 (1H, dd, *J* = 1.6 and 7.8 Hz, H-4'), 8.41 (1H, t, *J* = 5.8 Hz, NH), 12.37 (1H, s, NH-pyrrole); ^{13}C NMR (125 MHz, DMSO-d_6) δ ppm

15.3 (CH_3), 41.6 (NH-CH_2), 61.4 (CH_2), 100.2 (CH), 110.6 (C-Ar), 124.3 (C-Ar), 126.9 (C-Ar), 127.5 (C-Ar), 128.5 (C-Ar), 128.6 (C-Ar), 131.2 (C-Ar), 132.2 (C-Ar), 141.8 (C-Ar), 160.0 (CO), 187.4 (CO); HRMS calcd for $C_{18}H_{20}{}^{35}Cl_2N_2O_4$ $[M+H]^+$ 399.0873, found 399.0875.

3-(2,3-Dichlorobenzoyl)-1*H*-pyrrolo[2,3-c]pyridin-7(6*H*)-one, 437

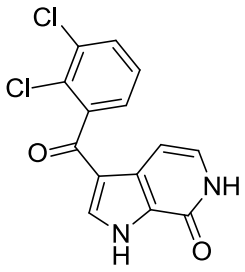

General procedure P: 4-(2,3-Dichlorobenzoyl)-*N*-(2,2-diethoxyethyl)-1*H*-pyrrole-2-carboxamide (2.30 g, 5.76 mmol). Purification *via* column chromatography (silica; 0-5% MeOH/DCM) gave **437** as a white solid (0.97 g, 55%). R_f 0.44 (9:1 DCM/MeOH); m.p. Degrades >200 ^oC; ˚C λ_{max} (EtOH/nm) 259.0, 216.5; IR υ_{max}/cm^{-1} 3087, 2956, 2915, 2869, 1774, 1633, 1527; ^1H NMR (500 MHz, DMSO-d_6) δ ppm 6.86 (1H, d, *J* = 6.9 Hz, CH-pyridone), 7.13 (1H, dd, *J* = 5.9 and 6.5 Hz, N-CH-pyridone), 7.48-7.50 (2H, m, H-6' and H-5'), 7.57 (1H, s, H-5), 7.79 (1H, dd, *J* = 3.8 and 5.8 Hz, H-4'), 11.34 (1H, s, CO-NH), 12.81 (1H, s, NH-pyrrole); ^{13}C NMR (125 MHz, DMSO-d_6) δ ppm 100.1 (C-pyridone), 117.2 (C-pyridone), 125.6 (C-Ar), 127.0 (C-Ar), 127.6 (C-Ar), 128.4 (C-Ar), 128.6 (C-Ar), 130.2 (C-Ar), 131.3 (C-Ar), 132.3 (C-Ar), 135.3 (C-Ar), 141.8 (C-Ar), 154.7 (CO), 187.5 (CO); HRMS calcd for $C_{14}H_8{}^{35}Cl_2N_2O_2$ $[M+H]^+$ 307.0036, found 307.0042.

3-(2,3-Dichlorobenzoyl)-1-((2-(trimethylsilyl)ethoxy)methyl)-*1H*-pyrrolo[2,3-c]pyridin-7(*6H*)-one, 438

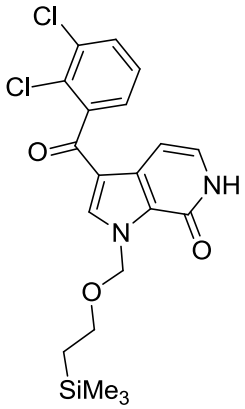

General procedure Q: 3-(2,3-Dichlorobenzoyl)-1*H*-pyrrolo[2,3-c]pyridin-7(6*H*)-one (0.61 g, 1.99 mmol), SEMCl (0.42 mL, 2.39 mmol), Et_3N (0.33 mL, 2.39 mmol), and DMAP (10 mol%). Purification *via* column chromatography (silica; 0-70% EtOAc/petrol) gave **438** as a colourless oil (0.63 g, 72%). R_f 0.39 (8:2 Petrol/EtOAc); λ_{max} (EtOH/nm) 260.5, 218.0; IR υ_{max}/cm^{-1} 2956, 1646, 1611, 1525; ^1H NMR (500 MHz, $CDCl_3$) δ ppm 0.01 (9H, s, CH_3), 0.91-0.94 (2H, m, Si-CH_2), 3.63-3.67 (2H, m, O-CH_2), 5.96 (2H, s, N-CH_2-O), 7.12 (1H, dd, *J* = 6.1 and 6.9 Hz, N-CH-pyridone), 7.29 (1H, d, *J* = 6.9 Hz, CH-pyridone), 7.33-7.34 (2H, m, H-6' and H-5'), 7.44 (1H, s, H-5), 7.61 (1H, dd, *J* = 3.4 and 6.1 Hz, H-4'), 9.87 (1H, s, CO-NH); ^{13}C NMR (125 MHz, $CDCl_3$) δ ppm 0.00 (CH_3), 19.3 (CH_2), 68.2 (O-CH_2), 76.1 (N-CH_2-O), 103.9 (C-pyridone), 104.6 (C-Ar), 119.3 (C-pyridone), 125.5 (C-Ar), 127.9 (C-Ar), 129.0 (C-Ar), 133.0 (C-Ar), 134.1 (C-Ar), 134.5 (C-Ar), 135.5 (C-Ar), 139.1 (C-Ar), 143.0 (C-Ar), 157.4 (CO), 189.6 (CO); HRMS calcd for $C_{20}H_{22}{}^{35}Cl_2N_2O_3Si$ $[M+H]^+$ 437.0850, found 437.0854.

3-(2,3-Dichlorobenzoyl)-6-(pyridin-4-yl)-1*H*-pyrrolo[2,3-c]pyridin-7(6*H*)-one, 439

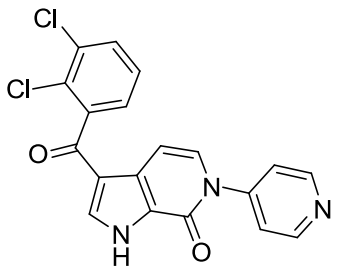

General procedure R: 3-(2,3-Dichlorobenzoyl)-1-((2-(trimethylsilyl)ethoxy)methyl)-1*H*-pyrrolo[2,3-c]pyridin-7(*6H*)-one (210 mg, 0.48 mmol), 4-bromopyridine HCl (122 mg, 0.63

mmol), K_2CO_3 (220 mg, 1.59 mmol) and CuI (10 mol%) gave 3-(2,3-dichlorobenzoyl)-6-(pyridin-4-yl)-1-((2-(trimethylsilyl)ethoxy)methyl)-1*H*-pyrrolo[2,3-c]pyridin-7(6*H*)-one which was used directly in the next step. General procedure H: 1M TBAF in THF (0.72 mL, 0.72 mmol). Purification *via* column chromatography (silica; 0-8% MeOH/DCM) gave **439** as a white solid (127 mg, 69%). R_f 0.26 (9:1 DCM/MeOH); m.p. Degrades >200 ^oC; λ_{max} (EtOH/nm) 253.0, 219.5; IR υ_{max}/cm^{-1} 3116, 3040, 2985, 1663, 1619, 1577; ^1H NMR (500 MHz, DMSO-d_6) δ ppm 7.01 (1H, d, *J* = 7.1 Hz, CH-pyridone), 7.49-7.52 (3H, m, N-CH-pyridone, H-4' and H-6'), 7.61 (2H, d, *J* = 6.1 Hz, CH-pyridine), 7.72 (1H, s, H-5), 7.81 (1H, dd, *J* = 4.8 and 4.9 Hz, H-5'), 8.76 (2H, d, *J* = 6.1 Hz, N-CH-pyridine), 13.23 (1H, s, NH-pyrrole); ^{13}C NMR (125 MHz, DMSO-d_6) δ ppm 101.6 (C-pyridone), 117.5 (C-pyridone), 121.9 (C-Ar), 124.9 (C-Ar), 127.0 (C-Ar), 127.6 (C-Ar), 128.7 (C-Ar), 129.6 (C-Ar), 131.5 (C-Ar), 131.8 (C-Ar), 132.4 (C-Ar), 136.2 (C-Ar), 141.7 (C-Ar), 147.6 (C-Ar), 150.6 (C-Ar), 153.4 (CO), 187.6 (CO); HRMS calcd for $C_{19}H_{11}{}^{35}Cl_2N_3O_2$ $[M+H]^+$ 384.0301, found 384.0304.

3-(2,3-Dichlorobenzoyl)-6-(pyridin-3-yl)-1*H*-pyrrolo[2,3-c]pyridin-7(6*H*)-one, 440

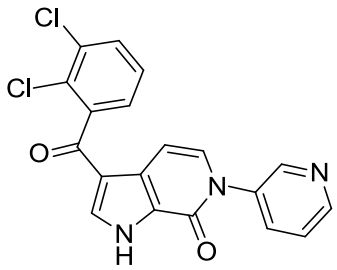

General procedure R: 3-(2,3-Dichlorobenzoyl)-1-((2-(trimethylsilyl)ethoxy)methyl)-1*H*-pyrrolo[2,3-c]pyridin-7(6*H*)-one (250 mg, 0.59 mmol), 3-bromopyridine HCl (150 mg, 0.77 mmol), K_2CO_3 (270 mg, 1.95 mmol) and CuI (10 mol%) gave 3-(2,3-Dichlorobenzoyl)-6-(pyridin-4-yl)-1-((2-(trimethylsilyl)ethoxy)methyl)-1*H*-pyrrolo[2,3-c]pyridin-7(6*H*)-one which was used directly in the next step. General procedure H: 1M TBAF in THF (0.89 mL, 0.89 mmol). Purification *via* column chromatography (silica; 0-8% MeOH/DCM) gave **440** as a white solid (90 mg, 40%). R_f 0.25 (9:1 DCM/MeOH); m.p. Degrades >200 ^oC; λ_{max} (EtOH/nm) 262.0, 219.5; IR υ_{max}/cm^{-1} 3079, 2935, 1653, 1591, 1573, 1517; ^1H NMR (500 MHz, DMSO-d_6) δ ppm 6.99 (1H, d, *J* = 6.9 Hz, CH-pyridone), 7.48-7.54 (3H, m, N-CH-pyridone, H-6' and H-4'), 7.60 (1H, dd, *J* = 4.7 and 8.0 Hz, CH-pyridine), 7.71 (1H, s, H-5), 7.81 (1H, dd, *J* = 4.7 and 4.8 Hz, H-5'), 7.98 (1H, ddd, *J* = 1.5, 2.5 and 8.0 Hz, CH-pyridine), 8.66 (1H, dd, *J* = 1.5 and 4.7 Hz, N-CH-pyridine), 8.72 (1H, d, *J* = 2.5 Hz, N-CH-pyridine),

13.21 (1H, s, NH-pyrrole); ^{13}C NMR (125 MHz, DMSO-d_6) δ ppm 101.2 (C-pyridone), 117.5 (C-pyridone), 123.9 (C-Ar), 124.9 (C-Ar), 127.0 (C-Ar), 127.6 (C-Ar), 128.7 (C-Ar), 129.7 (C-Ar), 131.5 (C-Ar), 132.4 (C-Ar), 132.6 (C-Ar), 134.9 (C-Ar), 136.0 (C-Ar), 137.2 (C-Ar), 141.7 (C-Ar), 147.9 (C-Ar), 148.8 (C-Ar), 153.9 (CO), 187.6 (CO); HRMS calcd for $C_{19}H_{11}{}^{35}Cl_2N_3O_2$ $[M+H]^+$ 384.0301, found 384.0304.

4-(2-Chloro-6-fluorobenzoyl)-*N*-(2,2-diethoxyethyl)-*1H*-pyrrole-2-carboxamide, 441

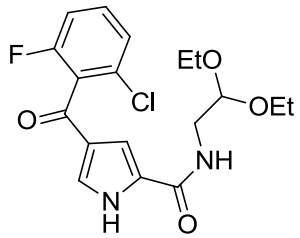

General procedure D: 4-(2-Chloro-6-fluorobenzoyl)-*1H*-pyrrole-2-carboxylic acid (0.74 g, 2.77 mmol), CDI (0.90 mg, 5.54 mmol) and aminoacetaldehyde diethyl acetal (1.01 mL, 6.93 mmol). Purification *via* column chromatography (silica; 10-70% EtOAc/petrol) gave **441** as a white solid (1.17 g, 64%). R_f 0.48 (9:1 DCM/MeOH); m.p. 142-145 ^{o}C; ˚C λ_{max} (EtOH/nm) 290.0, 236.0; IR υ_{max}/cm^{-1} 3372, 3182, 3132, 2976, 2884, 1621, 1571, 1534; ^{1}H NMR (500 MHz, DMSO-d_6) δ ppm 1.12 (6H, t, J = 7.0 Hz, CH_3), 3.29 (2H, dd, J = 5.5 and 6.1 Hz, NH-CH_2), 3.46-3.52 (2H, m, CH_2), 3.60-3.67 (2H, m, CH_2), 4.58 (1H, t, J = 5.5 Hz, CH), 7.21 (1H, br s, H-3), 7.33 (1H, br s, H-5), 7.38 (1H, dd, J = 8.3 and 8.9 Hz, H-5'), 7.45 (1H, d, J = 8.3 Hz, H-3'), 7.57 (1H, ddd, J = 6.3, 8.3 and 8.4 Hz, H-4'), 8.42 (1H, t, J = 6.1 Hz, CO-NH), 12.41 (1H, s, NH-pyrrole); ^{13}C NMR (125 MHz, DMSO-d_6) δ ppm 15.3 (CH_3), 41.6 (NH-CH_2), 61.4 (CH_2), 100.2 (CH), 110.1 (C-Ar), 114.9 (d, J_{CF} = 21.7 Hz, C-Ar), 125.0 (C-Ar), 125.8 (d, J_{CF} = 2.8 Hz, C-Ar), 128.1 (C-Ar), 128.3 (C-Ar), 128.7 (C-Ar), 130.4 (d, J_{CF} = 6.4 Hz, C-Ar), 131.7 (d, J_{CF} = 9.1 Hz, C-Ar), 158.6 (d, J_{CF} = 246.7 Hz, C-F), 159.9 (CO), 183.8 (CO); HRMS calcd for $C_{18}H_{20}{}^{35}ClFN_2O_4$ $[M+H]^+$ 383.1168, found 383.1172.

3-(2-Chloro-6-fluorobenzoyl)-1*H*-pyrrolo[2,3-c]pyridin-7(6*H*)-one, 442

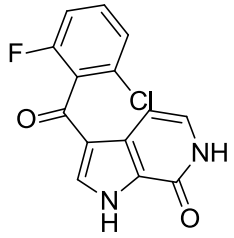

General procedure P: 4-(2-Chloro-6-fluorobenzoyl)-*N*-(2,2-diethoxyethyl)-1*H*-pyrrole-2-carboxamide (1.10 g, 2.88 mmol). Purification *via* column chromatography (silica; 0-5% MeOH/DCM) gave **442** as a white solid (0.44 g, 53%). R_f 0.43 (9:1 DCM/MeOH); m.p. Degrades >200 ^{o}C; ˚C λ_{max} (EtOH/nm) 260.0, 215.5; IR υ_{max}/cm^{-1} 3132, 3097, 2973, 1773, 1646, 1605, 1570, 1530; ^{1}H NMR (500 MHz, DMSO-d_6) δ ppm 6.80 (1H, br s, CH-pyridone), 7.14 (1H, dd, *J* = 6.5 and 6.9 Hz, N-CH-pyridone), 7.39 (1H, dd, *J* = 8.3 and 8.9 Hz, H-5'), 7.46 (1H, d, *J* = 8.3 Hz, H-3'), 7.58 (1H, ddd, *J* = 6.3, 8.3 and 8.4 Hz, H-4'), 7.66 (1H, d, *J* = 3.3 Hz, H-5), 11.37 (1H, br s, CO-NH), 13.02 (1H, s, NH-pyrrole); ^{13}C NMR (125 MHz, DMSO-d_6) δ ppm 99.8 (C-pyridone), 115.0 (d, J_{CF} = 21.8 Hz, C-Ar), 118.0 (C-pyridone), 125.6 (C-Ar), 125.8 (d, J_{CF} = 3.0 Hz, C-Ar), 128.2 (d, J_{CF} = 22.6 Hz, C-Ar), 128.6 (C-Ar), 129.8 (C-Ar), 130.5 (d, J_{CF} = 6.2 Hz, C-Ar), 131.8 (d, J_{CF} = 9.3 Hz, C-Ar), 135.0 (C-Ar), 154.6 (CO), 158.6 (d, J_{CF} = 247.8 Hz, C-F), 183.7 (CO); HRMS calcd for $C_{14}H_8{}^{35}ClFN_2O_2$ $[M+H]^+$ 291.0331, found 291.0336.

3-(2-Chloro-6-fluorobenzoyl)-1-((2-(trimethylsilyl)ethoxy)methyl)-1*H*-pyrrolo[2,3-c]pyridin-7(6*H*)-one, 443

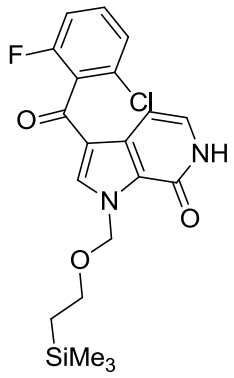

General procedure Q: 3-(2-Chloro-6-fluorobenzoyl)-1*H*-pyrrolo[2,3-c]pyridin-7(*6H*)-one (430 mg, 1.48 mmol), SEMCl (0.32 mL, 1.78 mmol), Et_3N (0.25 mL, 1.78 mmol) and DMAP (10 mol%). Purification *via* column chromatography (silica; 0-70% EtOAc/petrol) gave **443**

as a colourless oil (298 mg, 48%). R_f 0.39 (8:2 Petrol/EtOAc); λ_{max} (EtOH/nm) 259.5, 217.5; IR υ_{max}/cm^{-1} 2953, 2890, 1649, 1605, 1571, 1521; ^1H NMR (500 MHz, $CDCl_3$) δ ppm 0.02 (9H, s, CH_3), 0.86-0.90 (2H, m, Si-CH_2), 3.54-3.57 (2H, m, O-CH_2), 5.77 (2H, s, N-CH_2-O), 7.11-7.14 (1H, m, H-5'), 7.30 (1H, d, *J* = 8.2 Hz, H-3'), 7.40 (1H, ddd, *J* = 6.3, 8.3 and 8.4 Hz, H-4'), 7.54 (1H, s, H-5), 7.78 (1H, d, *J* = 5.6 Hz, CH-pyridone), 7.96 (1H, d, *J* = 5.6 Hz, N-CH-pyridone); ^{13}C NMR (125 MHz, $CDCl_3$) δ ppm 0.00 (CH_3), 19.5 (CH_2), 69.1 (O-CH_2), 79.6 (N-CH_2-O), 104.0 (C-pyridone), 113.0 (C-pyridone), 116.0 (d, J_{CF} = 21.7 Hz, C-Ar), 127.1 (d, J_{CF} = 3.3 Hz, C-Ar), 128.9 (C-Ar), 132.4 (d, J_{CF} = 9.1 Hz, C-Ar), 133.5 (d, J_{CF} = 5.8 Hz, C-Ar), 135.7 (C-Ar), 140.1 (C-Ar), 140.7 (C-Ar), 151.5 (CO), 160.8 (d, J_{CF} = 250.9 Hz, C-F), 185.3 (CO), one F split C-Ar not observed; HRMS calcd for $C_{20}H_{22}{}^{35}ClFN_2O_3Si$ $[M+H]^+$ 421.1145, found 421.1148.

3-(2-Chloro-6-fluorobenzoyl)-6-(pyridin-4-yl)-1*H*-pyrrolo[2,3-c]pyridin-7(6*H*)-one, 444

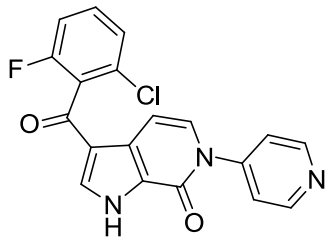

General procedure R: 3-(2-Chloro-6-fluorobenzoyl)-1-((2-(trimethylsilyl)ethoxy)methyl)-1*H*-pyrrolo[2,3-c]pyridin-7(6*H*)-one (100 mg, 0.24 mmol), 4-bromopyridine HCl (61 mg, 0.31 mmol), K_2CO_3 (109 mg, 0.79 mmol) and CuI (10 mol%) gave 3-(2-chloro-6-fluorobenzoyl)-6-(pyridin-4-yl)-1-((2-(trimethylsilyl)ethoxy)methyl)-1*H*-pyrrolo[2,3-c]pyridin-7(6*H*)-one which was used directly in the next step. General procedure H: 1M TBAF in THF (0.36 mL, 0.36 mmol). Purification *via* column chromatography (silica; 0-8% MeOH/DCM) gave **444** as a white solid (45 mg, 51%). R_f 0.26 (9:1 DCM/MeOH); m.p. Degrades >200 ^oC; λ_{max} (EtOH/nm) 254.0; IR υ_{max}/cm^{-1} 3121, 3035, 2971, 1636, 1599, 1577, 1518; ^1H NMR (500 MHz, DMSO-d_6) δ ppm 6.95 (1H, br s, CH-pyridone), 7.42 (1H, dd, *J* = 8.6 and 8.9 Hz, H-5'), 7.48-7.50 (2H, m, N-CH-pyridone and H-3'), 7.58-7.62 (3H, m, CH-pyridine and H-4'), 7.81 (1H, s, H-5), 8.76 (2H, d, *J* = 6.1 Hz, N-CH-pyridine), 13.29 (1H, s, NH-pyrrole); ^{13}C NMR (125 MHz, DMSO-d_6) δ ppm 101.3 (C-pyridone), 115.1 (d, J_{CF} = 21.5 Hz, C-Ar), 118.2 (C-pyridone), 121.9 (C-Ar), 125.0 (C-Ar), 125.9 (d, J_{CF} = 2.7 Hz, C-Ar), 129.2 (C-Ar), 130.4 (d, J_{CF} = 6.1 Hz, C-Ar), 132.0 (C-Ar), 132.1 (C-Ar), 136.0 (C-Ar),

147.6 (C-Ar), 150.7 (C-Ar), 153.3 (CO), 158.6 (J_{CF} = 246.8 Hz, C-F), 183.9 (CO), one C-Ar not visualised; HRMS calcd for $C_{19}H_{11}{}^{35}ClFN_3O_2$ $[M+H]^+$ 368.0597, found 368.0600.

3-(2-Chloro-6-fluorobenzoyl)-6-(pyridin-3-yl)-*1H*-pyrrolo[2,3-c]pyridin-7(*6H*)-one, 445

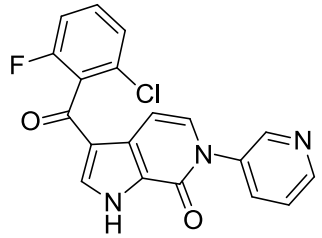

General procedure R: 3-(2-Chloro-6-fluorobenzoyl)-1-((2-(trimethylsilyl)ethoxy)methyl)-1*H*-pyrrolo[2,3-c]pyridin-7(6*H*)-one (120 mg, 0.29 mmol), 3-bromopyridine HCl (74 mg, 0.38 mmol), K_2CO_3 (138 mg, 1.00 mmol) and CuI (10 mol%) gave 3-(2-chloro-6-fluorobenzoyl)-6-(pyridin-3-yl)-1-((2-(trimethylsilyl)ethoxy)methyl)-1*H*-pyrrolo[2,3-c]pyridin-7(6*H*)-one which was used directly in the next step. General procedure H: 1M TBAF in THF (0.44 mL, 0.44 mmol). Purification *via* column chromatography (silica; 0-8% MeOH/DCM) gave **445** as a white solid (20 mg, 19%). R_f 0.26 (9:1 DCM/MeOH); m.p. Degrades >200 ^oC λ_{max} (EtOH/nm) 262.5, 217.5; IR υ_{max}/cm^{-1} 3057, 2816, 1645, 1560, 1568, 1528; ^1H NMR (500 MHz, DMSO-d_6) δ ppm 6.93 (1H, br s, CH-pyridone), 7.42 (1H, dd, *J* = 8.7 and 8.9 Hz, H-5'), 7.48-7.50 (2H, m, N-CH-pyridone and H-3'), 7.58-7.63 (2H, m, H-4' and CH-pyridine), 7.80 (1H, s, H-5), 7.99 (1H, ddd, *J* = 1.5, 2.4 and 8.2 Hz, CH-pyridine), 8.66 (1H, dd, *J* = 1.5 and 4.7 Hz, N-CH-pyridine), 8.72 (1H, d, *J* = 2.4 Hz, N-CH-pyridine), 13.27 (1H, s, NH-pyrrole); ^{13}C NMR (125 MHz, DMSO-d_6) δ ppm 100.8 (C-pyridone), 115.1 (d, J_{CF} = 21.4 Hz, C-Ar), 118.2 (C-pyridone), 123.9 (C-Ar), 125.1 (C-Ar), 125.9 (d, J_{CF} = 3.0 Hz, C-Ar), 129.4 (C-Ar), 130.4 (d, J_{CF} = 7.8 Hz, C-Ar), 132.0 (d, J_{CF} = 9.5 Hz, C-Ar), 132.9 (C-Ar), 135.0 (C-Ar), 135.9 (C-Ar), 137.2 (C-Ar), 147.9 (C-Ar), 148.8 (C-Ar), 153.8 (CO), 158.7 (d, J_{CF} = 247.8 Hz, C-F), 183.8 (CO), one C-Ar not visualised; HRMS calcd for $C_{19}H_{11}{}^{35}ClFN_3O_2$ $[M+H]^+$ 368.0597, found 368.0600.

4-(2-Bromo-6-fluorobenzoyl)-*N*-(2,2-diethoxyethyl)-1*H*-pyrrole-2-carboxamide, 446

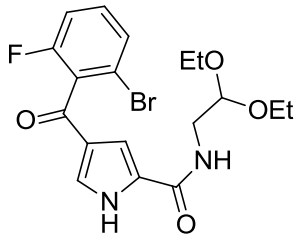

General procedure D: 4-(2-bromo-6-fluorobenzoyl)-1*H*-pyrrole-2-carboxylic acid (1.90 g, 6.09 mmol), CDI (1.97 g, 12.18 mmol) and aminoacetaldehyde diethyl acetal (2.21 mL, 15.33 mmol). Purification *via* column chromatography (silica; 10-70% EtOAc/petrol) gave **446** as a white solid (1.42 g, 57%). R_f 0.49 (9:1 DCM/MeOH); m.p. 152-154 ^{o}C; ˚C λ_{max} (EtOH/nm) 285.0, 234.0; IR υ_{max}/cm^{-1} 3368, 3174, 3130, 2979, 2899, 1620; ^{1}H NMR (500 MHz, DMSO-d_6) δ ppm 1.12 (6H, t, *J* = 7.0 Hz, CH_3), 3.28 (2H, dd, *J* = 5.5 and 5.8 Hz, NH-*CH*$_2$), 3.46-3.52 (2H, m, CH_2), 3.60-3.66 (2H, m, CH_2), 4.58 (1H, t, *J* = 5.5 Hz, CH), 7.20 (1H, br s, H-3), 7.30 (1H, br s, H-5), 7.41 (1H, dd, *J* = 8.3 and 8.9 Hz, H-5'), 7.49 (1H, ddd, *J* = 6.3, 8.3 and 8.4 Hz, H-4'), 7.59 (1H, d, *J* = 8.3 Hz, H-3'), 8.42 (1H, t, *J* = 5.8 Hz, CO-NH), 12.40 (1H, s, NH-pyrrole); ^{13}C NMR (125 MHz, DMSO-d_6) δ ppm 15.3 (CH_3), 41.6 (NH-CH_2), 61.4 (CH_2), 100.2 (CH), 110.2 (C-Ar), 115.3 (d, J_{CF} = 21.7 Hz, C-Ar), 119.0 (d, J_{CF} = 5.2 Hz, C-Ar), 124.7 (C-Ar), 125.8 (C-Ar), 128.3 (C-Ar), 128.8 (C-Ar), 130.1 (d, J_{CF} = 22.7 Hz, C-Ar), 132.0 (d, J_{CF} = 8.5 Hz, C-Ar), 158.5 (d, J_{CF} = 249.1 Hz, C-F), 159.9 (CO), 184.8 (CO); HRMS calcd for $C_{18}H_{20}{}^{79}BrFN_2O_4$ $[M+H]^+$ 427.0663, found 427.0666.

3-(2-Bromo-6-fluorobenzoyl)-1*H*-pyrrolo[2,3-c]pyridin-7(6*H*)-one, 447

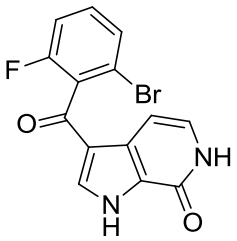

General procedure P: 4-(2-bromo-6-fluorobenzoyl)-*N*-(2,2-diethoxyethyl)-1*H*-pyrrole-2-carboxamide (1.40 g, 3.28 mmol). Purification *via* column chromatography (silica; 0-5% MeOH/DCM) gave **447** as a white solid (0.65 g, 59%). R_f 0.44 (9:1 DCM/MeOH); m.p. 301-302 ^{o}C; ˚C λ_{max} (EtOH/nm) 261.0, 215.5; IR υ_{max}/cm^{-1} 3117, 3094, 2916, 1729, 1650, 1602, 1568, 1530; ^{1}H NMR (500 MHz, DMSO-d_6) δ ppm 6.78 (1H, br s, CH-pyridone), 7.13 (1H, dd, *J* = 6.4 and 6.9 Hz, N-CH-pyridone), 7.42 (1H, dd, *J* = 8.5 and 9.1 Hz, H-5'), 7.51 (1H,

ddd, J = 6.3, 8.3 and 8.4 Hz, H-4'), 7.60 (1H, d, J = 8.3 Hz, H-3'), 7.63 (1H, s, H-5), 11.36 (1H, br s, CO-NH), 13.01 (1H,s, NH-pyrrole); ^{13}C NMR (125 MHz, DMSO-d_6) δ ppm 99.8 (C-pyridone), 115.4 (d, J_{CF} = 21.8 Hz, C-Ar), 117.7 (C-pyridone), 119.2 (d, J_{CF} = 5.1 Hz, C-Ar), 125.7 (C-Ar), 128.5 (C-Ar), 128.8 (d, J_{CF} = 2.8 Hz, C-Ar), 129.9 (C-Ar), 130.1 (d, J_{CF} = 22.6 Hz, C-Ar), 132.1 (d, J_{CF} = 8.7 Hz, C-Ar), 134.9 (C-Ar), 154.6 (CO), 158.6 (d, J_{CF} = 247.8 Hz, C-F), 184.7 (CO); HRMS calcd for $C_{14}H_8{}^{79}BrFN_2O_2$ $[M-H]^-$ 334.9826, found 334.9833.

3-(2-Bromo-6-fluorobenzoyl)-1-((2-(trimethylsilyl)ethoxy)methyl)-1*H*-pyrrolo[2,3-c]pyridin-7(6*H*)-one, 448

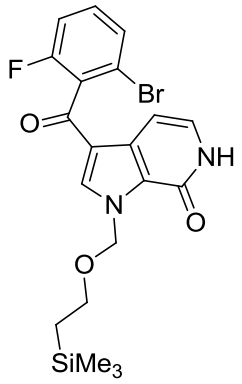

General procedure Q: 3-(2-bromo-6-fluorobenzoyl)-1*H*-pyrrolo[2,3-c]pyridin-7(6*H*)-one (450 mg, 1.34 mmol), SEMCl (0.28 mL, 1.61 mmol), Et_3N (0.22 mL, 1.61 mmol) and DMAP (10 mol%). Purification *via* column chromatography (silica; 0-70% EtOAc/petrol) gave **448** as a colourless oil (400 mg, 64%). R_f 0.40 (8:2 Petrol/EtOAc); λ_{max} (EtOH/nm) 260.5, 218.0; IR υ_{max}/cm^{-1} 2952, 2894, 1646, 1602, 1570, 1521; ^{1}H NMR (500 MHz, $CDCl_3$) δ ppm 0.01 (9H, s, CH_3), 0.89-0.82 (2H, m, Si-CH_2), 3.62-3.65 (2H, m, O-CH_2), 5.96 (2H, s, N-CH_2-O), 7.10 (1H, dd, J = 5.5 and 5.9 Hz, N-CH-pyridone), 7.14-7.18 (1H, m, H-5'), 7.21 (1H, d, J = 5.5 Hz, CH-pyridone), 7.32-7.36 (1H, m, H-4'), 7.46-7.48 (2H, m, H-5 and H-3'), 9.47 (1H, s, CO-NH); ^{13}C NMR (125 MHz, $CDCl_3$) δ ppm 0.01 (C-*CH*$_3$), 19.3 (CH_2), 68.3 (O-CH_2), 76.0 (N-CH_2-O), 104.6 (C-pyridone), 116.6 (d, J_{CF} = 21.6 Hz, C-Ar), 119.7 (C-pyridone), 121.5 (d, J_{CF} = 4.8 Hz, C-Ar), 125.6 (d, J_{CF} = 2.8 Hz, C-Ar), 129.3 (C-Ar), 130.3 (C-Ar), 131.7 (d, J_{CF} = 22.0 Hz, C-Ar), 133.0 (d, J_{CF} = 8.7 Hz, C-Ar), 134.3 (C-Ar), 138.9 (C-Ar), 157.4 (CO), 160.8 (d, J_{CF} = 252.1 Hz, C-F), 186.6 (CO); HRMS calcd for $C_{20}H_{22}{}^{79}BrFN_2O_3Si$ $[M+H]^+$ 465.0640, found 465.0635.

3-(2-Bromo-6-fluorobenzoyl)-6-(pyridin-4-yl)-*1H*-pyrrolo[2,3-c]pyridin-7(*6H*)-one, 449

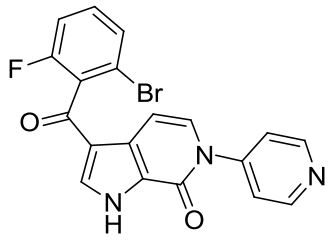

General procedure R: 3-(2-bromo-6-fluorobenzoyl)-1-((2-(trimethylsilyl)ethoxy)methyl)-1*H*-pyrrolo[2,3-c]pyridin-7(6*H*)-one (190 mg, 0.41 mmol), 4-bromopyridine HCl (86 mg, 0.44 mmol), K_2CO_3 (155 mg, 1.12 mmol), and CuI (10 mol%) gave 3-(2-bromo-6-fluorobenzoyl)-6-(pyridin-4-yl)-1-((2-(trimethylsilyl)ethoxy)methyl)-1*H*-pyrrolo[2,3-c]pyridin-7(6*H*)-one which was used directly in the next step. **General procedure H:** 1M TBAF in THF (0.62 mL, 0.62 mmol). Semi-preparative chromatography gave **449** as a white solid (16 mg, 9%). R_f 0.24 (9:1 DCM/MeOH); m.p. Degrades >200 ^oC; λ_{max} (EtOH/nm) 260.0; IR υ_{max}/cm^{-1} 3115, 3088, 2935, 1637, 1600, 1579, 1516; ^1H NMR (500 MHz, DMSO-d_6) δ ppm 6.92 (1H, br s, CH-pyridone), 7.44 (1H, dd, *J* = 8.7 and 9.1 Hz, H-5'), 7.48 (1H, d, *J* = 7.5 Hz, N-CH-pyridone), 7.52 (1H, ddd, *J* = 6.3, 8.3 and 8.4 Hz, H-4'), 7.61-7.63 (3H, m, CH-pyridine and H-3'), 7.78 (1H, s, H-5), 8.75 (2H, s, *J* = 6.1 Hz, N-CH-pyridine), 13.25 (1H, s, NH-pyrrole); HRMS calcd for $C_{19}H_{11}{}^{79}BrFN_3O_2$ $[M+H]^+$ 412.0091, found 412.0091.

Chapter 8: References

1. Hanahan, D.; Weinberg, R. A. The Hallmarks of Cancer. *Cell.* **2000,** 100, 57-70.
2. http://info.cancerresearchuk.org/cancerstats/incidence/all-cancers-combined/. (25/07/2012).
3. Jemal, A.; Siegel, R.; Ward, E.; Hao, Y.; Xu, J.; Murray, T.; Thun, M. J. Cancer Statistics, 2008. *CA. Cancer J. Clin.* **2008,** 58, 71-96.
4. http://info.cancerresearchuk.org/cancerstats/incidence/commoncancers/. http://info.cancerresearchuk.org/cancerstats/incidence/commoncancers/ (25/07/2012).
5. DeVita, V. T., Jr.; Chu, E. A history of cancer chemotherapy. *Cancer Res.* **2008,** 68, 8643-53.
6. Farber, S.; Diamond, L. K.; Mercer, R. D.; Sylvester, R. F.; Wolff, J. A. Temporary Remissions in Acute Leukemia in Children Produced by Folic Acid Antagonist, 4-Aminopteroyl-Glutamic Acid (Aminopterin). *N. Engl. J. Med.* **1948,** 238, 787-793.
7. Capdeville, R.; Buchdunger, E.; Zimmermann, J.; Matter, A. Glivec (STI571, imatinib), a rationally developed, targeted anticancer drug. *Nat. Rev. Drug Discov.* **2002,** 1, 493-502.
8. Drews, J. Drug Discovery: A Historical Perspective. *Science.* **2000,** 287, 1960-1964.
9. Jordan, V. C. Tamoxifen: a most unlikely pioneering medicine. *Nat. Rev. Drug Discov.* **2003,** 2, 205-213.
10. Lipinski, C. A.; Lombardo, F.; Dominy, B. W.; Feeney, P. J. Experimental and computational approaches to estimate solubility and permeability in drug discovery and development settings. *Adv. Drug Delivery Rev.* **1997,** 23, 3-25.
11. Ertl, P.; Rohde, B.; Selzer, P. Fast Calculation of Molecular Polar Surface Area as a Sum of Fragment-Based Contributions and Its Application to the Prediction of Drug Transport Properties. *J. Med. Chem.* **2000,** 43, 3714-3717.
12. Kramer, J. A.; Sagartz, J. E.; Morris, D. L. The application of discovery toxicology and pathology towards the design of safer pharmaceutical lead candidates. *Nat. Rev. Drug Discov.* **2007,** 6, 636-649.
13. Manning, G.; Whyte, D. B.; Martinez, R.; Hunter, T.; Sudarsanam, S. The Protein Kinase Complement of the Human Genome. *Science.* **2002,** 298, 1912-1934.
14. Manley, P. W.; Cowan-Jacob, S. W.; Buchdunger, E.; Fabbro, D.; Fendrich, G.; Furet, P.; Meyer, T.; Zimmermann, J. Imatinib: a selective tyrosine kinase inhibitor. *Eur. J. Cancer.* **2002,** 38, S19-S27.

15. Rask-Andersen, M.; Almén, M. S.; Schiöth, H. B. Trends in the exploitation of novel drug targets. *Nat. Rev. Drug Discov.* **2011,** 10, 579-590.
16. http://www.fda.gov/Drugs/default.htm. (26/07/2012).
17. Shepherd, F. A.; Rodrigues Pereira, J.; Ciuleanu, T.; Tan, E. H.; Hirsh, V.; Thongprasert, S.; Campos, D.; Maoleekoonpiroj, S.; Smylie, M.; Martins, R.; van Kooten, M.; Dediu, M.; Findlay, B.; Tu, D.; Johnston, D.; Bezjak, A.; Clark, G.; Santabárbara, P.; Seymour, L. Erlotinib in Previously Treated Non–Small-Cell Lung Cancer. *N. Engl. J. Med.* **2005,** 353, 123-132.
18. http://www.ukmi.nhs.uk. (28/08/2012).
19. Wells, S. A., Jr.; Gosnell, J. E.; Gagel, R. F.; Moley, J.; Pfister, D.; Sosa, J. A.; Skinner, M.; Krebs, A.; Vasselli, J.; Schlumberger, M. Vandetanib for the treatment of patients with locally advanced or metastatic hereditary medullary thyroid cancer. *J. Clin. Oncol.* **2010,** 28, 767-72.
20. Engelman, J. A.; Zejnullahu, K.; Mitsudomi, T.; Song, Y.; Hyland, C.; Park, J. O.; Lindeman, N.; Gale, C.-M.; Zhao, X.; Christensen, J.; Kosaka, T.; Holmes, A. J.; Rogers, A. M.; Cappuzzo, F.; Mok, T.; Lee, C.; Johnson, B. E.; Cantley, L. C.; Janne, P. A. MET Amplification Leads to Gefitinib Resistance in Lung Cancer by Activating ERBB3 Signaling. *Science.* **2007,** 316, 1039-1043.
21. Balak, M. N.; Gong, Y.; Riely, G. J.; Somwar, R.; Li, A. R.; Zakowski, M. F.; Chiang, A.; Yang, G.; Ouerfelli, O.; Kris, M. G.; Ladanyi, M.; Miller, V. A.; Pao, W. Novel D761Y and Common Secondary T790M Mutations in Epidermal Growth Factor Receptor–Mutant Lung Adenocarcinomas with Acquired Resistance to Kinase Inhibitors. *Clin. Cancer Res.* **2006,** 12, 6494-6501.
22. Gazdar, A. F. Activating and resistance mutations of EGFR in non-small-cell lung cancer: role in clinical response to EGFR tyrosine kinase inhibitors. *Oncogene.* **2009,** 28, S24-S31.
23. Chapman, P. B.; Hauschild, A.; Robert, C.; Haanen, J. B.; Ascierto, P.; Larkin, J.; Dummer, R.; Garbe, C.; Testori, A.; Maio, M.; Hogg, D.; Lorigan, P.; Lebbe, C.; Jouary, T.; Schadendorf, D.; Ribas, A.; O'Day, S. J.; Sosman, J. A.; Kirkwood, J. M.; Eggermont, A. M. M.; Dreno, B.; Nolop, K.; Li, J.; Nelson, B.; Hou, J.; Lee, R. J.; Flaherty, K. T.; McArthur, G. A. Improved Survival with Vemurafenib in Melanoma with BRAF V600E Mutation. *N. Engl. J. Med.* **2011,** 364, 2507-2516.
24. Dhillon, A. S.; Hagan, S.; Rath, O.; Kolch, W. MAP kinase signalling pathways in cancer. *Oncogene.* 26, 3279-3290.

25. Turjanski, A. G.; Vaque, J. P.; Gutkind, J. S. MAP kinases and the control of nuclear events. *Oncogene.* 26, 3240-3253.
26. Cargnello, M.; Roux, P. P. Activation and function of the MAPKs and their substrates, the MAPK-activated protein kinases. *Microbiol. Mol. Biol. Rev.* **2011,** 75, 50-83.
27. Lee, J. T., Jr.; McCubrey, J. A. The Raf/MEK/ERK signal transduction cascade as a target for chemotherapeutic intervention in leukemia. *Leukemia.* **2002,** 16, 486-507.
28. Drew, B. A.; Burow, M. E.; Beckman, B. S. MEK5/ERK5 pathway: The first fifteen years. *Biochim. Biophys. Acta, Rev. Cancer.* **2012,** 1825, 37-48.
29. Robinson, M. J.; Cobb, M. H. Mitogen-activated protein kinase pathways. *Curr. Opin. Cell Biol.* **1997,** 9, 180-186.
30. Wu, X.; Noh, S. J.; Zhou, G.; Dixon, J. E.; Guan, K. L. Selective activation of MEK1 but not MEK2 by A-Raf from epidermal growth factor-stimulated Hela cells. *J. Biol. Chem.* **1996,** 271, 3265-71.
31. Friday, B. B.; Adjei, A. A. Advances in targeting the Ras/Raf/MEK/Erk mitogen-activated protein kinase cascade with MEK inhibitors for cancer therapy. *Clin. Cancer Res.* **2008,** 14, 342-6.
32. Thompson, N.; Lyons, J. Recent progress in targeting the Raf/MEK/ERK pathway with inhibitors in cancer drug discovery. *Curr. Opin. Pharmacol.* **2005,** 5, 350-356.
33. Kloog, Y.; Cox, A. D. RAS inhibitors: potential for cancer therapeutics. *Mol. Med. Today.* **2000,** 6, 398-402.
34. Barrett, S. D.; Bridges, A. J.; Dudley, D. T.; Saltiel, A. R.; Fergus, J. H.; Flamme, C. M.; Delaney, A. M.; Kaufman, M.; LePage, S.; Leopold, W. R.; Przybranowski, S. A.; Sebolt-Leopold, J.; Van Becelaere, K.; Doherty, A. M.; Kennedy, R. M.; Marston, D.; Howard Jr, W. A.; Smith, Y.; Warmus, J. S.; Tecle, H. The discovery of the benzhydroxamate MEK inhibitors CI-1040 and PD 0325901. *Bioorg. Med. Chem. Lett.* **2008,** 18, 6501-6504.
35. Sebolt-Leopold, J. S.; Merriman, R.; Omer, C.; Tecle, H.; Bridges, A.; Klohs, W.; Loi, C.-M.; Valik, H.; Przybranowski, S.; Meyer, M.; Leopold, W. R. The biological profile of PD 0325901: A second generation analog of CI-1040 with improved pharmaceutical potential. *AACR Meeting Abstracts* **2004,** 2004, 925.
36. Davies, B. R.; Logie, A.; McKay, J. S.; Martin, P.; Steele, S.; Jenkins, R.; Cockerill, M.; Cartlidge, S.; Smith, P. D. AZD6244 (ARRY-142886), a potent inhibitor of mitogen-activated protein kinase/extracellular signal-regulated kinase kinase 1/2 kinases:

mechanism of action in vivo, pharmacokinetic/pharmacodynamic relationship, and potential for combination in preclinical models. *Mol. Cancer Ther.* **2007,** 6, 2209-2219.

37. Yeh, T. C.; Marsh, V.; Bernat, B. A.; Ballard, J.; Colwell, H.; Evans, R. J.; Parry, J.; Smith, D.; Brandhuber, B. J.; Gross, S.; Marlow, A.; Hurley, B.; Lyssikatos, J.; Lee, P. A.; Winkler, J. D.; Koch, K.; Wallace, E. Biological Characterization of ARRY-142886 (AZD6244), a Potent, Highly Selective Mitogen-Activated Protein Kinase Kinase 1/2 Inhibitor. *Clin. Cancer Res.* **2007,** 13, 1576-1583.
38. Leijen, S. M., M.R; Tresca, P; Kraeber-Bodere, F; Dieras, V; Scheulen, M; Gupta, A; Lopez-Valverde, V; Xu, Z-X; Rueger, R; Tessier, J; Shochat, E; Blotner, S; Naegelen, V.M; Schellens, J.H.M; Eberhardt W.E.E. Phase I Dose-escalation Study of the Safety, Pharmacokinetics and Pharmacodynamics of the MEK Inhibitor RO4987655 (CH4987655) in Patients with Advanced Solid Tumours. *Clin. Cancer Res.* **2012**.
39. Ohori, M.; Kinoshita, T.; Okubo, M.; Sato, K.; Yamazaki, A.; Arakawa, H.; Nishimura, S.; Inamura, N.; Nakajima, H.; Neya, M.; Miyake, H.; Fujii, T. Identification of a selective ERK inhibitor and structural determination of the inhibitor–ERK2 complex. *Biochem. Biophys. Res. Commun.* **2005,** 336, 357-363.
40. Kim, M. H.; Chung, J. Y.; Ryu, J. S.; Hah, J. M. Structure tuning of pyrazolylpyrrole derivatives as ERK inhibitors utilizing dual tools; 3D-QSAR and side-chain hopping. *Bioorg. Med. Chem. Lett.* **2011,** 21, 4900-4.
41. Johnson, G. L.; Lapadat, R. Mitogen-Activated Protein Kinase Pathways Mediated by ERK, JNK, and p38 Protein Kinases. *Science.* **2002,** 298, 1911-1912.
42. Herlaar, E.; Brown, Z. p38 MAPK signalling cascades in inflammatory disease. *Mol. Med. Today.* **1999,** 5, 439-47.
43. Bradham, C.; McClay, D. R. p38 MAPK in development and cancer. *Cell Cycle.* **2006,** 5, 824-8.
44. Losa, J. H.; Cobo, C. P.; Viniegra, J. G.; Lobo, V. J. S.-A.; Cajal, S. R. y.; Sanchez-Prieto, R. Role of the p38 MAPK pathway in cisplatin-based therapy. *Oncogene.* **2003,** 22, 3998-4006.
45. Davis, R. J. Signal Transduction by the JNK Group of MAP Kinases. *Cell.* **2000,** 103, 239-252.
46. Hope, H. R.; Anderson, G. D.; Burnette, B. L.; Compton, R. P.; Devraj, R. V.; Hirsch, J. L.; Keith, R. H.; Li, X.; Mbalaviele, G.; Messing, D. M.; Saabye, M. J.; Schindler, J. F.; Selness, S. R.; Stillwell, L. I.; Webb, E. G.; Zhang, J.; Monahan, J. B. Anti-inflammatory

properties of a novel N-phenyl pyridinone inhibitor of p38 mitogen-activated protein kinase: preclinical-to-clinical translation. *J. Pharmacol. Exp. Ther.* **2009,** 331, 882-95.

47. M. Bello, A.; K. Purohit, M.; Jun Yang Cui, T.; Brandon Stead, S.; P. Kotra, L. Immunological Targets in Inflammation from the Small Molecule Perspective. *Curr. Med. Chem.: Anti-Inflammatory Anti-Allergy Agents.* **2011,** 10, 121-131.
48. Yong, H. Y.; Koh, M. S.; Moon, A. The p38 MAPK inhibitors for the treatment of inflammatory diseases and cancer. *Expert. Opin. Investig. Drugs.* **2009,** 18, 1893-905.
49. Navas, T.; Hideshima, T.; Nguyen, A.; Henson, M.; Stebbins, L.; Kapoun, A. M.; O'Young, G.; Chakravarty, S.; Mavunkel, B.; Perumattam, J.; Luedtke, G.; Dugar, S.; Schreiner, G.; Anderson, K.; Higgins, L. S. The p38α MAPK inhibitor SCIO-469 enhances the apoptotic and anti-proliferative effects of proteasome inhibitors MG132 and PS341 (Velcade) in multiple myeloma cells. *AACR Meeting Abstracts*. **2004,** 2004, 775-776.
50. Manning, A. M.; Davis, R. J. Targeting JNK for therapeutic benefit: from junk to gold? *Nat. Rev. Drug Discov.* **2003,** 2, 554-565.
51. Pearson, G.; English, J. M.; White, M. A.; Cobb, M. H. ERK5 and ERK2 Cooperate to Regulate NF-kappa B and Cell Transformation. *J. Biol. Chem.* **2001,** 276, 7927-7931.
52. Wang, X.; Tournier, C. Regulation of cellular functions by the ERK5 signalling pathway. *Cell. Signalling.* **2006,** 18, 753-760.
53. Hayashi, M.; Lee, J.-D. Role of the BMK1/ERK5 signaling pathway: lessons from knockout mice. *J. Mol. Med.* **2004,** 82, 800-808.
54. English, J. M.; Pearson, G.; Hockenberry, T.; Shivakumar, L.; White, M. A.; Cobb, M. H. Contribution of the ERK5/MEK5 Pathway to Ras/Raf Signaling and Growth Control. *J. Biol. Chem.* **1999,** 274, 31588-31592.
55. Zhou, G.; Bao, Z. Q.; Dixon, J. E. Components of a New Human Protein Kinase Signal Transduction Pathway. *J. Biol. Chem.* **1995,** 270, 12665-12669.
56. Sun, W.; Wei, X.; Kesavan, K.; Garrington, T. P.; Fan, R.; Mei, J.; Anderson, S. M.; Gelfand, E. W.; Johnson, G. L. MEK Kinase 2 and the Adaptor Protein Lad Regulate Extracellular Signal-Regulated Kinase 5 Activation by Epidermal Growth Factor via Src. *Mol. Cell. Biol.* **2003,** 23, 2298-2308.
57. Dhanasekaran, D. N.; Kashef, K.; Lee, C. M.; Xu, H.; Reddy, E. P. Scaffold proteins of MAP-kinase modules. *Oncogene.* **2007,** 26, 3185-202.
58. Roberts, O. L.; Holmes, K.; Muller, J.; Cross, D. A.; Cross, M. J. ERK5 and the regulation of endothelial cell function. *Biochem. Soc. Trans.* **2009,** 37, 1254-9.

59. Nishimoto, S. MAPK Signalling: ERK5 versus ERK1/2. *EMBO reports.* **2006,** 7, 782-786.
60. Wada, T.; Penninger, J. M. Mitogen-activated protein kinases in apoptosis regulation. *Oncogene.* 23, 2838-2849.
61. Ranganathan, A.; Pearson, G. W.; Chrestensen, C. A.; Sturgill, T. W.; Cobb, M. H. The MAP kinase ERK5 binds to and phosphorylates p90 RSK. *Arch. Biochem. Biophys.* **2006,** 449, 8-16.
62. Carriere, A. R., H; Blenis, J; Roux, P. P. The RSK factors of activating the Ras/MAPK signaling cascade. *Front. Biosci.* **2008,** 13, 4258-4275.
63. Yang, Q.; Deng, X.; Lu, B.; Cameron, M.; Fearns, C.; Patricelli, M. P.; Yates Iii, J. R.; Gray, N. S.; Lee, J.-D. Pharmacological Inhibition of BMK1 Suppresses Tumor Growth through Promyelocytic Leukemia Protein. *Cancer Cell.* **2010,** 18, 258-267.
64. Kato, Y.; Tapping, R. I.; Huang, S.; Watson, M. H.; Ulevitch, R. J.; Lee, J.-D. Bmk1/Erk5 is required for cell proliferation induced by epidermal growth factor. *Nature.* **1998,** 395, 713-716.
65. Cude, K.; Wang, Y.; Choi, H.-J.; Hsuan, S.-L.; Zhang, H.; Wang, C.-Y.; Xia, Z. Regulation of the G2–M cell cycle progression by the ERK5–NFκB signaling pathway. *J. Cell Biol.* **2007,** 177, 253-264.
66. Girio, A.; Montero, J. C.; Pandiella, A.; Chatterjee, S. Erk5 is activated and acts as a survival factor in mitosis. *Cell Signal.* **2007,** 19, 1964-72.
67. Gilley, R.; Lochhead, P. A.; Balmanno, K.; Oxley, D.; Clark, J.; Cook, S. J. CDK1, not ERK1/2 or ERK5, is required for mitotic phosphorylation of BIMEL. *Cell Signal.* **2012,** 24, 170-80.
68. Sohn, S. J.; Sarvis, B. K.; Cado, D.; Winoto, A. ERK5 MAPK regulates embryonic angiogenesis and acts as a hypoxia-sensitive repressor of vascular endothelial growth factor expression. *J. Biol. Chem.* **2002,** 277, 43344-51.
69. Hayashi, M.; Fearns, C.; Eliceiri, B.; Yang, Y.; Lee, J.-D. Big Mitogen-Activated Protein Kinase 1/Extracellular Signal-Regulated Kinase 5 Signaling Pathway Is Essential for Tumor-Associated Angiogenesis. *Cancer Res.* **2005,** 65, 7699-7706.
70. Doebele, R. C.; Schulze-Hoepfner, F. T.; Hong, J.; Chlenski, A.; Zeitlin, B. D.; Goel, K.; Gomes, S.; Liu, Y.; Abe, M. K.; Nor, J. E.; Lingen, M. W.; Rosner, M. R. A novel interplay between Epac/Rap1 and mitogen-activated protein kinase kinase 5/extracellular signal-regulated kinase 5 (MEK5/ERK5) regulates thrombospondin to control angiogenesis. *Blood.* **2009,** 114, 4592-4600.

71. Reddy, K. B.; Nabha, S. M.; Atanaskova, N. Role of MAP kinase in tumor progression and invasion. *Cancer Metastasis Rev.* **2003,** 22, 395-403.
72. Westermarck, J.; Kahari, V. M. Regulation of matrix metalloproteinase expression in tumor invasion. *Faseb J.* **1999,** 13, 781-92.
73. Mehta, P. B.; Jenkins, B. L.; McCarthy, L.; Thilak, L.; Robson, C. N.; Neal, D. E.; Leung, H. Y. MEK5 overexpression is associated with metastatic prostate cancer, and stimulates proliferation, MMP-9 expression and invasion. *Oncogene.* 22, 1381-1389.
74. Sawhney, R. S.; Liu, W.; Brattain, M. G. A novel role of ERK5 in integrin-mediated cell adhesion and motility in cancer cells via Fak signaling. *J Cell Physiol* **2009,** 219, 152-61.
75. Bawn, R. Development of Small-Molecule Inhibitors of ERK5 for the Treatment of Cancer. Newcastle University, 2011.
76. www.moleculardevices.com/pages/reagents/imap_intro.html. (28/08/2012).
77.. http://info.cancerresearchuk.org/cancerstats/. (02/07/2012).
78. Consortium, T. B. C. L. Cancer Risks in BRCA2 Mutation Carriers. *J. Natl. Cancer Inst.* **1999,** 91, 1310-1316.
79. Stamey, T. A.; McNeal, J. E.; Yemoto, C. M.; Sigal, B. M.; Johnstone, I. M. Biological Determinants of Cancer Progression in Men With Prostate Cancer. *JAMA.* **1999,** 281, 1395-1400.
80. http://www.stjohnprovidence.org/InnerPage.aspx?PageID=1446. (02/07/2012).
81. Heidenreich, A.; Aus, G.; Bolla, M.; Joniau, S.; Matveev, V. B.; Schmid, H. P.; Zattoni, F. EAU Guidelines on Prostate Cancer. *Eur. Urol.* **2008,** 53, 68-80.
82. Heinlein, C. A.; Chang, C. Androgen receptor in prostate cancer. *Endocr. Rev.* **2004,** 25, 276-308.
83. Sharifi N, G. J. L. D. W. L. ANdrogen deprivation therapy for prostate cancer. *JAMA.* **2005,** 294, 238-244.
84. Emami, K. H.; Corey, E. When prostate cancer meets bone: Control by wnts. *Cancer Lett.* **2007,** 253, 170-179.
85. Wirth, M. P.; Hakenberg, O. W.; Froehner, M. Antiandrogens in the Treatment of Prostate Cancer. *Eur. Urol.* **2007,** 51, 306-314.
86. Tannock, I. F.; de Wit, R.; Berry, W. R.; Horti, J.; Pluzanska, A.; Chi, K. N.; Oudard, S.; Theodore, C.; James, N. D.; Turesson, I.; Rosenthal, M. A.; Eisenberger, M. A.; the, T. A. X. I. Docetaxel plus Prednisone or Mitoxantrone plus Prednisone for Advanced Prostate Cancer. *N. Engl. J. Med.* **2004,** 351, 1502-1512.

87. O'Donnell, A.; Judson, I.; Dowsett, M.; Raynaud, F.; Dearnaley, D.; Mason, M.; Harland, S.; Robbins, A.; Halbert, G.; Nutley, B.; Jarman, M. Hormonal impact of the 17[alpha]-hydroxylase//C17,20-lyase inhibitor abiraterone acetate (CB7630) in patients with prostate cancer. *Br. J. Cancer.* **2004,** 90, 2317-2325.
88. McPhaul, M. J. Mechanisms of prostate cancer progression to androgen independence. *Best Pract. Res. Clin. Endocrinol. Metab.* **2008,** 22, 373-388.
89. Vasaitis, T. S.; Bruno, R. D.; Njar, V. C. O. CYP17 inhibitors for prostate cancer therapy. *J. Steroid Biochem. Mol. Biol.* **2011,** 125, 23-31.
90. Kaku, T.; Hitaka, T.; Ojida, A.; Matsunaga, N.; Adachi, M.; Tanaka, T.; Hara, T.; Yamaoka, M.; Kusaka, M.; Okuda, T.; Asahi, S.; Furuya, S.; Tasaka, A. Discovery of orteronel (TAK-700), a naphthylmethylimidazole derivative, as a highly selective 17,20-lyase inhibitor with potential utility in the treatment of prostate cancer. *Bioorg. Med. Chem.* **2011,** 19, 6383-6399.
91. Tran, C.; Ouk, S.; Clegg, N. J.; Chen, Y.; Watson, P. A.; Arora, V.; Wongvipat, J.; Smith-Jones, P. M.; Yoo, D.; Kwon, A.; Wasielewska, T.; Welsbie, D.; Chen, C. D.; Higano, C. S.; Beer, T. M.; Hung, D. T.; Scher, H. I.; Jung, M. E.; Sawyers, C. L. Development of a Second-Generation Antiandrogen for Treatment of Advanced Prostate Cancer. *Science.* **2009,** 324, 787-790.
92. Scher, H. I.; Beer, T. M.; Higano, C. S.; Anand, A.; Taplin, M.-E.; Efstathiou, E.; Rathkopf, D.; Shelkey, J.; Yu, E. Y.; Alumkal, J.; Hung, D.; Hirmand, M.; Seely, L.; Morris, M. J.; Danila, D. C.; Humm, J.; Larson, S.; Fleisher, M.; Sawyers, C. L. Antitumour activity of MDV3100 in castration-resistant prostate cancer: a phase 1–2 study. *The Lancet.* 375, 1437-1446.
93. So, A.; Gleave, M.; Hurtado-Col, A.; Nelson, C. Mechanisms of the development of androgen independence in prostate cancer. *World J. Urol.* **2005,** 23, 1-9.
94. McDonnell, T. J.; Troncoso, P.; Brisbay, S. M.; Logothetis, C.; Chung, L. W. K.; Hsieh, J.-T.; Tu, S.-M.; Campbell, M. L. Expression of the Protooncogene bcl-2 in the Prostate and Its Association with Emergence of Androgen-independent Prostate Cancer. *Cancer Res.* **1992,** 52, 6940-6944.
95. McCracken, S. R. C.; Ramsay, A.; Heer, R.; Mathers, M. E.; Jenkins, B. L.; Edwards, J.; Robson, C. N.; Marquez, R.; Cohen, P.; Leung, H. Y. Aberrant expression of extracellular signal-regulated kinase 5 in human prostate cancer. *Oncogene.* **2007,** 27, 2978-2988.

96. McPherson, K.; Steel, C. M.; Dixon, J. M. Breast cancer—epidemiology, risk factors, and genetics. *BMJ.* **2000,** 321, 624-628.
97. King, M.-C.; Marks, J. H.; Mandell, J. B.; Group, T. N. Y. B. C. S. Breast and Ovarian Cancer Risks Due to Inherited Mutations in BRCA1 and BRCA2. *Science.* **2003,** 302, 643-646.
98. Song, H.; Jin, X.; Lin, J. Stat3 upregulates MEK5 expression in human breast cancer cells. *Oncogene.* **2004,** 23, 8301-8309.
99. Kamath, S.; Buolamwini, J. K. Targeting EGFR and HER-2 receptor tyrosine kinases for cancer drug discovery and development. *Med. Res. Rev.* **2006,** 26, 569-594.
100. Montero, J. C.; Ocaña, A.; Abad, M.; Ortiz-Ruiz, M. J.; Pandiella, A.; Esparís-Ogando, A. Expression of Erk5 in Early Stage Breast Cancer and Association with Disease Free Survival Identifies this Kinase as a Potential Therapeutic Target. *PLoS. ONE.* **2009,** 4, e5565.
101. Zen, K. Y., K.; Nakajima, T. et al. ERK5 is a target for gene amplification at 17p11 and promotes cell growth in hepatocellular carcinoma by regulating mitotic entry. *Genes, chromosomes. cancer.* **2009,** 48, 109-120.
102. Angtuaco, E. J. C.; Fassas, A. B. T.; Walker, R.; Sethi, R.; Barlogie, B. Multiple Myeloma: Clinical Review and Diagnostic Imaging. *Radiology.* **2004,** 231, 11-23.
103. Carvajal-Vergara, X.; Tabera, S.; Montero, J. C.; Esparís-Ogando, A.; López-Pérez, R.; Mateo, G.; Gutiérrez, N.; Parmo-Cabañas, M.; Teixidó, J.; San Miguel, J. F.; Pandiella, A. Multifunctional role of Erk5 in multiple myeloma. *Blood.* **2005,** 105, 4492-4499.
104. Tatake, R. J.; O'Neill, M. M.; Kennedy, C. A.; Wayne, A. L.; Jakes, S.; Wu, D.; Kugler Jr, S. Z.; Kashem, M. A.; Kaplita, P.; Snow, R. J. Identification of pharmacological inhibitors of the MEK5/ERK5 pathway. *Biochem. Biophys. Res. Commun.* **2008,** 377, 120-125.
105. Roth, J., G.; Heckel, A.; Walter, R.; Van Meel, J.; Redemann, N.; Tontsch-Grunt, U.; Spevak, W.; Hilberg, F.; Substituted indolines which inhibit receptor tyrosine kinases. 2004.
106. Lovric, M.; Cepanec, I.; Litvic, M.; Bartolincic, A.; Vinkovic, V. Scope and limitations of sodium and potassium trimethylsilanolate as reagents for conversion of esters to carboxylic acids. *Croat. Chem. Acta.* **2007,** 80, 109-115.
107. Shestopalov, A. M.; Nikishin, K. G.; Gromova, A. V.; Rodinovskaya, L. A. One-pot synthesis of 4,6-diaryl-3-cyanopyridine-2(1*H*)-thiones and their transformation to

substituted thieno[2,3-b;4,5-b]dipyridines and pyrido[3",2":4,5]thieno[3,2-d]pyrimidines. *Russ. Chem. Bull.* **2003,** 52, 2203-2206.

108. Krauze, A.; Germane, S.; Eberlins, O.; Sturms, I.; Klusa, V.; Duburs, G. Derivatives of 3-cyano-6-phenyl-4-(3'-pyridyl)-pyridine-2(1*H*)-thione and their neurotropic activity. *Eur. J. Med. Chem.* **1999,** 34, 301-310.

109. Fan, H.; Peng, J.; Hamann, M. T.; Hu, J.-F. Lamellarins and Related Pyrrole-Derived Alkaloids from Marine Organisms. *Chem. Rev.* **2007,** 108, 264-287.

110. Ferreira, V. F.; De Souza, M. C. B.; Cunha, A. C.; Pereira, L. O. R.; Ferreira, M. L. G. Recent Advances in the Synthesis of Pyrroles. *ChemInform.* **2001,** 32.

111. Paal, C. Synthese von Thiophen und Pyrrolderivaten. *Chem. Ber.* **1885,** 18, 367.

112. Amarnath, V.; Anthony, D. C.; Amarnath, K.; Valentine, W. M.; Wetterau, L. A.; Graham, D. G. Intermediates in the Paal-Knorr synthesis of pyrroles. *J. Org. Chem.* **1991,** 56, 6924-6931.

113. Trautwein, A. W.; Süßmuth, R. D.; Jung, G. Hantzsch pyrrole synthesis on solid support. *Bioorg. Med. Chem. Lett.* **1998,** 8, 2381-2384.

114. Williams, S. P.; Kuyper, L. F.; Pearce, K. H. Recent applications of protein crystallography and structure-guided drug design. *Curr. Opin. Chem. Biol.* **2005,** 9, 371-380.

115. Fox, T.; Coll, J. T.; Xie, X.; Ford, P. J.; Germann, U. A.; Porter, M. D.; Pazhanisamy, S.; Fleming, M. A.; Galullo, V.; Su, M. S.; Wilson, K. P. A single amino acid substitution makes ERK2 susceptible to pyridinyl imidazole inhibitors of p38 MAP kinase. *Protein Sci.* **1998,** 7, 2249-55.

116. Gramstad, T. Studies of hydrogen bonding—part VII: Hydrogen-bond association of phenol and pentachlorophenol with carbonyl compounds and ethers. *Spectrochim. Acta.* **1963,** 19, 497-508.

117. Kakushima, M.; Hamel, P.; Frenette, R.; Rokach, J. Regioselective synthesis of acylpyrroles. *J. Org. Chem.* **1983,** 48, 3214-3219.

118. Karplus, M. Vicinal proton coupling in nuclear magnetic resonance. *Am. Chem. Soc.* **1963,** 85, 2870-2871.

119. Mattsson, S.; Dahlström, M.; Karlsson, S. A mild hydrolysis of esters mediated by lithium salts. *Tet. Lett.* **2007,** 48, 2497-2499.

120. Hanessian, S.; Guindon, Y. Cleavage of methyl and benzyl ethers with thiotrimethylsilanes. *Tet. Lett.* **1980,** 21, 2305-2308.

121. Rebelo, R. A.; Rezende, M. C.; Nome, F.; Zucco, C. The Use of 2,2,2-Trichloro-1-Arylethanones as Benzoylating Agents. *Synth. Commun.* **1987,** 17, 1741-1748.
122. Shadnia, H.; Wright, J. S. Understanding the Toxicity of Phenols: Using Quantitative Structure−Activity Relationship and Enthalpy Changes To Discriminate between Possible Mechanisms. *Chem. Res. Toxicol.* **2008,** 21, 1197-1204.
123. Ethell, B. T.; Ekins, S.; Wang, J.; Burchell, B. Quantitative structure activity relationships for the glucuronidation of simple phenols by expressed human UGT1A6 and UGT1A9. *Drug Metab. Dispos.* **2002,** 30, 734-8.
124. Katritzky, A. R.; Suzuki, K.; Singh, S. K.; He, H.-Y. Regiospecific C-Acylation of Pyrroles and Indoles Using N-Acylbenzotriazoles. *J. Org. Chem.* **2003,** 68, 5720-5723.
125. Colombo, M.; Bossolo, S.; Aramini, A. Phosphorus Trichloride-Mediated and Microwave-Assisted Synthesis of a Small Collection of Amides Bearing Strong Electron-Withdrawing Group Substituted Anilines. *J. Comb. Chem.* **2009,** 11, 335-337.
126. Mehta, A.; Jaouhari, R.; Benson, T. J.; Douglas, K. T. Improved efficiency and selectivity in peptide synthesis: Use of triethylsilane as a carbocation scavenger in deprotection of t-butyl esters and t-butoxycarbonyl-protected sites. *Tet. Lett.* **1992,** 33, 5441-5444.
127. Down, K.; Bamborough, P.; Alder, C.; Campbell, A.; Christopher, J. A.; Gerelle, M.; Ludbrook, S.; Mallett, D.; Mellor, G.; Miller, D. D.; Pearson, R.; Ray, K.; Solanke, Y.; Somers, D. The discovery and initial optimisation of pyrrole-2-carboxamides as inhibitors of p38α MAP kinase. *Bioorg. Med. Chem. Lett.* **2010,** 20, 3936-3940.
128. Herberich, B.; Cao, G.-Q.; Chakrabarti, P. P.; Falsey, J. R.; Pettus, L.; Rzasa, R. M.; Reed, A. B.; Reichelt, A.; Sham, K.; Thaman, M.; Wurz, R. P.; Xu, S.; Zhang, D.; Hsieh, F.; Lee, M. R.; Syed, R.; Li, V.; Grosfeld, D.; Plant, M. H.; Henkle, B.; Sherman, L.; Middleton, S.; Wong, L. M.; Tasker, A. S. Discovery of Highly Selective and Potent p38 Inhibitors Based on a Phthalazine Scaffold. *J. Med.Chem.* **2008,** 51, 6271-6279.
129. Adams, J. L.; Boehm, J. C.; Kassis, S.; Gorycki, P. D.; Webb, E. F.; Hall, R.; Sorenson, M.; Lee, J. C.; Ayrton, A.; Griswold, D. E.; Gallagher, T. F. Pyrimidinylimidazole inhibitors of CSBP/P38 kinase demonstrating decreased inhibition of hepatic cytochrome P450 enzymes. *Bioorg. Med. Chem. Lett.* **1998,** 8, 3111-3116.
130. Leeson, P. Drug discovery: Chemical beauty contest. *Nature.* **2012,** 481, 455-456.
131. Veber, D. F.; Johnson, S. R.; Cheng, H. Y.; Smith, B. R.; Ward, K. W.; Kopple, K. D. Molecular properties that influence the oral bioavailability of drug candidates. *J. Med. Chem.* **2002,** 45, 2615-23.

132. Hitchcock, S. A. Structural Modifications that Alter the P-Glycoprotein Efflux Properties of Compounds. *J. Med. Chem.* **2012,** 55, 4877-4895.
133. Auerbach, R.; Lewis, R.; Shinners, B.; Kubai, L.; Akhtar, N. Angiogenesis assays: a critical overview. *Clin. Chem.* **2003,** 49, 32-40.
134. Knapp, D. M.; Gillis, E. P.; Burke, M. D. A General Solution for Unstable Boronic Acids: Slow-Release Cross-Coupling from Air-Stable MIDA Boronates. *J. Am. Chem. Soc.* **2009,** 131, 6961-6963.
135. Payne, S. L. Small-molecule inhibitors of mTOR and DNA-PK. Newcastle University, 2010.
136. Rose, J. D.; Secrist, J. A.; Montgomery, J. A. Certain 3,9-Dideazapurines as Inhibitors of Purine Nucleoside Phosphorylase. *Nucleos. Nucleot.* **1999,** 18, 2443-2461.
137. Sahoo, S. P. C., M-H; Dykstra, K.D; Koyama, H; Meinke, P.T; O'Keefe, S.J; Yang, G, X-Q;. Pyrrolo[2, 3-C]pyridine derivatives as p38 kinase inhibiting agents. 2009.
138. Wang, P.-S.; Liang, C.-K.; Leung, M.-k. An improved Ullmann–Ukita–Buchwald–Li conditions for CuI-catalyzed coupling reaction of 2-pyridones with aryl halides. *Tetrahedron.* **2005,** 61, 2931-2939.
139. Andrews, S. P.; Ladlow, M. Convenient Preparation and Use of a New Analytical Construct for the Analysis and Development of Solid-Phase Chemistries. *J. Org. Chem.* **2003,** 68, 5525-5533.
140. Stroba, A.; Schaeffer, F.; Hindie, V.; Lopez-Garcia, L.; Adrian, I.; Fröhner, W.; Hartmann, R. W.; Biondi, R. M.; Engel, M. 3,5-Diphenylpent-2-enoic Acids as Allosteric Activators of the Protein Kinase PDK1: Structure−Activity Relationships and Thermodynamic Characterization of Binding as Paradigms for PIF-Binding Pocket-Targeting Compounds†† PDB code of 2Z with PDK1: 3HRF. *J. Med. Chem.* **2009,** 52, 4683-4693.
141. Edwards, M. L.; Stemerick, D. M.; Sabol, J. S.; Diekema, K. A.; Dinerstein, R. J. Inhibition of Myeloperoxidase Release from Rat Polymorphonuclear Leukocytes by a Series of Azachalcone Derivatives. *J. Med. Chem.* **1994,** 37, 4357-4362.
142. Mroczkiewicz, M.; Ostaszewski, R. A new and general method for the synthesis of tripeptide aldehydes based on the multi-component Ugi reaction. *Tetrahedron.* **2009,** 65, 4025-4034.
143. Anderson, H. J.; Riche, C. R.; Costello, T. G.; Loader, C. E.; Barnett, G. H. Pyrrole chemistry. XIX. Reactions of 2-pyrrolecarbonitrile and its 4-substituted derivatives. *Can. J. Chem.* **1978,** 56, 654-657.